The Characterisation of the Hydrodynamic Vortex Separator using Residence Time Distribution Analysis

Philip Richard Higgins

A thesis submitted in partial fulfilment of the University's requirements for the Degree of Doctor of Philosophy

November 2000

Liverpool John Moores University
School of the Built Environment

Abstract

The hydrodynamic vortex separator (HDVS) is currently employed at wastewater treatment works and in the sewerage system as a combined sewer overflow (CSO) for the separation of solids from an incoming waste stream. This project presents the first stage in developing and aiding the existing design methodology for the optimisation of kinetic processes within the HDVS. The kinetic process design methodology combines hydraulic and kinetic principles by using the true mixing regime characteristics of a system and batch reactor data to determine a kinetic processes efficiency.

This project used residence time distribution (RTD) analysis to extensively characterise the mixing regime within a model and prototype HDVS. The HDVS was operated with and without a baseflow component and with and without the sludge hopper for a range of inlet flow rates and flow splits covering design flow rates for a number of existing applications. The RTD was obtained using a pulse tracer injection method and described using the complete range of data analysis techniques typical employed in RTD studies. This includes the axial dispersion model (ADM), tanks-in-series model (TISM), RTD indices and a RTD combined mathematical model. The combined model is configured to quantify the inactive flow behaviour within the HDVS i.e. stagnant and dead volumes.

The HDVS has a complex imperfect plug-flow mixing regime. This non-ideal flow behaviour is associated with both dispersion and dead volumes and results in short-circuiting. At low flow rates the HDVS operating without a baseflow contains fluid elements which conduct flow slower than the mean velocity. At high flow rates the inactive flow behaviour is associated with dead volumes and subsequently short-circuiting. The flow rate at which this change in mixing characteristics occurs is termed the transition flow rate and is approximately 15l/min and 90l/min for the model and prototype HDVS respectively. At all flow rates above the transition flow rate the HDVS has a very stable mixing regime, which is associated with both the inactive flow behaviour and the plug-flow mixing characteristics. The ADM and TISM parameters increase as the flow rate decreases and therefore, the HDVS has improved plug-flow mixing characteristics and reduced dispersion at low flow rates. Removing the sludge hopper reduces the inactive flow behaviour and improves the plug-flow mixing characteristics.

The inactive flow behaviour within the model HDVS operating with no baseflow occupies approximately 20-40% of the total volume and similarly for the prototype

HDVS 5-25% and increases as the inlet flow rate increases. The inactive flow behaviour occupies a smaller fraction of the total volume and the plug-flow mixing characteristics are also improved as the HDVS is scaled-up in size. Hence, the scale-up of the HDVS will provide a mixing regime with less short-circuiting and improved plug-flow mixing characteristics and therefore, more conducive for certain kinetic processes and particularly chemical disinfection processes.

The introduction of a baseflow component alters the total mixing regime within the HDVS. The baseflow component introduces an element of plug-flow mixing and subsequently the total plug-flow mixing characteristics of the HDVS operating with a baseflow component are greater than the HDVS operating without a baseflow. The baseflow component plug-flow mixing characteristics increase and the overflow component decrease as the inlet flow rate increases. Short-circuiting of the baseflow and overflow component occurs as the inlet flow rate decreases and increases respectively. Hence, there are different mixing regimes within the HDVS associated with the overflow and baseflow component. The HDVS operating with a baseflow component has improved plug-flow mixing characteristics when the sludge hopper is included.

This project was also extended to include an experimental kinetic process analysis, by investigating the first-order decomposition of hydrogen peroxide (H_2O_2) using catalase. This was undertaken to compare the actual kinetic process performance within the HDVS to that estimated using the RTD. The H_2O_2 decomposition results showed that the design of the HDVS for kinetic processes can be achieved using only the RTD and relevant batch reactor data. This enables the HDVS to be optimised for kinetic process applications and eliminates the need for costly and time consuming pilot trials.

The characterisation of the HDVS using RTD analysis creates scope for significant future research. This includes: alternative experimental RTD techniques, development of the RTD combined mathematical model to include a baseflow component and kinetic process principles, extensive kinetic process batch reactor investigations, application of both the hydraulic and kinetic data into chemical reactor design computer software and finally the scaling of the HDVS using the RTD and therefore the kinetic process optimisation.

This work is a proactive response by practitioners and Hydro International Plc to pressure from the regulators and EU Directives, placing emphasis on the use of sophisticated treatment processes based on good scientific principles, to meet current and future stringent water quality standards.

Acknowledgements

I would first like to collectively thank my project supervisors Dr Rafid Alkhaddar, Dr Dave Phipps (LJMU) and Professor Bob Andoh (Hydro International Plc) for providing me with the opportunity to participate in this research and their guidance, continuous support and patience particularly during the writing up period. Additionally I would like to thank my supervisors for their encouragement and the opportunities provided to produce publications and for sharing their knowledge of their respective fields. The commitment of Hydro International Plc to the supply of a prototype HDVS and funding, which contributed to the manufacture of the model HDVS and the time dedicated by Professor Bob Andoh.

I would like to thank Dr Alec James of UMIST and Chu Cheong from LJMU for their help and ideas in developing the RTD combined mathematical model (chapter 5). The technicians at Clarence Street and Byrom Street and especially Mr Paul Wright and the technicians who could never do enough particularly during the time spent building the model HDVS. The School of Biological Earth Sciences and School of Biomolecular Sciences at LJMU for use of their facilities.

My current employers Coventry University and particularly Professor Chris Pratt and Dr John Davies for their understanding and freedom provided during the writing of the thesis. Mr Paul Whitehall for his moral support and being a good friend.

Finally all my family and friends who never stopped listening and encouraging and those from whom I sought greatest inspiration - Claire O'Reilly and Bruce - thanks for those memorable nights in the garden and the dream was never a lie. This ones for you Marj and George and the 28 years of believing and supporting.

Contents **Page**

List of Figures **Page**

List of Tables **Page**

Glossary of Terms

AAS	Atomic Absorption Spectrophotometer
ADE	Advection-Dispersion Equation
ADF	Advanced Demonstration Facility
ADM	Axial Dispersion Model
ADZ	Aggregated Dead Zone Model
AS	Absorption Spectrophotometer
BOD	Biochemical Oxygen Demand
BWD	Bathing Water Directive
CFD	Computational Fluid Dynamics
CSTR	Continuous Stirred Tank Reactor
CT	Concentration (C)-Time (T) Product
D	Dispersion Number
Da	Damköhler Number (dimensionless)
DAF	Dissolved Air Flotation
Dead Volume	Isolated from the rest of the system and therefore reduces its 'true' volume
DP	Dosing Point
ESS	Sum of the Errors Squared
E(t)	Exit-Age Distribution Function
E(Θ)	Normalised Exit-Age Distribution Function
F(t)	Cumulative Distribution Function
HDVS	Hydrodynamic Vortex Separator
H_2SO_4	Sulphuric Acid
H_2O_2	Hydrogen Peroxide
I_2	Iodine
k	Reaction Rate Constant (min^{-1})
KI	Potassium Iodide
LiCl	Lithium Chloride
LJMU	Liverpool John Moores University
MW	Molecular Weight
N	Number of Tanks-in-Series
n	RTD Curve Moment
$Na_2S_2O_3$	Sodium Thiosulphate

P_e	Peclet Number
Qb	Baseflow Component Flow Rate
Qi	Inlet Flow Rate
Qo	Overflow Component Flow Rate
Q_2	Combined Model Flow Rate Through Tank 2 (Exchange Flow Rate)
RTD	Residence Time Distribution
R^2	Coefficient of Correlation
Sluggish Flow	Flow due to convection but at a rate much slower than the mean
SP1	Sample Point 1 (overflow)
SP2	Sample Point 2 (Baseflow)
SP3	Sample Point 3 (Baseflow)
Stagnant Flow	Flow due to molecular diffusion
SWTR	Surface Water Treatment Rule
TISM	Tank-in-Series Model
TSS	Total Suspended Solids
t_f	Time at which tracer first appears
t_p	Time of peak concentration
t_{10}	Time at which 10% of tracer passed through reactor
t_{50}	Time at which 50% of tracer passed through reactor
t_{90}	Time at which 90% of tracer passed through reactor
t_m	Experimental Mean Residence Time - centroid of curve
UK	United Kingdom
US	United Sates
USEPA	United States Environmental Protection Agency
UWWTD	Urban Wastewater Treatment Directive
V_4	Combined Model Volume of Tank 4 (Dead Volume)
W(t)	Washout Function
X	Conversion (%)
X(t)	Conversion after time t (%)
$\lambda(t)$	Intensity Function
$\lambda(\Theta)$	Normalised Intensity Function
Θ	Normalised Time
τ	Theoretical Mean Residence Time (t = V/Q)

1.0 Introduction

The treatment of wastewater and stormwater is predominantly addressed by two European Union (EU) Directives, the Urban Wastewater Treatment Directive (UWWTD) (Council of the European Communities, 1991) and the Bathing Water Directive (BWD) (Council of the European Communities, 1976). These directives identify three stages of treatment - primary, secondary and tertiary. The level of treatment increases as more stages are employed. In the UK, primary and secondary processes have generally been used to meet statutory EU water quality standards.

The UWWTD defines primary treatment as a means of treating urban wastewater by a physical and/or chemical process. This involves the settlement of suspended solids or other processes in which the biochemical oxygen demand (BOD) of the incoming wastewater is reduced to at least 20% before discharge and the total suspended solids (TSS) of the incoming wastewater are reduced by at least 50%. Secondary treatment has been defined in the UWWTD as treatment by a process generally involving biological treatment with a secondary settlement or other process in which the TSS and BOD are at a minimum reduced to 90% and 70-90% respectively. (Andoh, 1993).

The UWWTD requires the treatment of discharges to a certain level depending on the population of the contributing catchment and the classification of the receiving watercourse. Discharges to bathing waters are regulated by the BWD. In addition, discharges to bathing waters meeting the UWWTD must also meet the requirements of the BWD. The BWD provides microbiological standards, both mandatory and guideline limits for various microbiological indicators (Realey, 1995).

To meet these additional biological standards for discharges to bathing waters the third stage of treatment is sometimes employed. Tertiary treatment processes are generally used for bathing water discharges and discharges to receiving waters

classified as sensitive by the UWWTD e.g. where nutrient and microbial control is required. Typical processes used for tertiary treatment include chemical and physical disinfection.

At present, no EU legislation specifically controls or requires the use of any tertiary treatment processes to meet microbiological standards. The tried and tested traditional civil engineering approach relies upon standard treatment combined with outfalls discharging far enough away to allow dispersion, dilution and the natural biocidal action of the environment to reduce the levels of sewage derived microorganisms to acceptable levels (Realey, 1995). However, as concerns increase over the quantitative and qualitative nature of wastewater, and the associated costs and practicalities of the traditional approach, emphasis is being placed on innovative methods for achieving cost-effective wastewater treatment. There is also concern that although achieving microorganism indicator standards, long sea outfalls may permit accumulation of bacterial and viral pathogens in sediment reservoirs near the discharge point (Rudd and Hopkinson, 1989). This is highlighted by considering the new proposed amendments to the BWD. These propose lower statutory limits for various microbiological indicators and extend the current definition of a bathing water (Stedman, 1996). If implemented a bathing water may include many inland waters and as a consequence current discharge consents could fail EU microbiological standards. The combined effect of these amendments and impending legislation, together with other factors such as the availability of new technology may mean that the use of tertiary treatment and specifically wastewater disinfectant is an option that many of the water undertakers will consider seriously.

The choice to use the traditional approach or tertiary treatment has divided the water industry during its implementation of both the UWWTD and BWD EU directives. In terms of initial cost, the industry considers that there is little difference between the

two treatment methods. The difference in costs of simpler and complex treatment systems is offset against longer and shorter outfalls respectively (Stedman, 1997). The ultimate question becomes one of effectiveness – which approach produces water quality standards sufficient to meet the two relevant directives. Both techniques appear to provide effective treatment however, in several areas of the water industry it has been suggested that standards should be based on good science. Hence, standards are acceptable and can be justified to the public. Subsequently, the UK government have suggested the need for tertiary treatment at all sea outfalls (Environment Select Committee, 1998).

Tertiary treatment is been recognised as a primary weapon in the challenge to maintain BWD and UWWTD standards. Politics, tourist considerations and legislation are the main drivers for tertiary treatment and given the political climate and more stringent legislation pending, disinfection is likely to be a key factor in future improvements. Subsequently, several U.K. water companies have started to implement policies of installing tertiary treatment for discharges to bathing waters e.g. North West Water, Welsh Water and Wessex Water.

The above discussion is not only confined to discharges from wastewater treatment works (WWTW) but also to intermittent discharges to watercourses from combined sewer overflows (CSO) and stormwater discharges i.e. rainfall runoff. A CSO is a device used in the combined sewerage system i.e. foul and stormwater flow in the same pipe to provide relief during heavy periods of rainfall and therefore prevent flooding upstream. A CSO also has additional requirements to ensure that the excess flow i.e. overflow discharged to the nearest watercourse is of a required quality i.e. pollutant load. The latter unfortunately was not appreciated by the designers of the first and majority of CSO's currently installed in the UK drainage network. CSO discharges also have to meet the requirements of the UWWTD and BWD and are currently being

addressed by the water industry in their Asset Management Plans 2 and 3 (AMP2 and AMP3). The requirements and methods to achieve these standards are detailed in the Urban Pollution Management Manual for the UK (Foundation for Water Research, 1998).

CSO's at best only provide a level of treatment equal to primary treatment i.e. solids-liquid separation. However, self-cleansing screen mechanisms are being installed at CSO's to remove the threat of aesthetic pollution from gross solids and particularly neutrally buoyant material. Due to the problems outlined above and continuing concern over the quality of our watercourses due to the impact of CSOs the prospect of increasing the level of treatment at CSOs is coming ever closer. The United States (US) has been researching the idea of providing higher levels of treatment at CSO's since the 1970's (section 2.1.5). The processes considered include chlorine (Cl), ozone (O_3), ultra violet (UV) disinfection and chemical precipitation and dissolved air flotation (DAF). However, Europe still lags some way behind the US trend of screening, settlement and disinfecting as preferred CSO treatment options (Smith, 1999). The UK water industry is currently undertaking CSO rehabilitation projects generally included in drainage area studies (DAS). The removal of CSOs is a common option however if the design engineer had the option of sophisticated treatment processes mentioned above it may encourage CSOs to be considered and possibly provide the hydraulic and environmental benefits they are envisaged to offer.

An emphasis on sustainable development in the UK, following the UN Earth summit at Rio de Janeiro in 1992 resulted in the UK government publishing *Local Agenda 21 – A framework for Local sustainability* (CIRIA, 2000). This had implications for stormwater discharges and particularly from new developments. It is widely accepted that it is impractical to treat all stormwater discharges but localised treatment and particularly at its source is now becoming a preferred option i.e. sustainable urban

drainage systems (SUDS). Stormwater can be contaminated with levels of pollutants far exceeding those accepted from a WWTW discharge and include solids, oil and pathogenic organisms (Scottish Environment Protection Agency and Environment Agency, 1997).

This project is the first stage in developing a design methodology for the application of a hydrodynamic vortex separator (HDVS) for processes dependent on kinetic principles. This includes treatment processes used in wastewater and stormwater management as discussed above. However the approach adopted equally applies to a range of kinetic processes employed in a number of other applications. The term 'kinetic principle' refers to the mechanism by which the process occurs i.e. chemical as opposed to physical. Typical kinetic process mechanisms include chemical reactions, converting reactants into products and the inactivation of microorganisms using a disinfectant. The design methodology is dependent on both the hydraulic characteristics of the contact tank in which the process precedes and the specific kinetic principles of the process.

The first stage of the design methodology is achieved by characterising the HDVS mixing regime using residence time distribution (RTD) analysis. This is undertaken as the mixing regime characteristics are an integral design parameter for the optimisation of any kinetic process and describes the hydraulic stage of the design methodology. This project was also extended to include an experimental kinetic analysis investigating the first-order decomposition of hydrogen peroxide (H_2O_2) by a biological enzyme - catalase. Due to the reaction mechanism this kinetic process lends itself to direct comparison with the RTD prediction of the experimental H_2O_2 decomposition. Additionally this project presents experimental data to aid in the scaling of the HDVS and therefore the design methodology is not constrained by the size of a particularly HDVS and operating conditions. This study is part of a long term research project to

characterise and optimise the HDVS for kinetic process applications and runs in parallel with on-site trials into a range of such processes conducted in the US (section 2.1.5).

The HDVS is currently used in stormwater and wastewater management. The HDVS (Fig. 3.1) is a third generation vortex-style sedimentation device, which provides a controlled flow regime for the separation of solids from an incoming waste stream. The initial concept was provided by Smisson, (1967) and had its first full-scale investigation in the 1960's. The results and conclusions were presented at an Institution of Civil Engineers (ICE) symposium on storm sewage overflows (Smisson, 1967).

The HDVS used throughout this project is one of three patented designs used for the separation of the complete range of incoming solids from an incoming waste stream. The HDVS currently manufactured by Hydro International Plc, which are relevant to this project as they have developed from the first concept design (Smisson, 1967) and relevant research is cited in chapter 2, are described in Table 1.1.

Table 1.1 Summary of the Different Styles of HDVS Developed in the UK

HDVS	Solids	Application	Mode of Operation	General Comments
Swirl-Flo™	Colloidal Particles	Wastewater and industrial-chemically enhanced solids removal	Baseflow	Sludge Hopper
Storm King™	Particles in suspension	Wastewater and stormwater (CSO)	Baseflow	No Sludge Hopper
Grit King™	Grits and sands etc.	Wastewater, stormwater, industrial	No Baseflow	Grit Pot

Table 1.1 is not a comprehensive description of the different styles of HDVS and a number of modifications and operating conditions can be applied to each HDVS particularly as the information provided generally relates to the HDVS for solids-liquid separation processes. The three types of HDVS all have different internal and operating

configurations and parameters, which are optimised for the separation of their designed solids loading rate and properties. The Swirl-Flo™ HDVS operates at a lower flow rate compared to the Grit King™ and its internal configuration includes additional baffles to minimise turbulence which is detrimental to the removal of lighter particles. The HDVS's investigated and discussed throughout this project were developed in the UK (Table 1.1). Similar processes developed outside the UK are mentioned in chapter 2 (section 2.1.1).

The Swirl-Flo™ HDVS process is used for all experimental investigations throughout this project. In the experimental chapters and conclusions (chapter 3-8) the Swirl-Flo™ style of device is referred to as the HDVS. However, in the literature review (chapter 2) and when comparing experimental results e.g. section 4.4.9.3 the individual trade names are used so as to differentiate between the different styles of HDVS and ensure that cited references are correctly interpreted and relevance understood. The reader is occasionally referred to Fig. 3.1 showing a schematic representation of the Swirl-Flo™ HDVS used throughout this project when discussing the Grit King™ and Storm King™ HDVS, as the typical configuration i.e. inner and outer zones, position of inlet pipe and the dip plate are common to all styles of HDVS.

The HDVS is used at wastewater treatment plants where such treatment processes are required to provide a treated effluent suitable for further treatment, to meet water quality standards. The HDVS other main application is in the sewerage system as a CSO. Its purpose being to control the quantity of flow passed on to the treatment works and the quality of effluent discharged to the receiving watercourse during wet-weather flows.

The HDVS generally has one inlet pipe and two outlet pipes. The outlet pipes are referred to as the overflow and baseflow and the HDVS has several applications operating with and without the baseflow component (Fig. 3.1). Operating with a

baseflow the device can be used directly for high-rate primary sedimentation either at a WWTW or as a CSO. The device can also be used as a coagulation/flocculation tank and for the following sedimentation process. The device's main applications with no baseflow is for the separation of heavy particles such as grit and sand at WWTW and from stormwater discharges and as a contact tank for wastewater disinfection and/or dissolved air flotation. The HDVS principle of operation is described in more detail in chapter 3 (section 3.2).

The HDVS is used for two stages of the treatment process i.e. primary and secondary treatment. However by investigating the device's potential for other treatment processes and particularly chemical processes, it may be possible to provide the three stages of treatment by using one device e.g. a series of HDVS's could be used, providing different levels of treatment depending on the application and receiving watercourse. Alternatively the HDVS could be operated in a similar manner to a sequencing batch reactor (SBR) which are predominantly used for nitrification/denitrification treatment processes (Tchobanoglous and Burton, 1991). The SBR operates in a true batch mode with different treatment processes occurring in the same device. The major difference between a batch and continuous flow system is that the SBR technique carries out the process in a time sequence rather than the conventional space sequence. This provides flexibility with regards to the treatment time for each process i.e. primary, secondary and tertiary treatment within the HDVS. The HDVS potential as a contact tank for tertiary treatment processes will have to account for its particular application e.g. a CSO is typically located at a remote location and its operation is intermittent.

The traditional approach used to design a kinetic process has been to split the investigation into two separate parts – a hydraulic and kinetic analysis and finally to combine the two stages (Johnson *et al.*, 1997 and 1998).

It is widely recognised that the flow patterns expected within a mixing device would be non-ideal, as diffusion and dispersion are ever present. Turbulent regions, which often include flow recirculation and separation, cause the flow to be non-uniform and this results in short-circuiting and stagnant zones. The resulting consequence of these flow patterns is that the fluid leaving the device has a RTD i.e. different volumes reside within the device for different periods of time. The presence of a RTD results in the actual mixing regime being between the boundaries of the two theoretical mixing regimes of plug-flow and complete mixing, which are generally and incorrectly assumed for design processes. The two theoretical mixing regimes are described in more detail in chapter 4 (section 4.1).

The type of mixing regime provided by a particular device influence its performance for various applications. A plug-flow mixing regime is more conducive for liquid disinfection e.g. sodium hypochlorite and sedimentation processes. A complete mixing flow regime is typically used for mass transfer limited disinfection processes e.g. ozone. This is due to the rate limiting parameters for these processes. Contact time is the main rate limiting parameter for liquid disinfection and sedimentation processes whereas contact area between the two phases is more significant for mass transfer limited processes. Plug-flow mixing devices typically include tanks with a large length to width ratio e.g. baffled trains and tubular arrays and for complete mixing, stirred tanks and bubble columns. Therefore, for certain operations it is imperative that the flow regime is made to approach one of the above theoretical flow regimes – usually plug-flow mixing as existing non-ideal flow behaviour is analogous to a mixing regime approaching complete mixing.

The common approach used to design the kinetic process stage of the design methodology is based on batch-scale investigations and a mathematical model, describing either theoretical plug-flow or complete mixing principles and relating the

batch-scale operating parameters to the full-scale plant performance. Therefore the data from batch-scale experiments is scaled accordingly to the continuous flow system to provide a given kinetic process performance. However, these batch-scale tests are conducted under 'perfect' mixing conditions and do not account for any non-ideal flow behaviour within the continuous flow system as discussed above. The World Health Organisation (WHO) drinking water recommendation (World Health Organisation, 1993) illustrates the problem to the designer in that there is no indication as to whether the quoted standards apply to a batch situation, mixed tank or other system (Stevenson, 1995). Therefore, to provide an accurate representation of the full-scale plant some account of this non-ideal flow behaviour must be considered. Hence the approach adopted in this project accounts for these problems by combining the RTD with batch-scale results and therefore knowledge of the RTD enables the true and optimum hydraulic and kinetic process operating parameters to be obtained.

The experimental methodology investigated and considered in this study is currently being addressed and simplified for the design engineer. This is being achieved by the development of computer software packages, which provide fast and accurate design of contact tanks using both hydraulic and kinetic analysis (section 2.2.4). These specific software packages enable new designs and retrofits to be completed within a fraction of the time and cost required compared to conventional physical modelling techniques. However, for many new or existing devices for which experimental hydraulic or kinetic analysis does not exist, it is important that physical tests are undertaken. These aid in the validation and verification of any simulated computer model.

The design methodology discussed above has been extensively researched for the design and optimisation of contact tanks particularly for chlorine disinfection in potable water treatment (section 2.2). However the work described in this project relates to

stormwater and wastewater treatment systems and will possibly become recognised and accepted as wastewater disinfection is considered a necessary and preferred treatment process.

This project used a prototype and a model HDVS geometrically scaled from the prototype HDVS. The project investigates the results for the two HDVS devices using several data analysis techniques, particularly for the RTD investigations. To provide clarity for the reader and easier reference to each HDVS and technique the results and discussions have been separated accordingly. Additionally, experimental data for both devices can be directly compared and scaling relationships considered in future research (section 8.6). It is not the aim of this study to redesign the HDVS or investigate the effects of changing the HDVS internal configuration. However observations made during this project and particularly with respect to potential scaling effects should be considered in future research and the design of the HDVS for all its operating configurations and applications and not limited to the design of the HDVS for kinetic processes.

Chapter 2 in this study reviews work to date on the HDVS and the methods employed in the following chapters to achieve the hydraulic characterisation and future kinetic process optimisation of the HDVS. Additionally chapter 2 identifies the rationale based on existing research for conducting the characterisation of the HDVS using RTD analysis, which is presented in this project. Chapter 3 describes the materials and experimental methods used in the project. Chapters 4 - 6 detail the RTD hydraulic analysis by investigating the mixing regime of both the prototype and model HDVS for a range of operating configurations and parameters. Chapter 5 presents a RTD combined mathematical model specifically designed to describe the mixing regime of the HDVS operating without a baseflow component. This mathematical model accounts for non-ideal flow behaviour not represented by standard RTD flow models. The

combined model development and analysis is part of ongoing research at Liverpool John Moores University (LJMU) and will extend to representing the HDVS operating with a baseflow component and aid in establishing RTD analysis scaling relationships. Chapter 7 investigates reaction kinetics by determining the experimental first-order decomposition of hydrogen peroxide (H_2O_2) by a biological enzyme - catalase within the HDVS. This reaction is also undertaken for batch conditions and the results combined with the RTD to predict the H_2O_2 decomposition in the model and prototype HDVS. Subsequently this is compared to the continuously operated model and prototype HDVS operated with and without a baseflow component experimental H_2O_2 decomposition results. The final chapter concludes and summarises the results from the previous experimental chapters and identifies scope for further research. Supplementary data and information are contained in the appendices supplied on CD-ROM and microfiche.

2.0 Literature Review

This project investigates the Swirl-Flo™ HDVS (Table 1.1) using experimental methods, which are classified as physical and chemical techniques and are typically, applied in the field of environmental engineering. Due to the wide variety of work conducted in these areas the following discussion is an overview of the relevant work to date on the HDVS and in the subject areas below:

- Hydrodynamic Vortex Separator (HDVS)
- Residence Time Distribution (RTD)
- Chemical Kinetic Processes

This chapter presents the work conducted on the HDVS from its initial conception and during its development, for a range of applications in the water industry. This predominantly relates to the HDVS solids-liquid separation performance and has involved laboratory and field investigations. The HDVS has also been used as a contact tank or mixing device to provide chemical treatment processes dependent on kinetic principles.

The majority of this early research conducted on the HDVS has generally treated the HDVS as a 'black box' and was only concerned with the effluent concentration of pollutants and therefore provided little insight into its internal behaviour. However, this has been partially addressed recently by conducting RTD, CFD and hydraulic scaling investigations to support results and conclusions obtained from the HDVS solids-liquid separation efficiency investigations.

The application of RTD analysis to characterise the mixing regime has been applied to several processes in a range of scientific fields and most recently and extensively in

the water industry. Limited RTD investigations have been conducted on the HDVS mainly on the Grit King™ and Storm King™ HDVS (Table 1.1). These HDVS's have different internal geometry's, operating parameters and applications and therefore mixing regimes compared to the Swirl-Flo™ HDVS characterised using the RTD in this project. This existing RTD work did not characterise the HDVS for a range of operating conditions or parameters. Additionally the RTD results used to describe the Grit King™ and Storm King™ HDVS mixing regime are not consistent or maintain standard RTD experimental and data analysis protocol and more importantly investigated by comparing the results generated from different RTD data analysis techniques due to their individual limitations.

The RTD describes the mixing regime within a contact tank upon which the efficiency of the kinetic process undertaken is dependent. Hence, the design of a kinetic process in a continuously operated system should utilise the RTD combined with kinetic principles. However, this is typically conducted using a theoretical interpretation of the combined principles or the experimental RTD and theoretical kinetic principles and therefore the methodology is not supported with experimental kinetic data obtained from the full-scale process. This is highlighted by the optimisation of existing chemical processes within the HDVS. Batch-scale investigations are used to determine the required chemical dose e.g. coagulant however, this information is not combined with the RTD and therefore the effect of non-ideal flow behaviour in the HDVS is not considered. The presence of non-ideal flow behaviour results in discrepancies between the optimum reactants determined from batch-scale tests and that required in the continuously operated HDVS. This results in excessive operating costs or more dramatically failure of the process to meet the required environmental standards.

Therefore it is clear that a comprehensive and consistent RTD characterisation of the HDVS is required to provide detailed information regarding the internal mixing

regime. This will also ascertain the appropriate RTD data analysis combinations, which best describe the HDVS's mixing regime. Additionally the RTD will provide the information required to achieve the first stage in creating a design methodology for the optimisation of kinetic processes within the HDVS. Further work is also required to compare experimental kinetic process results to those predicted from the experimental RTD and batch-scale investigations to ensure that the methodology and final design of the process is correct. This has also been addressed in this project by investigating the first-order decomposition of hydrogen peroxide (H_2O_2) by a biological enzyme – catalase within the HDVS. Due to the reaction mechanism this kinetic process lends itself to direct comparison with the RTD and batch-scale results prediction of the experimental H_2O_2 decomposition. Subsequently the design methodology will enable batch-scale data, on the specific kinetic process, to be combined with the RTD to accurately design the full-scale continuously operated HDVS for kinetic process applications as opposed to conducting laboratory, pilot and field scale HDVS trials.

Based on the above résumé and detailed discussion below on the work currently undertaken on the HDVS this outlines the rationale for conducting the following research presented in this project and is undertaken in response to both product development and environmental legislation.

2.1 The Hydrodynamic Vortex Separator (HDVS) - Research and Development

2.1.1 Conception of the Hydrodynamic Vortex Separator (HDVS)

The existing design and development of the HDVS has evolved from its first conception in the 1960's (Smisson, 1967). This research carried out extensive work on models and full-scale devices culminating in identifying the flow patterns and design

recommendations for this type of HDVS. Performance monitoring of this first style of HDVS, undertaken in Bristol (UK), illustrated that even in its concept design the process of dynamic separation was capable of ensuring that more than 70% of the incoming solids could be retained in 5% of the flow carried forward to treatment (Qb) (Fig. 6.1). Fig. 2.1 shows a typical HDVS schematic arrangement and is provided to aid the reader in this chapter. The HDVS principle of operation and a more detailed illustration of the HDVS internal configuration are provided in chapter 3 (Fig. 3.1).

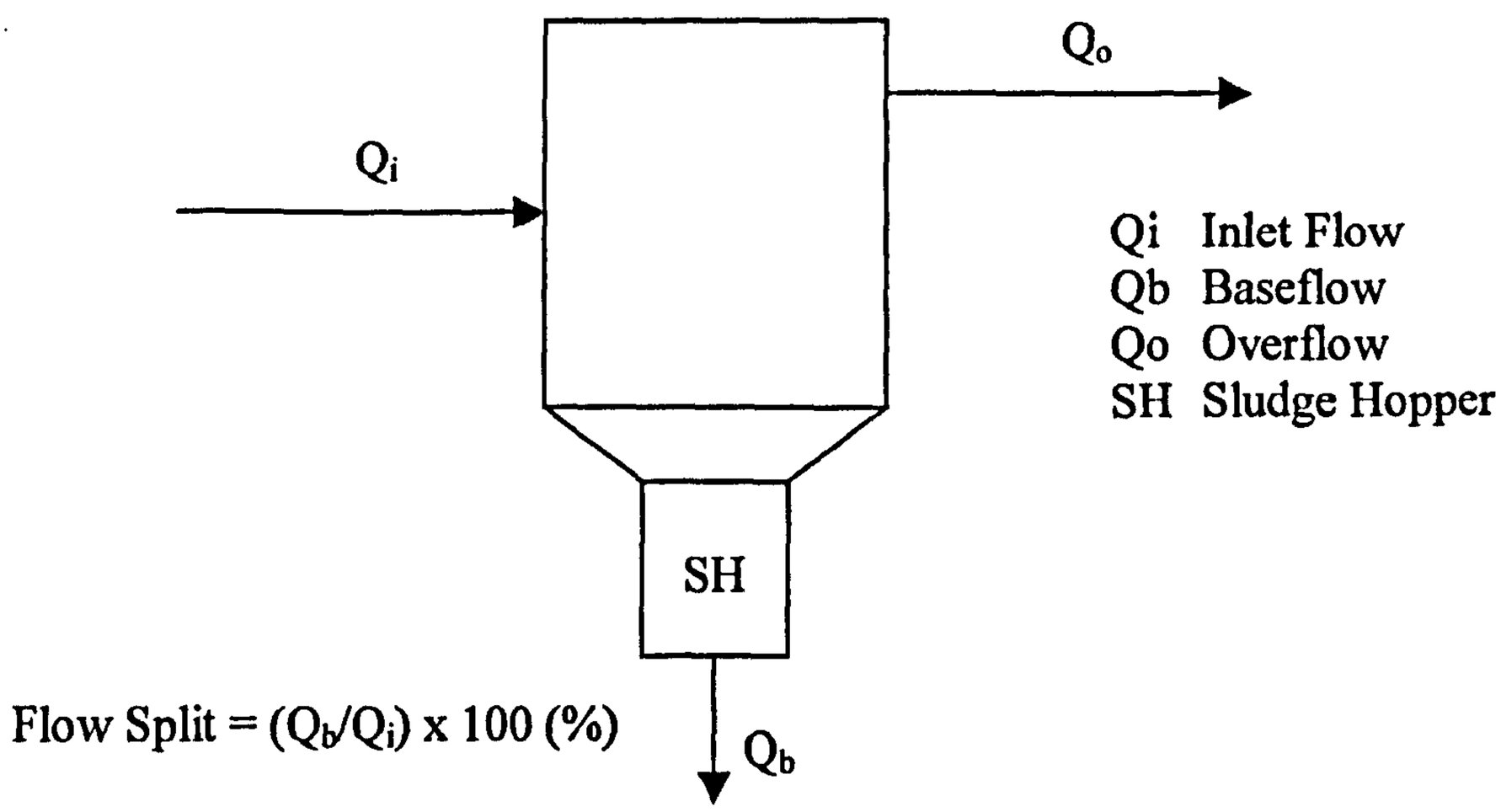

Fig. 2.1 HDVS Flow Component and General Configuration

The current range of HDVS's is a patented design and provides solids-liquid separation treatment for the complete spectrum of incoming solids (Table 1.1). This includes grits and sand which readily settle in a practical time period, colloidal solids e.g. diary industry waste products which do not settle in a practical time period and generally require additionally treatment processes to encourage their settlement and neutrally buoyant material which do not readily settle or float e.g. sanitary towels, condoms, cotton buds etc. The separation of solids takes place within a complex flow regime of upward and downward helical flow as discussed below and in chapter 3

(section 3.2). Additionally, as the HDVS is a high-rate settlement process other pollutants are also removed and include oil and grease and microorganisms associated with solids removal (Andoh, 1993). Since their introduction in the mid 1980's there has been approximately 500 installations of the HDVS in a wide variety of applications including wastewater, stormwater, and industrial effluent treatment (Andoh, 2000).

Existing devices that operate in a similar manner to the HDVS investigated in this project include the Fluid-Sep™ (Brombach, 1987 and 1992, Brombach *et al.*, 1993 and Pisano and Brombach, 1994), vortex overflow with peripheral spill (Balmforth *et al.*, 1984) and US Swirl concentrator (Field, 1974). Current research into these processes has largely focussed on their solids removal efficiency. A review of the various types of HDVS has been given by Field and O'Connor, (1996), Andoh, (1998) and Saul and Harwood, (1998). However, only the range of HDVS discussed previously (chapter 1) are currently being applied and researched extensively both in the UK and internationally for its potential wastewater and stormwater treatment process applications and in combination with existing treatment processes (Boner *et al.*, 1994). The Fluid-Sep™ process has also been subject to several research initiatives as mentioned in section 2.1.5.

The style of HDVS used throughout this project and vortex overflow with peripheral spill are both recommended for use in the UK drainage system as CSO structures (Foundation for Water Research, 1998). Two other CSO structures also recommended are the high-sided weir and stilling pond chamber although these chambers do not utilise the process of dynamic separation for the removal of solids and therefore are not applicable to the research undertaken in this project. The design of CSO's recommended for use in the UK sewer system is provided in the Foundation for Water Research (FWR) report 'Guide to the design of combined sewer overflow structures' (Balmforth *et al.*, 1994).

The hydrocyclone is also a device utilising rotary flow for sedimentation. It is typically used in the mining and chemical industries and is based principally on centrifugal separation in a vortex generated within a conocylindrical body. This contrasts with the HDVS, which uses its internal fixed geometry to create a controlled shear environment providing optimum conditions principally for gravitational forces to effect solids removal (Fenner and Tyack, 1997). The reliable scale-up of hydrocyclones has been demonstrated by Svarovsky, (1984).

2.1.2 Hydrodynamic Vortex Separator (HDVS) Solids Removal Efficiency Investigations

The HDVS (Table 1.1) has been the subject of many research projects undertaken independently by various organisations e.g. universities, Water Research Centre (WRc), water companies and also in collaboration with Hydro International Plc. Research and development on the HDVS has been published in several water and engineering periodicals both nationally and internationally, internally by Hydro International Plc and provides the focal discussion for many conferences in CSO technology and stormwater management. The work undertaken on the HDVS to date is not only driven by the manufactures product development but also legislation predominately related to the water industry (chapter 1).

The HDVS history, operation, design and performance in various laboratory and full-scale applications has been documented (Smisson, 1989, Hedges, 1991, 1993 and 1994, Fagan, 1993, Andoh and Smisson, 1993 and Andoh, 1994 and 1998). The majority of this early research has investigated the level of primary (physical) treatment provided by the device i.e. total suspended solids (TSS) and biochemical oxygen

demand (BOD) removals. The TSS removal efficiency has been investigated using both artificial solids and wastewater (Hedges, 1993).

Many authors discussing a particular HDVS refer to the inlet flow rate however, the manufacturers generally use the surface loading rate which is a function of the overall diameter and used in the design of the HDVS (Table 1.1) i.e. inlet flow rate/horizontal cross-sectional area ($l/s/m^2$). The HDVS diameter can be sized from the design inlet flow rate and the specified solids removal efficiency required. Therefore, throughout this project the inlet flow rate is used although were relevant the surface loading rate is presented.

Andoh, (1994) presented and discussed some of the findings from several investigations undertaken on the HDVS into its solids removal performance. This work discussed by Andoh, (1994) has contributed to verifying a semi-emperical model, developed from first principles relating to sedimentation theory, for the design of the HDVS based on its solids removal efficiency under steady state conditions (Andoh and Smisson, 1993). The empirical constants were initially obtained from previous extensive research, conducted internally by Hydro International Plc, on a variety of different sized HDVS. The model relates the internal dimensions of the HDVS to the operating conditions i.e. inlet flow rate and flow split (Fig. 6.1) and the solids characteristics in the incoming wastewater. Therefore the model provides the HDVS solids removal efficiency for a given solids settling velocity and HDVS operating conditions.

The solids characteristics are obtained from velocity-grading curves i.e. the fraction of solids in the incoming waste stream with settling velocities less than a given settling velocity. Therefore, obtaining the solids velocity-grading curve is a prerequisite of any performance investigation into the HDVS for solids-liquid separation (Tyack *et al.*, 1992). A test procedure used to obtain the solids velocity-grading curve of a waste stream for both settling and floating fractions has been developed (Tyack *et al.*, 1993)

and applied as a parameter for characterising wastewater solids (Hedges *et al.*, 1998). The HDVS internal configuration depends largely on the solids velocity-grading curve. The Grit King™ HDVS can be operated at higher incoming flow rates for the separation of grits and sand due to their rapid settling characteristics and therefore with increased turbulence. Hence, the internal geometry slightly differs compared to the Swirl-Flo™ HDVS used for the separation of colloidal particles where quiescent conditions are preferred, particularly to reduce shear forces resulting in the break-up of flocs and to prevent resuspension of the solid. However, for similar treatment processes e.g. settlement tanks using the same incoming waste stream the HDVS can operate at significantly higher loading rates or alternatively a smaller HDVS volume is required (Boner *et al.*, 1994). The general HDVS internal flow path and standard configuration components are as described in section 3.2.

More recent work has developed a physically-based deterministic mathematical model to estimate the Storm King™ HDVS solids removal efficiency (Luyckx *et al.*, 1998a) and compared the results against a similar model for a modified high-sided weir CSO (Luyckx *et al.*, 1998b). This work clearly shows the HDVS has greater solids removal efficiency at lower inlet flow rates and for the same inlet flow rate a greater efficiency at higher flow splits. As with the semi-emperical model previously developed and discussed above an integral design parameter is the sewage velocity grading curve. The solids removal efficiency model presented by Luyckx *et al.*, (1998a) has been compared to field tests on a prototype Storm King™ HDVS and the same efficiency results and curves obtained. Hence, the model is valid for differently scaled Storm King™ HDVS's with the same inlet pipe diameter and HDVS diameter ratio.

These investigations showed that the surface loading rate was the dominant parameter as the high-sided weir and Storm King™ HDVS removed the same amount of suspended solids for the same horizontal area. However, when both chambers have

the same horizontal area the volume of the Storm King™ HDVS is considerably greater than the high-sided weir and this will have a significant impact during real storm events with respect to storage requirements and the first flush of solids accumulated during antecedent dry periods in the sewerage system. Subsequently, further work was undertaken using the relevant flow data from four measured storm events and an assumed artificial settling velocity profile. The separating efficiency of the Storm King™ HDVS remains consistent irrespective of the size of the device and the majority of solids removal is associated with the available storage at higher efficiencies. Whereas in comparison the high-sided weir relies to a greater extent on the separating efficiency, which is not as effective as the efficiency associated with storage.

The workers also conducted a construction cost comparison between the two chambers and concluded that the Storm King™ HDVS becomes economically competitive with a modified high-sided weir when a solids removal efficiency of 70% is required (Luyckx *et al.*, 1998b). Unfortunately this scenario creates uncertainty in the design engineers decision making process regarding the requirements of the client specification and particularly costs over the environment, depending on the discharge consent.

Gross solids are visible to the public and therefore an aesthetic problem and subsequently result in a significant source of complaint to the water industry. The problematic removal of this neutrally buoyant material i.e. solids that neither readily settle or float and therefore have a terminal velocity (rise or fall) that is close to zero e.g. sanitary towels, condoms, cotton buds etc is highlighted by the solids settling velocity (Vs) / inlet flow rate (Vi) ratio approaching zero, which resulted in 'possible negative treatment', in the HDVS case study presented by Hedges, (1994). The poor removal of neutrally buoyant material is common to all solid-liquid separation processes and not only limited to the HDVS. Subsequently emission standards have been imposed where

the treatment process must remove solids greater than 6 or 10mm depending on the amenity use of the receiving watercourse to meet EU legislation requirements (UWWTD). These permissible solid dimensions have associated guidelines for meeting the required standards. The emission standards for the UK are set out in the Urban Pollution Management Manual 1st edition (1994) which formalised the basic procedures presented in the AMP2 guidelines (NRA, 1993). As stated above the sewage velocity grading curve is an important parameter in the design of a solids-liquid separation process. Subsequently this has been investigated considering only neutrally buoyant material (floatables) (Gagné *et al.*, 1998).

The HDVS has received considerable attention and improved modifications to combat and adequately remove the problem of neutrally buoyant material. This was initially provided by the inclusion of a physical barrier with a relative aperture size i.e. the Diverter™, located on the Storm King™ HDVS overflow pipe (Ruff, 1994) and the Integral Mesh Diverter™, located within the inner zone of the Storm King™ HDVS (Ruff *et al.*, 1994). These processes have been further developed to provide the Swirl-Cleanse™ (Harwood and Saul, 1996a) and Hydro-Jet Screen™ (Smith, 1999) processes for the removal of neutrally buoyant material. The former can be retrofitted, typically to the Storm King™ HDVS, if required to meet additional aesthetic standards. The Swirl-Cleanse™ and Hydro-Jet Screen™ are now marketed under the trade names of the Rotary and Linear Hydro-Jet Screen due to the flow path taken through the screens respectively (Andoh, 2000). These treatment processes remove the problem of screen blinding by using a self-automated backwash cleaning system activated by the rising water level in the chamber, which is controlled by a siphon arrangement. Full-scale testing of the Storm King™ HDVS and Swirl-Cleanse™ and Hydro-Jet Screen™ showed that an additional 40% of total solids were retained by the inclusion of the screen (Saul, 1998). These processes have the advantage that they are self-cleansing

devices and therefore relatively maintenance free compared to alternative processes such as mechanical screens. A full-scale study investigating various screen and chamber combination configurations considering their performance and maintenance requirements has been undertaken at the Wigan CSO test facility (Saul, 2000).

The previous research cited and discussed above has been undertaken in parallel with research designed to obtain a better understanding of the hydrodynamics within the range of HDVS (Table 1.1) i.e. the internal mixing patterns and their effect on the HDVS performance for a particular application. It can be seen from the above research that the HDVS has a proven track record in the field of wastewater and stormwater management providing high-rate solids-liquid treatment. However, the HDVS in these investigations is treated as a 'black box' and if further developments in the HDVS design are to be beneficial and potential applications identified, the internal operation needed consideration and a better understanding obtained. Subsequently, this has been addressed for the solids-liquid separation performance of the HDVS by conducting scaling and CFD investigations, which are discussed below and RTD tests which are discussed in section 2.2.2 on the different styles of HDVS (Table 1.1).

2.1.3 Hydrodynamic Vortex Separator (HDVS) Solids Removal Efficiency Scaling Investigations

The scaling relationships used to predict the performance of a particular size device for a given process are an integral stage in developing a design methodology and particularly for the solids removal efficiency of the HDVS. This has been investigated in detail for the Grit King™ HDVS operating with and without a baseflow component using artificial solids of known shape and density (Fenner and Tyack, 1997 and 1998).

This project used several model Grit King™ HDVS's (0.225, 0.300 and 0.600m diameter) and a prototype Grit King™ HDVS (1.6m diameter).

The traditional scaling approach considers the process performance of the HDVS for solids retention efficiency over a range of different sized HDVS and presents the removal efficiency as a function of a dimensional scaling factor. Therefore, from a range of parameters influencing the solids removal efficiency of a given HDVS (model) e.g. inlet pipe, HDVS diameter, flow rate, solids characteristics etc it is possible to predict the operating conditions for a different sized HDVS (prototype) to achieve the same process performance. To ensure that the prototype reproduces the conditions of the model accurately, a number of dimensionless groups should be identical in both devices i.e. Hazen number, Reynolds number, Weber number and Froude number. In most cases the exact number cannot be reproduced for two different sized devices and the dominant mechanism i.e. dimensionless number or numbers are identified by engineering judgement and supported by experimental data to best describe the relationship between the model and prototype scale device. The two common scaling laws applied to the HDVS are the Hazen (eqn. 3.1) and Froude (eqn. 3.2) scaling laws (chapter 3). The Hazen number is the ratio of the overflow flow rate to the particle settling velocity and the Froude scaling law is relevant where free surface gravitational effects predominate.

Initial scaling investigations commented that the Froude scaling law does not strictly hold for swirl flow conditions but is the best method currently available (Halliwell and Saul, 1980, Hedges, 1994 and Weiss and Michelbach, 1996). The scaling investigation on the Grit King™ HDVS clarified this observation and concluded that the Froudian scaled model flows provide a better experimental prediction for solids removal efficiencies up to 50% (higher flow rates) and Hazen scaled flow for efficiencies greater than 50% (lower flow rates) (Fenner and Tyack, 1997). These results were considered

acceptable as the Froude number is usually applied to a system, which has a significant free surface, and where gravitational forces dominate. Subsequently this research presented a hybrid scaling model using the two scaling protocols (eqn. 2.1), allowing the required scaling law to dominate for the preferred range of flow rates, and observed an excellent fit between the experimental and modelled data with a maximum difference of 5%. However, the scaling relationships are limited to the artificial solids used in the study referred to as large and small and their properties are provided by the authors. Therefore the model robustness needs to be extended to particles of different shapes and densities and wastewater with varying solids loading and characteristics.

$$Q_{prototype} = Q_{model}\left[(\eta_m L_r^2) + (1-\eta_m)L_r^{2.5} + \frac{B}{3}(1-\eta_m)L_r^{2.5}\right] \qquad (2.1)$$

Where: η_m = Model efficiency

L_r = Length ratio i.e. inlet pipe or overall HDVS diameter

$Q_{prototype}$ = Prototype inlet flow rate

Q_{model} = Model inlet flow rate

B =Average particle diameter (mm)

The head loss across the HDVS was also investigated and varied depending on the size of the HDVS and is therefore "a scale effect due to the impossibility of satisfying all dimensionless groups simultaneously e.g. Froude and Reynolds numbers and needs to be modelled once other significant scale effects have been identified and overcome". The workers also investigated scaling of the RTD experimental mean residence time and conducted CFD simulations to aid in obtaining a better understanding of the internal behaviour of the Grit King™ HDVS and its effect on the solids removal efficiency (Tyack and Fenner, 1997 and 1998a).

Scaling investigations using the same model (0.300m diameter) and prototype Grit King™ HDVS operating with a baseflow component (chapter 6) (Fenner and Tyack, 1998) confirmed earlier results discussed above for the Grit King™ HDVS operating with no baseflow (Fenner and Tyack, 1997). The scaling relationship for the Grit King™ HDVS operating with a baseflow component (eqn. 2.2) was obtained by modifying the hybrid scaling equation used for the no baseflow scaling investigations (eqn. 2.1) as the Hazen scaling law becomes dominant across the range of inlet flow rates. This suggested that the influence of gravitational forces is reduced when a baseflow component is introduced and the effects of surface overflow rate become more important.

$$Q_{prototype} = Q_{model}\left[(\eta_m L_r^2) + 0.75(1-\eta_m)L_r^{2.5}\right] \qquad (2.2)$$

The no baseflow hybrid scaling equation (eqn. 2.1) is partly dependent on the particle size (B) whereas operating with a baseflow component scaling is independent of the particle size (eqn. 2.2).

This work also highlighted the importance of considering scaling of the particles in addition to the flows which was discussed but not undertaken in the no baseflow scaling investigations. Model Grit King™ HDVS investigations using large solids (high settling velocity) produced consistently high efficiencies suggesting the need to scale the particle size, settling velocity and flow rate as opposed to using the same particles in both the model and prototype Grit King™ HDVS and assuming dimensional similarity. By applying the Hazen scaling law to the particle settling velocity and the Froude scaling law to the flow rate a good estimation of the prototype Grit King™ HDVS performance was achieved from the model Grit King™ HDVS experimental results

across the entire range of efficiencies. This study did not scale the baseflow flow rate and the workers commentated that the overflow and baseflow components are likely to follow different scaling laws.

The Grit King™ HDVS used in the above solids-liquid separation scaling investigations is originally configured to operate without a baseflow component (Fig. 2.1). The baseflow pipe is generally provided as a maintenance feature for the removal of collected solids (grits, sands etc). Subsequently the baseflow pipe diameter is not optimised for solids separation with respect to the inlet and overflow pipes and the Grit King™ HDVS overall diameter. The baseflow pipe diameter is generally smaller compared to the Swirl-Flo™ and Storm King™ HDVS configured for solids separation operating with a baseflow component. However, the Swirl-Flo™ and Storm King™ HDVS are employed for different solids removal applications, dependent on the incoming solids properties, compared to the Grit King™ HDVS (Table 1.1). Hence the above solids-liquid separation scaling results are specific to the Grit King™ HDVS and their comparison with any similar future studies on the Storm King™ or Swirl-Flo™ HDVS treated with caution.

2.1.4 Hydrodynamic Vortex Separator (HDVS) Computational Fluid Dynamics (CFD) Investigations

Computational fluid dynamic (CFD) investigations have been conducted on all the different styles of HDVS discussed in chapter 1 (Table 2.1). CFD is a computer software program commonly used in the aerospace and automobile industry capable of modelling fluid flow, heat transfer and chemical reactions and uses finite element methods to solve the governing equations of mass, momentum and energy. CFD investigation were conducted on the same prototype Grit King™ HDVS operating with

no baseflow used for the solids retention efficiency scaling investigations discussed above and by the same workers (Tyack and Fenner, 1998a), a Storm King™ HDVS operating with a baseflow component (Harwood and Saul, 1996b) and a Swirl-Flo™ HDVS operating without a baseflow component at low surface loading rates (Faram and Andoh, 2000).

The Grit King™ HDVS study compared the CFD results to three experimental inlet flow rates with no baseflow covering the design flow rate and the Storm King™ HDVS CFD study to one experimental inlet flow rate at a fixed flow split of 30% (chapter 6). The Swirl-Flo™ HDVS investigation used only CFD simulated flow rates. Tyack and Fenner, (1998b) also conducted RTD investigations to aid in interpreting the Grit King™ HDVS CFD and velocity measurements (section 2.2.2).

Table 2.1 Summary of CFD Investigations Undertaken on the Range of HDVS

HDVS	CFD Package	Diameter (m)	Operating Conditions	Workers
Swirl-Flo™	Fluent	12.000	Inlet- 113, 126 and 339l/s No Baseflow	Faram and Andoh, (2000)
Storm King™	Fluent	1.450	Inlet-60l/s Baseflow–20l/s	Harwood and Saul, (1996b)
Grit King™	FIDAP	1.600	Inlet-30, 52 and 63.6l/s No Baseflow	Tyack and Fenner, (1998a)

These investigations used CFD to describe the flow field i.e. velocity vectors within the HDVS. Tyack and Fenner, (1998a) used the k-ε (RNG) turbulence model to obtain a solution representative of swirl flow conditions and in situ velocity measurements (3D acoustic Doppler velocimetry) to verify the CFD model results for two of the three inlet flow rates investigated. This showed the general flow patterns within the Grit King™ HDVS are being modelled with a good level of accuracy. The potential effects of an intrusive probe within the flow field on the velocity measurements were investigated

and it was concluded that there was no detectable effect particularly as the probe measured the velocity at a point 50mm below its location. Harwood and Saul, (1996b) used the Reynolds stress model (RSM) solution to obtain a solution representative of swirl flow conditions and a video imaging system to record the position and movement of neutrally buoyant polystyrene beads which showed excellent agreement with the measured direction of the simulated velocity field. It was commented that the CFD model would be verified using in situ velocity measurements in future studies.

The simulated flow field observed within the HDVS using CFD confirms that the general pattern of flow is as described in section 3.2 and previous findings using scaling laws and residence time studies to investigate flow regimes within the Grit King™ HDVS (Tyack and Fenner, 1997 and 1998b). The flow patterns observed were very similar for the three flow rates investigated on the Grit King™ HDVS and only the relative magnitudes of the velocities changed (Tyack and Fenner, 1998a). This was slightly different to the in situ velocity measurements and suggested that the CFD model was not correctly calibrated for some variables e.g. wall roughness or the experimental velocity measurement procedure needed refining.

The adequate CFD model verification provides confidence in using the simulated flow field of the HDVS to predict its performance for a particularly application. Subsequently, Harwood and Saul, (1996b) investigated the potential of CFD to predict the solids retention efficiency of the Storm King™ HDVS compared to experimental data and also the effect of modifying the internal geometry of the Storm King™ HDVS CFD model only on the solids retention efficiency. This was achieved by extending the vertical dip plate towards the base of the Storm King™ HDVS adjacent to the cone (Fig. 3.1). This significantly changed the flow field within the Storm King™ HDVS by increasing the upward velocity and therefore, reducing the quiescent conditions in the inner zone preferable for optimum solids-liquid separation (Andoh, 1994). The

simulation of solids in the Storm King™ HDVS was achieved using the CFD particle tracking routine which allows the solids properties to be defined e.g. diameter and density. Good agreement between the simulated and experimental results was achieved. However, the modified Storm King™ HDVS showed a reduction in the retention efficiency and this was associated with an increase in the upward vertical velocity components. Smisson, (1987) also found that introducing a deep dip plate (Fig. 3.1) produced a region where random swirls were created and became known as the shear zone (section 3.2). The above CFD investigations have provided a greater insight into the shear zone and its effect on the solids removal performance of a Storm King™ HDVS and that the position of the shear zone may vary around the dip plate region rather than the simplified description commonly provided of directly under the dip plate (Andoh, 1994).

The work undertaken by Harwood and Saul, (1996b and 1999) is part of a larger study using CFD to estimate the particle retention efficiency of the four CSO chambers recommended for use in UK sewerage system as discussed above (Foundation for Water Research, 1998). Saul and Svejkovsky, (1994) also used CFD to investigate different particles trajectory in a vortex overflow with peripheral spill to predict its solids retention efficiency. This data was compared to existing experimental data and achieved some agreement but the simulated particle retention efficiency was generally overestimated.

The CFD investigations undertaken on the Swirl-Flo™ HDVS were conducted at three surface loading rates covering its typical applications operating with no baseflow and using the Reynolds stress (RSM) model of turbulence to describe the swirling flow conditions (Faram and Andoh, 2000). This study closely followed the approach taken on the Storm King™ HDVS (Harwood and Saul, 1996b). The primary objective was to verify the semi-emperical model discussed above, used to estimate the solids removal

efficiency of the HDVS for a given set of operating conditions (Andoh and Smisson, 1993), against the CFD solids removal predictions. Additionally this study modified the CFD simulated model internal configuration of the Swirl-Flo™ HDVS to assess its effect on the solids removal efficiency.

The particle tracking routine provided in the CFD software was used to simulate solids within the Swirl-Flo™ HDVS CFD model as employed by other workers on a number of different solid-liquid separation chambers and mentioned by Harwood and Saul, (1999). The CFD solids removal efficiency predictions correspond particularly well to the semi-empirical model for the two higher surface loading rates investigated. The CFD results also support the observed shift in the model efficiency curves as the surface loading rate increases and therefore "gives confidence in the use of CFD as a tool for the assessment of 'relative' effects" (Faram and Andoh, 2000). This work also illustrated that the semi-empirical model estimates the solids retention efficiency of the HDVS in the same manner, with respect to the inlet flow rate and flow split, as the physically-based deterministic model discussed above (Luyckx *et al.*, 1998a).

The modified Swirl-Flo™ HDVS CFD simulation model estimated marginally greater solids removal compared to the conventional Swirl-Flo™ HDVS and subsequently has been adopted in future designs and applications of the Swirl-Flo™ HDVS. The modified Swirl-Flo™ HDVS has also been subject to experimental testing although the results were not presented or discussed with respect to their correlation with the CFD simulated solids removal efficiency.

The Swirl-Flo™ HDVS investigation did not verify the simulated CFD flow field as previously undertaken e.g. using in situ velocity measurements (Tyack and Fenner, 1998a). However, as commented upon by the authors this has varying relevance depending on the study objectives. The study concentrated on the general flow characteristics and introducing internal modifications to assess their effect on process

performance rather than providing information for developing CFD coding and the relationship between these modifications and the flow field. A contribution to CFD coding specific to the HDVS could possibly be obtained by investigating the different CFD models used to simulate swirl flow conditions.

A fundamental problem with hydraulic models and scaling relationships (section 2.1.3) is their flexibility and robustness to changes that are outside the constraints of the processes on which they were undertaken. This relates to comparing data sets generated from different HDVS external and internal configurations and the specific experimental process properties e.g. sewage velocity grading curve. Although CFD is not sufficiently advanced to neglect these traditional experimental techniques it does provide increased flexibility as the process and investigative methods are developed and simulated on a computer. This allows information for different process configurations and operating parameters, which is difficult and time consuming to collect experimentally, to be investigated and directly compared. Hence, the modification and final design of a HDVS can be easier assessed and optimised using a computer simulation package.

2.1.5 Treatment Processes Combined with the Hydrodynamic Vortex Separator (HDVS)

The majority of the previous research discussed above has focussed on the Grit King™ and Storm King™ HDVS solids removal efficiency. However, three significant projects have investigated physico-chemical and chemical treatment process combined with the HDVS. These projects were conducted in parallel with the previous research discussed above and investigated the performance of coagulants to enhance the solids removal efficiency of the Swirl-Flo™ HDVS, the reduction in chemical and biological impacts on a watercourse due to discharges from a Storm King™ HDVS using a

chemical disinfectant and the potential and application of a range of treatment processes combined with the Storm King™ HDVS.

The coagulation treatment process in the HDVS has been investigated using several pilot and full-scale installations. These have been located across the UK, treating wastewater with different solids loading rates and properties. The results of performance evaluation work show a range of achievable performances depending on the process configuration and mode of operation (Andoh and Williams, 1995, Andoh *et al.*, 1993, and Andoh and Harper, 1994). When used with the appropriate types and dose levels of coagulant and flocculant, very high levels of suspended solids removal, solids associated BOD, grease, fats, oils and phosphates and significant reductions in bacterial numbers have been observed (Andoh, 1993). These trials have also been used to compare the actual TSS removals observed by the Swirl-Flo™ HDVS process to the semi-empirical model discussed above used for the design of a HDVS for solids-liquid separation and produced an excellent correlation (Faram and Andoh, 2000). The most detailed Swirl-Flo™ HDVS coagulation and flocculation study was conducted at Totnes WWTW.

Totnes Wastewater Treatment Works (1991-1993) – Following preliminary work by South West Water in 1991 the Water Research Centre (WRc) were commissioned to undertake an independent evaluation trial of the Swirl-Flo™ HDVS process (Dudley and Marks, 1993). The process was operated with and without chemicals using pilot-scale and prototype units and their performance compared to a full-scale installation to assess its feasibility as a process to meet the UWWTD requirements (Andoh and Williams, 1995). The results were also presented by Hydro International Plc (Andoh, 1993).

The following description and general findings relate to work conducted on the full-scale installation at Totnes WWTW. The two main modes of operation were with and without chemicals. The process configuration for both modes of operation consisted of two Swirl-Flo™ HDVS treatment trains with a common third sludge decant tank. The first Swirl-Flo™ HDVS acts as the coagulation/flocculation tank (4.24m diameter), were sewage and coagulant are mixed and a fraction of the gross solids are removed and passed to the existing sludge facility. The coagulated sewage passes to a much larger second Swirl-Flo™ HDVS (8.54m diameter) where the flocculant is added and the bulk solids settle out and clarified effluent discharged or passed forward for further treatment. The first Swirl-Flo™ HDVS provides the necessary reaction/contact time for the coagulation process and the second Swirl-Flo™ HDVS aids in the separation of the agglomerated flocs. The sludge from the flocculant tank flows to the third sludge decant tank (2.52m diameter) which is common to both process trains, from were it passes to the existing sludge facility. The sludge from each process i.e. operating with and without chemicals was collected separately to investigate their respective properties.

In the no-chemicals mode the Swirl-Flo™ HDVS meets the requirements for primary treatment as defined in the UWWTD (Council of the European Communities, 1991) for BOD but not for TSS and therefore should only be considered where the effluent is to be treated further before discharge. At the low chemical dose the effluent is acceptable for coastal discharges although the process showed little improvement over the no chemicals mode. The high chemical dose trials percentage removals observed for BOD and TSS typically exceeded 70 and 90% respectively and qualifies the process as an 'appropriate treatment' under the UWWTD for discharge to less and average sensitive areas. The high removal of bacteria would permit discharge close to bathing waters. However, these observations regarding the performance of the Swirl-Flo™ HDVS process are specific to the wastewater characteristics at the Totnes site i.e.

sewage velocity grading data and process operation i.e. flow rates and chemical dosing rates.

Due to project time constraints the process was not fully optimised and only a 'low' and 'high' chemical dosing level was used. Therefore, if optimisation is provided i.e. chemical dose, loading rate and wastewater characteristics the Swirl-Flo™ HDVS without chemicals meets the requirements for primary treatment and with chemicals the requirements for secondary treatment or appropriate treatment as defined in the UWWTD for the percentage reduction in TSS, BOD, COD and phosphorous. The results also support previous conclusions obtained for the process at lower inlet flow rates and therefore the scale up of the process with no reduction in performance. However, there is no nitrogen removal even with chemical dosing and therefore suitable downstream nitrification/denitrification treatment is required for discharges to sensitive waters where eutrophication may be a problem (Andoh, 1993). Additionally, the use of chemicals particularly at high dosing levels increases the quantity of sludge collected and may make the sludge more difficult to dewater and also potentially inhibit anaerobic digestion.

Bexhill-on-Sea: Egerton Park Streams (1988-1992) - This project considered the Storm King™ HDVS combined with chemical disinfection to reduce chemical and biological impacts on a watercourse as a result of intermittent discharges. The project planning, results and conclusions are discussed by Realey, (1989), Thomas, (1989) and Bennett and Farraday, (1990).

It was concluded that the intermittent discharges from the Storm King™ HDVS had no adverse long term impact on the ecological sensitive stream. Although the HDVS did not remove indicator bacteria in the stormwater, such bacteria associated with solids and considered difficult to inactivate using disinfection is reduced, due to the solids

separation performance of the HDVS. The Storm King™ HDVS is considered to reduce the discharge of material, which would normally deposit on the bed of streams, inhibit ecological development and cause chronic impacts (Andoh, 1994).

As the receiving watercourse flows to a designated bathing beach, bacteriological impacts were considered of significant importance and subsequently an investigation was conducted to demonstrate the potential of disinfecting stormwater and ensuring that EU Directives are met during storm events (Realey, 1989). This trial showed that there is a need to address the bacteriological quality of stormwater discharges and that stormwater could be disinfected, even when grossly polluted with sewage. Oxymaster™ (peracetic acid) was used as the disinfectant, at doses of 10, 15 and 25mg/l and reductions of 2-3 orders in magnitude of fecal coliforms and 4 orders in magnitude of fecal streptococci achieved. The disinfectant was introduced into the overflow pipe (Fig. 2.1) and hence does not provide any information regarding the Storm King™ HDVS potential as a disinfectant contact tank only that it provides an effluent suitable for chemical disinfectant with Oxymaster™.

In the UK no current water quality regulations specify the use of treatment processes to reduce the microbiological content from CSO discharges. Hence, it is currently left to the industry itself and particularly practitioners in those areas to identify suitable and practical solutions. Subsequently, in the late 1990's Hydro International Plc and researchers working on the HDVS started to consider and investigate its potential for different treatment processes either directly or in combination. Unsurprisingly this work was undertaken in the US where there has been far greater appreciation and acceptance that such processes are beneficial and potentially a necessity for discharges to meet current and future more stringent standards compared to the reactive approach adopted in the UK.

This is no better illustrated than by comparing the work previously undertaken in the US and UK. The US Environmental Protection Agency (USEPA) has published the results for over twenty investigations into CSOs with combined treatment from 1970 to the present. The studies considered chlorine, ozone and UV disinfection; coagulation, filtration and screening treatment processes; control equipment, maintenance and costs, conducted on pilot plants and full-scale devices. Hence, the work considers the intermittent operation of a CSO and the unsteady flows created by surface water run-off which have associated practical problems e.g. chemical dosing rates and adequate supply. This project has not cited any references in the text or reference listing however, the reader can access their details at www.epa.gov. This work is still ongoing and has investigated the effects of discontinuing disinfection on a receiving watercourse (Haas *et al.*, 1988), developed a mathematical model to describe the inactivation of indicator bacteria i.e. total coliform (Haas *et al.*, 1990) and investigated the behaviour and relationship of sediments with respect to indicator bacteria (Irvine and Pettibone, 1993) at CSOs in the field. Haas *et al.*, (1990) also provides a detailed literature review and discussion of the work undertaken to date.

The UK is still currently assessing the environmental impact of discharges from CSOs rather than implementing pilot-studies and investigating the efficacy and efficiency of suitable treatment processes. This work has generally identified and documented the potential polluting loads on the receiving watercourse and supported with field monitoring of CSOs (Hvitved-Jacobsen, 1982, Balmforth, 1990 and Mulliss *et al.*, 1997). However, the UK has considered the practical challenges and cost effectiveness of treating CSO discharges using chemical treatment process. This included chlorination and UV disinfection processes (Walsh *et al.*, 1994).

Columbus, Georgia US (1989-Present) - Following national CSO policy changes by the USEPA, for compliance with the Clean Water Act (CWA) 1972, under National Pollutant Discharge Elimination System (NPDES) permits, the City of Columbus, Georgia, through Columbus Water works initiated studies to examine its CSO problems. Details of the test programme and full-scale evaluation are provided in a Water Environmental Research Foundation (WERF) project report (Boner *et al.*, 1994). An objective of this work was to disseminate the ongoing results, findings and costs to an international audience and is being achieved through numerous publications (Ghosh and Boner, 1992, Boner *et al.*, 1993 and 1995, Arnett and Gurney, 1998 and Turner and Boner, 1998.

Bench-scale and pilot-scale tests were undertaken with the intention of investigating a range of treatment technologies and to aid in selecting the appropriate methods for full-scale operation and meeting quality standards. This was achieved in two stages and resulted in two treatment plants at different locations. The two treatment plants are a conventional vortex separator with chemical disinfectant plant (CV/DP) and a modified vortex separator with UV disinfectant (MVS/UV). The vortex separator refers to the Storm King™ HDVS (Table 1.1). Both configurations went on-line in December 1995 and are currently being monitored by the USEPA.

The first stage considered the CV/DP configuration. A number of bench-scale tests were used to determine the most suitable chemical disinfectant. Sodium hypochlorite, bromine chloride and peracetic acid were all considered at bench-scale with liquid sodium hypochlorite chosen for pilot-scale and full-scale trials. The disinfectant is introduced via the inlet pipe and hence in this application the Storm King™ HDVS is used as the contact tank for disinfection. Parallel studies were conducted using a contact chamber with mixer and comparable disinfectant efficiency data shows that the CV/DP provides equivalent treatment in approximately one-third of the volume of the tank with

mixer. This higher disinfectant performance is associated with a higher removal of solids, the reduction of volume due to the baseflow component and a mixing device, which operates in a plug-flow manner and therefore provides better chlorine utilisation. A 4.4 log fecal coliform reduction was observed for a 7min contact time using an 8mg/l chlorine dose. TSS and COD removals were significantly higher in the Storm King™ HDVS with maximum removals as high as 80 and 70% respectively, with corresponding values of 41 and 45% in the conventional mixed basin. The minimum removals observed in the Storm King™ HDVS were 40 and 45% respectively. A volumetric comparison with a conventional sedimentation basin (CSB) indicates a conventional vortex separator (CVS) would require to be approximately 1/4 of the size of a CSB.

The second stage considered the MVS/UV configuration. This is a conventional Storm King™ HDVS, mechanically altered to allow for chemical addition and air injection for coagulation and dissolved air filtration (DAF) treatment. The potential of using UV disinfection for treating the MVS overflow discharge was also considered. Bench-scale tests consisted of jar tests to obtain the optimum coagulant and flocculant doses and DAF operating parameters. Simultaneously UV tests were performed to determine dose-response relationships for untreated and pre-treated CSO discharges. Preliminary pilot-scale studies investigated the potential of these treatment technologies and in the final phase three storm generated CSO events were evaluated for direct treatment using a combination of coagulation and DAF. UV disinfection was performed during two of these CSO events. Samples were collected to quantify the removal of various contaminants, which include TSS, floatables, faecal coliforms, COD, BOD, nutrients and metals. These pilot studies demonstrated enhanced pollutant removal in the Storm King™ HDVS when using coagulation and DAF through various combinations and produced a highly clarified effluent suitable for UV disinfection.

One of the treatment plants is also constructed as an Advanced Demonstration Facility (ADF). This is a collaborative research programme to find improved solids removal and disinfection technologies at lower costs. The ADF is being used to investigate various treatment technologies including sodium hypochlorite, chlorine, peracetic acid, UV disinfection, dechlorination, chemical precipitation, dissolved air flotation (DAF), filtration and screening in combination with the Storm King™ HDVS and is currently ongoing. Previous and current results and other project information are published on the Internet at www.wwetco.com. (Andoh, 1998). The results to date for chemical disinfection trials use the concentration multiplied by contact time (CT) relationship for describing the Storm King™ HDVS performance (section 2.2.3 and section 4.3.4). An interesting aspect of the ADF programme is the development of design relationships between the effluent bacteria, solids concentration and disinfectant dose to the process influent properties. This has been presented for chlorine disinfection using different CT values (Arnett and Gurney, 1998). Unfortunately no RTD results, kinetic data i.e. rate constants (section 7.2) or alternatively the raw data have been published for the ADF. This information could be combined with the RTD data generated in this project and the inactivation of microorganisms determined using the various flow models as discussed in chapter 7 and compared to the ADF experimental data.

The Fluid-Sep™ vortex separator mentioned above (section 2.1.1) has also been used in combination with other treatment technologies in Toronto, Canada in a similar manner as employed with the HDVS at the ADF. The project planning, implementation and results have been reported by Pisano and Zukovs, (1992), Zukovs and Pisano, (1993) and Zukovs and Pisano, (1994).

2.2 The Residence Time Distribution (RTD)

2.2.1 Development and Applications

It is widely recognised that the mixing regime within a system does not readily conform to the two theoretical mixing regimes of plug-flow or complete mixing which are generally and incorrectly assumed in the design process (Danckwerts, 1953). This discrepancy can be investigated using the RTD, which describes the macromixing patterns within a mixing device. Characterisation of the mixing regime using the RTD dates from theoretical studies on laminar flow reactors (Bosworth, 1948) and experimental measurements on fluidised beds (Gilliland and Mason, 1952). The generalisation of this approach was due to pioneering work during the 1950s by Danckwerts, (1953) and Zwietering, (1959). These workers presented the general mathematical properties of residence time theory, with specific consideration to packed beds, blenders, reactors and tubular devices. Since this work several publications have presented and summarised the developments in the RTD experimental and data analysis techniques currently employed (Levenspiel, 1972, Wen and Fan, 1975, Nauman and Buffham, 1983 and Fogler, 1992). The contribution of these references to the development of the RTD and their specific relevance is highlighted by their numerous citations during the following chapters and sections discussing the RTD results presented in this project.

The RTD concept was pioneered in the field of chemical engineering. Subsequently chemical reactors on which RTD studies have been conducted include: bubble columns (Deckwer and Schumpe, 1993), pulsed baffle bubble columns (Ni, 1994) both of varying operating conditions i.e. cocurrent and countercurrent, screw extruders (Wolf and White, 1976), tubular reactors (Danckwerts, 1953), packed columns (Oliveros and

Smith, 1982) and fluidised beds (Danckwerts *et al.*, 1954 and Levenspiel, 1972). Due to the operating nature of some of these systems i.e. multiphase, the RTD investigations occasionally include the gas and solid phases. The RTD also has been employed in a wide range of scientific fields including the medical (Lee *et al.*, 1997), geophysics (Robinson and Tester, 1984), petroleum engineering (Hall and Hughes, 1993) and predominantly recently and most relevant, the water industry.

The RTD is gaining recognition in the water industry due to the emphasis being placed on design engineers to produce good scientific and accountable design of process applications. Treatment processes used in the water industry, which have been subject to RTD investigations are detailed in Table 2.2.

Table 2.2 Water Treatment Processes Investigated using the RTD

Process	Workers
Activated sludge plants	Burrows *et al.*, (1999)
Aerated lagoons and waste stabilization ponds	Naméche and Vassel, (1996)
Chlorine disinfection	Haas, (1988)
Oil-water separator	Muhammad *et al.*, (2000)
Ozone disinfection	Martin *et al.*, (1992).
Settlement tanks	Morrill, (1932)
Stormwater wetlands	Werner and Kadlec, (1996)
UV disinfection	Nieuwstad *et al.*, (1991)

The process configurations include hydraulic only and combined hydraulic and kinetic RTD investigations. The majority of hydraulic only RTD studies have been used to investigate and modify the mixing regime of the system rather than its performance for a particular process e.g. increasing plug-flow mixing and reducing short-circuiting. These investigations typically include the optimisation of baffle arrangements within a tank, mixer speeds, tank geometry and internal and inlet pipe configurations. Combined RTD and kinetic investigations are predominantly theoretical studies or based on batch-scale data as discussed below (section 2.2.3).

All systems are typically operated continuous and steady state however, RTD theory has been developed and experimental investigations undertaken for the application to a recycle system (Buffham and Nauman, 1975 and Battaglia *et al.*, 1993) and similarly for an unsteady-state system (Fernández-Sempere *et al.*, 1995). This is not a complete list of the different types of chemical reactors and water treatment processes, which have been subject to RTD investigations or the workers conducting the investigations, and more are cited throughout this chapter.

The RTD experimental tracer injection technique is typically conducted using either a pulse or step method and one of several commonly employed tracers as discussed in section 3.4. The majority of investigations cited in this chapter use these RTD experimental techniques. Wen and Fan, (1975) detail the RTD experimental procedure and data analysis techniques used to investigate several systems.

A novel RTD experimental technique has been proposed and described using a time-reaction (Denbigh *et al.*, 1962 and Danckwerts and Wilson, 1963). This method introduces two reactants and an indicator solution, which together turn a particular colour as the reaction proceeds. The principle is the same adopted for the sample analysis of hydrogen peroxide (H_2O_2) concentrations used in this project and is discussed in section 3.5.3 and Danckwerts and Wilson, (1963) also used similar reactants. The injection of a coloured dye injected into the fluid will only provide a momentary impression of the nature of the flow pattern. Whereas the time-reaction method will provide a stationary response, as the difference in colour will be a function only of the time spent in the reactor i.e. fluid 'age'. This is related to the theoretical time for the reactants to change colour, which is dependent on the reaction rate constant (k) (section 7.2) and can be set accordingly by varying the individual reactants concentration and feed rates. The distribution of colour will reveal a good deal about the pattern of flow and regions of dead and stagnant volumes and recirculation and a time-

exposure photograph yields the time average pattern. To prevent the reaction also depending on the micromixing effects (section 7.5) within the system the reactants are feed into the system completely mixed as provided using a non-reactive tracer.

The specific RTD data analysis techniques used throughout this project and relevant references are detailed in their respective chapters to provide the reader with continuity. The different data analysis categories used to describe the RTD are outlined in section 4.3. The typical procedure usually selects one or part of these methods to investigate the RTD experimental data from a system. This project has used one or more techniques from each category and therefore used the range of RTD data analysis techniques commonly employed by other workers to date as detailed in section 4.3 and chapter 5. This includes the indirect method of moments and direct non-linear regression axial dispersion model (ADM) and tanks-in-series model (TISM) parameter estimation techniques (Levenspiel, 1972, Fogler, 1992, Haas *et al.*, 1995 and 1997), RTD indices (Stover *et al.*, 1986), the intensity function (λ) (Naor and Shinnar, 1963 and Himmelblau and Bischoff, 1968) and a RTD combined mathematical model discussed below (Wen and Fan, 1975).

The ADM and TISM are one parameter models, which have been developed from first principles to describe the macromixing within a flow system. The ADM (eqn. 4.11) is developed from mass balance equations through a tubular reactor, which also account for the presence of any dispersion along the length of the reactor. The TISM (eqn. 4.9) is also developed from mass balance equations across an infinite number of completely mixed tanks in series. The former is solved analytically and the latter provides a direct solution from the mass balance equations (Levenspiel, 1972) The ADM describes the mixing regime deviation from plug-flow mixing towards complete mixing whereas the TISM uses the opposite relationship. Neither models concept is associated with one particular worker although Levenspiel, (1972) presented and discussed both the TISM

and ADM and developed the latter with respect to systems with small and large amounts of dispersion and open and closed boundary conditions and related the model parameters to the first and second moments of the RTD curve. However, it has been shown that it is best to fit to the model directly rather than to first fit to the moments and is true even for the ADM, which is closely associated with the analysis of moments (Nauman, 1981). Haas *et al.*, (1997) commented that the non-linear regression technique is superior to the method of moments. Laplace and Fourier transforms (Westerterp *et al.*, 1984) and the holdup function H(t) (Buffham and Mason, 1993) have also been used to calculate the first and second moments of the RTD curve and subsequently the ADM and TISM parameters. The flow regime, investigated using the data analysis techniques discussed and employed in this project, is turbulent and the velocity profile is flat (section 4.4). If this is not the case and laminar flow conditions exist resulting in a parabolic velocity profile alternative techniques require consideration to describe the RTD (Fogler, 1992).

Alternative techniques used for interpreting the RTD and degree of non-ideal flow behaviour exist and are still currently being developed. This includes the holdback function (χ) (Danckwerts, 1953 and Robinson and Tester, 1986), internal-age distribution function $\phi(t)$ (Buffham, 1983) and internal cumulative residence time distribution $\Phi(t)$ (Robinson and Tester, 1986) which are all used to identify the extent of relative stagnancy. A recent RTD interpretation technique is the use of an index system, which describes the RTD by splitting the curve into two sections (Morgan-Sagastume *et al.*, 1999). The sections correspond to the portion of the curve describing a normal distribution and the other to the tail part of the curve. This method was calibrated against a number of different mixing devices and operating conditions e.g. aeration, packing and baffling arrangements.

This project has also used a RTD combined model to attempt to describe the mixing regime within the HDVS (chapter 5). This procedure uses a number of mixing regions e.g. plug-flow, complete mixing and dead zones interconnected in a variety of combinations e.g. bypass, recycle or crossflow represented by theoretical mathematical equations and modifications to ensure practical realism (Wen and Fan, 1975). Due to the potential number of parameters a RTD combined model can provide an accurate fit to the experimental RTD curve although its mathematical solution is more complex (appendix D.1).

RTD combined models have been used with success to represent the hydraulic behaviour of some biological systems using a completely mixed tank with a bypass and dead zone (Cholette and Cloutier, 1959). Additionally, combined models have been applied in the study of anaerobic sludge digesters (Montieth and Stephenson, 1981), anaerobic filters (Samson *et al.*, 1984, Hall, 1985 and Young and Young, 1988) and in aerobic submerged filters (Hamoda and Abd-El-Bary, 1987). Other workers have also presented the analytical solutions to less complex combined models and the stages required in developing a solution using graphical methods (Levenspiel, 1972 and Fogler, 1992).

A problem with the combined model approach is that the model is not unique to the device under investigation and likewise the device is not unique to the model. Hence, the RTD data is not consistent because many configurations of combined model fit the experimental RTD curve. Subsequently different information is provided depending on the model configuration. These models require more effort and specialised knowledge compared to other RTD data analysis techniques e.g. numerical solution of differential equations. Hahn, (1990) commentated that a "global assessment may suffice to allow first quantifications of possible positive or negative modifications on tank flow patterns". This refers to the optimisation of a system's configuration for a specific

application. However, the RTD investigations undertaken in this project on the HDVS are aimed at assessing its potential for kinetic processes by providing information regarding the mixing regime and maintaining its current internal configuration (Fig. 3.1). Hence, the detailed development and analysis of the RTD combined model (chapter 5) is justified and particularly if recommendations for further research (section 8.6) are implemented by incorporating a reaction rate constant (k) (section 7.2) into the combined model solution (appendix D.1). The inclusion of a reaction rate constant (k) enables the combined model to estimate the kinetic process performance e.g. chemical conversion or microbial inactivation within a continuously operated system accounting for non-ideal flow behaviour. Wen and Fan, (1975) provide the solution for various combined model configurations including a reaction rate constant (k) (section 7.2).

2.2.2 Existing Residence Time Distribution (RTD) Investigations on the Hydrodynamic Vortex Separator (HDVS)

Limited full-scale and laboratory (model and prototype) RTD investigations have been conducted on the three different types of HDVS (Table 1.1). Two investigations used lithium chloride (LiCl) as the tracer and a pulse injection technique to introduce the tracer into the inlet pipe. The concentration of free lithium (Li) was measured using an atomic absorption spectrophotometer in both investigations. The remaining RTD investigation also used a pulse injection technique and fluorescein as the tracer, which was measured using an absorption spectrophotometer. The above RTD experimental techniques are discussed in more detail in section 3.4. The advantages and disadvantages of these methods e.g. tracer, tracer injection and sample concentration analysis techniques are discussed in BS 3680 2C: 1993 and BS 3680 2D: 1993. A

summary of the existing RTD investigations conducted on the range of HDVS is provided in Table 2.3.

Table 2.3 Summary of RTD Investigations Undertaken on the Range of HDVS

HDVS	Injection/ Tracer	Data Analysis	Diameter (m)	Operating Conditions	Workers
Swirl-Flo™	Pulse/Lithium Chloride	Method of Moments, ADM and TISM	4.24 8.54	No Baseflow	Dudley and Marks, (1993)
Storm King™	Pulse/ Fluorescein	RTD Indices	1.000	Baseflow Only	Luyckx *et al.*, (1998a)
Grit King™	Pulse/Lithium Chloride	Method of Moments and ADM	0.300 1.600	No Baseflow and Baseflow	Tyack and Fenner, (1997 and 1998b)

The RTD experimental results presented by previous workers on the HDVS are discussed in detail and compared to the RTD results obtained in this project in the relevant chapters i.e. no baseflow (chapter 4) and with a baseflow component (chapter 6).

The only existing RTD data published for the Swirl-Flo™ HDVS was conducted separately on the coagulation and flocculation tanks used in the Totnes WWTW trials discussed above (section 2.1.5) (Dudley and Marks, 1993). This investigation produced RTD results at two flow rates, the design flow rate and twice the design flow rate. The project report does not provide a comprehensive description of the RTD of the Swirl-Flo™ HDVS although it does provide comparable data for the TISM and ADM parameters (section 4.3.3) and indicates a similar type of mixing regime with high dispersion, as illustrated in this project (section 4.4). The coagulation and flocculation tanks were both operated with no baseflow and therefore these existing RTD investigations correspond to the Swirl-Flo™ HDVS RTD data presented in chapter 4 (section 4.4.9.3). It should be noted that the first HDVS in the Totnes treatment train

providing coagulation and flocculation has a sludge hopper (Fig. 2.1) and the second HDVS providing optimum conditions for flocculation does not have a sludge hopper. Therefore the second HDVS has a similar configuration to the Storm King™ HDVS. The difference between the range of HDVS configurations and applications is provided in chapter 1 (Table 1.1).

General conclusions observed from the coagulation and flocculation tanks RTD include the former has very little dead space and the mixing regime progresses towards plug-flow at higher flow rates (section 4.1). Alternatively, the flocculation tank has a dead volume which increases with higher flow rates and the mixing regime deviates from plug-flow as the flow rate is increased. These observations regarding the presence of short-circuiting appear to be made from the RTD normalised curves $E(\Theta)$ e.g. Fig. 4.8 using the experimental mean residence time and are based only on two inlet flow rates reducing confidence in the final conclusions. However, the RTD curves also have a long tail, which suggests that there are fluid elements with extended mean residence times, greater than the theoretical mean residence time (eqn. 4.2) and provide confirmation that stagnant regions exist. The workers also commentated that differential equations could be developed using the TISM to estimate pollutant 'spot' percentage removals through the Swirl-Flo™ HDVS. This technique has been partially utilised in the development of the RTD combined model presented in chapter 5 and will be fully implemented if a reaction rate constant (k) (section 7.2) is introduced into the RTD combined model solution (appendix D.1) as suggested in the recommendations for further research (section 8.6).

The work undertaken in this project, also on the Swirl-Flo™ HDVS (Table 1.1), has generated several publications describing the RTD obtained from the HDVS operating with and without a baseflow component (Higgins *et al.*, 1998, Higgins *et al.*, 1999 and Alkhaddar, Higgins, Phipps and Andoh, 1999). The work presented in these

publications is further investigated and discussed in the relevant chapters in this project (chapter 4-6). The publications generated by the research conducted in this project are presented in a separate section at the back of the thesis.

RTD investigations have also been conducted by the same workers on the model and prototype Grit King™ HDVS used in the solids removal efficiency scaling and CFD investigations discussed above. This work presented the use of scaling laws to characterise the RTD (Tyack and Fenner, 1997) and identify flow regimes within the Grit King ™ HDVS (Tyack and Fenner, 1998b). The former investigation operated the model and prototype Grit King™ HDVS with no baseflow (Fig. 2.1) and the latter using only the prototype Grit King™ HDVS with and without a baseflow component i.e. flow split (chapter 6). The RTD scaling investigation showed that the experimental mean residence time of the model Grit King™ HDVS, when scaled using the Froude scaling protocol for flows (section 2.1.3), provides a very good fit to the prototype Grit King™ HDVS experimental results over a range of inlet flow rates.

Research by Tyack and Fenner, (1998b) into the flow regimes within a prototype Grit King™ HDVS presented and analysed the RTD data in a similar format to the work presented in this project. The prototype Grit King™ HDVS was operated without a baseflow component for twelve inlet flow rates and with a baseflow component for four inlet flow rates. A single baseflow flow rate was used for all four inlet flow rates and varied with 'head loss' through the device between 8 and 10l/s and provided flow splits ranging from 15-70% depending on the inlet flow rate (chapter 6). This study presented the ADM parameter i.e. dispersion number (D) for both flow components and operating conditions. The experimental results are presented and discussed in section 4.4.9.4 and 6.2.7.1 for the prototype Grit King™ HDVS operating with no baseflow and with a baseflow component respectively. These sections compare the Grit King™ HDVS RTD results to the prototype Swirl-Flo™ HDVS used throughout this project operating with

the sludge hopper in the no baseflow and baseflow (SP3) (Fig. 3.1) mode of operation (section 3.3). This configuration is considered to closely replicate the Grit King™ HDVS operating with a grit pot used in the study undertaken by Tyack and Fenner, (1998b) and the overall diameters are also similar. The main conclusions with regards to the RTD tests are detailed below.

The mixing regime and recirculation observed within the Grit King™ HDVS is very similar when operated with and without a baseflow component and there is a large amount of mixing. Short-circuiting of the flow occurs causing the peak in the RTD to skew towards the origin although no relationship with the inlet flow rate or flow split was observed. The workers identified the active zone to occur between the dip plate and outer wall where most of the flow activity occurs due to the turbulent nature of the flow in this region (Fig. 3.1). The results also implied that there maybe more than one flow regime within the Grit King™ HDVS associated with the overflow and baseflow component. However, the summation of the individual flow component dispersion numbers (ADM) provide a very similar dispersion number as the no baseflow operating conditions, although the spread of the results i.e. variance is far greater.

RTD tests have also been conducted on the Storm King™ HDVS operating with a baseflow component only (Luyckx *et al.*, 1998a). These tests used a greater range of operating conditions compared to the previous RTD baseflow experiments (Tyack and Fenner, 1998b) and a range of flow splits exceeding but comparable to those used in this project i.e. 10-50% and 10-40% at increments of 10% respectively (chapter 6). The RTD indices data analysis technique was used to investigate the degree of short-circuiting from the RTD curve (section 4.3.4). Unfortunately only the t_{50}/τ index was calculated and presented and is therefore not a detailed RTD index assessment of the Storm King™ HDVS RTD as provided in this project for the model and prototype Swirl-Flo™ HDVS in chapters 4 and 6. The index was calculated using the theoretical

mean residence time (τ) as the denominator expression (eqn. 4.2). However, following the USEPA RTD parameter guidelines (Stover *et al.*, 1986) (section 4.3.4) the experimental mean residence time (t_m) calculated using the method of moments should be used as the denominator as followed for the RTD investigations conducted in this project. Therefore it is difficult to conclude if the t_{50}/τ index provides comparable data to the t_{50}/t_m index presented in section 6.2.6.1 for the prototype Swirl-Flo™ HDVS as the experimental mean residence time and difference compared to the theoretical mean residence time is not presented (section 6.2.7.2). Additionally, it is not clear from the data presented as to whether the t_{50}/τ index is calculated from the overflow or baseflow component RTD or a combination. Subsequently, the dead volume estimation of 25% of the total volume is vague as it does not refer to the fraction of the total volume associated with either the overflow or baseflow component.

The concentration-time data for both the overflow and baseflow component appear to be normalised with respect to the total injected concentration only and not the theoretical or experimental mean residence time which allows direct comparison of different flow rates which occurs for both the overflow and baseflow component as the flow split is changed (section 6.2.1.1). Additionally using the total injected concentration as opposed to the quantity of tracer passed through each flow component can result in problems in fitting the experimental curves to the ADM and TISM as discussed in section 6.2.1.2.

The theoretical mean residence time (eqn. 4.2) for both the overflow and baseflow components of the Grit King™ HDVS were not presented by Tyack and Fenner, (1998b), as it was "not possible to determine with any meaning". This interpretation was not adopted for the baseflow component experiments conducted in this project and the theoretical mean residence time values are presented with the assumption that both flow components occupy a fraction of the total volume proportional to the inlet flow

rate flow split (chapter 6). Luyckx *et al.*, (1998a) operated the Storm King™ HDVS with a baseflow component and used the theoretical mean residence time. Although, no comment is made as to the method or assumptions used in calculating the theoretical mean residence time.

The previous RTD experiments appear to be preliminary studies to aid in supporting conclusions obtained from solids-liquid separation and CFD investigations undertaken on the HDVS (section 2.1) and the RTD data analysis techniques are not consistent or comprehensive for all investigations and different styles of HDVS (Table 1.1). However, as the mixing characteristics are an integral parameter in the design and optimisation of any kinetic process, this project investigates and presents the RTD data for the Swirl-Flo™ HDVS in detail. The RTD is obtained for a model and prototype Swirl-Flo™ HDVS operating in several different configurations and presented consistently using a variety of data analysis techniques commonly used in RTD investigations (section 4.3). Additionally the Swirl-Flo™ HDVS process has received the least attention with regards to its RTD.

2.2.3 Combined Hydraulic and Kinetic Process Investigations

The development of the RTD is closely associated with chemical reaction kinetics and subsequently disinfection kinetics. The latter is receiving considerable attention due to reasons previously discussed in chapter 1 and is of particularly relevance to the HDVS as it is predominantly used in the water industry and therefore its potential of providing combined high-rate solids separation treatment and disinfection. Subsequently more research has considered the combination of hydraulic and kinetic principles for disinfection processes as opposed to chemical reactions. This is possibly

due to the practical challenges posed by adapting chemical kinetic processes for use in the water industry and particularly wastewater treatment.

Process operation in the chemical industry is generally known and controlled in such a manner so as the characteristics of the reactants and mixing regime are known and physical characteristics of the system controlled e.g. temperature, pH etc. The mixing regime is generally maintained in the vicinity of a theoretical mixing regime and therefore the process design simplified (section 4.1). Whereas process operation in the water industry is often limited by the surface loading rates of a particularly style of contact tank, subject to varying pollutant loads i.e. first flush effect and pollutant properties i.e. contributing catchment and intermittent operation controlled by the environment as opposed to the design engineer i.e. rainfall. Additionally the residual disinfectant concentration also requires control with respect to providing palatable drinking water and preventing excessive concentrations from being discharged into the aquatic environment. Chlorine disinfection residual has received considerable attention due the formation of carcinogenic compounds.

Chapter 1 discussed the water industry's dilemma of opting for sophisticated tertiary treatment systems or the traditional outfall and that the latter design fails to be based on 'good science'. However, Trussell and Chao, (1977) concluded that the best reactor configurations they investigated were long pipelines i.e. outfalls and the degree of dispersion (ADM) and therefore kinetic process efficiency can be predetermined using an empirical relationship developed from field data. This shows that combined hydraulic and kinetic design methodologies can be employed to design traditional treatment processes and that their adoption for the characterisation and optimisation of new treatment processes is not a new concept. Additionally the conventional treatment process design can be based on the 'good science' approach which is being promoted for the design of new sophisticated treatment processes (chapter 1). This implies that the

current focus on developing sophisticated treatment processes to improve water quality standards is predominantly driven by practitioners and treatment process manufacturers. Additionally this also highlights the problem faced by practitioners working in the mutli-disciplinary field of environmental engineering and collating and interpreting all relevant information.

The general RTD references cited above continue the development of the RTD to include its application with chemical reaction kinetics and those cited below also discuss the RTD with disinfection kinetics and chemical kinetics relevant to the work presented in chapter 7.

The RTD becomes significantly important for a reaction system when contacting is a relatively fast process, and the reaction kinetics are relatively slow (Levenspiel, 1979). Disinfection systems and kinetics generally conform to this situation and RTD investigations undertaken as mentioned above (Table 2.2). The term disinfection kinetics refers to the classic first-order reaction (section 7.2) as investigated and presented by Chick, (1908) and Watson, (1908) with more recent developments discussed in section 7.2 (Haas *et al.*, 1995).

Considering the theoretical mixing regimes discussed in section 4.1, the worst case for a disinfection reactor is complete mixing. In this flow system a fraction of the input will be immediately discharged without significant time for contact with the disinfectant. This is totally unacceptable for a disinfection process, as the inactivation of microorganisms requires a time element and hence in a completely mixed tank a significant fraction of microorganisms in the wastewater will exit with little chance of being inactivated. The ideal case is the plug-flow reactor, however in real systems some degree of dispersion will be present and in the design of disinfection systems, the object is generally to minimise any spreading of the RTD curve. Thus the ADM and TISM parameters (section 4.3.3) and RTD indices (section 4.3.4) are important design tools.

The disinfection process is generally in the liquid phase e.g. sodium hypochlorite as opposed to the gas phase e.g. ozone. The latter is more complex, due to the high degree of mixing required to dissolve the ozone into the wastewater. Although this can increase the contact between the disinfectant and the microorganisms backmixing can also increase and hence the amount of dispersion.

The ADM and TISM mathematical models used to describe the RTD can be further developed to estimate the chemical conversion of a reactant (Levenspiel, 1972) or the microbiological inactivation by disinfection processes (Johnson *et al.*, 1997 and 1998). The RTD tells us how long various fluid elements have stayed in the reactor i.e. macromixing, but does not provide information about the exchange of matter between fluid elements i.e. micromixing. Two models, with zero parameters can be used to define the boundaries of micromixing - complete segregation and maximum mixedness, and provide the upper and lower limits of micromixing conversion in a non-ideal reactor respectively. The principles of micromixing were first described by Danckwerts, (1958) and Zwietering, (1959). These models define the boundaries of microscopic mixing in terms of late and early mixing respectively. They can be considered as the boundaries of microscopic mixing as plug-flow and complete mixing are to macroscopic mixing (section 4.1).

Haas, (1988) concluded, "the effect of micromixing becomes particularly important at high degrees of inactivation. Thus for reuse applications or in the disinfection of poorly treated wastewater e.g. combined stormwater overflows, the effect of micromixing may be important to consider". This is of particular significance with respect to the HDVS as one of its main applications is as a CSO in the sewerage system. Additionally, for a practical application, minimising the micromixing will reduce the required disinfectant dose or contact time and can be achieved by minimising the head loss across the contact tank (Haas, 1988).

In a similar manner as to the parameters discussed throughout this project and mentioned above to describe the RTD i.e. macromixing, Zwietering, (1959) and Haas, (1988) presented three parameters to identify and define the extent of micromixing. The former developed the degree of segregation (J) which is analogous to the normalised variance for macromixing (section 4.3.1) and the latter presented the segregation number (Sg) and the minimum eddy radius number (rp). Additionally Robinson and Tester, (1986) presented a method of estimating the chemical conversion directly from the RTD using the holdback function (χ) (Danckwerts, 1953). Further discussion on micromixing theory and particularly regarding its importance for different kinetic mechanisms is provided by Douglas, (1964) and relevant references are also cited in chapter 7.

Initial research into the RTD and subsequently the performance of a device for kinetic processes was one of a theoretical analysis. This work was simplified and allowed the methodology to be adopted by engineers not necessarily with a relevant background to perform RTD tests and analyse the results easily (Levenspiel, 1972, Fogler, 1992 and Haas *et al.*, 1995). Unfortunately despite many workers now conducting practical RTD tests, the kinetic aspect of the design still remains predominantly a theoretical investigation or limited to batch-scale investigations (Haas *et al.*, 1997). This sequence of research is possibly due to the late arrival of the RTD concept with respect to the research undertaken into chemical and particularly disinfection kinetics. Chick, (1908) and Watson, (1908) investigated and presented the disinfection mechanism in the early 1900s whereas the RTD received consideration and particularly combined with kinetic theory in the 1950s.

The USEPA Surface Water Treatment Rule (SWTR) developed the CT (concentration x time) concept for achieving various degrees of inactivation of pathogenic microorganisms for potable water treatment (American Waterworks

Association, 1991). This technique utilises kinetic and hydraulic models to accurately determine the optimum concentration and contact time to achieve a required efficiency. The SWTR published CT values have been demonstrated to achieve specific degrees of inactivation for various water quality conditions from batch experiments (Teefy and Singer, 1990). The CT method was principally developed for potable water but can equally be applied to wastewater. The only significant differences are the presence of solids in the wastewater effecting the bulk flow characteristics and an increased demand placed on the initial disinfection concentration due to the presence of organic pollutants.

Several workers have investigated the CT experimental approach and alternative methods to determine the individual parameters however, they have also expressed concern over their true representation of the full-scale continuous process (Teefy and Singer, 1990 and Lawler and Singer, 1993). Subsequently theoretical studies have been conducted due to the universal acceptance that the CT concept i.e. the product of the concentration and time providing 99.9% or 99.99% microorganism inactivation under batch conditions, for designing continuously operated disinfection and contact tanks, does not consider all or if any non-ideal flow behaviour in determining the T element i.e. the RTD. Additionally, the disinfection element (C) is assumed not to decay with time but in practice it is consumed during the disinfection mechanism (Haas *et al*, 1995). The T component is discussed further is section 4.3.4 and presented for the model and prototype HDVS in section 4.4 and 6.2.

This is illustrated by Johnson *et al.*, (1997 and 1998), who presented two theoretical papers combining the ADM, TISM and RTD indices (section 4.3) with disinfection kinetics (section 7.2). This combined theoretical hydraulic and kinetic investigation showed that for an ADM Peclet number (P_e) of 50 and TISM parameter of 20, improving the RTD towards plug-flow (section 4.1) will not significantly increase the overall disinfection performance of the device and is supported by Stevenson, (1995).

Hence, the elusive target of designing a system that demonstrates near perfect plug-flow behaviour is not necessary (Johnson *et al.*, 1998). The workers also collated and presented existing experimental inactivation rates for a number of different microbes for a given initial chlorine concentration and physical conditions. However, the data is not entirely consistent and need to be confirmed (Stevenson, 1995). It must be stressed that this study was completely theoretical and therefore the conclusions also need verifying in practice.

In a similar manner Stevenson, (1995) combined theoretical hydraulic and kinetic principles to characterise contact tanks, accepting that batch conditions are not truly representative of the continuous operating system. This work developed the CT concept by presenting the 'compensation factor' which compensates between the concentration or time element required to achieve a given performance under batch conditions to the concentration or time element required to provide the same performance, considering the ADM and TISM description of the RTD, in a continuous flow system. The 'compensation factor' which is a function of the 'disinfection index' i.e. $\log_{10}$ (concentration in/concentration out) is applied to either the concentration (C) or time (T) element as a multiple. Stevenson, (1995) also discussed the use of CONTANK™ computer software (section 2.2.4) to modify rectangular and square tanks internal configurations to achieve a required disinfection index and resulting compensation factor.

The kinetic process investigated in this project using batch and HDVS experiments is the decomposition of H_2O_2 by a biological enzyme - catalase and the results are compared to RTD flow model predictions (chapter 7). The application of H_2O_2 and catalase either in combination or as individual reactants has been detailed in section 7.1. This project is generally concerned with the RTD flow models prediction of the experimental conversion rather than the reaction mechanism or individual reactants.

However, this reaction rigorously follows a first-order reaction mechanism (Dennis, 1984) and is therefore similar to that used to model disinfection systems (Chick, 1908 and Watson, 1908). The relevant literature is cited in chapter 7 and predominately considers the H_2O_2 concentration sample analysis technique Dennis, (1984) and physical factors influencing the experimental results Aldershof *et al.*, (1997). The interpretation of a first-order reaction is provided by many chemical engineering text books for both the batch and continuously operated HDVS experiments along with its relationship with the RTD (Levenspiel, 1972 and Fogler, 1992). The approach adopted in this project is similar to that used by Worrell and Eagleton, (1964). This work used a different reaction mechanism and was undertaken using a continuously operated mixed tank, which simplifies the data analysis as the RTD closely follows a theoretical mixing regime (section 4.1). The decomposition of H_2O_2 has also been investigated using a range of chemical catalysts (Dennis, 1984, Conklin, 1996, Hansen, 1996, Aldershof *et al.*, 1997, Kuznetsov *et al.*, 1997, Gustavsson *et al.*, 1998).

Preliminary disinfection investigations conducted on the model HDVS used throughout this project showed that the overflow and baseflow components microbiological RTD follow a similar trend as the hydraulic RTD. Hence, the model HDVS disinfection experimental results could reliable be obtained from the RTD and batch-scale data. Subsequently the HDVS experimental inactivation of a non-pathogenic bacteria compared to the RTD and TISM estimation, provided satisfactory results considering the inaccuracies in measuring bacterial concentrations (Alkhaddar, Higgins and Phipps, 1999 and 2000). The publications generated by the research conducted in this project are presented in a separate section at the back of the thesis.

2.2.4 Hydraulic and Kinetic Process Computer Aided Design

The advent of fast and cheap personal computers together with a better understanding of the RTD, provided by previous research and coupled with improved user friendly computer programming, has resulted in the development of CFD and subsequently RTD computer software packages to simulate and modify the RTD of a continuously operated system. As discussed above CFD has been used to investigate the mixing regime within the HDVS and also to predict its solids removal efficiency (section 2.1.4). However, as several CFD packages can also model chemical reactions it appears a natural progression to utilise CFD principles to provide a software package specifically to investigate both the hydraulic and kinetic properties of a process simultaneously. This has been accomplished by two software packages known as CONTANK™ and DISINFEX™. These have primarily been developed to optimise chlorine contact tank configurations for treating potable water supplies. However, a similar principle applies for wastewater disinfection and disinfectants other than chlorine in the liquid phase.

CONTANK™ is a finite difference analysis program, which represents the system as a set of small cells and calculates the progress and simultaneously the properties of the bulk flow and process under investigation using the equations of mass, energy and momentum. The program allows the proposed tank to be drawn on screen, and various options selected e.g. inlet and outlet arrangements, baffles, weirs etc. The program accepts reaction constants (section 7.2) and physical parameters e.g. temperature, pH etc and outputs the ADM parameter as the dispersion number (D) (section 4.3.3), the disinfection index as discussed above (section 2.2.3), flow vectors and the RTD (Stevenson, 1995).

The DISINFEX™ program operation and output data is very similar to CONTANK™. However, DISINFEX™ also supports a database of RTDs for a number of tank configurations, which provides future comparative data and considers chlorine decay mechanisms and subsequently the formation of trihalomethane (THM). This is a known carcinogenic and its concentration levels subject to existing and possibly more stringent European regulations (Dawson, 1998). IMPULSE is also computer program which models the RTD, by using various theoretical mixing regimes, in a similar manner used for the RTD combined mathematical model presented in this project (chapter 5) (Brouckaert *et al.*, 1995). Hence, reducing the time and mathematical expertise required in developing such a model (appendix D.1).

This use of such software can dramatically reduce the time and expense in conducting model, prototype and full-scale RTD and kinetic experimental investigations and ultimately minimise capital and operating costs by designing an optimised tank and process. It also provides operating personnel with the opportunity to directly use the RTD to characterise the mixing regime, not previously considered due to its mathematical complexity. The literature cited describing these computer programs do not discuss the hydraulic and kinetic algorithms used during their simulation. Therefore, it is not possible to comment on their relative advantages or limitations due to the likely 'inbuilt' assumptions made during the development procedure.

2.3 Chapter Overview

The development, design and process optimisation of the HDVS for solids-liquid separation has evolved over 30 years. Existing research generated during this work on the HDVS has followed a structured and logical progression in response to both product development and legislation in the water industry. The research presented in the

following chapters on the Swirl-Flo™ HDVS is the first stage in assessing its potential for kinetic process applications in stormwater and wastewater management and will aid in producing a design methodology based on the RTD and chemical kinetic principles. The long term objectives and future research initiatives undertaken to achieve this design methodology should follow the previous research considering kinetic processes as opposed to solids-liquid separation (section 8.6).

The majority of existing work undertaken on the HDVS investigates its solid-liquid separation efficiency. Additionally alternative experimental techniques have been used to support these results and conclusions. This includes RTD, CFD, and hydraulic scaling investigations. The HDVS has also been employed as contact tank for several chemical process applications, which are dependent on kinetic principles. It is the latter processes combined with the RTD were no research at present has been undertaken on the HDVS. Subsequently the HDVS has not been comprehensively characterised using RTD analysis and the data presented in a suitable manner for determining its performance for a range of kinetic processes. Additionally the design of current HDVS kinetic process applications, which are dependent on the RTD and kinetic principles, are not combined with RTD analysis. Therefore the relationship between the predicted performance of the HDVS using RTD analysis and the actual experimental kinetic process performance has also not been addressed.

The HDVS is not unique by a lack of research in this area as many kinetic process applications in a range of scientific fields and particularly the water industry only use the RTD to characterise the mixing regime and therefore do not continue the design methodology by combining the RTD with kinetic process principles and optimising the performance of the continuously operated system. The importance and recognition of this procedure and combination of principles is highlighted by recent work presented and discussed using generic combined theoretical RTD and kinetic principles. This

work can be initially used to assess the HDVS's performance as a contact tank and also to provide verification data for any future kinetic and particularly disinfection experimental process investigations within the HDVS, using the RTD data presented in the following chapters. RTD computer packages currently available have also been discussed and could possibly aid and simplify the development of the design methodology.

3.0 Materials and Methods

3.1 Experimental Plan

Two different size hydrodynamic vortex separators (HDVS) (Fig. 3.1) were used throughout the project and are termed the prototype HDVS (Fig. 3.2a/b) and model HDVS (Fig. 3.3a/b). As discussed in chapter 1 this study has been approached in two stages, a hydraulic and kinetic analysis. This is reflected by the experimental investigations undertaken:

- Residence Time Distribution (RTD)
- Hydrogen Peroxide (H_2O_2) Decomposition

The RTD experiments investigated the hydraulic mixing regime and the H_2O_2 decomposition experiments investigated kinetic processes within the HDVS. All residence time distribution (RTD) and hydrogen peroxide (H_2O_2) - catalase decomposition experiments were conducted on both the model and prototype HDVS operating with and without a baseflow component.

All RTD experiments were performed at least 3 times for the same HDVS operating configuration i.e. with and without a baseflow and the sludge hopper and operating parameters i.e. inlet flow rate and flow split. This approach was also adopted for the HDVS and batch reactor H_2O_2 decomposition experiments. The final RTD curve and H_2O_2 conversion results presented and used for analysis were obtained from an average of the individual experiments. The experimental methods employed provided consistent replication of the experimental results. The experimental sequence adopted and the approximate time scales involved are shown in Table 3.1.

Table 3.1 HDVS Experimental Sequence and Time Scales

Experiments	Operating Conditions	Months
RTD	Prototype HDVS no baseflow	3
	Prototype HDVS no sludge hopper	1
	Prototype HDVS baseflow	3
	Model HDVS no baseflow	1
	Model HDVS no sludge hopper	1
	Model HDVS baseflow	2
H_2O_2 Decomposition	Model HDVS no baseflow	2
	Batch Reactor	1
	Prototype HDVS no baseflow	1
	Model HDVS baseflow	2
	Prototype HDVS baseflow	2

For all experimental methods and chemicals used throughout the project health and safety risk assessments were undertaken and approved by the Liverpool John Moores University (LJMU) health and safety officer and project supervisors.

3.2 Hydrodynamic Vortex Separator (HDVS) Principle of Operation

The HDVS (Fig. 3.1) is normally considered as a vortex-style-separating device, which provides a controlled flow regime for the separation of solids from an incoming waste stream. The mixing patterns within the HDVS are provided by the position of the inlet pipe, fixed geometry and internal configuration (Andoh, 1994). The following discussion describes the flow patterns within the HDVS with respect to its internal components and application for solids-liquid separation. The established flow patterns are considered present regardless of the constituents of the inlet stream and application of the HDVS.

Referring to Fig. 3.1, the inlet stream (A) enters the HDVS tangentially at a height of approximately half its operating height. The flow first moves in a radial manner around the outer zone (B), confined between the outer wall and internal vertical dip plate (C). A portion of the flow is removed via the baseflow pipe (D) and the remainder

passes up through the inner zone (E), located within the circular vertical dip plate (C). This description assumes a baseflow component is present but it can be removed and hence, all the flow will pass up through the inner zone (E). A horizontal baffle plate (F) is located at the top of the dip plate and once passed the flow leaves the device via a weir (G), along a spillway and through the overflow pipe (H).

The combination of a baseflow and overflow component result in a non-uniform axial velocity profile with higher velocities located in the outer zone (B) and quiescent conditions in the inner zone (E) relative to each other. At the position where these two flow regimes are adjacent to each other a shear plane exists, with zero velocity, which creates optimum conditions for flocculation of solids. The position and size of the shear plane depends on the depth of the vertical dip plate (C) and central cone (J). The cone helps to direct solids towards the baseflow pipe, stabilises the flow passing up through the dip plate (C) and aids in preventing siltation. In its normal mode of operation the waste stream passes through the baseflow pipe (D) and the treated water out via the overflow pipe (H). The separation of solids from a liquid is largely achieved by extending the flow path that a particle takes and hence provides greater time for gravitational forces to act which are aided by inertial and other forces. A secondary flow pattern is superimposed on top of the primary flow as a result of velocity gradients established. This aids in sweeping solids towards the base of the device, which are collected in the sludge hopper (K) and therefore prevents solids resuspension and provides a controlled flow regime for optimum solids separation (Andoh, 1994).

The design of the HDVS used throughout this study is predominantly employed for the separation of colloidal particles i.e. particles that do not settle in a practical time period (Table 1.1). This separation can be encouraged and enhanced with the use of chemicals i.e. coagulants and flocculants however, no trials were conducted in this project to investigate the solids separation performance of the device with or without the

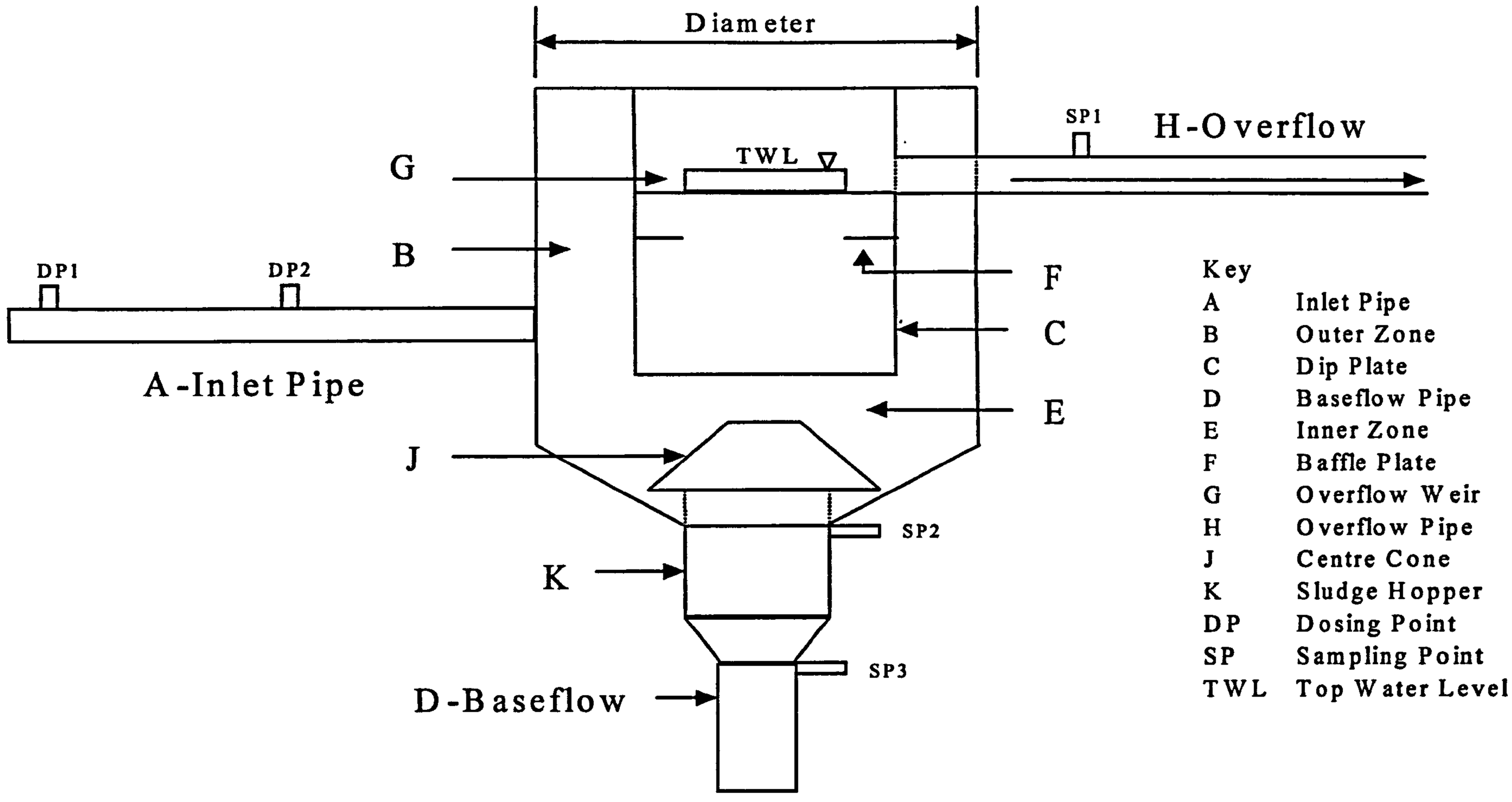

Fig. 3.1 Model and Prototype HDVS Internal and Experimental Configuration

use of chemicals. Previous research into the HDVS solids-liquid separation performance has been discussed in chapter 2.

3.3 Hydrodynamic Vortex Separator (HDVS) Experimental Configuration

The model and prototype HDVS were operated in a continuous flow-through mode for all experiments. The volume of each device was calculated from engineering drawings (appendix A.1 and A.2) and checked against the volume calculated by feeding a calibrated flow rate into the device and measuring the time taken for the device to overflow. The estimated volumes do not include any connecting pipework.

For all experiments operating with no baseflow a gate valve or blank flange was positioned directly below the sludge hopper (Fig. 3.1). This ensured that the HDVS would be operating in a similar manner as a device constructed with a sludge hopper and without a baseflow component. Additionally, experiments were conducted omitting the sludge hopper from the active volume of the HDVS. This was achieved by temporally removing all internal components from the HDVS and placing a blank plate across the sludge hopper and below SP2 (Fig. 3.1).

3.3.1 Prototype Hydrodynamic Vortex Separator (HDVS)

The prototype HDVS device is a 750mm diameter, mild-steel freestanding HDVS. Its size and operating conditions are such that it is considered a pilot-scale rig (Fig. 3.2a/b and appendix A.1). The prototype HDVS estimated volume is 464 litres, including the sludge hopper. The sludge hopper has a volume of approximately 35 litres. An 80mm diameter horizontal pipe approximately 24-pipe diameters long directs the flow into the device. This length of pipe was used to minimise any turbulence

effects before the flow entered the HDVS. Approximately 20-pipe diameters from the HDVS entrance a dosing point (DP1) is located and similarly at 12-pipe diameters, a dosing point (DP2) is also located. A sample point (SP1) was placed on the 80mm diameter overflow pipe and two sampling points located on the baseflow outlet. The baseflow SP's were positioned above (SP2) and directly below (SP3) the sludge hopper (Fig. 3.1). SP3 is located on the 100mm diameter baseflow pipe.

Inlet flow control is provided by a gate valve and flow measurement by a calibrated Helix 4000™ turbine-style flowmeter manufactured by ABB Kent Meters. This type of flowmeter measures and records the volume of flow passed and hence the total volume passed, in the duration of an experiment, can be measured and an average flow rate calculated. Additionally the flow rate was checked volumetrically at the overflow, by measuring the time taken for the flow to fill a container of a known volume. The two techniques employed to measure the inlet flow rate are considered to aid in minimising any experimental errors. The inlet flow was pumped to the prototype HDVS using two different capacity pumps for flow rates above and below 90l/min.

Experiments were conducted for a range of flow rates (15-480l/min), providing theoretical retention times of approximately 1-30min (eqn. 4.2). The maximum flow rate without hydraulic overloading of the prototype HDVS occurring, when operating with no baseflow, is approximately 540l/min. The baseflow flow rate was measured using the same procedure as the inlet flow rate discussed above and then checked against the required overflow flow rate with respect to the inlet flow rate. The baseflow flow rate ranged from 10-60% of the inlet flow rate i.e. flow split (Fig. 6.1) depending on the experimental investigation. The range of flow rates and flow splits investigated cover all design flow rates for the HDVS current applications operating with and without a baseflow component (Andoh, 2000).

Fig. 3.2a Prototype Hydrodynamic Vortex Separator (HDVS) Elevation

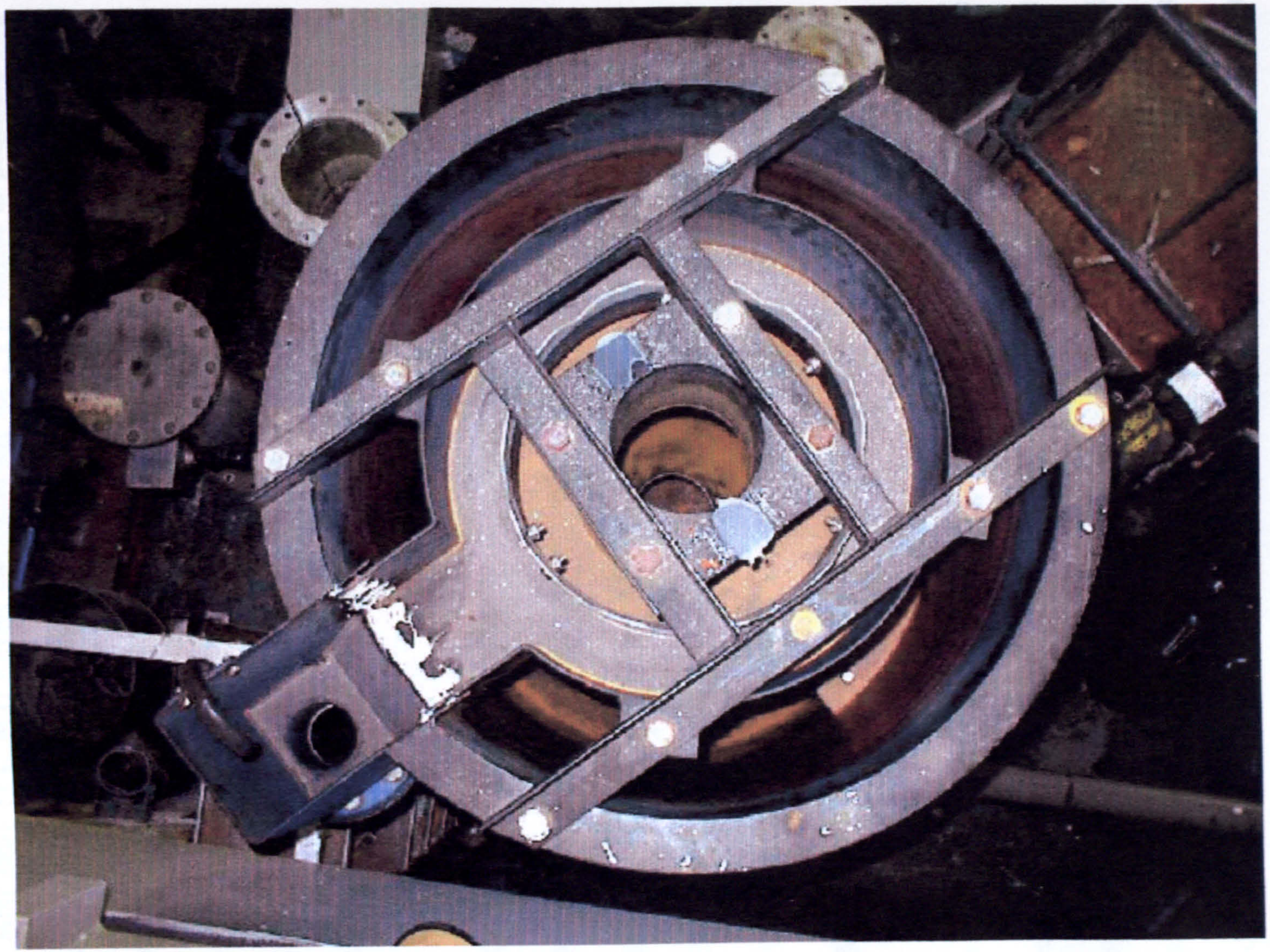

Fig. 3.2b Prototype Hydrodynamic Vortex Separator (HDVS) Plan View

3.3.2 Model Hydrodynamic Vortex Separator (HDVS)

The model HDVS (Fig. 3.3a/b) was constructed from 6mm thick clear plastic enabling visual inspection of the internal flow patterns. A specialist plastics company manufactured the outer shell of the model HDVS. It was produced as one complete unit and therefore eliminated any leakage problems. All internal components and connecting pipework were constructed by the engineering workshop at Byrom Street, LJMU. The model HDVS construction was jointly financed by Hydro International Plc and LJMU and constructed to investigate scaling effects on the HDVS mixing regime in future research.

The model HDVS (Fig. 3.3a/b and appendix A.2) is a half-geometric scale replica of the prototype HDVS. The dimensions of the model HDVS (appendix A.2) were obtained by applying a dimensional scaling factor of 0.5 to the prototype HDVS dimensions (appendix A.1) as the exact hydraulic scaling relationships of the HDVS are not known. The scaling relationships, which are considered to most likely represent the HDVS, are Hazen and Froude scaling (Fenner and Tyack, 1997 and 1998) and are discussed below and in chapter 2 (section 2.1.3).

The model HDVS diameter is 375mm and its estimated volume is 60 litres, including the sludge hopper. The sludge hopper has a volume of approximately 5 litres. A 40mm diameter horizontal pipe approximately 30-pipe diameters long directs the flow into the device. The dosing and sampling point arrangements and labels for both the overflow (40mm diameter) and baseflow (50mm diameter) pipes are the same as that described in section 3.3.1 for the prototype HDVS (Fig. 3.1). Inlet flow control is provided by a gate valve and flow measurement by a calibrated rotameter. Additionally, the flow rate was checked volumetrically at the overflow. The inlet flow to the model HDVS was delivered directly from the laboratory ring main. Care was taken to ensure

Fig. 3.3a Model Hydrodynamic Vortex Separator (HDVS) Elevation

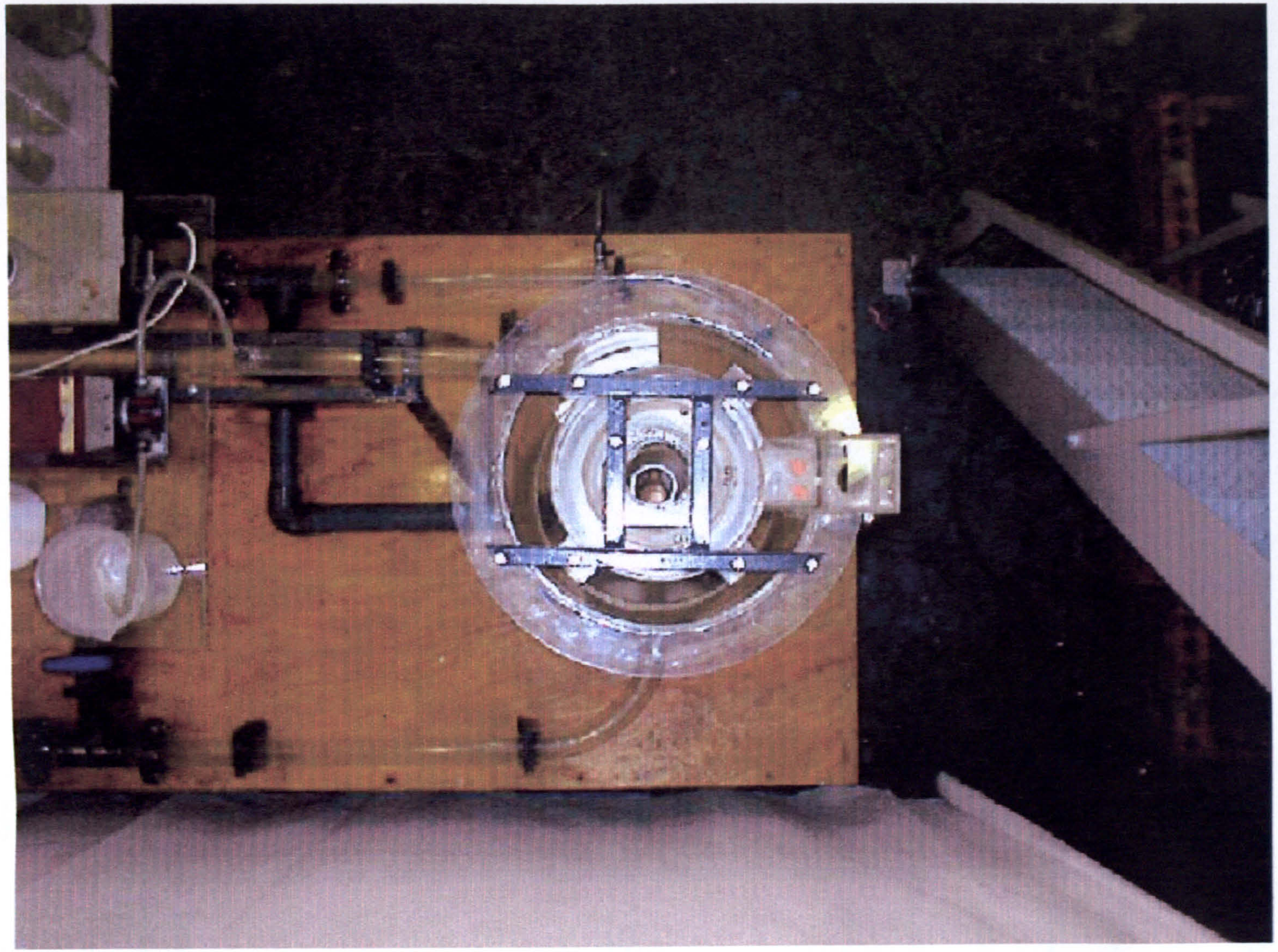

Fig. 3.3b Model Hydrodynamic Vortex Separator (HDVS) Plan View

that the calibrated rotameter maintained the required reading for the duration of the experiment due to the possibility of 'pressure drop' across the ring main. Experiments were conducted for a range of flow rates (4-90l/min), providing theoretical retention times of approximately 0.5-15min (eqn. 4.2).

The range of flow rates investigated for the model HDVS cover the equivalent Hazen (eqn. 3.1) and Froude (eqn. 3.2) scaled range of operating flow rates for the prototype HDVS. This was achieved by applying Hazen and Froude hydraulic scaling relationships to the prototype HDVS flow rates using the model HDVS dimensional scaling factor of 0.5 (L) (Table 3.2). Hence, the range of flow rates and flow splits investigated will also cover all design flow rates for the model HDVS (Andoh, 2000). Table 3.2 details the model HDVS equivalent prototype HDVS inlet flow rate using the above scaling laws and their relationships below:

$$\text{Hazen Scaling - } \frac{Qm}{Qp} = L^2 \qquad (3.1)$$

$$\text{Froude Scaling - } \frac{Qm}{Qp} = L^{2.5} \qquad (3.2)$$

Where: Qm = Model HDVS Flow Rate (l/min)

Qp = Prototype HDVS Flow Rate (l/min)

L = Dimensional Scaling Factor i.e. 0.5

Table 3.2 Hydraulic Scaling Relationships for the Model and Prototype HDVS

Qp (l/min)	Hazen – Qm (l/min)	Froude – Qm (l/min)
15	3.750	2.650
30	7.500	5.300
45	11.25	7.950
60	15.00	10.61
90	22.50	15.91
120	30.00	21.21
240	60.00	42.43
360	90.00	63.64
480	120.0	84.85

The maximum flow rate without hydraulic overloading of the model HDVS occurring, when operating with no baseflow, is approximately 120l/min. Hence, the Hazen scaled flow rate of 120l/min, which is equivalent to 480l/min for the prototype HDVS, could not be achieved and therefore investigated on the model HDVS.

The baseflow flow rate was measured using the same procedure as the inlet flow rate discussed above and then checked against the required overflow flow rate with respect to the inlet flow rate. The baseflow flow rate ranged from 10-60% of the inlet flow rate i.e. flow split (Fig. 6.1) depending on the experimental investigation.

3.4 Residence Time Distribution (RTD) Experiments

The RTD tests are stimulus-response experiments. The RTD is obtained experimentally by injecting an inert substance (tracer), in solution, into the reactor at time t = 0 and then measuring the tracer concentration, in the outlet stream(s) as a function of time i.e. overflow or overflow and baseflow. The most commonly used tracers are coloured and radioactive materials and salts e.g. potassium chloride, lithium chloride and sodium chloride. The use of radioactive tracers was rejected, so to avoid added health and safety requirements e.g. trained personnel and control equipment. The two tracers used for the RTD experiments conducted on the HDVS in this project were a coloured dye and lithium chloride (LiCl). The tracer should have the following characteristics to ensure its behaviour accurately reflects that of the liquid phase:

- Non reactive species
- Physical properties similar to those of the liquid phase
- Non absorbance by contact surfaces
- Not present at significant levels in the liquid phase

Other general considerations include:

- Easily detectable at low concentrations by in house methods
- Cheap and readily available
- Suitable levels for human contact
- Prevent the build up of dangerous levels and suitable to discharge to drain

There are several techniques that can be adopted to inject the tracer into the incoming feed e.g. pulse, step, oscillating, wave, sinusoidal etc (Wen and Fan, 1975). A pulse (LiCl) and step (coloured dye) injection technique were used to obtain the RTD from both the model and prototype HDVS. The RTD experimental tracer and injection technique and model and prototype HDVS operating condition combinations are shown below. The baseflow SP2 and SP3 RTD experiments were conducted completely separately, as it was not practical to manually sample 3 outlets simultaneously. This approach provides several comparable RTD curves for the overflow component.

- No baseflow – Pulse tracer injection (SP1)
- No sludge hopper – Pulse tracer injection (SP1)
- No baseflow – Continuous tracer feed (step) (SP1)
- Baseflow – Pulse tracer injection (SP2)
- Baseflow – Pulse tracer injection (SP3)

To provide clarity for the reader no baseflow implies the sludge hopper is included in the HDVS volume whereas the no sludge hopper experiments also have no baseflow but the sludge hopper is not included in the HDVS volume for the RTD investigations. The baseflow experiments have both an overflow and baseflow component as described

in section 6.1 and due to the HDVS configuration (Fig. 3.1) must include the sludge hopper in the HDVS volume. However, the influence of the sludge hopper on the baseflow component RTD was investigated by sampling the baseflow component RTD above (SP2) and below (SP3) the sludge hopper (Fig. 3.1). The RTD results are presented and discussed for the HDVS operating without a baseflow in chapter 4 and with a baseflow component in chapter 6.

The pulse RTD experimental procedure discussed below i.e. tracer, sample collection and analysis adopted in this project is the same as previously used for RTD investigations on the Swirl-Flo™ (Dudley and Marks, 1993) and Grit King™ HDVS (Tyack and Fenner, 1997 and 1998b) (section 2.2.2).

3.4.1 Residence Time Distribution (RTD) Pulse Injection Technique

The lithium chloride (LiCl) tracer was injected, using a syringe, into the centre of the flow of the inlet pipe at the dosing point (DP2) (Fig. 3.1). The tracer injection arrangement on the inlet pipe consisted of a pipe with a gate clamp, connected through the inlet pipe by a saddle arrangement. Prior to injection the gate clamp was opened and once completed closed again. A 5ml and 20 or 30ml syringe volume were used for the model and prototype HDVS experiments respectively. A stock solution of dilute lithium chloride (LiCl) was made prior to all RTD experiments. Care was taken to ensure that the correct dilution and subsequent concentrations were achieved as when lithium chloride (LiCl) is added to water heat is given off as an exothermic reaction occurs. The tracer stock solution was as dilute as practically possible to minimise any density differences between the tracer and liquid phase. The volume and concentration of lithium chloride (LiCl) initially injected was determined by trial and error and is not just dependent upon the flow rates and subsequent dilution factors but also the sensitivity of

the atomic absorption spectrophotometer (AAS) (Perkin-Elmer 372) used for the lithium (Li) sample analysis.

The AAS provides an absorption reading, which is related to the lithium (Li) component concentration of the injected lithium chloride (LiCl) tracer only. The absorption reading is converted to lithium (Li) concentration using calibration standards discussed below. The AAS method of operation and measurement principal is described by Sawyer *et al.*, (1994) and the lithium (Li) concentration measurement is optimised at a wavelength of 670.8nm.

Operating with and without a baseflow component the lithium (Li) tracer concentrations for the model HDVS ranged from 100-250mg/l and for the prototype HDVS from 500-2000mg/l. The RTD experiments for both the model and prototype HDVS operating with a baseflow at SP2 generally required a smaller tracer concentration. A range of concentrations were used due to the variation in sensitivity of the AAS. However, this will not prevent comparison of any RTD curves as the AAS lithium (Li) samples absorption readings are calibrated against standard lithium (Li) concentration solutions absorption readings. A manufactures lithium (Li) solution and 1-5mg/l lithium (Li) samples prepared for this investigation were used as calibration standards. The above concentrations ensured that the absorption readings ranged from approximately 0-0.6 units and with a linear trend with respect to the lithium (Li) concentration.

The 'mixing-cup' method i.e. discrete samples, was used for collecting samples at the overflow and baseflow outlet as opposed to the 'through-the-wall' method. The 'mixing-cup' method closely represents closed vessel boundary conditions i.e. there is a change in the flow pattern at the devices inlet and outlet boundaries (Levenspiel, 1972). These boundary conditions are considered to occur for the HDVS and are representative of a disinfectant contact tank (Teefy and Singer, 1990). The 'through-the-wall' method

is more in accord with open vessel flow where the flow is not disturbed as it passes the monitoring point (Levenspiel, 1972).

Samples were taken at a higher frequency up to the theoretical mean residence time (eqn. 4.2) so to ensure that the peak of the experimental RTD curve would be well defined. Sample frequency was also dependent on the mean residence time and increased as the mean residence time decreased and therefore as the flow rates increased. This sample frequency procedure also applies to the baseflow SP2 and SP3 experiments as the RTD at SP2 peaks before SP3 hence, a different sample frequency is required for each sample point for the same inlet flow rate. Samples were analysed immediately after collection using the AAS and as all the HDVS RTD experiments were operated in a continuous flow mode there were no problems with background levels of lithium (Li) as encountered when operating in a recycle mode.

The RTD experiments were conducted for approximately 6 times the theoretical mean residence time (eqn. 4.2) in this project. This was to ensure an accurate tracer recovery (mass balance) was achieved and the results for the recommended truncation time of to 3-4 times the theoretical mean residence time (eqn. 4.2) (Nauman, 1981) can be obtained by a truncation analysis. Maintaining the same RTD experimental duration for all HDVS operating conditions and inlet flow rates allows a direct comparison of all the results and data analysis techniques used to describe the RTD (chapter 4-6).

The experimental procedures and calibration standards are detailed in appendix B.1 and B.2 respectively and were followed in accordance with BS 3680 2C: 1993 and BS 3680 2D: 1993.

3.4.2 Residence Time Distribution (RTD) Continuous Feed (Step) Technique

The step injection technique is obtained experimentally by continuously feeding a tracer into the incoming flow of the device and measuring the outlet concentration from t=0, until a constant reading is obtained i.e. steady state. The tracer was injected using a steady state continuous feed self-priming rotary pump. The pump was selected as it could maintain a constant feed, as opposed to a peristaltic pump and could operate against the natural head imposed by the HDVS.

A coloured dye was chosen as the tracer due to few problems with handling, easy detection and possible visual inspection of the model HDVS and collected samples. The dye used was relatively inexpensive and could be easily obtained in bulk. The dye is manufactured by Dylon International Ltd and used for the permanent colouring of fabrics. Due to the high flow rates for both the prototype and model HDVS and subsequent dilution factors, large amounts of dye were required for easy detection. The tracer was supplied in solid form and dissolved into a feeder reservoir, from which the pump supplied the continuous feed. Several tests were required to optimise the tracer feed concentration and flow rate for suitable detection concentrations. A tracer feed flow rate of 4l/min was used for all experiments on the prototype HDVS with a feed volume and hence tracer mass (200-400g) dependent on the experiments duration and inlet flow rate dilution factor. The tracer feed flow rate and coloured dye mass for the model HDVS experiments were 1l/min and 100-200g respectively. The feed was delivered by the pump at DP2 (Fig. 3.1) and measured and controlled by a calibrated rotameter.

An absorption spectrophotometer (AS) (Cecil Instruments CE 272) was used for all coloured dye sample analysis. The AS provides an absorption reading, which is a function of the coloured dye sample concentration. However as the step RTD data

analysis procedure (section 4.2 and 4.3.2) does not require an estimation of the tracer concentration recovered (mass balance) the absorption readings were used directly to obtain and investigate the step RTD. The AS method of operation and measurement principal is described by Sawyer *et al.*, (1994). The AS optimum coloured dye detection wavelength was obtained using a digital spectrophotometer wavelength scanner and this was compared to the optimum wavelength estimated using the dial indicator on the AS used for the sample analysis. The optimum wavelength ranged from approximately 570-590nm using a deuterium light source. The experimental procedures are detailed in appendix B.3 and were also followed in accordance with BS 3680 2C: 1993 and BS 3680 2D: 1993.

3.5 Hydrogen Peroxide (H_2O_2) Decomposition Experiments

This experimental procedure consisted of determining the rate at which hydrogen peroxide (H_2O_2) is decomposed by catalase (section 7.1). Subsequently, experiments were conducted on both the model and prototype HDVS, continuously feeding both H_2O_2 and catalase, to measure the actual H_2O_2 decomposition in the HDVS. The materials and methods used to perform these experiments are outlined below and in appendix B.4 and B.5 and the H_2O_2 decomposition results are presented and discussed in chapter 7.

The H_2O_2 used for all experiments was supplied by Fisher Scientific and had a 30% weight to volume (w/v) ratio i.e. 300g/l resulting in approximately a 8.8 molar stock solution (appendix B.4). However, due to problems with the natural decomposition of H_2O_2 the concentration of H_2O_2 in the stock solution was checked before each experiment. The catalase (bovine liver) has a specific activity of 1300μmol of H_2O_2 per minute per mg of catalase at a neutral pH and 25°C under saturated conditions.

The concentrations of H_2O_2 and catalase used to obtain a practical decomposition rate with respect to time were predicted by trial and error. This was first undertaken using the model HDVS to ensure that the H_2O_2 decomposition for the range of contact times, provided by the range of flow rates investigated, is between 0-100% of the initial H_2O_2 concentration. The concentration of H_2O_2 and catalase used in the batch reactor experiments were the same as those used in the model and prototype HDVS continuous flow experiments. The H_2O_2 and catalase feed concentrations and flow rates, for both the model and prototype HDVS, are presented in Tables 3.3 and 3.4 respectively and equivalent batch reactor H_2O_2 and catalase concentrations were 0.5ml (30% w/v) and 5mg for a 2 litre operating volume respectively.

Table 3.3 Model HDVS - Hydrogen Peroxide (H_2O_2) and Catalase Experimental Concentrations and Feed Flow Rates

Flow Rate (l/min)	Feed Rate (l/min)	Catalase Concentration	H_2O_2 Concentration (*)
6	0.3	1g / 20L	100ml / 20L
10	0.5	1g / 20L	100ml / 20L
20	1.0	1g / 20L	100ml / 20L
30	1.0	1.5g / 20L	150ml / 20L
60	1.0	3g / 20L	300ml / 20L

Table 3.4 Prototype HDVS - Hydrogen Peroxide (H_2O_2) and Catalase Experimental Concentrations and Feed Flow Rates

Flow Rate (l/min)	Feed Rate (l/min)	Catalase Concentration	H_2O_2 Concentration (*)
45	0.3	7.5g / 20L	750ml / 20L
60	0.5	6g / 20L	600ml / 20L
120	1.0	6g / 20L	600ml / 20L
240	1.0	12g / 20L	1200ml / 20L
360	1.0	18g / 20L	1800ml / 20L

* The H_2O_2 concentration is presented as either mg/l or mol/l (section 3.5.3)

3.5.1 Batch Reactor Experiments

The batch reactor experiments were carried out in a fermentor with a 3 litre operating volume. The fermentor was a self-contained unit with an in-built mixer and control. The mixer was set at 500rpm and the fermentor filled with 2 litres of mains water for all experiments. Mains water was used for all batch experiments as this was used for the experiments on the model and prototype HDVS (section 3.5.2).

The H_2O_2 was diluted to the required concentration and a measured volume added using a pipette. Samples of the fermentor, containing only 2 litres of water and the required concentration of H_2O_2 were taken to check the concentration of H_2O_2 against the neat H_2O_2 dilution samples and the manufacturers stated concentration. The catalase was dissolved in 100ml of mains water and at time t=0 the measured volume and concentration of catalase was added using a pipette to the fermentor and discrete samples taken at different time intervals. Samples were taken at a greater frequency at the beginning of the experiment as the decomposition of H_2O_2 is proportional to its initial concentration and hence is greater at the beginning of the experiment i.e. exponential decay. The complete batch reactor H_2O_2 decomposition experimental procedure is presented in appendix B.4.

3.5.2 Model and Prototype Hydrodynamic Vortex Separator (HDVS) Experiments

The flow rates investigated for the H_2O_2 decomposition experiments on the model HDVS were 6, 10, 20, 30 and 60l/min and similarly for the prototype HDVS 45, 60, 120, 240 and 360l/min and the flow splits ranged from 10-60% at increments of 10%. The experimental technique and procedure is the same for both devices (appendix B.5).

These experiments consisted of simultaneously feeding both the H_2O_2 and catalase into the inlet pipe of the HDVS until a steady state H_2O_2 concentration in the outlet(s) is achieved. Two small capacity, self-priming rotary pumps were used to separately feed both the reactants into the HDVS inlet pipe at DP2 (Fig. 3.1). The inlet feed arrangement consisted of a 'Y' shape connection, which mixed both flows prior to entering the inlet pipe (section 7.3). The H_2O_2 and catalase feed reservoirs were both filled with 20 litres of mains tap water using a measuring cylinder. The required volumes of H_2O_2 and catalase were added and mixed thoroughly (Table 3.3 and 3.4). Plastic tubing was used for all the connecting pipework feeding the H_2O_2 and catalase.

At the time at which both flows entered the inlet pipe the clock was started and the experiment conducted for approximately 4-5 times the theoretical mean residence time (eqn. 4.2), ensuring steady state conditions. Several samples were taken over a period of time once steady state conditions were considered to be achieved. Therefore, the sample results also provided a check on steady state conditions. The reactants feed flow rates were set at time t=0 and were carefully measured, using a calibrated rotameter and monitored throughout the experiment to prevent any fluctuation.

All samples for both devices operating with a baseflow were taken from SP3 i.e. directly below the sludge hopper (Fig. 3.1). The experimental procedure for the HDVS operating with a baseflow is the same as operating without a baseflow. The sample analysis for all H_2O_2 decomposition experiments is described in section 3.5.3 and a breakdown of the above procedures is detailed in appendix B.4 and B.5.

For both the model and prototype HDVS an experimental check on the dilution factors, inlet and feed flow rates and the natural decomposition of H_2O_2 due to oxidation and contact materials was undertaken before the introduction of any catalase. This was investigated by feeding only dilute H_2O_2 of a known concentration into the HDVS inlet pipe operating with no baseflow. Samples were taken from the overflow pipe and the

measured concentrations of H_2O_2 compared to the initial feed concentrations taking into account the dilution factors due to the inlet flow rate and H_2O_2 feed flow rate. The effects of H_2O_2 absorption by materials in contact with the bulk flow are particularly important for the prototype HDVS as this is constructed from mild steel which can promote the decomposition of H_2O_2 compared to Perspex used to construct the model HDVS. These experiments showed that there is no natural decomposition of the H_2O_2 and also proved the inlet and reactants feed flow rates were correct for both the model and prototype HDVS (section 7.6).

Care was taken to prevent cross contamination hence, separate glassware for the H_2O_2 and catalase was used at all times. The HDVS was rinsed through with dilute H_2O_2 after each experiment to remove any excess catalase and then rinsed with mains water and detergent. Additionally, during experimental start-up mains water was allowed to continuously run through the HDVS removing any reactants and cleaning products and samples were also taken and checked to ensure no H_2O_2 remained in the device.

No temperature control was provided for any of the H_2O_2-catalase decomposition experiments. However, the temperature was measured throughout each experiment and there was no significant difference in temperature for all experiments i.e. 11-15°C. This allows a direct comparison of the results and no temperature correction factor is required. Additionally the pH of the water also remained relatively constant at approximately 6.3-6.6 (section 7.6.1).

3.5.3 Hydrogen Peroxide (H_2O_2) Sample Analysis

The potassium iodide (KI) - sodium thiosulphate ($Na_2S_2O_3$) titration technique was used to determine the concentration of H_2O_2 in all samples. This titration depends on the

release of iodine (I_2) from KI by the presence of H_2O_2 and the subsequent titration (reaction) of the liberated I_2 with $Na_2S_2O_3$ carried out in acidic conditions provided by sulphuric acid (H_2SO_4). Therefore, the concentration of I_2 is equal to the concentration of H_2O_2 and the volume and concentration of titre ($Na_2S_2O_3$) added to the sample is also directly related to the concentration of H_2O_2. The advantages and limitations of this method for measuring H_2O_2 have been discussed by many workers and dates as far back as 1880 (Dennis, 1984). H_2O_2 reacts with iodide, provided in the form of KI to produce I_2, in an acidic solution in accordance with the following equation:

$$H_2O_2 + 2H^+ + 2I^- = I_2 + 2H_2O \qquad (3.3)$$

From the above reaction, the relationship between the volume of titrated $Na_2S_2O_3$ and concentration of H_2O_2 is as follows:

(Volume $Na_2S_2O_3$.Concentration $Na_2S_2O_3$) ≡ 2 (Volume H_2O_2.Concentration H_2O_2)

The concentration of selected reactants used in this project are occasionally presented as mole/l as opposed to mg/l, where 1 mole is equal to the molecular weight (mw) of the reactant e.g. mw of H_2O_2 = 34.01g. The molecular weights for all titration reactants used in this project are provided in appendix B.4.

The titration reactants were all prepared and placed into a 250ml flask prior to starting the experiment. The reactants do not require being of an exact concentration only in excess and therefore not rate limiting in the titration reaction. The end point of the titration reaction is observed by visual inspection of the reaction solution. This is provided by the introduction of a starch solution, which creates a deep purple colour in the presence of the liberated I_2. Therefore the reaction solution becomes colourless, as

the $Na_2S_2O_3$ reacts with the I_2 and the end point is approached. The H_2O_2 sample was added immediately to the titration reactants after collection to minimise any further H_2O_2 decomposition. The samples were allowed to stand for approximately 15 minutes as the reaction velocity is comparatively slow, but increases with increasing concentration of acid (Aldershof *et al.*, 1997). The addition of ammonium molybdate ($(NH_4)_2 MoO_4$) solution renders the reaction almost instantaneous by acting as a catalyst and accelerating the rate at which the I_2 is liberated (Dennis, 1984).

The concentrations of $Na_2S_2O_3$ varied depending on the H_2O_2 concentration. The different $Na_2S_2O_3$ concentrations were obtained by diluting the stock solution prepared for all the H_2O_2 decomposition experiments. 10ml volume samples were taken in a discrete manner for all batch reactor, model and prototype HDVS experiments. Several blank samples containing only KI, H_2SO_4 and starch indicator were titrated with $Na_2S_2O_3$ solution during all experiments. This tested for any natural oxidation of the KI to I_2, which would falsely imply a greater concentration of H_2O_2.

4.0 Hydrodynamic Vortex Separator (HDVS) Operating without a Baseflow Component Residence Time Distribution (RTD) Analysis

The characterisation of the mixing regime within the HDVS using RTD analysis is split into two stages. This chapter presents the first stage of the characterisation process by investigating the model and prototype HDVS operating without a baseflow component (Fig. 3.1). The RTD will identify and describe any deviation from the two theoretical mixing regimes due to non-ideal flow behaviour i.e. dispersion and dead volumes (section 4.1). Subsequently the RTD provides an accurate description of the true mixing regime and is used in the design and optimisation of a system for kinetic process applications.

The HDVS RTD is obtained using a pulse injection technique (section 3.4.1) measured at SP1 only (Fig. 3.1) and characterised using a range of RTD data analysis techniques (section 4.3). This includes the axial dispersion model (ADM) and tanks-in series model (TISM) parameters solved indirectly and directly using the method of moments and non-linear regression techniques respectively. The model goodness of fit is assessed using typical RTD correlation parameters. The RTD experimental curves were also subject to a truncation analysis to investigate the effect of the experimental duration on the ADM and TISM parameters calculated using the method of moments and non-linear regression. RTD indices are also used to describe the spread of the RTD curves and presented to support conclusions obtained from other data analysis techniques. The HDVS RTD was also obtained using a step injection technique (section 3.4.2), described using the method of moments data analysis technique, to aid in supporting the detailed RTD data obtained from the pulse method.

The HDVS used throughout this project has a sludge hopper (Fig. 3.1) located at the base to collect solids during the solids-liquid separation process (section 3.2). The

sludge hopper is generally employed for low inlet flow rate and high solids loading rate operating conditions and therefore is not always required. Subsequently, RTD investigations were undertaken with the sludge hopper removed from the HDVS (Fig. 3.1). This will investigate the mixing characteristics of the sludge hopper and it's contribution to the overall mixing regime within the HDVS. This project investigated a Swirl-Flo™ HDVS and by operating it with and without the sludge hopper provided a similar configuration as the Storm King™ and Grit King™ HDVS (Table 1.1). The former operates without a sludge hopper and the latter has a grit pot and therefore a similar collection area for solids as the Swirl-Flo™ HDVS.

The RTD results from the model and prototype HDVS investigated in this project are compared with existing limited RTD data on the different styles of HDVS discussed above (Table 1.1). The RTD data is also presented in a manner suitable for kinetic process investigations, as considered in chapter 7 and potential future research in chapter 8 (section 8.6). The second RTD characterisation stage investigates the HDVS operating with a baseflow component (Fig. 3.1) and the results and conclusions are presented in chapter 6.

4.1 Theoretical Mixing and its Relationship with the Residence Time Distribution (RTD)

The need to investigate and model the hydraulic behaviour of a device, in which some form of mixing process occurs, arises as the hydraulic flow regime achieved in a full-scale continuous flow system does not generally conform to a theoretical mixing regime. The two theoretical mixing regimes, used in the design of a process dependent on mixing, are plug-flow mixing and complete mixing (Fig. 4.1 and 4.2).

Generally, when a stream of material flows steadily through a vessel such as a pipe or tank, in which it takes part in some process such as a chemical reaction, heat and mass transfer, sedimentation or simple mixing, it is usual to make use of one of the following assumptions in the design process (Danckwerts, 1953):

Complete Mixing - e.g. continuous stirred tank reactor (CSTR) - The feed introduced into a CSTR at any given time becomes completely mixed with the material already present in the vessel. Hence, some of the fluid elements entering the CSTR leave it almost immediately as material is continuously withdrawn. Alternatively, other fluid elements may stay in the vessel for an infinite time, as all the material is never removed from the reactor at one time. The majority of material leaves the reactor after a time in the vicinity of the theoretical mean residence time (eqn. 4.2).

Plug-Flow Mixing - In an ideal plug-flow reactor, all the fluid elements leave the reactor after having been inside it for exactly the same time. The fluid is considered to move with a constant and equal velocity on parallel paths and leave at the same moment i.e. the mean residence time. This type of flow is associated with high length to diameter ratios (aspect ratio) e.g. flow through a pipe.

The characterisation of a mixing device using RTD analysis describes the difference between the assumed i.e. theoretical and the actual mixing regime due the presence of non-ideal flow behaviour. In batch processes, mixing is defined with respect to compositional differences, which exist in 3-dimensional space. However, a fluid element in a continuous flow system has another attribute termed 'age' and is the time that a fluid element, molecule, particle etc has spent in the system.

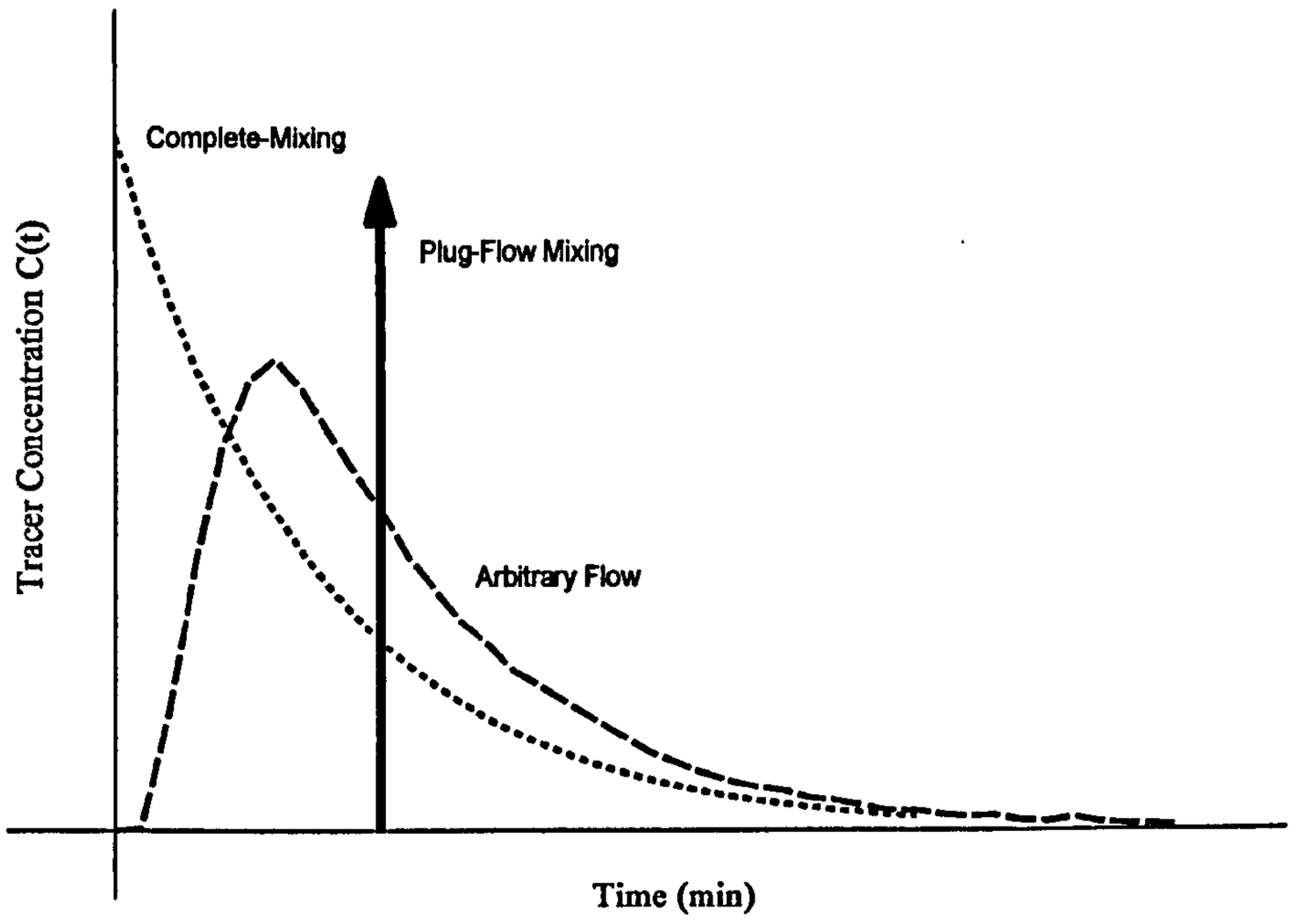

Fig. 4.1 Properties of the C(t) Curves for Different Mixing Regimes (Pulse Injection)

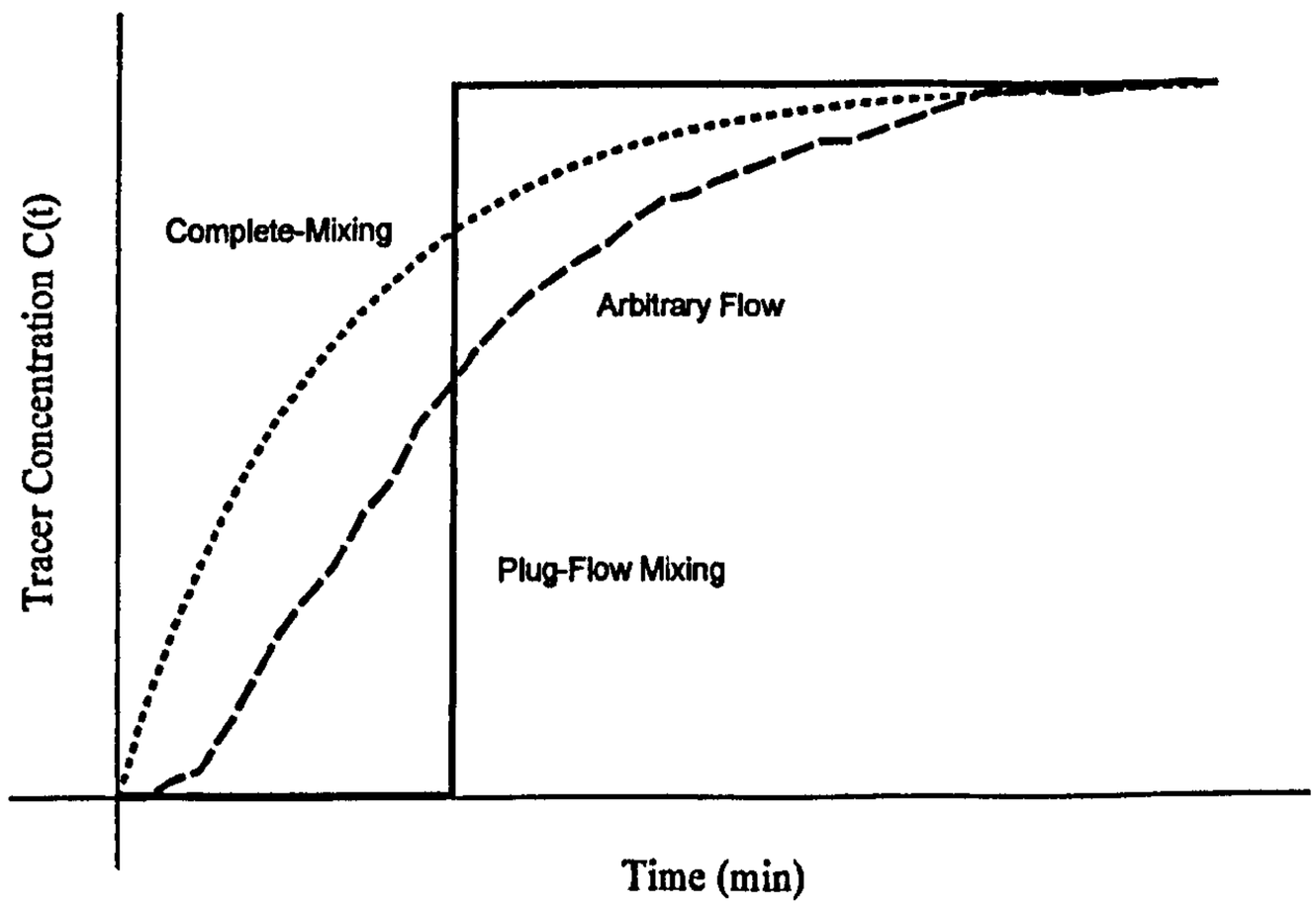

Fig. 4.2 Properties of the C(t) Curves for Different Mixing Regimes (Step Injection)

Characterisation of mixing in terms of 'ages' is called residence time theory and produces a RTD of the flow through the system (section 2.2).

The RTD describes the macromixing patterns within a system and therefore, the types of mixing provided between the theoretical boundaries of plug-flow mixing and complete mixing (Fig. 4.1 and 4.2). The RTD is used to identify the type of non-ideal flow behaviour and the quality of mixing in the reactor and can also be used to establish mathematical models to describe the system's mixing. Non-ideal flow behaviour includes dispersion and dead volumes which cause short-circuiting of the flow i.e. fluid passing through the system in a time less than the theoretical mean residence time (eqn. 4.2). The presence of a RTD can significantly affect the performance of a mixing device however, by characterising the HDVS RTD it is possible to predict and optimise it's performance for a range of kinetic processes. Additionally, the HDVS can also be compared to other reactors, blenders, contactors etc, which have been subject to RTD investigations (section 2.2). The kinetic process optimisation procedure first involves conducting batch-scale investigations to determine the operating parameters i.e. concentrations, contact time etc which provide the required efficiency e.g. chemical conversion. This information is combined with the RTD to predict the performance of the full-scale continuously operated system and therefore, the design process accounts for any non-ideal flow behaviour (chapter 7). The term 'kinetic process' refers to the mechanism by which the process occurs i.e. chemical as opposed to physical. Typical kinetic process mechanisms include chemical reactions, converting reactants into products and the inactivation of microorganisms using a disinfectant.

4.2 Residence Time Distribution (RTD) Experimental Techniques

The RTD is obtained by injecting a substance, termed a tracer, into the inlet stream and measuring it's concentration at the outlet(s). The principle function of the tracer is to have similar physical characteristics as the bulk flow and to provide a traceable solution in the outlet(s). Two different injection techniques, using different tracers, were employed in this project. These were a pulse technique using lithium chloride (LiCl) as the tracer and a step injection technique using coloured dye. The RTD experimental tracer, injection technique and HDVS operating condition combinations used to characterise the HDVS's mixing regime are described in chapter 3 and appendix B. The theoretical and experimental responses to a pulse and step injection technique are shown in Fig. 4.1 and 4.2 respectively. The theoretical RTD curves are analogous to the above descriptions of the two theoretical types of mixing i.e. complete mixing and plug-flow mixing.

If perfect plug-flow mixing is present the pulse injection technique will provide a well-defined spike occurring at the device's theoretical mean residence time (eqn. 4.2). Alternatively, if complete mixing conditions are present the curve will be exponentially decreasing, until the tracer is washed out (Fig. 4.1). The step injection produces a square wave response to perfect plug-flow conditions (Fig. 4.2). The final steady state concentration is dependent on the initial tracer concentration and dilution factors, due to the inlet flow rate and the system volume. If complete mixing conditions are present the systems response to a positive step injection will be exponentially increasing, until steady state conditions are achieved.

The principle difficulty with the pulse method is ensuring an accurate representation of a pulse signal i.e. dispersion of the tracer between its injection point and reactor entrance should be negligible and the injection time less than the response time of the

system. If these conditions are ensured, the pulse method is a simple and direct way of obtaining the RTD.

The step input method is usually considered easier to carry out experimentally than the pulse technique and has the additional advantage that the total amount of tracer, in the feed over the period of the test, does not need to be known as in the pulse method. A possible limitation of the step method is ensuring a constant tracer feed concentration is maintained for the duration of the test and a large amount of tracer is generally required. Additionally, obtaining the RTD curve parameters from a positive step test can involve differentiation of the data and this on occasion may lead to large errors. In this project the step RTD parameters were determined directly from the step distribution and hence eliminating any such errors (section 4.3.2).

4.3 Residence Time Distribution (RTD) Data Analysis Techniques

In order to analyse the RTD curves obtained from tracer studies, three methods are typically employed:

1. Determination of the mean residence time and the variance by the method of moments.
2. The use of mathematical models in order to assess the flow pattern by fitting to the RTD experimental curves.
3. The calculation of indices or parameters that have an empirical or semi-empirical nature.

All of the above RTD data analysis techniques are used to describe the HDVS RTD in this project and are presented and discussed using the same parameters employed in

existing chemical engineering literature (Levenspiel, 1972). The method of moments is used to determine the first and second moment (n) of the RTD curve. These moments correspond to the experimental mean residence time (t_m) and the variance (σ^2) respectively (section 4.3.1 and 4.3.2). The ratio of the variance to the square of the mean residence time provides a normalised variance (σ_θ^2). Two commonly used mathematical models employed in this project to describe the HDVS's mixing regime are the axial dispersion model (ADM) and tanks-in-series model (TISM) (section 4.3.3). The method of moments indirectly estimates the ADM and TISM parameters using the normalised variance (σ_θ^2). A non-linear regression direct ADM and TISM parameter estimation technique was also performed against the complete RTD experimental data. This study has also used a RTD combined mathematical model, developed specifically to describe and provide physical realism of the model and prototype HDVS mixing regime (chapter 5). The combined model configuration was established from initial observations and results obtained from the RTD curves and the ADM and TISM parameters. The final data analysis method is addressed by using RTD indices (section 4.3.4) and the intensity function (λ) (section 4.3.5).

4.3.1 Residence Time Distribution (RTD) Pulse Injection Technique

The lithium chloride (LiCl) pulse injection data is presented using the exit-age distribution function E(t) which has units of min^{-1} and is defined as the fraction of material which has left the device between time t and t + dt. C(t) is the concentration of tracer measured at the overflow (SP1) and baseflow outlets (SP2 and SP3) (chapter 6) at time t (Fig. 3.1):

$$E(t) = \frac{C(t)}{\int_0^\infty C(t)\,dt} \tag{4.1}$$

The denominator in equation 4.1 is the experimental quantity of the pulse injection tracer recovered (mass balance) in the overflow or overflow and baseflow components (Fig. 3.1). The RTD data can also be presented in its normalised form if the parameter Θ is defined as:

$$\Theta = \frac{t}{\tau} \qquad \text{and} \qquad \tau = \frac{\text{Volume (V) (l)}}{\text{Flow Rate (Q) (l/min)}} \tag{4.2}$$

Where: τ = theoretical mean residence time

Θ = normalised time

and therefore $\Theta = 1$ at the theoretical mean residence time

A dimensionless function $E(\Theta)$ can be defined as,

$$E(\Theta) = \tau E(t) \tag{4.3}$$

and plotted as a function of Θ e.g. Fig. 4.8. Appendix C shows the RTD experimental data in its C(t), E(t) and $E(\Theta)$ format for all model and prototype HDVS no baseflow operating conditions. The quantity Θ represents the number of reactor volumes of fluid that have passed through the reactor in time t. The RTD in its normalised form enables data for different flow rates and reactors of different sizes to be directly compared (Fogler, 1992).

The recommended RTD experimental duration is 3-4 times the theoretical mean residence time when using the methods of moments RTD data analysis technique (Nauman, 1981). However, all RTD experiments were stopped at approximately 5-6 times the theoretical mean residence time in this project. This RTD experimental duration was used to ensure that the maximum tracer recovery (mass balance) was obtained and also to provide consistent data, for all HDVS operating conditions, suitable for a truncation analysis. The truncation analysis was undertaken to investigate the effects of the experimental duration on the RTD moments (eqn. 4.4 and 4.5) and ADM and TISM parameters (section 4.3.3). The mean residence time is calculated from the first moment (n) about the origin:

$$t_m = \frac{\int_0^\infty E(t)\,t\,dt}{\int_0^\infty E(t)\,dt} \tag{4.4}$$

and the variance from the second moment (n) about the mean:

$$\sigma^2 = \frac{\int_0^\infty E(t)\,(t-t_m)^2 dt}{\int_0^\infty E(t)\,dt} \tag{4.5}$$

The variance is related to the spread of the RTD curve, which indicates the presence of dispersion and is particularly useful for comparing experimental and theoretical curves (Levenspiel, 1972). By normalising the variance with respect to the mean residence time (eqn. 4.6), it is possible to gauge the type of mixing i.e. a value of zero corresponds to a plug-flow mixing regime and a value of one to complete mixing (Fig. 4.1 and 4.2). The normalised variance (σ_θ^2) is used directly to predict the ADM and TISM parameters discussed below (section 4.3.3).

$$\sigma_\theta^2 = \frac{\sigma^2}{t_m^{\,2}} \tag{4.6}$$

Sample calculations using the method of moments technique are shown for the model HDVS operating with and without the sludge hopper in appendix C.1.1 and C.3.1 respectively. The same calculations where performed for all the flow rates investigated and the prototype HDVS.

4.3.2 Residence Time Distribution (RTD) Continuous Feed (Step) Technique

The positive step tracer injection technique provides the cumulative distribution function F(t), which is defined as the fraction of material with a residence time of t or less (Danckwerts, 1953). The exit-age distribution function E(t) is related to the cumulative distribution function F(t) by the following equation.

$$F(t) = \int_0^t E(t)\,dt \tag{4.7}$$

Rather than determining the exit-age distribution function E(t) by differentiation using equation 4.7, which is subject to errors, to analyse the RTD curve, the undifferentiated data may be used directly to obtain the RTD curve moments (n). This method converts the cumulative distribution function F(t) into the equivalent negative step and provides the washout function W(t) i.e. W(t) = 1 - F(t) (Nauman and Buffham, 1983). The washout function W(t) is the fraction of material with a residence time of t or greater and both F(t) and W(t) are dimensionless. The first and second moments (n) can be obtained directly from the general equation below, where n = moment (Nauman and Buffham, 1983).

$$n = \int_0^\infty W(t)\, t^{n-1}\, dt \qquad (4.8)$$

The washout function W(t) method is considered to reduce the time weighting factor by calculating the moments using t^{n-1} compared to t^n for the exit-age distribution function E(t) (section 4.3.1) (Nauman, 1981). A sample calculation using the washout function W(t) technique is shown for the model HDVS operating with no baseflow in appendix C.6.1. The same calculations where performed for all the flow rates investigated and the prototype HDVS.

All integrals used in the method of moments solution were solved using the trapezoidal rule. This is considered to have less bias when calculating the moments compared to alternative methods i.e. moment of inertia approach (Haas, 1996).

4.3.3 Residence Time Distribution (RTD) Hydraulic Flow Models

The two theoretical flow models used in this project to characterise the shape of the RTD curve are the ADM and TISM and are both single parameter models. These flow models are commonly used in environmental engineering and will therefore allow future comparison of the HDVS to other mixing devices.

The TISM arises from a system of perfectly mixed tanks-in-series with fluid flowing from one tank to the next. The TISM solution is obtained by solving the tracer mass balance across 3 tanks-in-series and then generalising for an infinite number of tanks (N) (eqn. 4.9).

$$E(t) = \frac{N^N . t^{N-1}}{t_m{}^N . (N-1)!} \exp\left(\frac{-N.t}{t_m}\right) \qquad (4.9)$$

The normalised variance (σ_θ^2) is related to the model parameter N by:

$$N = \frac{1}{\sigma_\Theta^2} \tag{4.10}$$

The model parameter N is the equivalent number of tanks-in-series. When N=1, the device under investigation is equal to one stirred tank and as N increases the mixing regime closer approximates plug-flow mixing. Fig. 4.3 shows the TISM curves for a range of model parameter (N) values (Fogler, 1992).

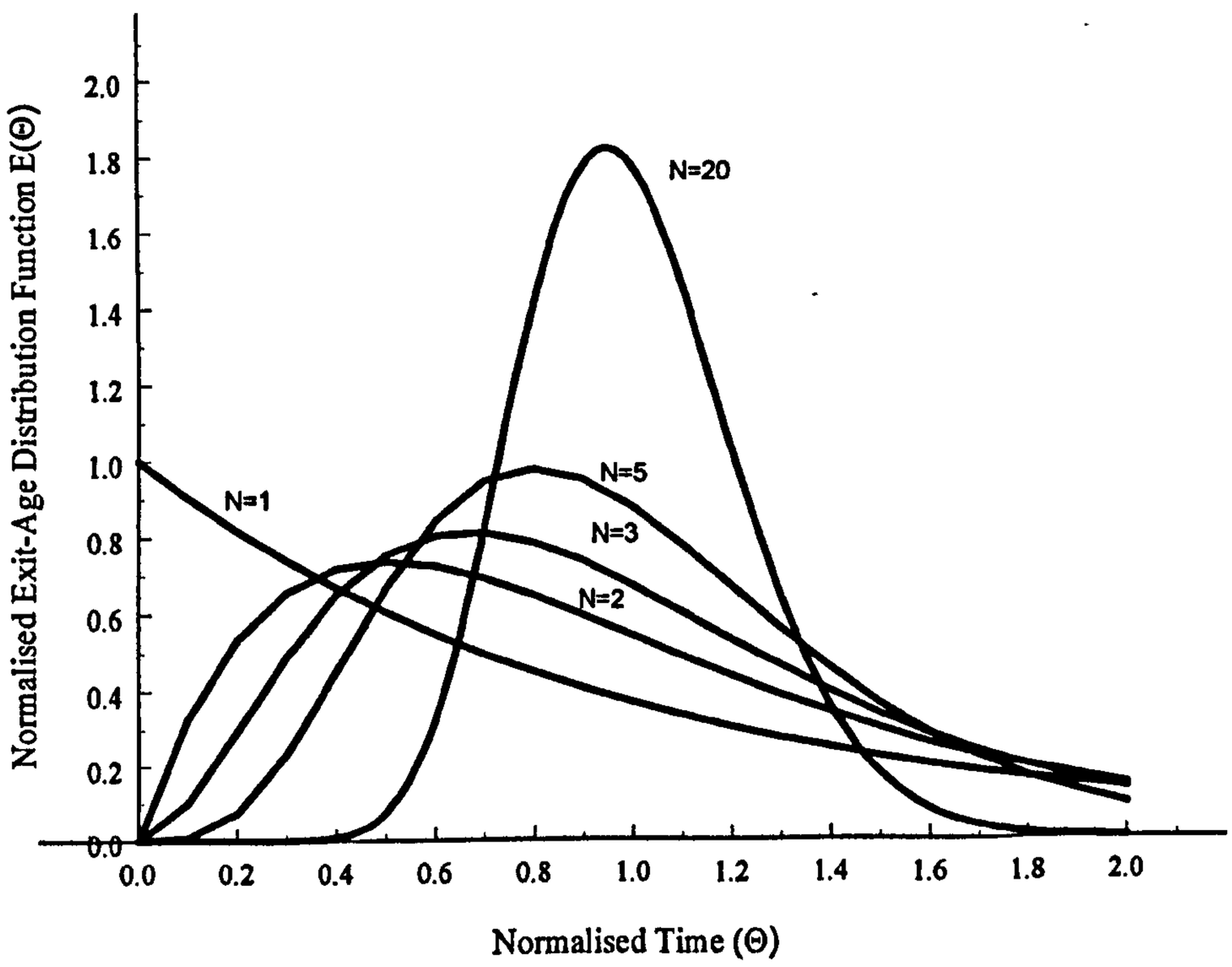

Fig. 4.3 Tanks-in-Series Model (TISM) Curves for Selected Model Parameter Values (N)

The ADM superimposes a degree of backmixing or intermixing on the perfect plug-flow model (section 4.1) and does not consider radial dispersion. The ADM model is characterised using a dispersion number (D) or its inverse the Peclet number (P_e). The Peclet number (P_e) can be defined as:

$$P_e = \frac{\text{Rate of transport by convection}}{\text{Rate of transport by diffusion or dispersion}}$$

The following Peclet number (P_e) values are used to classify the degree of dispersion (Levenspiel, 1972).

P_e = <10 – High, P_e = 10-100 – Moderate, P_e = >100 - Low

The ADM parameter is presented as the Peclet number (P_e), as opposed to the dispersion number (D), so that its trend in describing the mixing regime corresponds to that provided by the TISM parameter i.e. as the mixing regime approaches plug-flow mixing both the ADM and TISM parameters approach infinity. Fig. 4.4 shows the ADM for selected values of the Peclet number (P_e).

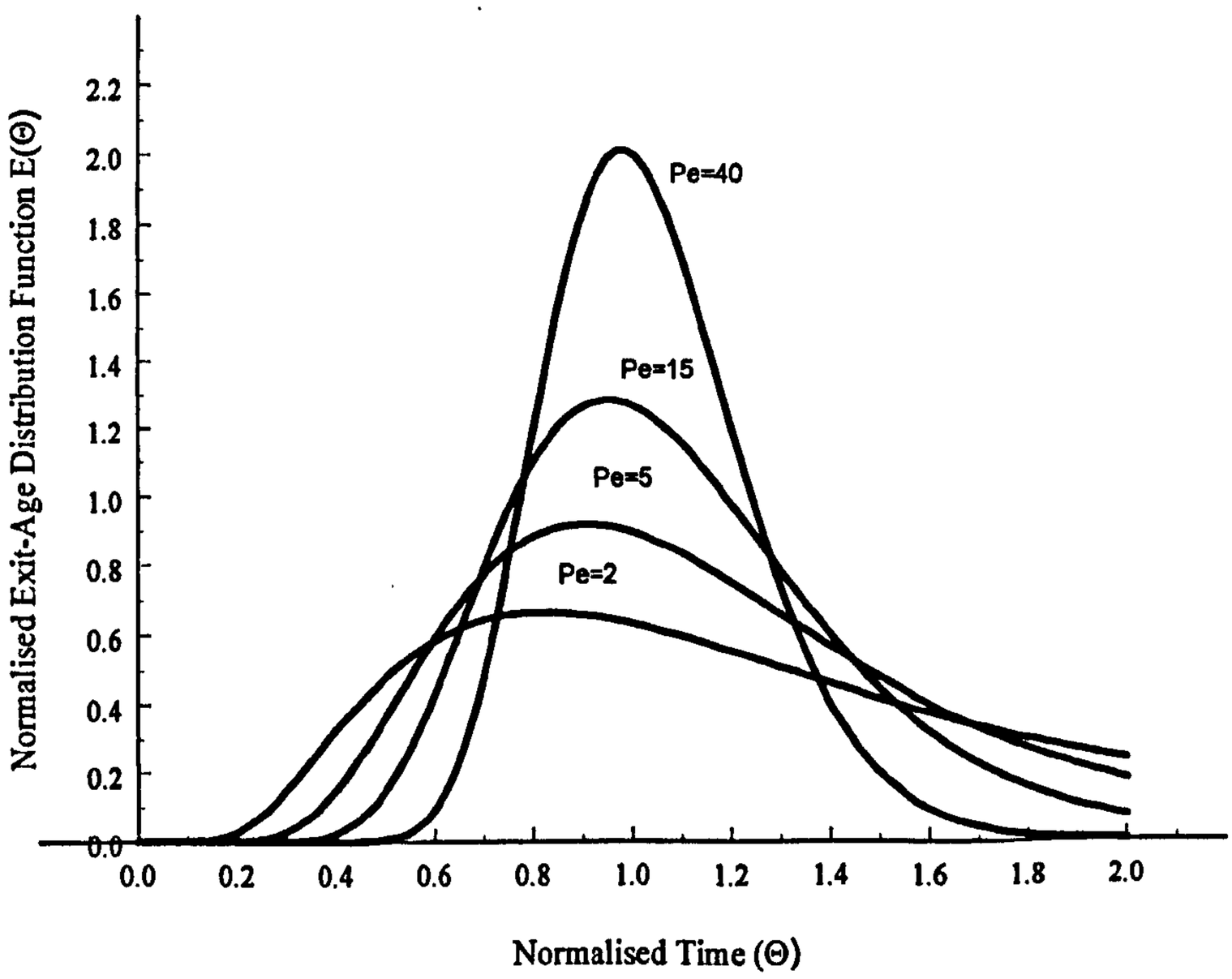

Fig. 4.4 Axial Dispersion Model (ADM) Curves for Selected Model Parameter Values (P_e)

The ADM solution is shown in equation 4.11 and is a convenient approximation of the exact ADM solution, as it directly provides the normalised variance and mean residence time parameters as opposed to only a dispersion number (D). These parameters allow a direct comparison between the indirect method of moments and the direct non-linear regression ADM parameter estimation technique discussed below. This ADM solution has been employed by several other workers conducting RTD investigations (Nauman and Buffham, 1983 and Haas *et al.*, 1995 and 1997). The ADM closed-closed boundary conditions are considered representative of the mixing at the inlet and outlet of a disinfection system (Teefy and Singer, 1990). A closed-closed system is one where no mixing occurs at the inlet or outlet i.e. plug-flow mixing conditions are present (section 4.1). These conditions are also considered representative of the HDVS and this is related to the sample withdrawal technique adopted (section 3.4.1).

$$E(t)=\sqrt{\frac{t_m}{2.\pi.t^3.\sigma_\theta^2}}\exp\left(-\frac{(t-t_m)^2}{2.t_m.t.\sigma_\theta^2}\right) \qquad (4.11)$$

The normalised variance (σ_θ^2) is related to the model parameter P_e by:

$$\sigma_\Theta^2=\frac{2}{P_e}-\frac{2}{P_e^2}(1-e^{-P_e}) \qquad (4.12)$$

The ADM solution used throughout this project (eqn. 4.11) has an error of approximately 5% for a Peclet number (P_e) of 5 compared to the exact solution (Haas *et al.*, 1997). As the normalised variance decreases and the flow approaches the characteristics of a plug-flow system, both the ADM and TISM become indistinguishably close to each other. However, as the mixing regime deviates from

plug-flow, the ADM and TISM curves show different distributions for the same normalised variance. The TISM produces a smaller peak and broader shoulders compared to the ADM for the same first and second moment (n). This can result in significantly different estimated effluent concentrations as the normalised variance increases above a value of 0.2 (Haas *et al.*, 1997) (chapter 7). However, with increased dispersion it becomes increasingly unlikely that the assumptions of the ADM will be satisfied by the real system. Additionally, the RTD curves first and second moments (n) are not effected by the inlet and outlet boundary conditions or the method of tracer injection and sample collection in the TISM parameter calculation (Levenspiel, 1972). The ADM and TISM solution only describe the non-ideal flow behaviour associated with a deviation from the two theoretical mixing regimes of plug-flow and complete mixing respectively (section 4.1). Therefore neither model accounts for dead volumes and subsequently short-circuiting of the flow (Morgan-Sagastume *et al.*, 1999).

In addition to using the method of moments, the ADM and TISM parameters were also calculated using a direct fitting non-linear regression method. This procedure was apparently first suggested by Michelsen, (1972) and has been employed in environmental engineering RTD investigations (Haas *et. al.*, 1997). The ADM non-linear regression analysis provides the normalised variance (σ_θ^2), which was substituted into equation 4.12 to obtain the model parameter (P_e). However, the TISM non-linear regression analysis directly provides the model parameter (N).

Due to these characteristics and limitations of the ADM and TISM, the complete experimental RTD curve and ADM and TISM modelled curves are compared to satisfy their suitability and the goodness of fit is assessed using correlation parameters. This approach is recommended by Levenspiel, (1972). The coefficient of correlation (R^2) and the sum of the errors squared (ESS) correlation parameters were used throughout this project to assess the modelled data goodness-of-fit to the RTD experimental data, for

both the method of moments and non-linear regression techniques. These correlation parameters are commonly used for RTD investigations (Haas *et al.*, 1995). The model yielding the best correlation parameters i.e. the highest coefficient of correlation (R^2) or lowest sum of the errors squared (ESS) is that which provides the best-fit to the experimental data. These correlation parameters were used to compare all other experimental and modelled data throughout this project (chapter 5-7).

The computation of moments and the non-linear regression ADM and TISM parameters from the RTD curve was performed using the EXCEL SOLVER function, MATHCAD 6 PLUS and AXUM 6. The non-linear regression was performed using the SOLVER routine available in the tools toolbox of EXCEL. This allows the correlation parameters ESS and R^2 to be minimised or maximised by setting a target cell to tend towards 0 or 1 respectively. The correlation parameter target cell is a function of the model parameters i.e. ADM or TISM and the experimental data.

The ADM and TISM are only two of a number of available flow models, which describe the RTD. The advection-dispersion equation (ADE) and aggregated dead zone (ADZ) models are also used to describe longitudinal dispersion and have been applied to describe the mixing regime within a high-sided weir CSO structure (Shepherd *et al.*, 2000). These models have two parameters and describe the amount of dispersion by relating the inlet and outlet concentrations of the RTD tracer. In chemical engineering a number of other models have been developed, typically using the RTD combined mathematical model approach, as undertaken in this project for the HDVS (chapter 5) (Wen and Fan, 1975 and Nauman and Buffham, 1983).

4.3.4 Residence Time Distribution (RTD) Indices

In the traditional design of potable water disinfectant tanks, although the principle can equally be applied to wastewater and stormwater treatment processes, it is common to use the concentration–time (CT) product. The concentration component (C) accounts for the reaction kinetics of the disinfection process and the time element (T) for the hydraulic characteristics of the system i.e. the RTD. This method is used extensively by designers in the US following the USEPA SWTR guidelines (American Waterworks Association, 1991) (section 2.2.3).

A number of parameters can be used to describe the RTD curve and therefore the time element (T) of the CT product (Fig. 4.5). These parameters can be combined to provide a series of indices that describe the hydraulic behaviour of a system and are defined below. The main objective for determining the RTD indices is to compare the plug-flow mixing characteristics and the degree of short-circuiting within the HDVS for different operating conditions. Additionally the main parameters used to determine the T element in the CT relationship are also presented. Recent work on the HDVS has also used the CT approach, as mentioned in chapter 2 (section 2.1.5).

In the evaluation of reactors specifically for disinfection, the crucial areas of the RTD curve are the initial portions and their relationship to the theoretical (τ) and experimental (t_m) mean residence time (Stover *et al.*, 1986). The time element (T) parameter is usually obtained from tracer tests and taken as t_{10} i.e. the time for 10% of the tracer to pass through the system (Teefy and Singer, 1990 and Johnson *et al.*, 1998) or alternatively the Morrill Dispersion Index (t_{90}/t_{10}) described below (Stevenson, 1995). The t_{10} parameter results in a conservative design, as 90% of the fluid leaving the system has a greater contact time than the design value.

Despite a shift in the CT design methodology, as discussed in chapter 2 (section 2.2.3), the parameters used to describe the RTD and predict the time component in the CT method are provided for the HDVS. This will aid any future design work using the CT technique and also provide an alternative interpretation of the HDVS's mixing regime, in addition to the conventional RTD data analysis techniques discussed above i.e. RTD normalised curves and the ADM and TISM parameters. Fig. 4.5 illustrates the various parameters used to describe the RTD for the design of disinfection contact tanks using the CT method.

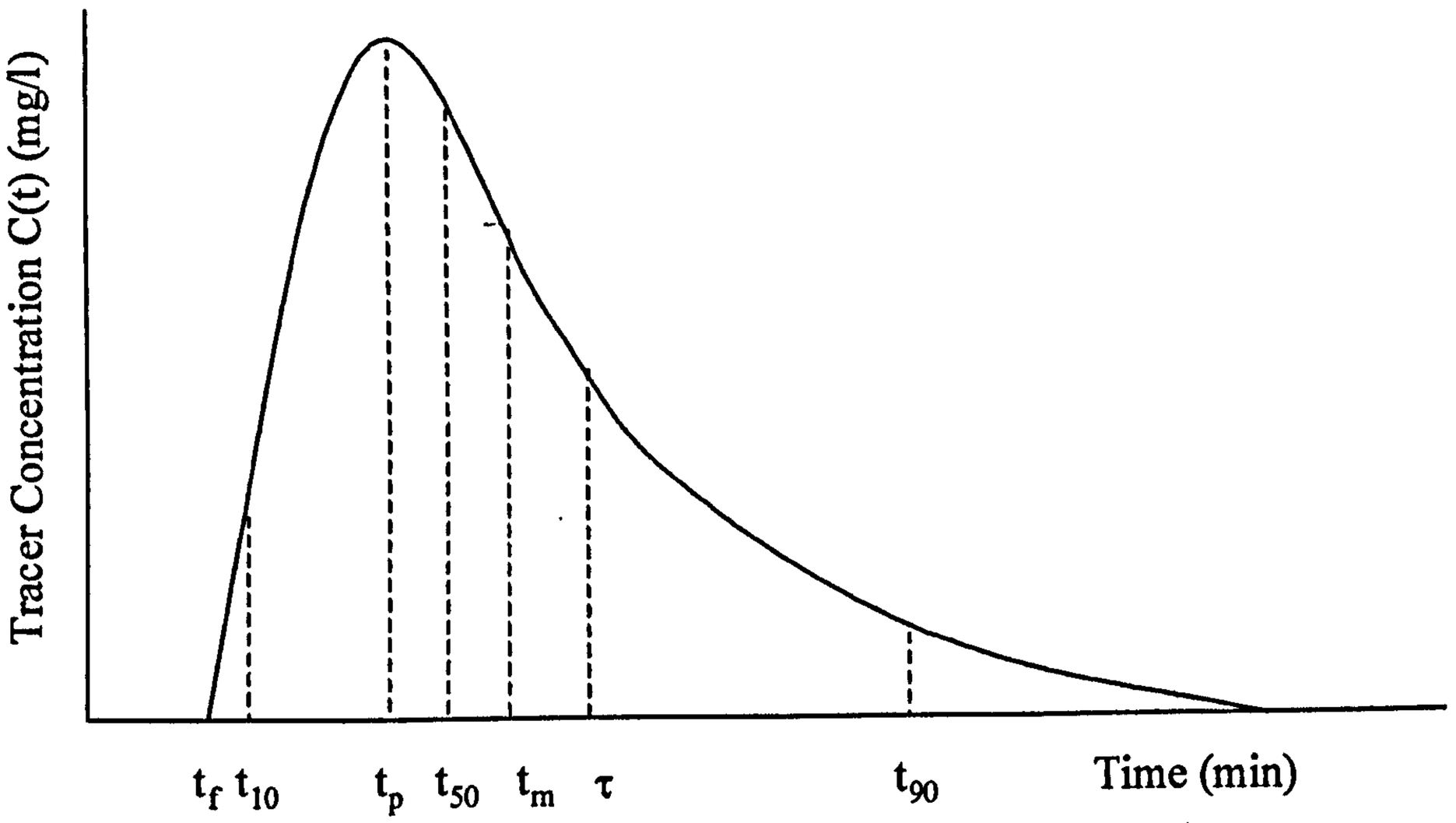

Fig. 4.5 Residence Time Distribution (RTD) Parameters

Where: t_f time at which tracer first appears

t_p time of peak concentration

t_{10} time at which 10% of tracer passed through reactor

t_{50} time at which 50% of tracer passed through reactor

t_{90} time at which 90% of tracer passed through reactor

t_m experimental mean residence time - centroid of curve

τ theoretical mean residence time (eqn. 4.2)

These parameters can be combined into a series of indices to describe the hydraulic behaviour of a system (Stover *et al.*, 1986).

t_f/τ - Measures the most severe short-circuiting. In an ideal plug-flow reactor the ratio is one, and approaches zero with increased mixing.

t_p/τ - Measures the average degree of short-circuiting and will indicate the presence of significant dead space areas. This in turn provides an estimate of the effective volume of the reactor. This ratio will approach one in a plug-flow reactor and zero with increased mixing.

t_{90}/t_{10} - This is the Morrill Dispersion Index and is the ratio of the time for 90% of the tracer to pass through the system to the time for 10% of the tracer to pass. This index provides a measure of the spread of the RTD curve and a value of 1.0 would indicate perfect plug-flow mixing and 21.9 for complete mixing. Reactor designs should allow for this index to be less than 2.0 for an effective design.

t_m/τ - For any reactor this should equal 1.0 and therefore full use is being made of the system volume. When this value is significantly less than 1.0, it indicates that the effective volume is much less than the actual volume.

t_{50}/t_m - In an effective plug-flow reactor, the RTD curve is very similar to a normal or Gaussian distribution. The ratio of the median (t_{50}) to the centroid (t_m) is a measure of the skew of the RTD curve. A skew to the left, in which t_{50}/t_m is less than 1.0, would be detrimental to an effective reactor design.

The two most important parameters are the t_{10} parameter and Morrill Dispersion Index (t_{90}/t_{10}). The t_{10} parameter is generally used in the CT product as the time element and both this parameter and the t_{90}/t_{10} index have been directly related to the ADM and TISM parameters (Stevenson, 1995 and Johnson *et al.*, 1998). This provides a relatively simple conversion from the original CT design method to the use of flow models (section 4.3.3) to design a contact tank for kinetic process applications (chapter 7).

The RTD indices were determined by converting the effluent tracer concentration values C(t) into cumulative concentration values and then displaying as a percentage of the total tracer recovered (mass balance). The corresponding time values for each parameter were obtained and each index calculated. The experimental mean residence time (t_m) was calculated using the method of moments (eqn. 4.4).

4.3.5 The Intensity Function (λ)

The intensity function (λ) is used to verify the existence of dead spaces and bypassing. It was first presented by Naor and Shinnar, (1963) and is described by the following equation:

$$\lambda(t)=\frac{E(t)}{1-F(t)} \qquad (4.13)$$

λ(t) dt is the fraction of the remaining volume leaving between time t and t + dt, i.e. λ(t) is an 'escape probability' of the volume remaining in the system at time t. If the intensity function (λ) curve decreases over some range of t, then this is evidence of non-ideal flow behaviour associated with inactive volumes i.e. stagnant and dead volumes (Himmelblau and Bischoff, 1968). The intensity function (λ) was calculated by

converting the pulse RTD exit-age distribution function E(t) into the cumulative distribution function F(t) using equation 4.7 (section 4.3.2) and then substituting into equation 4.13.

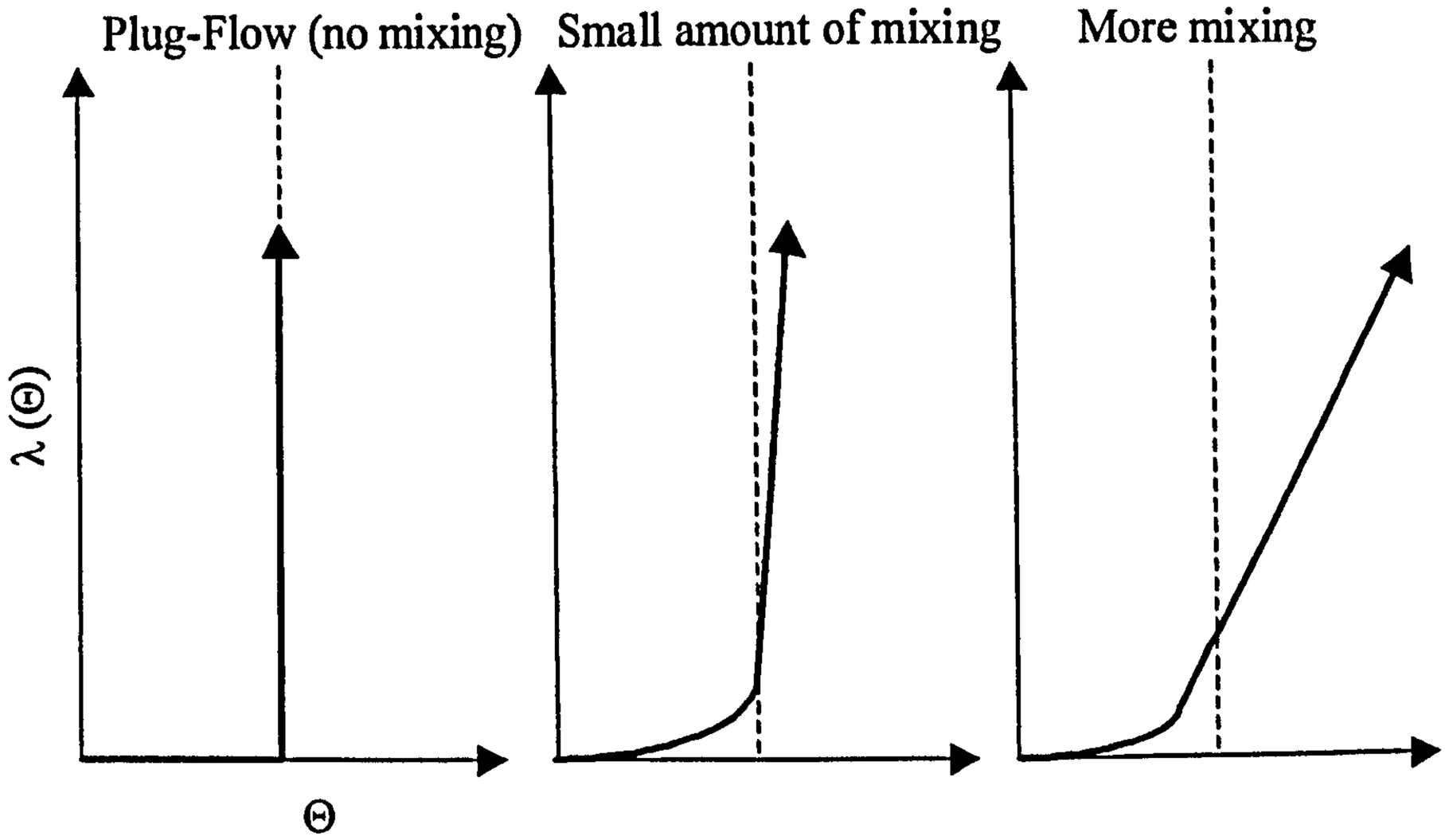

Fig. 4.6 Intensity Function λ(Θ) for a Relatively Small Degree of Mixing

Fig. 4.6 illustrates the intensity function (λ) for varying extents of mixing. As mixing increases the intensity function (λ) approaches a horizontal line and if stagnancy exists it takes on different shapes. Fig. 4.7 illustrates the intensity function (λ) distribution for dead space and bypassing (Himmelblau and Bischoff, 1968).

Dead Space: The main portion of the flow will have an intensity function (λ) curve similar to Fig. 4.7. The stagnant fluid has a low probability of leaving until a time equal to its long residence time is reached. The curve then has a decreasing portion until eventually all the fluid will leave and so the intensity function (λ) will increase again for these very long residence times.

Bypassing: For a short time period the bypassing fluid will have an increasing intensity function (λ). After this fluid leaves, the remaining fluid will have a low probability of leaving until the mean residence time is approached, after which the intensity function (λ) will start to increase again (Fig. 4.7).

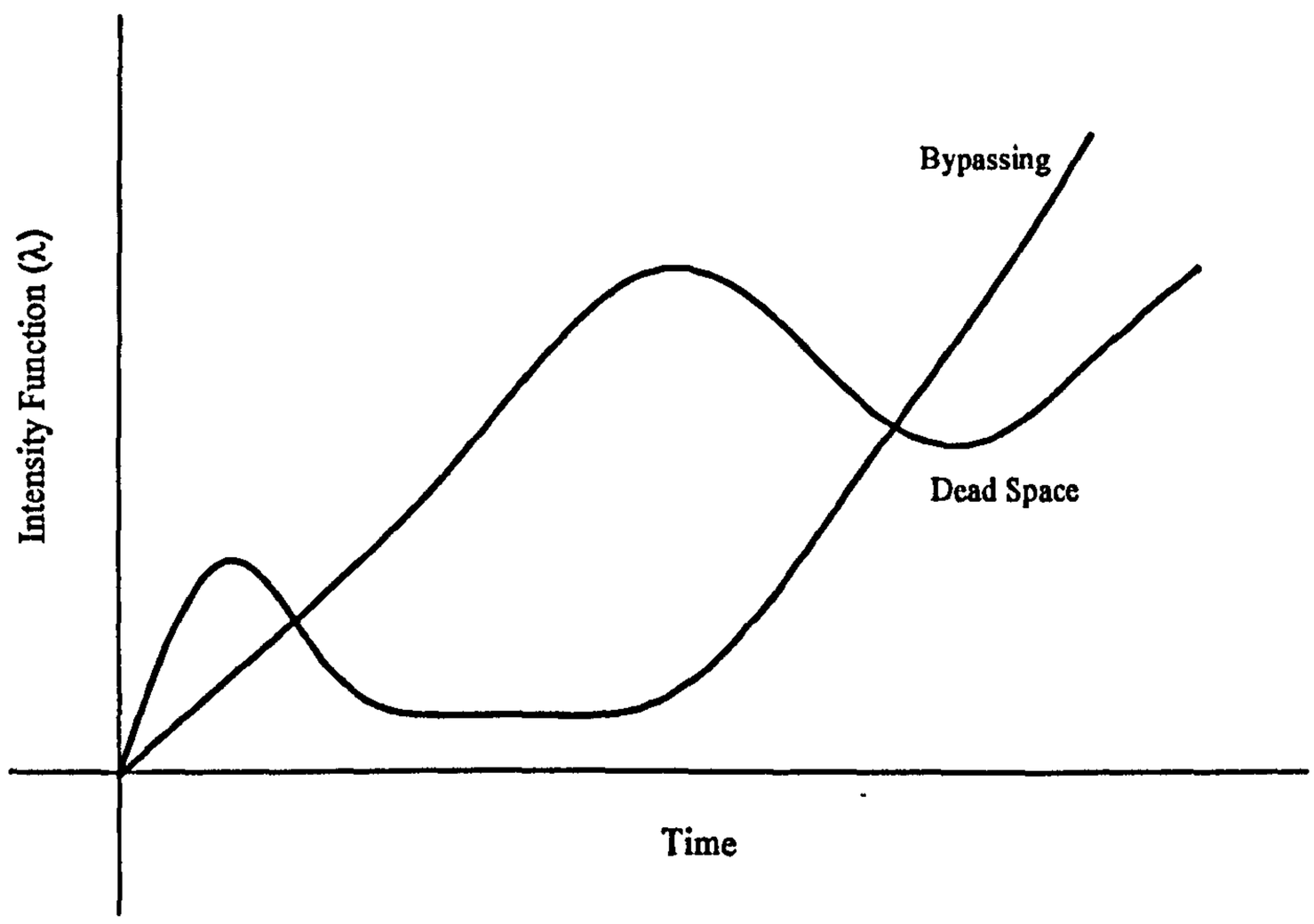

Fig. 4.7 The Effect of Bypassing and Dead Space in the Intensity Function (λ)

The intensity function (λ), unlike the normalised exit-age distribution function E(Θ) (section 4.3.1), maintains the same shape with respect to the maximum values no matter what the time scale. Therefore it enables a better understanding of stagnancy, especially when the true theoretical mean residence time is unknown (section 4.4.1). The intensity function (λ) can also be normalised with respect to the theoretical mean residence time, so enabling a comparison of different flow rates i.e. $\lambda(\Theta)$ (section 4.3.1).

4.4 Results and Discussion

4.4.1 Model Hydrodynamic Vortex Separator (HDVS) No Baseflow - Residence Time Distribution (RTD) Pulse Experiments

4.4.1.1 Method of Moments Data Analysis

Fig. 4.8 compares the model HDVS normalised exit-age distribution function E(Θ) curves, for the range of flow rates investigated (appendix C.1.4). These curves illustrate a plug-flow mixing device with a degree of non-ideal flow behaviour. This is evident, as there is a significant peak on the curve however, some of the tracer leaves the device before the theoretical mean residence time (eqn. 4.2). There is also a substantial tailing effect of the curve, with tracer concentrations still being measured at times of approximately 6 times the theoretical mean residence time. These effects demonstrate that stagnant volumes are present resulting in dead-spaces and short-circuiting within the HDVS (Nauman and Buffham, 1983).

There appears to be two sets of curves with a transition point occurring at approximately 15l/min. The first set of curves 20-90l/min, illustrate a very stable flow regime for the range of flow rates investigated. This has been suggested by other workers investigating the HDVS solids-liquid separation performance (Andoh and Harper, 1994). The second set of curves <15l/min, show that the largest fraction of tracer or similarly the internal volume, tends to leave closer to the theoretical mean residence time i.e. $\Theta = 1$, suggesting that the total volume is active in the mixing process. The second set of curves also show that at low flow rates a greater volume resides in the HDVS for residence times greater than the theoretical mean residence time. For the first set of curves the largest portion of flow leaves the device before the

theoretical mean residence time, due to short-circuiting and dead spaces and therefore may pass through the device with inadequate contact time for the desired process efficiency. Hence, this must be compensated for when determining the contact time for this range of flow rates. The first set of curves also has a well defined peak, which is a characteristic of plug-flow mixing (section 4.2).

Previous RTD investigations on a Grit King™ HDVS (Table 1.1) also suggested the presence of an active zone, subsequently resulting in short-circuiting of the flow and stagnant regions (Tyack and Fenner, 1998b) (section 2.2.2). A fraction of the tracer and therefore flow, was observed to pass into the central cone and grit pot region and combined with the inner zone, contributed to the extended tail on the RTD curves, which is a characteristic of stagnant regions (Fig. 3.1). The active zone was identified between the shear zone and outer wall (section 3.2). The workers proposed that only this active volume should be considered for the design of the Grit King™ HDVS as a chemical reactor i.e. kinetic processes dependent in contact time. However, this approach would underestimate the contact time and therefore reactor performance, as the fluid elements with long residence times i.e. greater than the theoretical mean residence time, which exist in the HDVS, would not be considered. The active volume method would introduce a factor of safety, which is advantageous to any design process, but it is preferable to also know the upper and lower limits of performance to determine the true operating efficiency and costs. CFD investigations undertaken on the range of HDVS's (Table 1.1) have also identified the location of recirculation zones and partially commented on the presence and likely location of stagnant regions within the HDVS (section 2.1.4). Although the relationship with the inlet flow rate was not discussed (Harwood and Saul, 1996b, Tyack and Fenner, 1998a and Faram and Andoh, 2000).

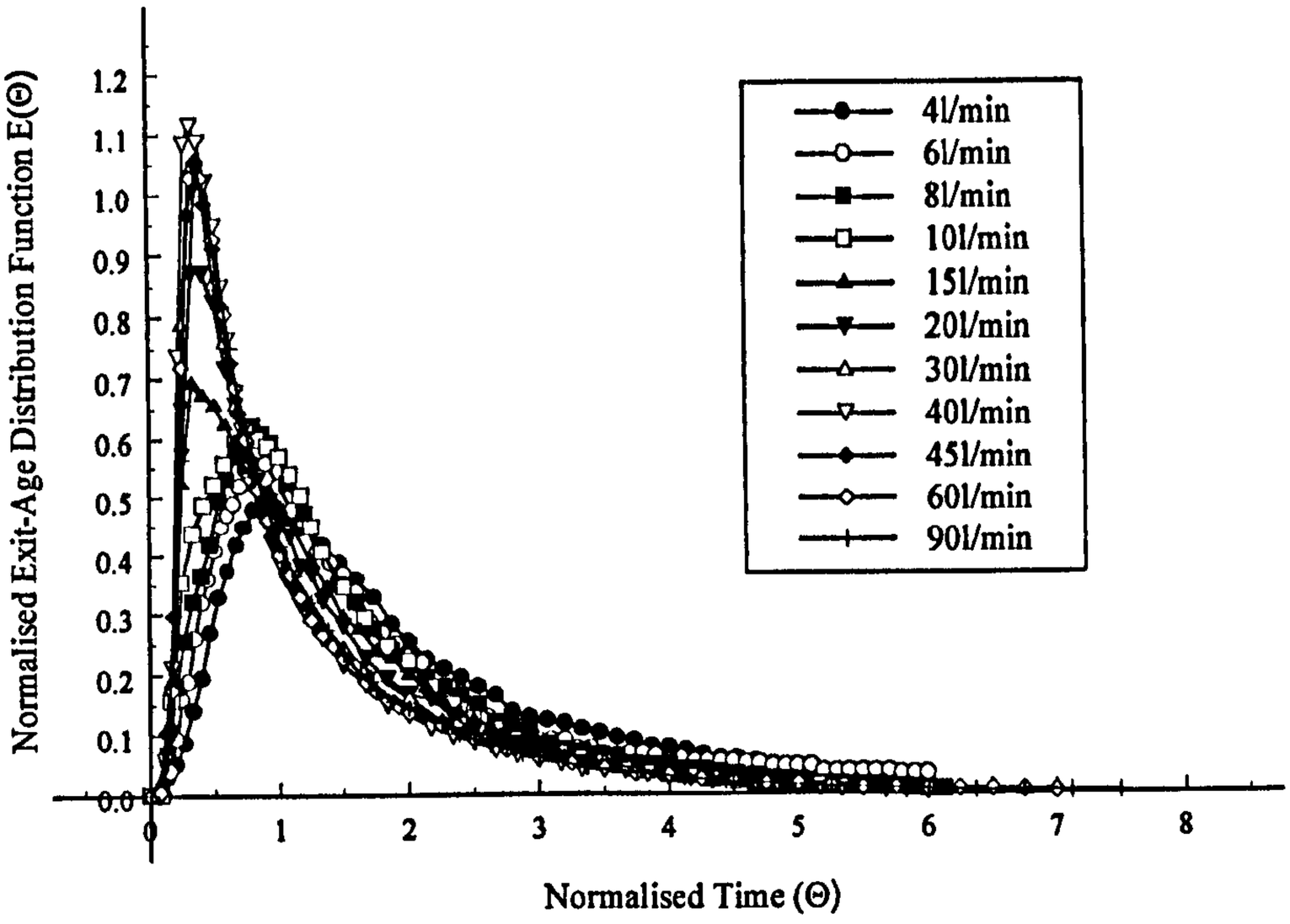

Fig. 4.8 Model HDVS No Baseflow - Comparison of Normalised Exit-Age Distribution Curves E(Θ)

Table 4.1 contains the RTD experimental mean residence time (t_m) and variance (σ^2) calculated using the method of moments, the experimental tracer recovery (mass balance) and their associated errors. The estimated experimental mean residence time is significantly greater than the theoretical mean residence time (eqn. 4.2), with the largest error at low flow rates / longer contact times. Due to the peak of the RTD curves generally occurring before their respective theoretical mean residence time i.e. $\Theta = 1$, it was expected that the experimental mean residence time calculated using the method of moments would be very close or less than the theoretical mean residence time. This is due to the presence of dead spaces, which result in a smaller effective volume and therefore a smaller mean residence time than that calculated from first principles (eqn. 4.2). The theory of the method of moments applied to the continuous flow through a system also shows that the experimental method of moments estimation of the mean residence time cannot be greater than the theoretical mean residence time calculated from first principles (eqn. 4.2) (Fogler, 1992). Subsequently the model and prototype

HDVS normalised exit-age distribution curves E(Θ), for all operating conditions e.g. Fig. 4.8, presented and discussed in this chapter, are calculated using the theoretical mean residence time (eqn. 4.2 and 4.3). The normalised time (Θ) values (eqn. 4.2) and subsequently the scaling of the RTD normalised curves E(Θ), are greatly affected if the experimental mean residence time is used for the normalisation procedure (section 4.3.1).

Table 4.1 Model HDVS No Baseflow - Comparison of First and Second Moments Calculated from RTD Experimental Data

Flow Rate (l/min)	Theoretical Mean Residence Time (min)	Experimental Mean Residence Time (min)	Variance (min^2)	Experimental Mean Residence Time % Error	Tracer Mass Balance (%)
4	15.0	28.835	345.075	+92.23	87.100
6	10.0	18.141	167.529	+81.41	78.000
8	7.50	11.836	69.2760	+57.81	93.650
10	6.00	8.6100	37.6350	+43.50	92.170
15	4.00	5.4020	16.7140	+35.05	109.00
20	3.00	3.8120	9.04100	+27.07	106.50
30	2.00	2.5350	5.00900	+26.75	104.40
40	1.50	1.6750	2.14100	+11.67	106.00
45	1.33	1.6600	2.15100	+24.53	100.50
60	1.00	1.2310	1.26500	+23.10	108.00
90	0.67	0.8180	0.53600	+22.64	110.50

The RTD normalised curves E(Θ) (Fig. 4.8) all exhibit an exponential tail. This is associated with velocity gradients and secondary flow patterns within the HDVS and results in diffusion occurring between slower and faster moving flow elements. The sludge hopper is considered to significantly contribute to this effect by acting as a stagnant volume i.e. slow moving fluid with little or no hydrodynamic velocity due to its isolated position relative to the rest of the system (Fig. 3.1). In the absence of diffusion this volume would not communicate with the rest of the system however, in real systems diffusion is present. This rate of interchange determines the form of the RTD and it is considered to have its greatest effect at low flow rates by increasing the

residence time of the stagnant volume. This is clearly shown in Fig. 4.8, as at flow rates below the transition flow rate, a greater fraction of the total volume has long residence times compared to that at high flow rates. Additionally the mass balance at 6l/min is approximately 78% and the experimental mean residence time is approximately 80% greater than the theoretical mean residence time, compared to 101% and 25% at 45l/min respectively (Table 4.1). The mean residence time error and tracer recovered (mass balance) values presented in Table 4.1 decrease and increase respectively up to the transition flow rate of 15l/min and then remain relatively stable. These observations imply that a significant portion of the tracer is being held within the sludge hopper region for times up to and greater than 6 times the theoretical mean residence time, particularly at low flow rates and is characteristic of stagnant regions.

The method of moments calculates the mean residence time i.e. first moment (n) by using a time weighting factor i.e. E(t)t (eqn. 4.4). Hence this will also have it greatest effect at low flow rates due to the shape of the HDVS RTD curve i.e. greater volumes E(t) at longer residence times (t). Therefore the combined effect of the RTD curves shape and method of moments data analysis technique, results in the error between the theoretical and experimental mean residence time. This is a limitation of the method of moments technique however, Fogler, (1992) illustrated that the method of moments experimental estimation of the mean residence time cannot be greater than the theoretical mean residence time (eqn. 4.2). Subsequently the work presented by Fogler, (1992) maybe applicable to theoretical interpretations of the RTD however, it appears not to apply to all forms of the experimental RTD and particularly if stagnant regions are present. Any limitations in the method of moments data analysis technique are reduced by using the same RTD experimental duration for all flow rates. Additionally an experimental mean residence time greater than the theoretical mean residence time implies there could be accumulation of the flow within the device. This is impractical

and therefore is due to partial accumulation or tracer hold-up i.e. volume elements with long residence times. The tracer recovered (mass balance) would approach 100% for all flow rates if the experimental duration was increased.

At high flow rates an error still exists between the theoretical and calculated experimental mean residence time, although it is smaller compared to that at low flow rates, as discussed above. This occurs, as all RTD data analysis techniques are dependent on the RTD experimental duration. Subsequently the effect of truncating the RTD curves has been investigated to provide an insight into the error between the experimental and theoretical mean residence time and is discussed below. The truncation analysis will also illustrate the sensitivity of the ADM and TISM parameters to the experimental duration. Additionally, RTD experiments were conducted omitting the sludge hopper from the HDVS (Fig 3.1) to aid the above discussion and also investigate its effect on the mixing regime (section 4.4.5).

In the traditional design of kinetic process applications the theoretical mean residence time (eqn. 4.2) is an important parameter and the presence of non-ideal flow behaviour can result in a significantly under or overestimated value. However, obtaining the residence time of individual volumes i.e. RTD, eliminates the need to use either the theoretical or experimental mean residence time, as a kinetic processes efficiency can be determined as a function of each volume and the contact time it provides (section 7.5). Therefore by obtaining the RTD there is also no need to assume an active volume for the design process, as suggested by Tyack and Fenner, (1998b).

Existing Swirl-Flo™ HDVS CFD results also support the RTD observations discussed above, regarding the presence of a stagnant volume i.e. low velocities relative to the remainder of the device, in and around the sludge hopper region (Fig. 3.1), for the HDVS operating with no baseflow (Faram and Andoh, 2000). The authors also indirectly highlight the conflict which arises from adapting a process originally

configured for a particular application, as the sludge hopper region is considered conducive for optimum solids separation and preventing solids resuspension (section 3.2). Whereas for kinetic process applications it is preferable to provide the same mixing regime throughout the device i.e. plug-flow or complete mixing (section 4.1). However, as mentioned above the RTD describes the active volume properties and any deviation from the theoretical mixing regimes (section 4.1) by providing the true residence time of individual volumes within the HDVS.

Two potential physical factors effecting the properties and therefore behaviour of the RTD tracer relative to the liquid phase are absorption and density differences. The former is due to contact surfaces and is dismissed as for the majority of experiments approximately 100% tracer recovery is obtained and low recoveries are considered due to the sludge hopper effect as discussed above. A main feature of the RTD curves is the long tail (Fig. 4.8), which is due to a quiescent zone i.e. sludge hopper (Fig. 3.1). The RTD data analysis techniques used throughout this project (chapter 4-6), do not allow for the possibility that the RTD pulse tracer (LiCl) sinks, because of density differences between the tracer and bulk flow i.e. buoyancy effects, before it is properly dispersed in the inlet zone. However, it maybe possible to estimate these effects by comparing the potential energy per unit volume associated with the initial density differences between the tracer and bulk flow with the local kinetic energy per unit volume associated with the fluid motion in the HDVS (James, 1999). If the latter is very much larger than the former then the tracer and liquid phase mixing will be fairly rapid. Alternatively, if they are very similar then there will definitely be a sinking plume and this would contribute to the poor tracer recoveries (mass balance) and the long tail on the RTD experimental curves (Fig. 4.8).

Table 4.2 Model HDVS No Baseflow - Comparison of ADM and TISM Parameters Calculated from RTD Experimental Data using the Method of Moments

Flow Rate (l/min)	Normalised Variance (σ_θ^2)	Peclet Number (P_e)	N-Tanks
4	0.415	3.48	2.410
6	0.509	2.48	1.965
8	0.495	2.60	2.020
10	0.508	2.48	1.969
15	0.573	1.96	1.745
20	0.622	1.63	1.608
30	0.779	0.80	1.284
40	0.763	0.87	1.311
45	0.781	0.79	1.280
60	0.835	0.57	1.198
90	0.801	0.70	1.248

Table 4.2 details the ADM (P_e) and TISM (N) parameters and the normalised variance (σ_θ^2), calculated using the method of moments (section 4.3.3). The normalised variance provides an indication as to the type of flow regime, relative to the extremes of perfect plug-flow and complete mixing (section 4.1). A value of one corresponds to complete mixing and zero to perfect plug-flow mixing. The ADM and TISM parameters both show a similar decreasing exponential trend as the flow rate is increased (Fig. 4.18). This relative trend in both model parameters is expected as the RTD curve moments (n), represented by the normalised variance, are used to indirectly determine both model parameters (section 4.3.3).

The Peclet number (P_e), which is the inverse of the dispersion number (D), describes a device with a plug-flow mixing regime and high dispersion (P_e<10) (section 4.3.3). The Peclet number (P_e) ranges from less than 1-3.48 depending on the flow rate. At all flow rates greater than 20l/min i.e. above the transition flow rate, the Peclet number (P_e) is less than 1. Referring to the definition of the Peclet number (P_e) in section 4.3.3, this implies that the rate of dispersion is greater than the rate of convection. This arises due to the method of moments Peclet number (P_e) estimation technique, based on equation 4.6, as the variance is high due to a large amount of dispersion and the mean residence time is decreasing as the flow rate increases. This

results in a high normalised variance value and therefore a small Peclet number (P_e). A normalised variance greater than 0.736 results in a Peclet number (P_e) less than 1 (eqn. 4.12). The Peclet numbers (P_e) less than 1 are relatively consistence, particularly for the stable flow regime achieved at high flow rates (Fig. 4.8). The model HDVS is equivalent to approximately 1.198–2.41 tanks-in-series (N) depending on the flow rate. The ADM and TISM parameters decrease as the flow rate increases and therefore the model HDVS has improved plug-flow mixing characteristics at low flow rates and dispersion and mixing effects decrease.

The previous discussion creates two conflicts between observational descriptions of the mixing regime within the HDVS provided by the RTD normalised curves E(Θ) (Fig. 4.8) and the RTD parameters i.e. tracer recovery (mass balance), experimental mean residence time and the ADM and TISM parameters. These conflicts are referred to as conflict (1) and conflict (2) throughout this chapter and following chapters:

1 - At low flow rates poor tracer recovery, a greater fraction of the volume with extended residence times and a substantially large experimental mean residence time calculation, are all attributed to dead volumes within the model HDVS i.e. sludge hopper region (Fig. 3.1). However the RTD normalised curves E(Θ) (Fig. 4.8) suggest that a greater fraction of the total volume of the model HDVS is active at low flow rates. This is due to the peak of the RTD curves occurring in the vicinity of a normalised time (Θ) value of 1 (eqn. 4.2).

2 - At high flow rates there is a more defined peak of the RTD curves, implying that the majority of the flow leaves the HDVS in the vicinity of certain contact time, although before a normalised time (Θ) value of 1 and therefore, short-circuiting and dead spaces are present. The former RTD characteristics, are representative of plug-flow mixing

however, the ADM and TISM parameters do not account for any short-circuiting or stagnant zones (Morgan-Sagastume *et al.*, 1999). Subsequently this could account for the ADM and TISM parameters decreasing as the flow rate is increased and create a possible conflict with visual observations. Hence, it is possible for the HDVS to have a greater element of plug-flow mixing at high flow rates, compared to low flow rates, in a volume smaller than the total volume of the HDVS. This conflict is purely visual and not supported by any other experimental or RTD parameters e.g. RTD indices (section 4.4.4).

It is not possible to further investigate these conflicts (1 and 2) other than by developing a more complex mathematical model, which describes a combination of non-ideal mixing characteristics e.g. dead volumes and dispersion. This has been addressed in this project by developing a RTD combined mathematical model (chapter 5). The combined model describes a mixing regime equal to 3 tanks-in-series (N) (TISM) and models the HDVS's dead volume as a function of an exchange flow rate located between the active and non-active volumes (Fig. 5.1). Therefore the combined model describes the HDVS's mixing regime using a combination of non-ideal flow behaviour i.e. dead volumes and dispersion. The combined model results are presented and discussed in detail in chapter 5.

Fig. 4.9 compares the experimental exit-age distribution function E(t) curve (eqn. 4.1), to the TISM (eqn. 4.9) and ADM (eqn. 4.11) curves, obtained using the method of moments, for selected flow rates. The remaining flow rates and all correlation parameters are presented in appendix C.1.5 and C.1.6. From visual comparison of the curves, the ADM appears to closer approximate the experimental RTD compared to the TISM. This is supported by the coefficient of correlation (R^2) and sum of the errors squared (ESS) correlation parameters, which show that the ADM generally provides the

best-fit to the experimental curve compared to the TISM at the same flow rate. The ADM correlation parameter (R^2) for flow rates below the transition flow rate of 15l/min all remain relatively constant. At the transition flow rate the poorest fit is obtained after which the correlation improves up to its maximum achieved at 90l/min. The TISM parameter N=2 provides the best correlation for all flow rates compared to N=1 and N=3. The TISM correlation parameter (R^2) increases for flow rates up to the transition flow rate, where it reaches a maximum and then reduces for all subsequent flow rates. Hence the TISM correlation parameters (R^2) generally show an opposite trend compared to the ADM correlation parameters. The relationship between the ADM and TISM correlation parameters and the HDVS's non-ideal flow behaviour is discussed in section 4.4.3.

It must be stressed that although the sum of the errors squared (ESS) correlation parameter is presented when comparing all ADM, TISM and RTD experimental curves, it is not generally used in assessing the goodness of fit. This is due to comparing the experimental and model RTD curves using the exit-age distribution function E(t) (section 4.3.1). The exit-age distribution function E(t) is effectively a normalised expression and for a given normalised sample time (Θ) it's value will increase as the flow rate increases due to the shape of the RTD curves (Fig. 4.8). Hence, the sum of the errors squared (ESS) correlation parameter will naturally decrease as the flow rate decreases and therefore not necessarily provide an accurate representation of the goodness of fit. However, the maximum coefficient of correlation (R^2) did generally provide the minimum sum of the errors squared (ESS) and therefore provide confidence in the correlation parameters. Subsequently the best-fit criteria, is based on the coefficient of correlation (R^2) combined with visual inspection. This applies to all RTD correlation parameter investigations using either the method of moments or non-linear regression (section 4.4.1.2) ADM and TISM parameter estimation techniques.

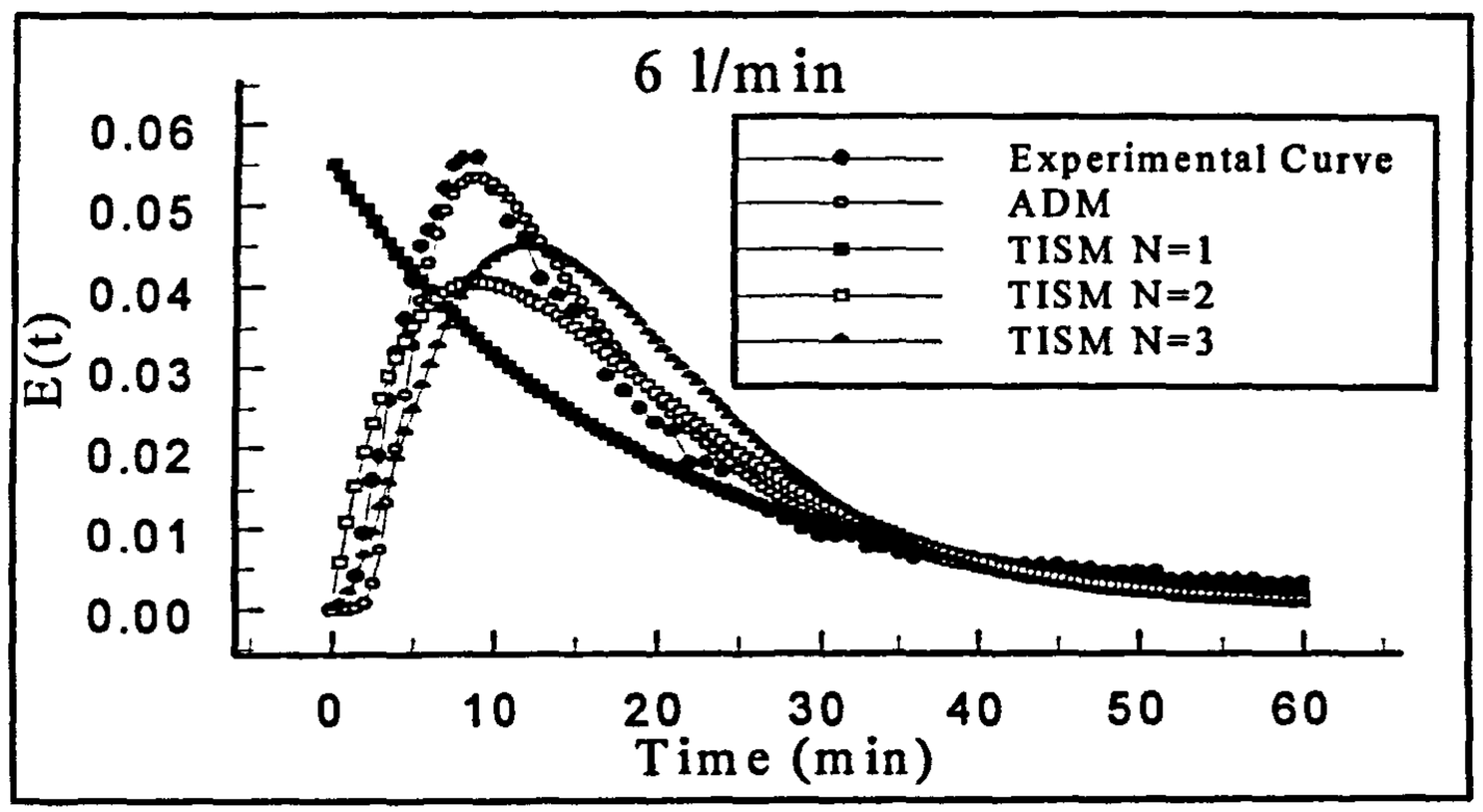

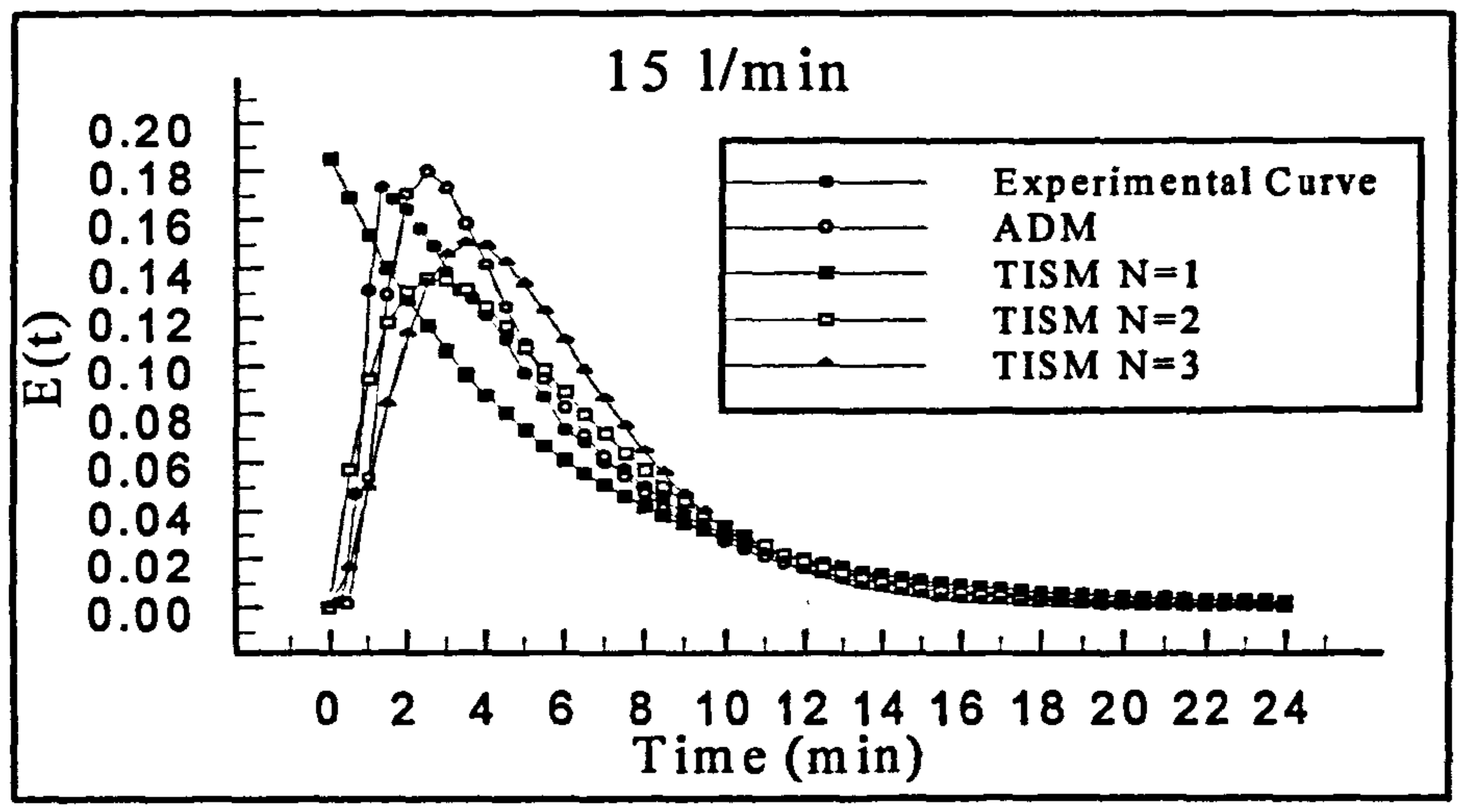

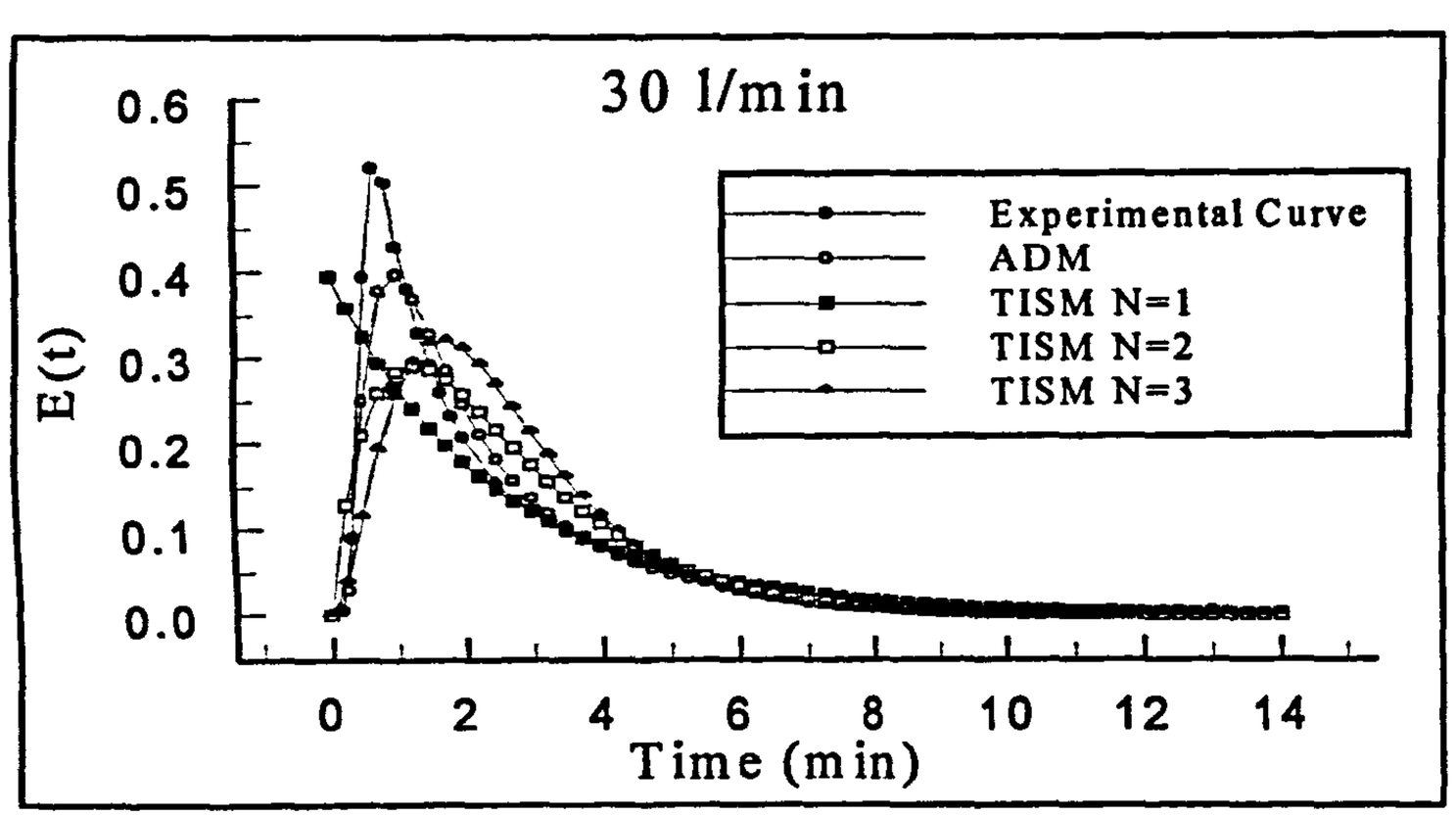

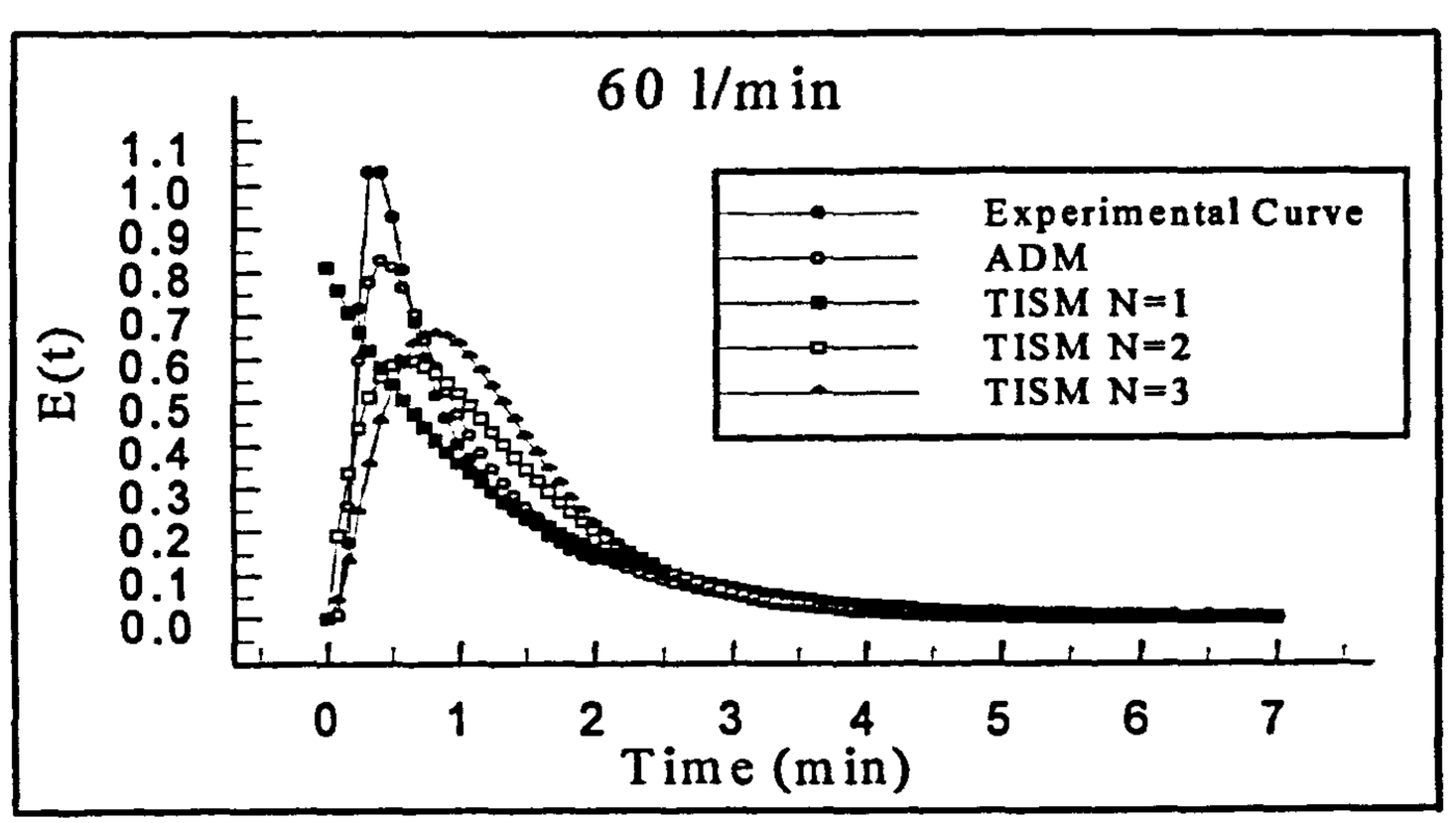

Fig. 4.9 Model HDVS No Baseflow - Comparison of E(t), ADM and TISM Curves Calculated Using the Method of Moments for Selected Flow Rates

Appendix C.1.7 shows the same RTD, ADM and TISM parameters, as presented in Table 4.1 and 4.2, for various RTD curve truncation times. The data analysis procedure adopted for the truncation investigation involves assuming the RTD experiments were terminated at certain times. The RTD data was truncated at 2,3,4 and 5 times the theoretical mean residence time and the same data analysis procedure conducted, as for the full experimental data discussed above. The results for 6 times the theoretical mean residence time (6t) in appendix C.1.7 correspond to the full RTD experimental duration i.e. Table 4.1 and 4.2. The truncation results show that for the lowest flow rates of 4 and 6l/min, the experimental mean residence time at each truncation time is still greater than the theoretical mean residence time. Between 8 and 30l/min the experimental mean residence time approximates the theoretical mean residence time at 2-3 times the theoretical mean residence time. At all flow rates greater than 30l/min the experimental mean residence time approximates the theoretical mean residence time between the truncation times of 3-4 times the theoretical mean residence time. This is the recommended RTD experimental duration when the method of moments is used for the RTD data analysis (Nauman, 1981).

The truncation results suggest that for high flow rates the truncation procedure is acceptable. However, at low flow rates other experimental and data analysis factors are influencing the results. This is illustrated by the experimental mean residence time following an exponential trend, across the range of truncation times, for the same flow rate (Fig. 4.10). The exponential trend arises due to a greater increase in the volume associated with long residence times at smaller truncation times i.e. shorter experiments, compared to that at large truncation times, as it approaches zero. This is due to the weighting created by the term $E(t)t^n$, where n is the first or second moment, in equation 4.4 and 4.5 and is exaggerated at low flow rates due to the greater tailing of the RTD curve. Therefore the trend in the truncated parameters is also a function of the shape of

the HDVS RTD curve and the method of moments calculation technique discussed above. Subsequently there is also a greater difference between the ADM and TISM parameters at 2 and 5 times the theoretical mean residence time at low flow rates compared to high flow rates as discussed below.

At the lowest flow rate of 4l/min the Peclet number (P_e) ranges from 3.48–12.39 and the number of tanks-in series (N) ranges from 2.41–6.72. Therefore the Peclet number (P_e) describes a system with moderate dispersion at 4l/min (section 4.3.3). At the highest flow rate of 90l/min the Peclet number (P_e) ranges from 1–5 and the number of tanks-in series (N) ranges from 1.25–3.12. Fig. 4.10 illustrates the trend in the truncated parameters at a low and high flow rate. The remaining flow rates are shown in appendix C.1.8.

The ADM and TISM parameters all increase as the truncation time is decreased i.e. shorter experiment, as the normalised variance also decreases. This is due to the relationship between the normalised variance and the TISM and ADM parameters in equations 4.10 and 4.12 respectively. The normalised variance (eqn. 4.6) decreases largely due to the variance term having a greater sensitivity to the time element and therefore, the fraction of the total volume residing in the device for long residence times i.e. the time element is raised to the power 2 (eqn. 4.5). Whereas the experimental mean residence time is raised to the power 1 (eqn. 4.4). Subsequently, due to the shape of the RTD curves the ADM and TISM parameter range will be greater at low flow rates across the range of truncation times (Fig. 4.10). The method of moments truncation results highlight the importance of gaining prior knowledge of the RTD experimental duration and data analysis technique before comparing RTD data sets.

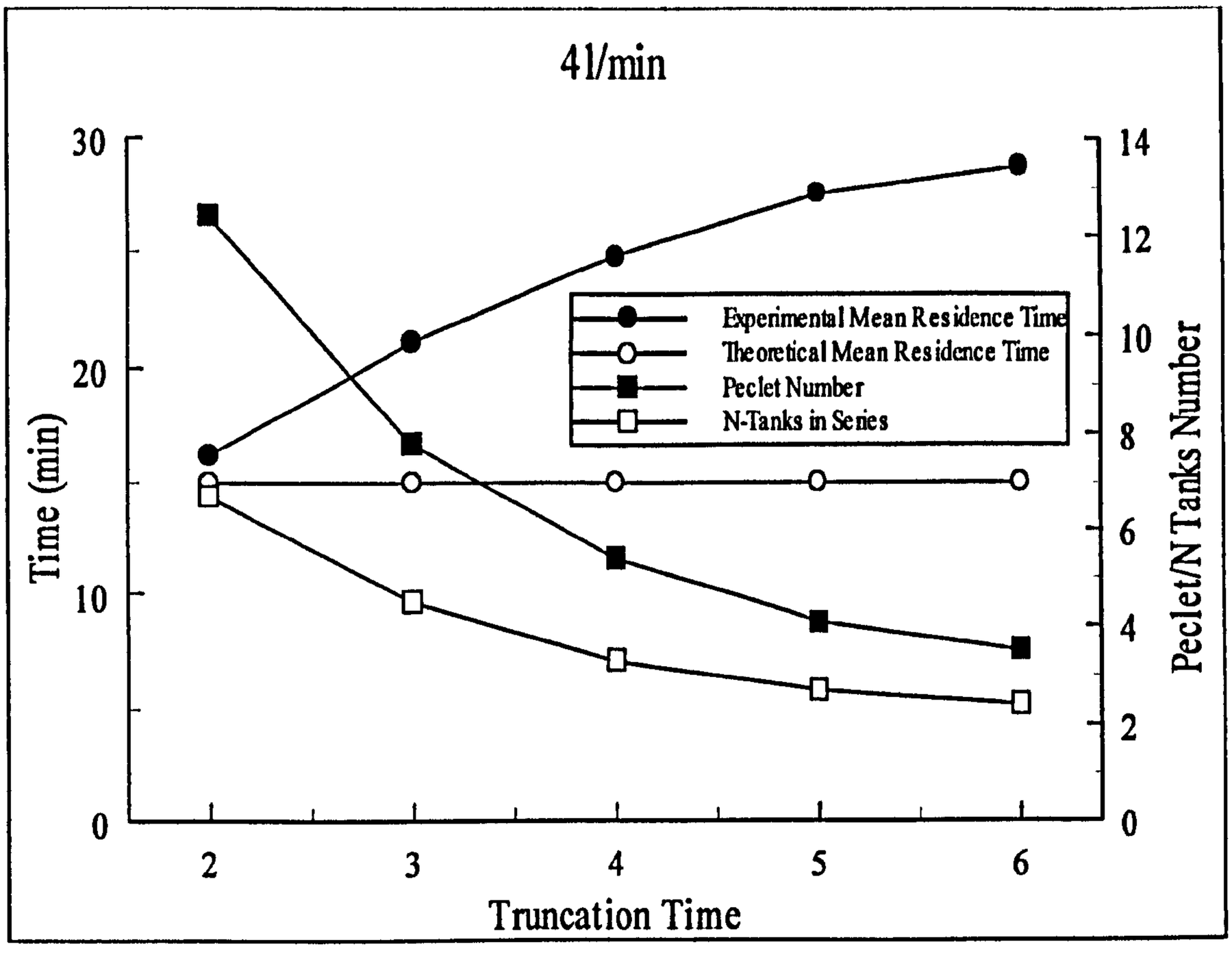

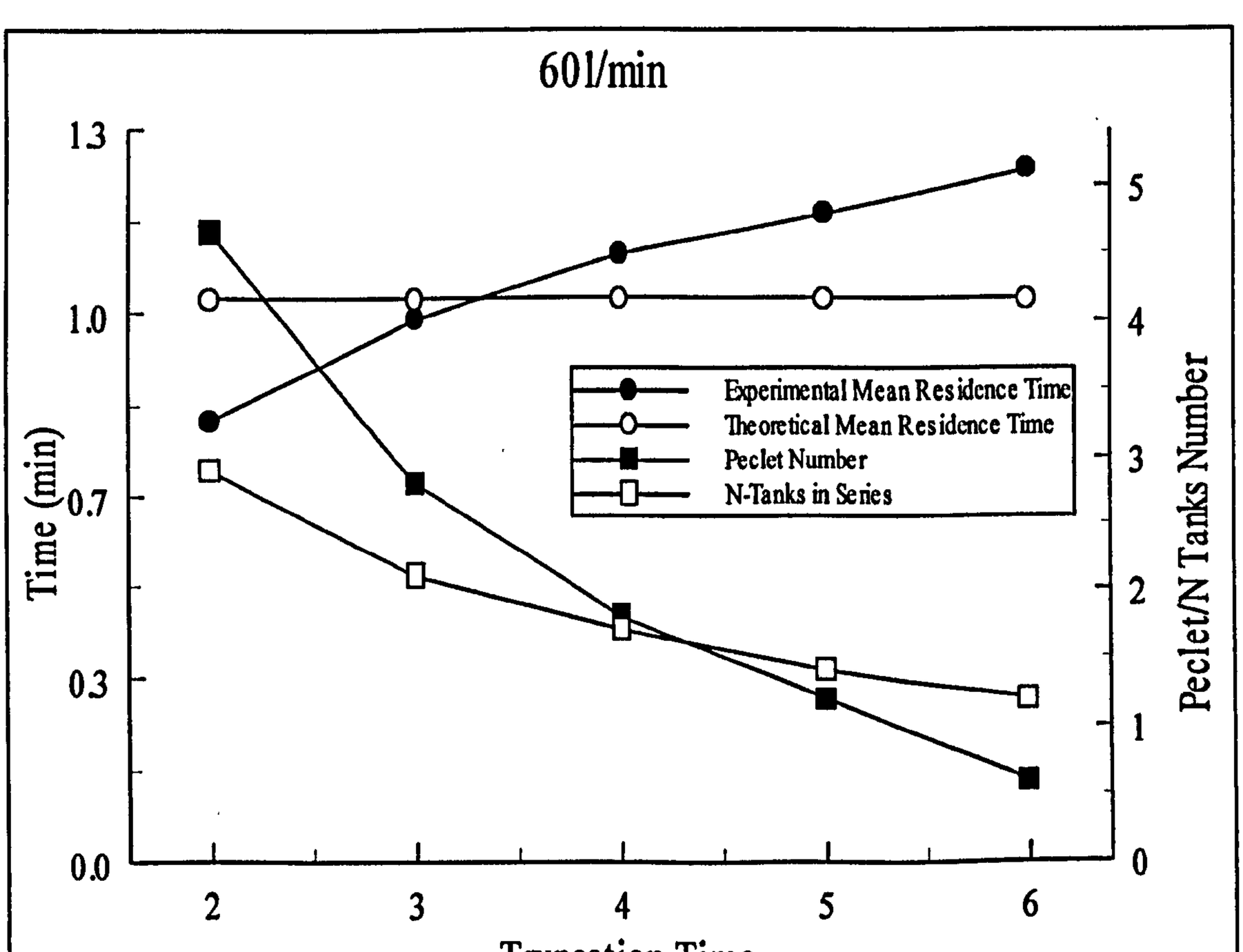

Fig. 4.10 Model HDVS No Baseflow - Effect of RTD Experiment Truncation on Mean Residence Time and ADM and TISM Parameters using the Method of Moments

Fig. 4.11 shows the normalised intensity function $\lambda(\Theta)$ for the model HDVS (appendix C.1.9). Following the discussion in section 4.3.5, the intensity function $\lambda(\Theta)$ describes a device with a large degree of mixing and short-circuiting. This is shown by the increasing probability in the early part of the intensity function $\lambda(\Theta)$ curve, implying that some of the volume leaves before the mean residence time i.e. $\Theta = 1$. This is followed by a horizontal section suggesting that the fluid for this time period has the same probability of leaving the device i.e. complete mixing (section 4.1). Finally after a long residence time, approximately equal to 5 times the theoretical mean residence time for all flow rates, the intensity function $\lambda(\Theta)$ rapidly increases as all the fluid leaves the device and then reduces to zero. Therefore the intensity function $\lambda(\Theta)$ supports the conclusions obtained from the RTD normalised curves $E(\Theta)$ (Fig. 4.8) and the ADM and TISM parameters discussed above. However, the intensity function $\lambda(\Theta)$ does not illustrate the previously identified transition flow rate, above and below which, the RTD normalised curves $E(\Theta)$ have different mixing regime characteristics.

The normalised intensity function $\lambda(\Theta)$ for flow rates of 4 and 6l/min have been omitted as at high normalised time values (Θ) the probability of the fluid leaving is extremely high and significantly effects the scaling for the remaining flow rates. However, their curves exhibit the same trend as achieved for the flow rates illustrated below (Fig. 4.11). The intensity function (λ) is a parameter in the maximum mixedness model and is therefore also presented to enable this model's principles to be used to investigate the performance of the HDVS for kinetic processes. The maximum mixedness model and other kinetic process models, which are combined with the RTD, are discussed in chapter 7 (section 7.5).

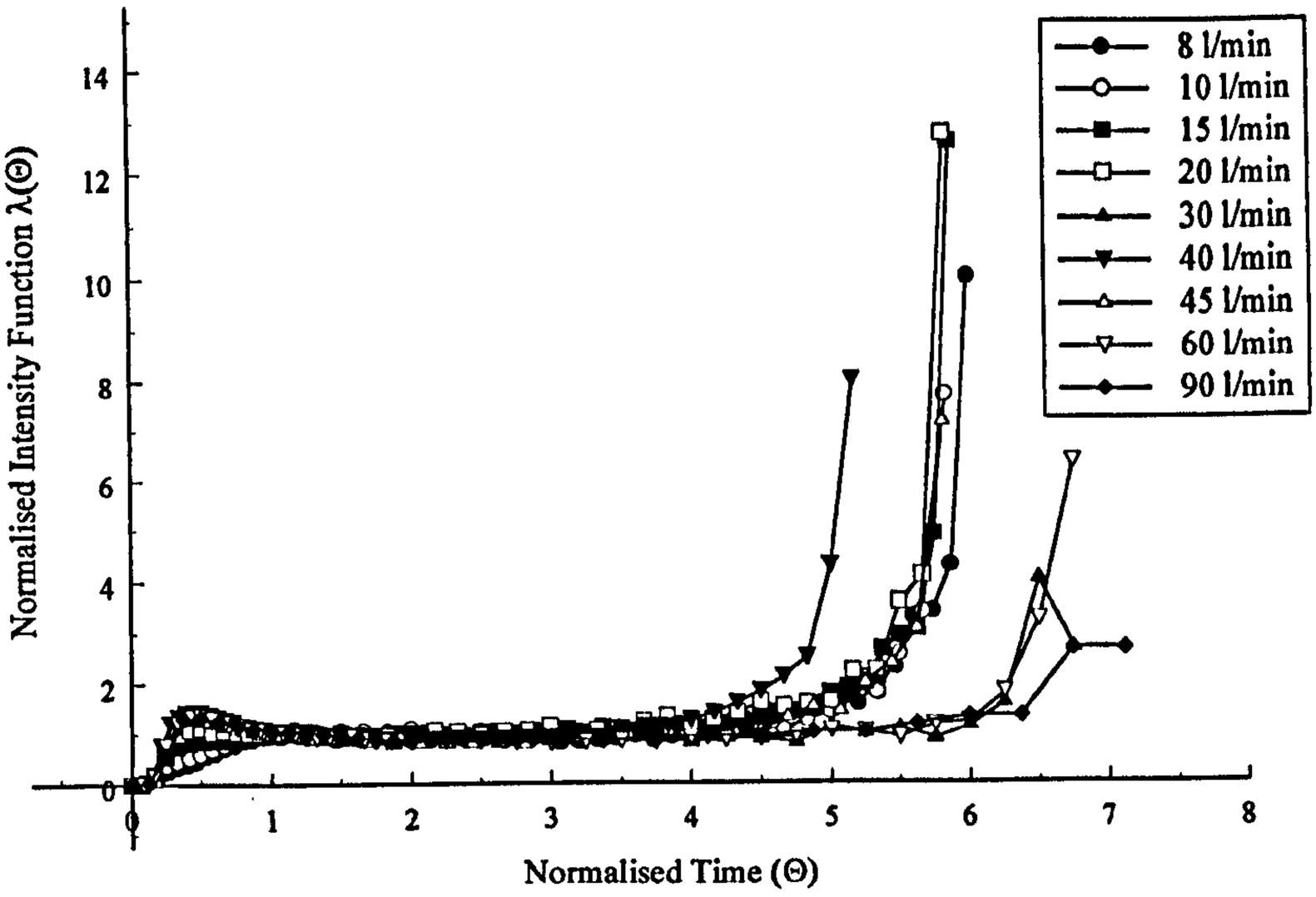

Fig. 4.11 Model HDVS No Baseflow - Normalised Intensity Function λ(Θ)

An associated problem with tracer techniques can arise due to laminar flow and backmixing of the tracer at its injection point (Fogler, 1992). This can result in an extended tracer plug width entering the device and therefore a system response occurring before the input signal is complete, as mentioned in section 4.2. At the lowest model HDVS experimental flow rates of 4 and 6l/min the flow regime in the inlet pipe is neither laminar or turbulent and is therefore transitional, as it has a Reynolds number (Re) of approximately 2000. The injected pulse has a maximum transit time and therefore width of approximately 20 seconds from the injection point to the entrance of the HDVS. Comparing this to the theoretical mean residence time of 15 and 10 minutes provided by the above flow rates respectively, if the flow regime in the inlet pipe approximates perfect plug-flow, the error associated with producing an instantaneous pulse of negligible width would be approximately 2.5%. At the highest flow rate of 90l/min the transit time of the tracer pulse from the injection point to the HDVS entrance is less than 1 second compared to a theoretical mean residence time of 40

seconds and similarly the associated error is approximately 2.5%. Additionally the time at which the tracer first appears (t_f) for each flow rate, is after the maximum theoretical time required for the pulse to travel from the injection point to the entrance of the HDVS i.e. the input signal is complete before any system response. Therefore the effects of any laminar flow conditions or backmixing at the tracer injection point are deemed not to significantly effect the RTD results. This is also supported by visual observations of the tracer behaviour within the transparent model HDVS inlet pipe. Section 8.6 mentions an existing RTD experimental technique, which accounts for non-ideal flow behaviour of the pulse tracer between the injection point and the entrance to a system.

4.4.1.2 Non-Linear Regression Data Analysis

Tables 4.3 and 4.4 show the ADM and TISM non-linear regression parameter estimation technique results. The experimental mean residence time values calculated using non-linear regression are of a similar order of magnitude as calculated using the method of moments (section 4.4.1.1), regardless of the flow model used for the non-linear regression iteration i.e. TISM (eqn. 4.9) or ADM (eqn. 4.11). However the error between the theoretical and experimental mean residence time at high flow rates, greater than the transitional flow rate of 15l/min, is less compared to the method of moments technique. This error for certain flow rates also changes from a positive to a negative error and therefore, the experimental mean residence time is less than the theoretical mean residence time, even for an experimental duration of 6 times the theoretical mean residence time. This is the expected relationship as discussed above (section 4.4.1.1) and implies that the non-linear regression technique, particularly when combined with the TISM, is less sensitive to the tailing section of the RTD curves (Fig. 4.8). However

at flow rates less than the transition flow rate, a positive error is always obtained and therefore the shape of the RTD curve still effects the non-linear regression results. The non-linear regression analysis technique was also used to investigate the truncated RTD curves as discussed below. This will provide information regarding the sensitivity of the non-linear regression parameter estimation technique to the experimental duration and therefore the RTD curve tailing section, compared to the method of moments technique (section 4.4.1.1).

The ADM Peclet number (P_e) ranges from less than 1–1.74 with the highest value occurring at the lowest flow rate and generally decreasing as the flow rate increases. The TISM parameter (N) remains relatively stable for all flow rates ranging from 1.952–2.195, with the highest value also occurring at the lowest flow rate. Therefore the ADM and TISM parameters calculated using non-linear regression describe a system with increased plug-flow mixing characteristics as the flow rate is decreased and is the same relationship as obtained using the method of moments to calculate the ADM and TISM parameters (section 4.4.1.1). The ADM Peclet numbers (P_e) were calculated from the normalised variance, obtained directly from the non-linear curve fitting technique and equation 4.12 and the TISM number of tanks (N) obtained directly from the non-linear curve fitting technique (eqn. 4.9).

Table 4.3 Model HDVS No Baseflow - Comparison of ADM Parameters using Non-Linear Regression

Flow Rate (l/min)	Experimental Mean Residence Time (min)	Normalised Variance (σ_θ^2)	Peclet Number (P_e)	Coefficient of Correlation (R^2)	Sum of the Errors Squared (ESS)	Experimental Mean Residence Time % Error
4	30.504	0.604	1.74	0.998	0.000036	+103.36
6	18.221	0.658	1.41	0.994	0.000218	+82.210
8	12.344	0.633	1.56	0.990	0.000847	+64.587
10	9.3720	0.694	1.21	0.988	0.001525	+56.200
15	6.0930	1.000	0.01	0.994	0.001902	+52.325
20	3.7920	0.913	0.28	0.996	0.002745	+26.400
30	2.2020	0.826	0.60	0.988	0.022650	+10.100
40	1.4670	0.762	0.88	0.986	0.072300	-2.2000
45	1.4760	0.817	0.64	0.987	0.066590	+10.977
60	1.0600	0.762	0.88	0.989	0.088400	+6.0000
90	0.7360	0.755	0.91	0.989	0.127000	+9.8510

Table 4.4 Model HDVS No Baseflow - Comparison of TISM Parameters using Non-Linear Regression

Flow Rate (l/min)	Experimental Mean Residence Time (min)	N-Tanks	Coefficient of Correlation (R^2)	Sum of the Errors Squared (ESS)	Experimental Mean Residence Time % Error
4	28.514	2.195	0.980	0.0004352	+90.093
6	12.741	2.134	0.980	0.0014130	+27.410
8	9.3420	2.165	0.983	0.0014160	+24.560
10	7.3200	2.126	0.982	0.0009878	+22.000
15	4.3290	1.952	0.982	0.0059470	+8.2250
20	2.4660	1.959	0.967	0.0233000	-17.800
30	1.8490	2.014	0.936	0.1152000	-7.5500
40	1.2460	1.996	0.924	0.3782000	-16.933
45	1.2100	1.964	0.930	0.3515000	-9.0230
60	0.8970	1.991	0.934	0.5070000	-10.300
90	0.6290	2.005	0.938	0.7242000	-6.1190

Fig. 4.12 compares the experimental exit-age distribution E(t) curve, to the TISM (eqn. 4.9) and ADM (eqn. 4.11) curves obtained using the non-linear regression analysis technique for selected flow rates. The remaining flow rates and also the correlation parameters (R^2 and ESS) are presented in appendix C.1.10 and C.1.11. The ADM provides a better fit to the experimental data compared to the TISM. This is shown by

the coefficient of correlation (R^2) and the sum of the errors squared (ESS) values in Table 4.3 and 4.4. The coefficient of correlation (R^2) values for the ADM are greater than the TISM for the same flow rate. The better fit generally occurs as the HDVS flow rate decreases for both models and therefore as the device's mixing regime tends towards plug-flow mixing. This trend in the correlation parameters is a function of the ADM and TISM as they assume that the total system is active in the mixing process and therefore no dead volumes are present (section 4.3.3). The RTD normalised curves E(Θ) at low flow rates suggest that a larger volume of the HDVS is active, as the curves peak at approximately the theoretical mean residence time i.e. normalised time (Θ) = 1 (Fig. 4.8). Whereas at high flow rates the peak of the RTD curve shifts towards the origin suggesting the presence of dead volumes. Hence this trend in the correlation parameters is expected, due to the HDVS's RTD curves characteristics and the limitations of the ADM and TISM with respect to the flow rate.

Due to the large number of data sets generated by the RTD experimental truncation data analysis investigation presented and discussed for all flow rates using the method of moments (section 4.4.1.1), only three flow rates covering the range of flow rates for the model HDVS operating without a baseflow component are investigated and presented using the non-linear regression technique. This was undertaken to investigate the tail portion of the RTD curve and if it significantly effects the non-linear regression analysis technique for estimating the RTD parameters i.e. experimental mean residence time, ADM and TISM parameters. The non-linear regression technique is considered less sensitive to the RTD experimental truncation time compared to the method of moments (Haas *et al.*, 1997).

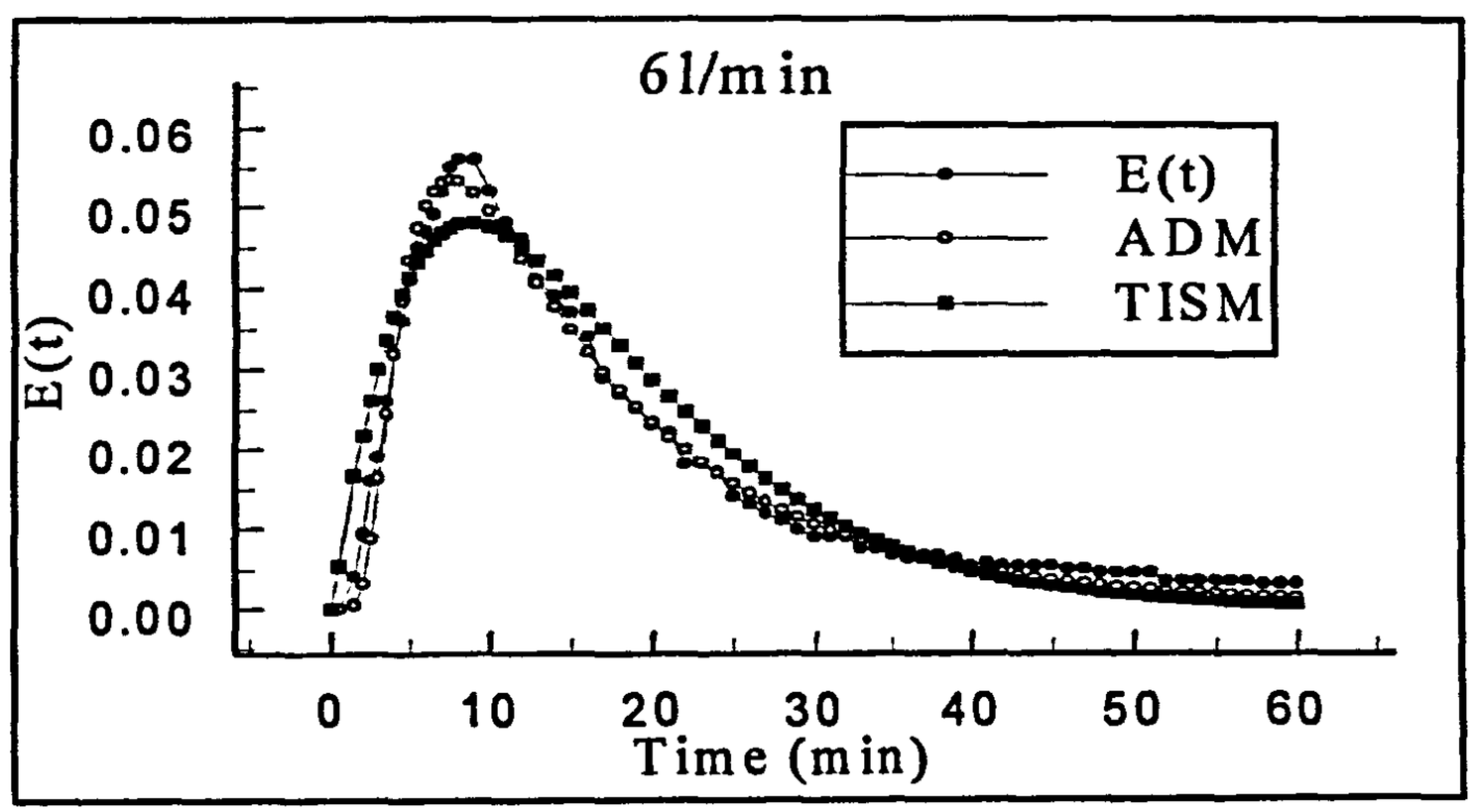

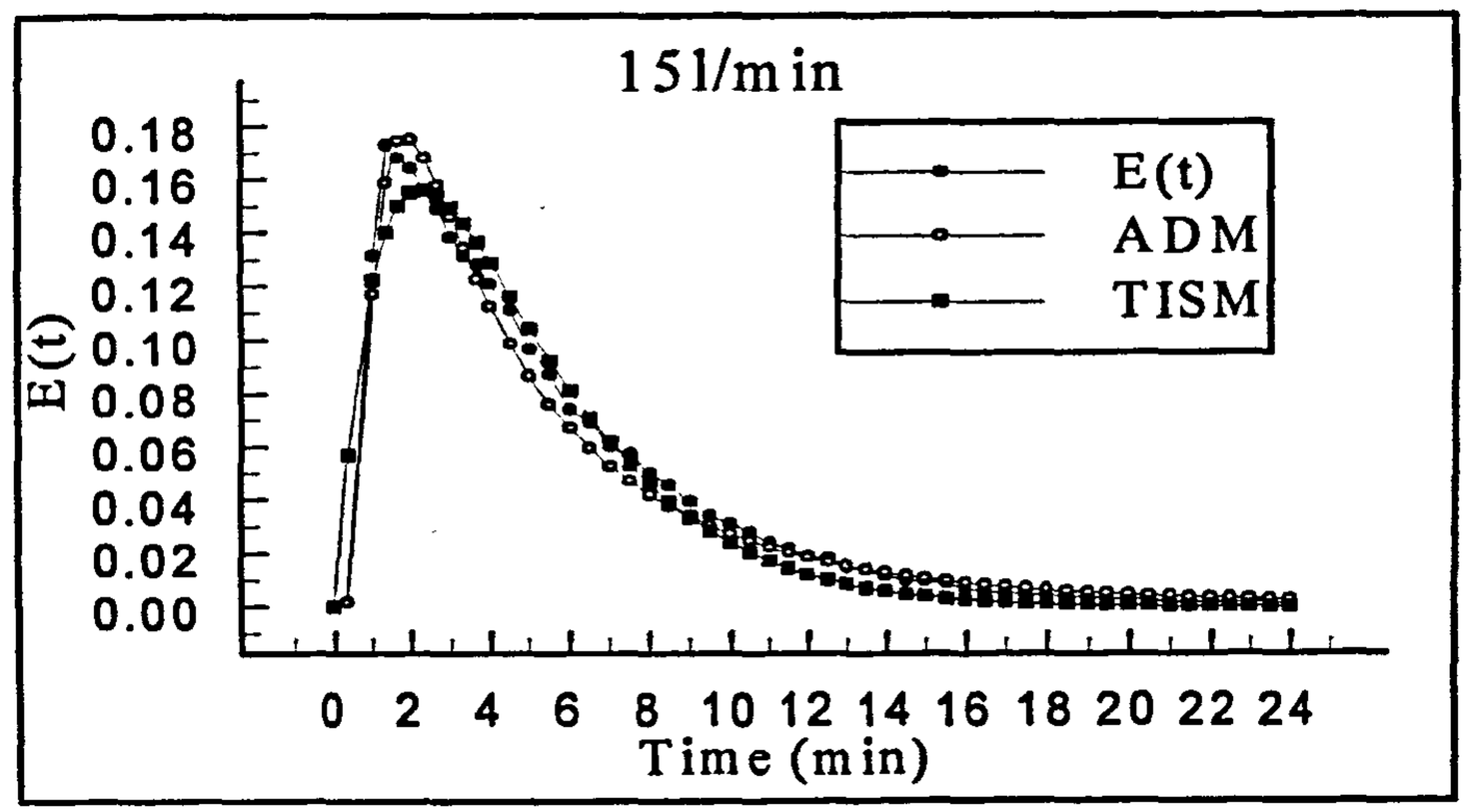

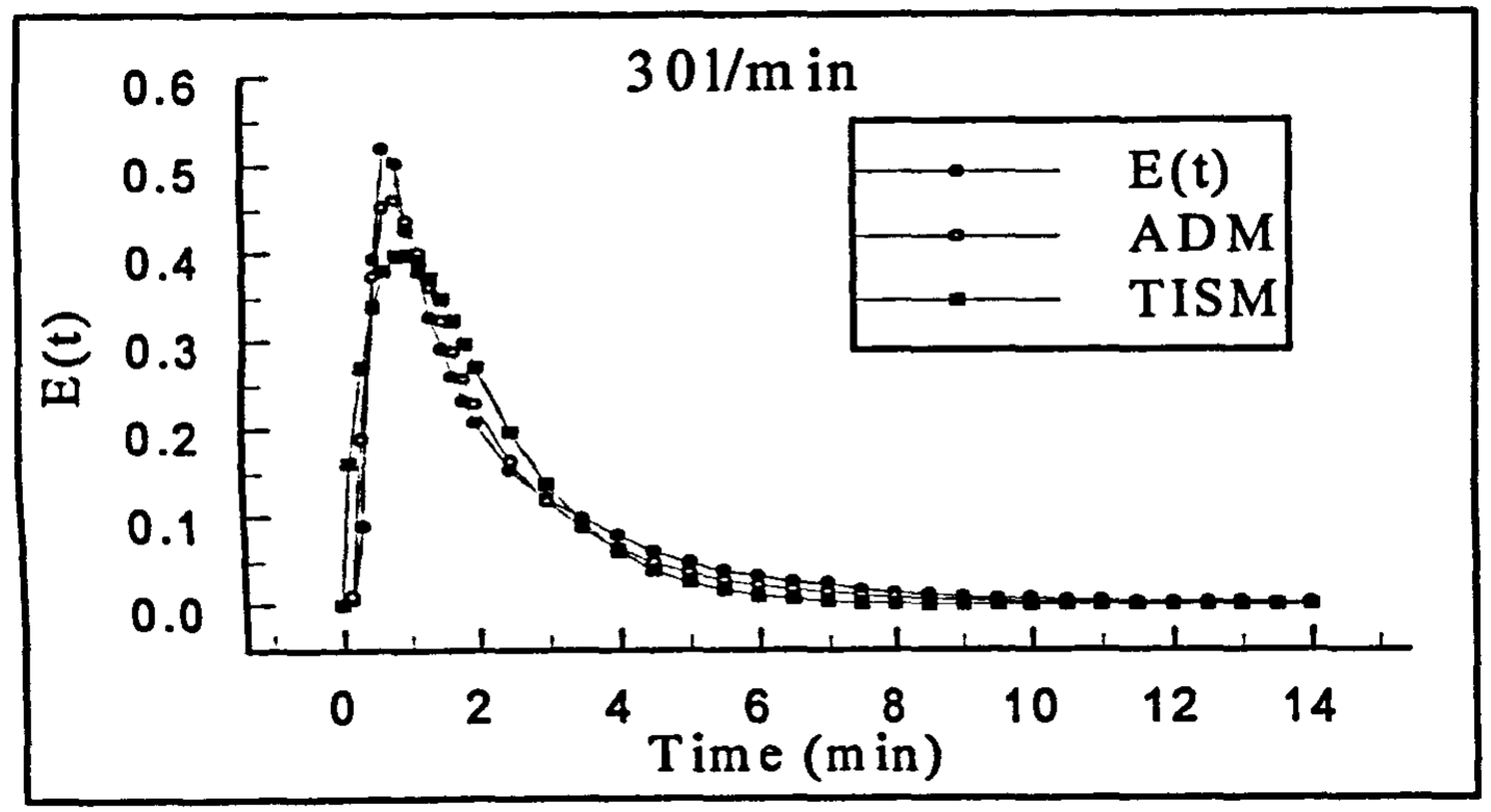

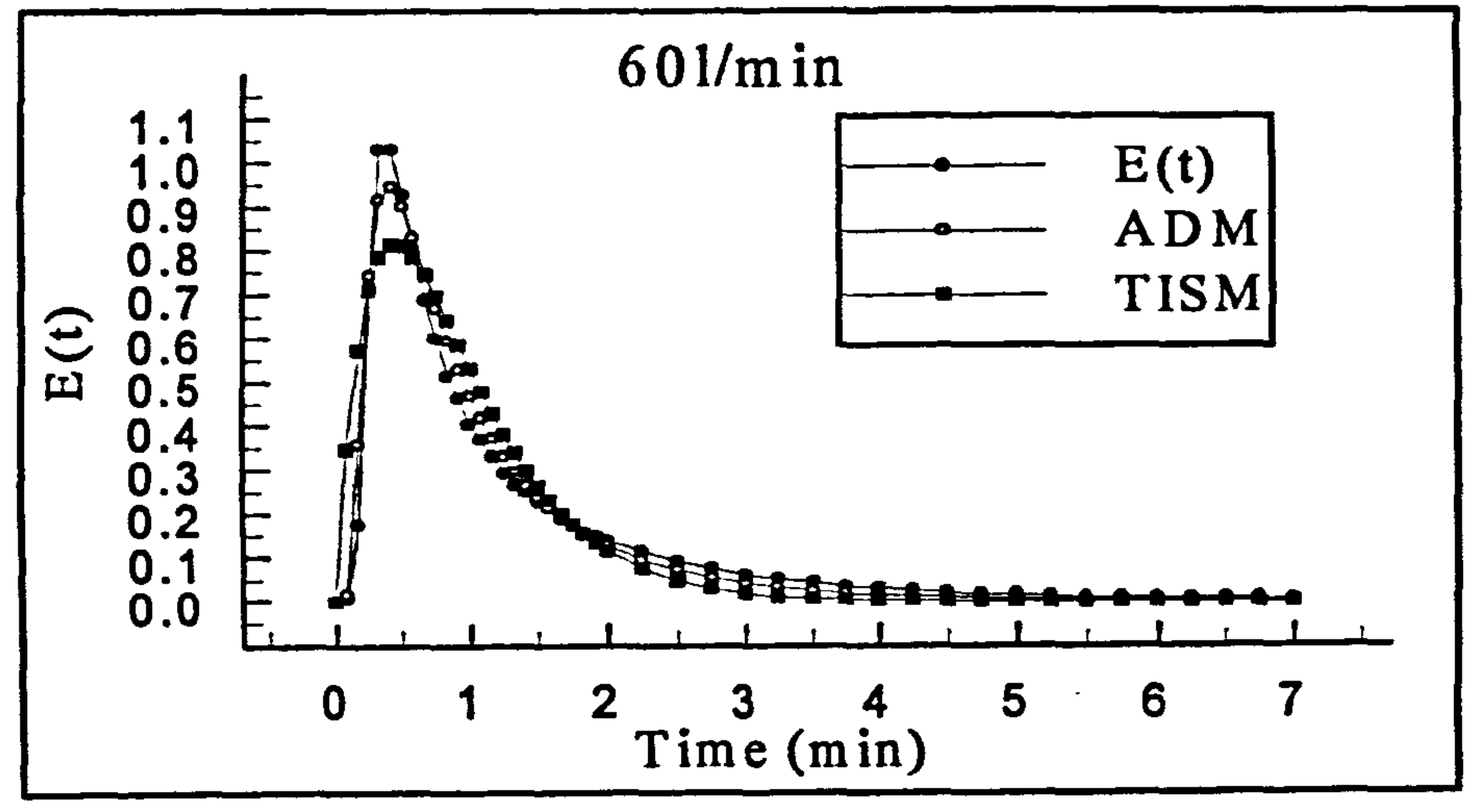

Fig. 4.12 Model HDVS No Baseflow - Comparison of E(t), ADM and TISM Curves Calculated Using Non-Linear Regression for Selected Flow Rates

The three flow rates investigated were 4, 30 and 90l/min and the results are presented in appendix C.1.7. The results clearly show that the ADM parameters are effected by the truncation time whereas the TISM parameter remains very stable for all truncation times and the mean residence time is also less effected compared to the ADM. At the lowest flow rate of 4l/min the ADM parameter increases by 276% from the minimum to the maximum truncation time and similarly for 30l/min, 341% and 90l/min, 253%. This compares to 356%, 578% and 714% using the method of moments respectively (appendix C.1.7). Additionally for flow rates of 30 and 90l/min, an experimental mean residence time value in the vicinity of the theoretical mean residence time is obtained for all truncation times, particularly when using the TISM. Whereas using the method of moments a greater truncation time i.e. shorter experiment is required to obtain an experimental mean residence time in the vicinity of the theoretical mean residence time for these flow rates (section 4.4.1.1). Therefore the non-linear regression technique is also effected by the RTD experimental truncation time i.e. the fraction of the total volume with residence times greater than the theoretical mean residence time, although to a lesser extent compared to the method of moments. This is in agreement with previous conclusions presented by Haas *et al.*, (1997).

The goodness of fit represented by the coefficient of correlation (R^2) and the sum of the errors squared (ESS) generally improves as the truncation time is increased i.e. as the data approaches the full experimental data (6t). The TISM goodness of fit to the experimental curve is inferior to that achieved for the ADM. It should be noted that the effect of truncating the RTD curve is a function of both the mathematical data analysis technique and the shape of the RTD and therefore, the conclusions observed in this project are not universal for all RTD curves. Additionally it is preferable to conduct the RTD experiment for a significant duration to achieve a comprehensive description of the mixing regime for the range of flow rates investigated. This will also provide an

ADM and TISM curve, which has an improved correlation with the experimental RTD curve.

Alternative RTD data analysis techniques include Laplace and Fourier transforms. These techniques reduce the time weighting factors that are applied in the method of moments analysis however, existing literature suggests that these techniques will not greatly affect the first and second moment (n) RTD calculations (Westerterp *et al.*, 1984). These techniques were not investigated due to the number of RTD experiments conducted during this project, generated by the range of HDVS operating conditions investigated.

4.4.2 Prototype Hydrodynamic Vortex Separator (HDVS) No Baseflow - Residence Time Distribution (RTD) Pulse Experiments

4.4.2.1 Method of Moments Data Analysis

The same conclusions observed for the model HDVS RTD normalised curves E(Θ) (Fig. 4.8) can be applied to the prototype HDVS (Fig. 4.13) (appendix C.2.3). Hence, the prototype HDVS RTD curves illustrate a plug-flow mixing device with a degree of non-ideal flow behaviour for the reasons discussed in section 4.4.1.1. The prototype HDVS RTD curves also support the model HDVS observations that there appears to be a transition flow rate above and below which, the HDVS has a different RTD and therefore mixing characteristics. The transition flow rate for the prototype HDVS occurs at approximately 90l/min. The mixing characteristics of the prototype HDVS RTD curves, for flow rates above and below the transition flow rate, are the same as the model HDVS (section 4.4.1.1).

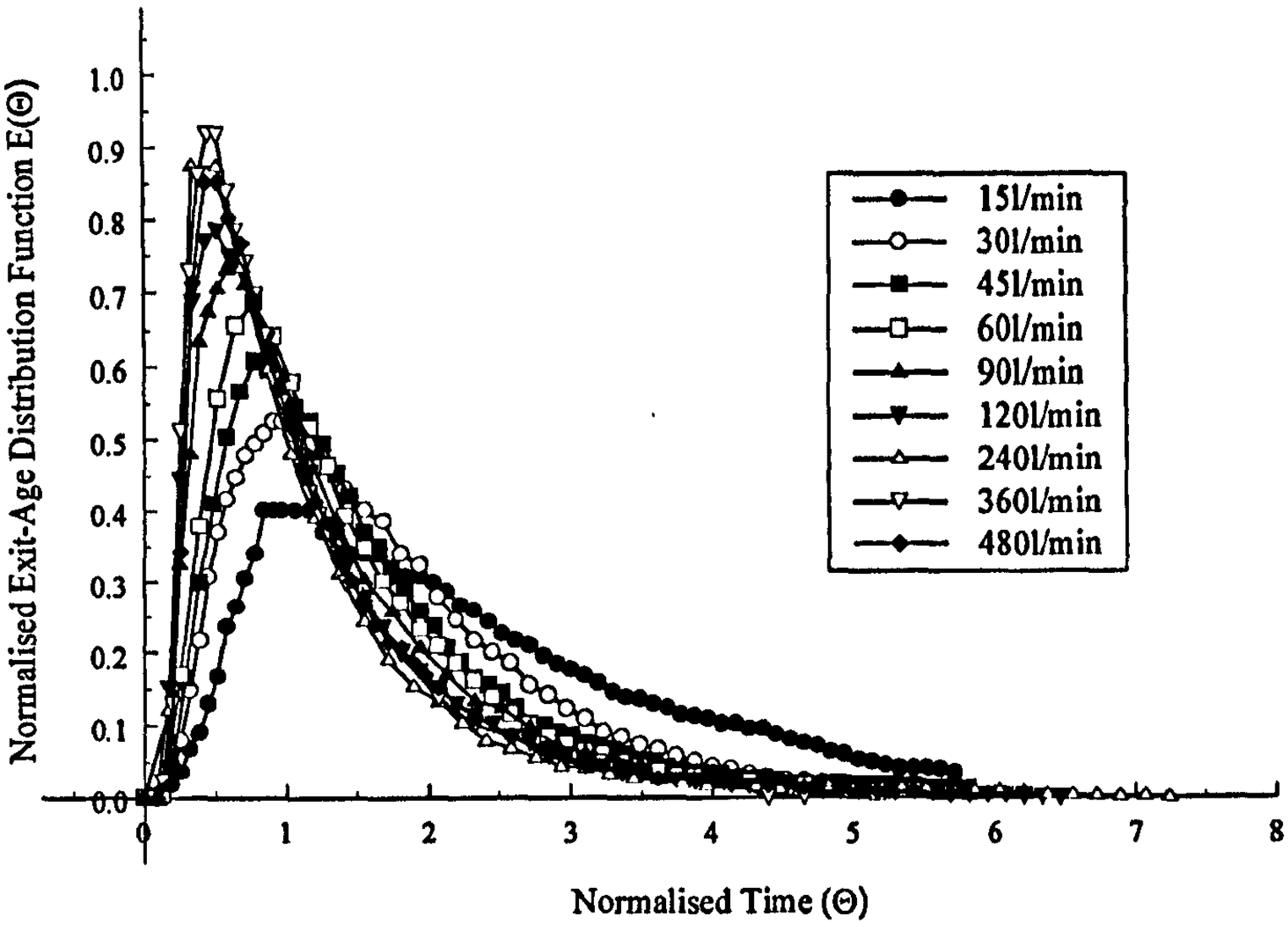

Fig. 4.13 Prototype HDVS No Baseflow - Comparison of Normalised Exit-Age Distribution Curves E(Θ)

Table 4.5 contains the RTD experimental mean residence time and variance calculated using the method of moments, the experimental tracer recovery (mass balance) and their associated errors. The experimental mean residence time estimated is significantly greater than the theoretical mean residence time, with the largest error at low flow rates / longer contact times. The mass balance at 15l/min is approximately 67% and the mean residence time is approximately 120% greater than the theoretical mean residence time, compared to 99% and 25% at 480l/min respectively. The errors associated with these results were discussed in section 4.4.1.1 and the same RTD investigations were undertaken for the prototype HDVS as for the model HDVS. This includes a RTD curve truncation analysis, which is discussed below and RTD experiments omitting the sludge hopper from the HDVS configuration (Fig. 3.1) (section 4.4.6).

Table 4.5 Prototype HDVS No Baseflow - Comparison of First and Second Moments Calculated from RTD Experimental Data

Flow Rate (l/min)	Theoretical Mean Residence Time (min)	Experimental Mean Residence Time (min)	Variance (min^2)	Experimental Mean Residence Time % Error	Tracer Mass Balance (%)
15	30.933	67.448	1645.00	+118.05	67.3500
30	15.467	26.526	246.869	+71.500	70.5600
45	10.311	15.839	108.517	+53.610	81.5600
60	7.7330	10.662	45.8600	+37.880	96.1200
90	5.1560	7.9060	30.2090	+53.340	106.663
120	3.8670	4.6990	12.5900	+21.520	90.6800
240	1.9330	2.2660	3.84600	+17.230	91.3600
360	1.2890	1.5070	1.31800	+16.910	100.133
480	0.9670	1.2070	0.86000	+24.820	99.0670

Table 4.6 details the ADM and TISM parameters and the normalised variance calculated using the method of moments. The Peclet number (P_e) describes a device with a plug-flow mixing regime and high dispersion, $P_e<10$ (section 4.3.3). The prototype HDVS Peclet number (P_e) ranges from less than 1–4.42 and is equivalent to 1.333–2.849 tanks-in-series (N) depending on the flow rate. All the Peclet numbers (P_e), besides the flow rate of 240l/min, are greater than 1 and therefore, the flow due to convection is generally greater than the rate of dispersion (section 4.4.1.1). The ADM and TISM parameters decrease as the flow rate increases and therefore the prototype HDVS has improved plug-flow mixing characteristics at low flow rates and dispersion and mixing effects decrease. The conflicts (1) and (2) identified for the model HDVS, between the RTD curves and parameters, equally apply to the prototype HDVS (section 4.4.1.1).

Table 4.6 Prototype HDVS No Baseflow - Comparison of ADM and TISM Parameters Calculated from RTD Experimental Data using the Method of Moments

Flow Rate (l/min)	Normalised Variance (σ_0^2)	Peclet Number (P_e)	N-Tanks
15	0.362	4.24	2.762
30	0.351	4.42	2.849
45	0.433	3.25	2.309
60	0.403	3.63	2.481
90	0.483	2.72	2.070
120	0.570	1.98	1.754
240	0.750	0.93	1.333
360	0.580	1.91	1.724
480	0.590	1.84	1.695

Fig. 4.14 compares the experimental exit-age distribution function E(t) curve to the TISM (eqn. 4.9) and ADM (eqn. 4.11) curves obtained using the method of moments for selected flow rates. The remaining flow rates and all correlation parameters (R^2 and ESS) are presented in appendix C.2.4 and C.2.5. The TISM provides the best-fit for the two lowest flow rates of 15 and 30l/min and the ADM provides the better fit for the remaining higher flow rates. The ADM correlation parameters (R^2) are stable across the range of flow rates except at the transition flow rate of 90l/min where the poorest fit is obtained. The TISM parameter N=3 provides the best-fit for flow rates of 15-60l/min. The TISM correlation (R^2) is uniform for this range of flow rates with the best-fit occurring at 30l/min. At flow rates including and above 90l/min the TISM parameter N=2 provides the better fit and the correlation generally decreases as the flow rate is increased. Therefore the trend in the correlation parameters (R^2) for the TISM parameter N=2 and N=3 support the reduction in the plug-flow mixing characteristics of the HDVS as the flow rate is increased as mentioned above. The relationship between the ADM and TISM correlation parameters and the HDVS's non-ideal flow behaviour is discussed in section 4.4.3.

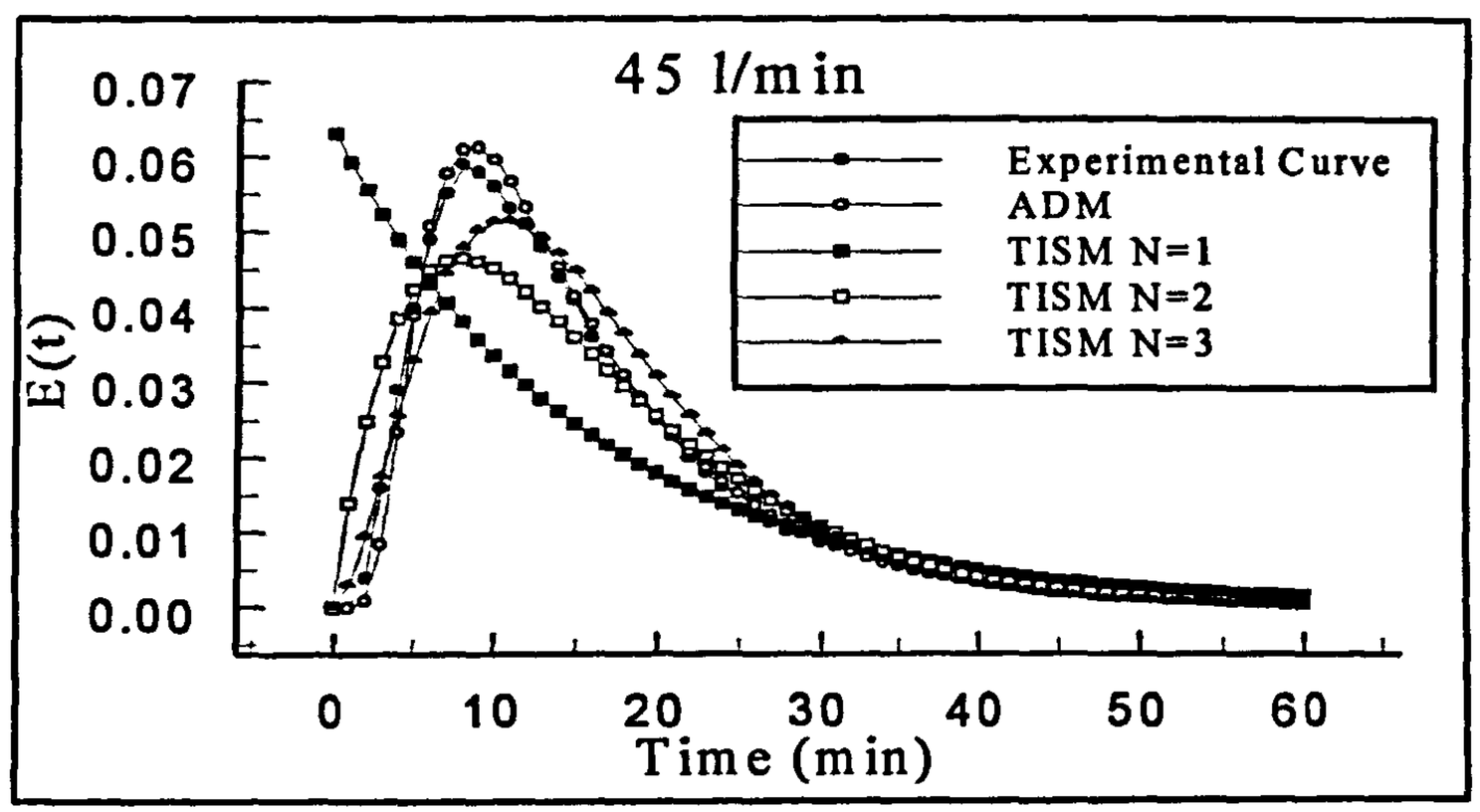

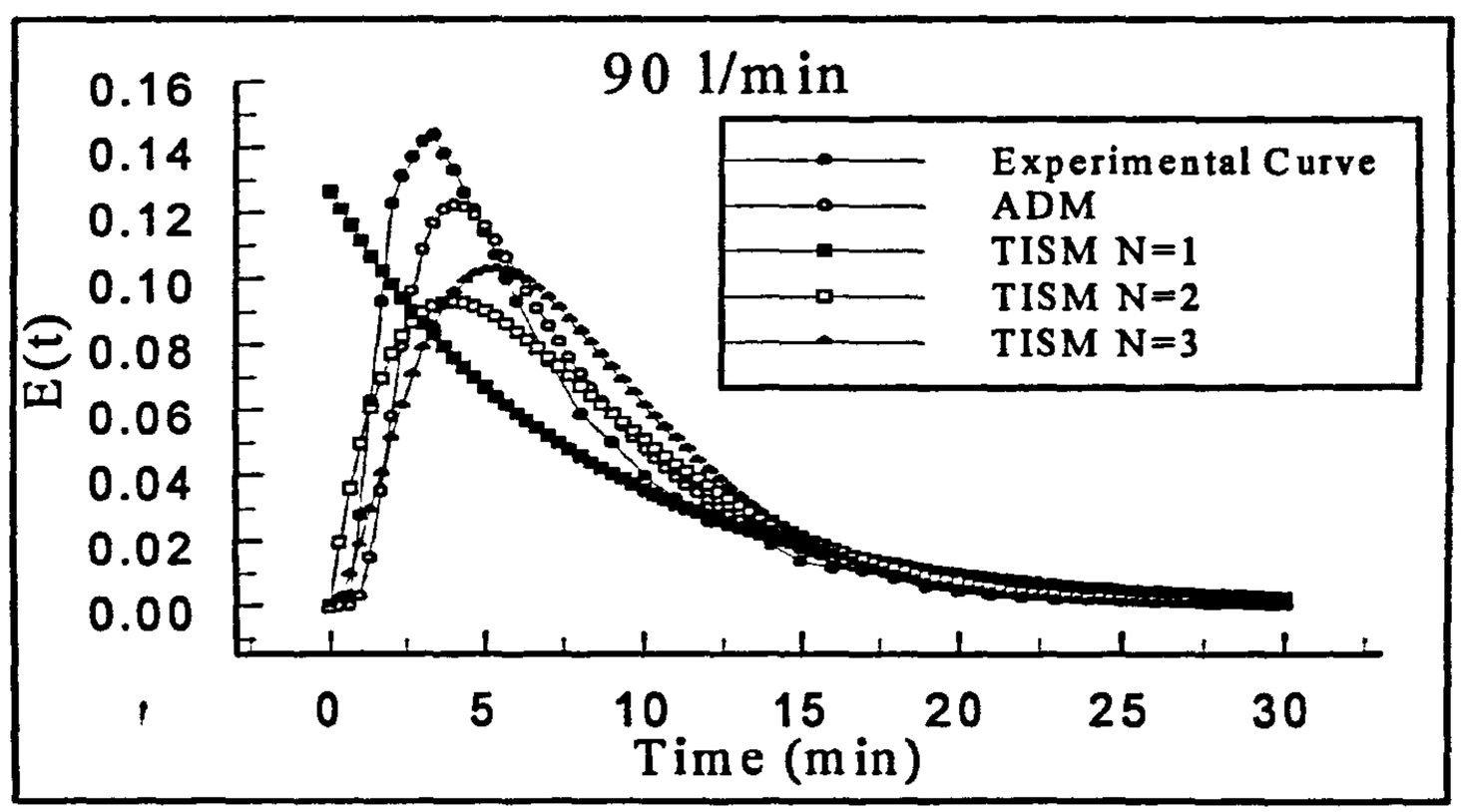

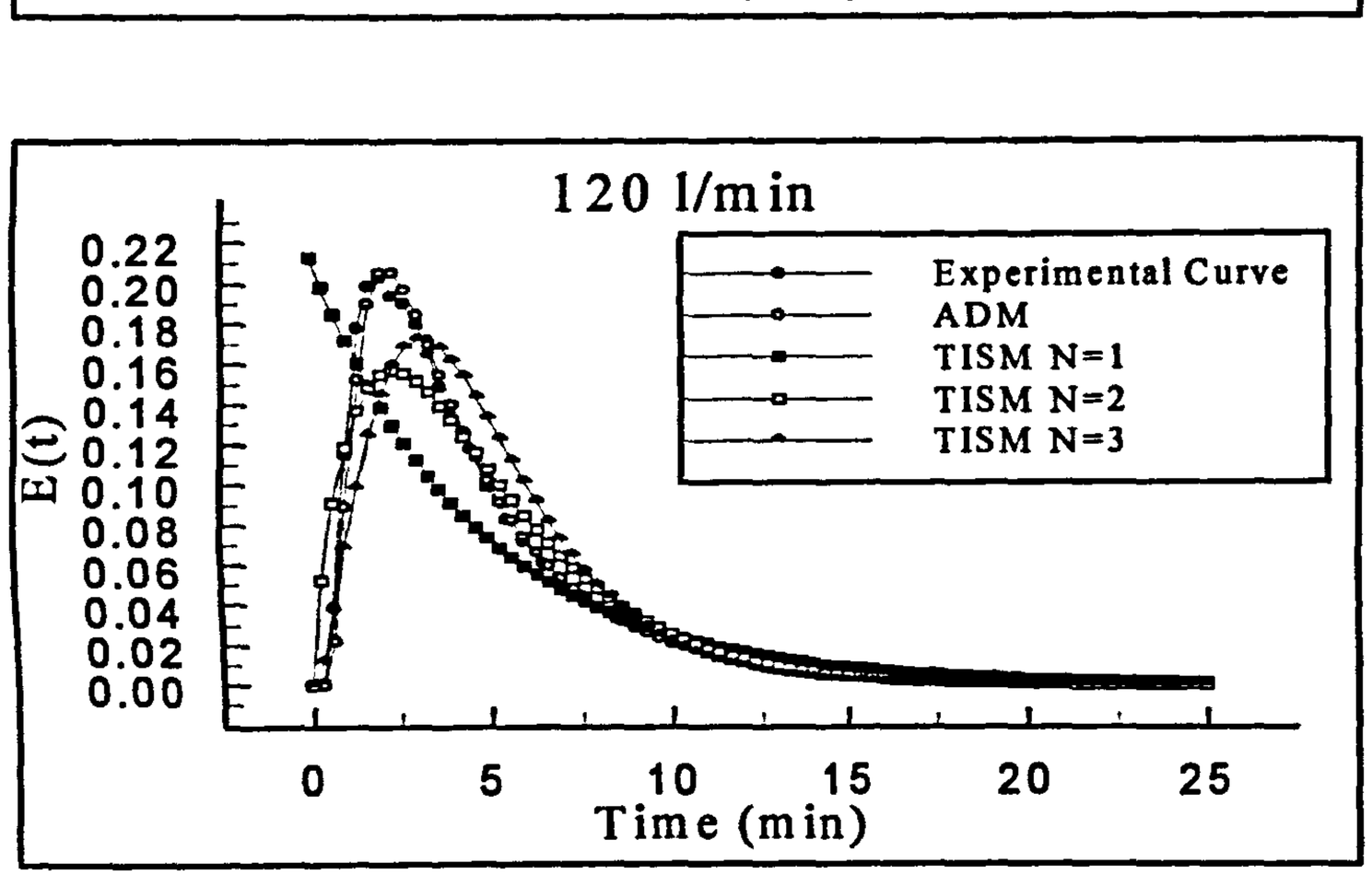

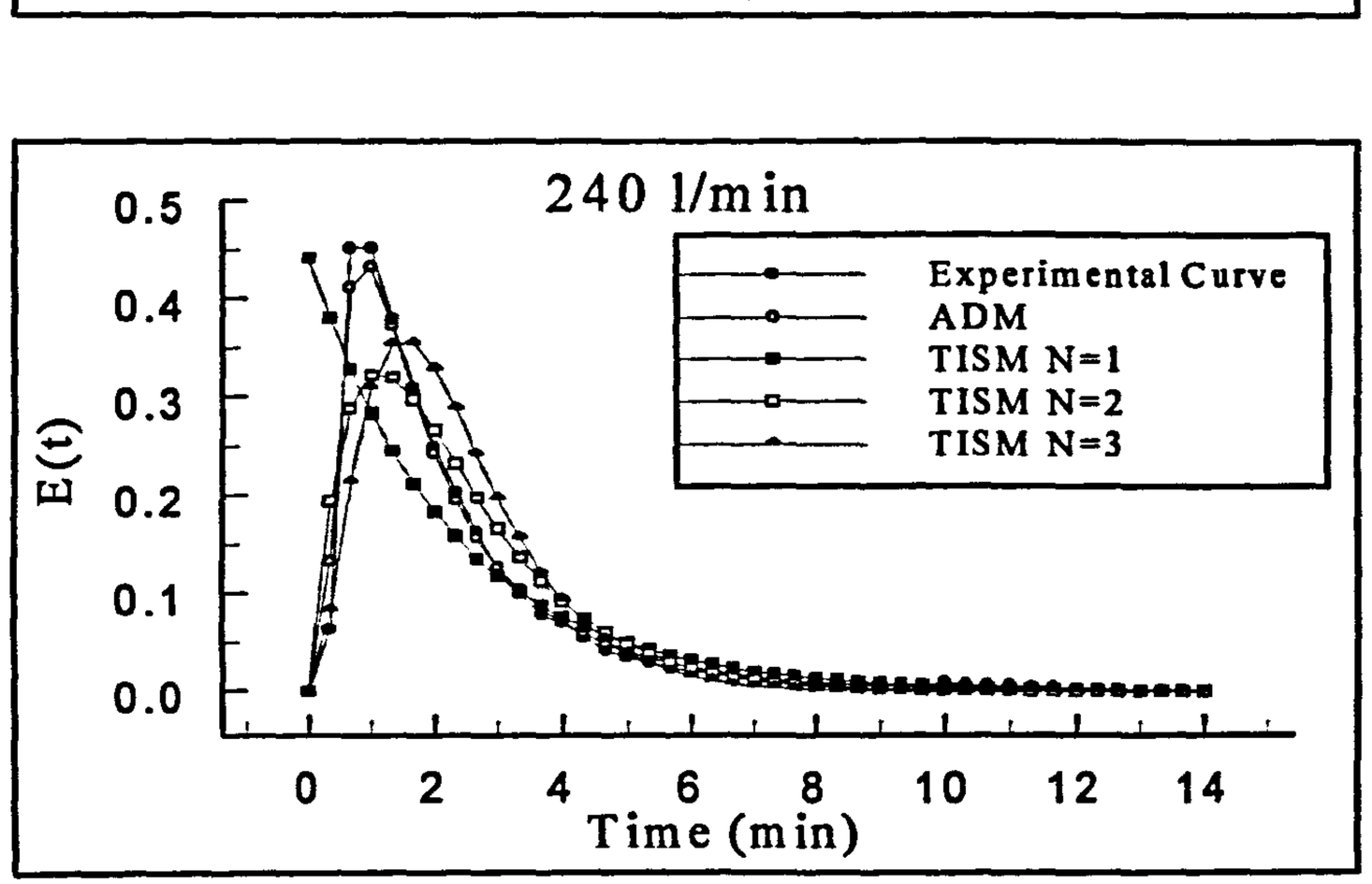

Fig. 4.14 Prototype HDVS No Baseflow - Comparison of E(t), ADM and TISM Curves Calculated Using the Method of Moments for Selected Flow Rates

Appendix C.2.6 shows the same RTD, ADM and TISM parameters, as presented in Table 4.5 and 4.6, for various RTD curve truncation times. The truncation times and data analysis procedure using the method of moments is the same as described for the model HDVS (section 4.4.1.1). Fig. 4.15 illustrates the trend in the truncated parameters at a low and high flow rate. The remaining flow rates are shown in appendix C.2.7. The results show that at flow rates less than 60l/min the experimental mean residence time at each truncation time is still greater than the theoretical mean residence time. Between 60 and 120l/min the experimental mean residence time approximates the theoretical mean residence time for a truncation time of 2-3 times the theoretical mean residence time. At all flow rates greater than 120l/min the experimental mean residence time approximates the theoretical mean residence time between the truncation times of 3-4 times the theoretical mean residence time (section 4.4.1.1).

At the lowest flow rate of 15l/min the Peclet number (P_e) ranges from 4.24–11.81 and the number of tanks-in series (N) ranges from 2.8–6.5. The Peclet number (P_e) at 15l/min describes a system with moderate dispersion (section 4.3.3). At the highest flow rate of 480l/min the Peclet number (P_e) ranges from 1.84–6.5 and the number of tanks-in series (N) ranges from 1.84–3.8. The same observations and conclusions obtained for the model HDVS RTD curve truncation investigation can be applied to the prototype HDVS (section 4.4.1.1).

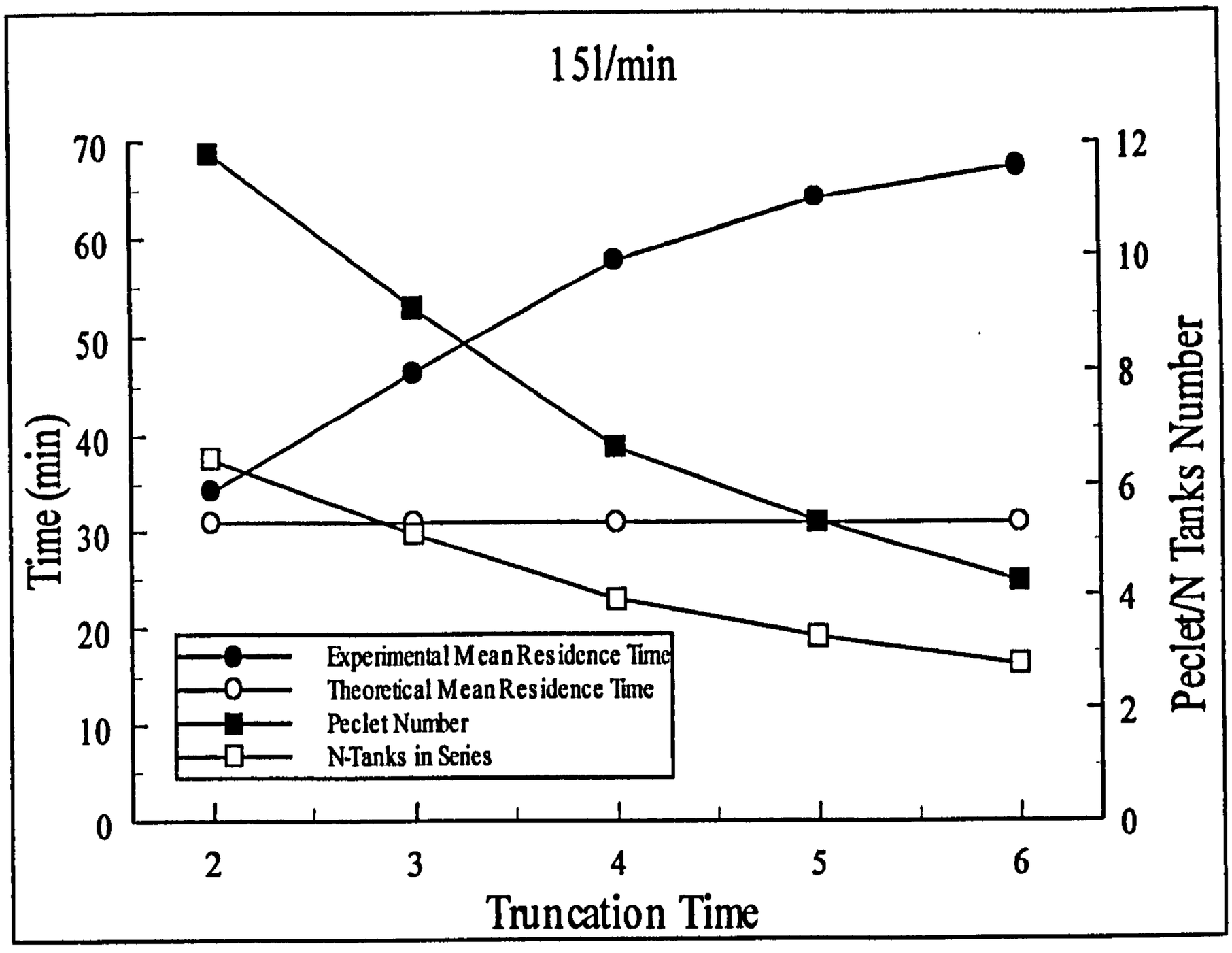

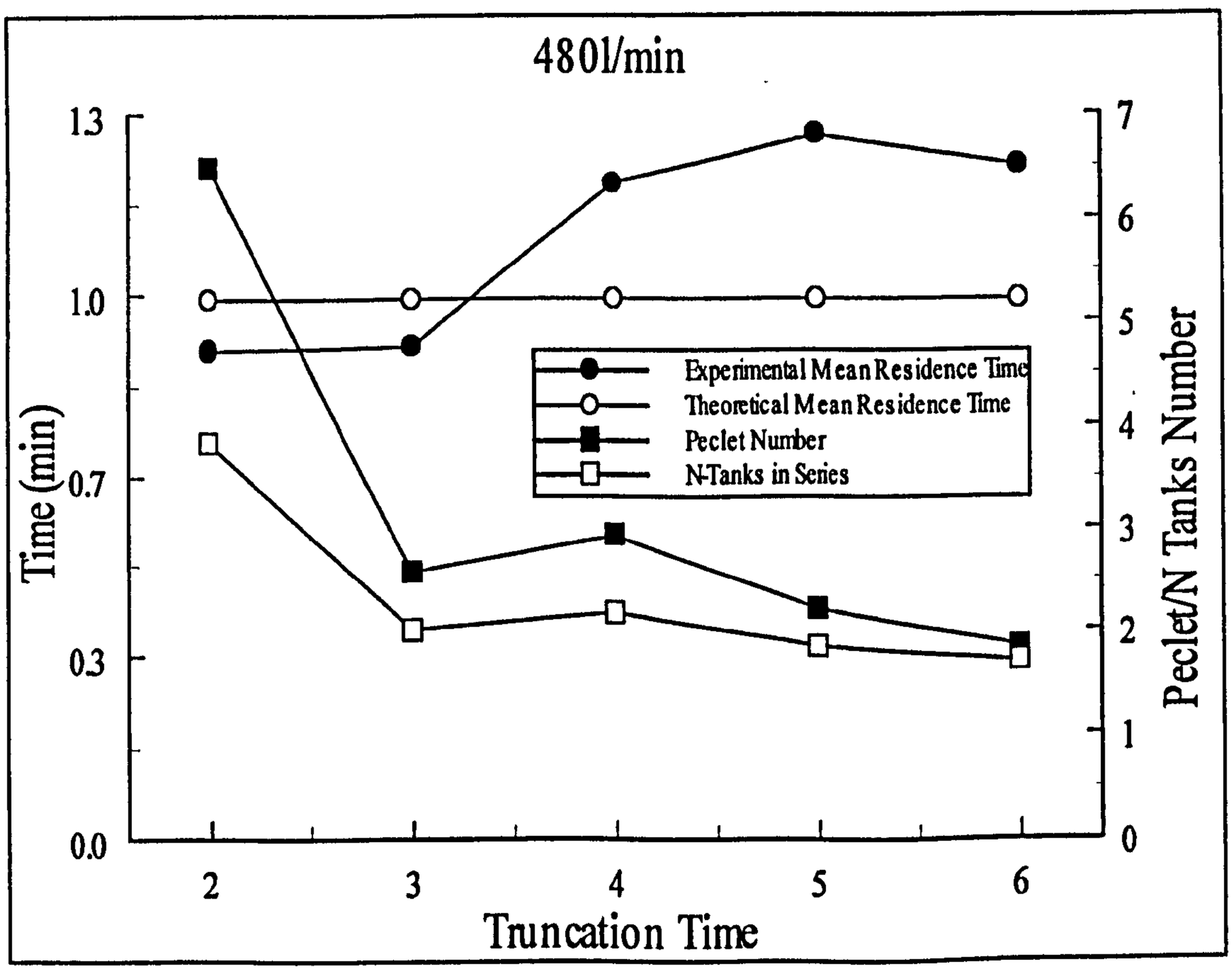

Fig. 4.15 Prototype HDVS No Baseflow - Effect of RTD Experiment Truncation on Mean Residence Time and ADM and TISM Parameters using the Method of Moments

The prototype HDVS normalised intensity function $\lambda(\Theta)$ curves (Fig. 4.16 and appendix C.2.8) exhibit a very similar shape to the model HDVS intensity function $\lambda(\Theta)$ curves (Fig. 4.11). Hence, the prototype HDVS intensity function $\lambda(\Theta)$ describes a similar mixing regime, as identified above using different RTD data analysis techniques and the same conclusions obtained for the model HDVS apply (section 4.4.1.1).

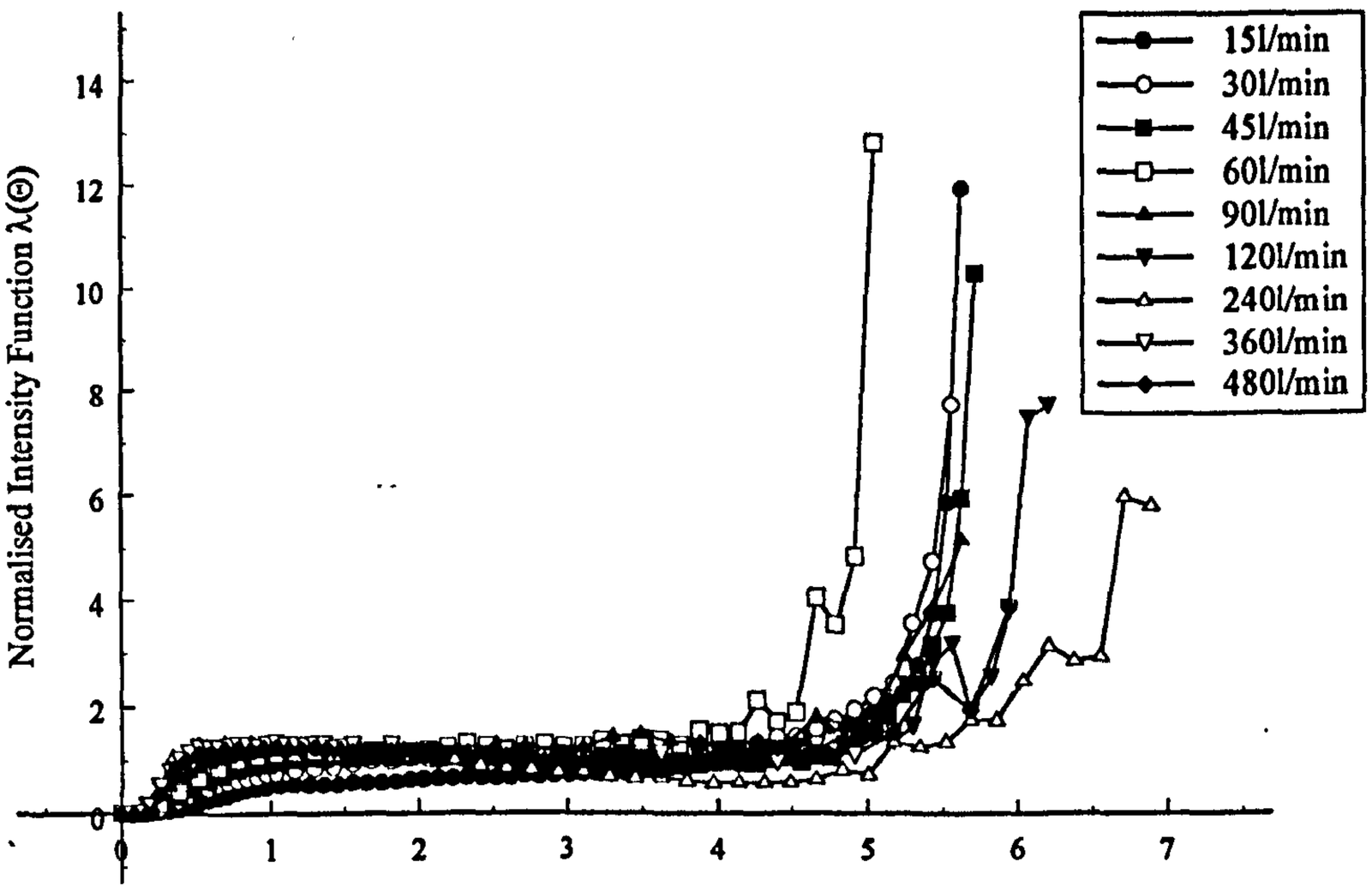

Fig. 4.16 Prototype HDVS No Baseflow - Normalised Intensity Function $\lambda(\Theta)$

The inlet flow regime for the prototype HDVS is turbulent for all operating flow rates i.e. Re > 4000. The same observations and similar errors obtained for the model HDVS, associated with the tracer pulse width and therefore the systems response relative to the input, apply to the prototype HDVS (section 4.4.1.1). Hence, no significant errors are envisaged due to the effects of tracer backmixing and laminar flow conditions, at the injection point and within the inlet pipe respectively.

4.4.2.2 Non-Linear Regression Data Analysis

Table 4.7 and 4.8 show the ADM and TISM parameters calculated using non-linear regression. A similar discussion for the model HDVS experimental mean residence time values calculated using non-linear regression can be applied to the prototype HDVS (section 4.4.1.2). The only significant difference for the prototype HDVS results is that the experimental mean residence time is greater than the theoretical mean residence time for all flow rates i.e. positive error. However the non-linear regression technique is still superior to the method of moments technique as discussed in section 4.4.1.2. The ADM Peclet number (P_e) ranges from 1.43–2.60 with higher values occurring at low flow rates. The TISM parameter (N) obtained directly from the non-linear curve fitting technique range from 2.092–2.285 also with higher values occurring at low flow rates. Therefore the non-linear regression technique supports the method of moments description of the HDVS's mixing regime i.e. improved plug-flow mixing characteristics as the flow rate decreases (section 4.4.2.1).

Table 4.7 Prototype HDVS No Baseflow - Comparison of ADM Parameters using Non-Linear Regression

Flow Rate (l/min)	Experimental Mean Residence Time (min)	Normalised Variance (σ_θ^2)	Peclet Number (P_e)	Coefficient of Correlation (R^2)	Sum of the Errors Squared (ESS)	Experimental Mean Residence Time % Error
15	74.986	0.569	1.99	0.999	0.000018	+142.414
30	28.327	0.526	2.33	0.998	0.000076	+83.1450
45	16.421	0.495	2.60	0.998	0.000067	+59.2570
60	11.129	0.498	2.57	0.999	0.000072	+43.9160
90	6.7550	0.605	1.74	0.999	0.000261	+31.0120
120	4.7360	0.655	1.43	0.999	0.000258	+22.4720
240	2.1140	0.637	1.53	0.997	0.004390	+9.36400
360	1.4190	0.592	1.83	0.997	0.015200	+10.0850
480	1.1250	0.578	1.93	0.996	0.026600	+16.3390

Table 4.8 Prototype HDVS No Baseflow - Comparison of TISM Parameters Using Non-Linear Regression

Flow Rate (l/min)	Experimental Mean Residence Time (min)	N-Tanks	Coefficient of Correlation (R^2)	Sum of the Errors Squared (ESS)	Experimental Mean Residence Time % Error
15	73.318	2.237	0.980	0.00008615	+137.022
30	27.973	2.285	0.978	0.00046230	+80.8560
45	15.916	2.207	0.973	0.00128500	+54.3590
60	10.822	2.211	0.971	0.00199500	+39.9460
90	6.464	2.229	0.975	0.00643600	+25.3690
120	4.306	2.144	0.970	0.01070000	+11.3520
240	1.939	2.092	0.960	0.05060000	+0.31000
360	1.344	2.152	0.952	0.24850000	+4.26700
480	1.065	2.146	0.948	0.36270000	+10.1340

Fig. 4.17 compares the experimental RTD normalised curves E(Θ) to the TISM (eqn. 4.9) and ADM (eqn. 4.11) curves obtained using the non-linear regression analysis technique for selected flow rates. The remaining flow rates and also the correlation parameters (R^2 and ESS) are presented in appendix C.2.9 and C.2.10. The ADM provides a better fit to the experimental data compared to the TISM. This is shown by the coefficient of correlation (R^2) and the sum of the errors squared (ESS) values (Table 4.7 and 4.8). The coefficient of correlation (R^2) values for the ADM are greater than the TISM for the same flow rate. Both models generally provide a better fit to the experimental data, as the flow rate decreases and therefore, as the HDVS's mixing regime has improved plug-flow mixing characteristics. The relationship between the ADM and TISM correlation parameters and the experimental RTD curves characteristics is discussed in section 4.4.1.2.

The prototype HDVS RTD curves were not subject to a truncation investigation using non-linear regression and the reader is referred to the model HDVS results (section 4.4.1.2). A truncation analysis is largely dependent on the shape of the RTD curve, which is very similar for both the model and prototype HDVS operating with no baseflow, with respect to the inlet flow rate and therefore the same observations apply.

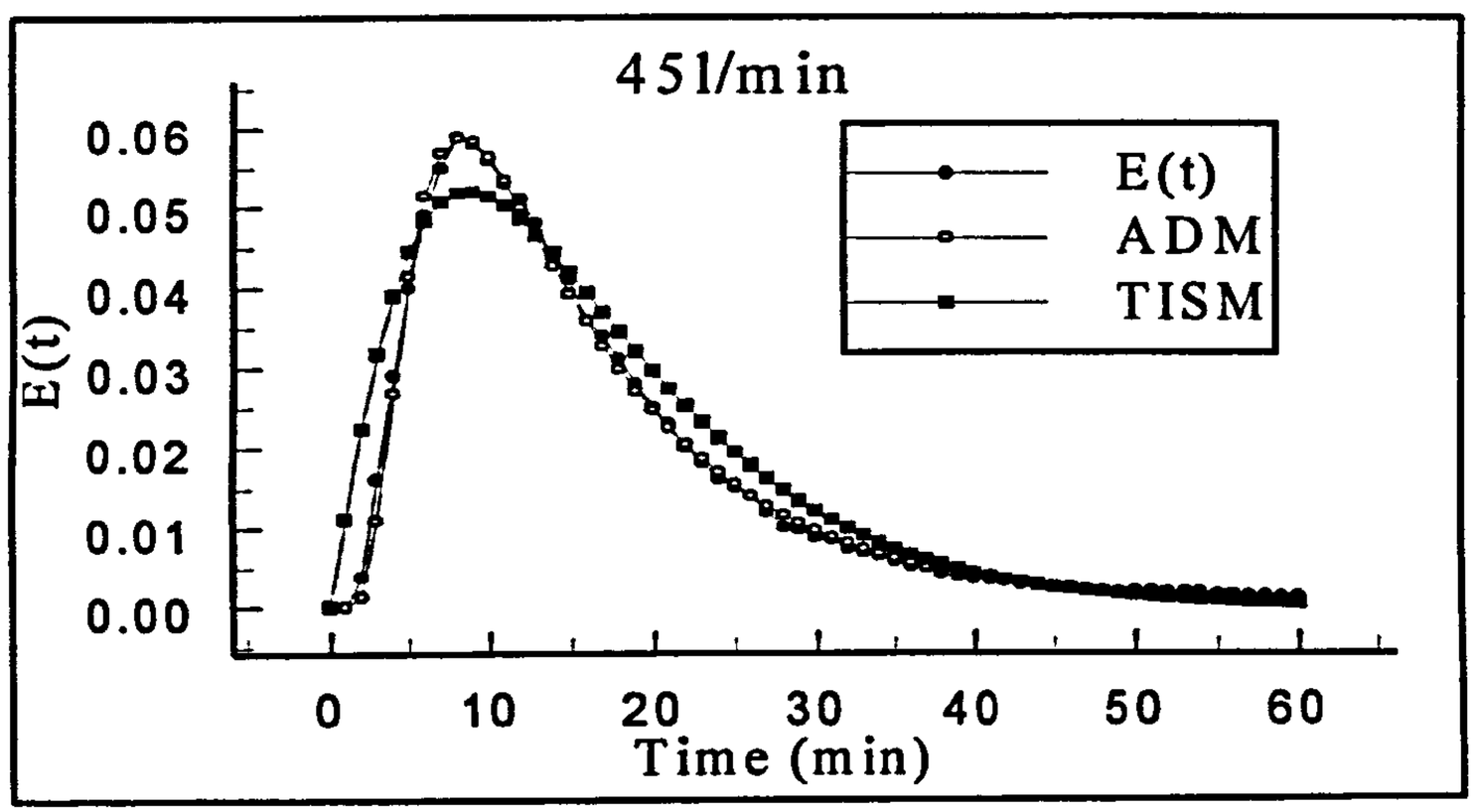

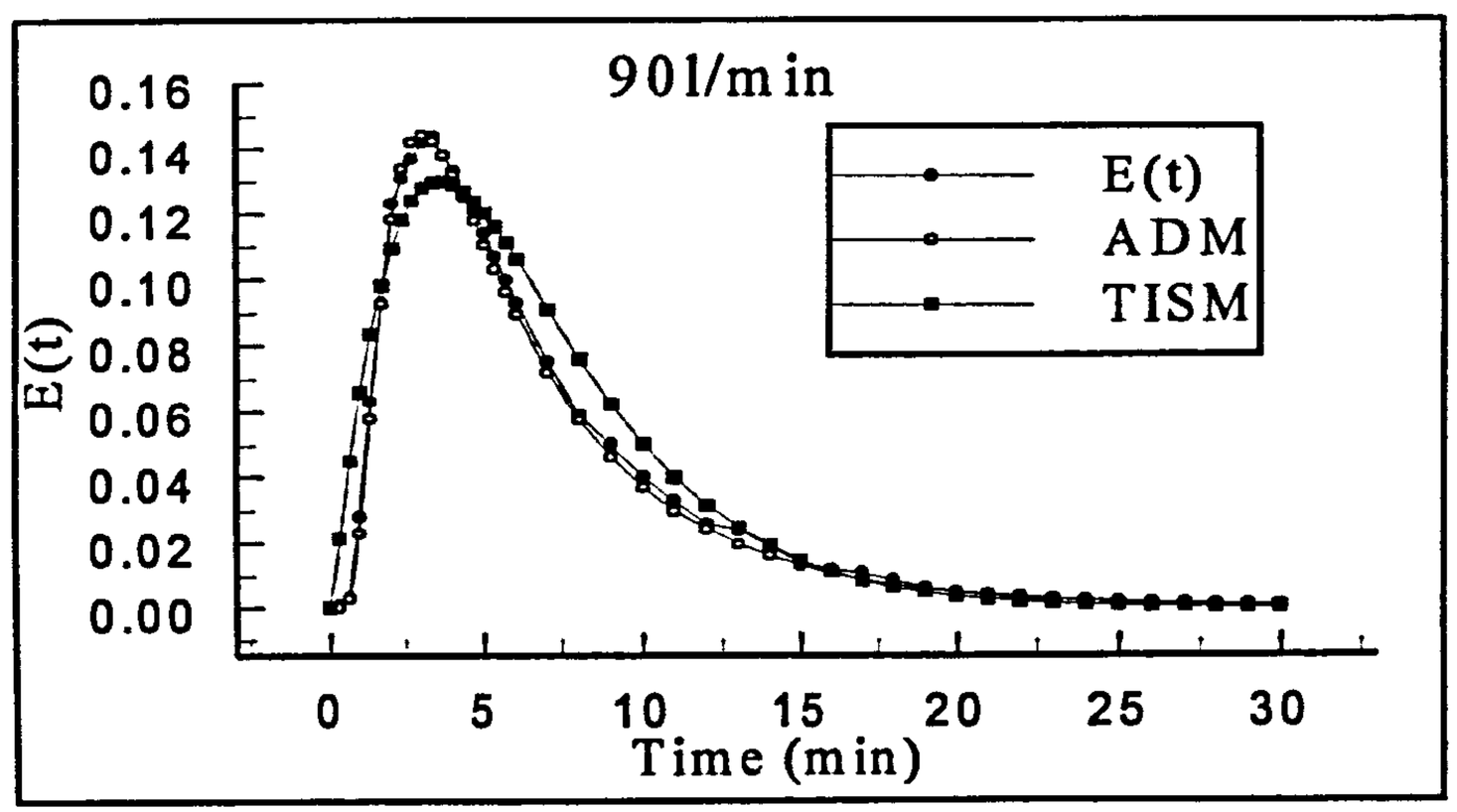

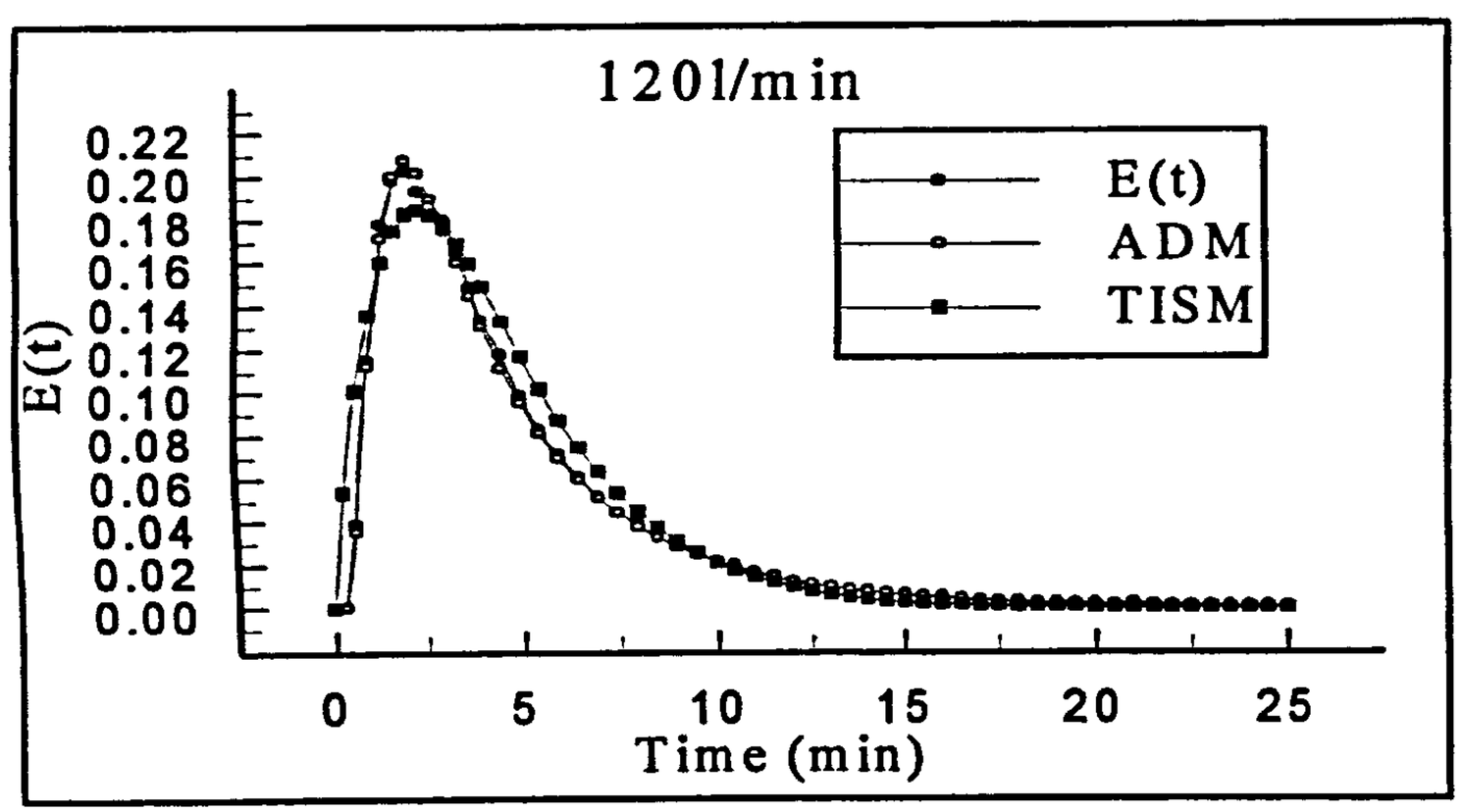

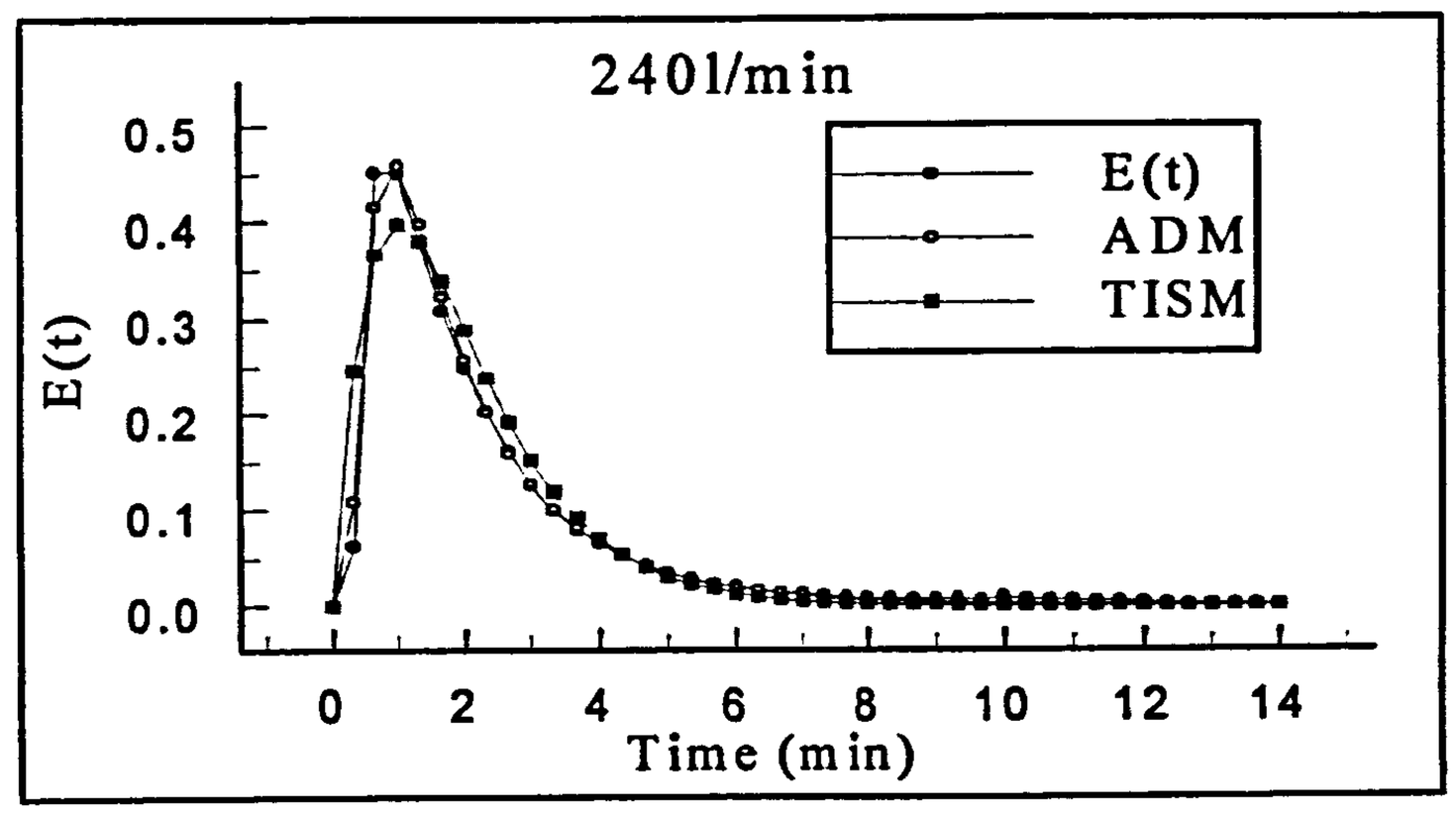

Fig. 4.17 Prototype HDVS No Baseflow - Comparison of E(t), ADM and TISM Curves Calculated Using Non-Linear Regression for Selected Flow Rates

4.4.3 Comparison of the Model and Prototype Hydrodynamic Vortex Separator (HDVS) No Baseflow RTD Pulse Injection Results

Appendix C.5.1 compares the model and prototype HDVS RTD normalised curves E(Θ) at flow rates above and below their transition flow rates. The RTD curves at high flow rates i.e. greater than 15l/min for the model HDVS and 90l/min for the prototype HDVS clearly show a very similar distribution and therefore the mixing regime for any size of HDVS above its transition flow rate is stable. The tail portions of the RTD curves after approximately twice the theoretical mean residence time are also very similar. The RTD curves at flow rates below the transition flow rate do not provide the same goodness of fit. However, they do show that as the flow rate increases for both devices, the peak of the RTD curve shifts towards the origin, implying that a smaller volume is active in the mixing process. The prototype HDVS RTD curves at low flow rates appears to peak closer to a normalised time (Θ) value of 1 compared to the model HDVS. Therefore at low flow rates the prototype HDVS has improved plug-flow mixing characteristics and a greater active volume compared to the model HDVS. The RTD curves are presented using the normalised exit-age distribution function E(Θ) (section 4.3.1). This allows a direct comparison of the RTD curves obtained from systems with different volumes and operating flow rates i.e. the model and prototype HDVS. However, it should be noted that no operating flow rates investigated for each device provide the same theoretical mean residence time. Table 4.9 shows the model and prototype HDVS operating flow rates, which provide similar theoretical mean residence times for each device.

A comparison of the model and prototype HDVS ADM and TISM parameters calculated using the method of moments and non-linear regression is shown in Fig. 4.18 and 4.19.

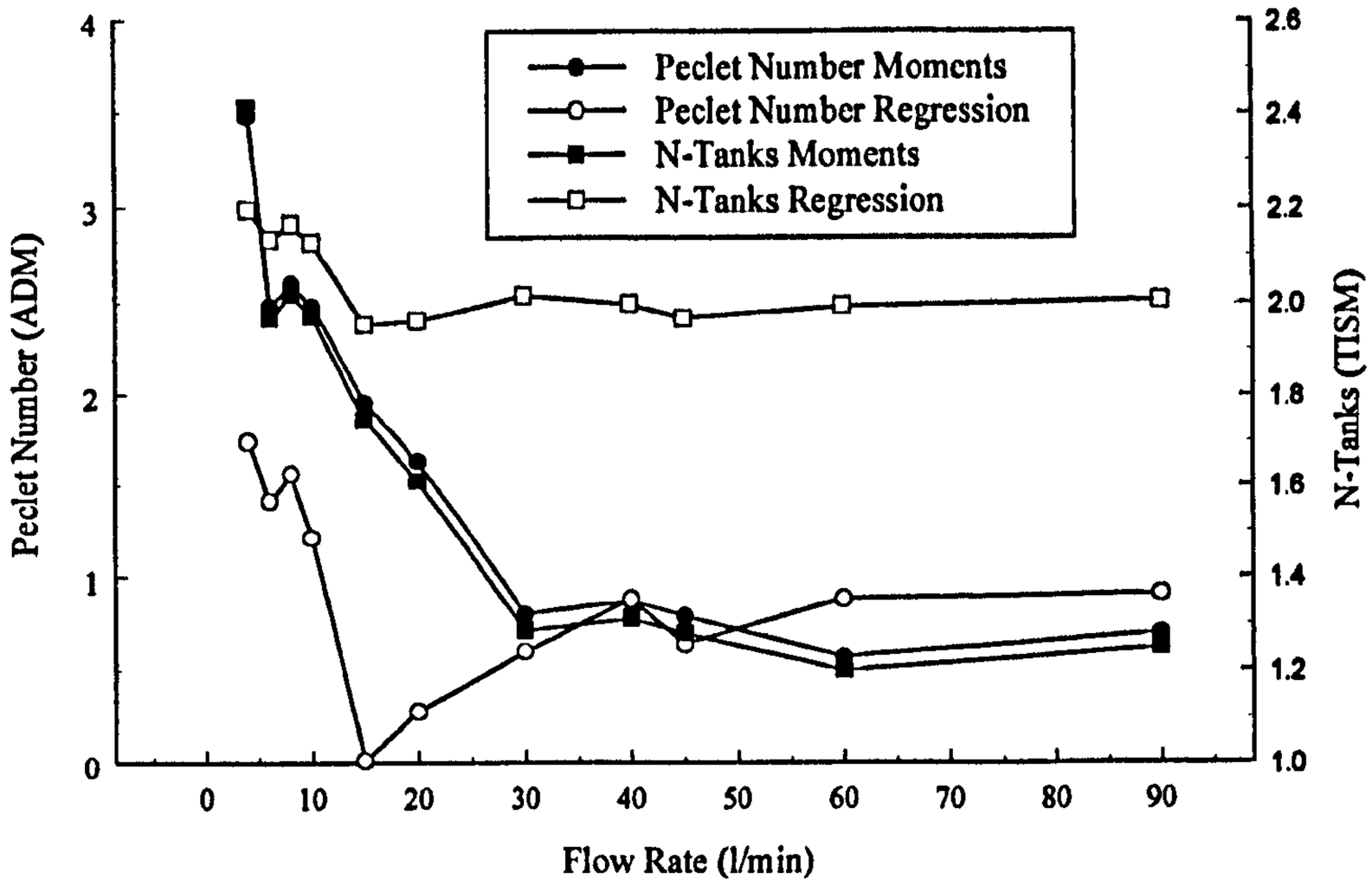

Fig. 4.18 Model HDVS No Baseflow - Comparison of ADM and TISM Parameters Calculated using the Method of Moments and Non-Linear Regression

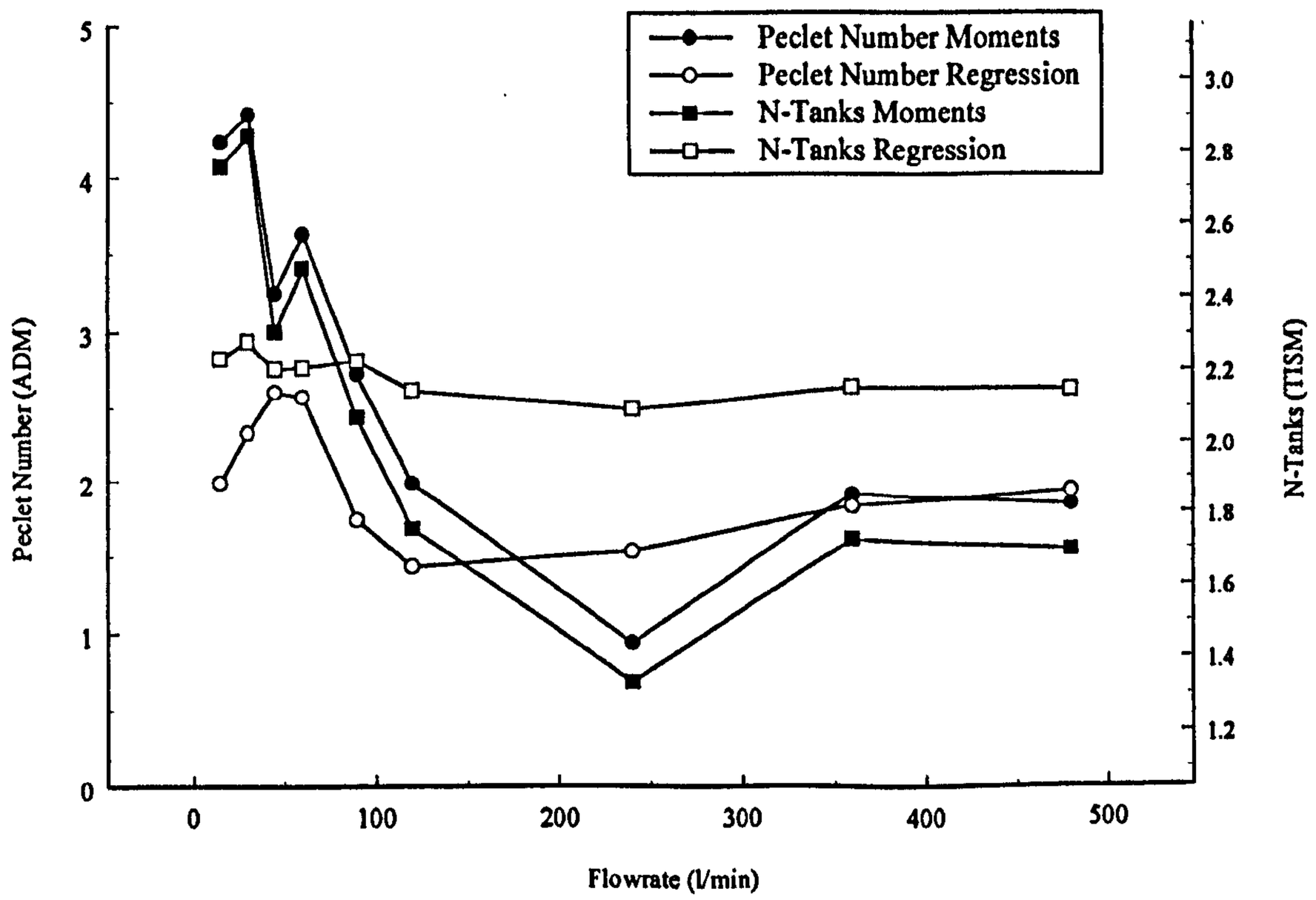

Fig. 4.19 Prototype HDVS No Baseflow - Comparison of ADM and TISM Parameters Calculated using the Method of Moments and Non-Linear Regression

The ADM and TISM parameters calculated using the method of moments, for both the model and prototype HDVS, show the same decreasing trend as the flow rate increases and then become relatively stable (Fig. 4.18 and 4.19). This parameter stability occurs at approximately 30l/min for the model HDVS and 120l/min for the prototype HDVS. The evidence of a transition flow rate i.e. a change in HDVS mixing characteristics, is provided by the falling section of the curves, between the lowest flow rate and the transition flow rate, where after the ADM and TISM parameters remain stable. This corresponds with the normalised exit-age distribution curves E(Θ) characteristics (Fig. 4.8 and 4.13) and therefore supports the stable mixing regime identified above, at high flow rates, for both the model and prototype HDVS. The model HDVS ADM and TISM parameters calculated using the method of moments range from less than 1–3.48 and 1.98-2.41 respectively and for the prototype HDVS 1-4.42 and 1.333-2.849 respectively. The ADM parameter for both device's, at their lowest flow rates and a truncation time of 2-3 times the theoretical mean residence time, provide a Peclet number (P_e) for a device with moderate dispersion, as opposed to high dispersion for all other flow rates (section 4.3.3). Similarly the TISM parameter implies that the HDVS is equal to approximately 6 tanks-in-series (N). Therefore the RTD experimental duration is a critical parameter in characterising the HDVS mixing regime and the author encourages the use of the entire RTD as opposed to individual RTD parameters to estimate the HDVS's efficiency for specific kinetic process applications (chapter 7).

The ADM provides the best-fit for all the model HDVS flow rates compared to the TISM using the method of moments. The TISM parameter N=2 provides the better fit compared to N=1 and N=3 (section 4.3.3). The ADM provides the best-fit for all the prototype HDVS flow rates above the transition flow rate and for flow rates less than the transition flow rate the TISM provides the best-fit using the method of moments. The TISM parameter N=3 provides the best-fit for flow rates less than the transition

flow rate and for higher flow rates N=2 provides the best-fit. Therefore the TISM correlation parameters support previous observations that the prototype HDVS has better plug-flow mixing characteristics compared to the model HDVS and particularly at low flow rates. This is also illustrated by the ADM and TISM parameters below (Table 4.9).

The model HDVS ADM and TISM parameters calculated using non-linear regression range from less than 1–1.74 and 1.952-2.195 respectively and for the prototype HDVS 1.43-2.60 and 2.092-2.285 respectively. The ADM provides the best-fit for all the model and prototype HDVS flow rates, compared to the TISM using non-linear regression. The ADM and TISM parameters obtained using non-linear regression remain relatively constant across the range of model and prototype HDVS flow rates investigated (Table 4.10). However the values do show a slight decreasing trend as the flow rate increases, although not to the same extent as the ADM and TISM parameters calculated using the method of moments (Table 4.9) and therefore provide less evidence of a transition flow rate. This is shown in Fig. 4.18 and 4.19, as the ADM and TISM parameters decrease up to the transition flow rate and then remain stable. Therefore the model and prototype HDVS ADM and TISM parameters, calculated using both the method of moments and non-linear regression, show that plug-flow mixing characteristics increase and dispersion and mixing effects decrease, as the flow rate decreases (section 4.1). Additionally the stable mixing regime identified within the HDVS at high flow rates is associated with both the inactive flow behaviour and the plug-flow mixing characteristics.

Table 4.9 Model and Prototype HDVS No Baseflow – Comparison of ADM and TISM Parameters Calculated using the Method of Moments

Model HDVS		Prototype HDVS		Peclet Number (P_e)		N-Tanks	
Flow Rate (l/min)	Theoretical Mean Residence Time (min)	Flow Rate (l/min)	Theoretical Mean Residence Time (min)	Model HDVS	Prototype HDVS	Model HDVS	Prototype HDVS
4	15.000	30	15.467	3.48	4.42	2.410	2.849
6	10.000	45	10.311	2.48	3.25	1.965	2.309
8	7.500	60	7.733	2.60	3.63	2.020	2.481
10	6.000	90	5.156	2.48	2.72	1.969	2.070
15	4.000	120	3.867	1.96	1.98	1.745	1.754
30	2.000	240	1.933	0.80	0.93	1.284	1.333
45	1.333	360	1.289	0.79	1.91	1.280	1.724
60	1.000	480	0.967	0.57	1.84	1.198	1.695

Table 4.10 Model and Prototype HDVS No Baseflow – Comparison of ADM and TISM Parameters Calculated using Non-Linear Regression

Model HDVS		Prototype HDVS		Peclet Number (P_e)		N-Tanks	
Flow Rate (l/min)	Theoretical Mean Residence Time (min)	Flow Rate (l/min)	Theoretical Mean Residence Time (min)	Model HDVS	Prototype HDVS	Model HDVS	Prototype HDVS
4	15.000	30	15.467	1.74	2.33	2.195	2.285
6	10.000	45	10.311	1.41	2.60	2.134	2.207
8	7.500	60	7.733	1.56	2.57	2.165	2.211
10	6.000	90	5.156	1.21	1.74	2.126	2.229
15	4.000	120	3.867	0.01	1.43	1.952	2.144
30	2.000	240	1.933	0.60	1.53	2.014	2.092
45	1.333	360	1.289	0.64	1.83	1.964	2.152
60	1.000	480	0.967	0.88	1.93	1.991	2.146

The model and prototype HDVS ADM and TISM parameters are of a similar order of magnitude and therefore, operate with a very similar and stable mixing regime, particularly above their respective transition flow rates. However the prototype HDVS ADM and TISM parameters are generally greater than the model HDVS, at a flow rate providing a similar theoretical mean residence time within each device. This is illustrated by the ADM and TISM parameters calculated using either the method of moments or non-linear regression (Table 4.9 and 4.10). Therefore the prototype HDVS has marginally improved plug-flow mixing characteristics compared to the model HDVS. Hence from the previous observations, as the HDVS is scaled-up, its plug-flow

mixing and active volume characteristics are improved.

The method of moments ADM correlation parameter (R^2) either remains stable or generally improves as the flow rate is increased, whereas the TISM correlation parameter generally improves as the flow rate is decreased. It should be noted that the ADM used throughout this project (eqn. 4.11) and commonly employed by other workers conducting RTD studies is an analytical solution obtained from the ADM first principles and will therefore contain mathematical errors (section 4.3.3). It is not an objective of this project to investigate these errors however, the reader should be aware, particularly when comparing ADM parameters obtained from different ADM solutions. Additionally, as the ADM parameter is approaching a value describing a system with high dispersion, confidence in its accuracy and true description of the HDVS's mixing regime reduces, as it is approaching it's lower confidence limits (section 4.3.3). Whereas the TISM is not subject to such confidence limits (Levenspiel, 1972). The non-linear regression ADM and TISM correlation parameters generally improve as the flow rate is decreased. The trend in the method of moments TISM correlation parameters and non-linear regression ADM and TISM correlation parameters is expected, as these two flow models do not account for the fraction of dead volume and subsequently short-circuiting within the HDVS. This non-ideal flow behaviour is evidently present due to the shape of the RTD normalised curves $E(\Theta)$ and increases as the flow rate increases. Hence the correlation between the ADM and TISM and the experimental data should improve as the flow rate decreases.

The ADM and TISM parameters obtained using non-linear regression provide a better correlation between the experimental and model generated RTD curve i.e. higher coefficient of correlation (R^2). This is due to the flexibility provided by the non-linear regression technique, as it directly fits the ADM and TISM curve to the experimental curve. Whereas the method of moments is an indirect parameter estimation technique,

as it relies on only two parameters i.e. first and second moments (n) to describe the shape of the RTD curve, from which the ADM and TISM parameters are calculated (section 4.3.3).

There is a numerical difference between the ADM and TISM parameters calculated using the method of moments and non-linear regression technique however, they both describe a similar mixing regime with improved plug-flow mixing characteristics at low flow rates. The difference, is due to the method of moments biased prediction of the first and second moments (n), as a result of the methods sensitivity to the tailing effects of the RTD (section 4.4.1.1). The non-linear regression ADM and TISM parameter estimation technique is less sensitive to RTD curve truncation effects and therefore the RTD curves tail section, particularly when combined with the TISM. This is shown by a reduction in the error between the theoretical and the experimental mean residence time calculated using non-linear regression compared to the method of moments. Additionally the non-linear regression RTD curve truncation investigation, provided more consistent ADM and TISM parameters across the range of truncation times for the same flow rate compared to the method of moments (section 4.4.1 and 4.4.2).

The ADM and TISM parameters calculated using the method of moments and non-linear regression do not directly illustrate which parameters best describe the HDVS. However, based on the above discussion, the non-linear regression parameter estimation technique is superior compared to the method of moments and particularly when combined with the TISM, to describe the HDVS's mixing regime. Haas *et al.*, (1997) used Monte Carlo studies (parameter optimisation) to investigate the discrepancy between the ADM and TISM parameters calculated using the method of moments and non-linear regression and concluded that the latter approach should be used to characterise the RTD.

4.4.4 Model and Prototype Hydrodynamic Vortex Separator (HDVS) No Baseflow - Residence Time Distribution (RTD) Indices

Table 4.11 and 4.12 present the model and prototype HDVS RTD indices, calculated from the parameters described in section 4.3.4. The t_f/τ index measures the most severe short-circuiting. A value of 1 corresponds to plug-flow mixing and 0 to complete mixing (section 4.3.4). Both the model and prototype HDVS exhibit a large degree of short-circuiting with values approaching that expected for complete mixing conditions. The t_f/τ values for both device's decrease as the flow rate increases. Subsequently the t_p/τ index, which gives an indication of the effective volume of the device, provides the same trend for both the model and prototype HDVS. Both the t_f/τ and t_p/τ indices support the RTD normalised curves $E(\Theta)$ description of the mixing regime (Fig. 4.8 and 4.13). At high flow rates (>15l/min model HDVS and >90l/min prototype HDVS) the peak of the RTD curve shifts towards the origin and therefore dead volumes and subsequently short-circuiting is present. Whereas at low flow rates the RTD curve peak occurs close to a normalised time (Θ) value of 1 (eqn. 4.2) implying a greater volume of the HDVS is active in the mixing process. Therefore the RTD indices support the conflict (1) identified between the RTD normalised curves $E(\Theta)$ and RTD experimental parameters (section 4.4.1.1). The prototype HDVS t_p/τ index is generally greater than the model HDVS and therefore, supports previous conclusions, that the prototype HDVS has a greater active volume compared to the model HDVS (section 4.4.3). This comparison is based on the flow rate, which provides the closest theoretical mean residence time through each HDVS (Table 4.9) and is also used for comparing other model and prototype HDVS RTD indices discussed below.

Table 4.11 Model HDVS No Baseflow - RTD Indices Calculated from Experimental Curves using the Method of Moments

Flow Rate (l/min)	t_f/τ	t_p/τ	t_{90}/t_{10}	t_m/τ	t_{50}/t_m
4	0.133	0.933	6.222	1.922	0.763
6	0.150	0.800	7.600	1.814	0.717
8	0.133	0.800	6.571	1.578	0.760
10	0.167	0.750	6.400	1.435	0.755
15	0.333	0.333	8.252	1.351	0.740
20	0.167	0.417	8.000	1.271	0.721
30	0.083	0.334	11.00	1.268	0.592
40	0.111	0.333	9.000	1.117	0.647
45	0.062	0.375	9.000	1.245	0.653
60	0.083	0.417	10.00	1.231	0.609
90	0.125	0.375	10.50	1.226	0.611

Table 4.12 Prototype HDVS No Baseflow - RTD Indices Calculated from Experimental Curves using the Method of Moments

Flow Rate (l/min)	t_f/τ	t_p/τ	t_{90}/t_{10}	t_m/τ	t_{50}/t_m
15	0.129	1.067	5.375	2.180	0.890
30	0.194	0.970	5.333	1.715	0.829
45	0.194	0.776	5.800	1.536	0.821
60	0.129	0.776	6.667	1.379	0.750
90	0.065	0.646	6.500	1.533	0.632
120	0.086	0.517	6.752	1.215	0.709
240	0.172	0.517	6.496	1.172	0.736
360	0.065	0.517	7.199	1.169	0.719
480	0.086	0.517	6.757	1.248	0.690

The t_{90}/t_{10} index (Morrill Dispersion Index) increases as the flow rate increases. Therefore, there is greater spreading of the RTD curve and subsequently more mixing and dispersion within the HDVS at high flow rates (section 4.1). This is also illustrated by the ADM and TISM parameters and hence, the RTD indices do not support the conflict (2) suggesting that the RTD normalised curves $E(\Theta)$ at high flow rates possibly have greater plug-flow mixing characteristics compared to low flow rates. This conflict (2) is purely a visual observation (section 4.4.1.1). The theoretical values for this index are 1 for plug-flow mixing and 21.9 for complete mixing. The t_{90}/t_{10} values range from approximately 25-50% of the theoretical value for complete mixing conditions. The recommended design value for the t_{90}/t_{10} index is no greater than 2 for potable water

disinfection systems (Stover *et al.*, 1986). The prototype HDVS t_{90}/t_{10} index is generally less than the model HDVS and therefore, supports previous conclusions, that the prototype HDVS has greater plug-flow mixing characteristics compared to the model HDVS (section 4.4.3).

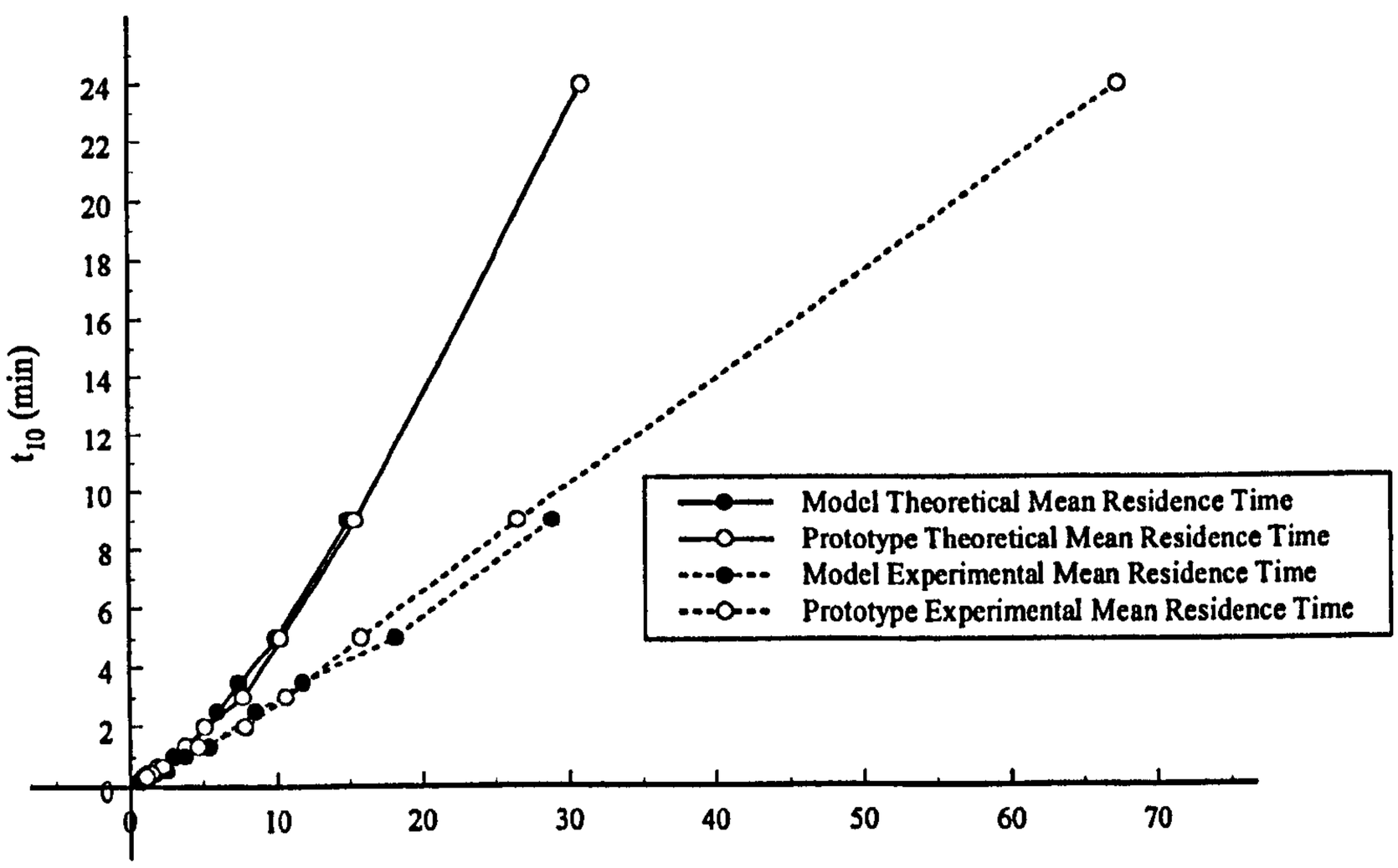

Fig. 4.20 Model and Prototype HDVS No Baseflow - Relationship Between RTD t_{10} Parameter and Mean Residence Time for all Flow Rates using the Method of Moments

The USEPA SWTR disinfection contact tank design methodology, using the CT product, generally uses the t_{10} parameter as the time element (T) (section 4.3.4). The values for the model and prototype HDVS operating with no baseflow are illustrated in Fig. 4.20.

The t_{10} parameter values, using the experimental mean residence time, would provide a conservative CT design, in addition to the factor of safety already provided by using the t_{10} parameter as the time element (T) (section 4.3.4). The t_{10} parameter values using the experimental mean residence time clearly show a linear trend and increase as the flow rate decreases i.e. longer mean residence time. However, using the theoretical

mean residence time, provides the relationship that is possibly more comparable with the mixing regime of the model and prototype HDVS, due to the error between the theoretical and experimental mean residence time results (section 4.4.1.1 and 4.4.2.1). At a theoretical mean residence time of approximately 5-7 minutes there is a change in gradient of the t_{10} curve (Fig. 4.20). This coincides with the model and prototype HDVS transition flow rates previously identified (section 4.4.1.1 and 4.4.2.1). The gradient becomes steeper, implying that for a small change in the mean residence time there is a greater increase in the t_{10} parameter, compared to the earlier part of the curve. This supports previous conclusions that at low flow rates i.e. longer mean residence times, both the model and prototype HDVS have improved plug-flow mixing characteristics (section 4.4.1.1 and 4.4.2.1) i.e. at low flow rates the ratio of t_{10} to the mean residence time increases. The model and prototype HDVS t_{10} parameter values both show similar trends and therefore, when using this parameter for the design of the HDVS for kinetic processes i.e. the time element of the CT product, it is independent of the size of the HDVS.

By definition the t_m/τ index should not be greater than 1. However, for both the model and prototype HDVS, this index is greater than 1 and only approaches 1 as the flow rate increases. This is due to the experimental mean residence time (t_m) being greater than the theoretical mean residence time (τ) and is discussed in detail in section 4.4.1.1. The t_{50}/t_m index measures the skew of the RTD curve to the left-hand side i.e. towards the origin. Referring to the RTD normalised curves E(Θ) (Fig. 4.8 and 4.13), this evidently occurs for both device's, as the peak of the RTD curves is before a normalised time (Θ) value of 1 and subsequently the t_{50}/t_m index is less than 1. The t_{50}/t_m index is closer to 1 at low flow rates (model HDVS < 20l/min and prototype HDVS < 60l/min) however, it generally remains constant thereafter and supports previous observations that the HDVS has a stable mixing regime at high flow rates. The

prototype HDVS t_{50}/t_m index is generally greater than the model HDVS and therefore, the prototype HDVS has improved plug-flow mixing characteristics compared to the model HDVS (section 4.4.3). A t_{50}/t_m index value of 1 would imply that the RTD curve is of a normal distribution and symmetrical about the mean i.e. first moment (n), which is preferred for effective reactor design (section 4.3.4).

All RTD indices either increase or decrease at low flow rates, depending on their individual properties and then remain stable as the flow rate increases. This supports previous conclusions that a transition flow rate exists, above and below which the HDVS's mixing regime has different characteristics and that the HDVS has a stable mixing regime at high flow rates (section 4.4.3).

The RTD indices and subsequently the conclusions obtained are influenced by the truncation time of the RTD curve. Hence, this must be considered when determining the final value of an index for the design of kinetic process applications using the CT methodology (section 4.3.4) or when comparing the efficiency of different systems.

4.4.5 Model Hydrodynamic Vortex Separator (HDVS) No Sludge Hopper - Residence Time Distribution (RTD) Pulse Experiments

The following sections present and discuss the RTD analysis undertaken on the model and prototype HDVS operating with no baseflow component and without the sludge hopper (Fig. 3.1). This was undertaken to investigate the contribution of the sludge hopper to the HDVS's mixing regime and to aid in supporting previous observations suggesting that the sludge hopper contributes to the inactive flow behaviour within the HDVS i.e. stagnant and dead volumes (section 4.4.1.1). The term 'no baseflow' refers to the HDVS operating with the sludge hopper and the RTD results are presented in the previous sections (section 4.4.1 and 4.4.2). As the general RTD

characteristics are very similar for the HDVS operating with i.e. no baseflow and without the sludge hopper, the reader is occasionally referred to section 4.4.1 and 4.4.2, which discuss the model and prototype HDVS no baseflow RTD results respectively. Additionally, as the same RTD data analysis techniques were applied to the HDVS operating with and without the sludge hopper this will aid in preventing any unnecessary repetition. The HDVS operating without the sludge hopper RTD experiments were conducted for a selection of the flow rates used for the HDVS operating with the sludge hopper.

4.4.5.1 Method of Moments Data Analysis

The same observations and conclusions for the model HDVS operating with the sludge hopper i.e. no baseflow RTD curves (section 4.4.1.1) can be applied to the RTD normalised curves E(Θ) for the model HDVS operating without the sludge hopper (Fig. 4.21). Hence, the RTD normalised curves E(Θ) (appendix C.3.4) illustrate a plug-flow mixing device, with a degree of non-ideal flow behaviour, for the reasons discussed in section 4.4.1.1. The RTD normalised curves E(Θ) also support the previous observations that there appears to be a transition flow rate, at which point the RTD curves change shape and subsequently, the mixing characteristics of the HDVS. This occurs at approximately 15l/min for the model HDVS operating without the sludge hopper and is the same as the model HDVS operating with the sludge hopper (section 4.4.1.1). The mixing characteristics of the model HDVS operating without the sludge hopper, for flow rates above and below the transition flow rate, are the same as the model HDVS operating with the sludge hopper (section 4.4.1.1).

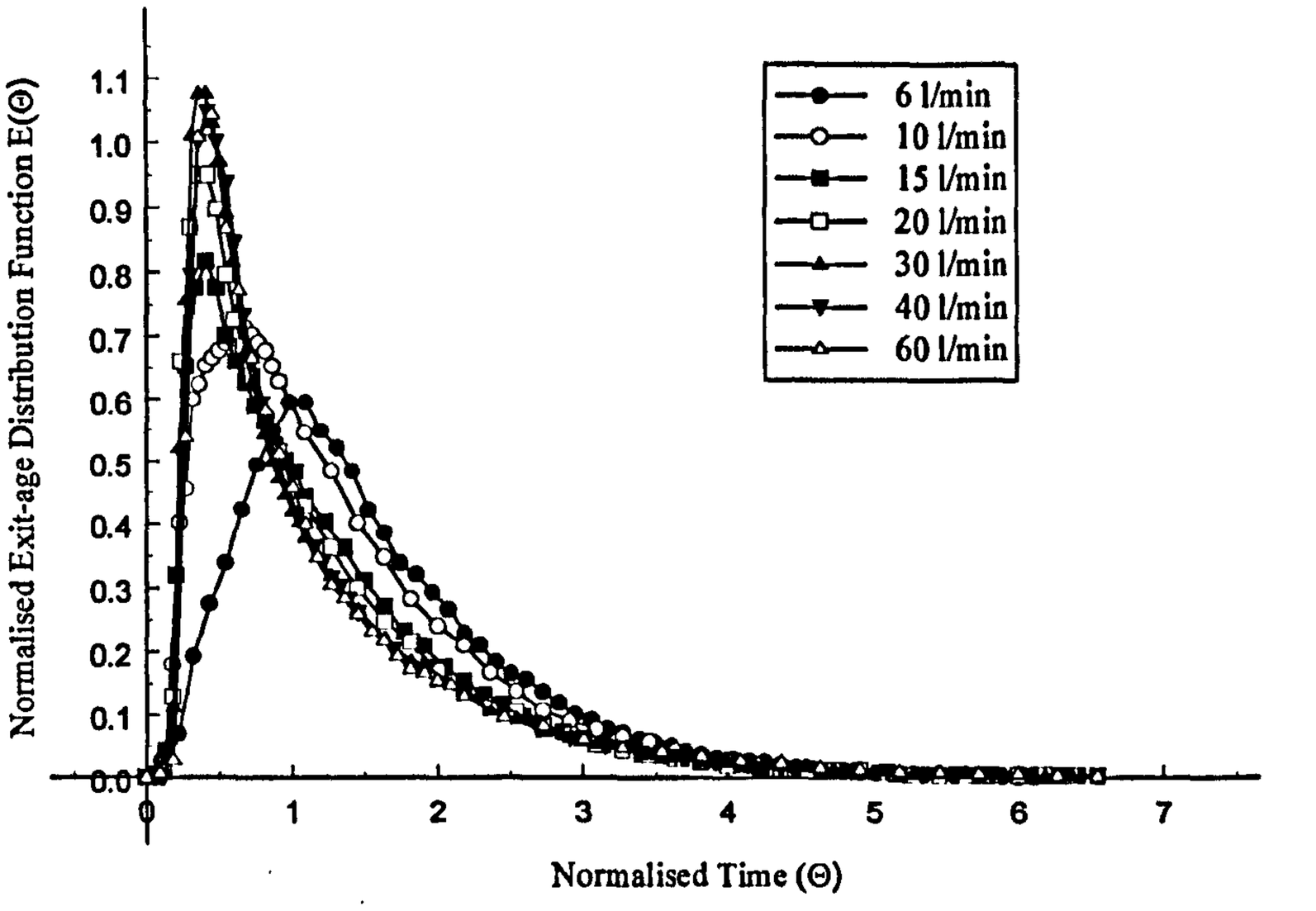

Fig. 4.21 Model HDVS No Sludge Hopper - Comparison of Normalised Exit-Age Distribution Curves E(Θ)

Table 4.13 contains the RTD experimental mean residence time and variance, calculated using the method of moments, the experimental tracer recovery (mass balance) and their associated errors. The estimated experimental mean residence time is greater than the theoretical mean residence time, with the largest error at low flow rates / longer contact times. The mass balance at 6l/min is approximately 102% and the mean residence time is approximately 57% greater than the theoretical mean residence time, compared to 106% and 25% at 60l/min respectively. The error between the experimental and theoretical mean residence time decreases up to the transition flow rate of 15l/min and then remains stable. This error between the experimental and theoretical mean residence time is discussed in detail in section 4.4.1.1. A better tracer recovery (mass balance) and a reduction in the experimental mean residence time error, particularly at low flow rates, is achieved compared to the model HDVS operating with the sludge hopper (Table 4.25). Based on the previous discussion in section 4.4.1.1, this implies that the sludge hopper contributes to the stagnant volume within the HDVS,

especially at low flow rates and therefore removing it reduces the fraction of the HDVS volume with residence times greater than the theoretical mean residence time. Subsequently this reduces the method of moments biased estimation of the first and second moments (n) and also reduces tracer hold-up (section 4.4.1.1). These combined effects result in an experimental mean residence time value closer to the theoretical mean residence time and a better tracer recovery, over the duration of the RTD experiment i.e. 6 times the theoretical mean residence time. The model HDVS operating with and without the sludge hopper RTD results are discussed and compared in section 4.4.9.1.

Table 4.13 Model HDVS No Sludge Hopper - Comparison of First and Second Moments Calculated from RTD Experimental Data

Flow Rate (l/min)	Theoretical Mean Residence Time (min)	Experimental Mean Residence Time (min)	Variance (min^2)	Experimental Mean Residence Time % Error	Tracer Mass Balance (%)
6	9.167	14.366	70.693	+56.714	102.000
10	5.500	7.7400	28.854	+40.727	99.8000
15	3.667	4.5900	12.170	+25.170	102.200
20	2.750	3.3750	7.0160	+22.727	99.4000
30	1.833	2.2180	3.6250	+21.004	104.933
40	1.375	1.6460	2.1600	+19.709	107.333
60	0.917	1.1450	0.9180	+24.864	106.000

Table 4.14 details the ADM and TISM parameters and the normalised variance calculated using the method of moments. The Peclet number (P_e) describes a device with a plug-flow mixing regime and high dispersion, $P_e<10$ (section 4.3.3). The model HDVS Peclet number (P_e) ranges from less than 1–4.57 and is equivalent to approximately 1.254–2.919 tanks-in-series (N), depending on the flow rate. All the Peclet numbers (P_e), besides the flow rates of 30 and 40l/min, are greater than 1 and therefore, the flow due to convection is generally greater than the rate of dispersion (section 4.4.1.1). The ADM and TISM parameters decrease as the flow rate increases and therefore the model HDVS has improved plug-flow mixing characteristics at low

flow rates and dispersion and mixing effects decrease. The model HDVS operating with and without the sludge hopper ADM and TISM parameters are directly compared in section 4.4.9.1 (Table 4.27).

The conflict (1) identified between the RTD curves and parameters for the model HDVS operating with the sludge hopper, does not equally apply to the model HDVS operating without the sludge hopper (section 4.4.1.1). This is due to a reduction in the stagnant volume associated with the sludge hopper and subsequently a reduced experimental mean residence time error and an improved tracer recovery (mass balance) at low flow rates as discussed above (Table 4.25). Therefore, a greater fraction of the HDVS's volume is active in the mixing process at low flow rates and the RTD parameters generally support the RTD normalised curves E(Θ) i.e. the peak of the RTD curve occurs closer to a normalised time (Θ) value of 1 (Fig. 4.21). However conflict (2), also identified for the model HDVS operating with the sludge hopper, does equally apply, although it is only a visual observation as previously stated (section 4.4.1.1).

Table 4.14 Model HDVS No Sludge Hopper - Comparison of ADM and TISM Parameters Calculated from RTD Experimental Data using the Method of Moments

Flow Rate (l/min)	Normalised Variance (σ_θ^2)	Peclet Number (P_e)	N-Tanks
6	0.343	4.57	2.919
10	0.482	2.73	2.076
15	0.578	1.93	1.731
20	0.616	1.67	1.624
30	0.737	0.99	1.357
40	0.797	0.72	1.254
60	0.700	1.18	1.428

Fig. 4.22 compares the experimental exit-age distribution function E(t) curve, to the TISM (eqn. 4.9) and ADM (eqn. 4.11) curves obtained using the method of moments, for selected flow rates. The remaining flow rates and all correlation parameters (R^2 and ESS) are presented in appendix C.3.5 and C.3.6. At flow rates below the transition flow rate of 15l/min, the TISM provides the best-fit and for higher flow rates the ADM

provides the best-fit. The best-fit for the ADM occurs at the lowest flow rate of 6l/min and the trend (R^2) is stable for the range of flow rates investigated. The TISM parameter N=3 provides the best-fit at the lowest flow rate and for all remaining flow rates N=2 provides the best-fit. The TISM correlation (R^2) decreases as the flow rate increases. The TISM correlation parameters (R^2) suggest that at the lowest flow rate, the model HDVS has marginally improved plug-flow mixing characteristics compared to all higher flow rates investigated. The relationship between the ADM and TISM correlation parameters and the HDVS's non-ideal flow behaviour is discussed in section 4.4.7.

Appendix C.3.7 shows the same RTD, ADM and TISM parameters, as presented in Table 4.13 and 4.14, for various RTD curve truncation times. The truncation times and data analysis technique using the method of moments, is the same as described for the model HDVS operating with the sludge hopper (section 4.4.1.1). Fig. 4.23 illustrates the trend in the truncated parameters at a low and high flow rate. The remaining flow rates are shown in appendix C.3.8. The results show that at the lowest flow rate of 6l/min, the experimental mean residence time at each truncation time is still greater than the theoretical mean residence time. Between 10 and 20l/min the experimental mean residence time approximates the theoretical mean residence time at truncation times of 2-3 times the theoretical mean residence time. At all flow rates greater than 20l/min the experimental mean residence time approximates the theoretical mean residence time between the truncation times of 3-4 times the theoretical mean residence time (section 4.4.1.1).

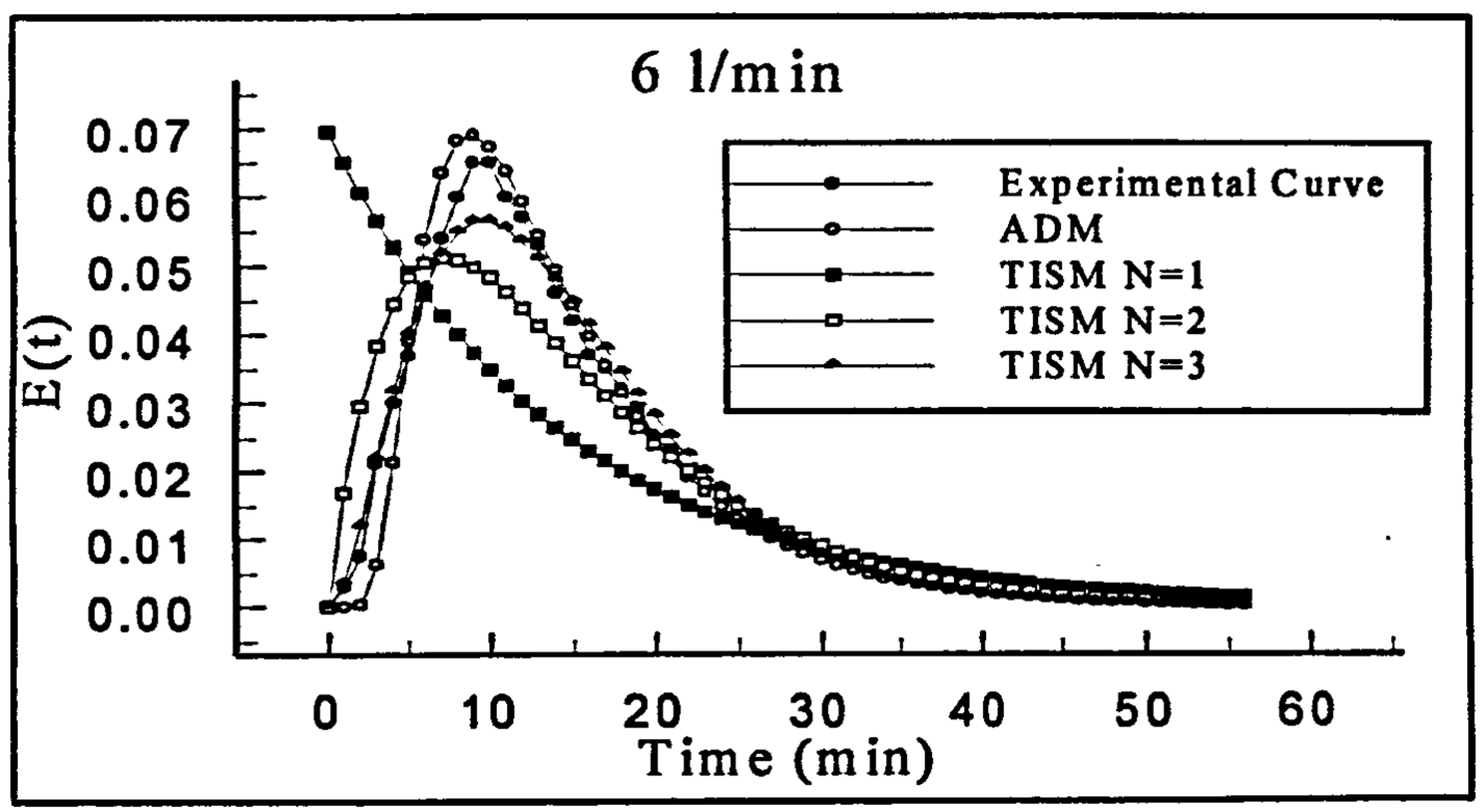

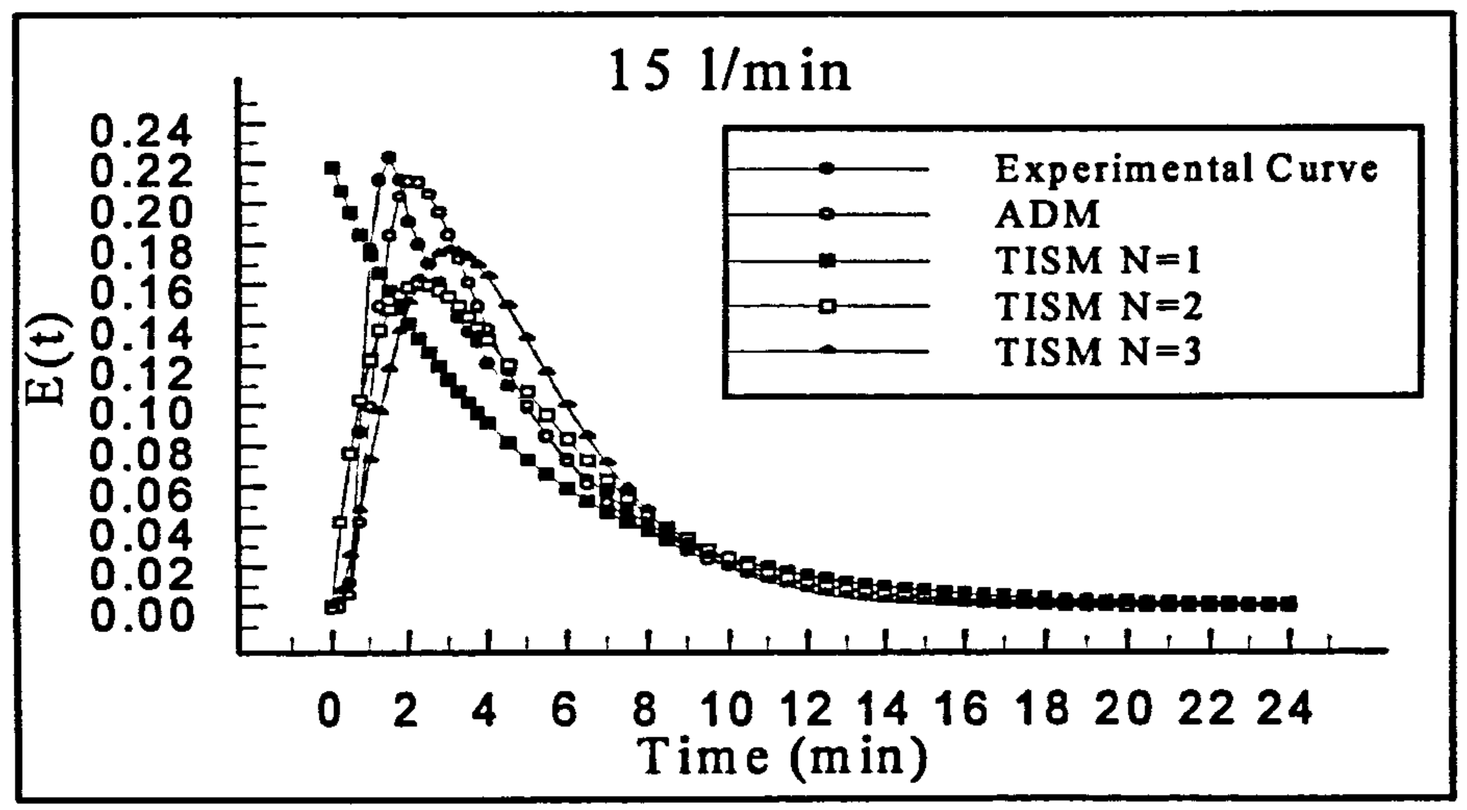

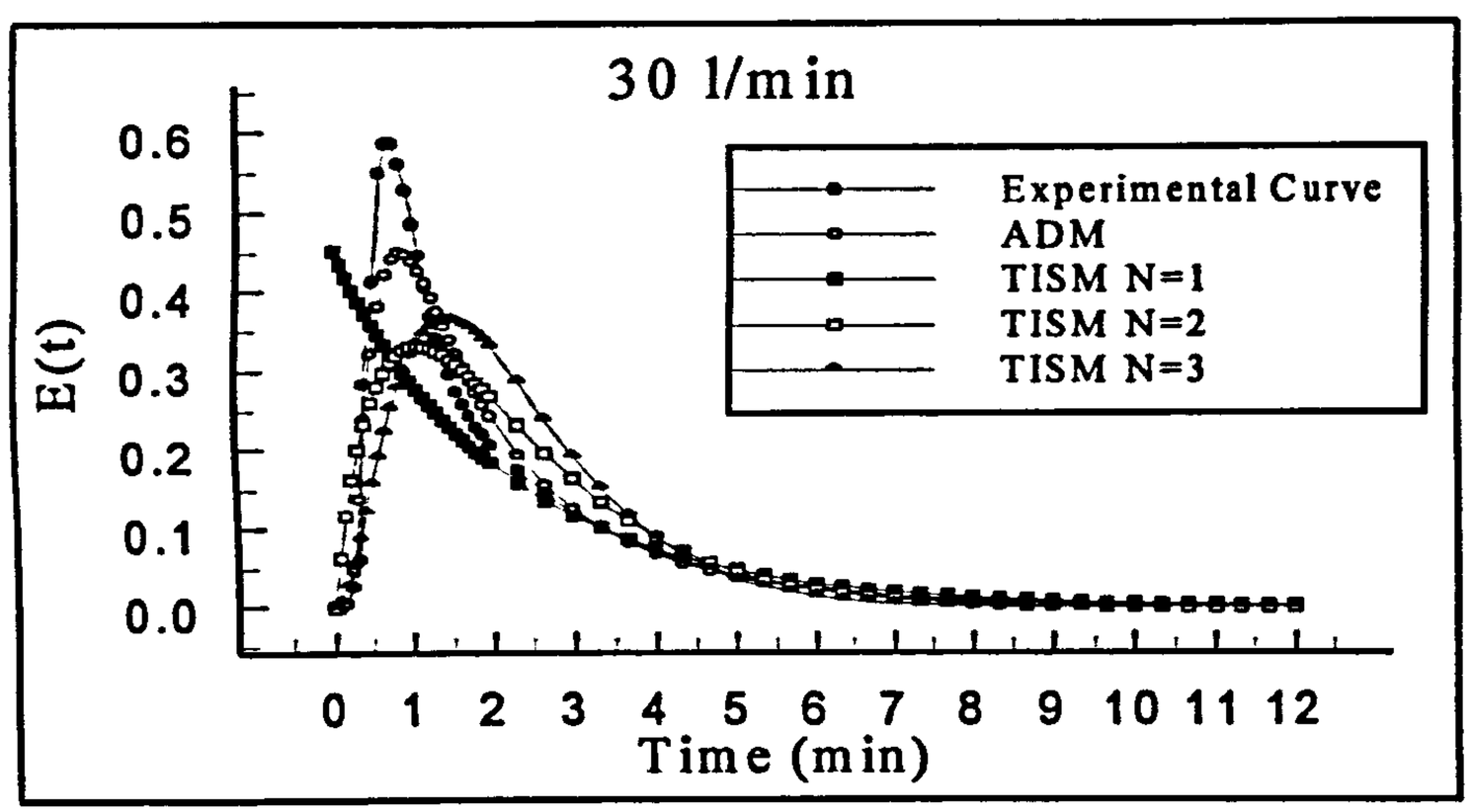

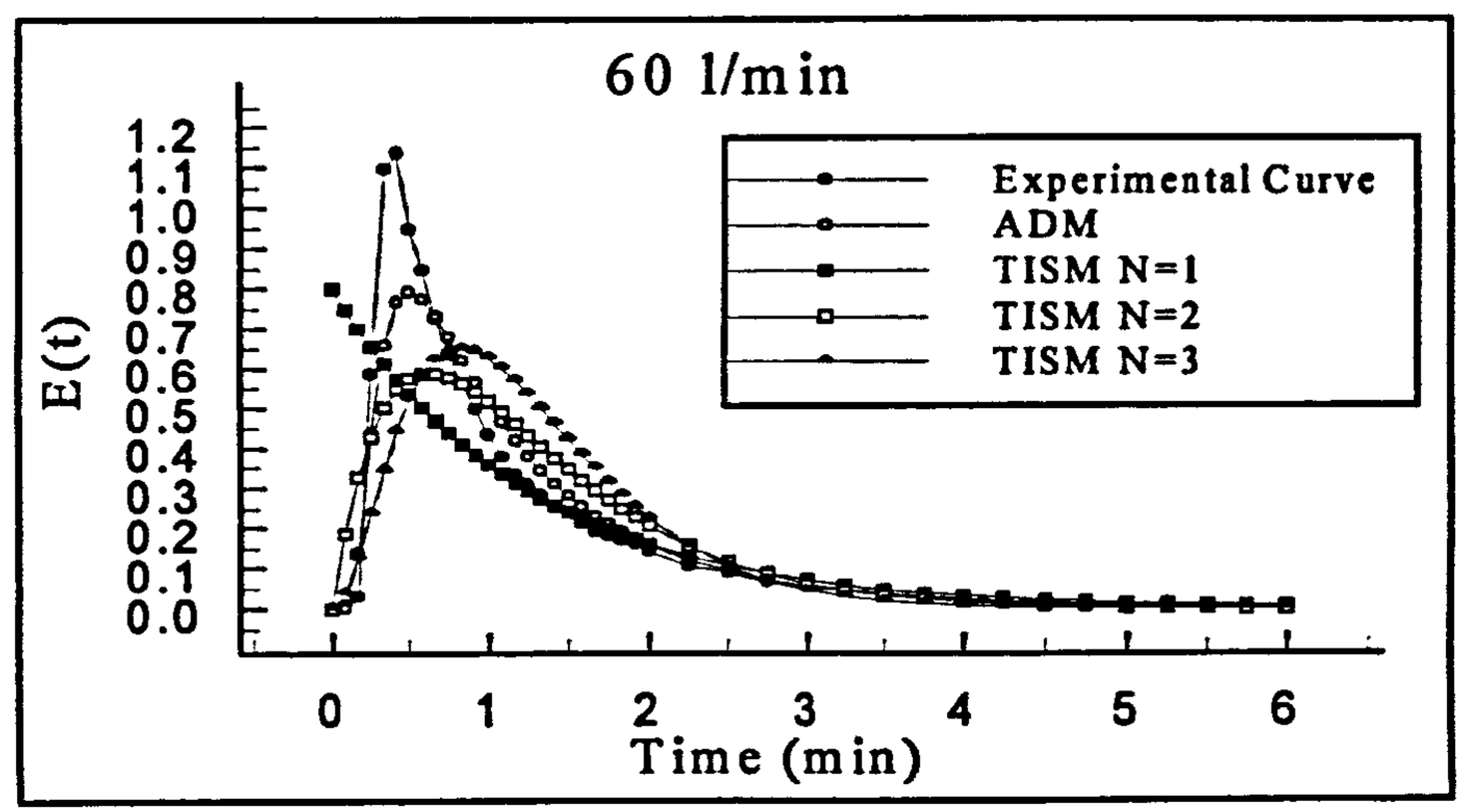

Fig. 4.22 Model HDVS No Sludge Hopper - Comparison of E(t), ADM and TISM Curves Calculated Using the Method of Moments for Selected Flow Rates

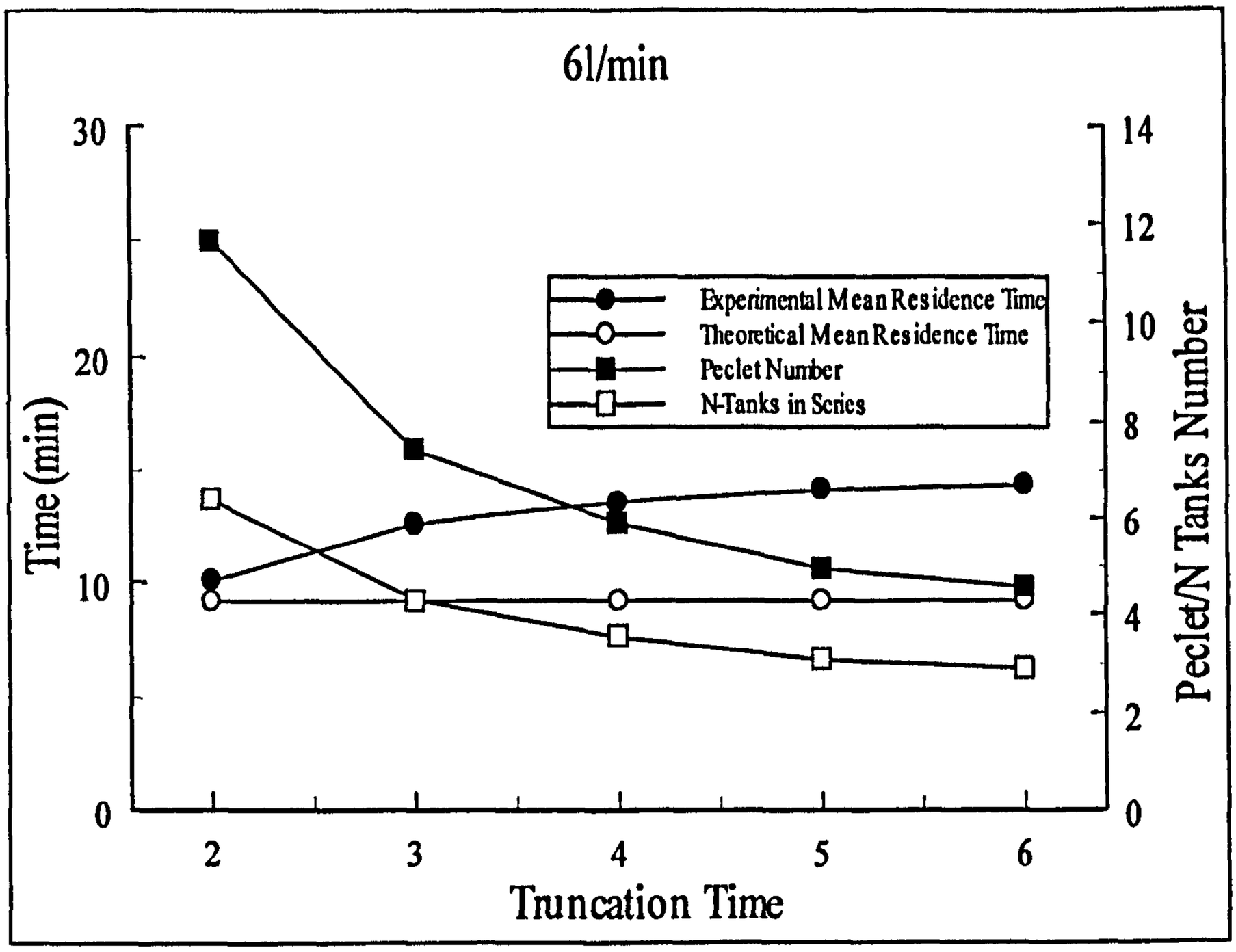

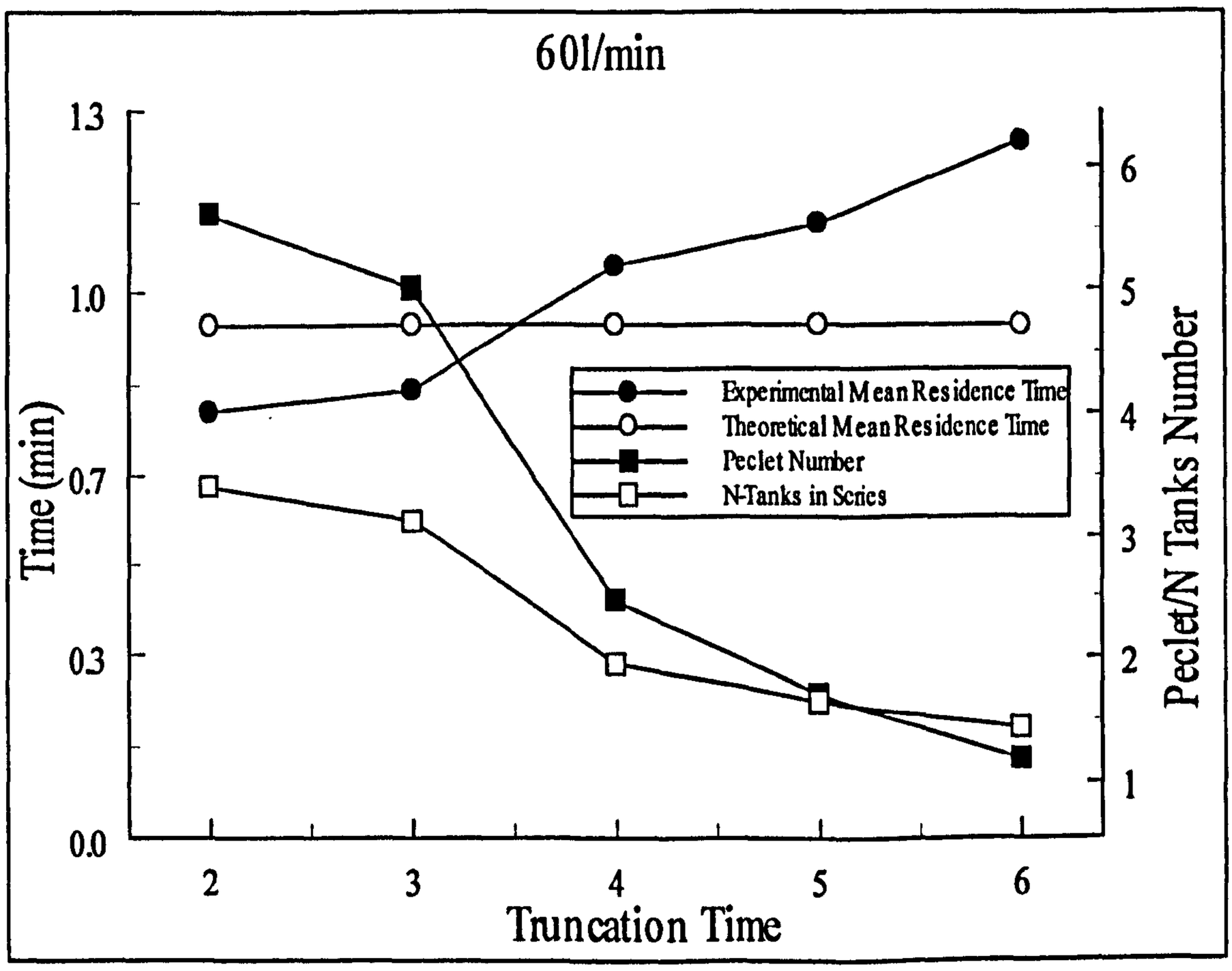

Fig. 4.23 Model HDVS No Sludge Hopper - Effect of RTD Experiment Truncation on Mean Residence Time and ADM and TISM Parameters using the Method of Moments

At the lowest flow rate of 6l/min the Peclet number (P_e) ranges from 4.57–11.65 and the number of tanks-in series (N) ranges from 2.92–6.381. Therefore the Peclet number (P_e) describes a system with moderate dispersion at 6l/min (section 4.3.3). At the highest flow rate investigated of 60l/min, the Peclet number (P_e) ranges from 1.18–5.60 and the number of tanks-in series (N) ranges from 1.43–3.402. The same observations and conclusions obtained for the model HDVS operating with the sludge hopper RTD curve truncation investigation, can be applied to the model HDVS operating without the sludge hopper (section 4.4.1.1).

The normalised intensity function $\lambda(\Theta)$ curves for the model HDVS operating without the sludge hopper (appendix C.3.9 and C.3.10) exhibit a very similar shape to the model HDVS operating with the sludge hopper intensity function $\lambda(\Theta)$ curves (Fig. 4.11). Hence, the model HDVS operating without the sludge hopper intensity function $\lambda(\Theta)$ describes a similar mixing regime as identified above, using different RTD data analysis techniques and the same conclusions obtained for the model HDVS operating with the sludge hopper apply (section 4.4.1.1).

4.4.5.2 Non-Linear Regression Data Analysis

Table 4.15 and 4.16 show the ADM and TISM parameters calculated using non-linear regression. The experimental mean residence time values calculated using non-linear regression are of a similar order of magnitude to those calculated directly from the method of moments (section 4.4.5.1). The experimental mean residence time values are also very similar regardless of the flow model used for the non-linear regression iteration i.e. TISM (eqn. 4.9) and ADM (eqn. 4.11). However for the TISM, at flow rates greater than 20l/min, the experimental mean residence time values are less than the theoretical mean residence time, which is expected from RTD studies (section 4.4.1.1).

This is shown by the mean residence time errors, which are either negligible or change from a positive to a negative error, particularly at high flow rates. This is the same relationship, as achieved for the model HDVS operating with the sludge hopper and is discussed in more detail in section 4.4.1.2. This also implies that the TISM non-linear regression parameter estimation technique is less effected by the RTD curve tail section compared to the method of moments (section 4.4.1.2). This RTD data analysis combination generally produces consistent parameters for the model HDVS operating with and without the sludge hopper compared to the method of moments (section 4.4.5.1).

The ADM Peclet number (P_e) ranges from less than 1–3.50 with the highest value occurring at the lowest flow rate. The TISM number-of-tanks (N) obtained directly from the non-linear regression technique range from 2.042–2.261, with the highest value also occurring at the lowest flow rate. The ADM and TISM parameters decrease as the flow rate increases and therefore the model HDVS has improved plug-flow mixing characteristics at low flow rates and dispersion and mixing effects decrease. The ADM and TISM parameters calculated using non-linear regression support the relationship provided by the method of moments with respect to the flow rate (section 4.4.5.1). The model HDVS operating with and without the sludge hopper ADM and TISM parameters are directly compared in section 4.4.9.1 (Table 4.28).

Table 4.15 Model HDVS No Sludge Hopper - Comparison of ADM Parameters using Non-Linear Regression

Flow Rate (l/min)	Experimental Mean Residence Time (min)	Normalised Variance (σ_θ^2)	Peclet Number (P_e)	Coefficient of Correlation (R^2)	Sum of the Errors Squared (ESS)	Experimental Mean Residence Time % Error
6	15.426	0.413	3.50	0.992	0.000396	+68.284
10	8.5040	0.803	0.70	0.985	0.003010	+54.618
15	4.9060	0.880	0.40	0.995	0.002950	+33.800
20	3.0960	0.743	0.97	0.989	0.012840	+12.582
30	1.8900	0.684	1.27	0.983	0.067000	+3.0910
40	1.4370	0.636	1.54	0.984	0.085400	+4.5090
60	0.9890	0.624	1.62	0.979	0.175000	+7.8910

Table 4.16 Model HDVS No Sludge Hopper - Comparison of TISM Parameters using Non-Linear Regression

Flow Rate (l/min)	Experimental Mean Residence Time (min)	N-Tanks	Coefficient of Correlation (R^2)	Sum of the Errors Squared (ESS)	Experimental Mean Residence Time % Error
6	15.407	2.261	0.976	0.00145	+68.076
10	7.3640	2.175	0.984	0.00329	+33.891
15	4.0630	2.042	0.965	0.01920	+10.809
20	2.7770	2.162	0.944	0.06390	+0.9820
30	1.7160	2.077	0.921	0.30160	-6.4000
40	1.3240	2.075	0.917	0.42290	-3.7090
60	0.9100	2.067	0.912	0.70000	-0.7270

Fig. 4.24 compares the experimental exit-age distribution function E(t) curve to the TISM (eqn. 4.9) and ADM (eqn. 4.11) curves obtained using non-linear regression for selected flow rates. The remaining flow rates and all correlation parameters (R^2 and ESS) are also presented in appendix C.3.11 and C.3.12. The ADM provides a better fit to the experimental data compared to the TISM, as the coefficient of correlation (R^2) values for the ADM are greater than the TISM at the same flow rate (Table 4.15 and 4.16). The better fit generally occurs as the flow rate decreases for both models and therefore, as the HDVS's mixing regime has improved plug-flow mixing characteristics. This is the same relationship as achieved for the model HDVS operating with the sludge hopper (section 4.4.1.2). The relationship between the ADM and TISM correlation parameters and the non-ideal flow behaviour is discussed in section 4.4.1.2.

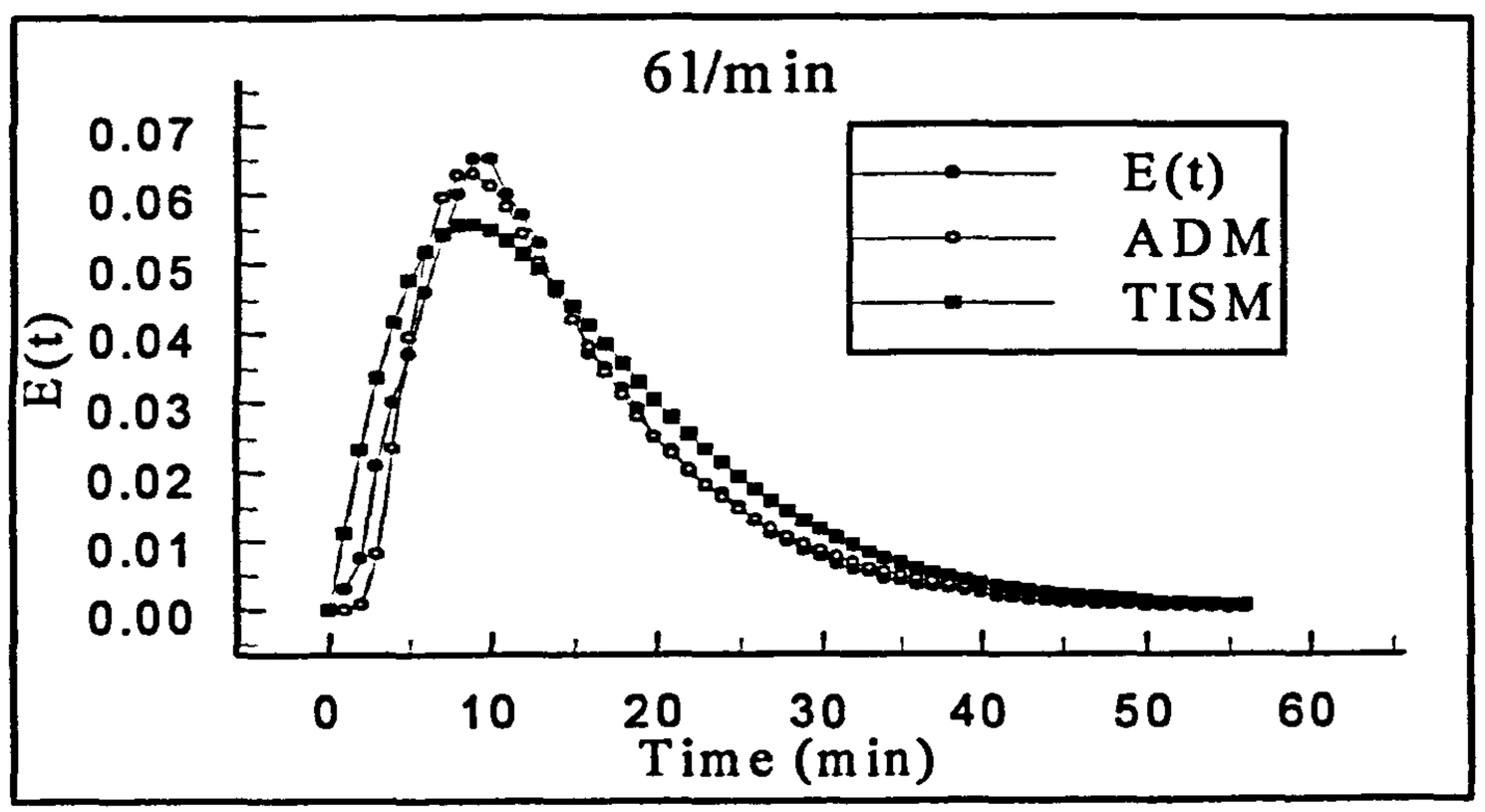

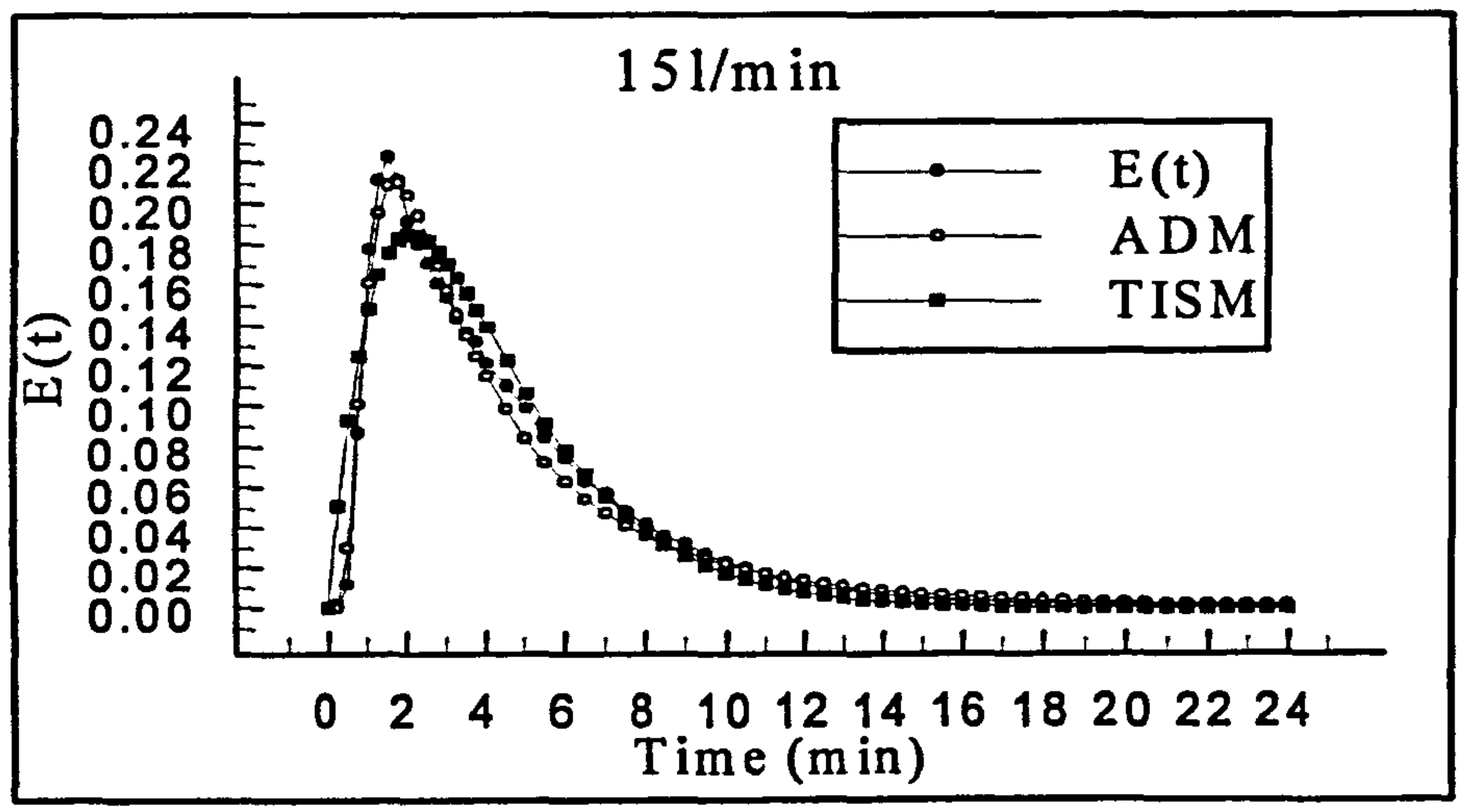

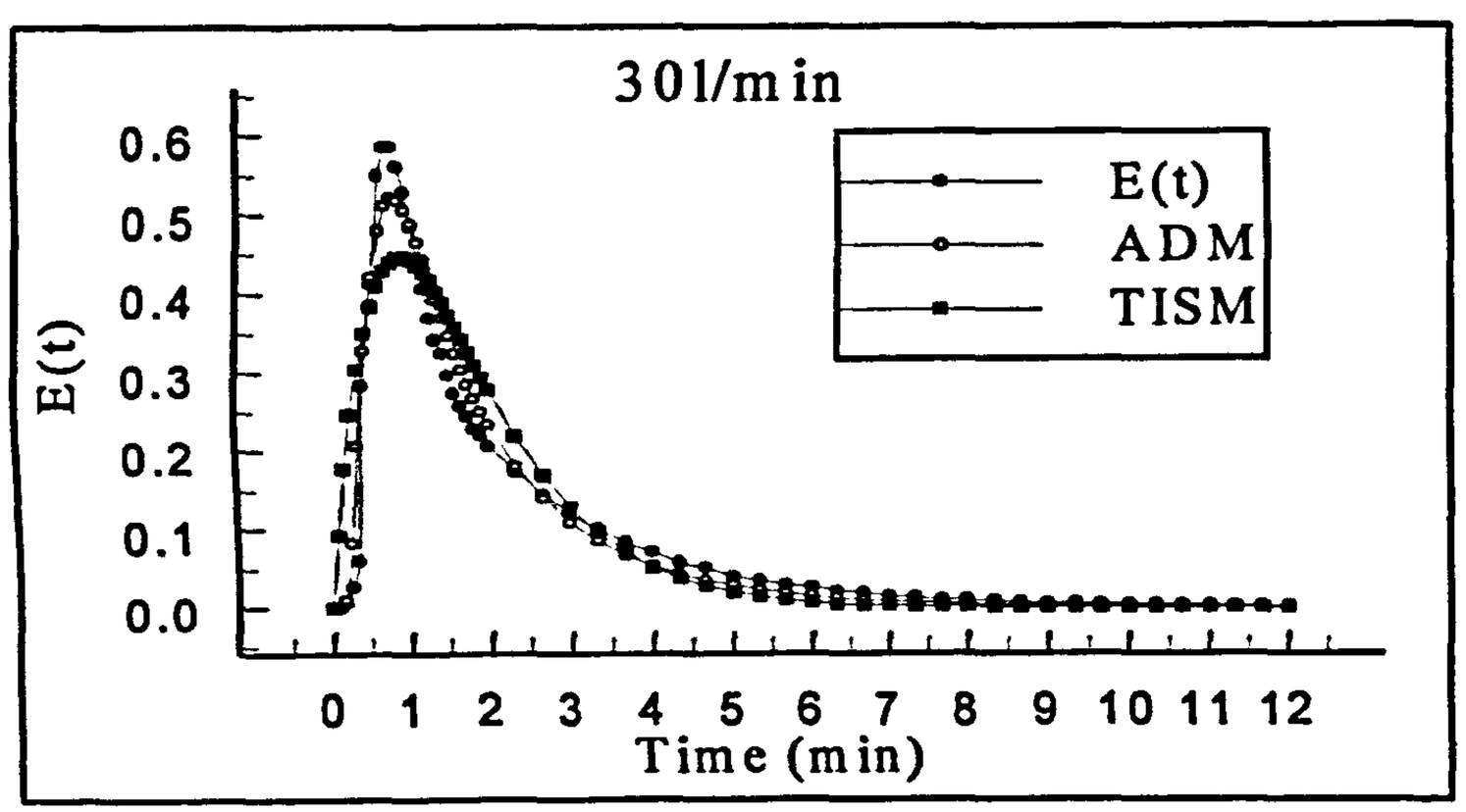

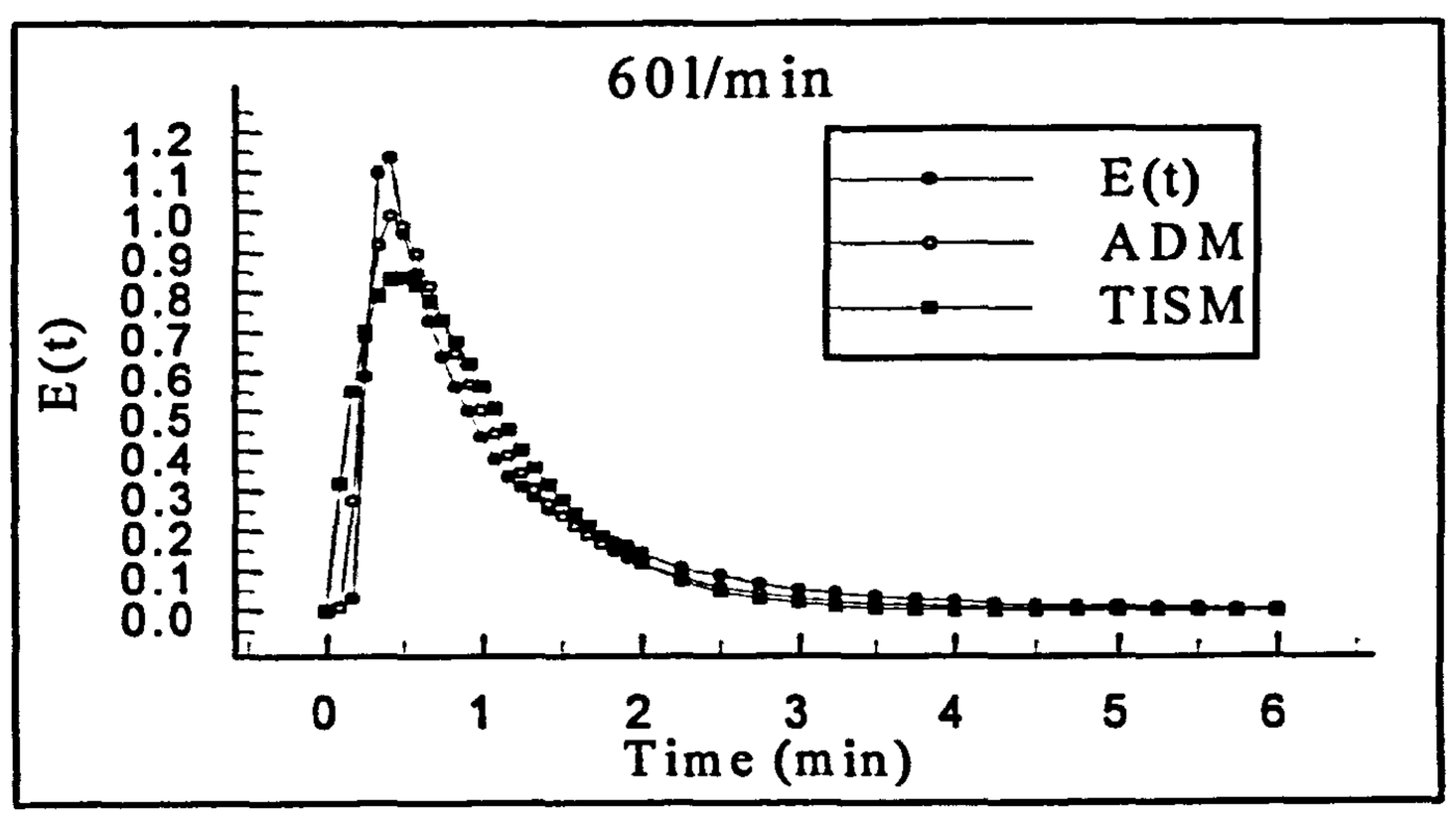

Fig. 4.24 Model HDVS No Sludge Hopper - Comparison of E(t), ADM and TISM Curves Calculated Using Non-Linear Regression for Selected Flow Rates

The model HDVS operating without the sludge hopper RTD curves were not subject to a truncation investigation using the non-linear regression technique and the reader is referred to the model HDVS operating with the sludge hopper truncation results and discussion (section 4.4.1.2). The truncation analysis is largely dependent on the shape of the RTD, which is very similar for both model HDVS operating conditions, with respect to the inlet flow rate and therefore the same general observations will apply.

4.4.6 Prototype Hydrodynamic Vortex Separator (HDVS) No Sludge Hopper - Residence Time Distribution (RTD) Pulse Experiments

4.4.6.1 Method of Moments Data Analysis

The same observations and conclusions for the prototype HDVS operating with the sludge hopper RTD curves (section 4.4.2.1), can be applied to the RTD normalised curves E(Θ) for the prototype HDVS operating without the sludge hopper (Fig. 4.25). Hence, the RTD normalised curves E(Θ) (appendix C.4.3) illustrate a plug-flow mixing device, with a degree of non-ideal flow behaviour, for the reasons discussed in section 4.4.1.1. The RTD normalised curves E(Θ) also support previous observations that there appears to be a transition flow rate (section 4.4.1.1). This occurs between 60-120l/min for the prototype HDVS operating without the sludge hopper and is the same as the prototype HDVS operating with the sludge hopper (section 4.4.2.1). The mixing characteristics of the prototype HDVS operating without the sludge hopper, for flow rates above and below the transition flow rate are described in section 4.4.1.1.

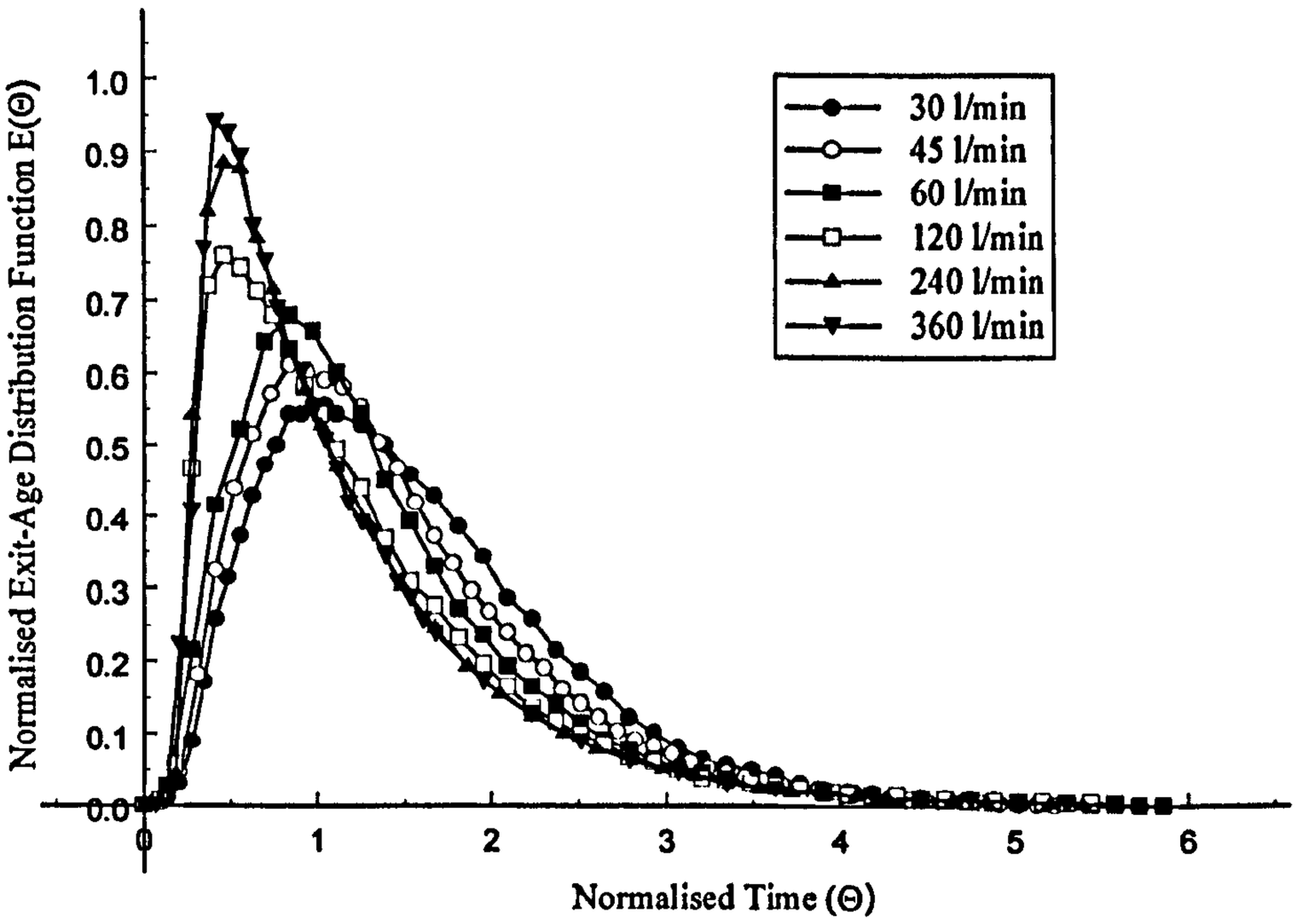

Fig. 4.25 Prototype HDVS No Sludge Hopper - Comparison of Normalised Exit-Age Distribution Curves E(Θ)

Table 4.17 contains the RTD experimental mean residence time and variance, calculated using the method of moments, the experimental tracer recovery (mass balance) and their associated errors. The estimated experimental mean residence time is greater than the theoretical mean residence time, with the largest error at low flow rates / longer contact times. The mass balance at 30l/min is approximately 91% and the mean residence time is approximately 58% greater than the theoretical mean residence time, compared to 100% and 19% at 360l/min respectively. The error between the experimental and theoretical mean residence time decreases up to the transition flow rate of 90l/min and then remains stable. As for the model HDVS operating without the sludge hopper (section 4.4.5.1), the prototype HDVS also has a better tracer recovery (mass balance) and a reduction in the experimental mean residence time error, particularly at low flow rates, compared to the prototype HDVS operating with the sludge hopper (section 4.4.2.1). Therefore the improved tracer recovery (mass balance) and reduced experimental mean time residence error, are due to the removal of the

sludge hopper, which results in a reduction of the stagnant volume within the HDVS i.e. fluid elements with residence times greater than the theoretical mean residence time (section 4.4.5.1). The prototype HDVS operating with and without the sludge hopper RTD parameters are discussed and compared in section 4.4.9.2 (Table 4.29).

Table 4.17 Prototype HDVS No Sludge Hopper - Comparison of First and Second Moments Calculated from RTD Experimental Data

Flow Rate (l/min)	Theoretical Mean Residence Time (min)	Experimental Mean Residence Time (min)	Variance (min^2)	Experimental Mean Residence Time % Error	Tracer Mass Balance (%)
30	14.333	22.705	150.752	+58.411	91.067
45	9.5560	13.641	58.8650	+42.748	99.533
60	7.1670	9.5480	33.2710	+33.222	99.467
120	3.5830	4.4330	9.58700	+23.723	103.20
240	1.7920	2.1040	2.20500	+17.411	98.000
360	1.1940	1.4240	1.03300	+19.263	99.550

Table 4.18 details the ADM and TISM parameters and the normalised variance calculated using the method of moments. The Peclet number (P_e) describes a device with a plug-flow mixing regime and high dispersion, $P_e<10$ (section 4.3.3). The prototype HDVS Peclet number (P_e) ranges from 2.48–5.65 and is equivalent to approximately 1.965–3.425 tanks-in-series (N), depending on the flow rate. The ADM and TISM parameters decrease as the flow rate increases and therefore the prototype HDVS has improved plug-flow mixing characteristics at low flow rates and dispersion and mixing effects decrease. The prototype HDVS operating with and without the sludge hopper ADM and TISM parameters are directly compared in section 4.4.9.2 (Table 4.31).

The conflict (1) identified between the RTD curves and parameters, for the prototype HDVS operating with the sludge hopper, does not equally apply to the prototype HDVS operating without the sludge hopper (section 4.4.2.1), for reasons discussed in section 4.4.5.1. However conflict (2), also identified for the prototype

HDVS operating with the sludge hopper, does equally apply, although it is only a visual observation as previously stated (section 4.4.1.1).

Table 4.18 Prototype HDVS No Sludge Hopper - Comparison of ADM and TISM Parameters Calculated from RTD Experimental Data using the Method of Moments

Flow Rate (l/min)	Normalised Variance (σ_θ^2)	Peclet Number (P_e)	N-Tanks
30	0.292	5.65	3.425
45	0.316	5.10	3.165
60	0.365	4.20	2.740
120	0.488	2.67	2.049
240	0.498	2.58	2.008
360	0.509	2.48	1.965

Fig. 4.26 compares the experimental exit-age distribution function E(t) curve, to the TISM (eqn. 4.9) and ADM (eqn. 4.11) curves obtained using the method of moments, for selected flow rates. The remaining flow rates and all correlation parameters (R^2 and ESS) are presented in appendix C.4.4 and C.4.5. At flow rates below the transition flow rate of 90l/min, the TISM provides the best-fit and for higher flow rates, the ADM provides the best-fit. The best-fit for the ADM occurs at a flow rate of 60l/min and the trend (R^2) is stable for the range of flow rates investigated. The TISM parameter N=3 provides the best-fit for flow rates less than the transition flow rate of 90l/min and the TISM parameter N=2 provides the best-fit for all the remaining flow rates. The TISM correlation (R^2) decreases as the flow rate increases. The TISM correlation parameters (R^2) suggest that at low flow rates the prototype HDVS has marginally improved plug-flow mixing characteristics compared to high flow rates. The relationship between the ADM and TISM correlation parameters and the HDVS's non-ideal flow behaviour is discussed in section 4.4.7.

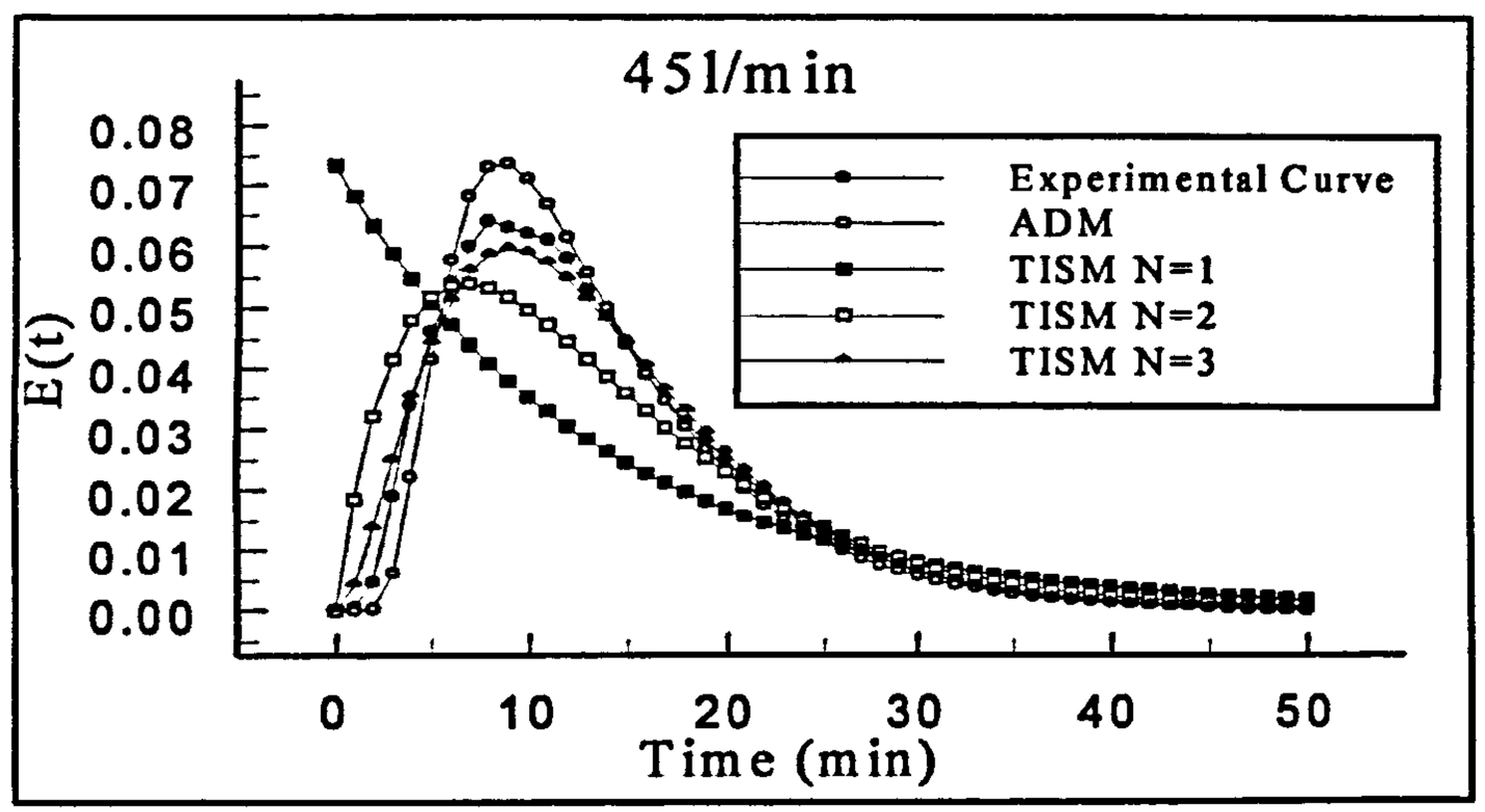

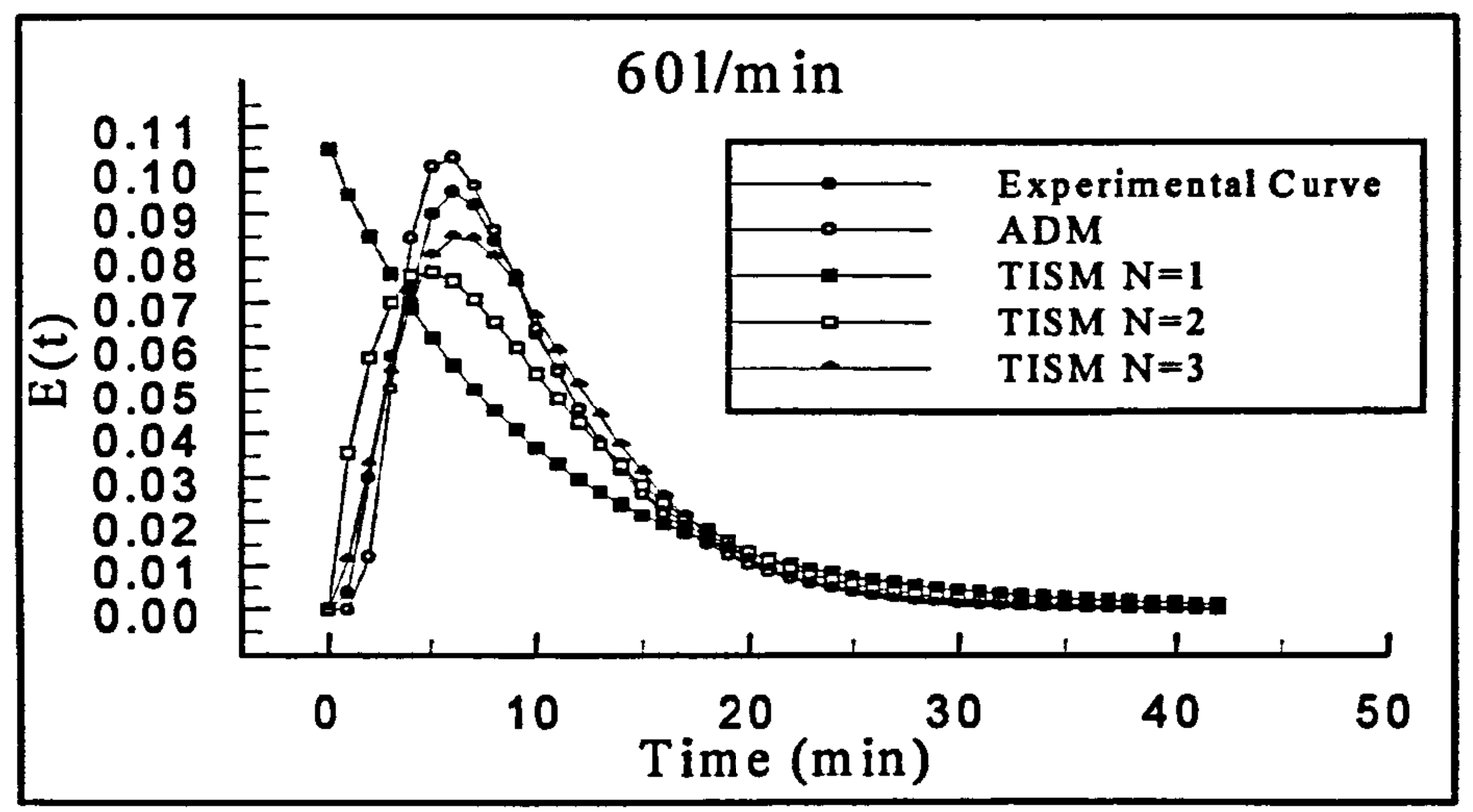

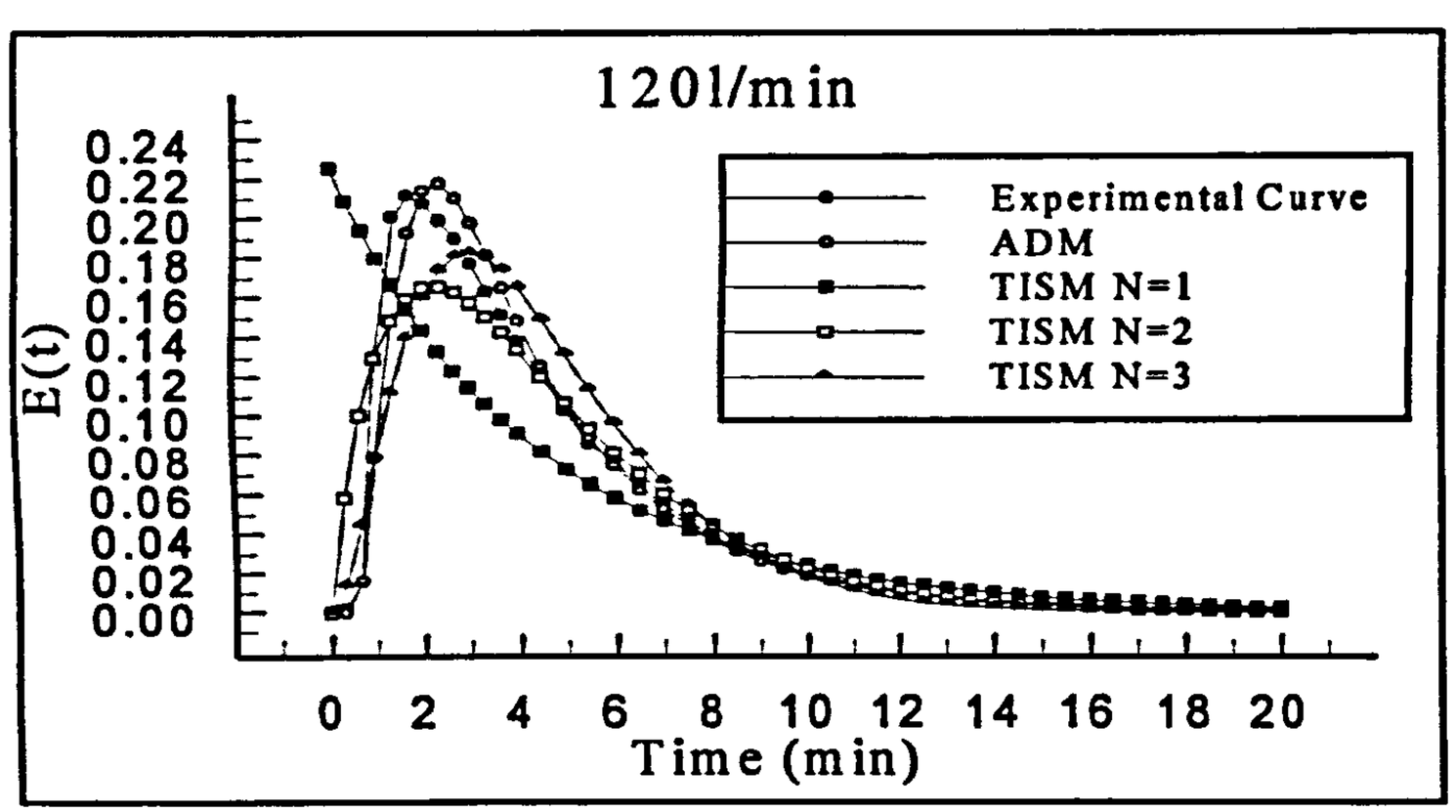

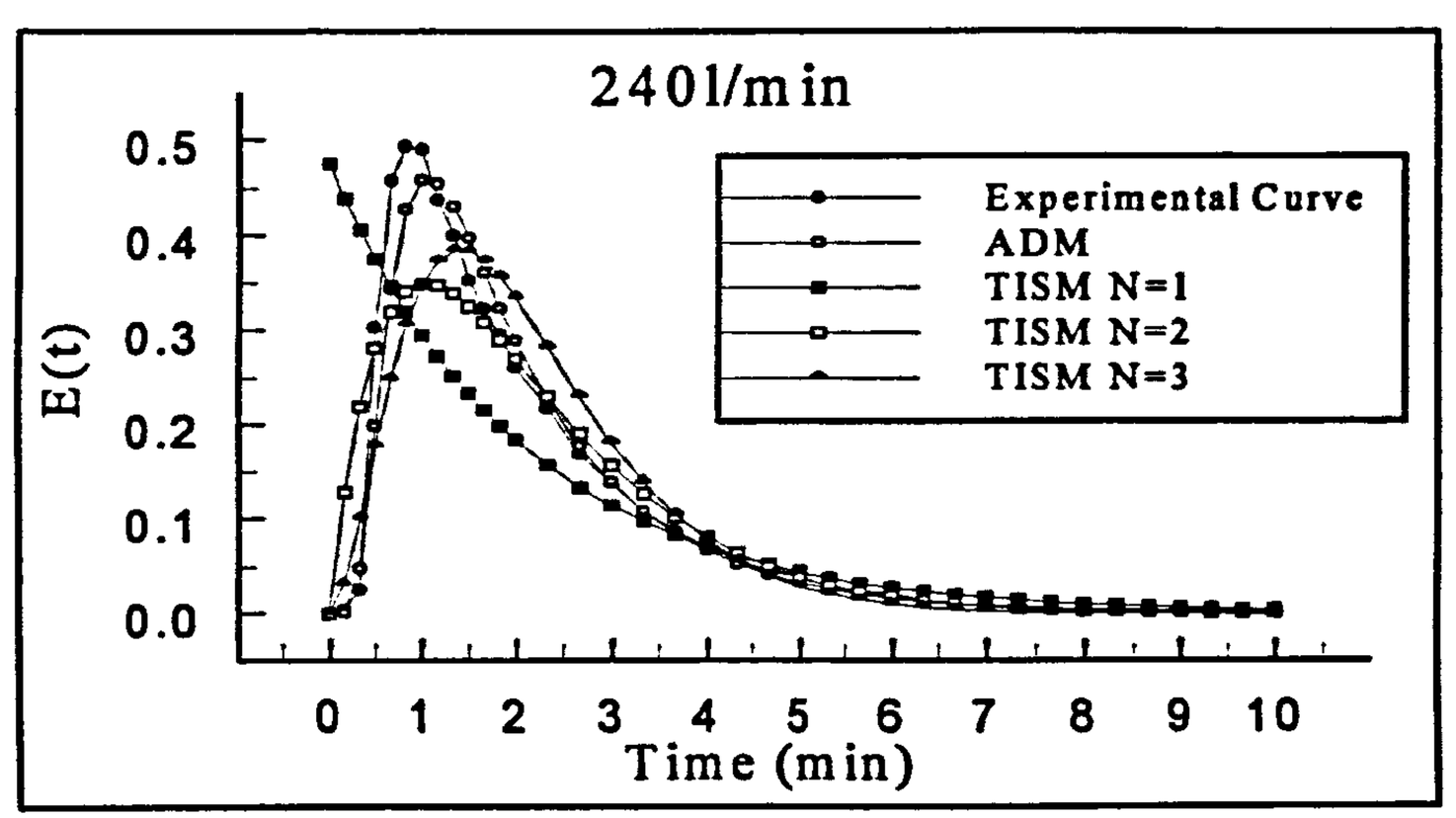

Fig. 4.26 Prototype HDVS No Sludge Hopper - Comparison of E(t), ADM and TISM Curves Calculated Using the Method of Moments for Selected Flow Rates

Appendix C.4.6 shows the same RTD, ADM and TISM parameters, as presented in Table 4.17 and 4.18, for various RTD curve truncation times. The truncation times and data analysis technique using the method of moments, is the same as described for the model HDVS operating with the sludge hopper (section 4.4.1.1). Fig. 4.27 illustrates the trend in the truncated parameters at a low and high flow rate. The remaining flow rates are shown in appendix C.4.7. The results show that for flow rates of 30-60l/min, the experimental mean residence time at each truncation time is still greater than the theoretical mean residence time. At all flow rates greater than 60l/min, the experimental mean residence time approximates the theoretical mean residence time between the truncation times of 2-3 times the theoretical mean residence time (section 4.4.1.1).

At the lowest flow rate of 30l/min the Peclet number (P_e) ranges from 5.65–12.5 and the number of tanks-in series (N) ranges from 3.425–6.807. Therefore the Peclet number (P_e) describes a system with moderate dispersion at 30l/min (section 4.3.3). At the highest flow rate investigated of 360l/min the Peclet number (P_e) ranges from 2.48–7.80 and the number of tanks-in series (N) ranges from 1.965–4.477. The same observations and conclusions obtained for the prototype HDVS operating with the sludge hopper RTD curve truncation investigation, can be applied to the prototype HDVS operating without the sludge hopper (section 4.4.2.1).

The normalised intensity function $\lambda(\Theta)$ curves for the prototype HDVS operating without the sludge hopper (appendix C.4.8 and C.4.9) exhibit a very similar shape to the prototype HDVS operating with the sludge hopper (Fig. 4.16). Hence, the same observations and conclusions apply (section 4.4.2.1) and are supported by the description of the HDVS's mixing regime provided above using different RTD data analysis techniques.

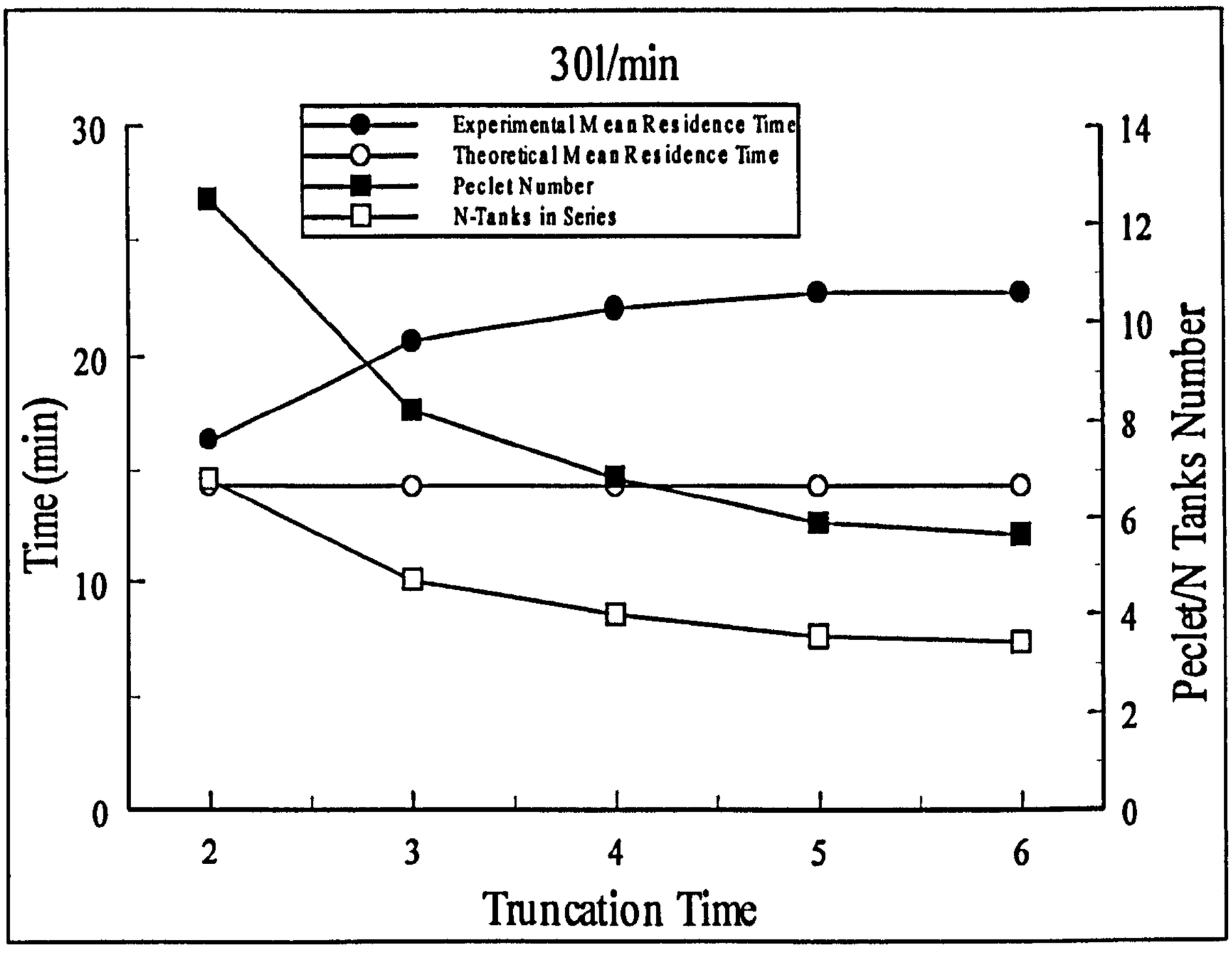

Fig. 4.27 Prototype HDVS No Sludge Hopper - Effect of RTD Experiment Truncation on Mean Residence Time and ADM and TISM Parameters using the Method of Moments

4.4.6.2 Non-Linear Regression Data Analysis

Tables 4.19 and 4.20 show the ADM and TISM parameters calculated using non-linear regression. The experimental mean residence time values calculated using non-linear regression are of a similar order of magnitude to those calculated directly from the method of moments (section 4.4.6.1). The experimental mean residence time values are also very similar regardless of the flow model used for the non-linear regression iteration i.e. TISM (eqn. 4.9) and ADM (eqn. 4.11). The experimental mean residence time values are greater than the theoretical mean residence time values for all flow rates. This is shown by the mean residence time errors, which all show a positive error. This is the same relationship as the prototype HDVS operating with the sludge hopper (section 4.4.2.2). Therefore the non-linear regression technique appears to be less effected by the RTD curve tail section, which is partly associated with the sludge hopper, compared to the method of moments. The prototype HDVS operating with and without the sludge hopper RTD parameters are discussed and compared in section 4.4.9.2 (Table 4.30).

The ADM Peclet number (P_e) ranges from 1.570–3.480, with higher values occurring at low flow rates. The TISM number of tanks (N), obtained directly from the non-linear regression curve fitting technique, range from 2.169–2.351 with the highest value occurring at the lowest flow rate and gradually decreasing as the flow rate increases. The ADM and TISM parameters decrease as the flow rate increases and therefore the prototype HDVS has improved plug-flow mixing characteristics at low flow rates and dispersion and mixing effects decrease. The ADM and TISM parameters calculated using non-linear regression support the relationship provided by the method of moments with respect to the flow rate (section 4.4.6.1). The prototype HDVS operating with and without the sludge hopper ADM and TISM parameters are directly compared in section 4.4.9.2 (Table 4.32).

Table 4.19 Prototype HDVS No Sludge Hopper - Comparison of ADM Parameters using Non-Linear Regression

Flow Rate (l/min)	Experimental Mean Residence Time (min)	Normalised Variance (σ_θ^2)	Peclet Number (P_e)	Coefficient of Correlation (R^2)	Sum of the Errors Squared (ESS)	Experimental Mean Residence Time % Error
30	24.483	0.421	3.400	0.998	0.000192	+70.812
45	14.721	0.415	3.480	0.995	0.000246	+54.057
60	10.126	0.431	3.280	0.994	0.000443	+41.293
120	4.5350	0.632	1.570	0.992	0.001660	+26.558
240	2.0160	0.577	1.930	0.992	0.009610	+12.521
360	1.3240	0.562	2.040	0.991	0.032300	+10.847

Table 4.20 Prototype HDVS No Sludge Hopper - Comparison of TISM Parameters using Non-Linear Regression

Flow Rate (l/min)	Experimental Mean Residence Time (min)	N-Tanks	Coefficient of Correlation (R^2)	Sum of the Errors Squared (ESS)	Experimental Mean Residence Time % Error
30	25.518	2.351	0.980	0.000712	+78.033
45	14.825	2.282	0.977	0.001553	+55.145
60	10.068	2.257	0.978	0.002120	+40.484
120	4.2280	2.172	0.968	0.014770	+17.991
240	1.9560	2.199	0.954	0.092800	+9.1720
360	1.2730	2.169	0.945	0.290000	+6.5770

Fig. 4.28 compares the experimental exit-age distribution E(t) curve, to the TISM (eqn. 4.9) and ADM (eqn. 4.11) curves obtained using non-linear regression, for selected flow rates. The remaining flow rates and all correlation parameters (R^2 and ESS) are also presented in appendix C.4.10 and C.4.11. The ADM provides a better fit to the experimental data compared to the TISM, as the coefficient of correlation (R^2) values for the ADM are greater than the TISM at the same flow rate (Table 4.19 and 4.20). The better fit generally occurs as the flow rate decreases for both models and therefore, as the HDVS's mixing regime has improved plug-flow mixing characteristics. This is the same relationship as achieved for the prototype HDVS operating with the sludge hopper (section 4.4.2.2). The relationship between the ADM and TISM correlation parameters and the non-ideal flow behaviour is discussed in section 4.4.1.2.

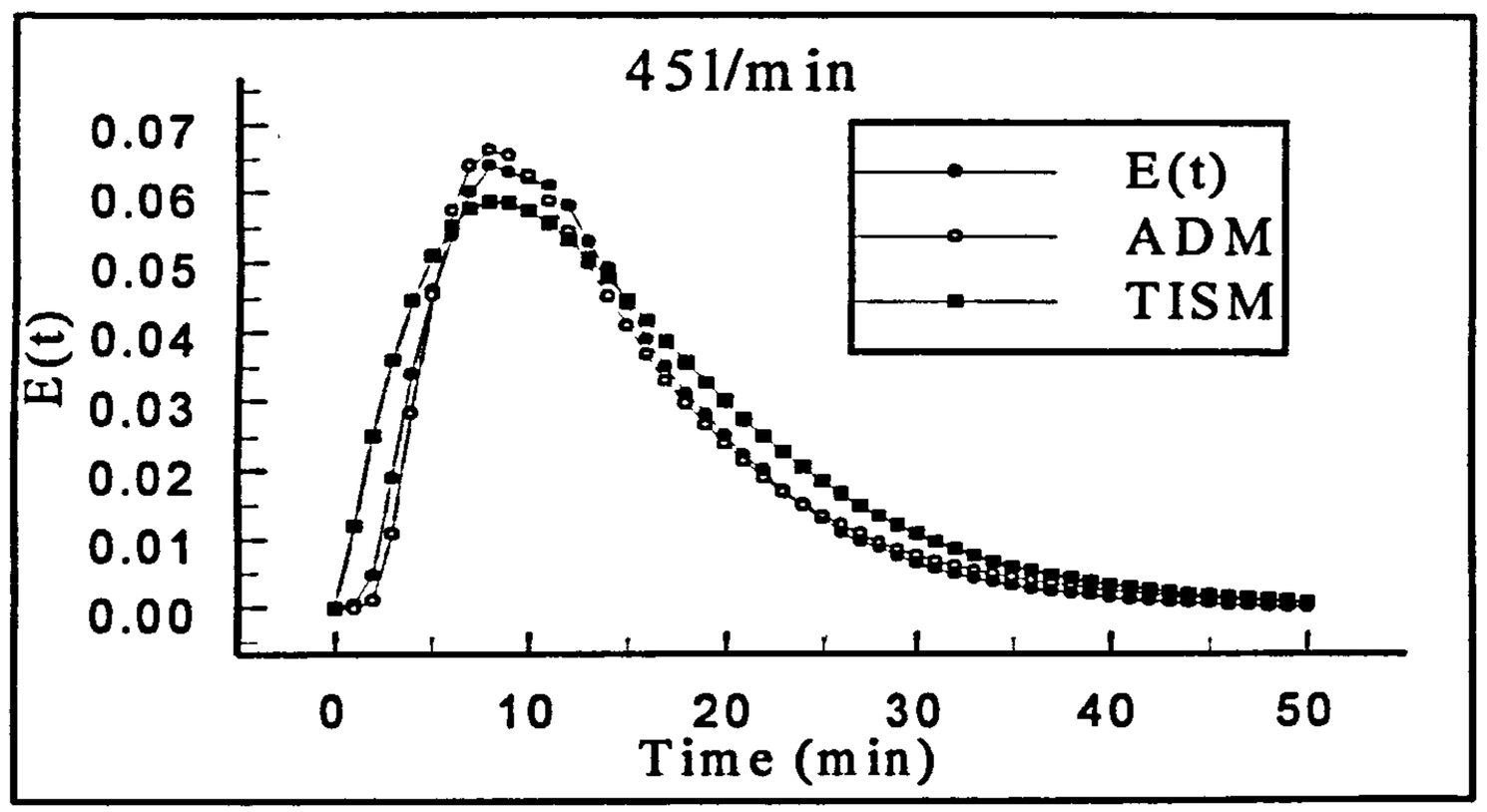

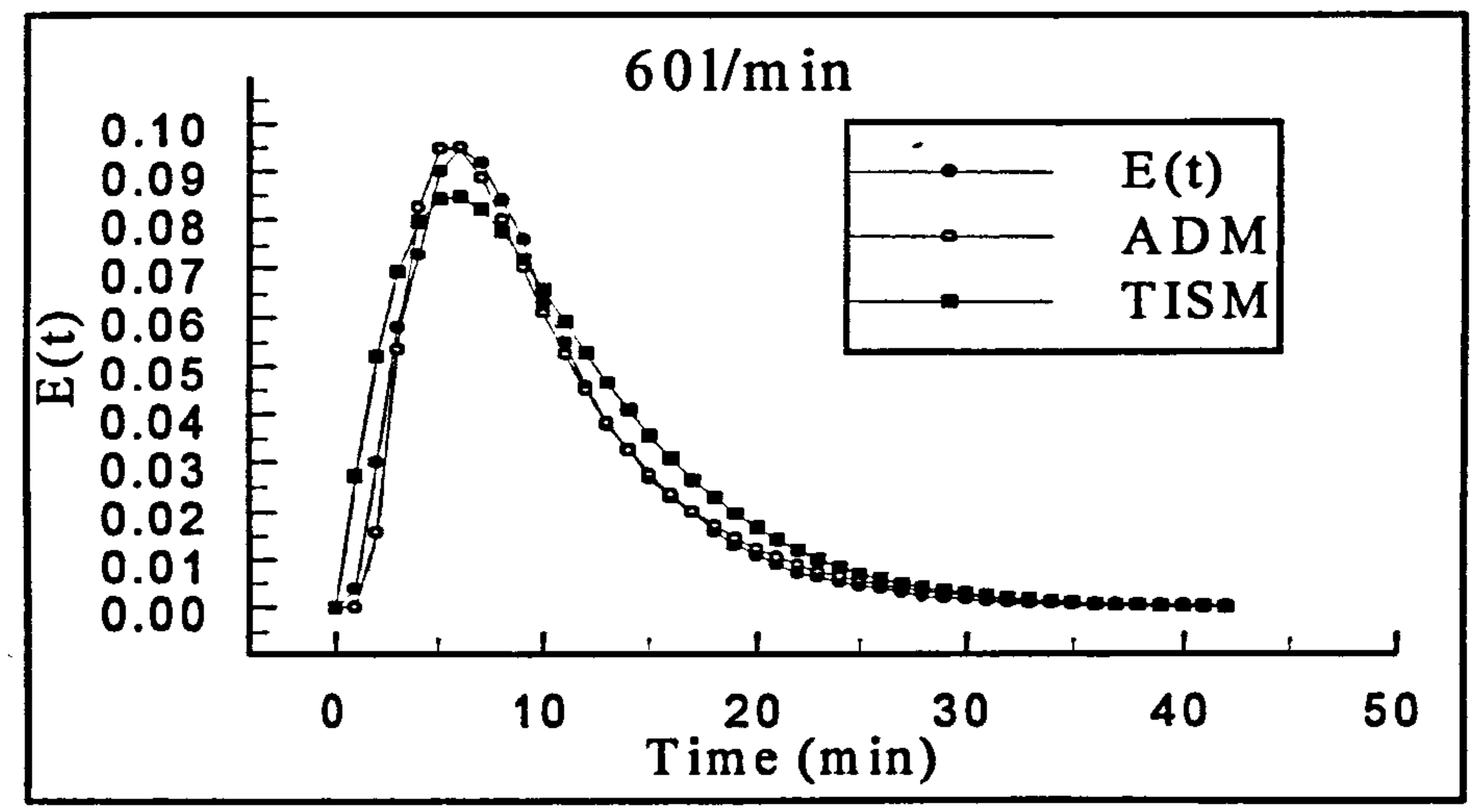

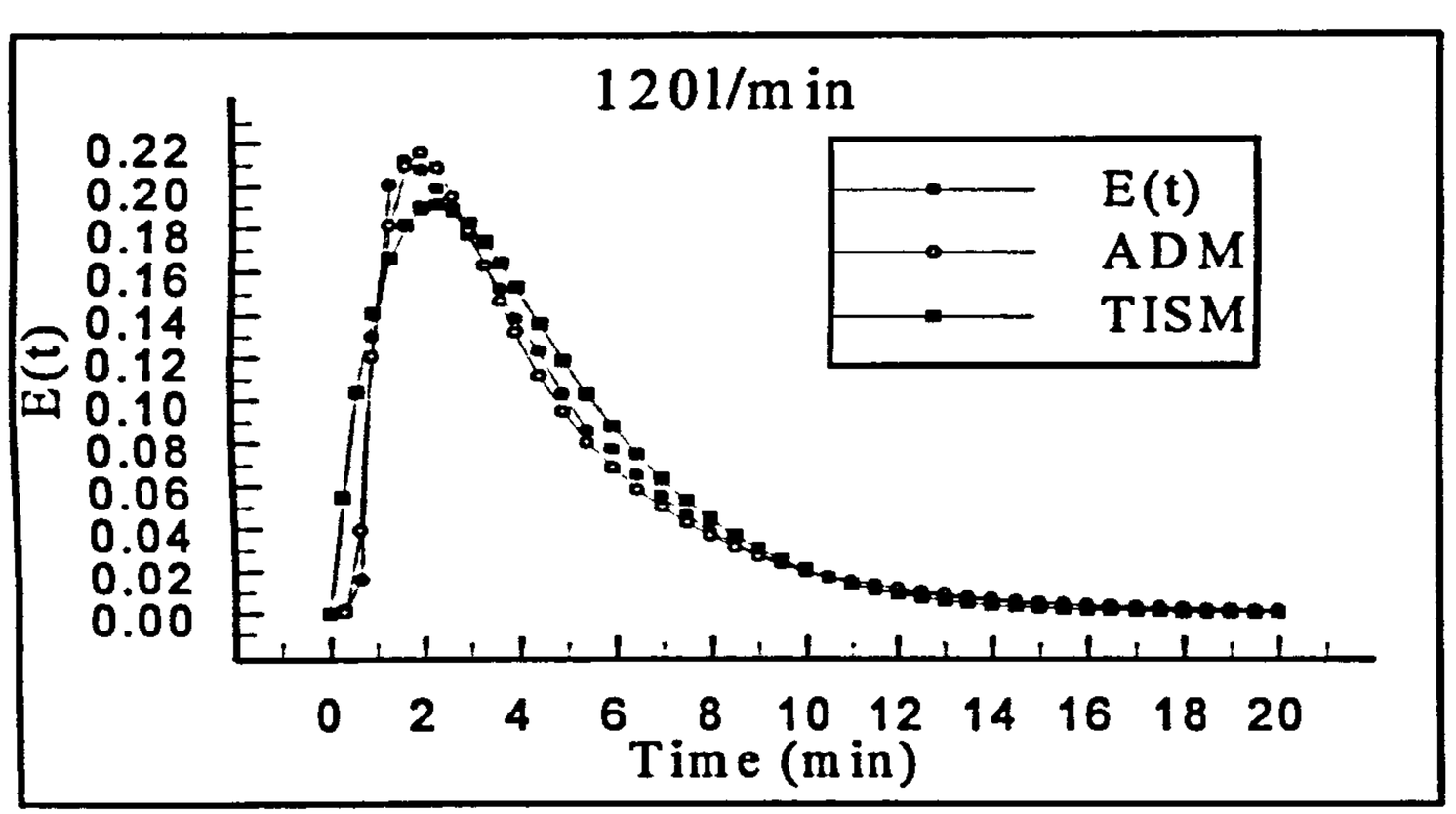

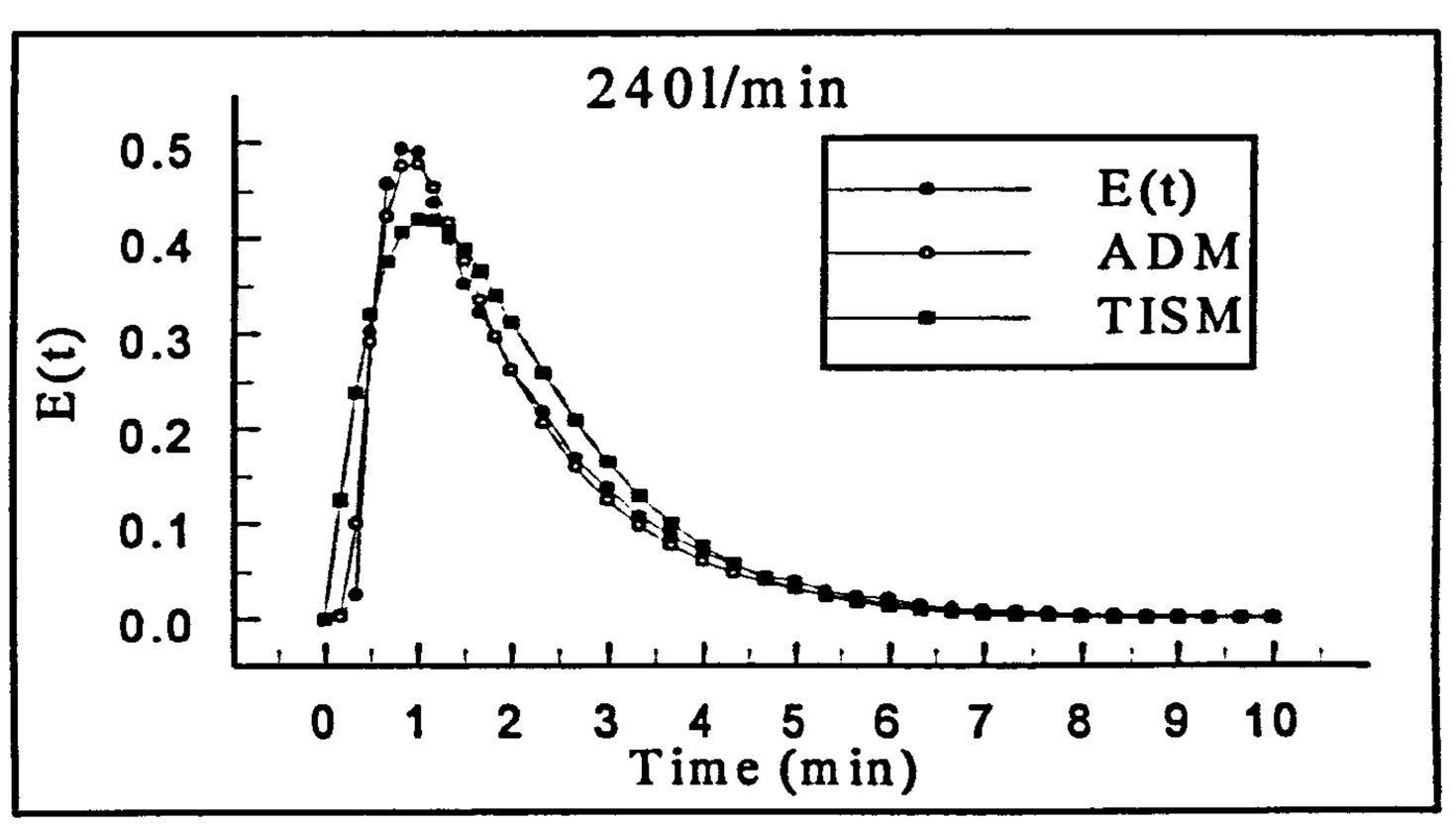

Fig 4.28 Prototype HDVS No Sludge Hopper - Comparison of E(t), ADM and TISM Curves Calculated Using Non-Linear Regression for Selected Flow Rates

The prototype HDVS operating without the sludge hopper RTD curves were not subject to a truncation investigation using the non-linear regression technique and the reader is referred to the model HDVS operating with the sludge hopper truncation results and discussion (section 4.4.1.2). The truncation analysis is largely dependent on the shape of the RTD, which is very similar for both the model and prototype HDVS operating conditions, with respect to the inlet flow rate and therefore the same general observations will apply.

4.4.7 Comparison of the Model and Prototype Hydrodynamic Vortex Separator (HDVS) No Sludge Hopper RTD Pulse Injection Results

The general RTD characteristics of the model and prototype HDVS operating with and without the sludge hopper are very similar and subsequently, throughout this section, the reader will be frequently referred to section 4.4.3. A comparison of the model and prototype HDVS operating with and without the sludge hopper is provided in section 4.4.9.

Appendix C.5.2 compares the model and prototype HDVS RTD normalised curves $E(\Theta)$ at flow rates above and below their transition flow rates i.e. 15l/min and 60-120l/min respectively. The same conclusions for both the model and prototype HDVS operating with the sludge hopper (section 4.4.3) apply to the HDVS operating without the sludge hopper. This is anticipated as removing the sludge hopper is only considered to reduce the stagnant volume within the HDVS. This would modify the RTD normalised curves $E(\Theta)$, by shifting the curves peak towards a normalised time (Θ) value of 1 and imply that a larger volume is active in the mixing process. However, this effect will be very small due to the percentage reduction in the total volume by removing only the sludge hopper. The model HDVS sludge hopper occupies 8.3% of

total volume and similarly for the prototype HDVS 7.5%. The model and prototype HDVS operating with and without the sludge hopper RTD normalised curves E(Θ) are directly compared in Fig. 4.32 and Fig. 4.33 respectively (section 4.4.9).

As for the model and prototype HDVS operating with the sludge hopper (section 4.4.3), the RTD curves are compared using the normalised exit-age distribution function E(Θ) (section 4.3.1). Similarly no operating flow rates investigated for each device provide the same theoretical mean residence time. Table 4.21 shows the model and prototype HDVS operating flow rates, which provide similar theoretical mean residence times for each device.

A comparison of the model and prototype HDVS ADM and TISM parameters calculated using the method of moments and non-linear regression is shown in Fig. 4.29 and 4.30.

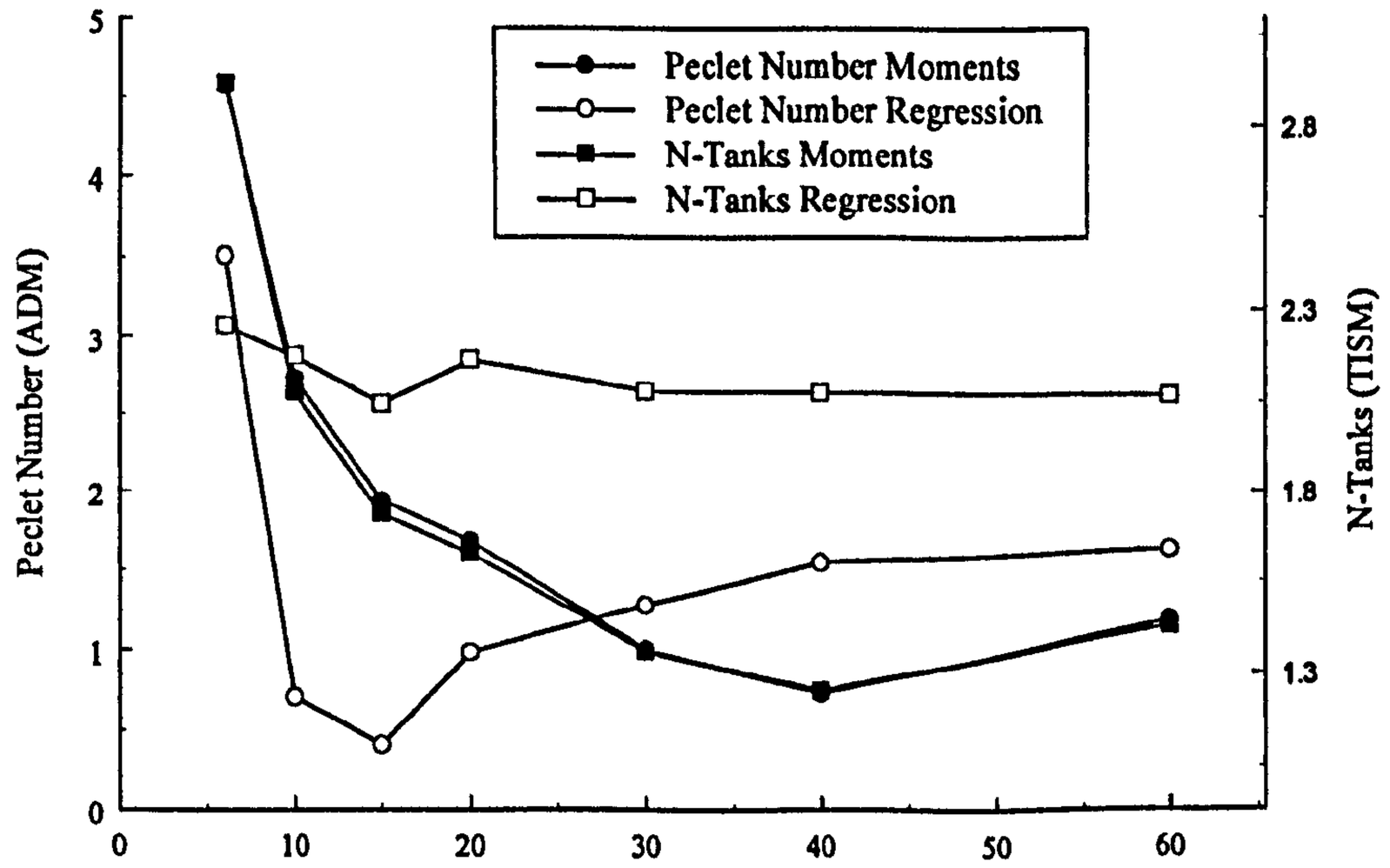

Fig. 4.29 Model HDVS No Sludge Hopper - Comparison of ADM and TISM Parameters Calculated using the Method of Moments and Non-Linear Regression

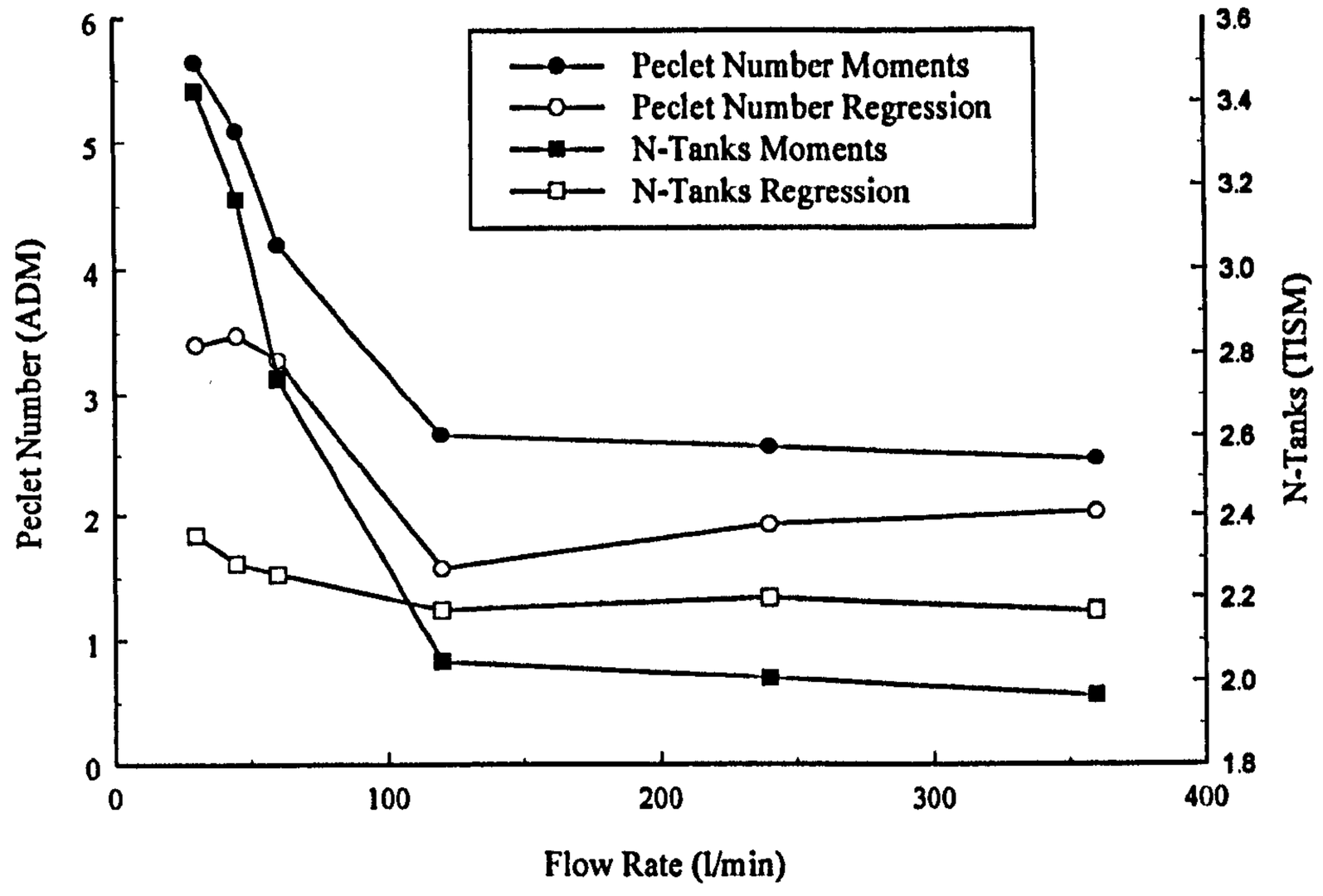

Fig. 4.30 Prototype HDVS No Sludge Hopper - Comparison of ADM and TISM Parameters Calculated using the Method of Moments and Non-Linear Regression

The ADM and TISM parameters calculated using the method of moments, for both the model and prototype HDVS, show the same decreasing trend as the flow rate increases and then become relatively stable (Fig. 4.29 and 4.30). The evidence of a transition flow rate i.e. a change in mixing characteristics, is provided by the falling section of the curves, between the lowest flow rate and the transition flow rate, where after the ADM and TISM parameters remain stable. This corresponds with the normalised exit-age distribution curves E(Θ) characteristics (Fig. 4.21 and 4.25) and therefore, supports the stable mixing regime identified at high flow rates for both the model and prototype HDVS. The model HDVS ADM and TISM parameters calculated using the method of moments range from less than 1–4.57 and 1.254-2.919 respectively and for the prototype HDVS 2.48-5.65 and 1.965-3.425 respectively. The ADM parameter for both device's, at their lowest flow rates and a truncation time of 2-3 times the theoretical mean residence time, provide a Peclet number (P_e) for a device with moderate dispersion, as opposed to high dispersion for all other flow rates (section

4.3.3). Similarly the TISM parameter implies that the HDVS is equal to approximately 6 tanks-in-series (N). Therefore the RTD experimental duration is an important parameter when classifying the HDVS's mixing regime and subsequently, for selecting the appropriate RTD design parameter to design the HDVS for kinetic process applications (section 4.4.3).

At flow rates below the transition flow rate of 15l/min, the model HDVS TISM provides the best-fit to the experimental RTD curve and for higher flow rates the ADM provides the best-fit, using the method of moments. The TISM parameter N=2 provides the best-fit to all flow rates, except at the lowest flow rate, where N=3 provides the better fit. The ADM provides the best-fit for all prototype HDVS flow rates above the transition flow rate and for flow rates less than the transition flow rate the TISM provides the best-fit. The TISM parameter N=3 provides the best-fit for flow rates less than the transition flow rate and for higher flow rates N=2 provides a better fit. Therefore the TISM correlation parameters suggest that the model and prototype HDVS have better plug-flow mixing characteristics at low flow rates. Additionally the prototype HDVS has improved plug-flow mixing characteristics for a greater range of flow rates compared to the model HDVS.

The model HDVS ADM and TISM parameters calculated using non-linear regression range from less than 1–3.50 and 2.042-2.261 respectively and for the prototype HDVS 1.57-3.48 and 2.169-2.351 respectively. The ADM provides the best-fit for all model and prototype HDVS flow rates compared to the TISM. The ADM and TISM parameters obtained using non-linear regression remain relatively constant across the range of model and prototype HDVS flow rates investigated (Table 4.22). However the values do show a slight decreasing trend as the flow rate increases, although not to the same extent as the ADM and TISM parameters calculated using the method of moments (Table 4.21) and therefore provide less evidence of a transition flow rate. This

is shown in Fig. 4.29 and 4.30 as the ADM and TISM parameters decrease up to the transition flow rate and then remain stable. Therefore the model and prototype HDVS ADM and TISM parameters, calculated using both the method of moments and non-linear regression, show that plug-flow mixing characteristics increase and dispersion and mixing effects decrease, as the flow rate decreases (section 4.1). Additionally the stable mixing regime identified within HDVS at high flow rates is associated with both the inactive flow behaviour and the plug-flow mixing characteristics.

Table 4.21 Model and Prototype HDVS No Sludge Hopper – Comparison of ADM and TISM Parameters Calculated using the Method of Moments

Model HDVS		Prototype HDVS		Peclet Number (P_e)		N-Tanks	
Flow Rate (l/min)	Theoretical Mean Residence Time (min)	Flow Rate (l/min)	Theoretical Mean Residence Time (min)	Model HDVS	Prototype HDVS	Model HDVS	Prototype HDVS
6	9.167	45	9.556	4.57	5.10	2.919	3.165
15	3.667	120	3.583	1.93	2.67	1.731	2.049
30	1.833	240	1.792	0.99	2.58	1.357	2.008
60	0.917	360	1.194	1.18	2.48	1.428	1.965

Table 4.22 Model and Prototype HDVS No Sludge Hopper – Comparison of ADM and TISM Parameters Calculated using Non-Linear Regression

Model HDVS		Prototype HDVS		Peclet Number (P_e)		N-Tanks	
Flow Rate (l/min)	Theoretical Mean Residence Time (min)	Flow Rate (l/min)	Theoretical Mean Residence Time (min)	Model HDVS	Prototype HDVS	Model HDVS	Prototype HDVS
6	9.167	45	9.556	3.50	3.48	2.261	2.282
15	3.667	120	3.583	0.40	1.57	2.042	2.172
30	1.833	240	1.792	1.27	1.93	2.077	2.199
60	0.917	360	1.194	1.62	2.04	2.067	2.169

The model and prototype HDVS ADM and TISM parameters are of a similar order of magnitude and therefore, operate with a very similar and stable mixing regime, particularly above their respective transition flow rates. However the prototype HDVS ADM and TISM parameters are generally greater than the model HDVS, at a flow rate

providing a similar theoretical mean residence time within each device. This is illustrated by the ADM and TISM parameters calculated using either the method of moments or non-linear regression (Table 4.21 and 4.22). Therefore the prototype HDVS has marginally improved plug-flow mixing characteristics compared to the model HDVS. Hence, as the HDVS is scaled-up its plug-flow mixing and active volume characteristics are improved.

The same observations and conclusions obtained from the correlation parameters (R^2 and ESS) for the HDVS operating with the sludge hopper, apply to the HDVS operating without the sludge hopper (section 4.4.3). This includes a comparison of the ADM and TISM correlation parameters obtained using the method of moments and non-linear regression parameter estimation techniques, their relationship with the HDVS non-ideal flow behaviour and the limitations of both model's, with respect to the flow rate.

4.4.8 Model and Prototype Hydrodynamic Vortex Separator (HDVS) No Sludge Hopper - Residence Time Distribution (RTD) Indices

Table 4.23 and 4.24 present the model and prototype HDVS operating without the sludge hopper RTD indices, calculated from the parameters described in section 4.3.4. The t_f/τ index measures the most severe short-circuiting. Both the model and prototype HDVS exhibit a large degree of short-circuiting with values approaching that expected for complete mixing conditions. The values for both device's decrease as the flow rate increases. Subsequently the t_p/τ index, which gives an indication of the effective volume of the device, provides the same trend for both the model and prototype HDVS.

Table 4.23 Model HDVS No Sludge Hopper - RTD Indices Calculated from Experimental Curves using the Method of Moments

Flow Rate (l/min)	t_f/τ	t_p/τ	t_{90}/t_{10}	t_m/τ	t_{50}/t_m
6	0.109	0.982	5.200	1.567	0.835
10	0.136	0.727	7.000	1.407	0.775
15	0.068	0.409	7.200	1.252	0.763
20	0.121	0.364	7.800	1.227	0.741
30	0.091	0.364	7.429	1.210	0.639
40	0.182	0.424	8.000	1.197	0.658
60	0.091	0.454	6.757	1.249	0.655

Table 4.24 Prototype HDVS No Sludge Hopper - RTD Indices Calculated from Experimental Curves using the Method of Moments

Flow Rate (l/min)	t_f/τ	t_p/τ	t_{90}/t_{10}	t_m/τ	t_{50}/t_m
30	0.070	1.047	4.222	1.584	0.881
45	0.105	0.837	4.800	1.427	0.880
60	0.140	0.837	5.667	1.332	0.838
120	0.093	0.465	6.377	1.237	0.752
240	0.093	0.465	6.000	1.174	0.713
360	0.070	0.419	6.400	1.193	0.702

The t_{90}/t_{10} index (Morrill Dispersion Index) increases as the flow rate increases and therefore there is greater spreading of the RTD curve at high flow rates. The theoretical values for this index are 1 for plug-flow mixing and 21.9 for complete mixing. The values range from approximately 30-50% of the theoretical value for complete mixing conditions (section 4.4.4). The model and prototype HDVS t_{10} parameter, which is occasionally used as the time element (T) in the design of contact tanks using the CT methodology (section 4.3.4), is illustrated in Fig. 4.31. The same conclusions obtained for the HDVS operating with the sludge hopper t_{10} parameter curves (section 4.4.4), apply to the model and prototype HDVS operating without the sludge hopper.

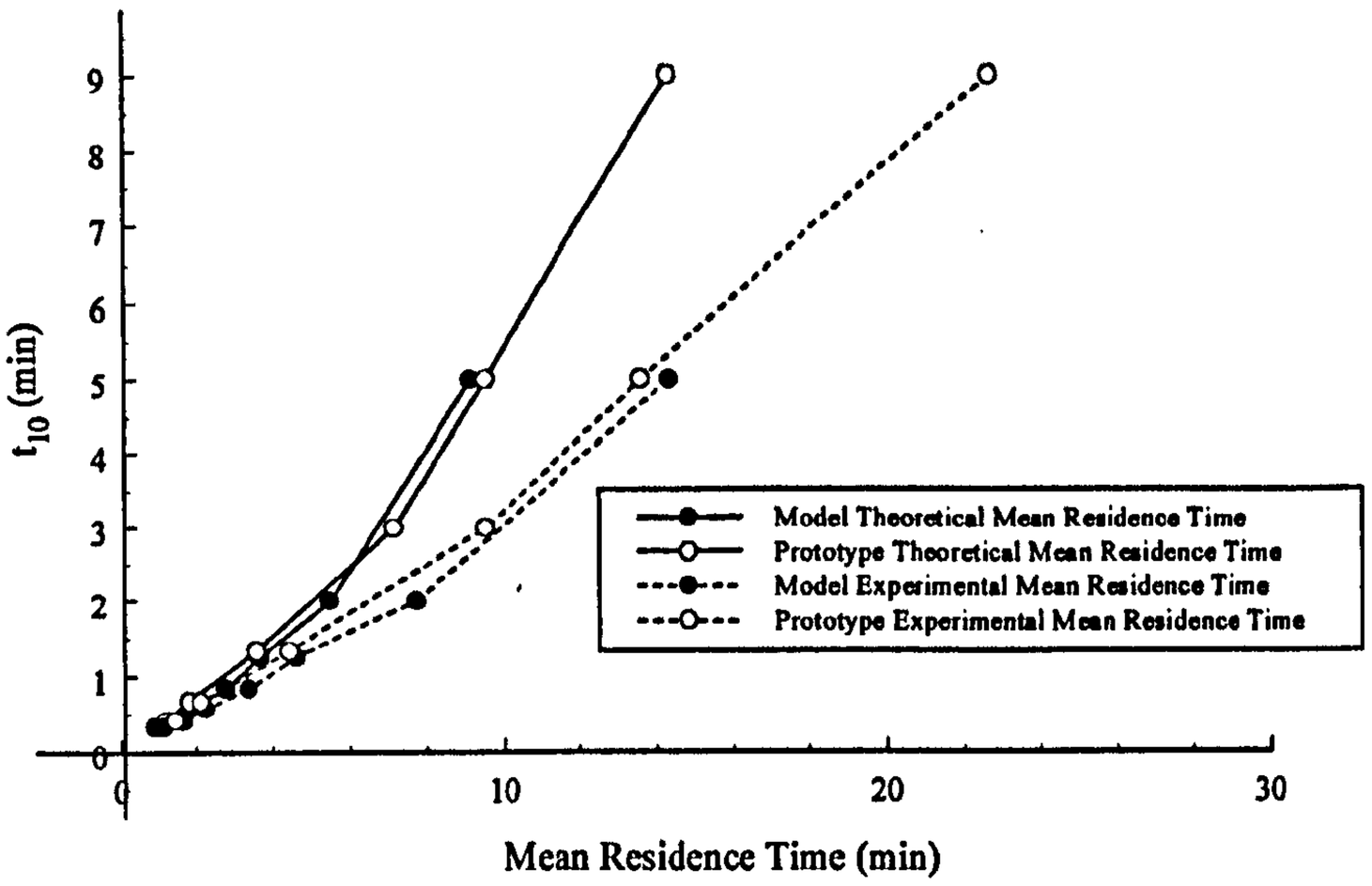

Fig. 4.31 Model and Prototype HDVS No Sludge Hopper - Relationship Between RTD t_{10} Parameter and Mean Residence Time for all Flow Rates using the Method of Moments

By definition the t_m/τ index should not be greater than 1. However, for both the model and prototype HDVS, this index is greater than 1 and only approaches 1 as the flow rate increases. This is due to the experimental mean residence time (t_m) being greater than the theoretical mean residence time (τ) and is discussed in detail in section 4.4.1.1. The t_{50}/t_m index measures the skew of the RTD curve to the left-hand side. Referring to the RTD normalised distribution curves E(Θ) (Fig. 4.21 and 4.25), this evidently occurs for both device's. The t_{50}/t_m index is closer to 1 at low flow rates however it generally remains constant at high flow rates (section 4.4.4).

The following conclusions were obtained by comparing the model and prototype HDVS operating with the sludge hopper RTD indices (section 4.4.4) and generally apply to the HDVS operating without the sludge hopper, unless otherwise stated. These comparisons are based on the flow rate, which provides the closest theoretical mean residence time through each HDVS (Table 4.21).

- Both the t_f/τ and t_p/τ indices support the RTD normalised curves E(Θ) description of the HDVS's mixing regime (Fig. 4.21 and 4.25). At high flow rates the peak of the RTD curve shifts towards the origin and therefore dead volumes and subsequently short-circuiting is present. Whereas at low flow rates, the RTD curve peak occurs close to a normalised time (Θ) value of 1 (eqn. 4.2), implying that a greater volume of the HDVS is active in the mixing process.

- The prototype HDVS t_p/τ index is generally greater than the model HDVS and therefore, supports previous conclusions suggesting that the prototype HDVS has a greater active volume compared to the model HDVS (section 4.4.7).

- The prototype HDVS t_{90}/t_{10} index, is generally less than the model HDVS and therefore, the prototype HDVS has greater plug-flow mixing characteristics compared to the model HDVS. The model and prototype HDVS t_{90}/t_{10} index increases as the inlet flow rate increases. Subsequently, there is more mixing and dispersion within the HDVS at high flow rates (section 4.1). This is supported by the ADM and TISM parameters (section 4.4.7).

- The model and prototype HDVS t_{10} parameter values both show similar trends with respect to the flow rate (Fig. 4.31). Therefore, when using this parameter for the design of the HDVS for kinetic processes i.e. the time element of the CT product, it is independent of the size of the HDVS.

- The prototype HDVS t_{50}/t_m index is generally greater than the model HDVS and therefore the prototype HDVS has improved plug-flow mixing characteristics compared to the model HDVS (section 4.4.4). This is supported by the t_{90}/t_{10} index

and the ADM and TISM parameters (section 4.4.7).

All RTD indices either increase or decrease at low flow rates, depending on their individual properties and then remain stable as the flow rate increases. This supports previous conclusions that a transition flow rate exists, above and below which the HDVS's mixing regime has different characteristics and that the HDVS has a stable mixing regime at high flow rates (section 4.4.3 and 4.4.7).

The RTD indices and subsequently the conclusions obtained are influenced by the truncation time of the RTD curve. Hence, this must be considered when determining the final value of an index for the design of kinetic process applications using the CT methodology (section 4.3.4) or when comparing the efficiency of different systems.

4.4.9 Comparison of the Model and Prototype Hydrodynamic Vortex Separator (HDVS) Operating with and without the Sludge Hopper

4.4.9.1 Model Hydrodynamic Vortex Separator (HDVS)

Fig. 4.32 and appendix C.5.3 compares the model HDVS operating with and without the sludge hopper RTD normalised exit-age distribution function E(Θ) curves. The model HDVS operating with and without the sludge hopper has a transition flow rate, above and below which, the HDVS mixing characteristics are different, as described in section 4.4.1.1. This occurs at approximately 15l/min for both operating conditions. The RTD curves show a very similar distribution and therefore mixing regime, particularly at flow rates greater than the transition flow rate. Hence the HDVS mixing regime is stable for both operating conditions above 15l/min.

At flow rates below the transition flow rate the RTD curve peak is slightly higher

for the HDVS operating without the sludge hopper, although it generally occurs at a similar time as the HDVS operating with the sludge hopper. Therefore a greater volume passes through the HDVS operating without the sludge hopper, at the same time interval at which the peak occurs, compared to the model HDVS operating with the sludge hopper. This suggests a reduction in the stagnant volume, as a greater volume of the HDVS is conducted closer to the mean velocity. Additionally, at the lowest flow rate investigated of 6l/min, the model HDVS operating without the sludge hopper RTD curve peak is closer to a normalised time (Θ) value of 1 (section 4.3.1) compared to the model HDVS operating with the sludge hopper. Significantly, the tail part of the model HDVS operating without the sludge hopper RTD curve (6l/min) also shows a reduction in the fraction of the total volume with residence times greater than the theoretical mean residence time and therefore stagnant volumes. These observations provide further evidence of a reduction in the stagnant volume and therefore a greater active volume within the model HDVS operating without the sludge hopper. Hence the sludge hopper does contribute to the stagnant volume within the HDVS.

The model HDVS operating without the sludge hopper t_{90}/t_{10} index (section 4.3.4) is smaller compared to the model HDVS operating with the sludge hopper and therefore, implies a smaller extent of mixing and dispersion is present (section 4.4.4 and 4.4.8). This is also illustrated by comparing the ADM and TISM parameters calculated for both HDVS operating conditions as discussed below. Due to the similarities between the RTD normalised curves E(Θ) for the model HDVS operating with and without the sludge hopper, the resulting intensity function λ(Θ) (section 4.4.1.1 and 4.4.5.1) and the remaining RTD indices (section 4.4.4 and 4.4.8) follow a similar trend and magnitude. Subsequently these RTD data analysis techniques do not provide any further insight into the different mixing characteristics between the two HDVS operating conditions.

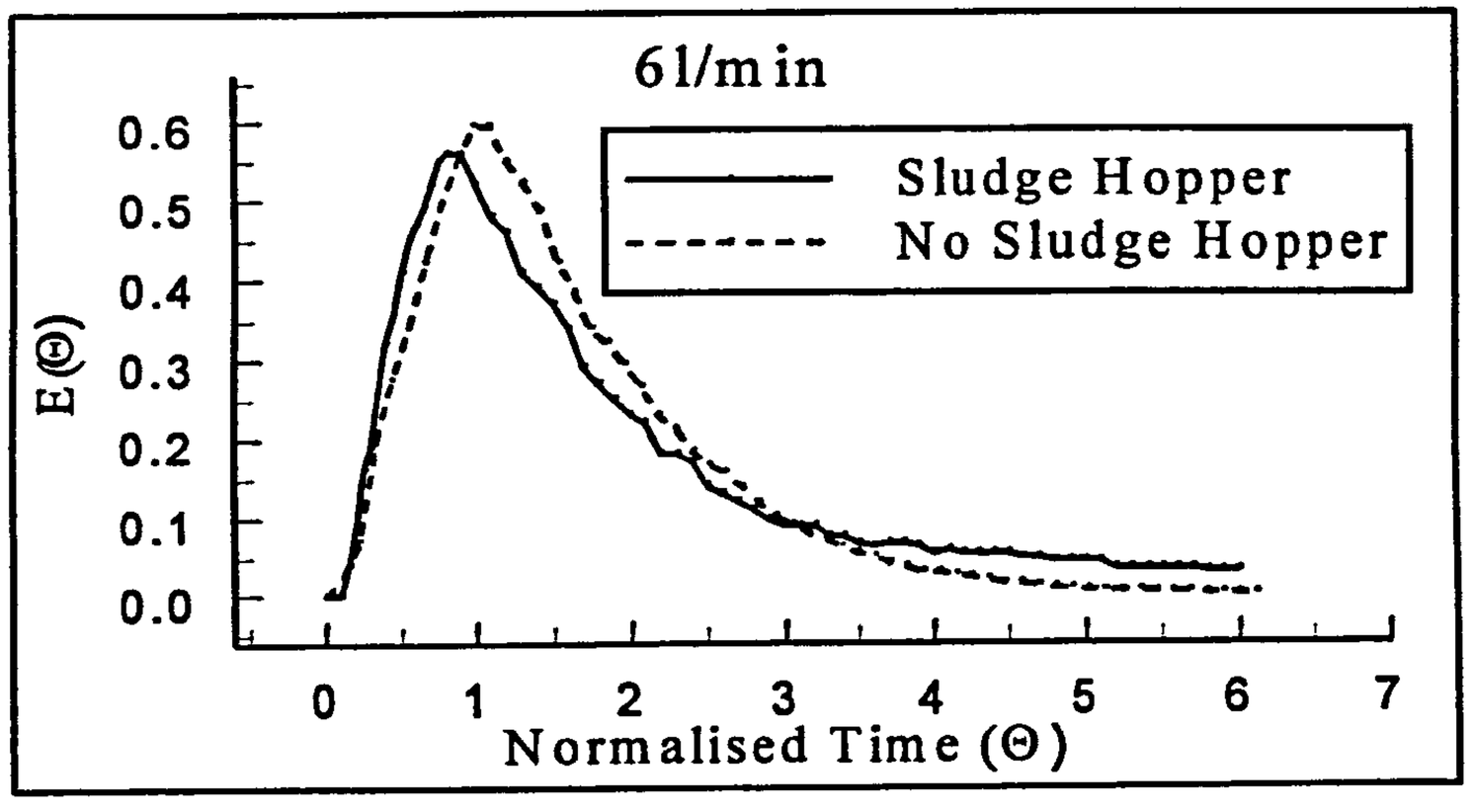

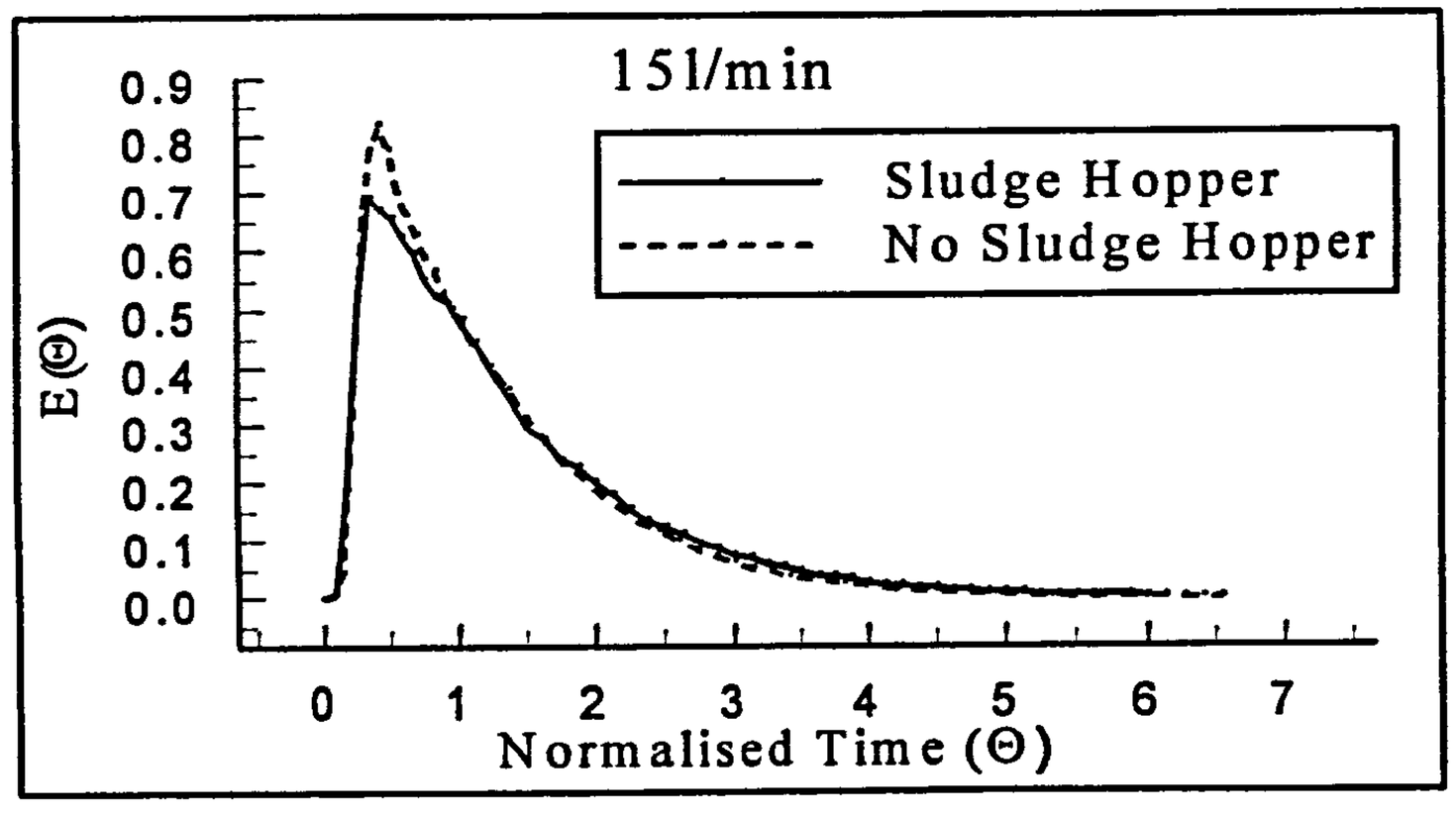

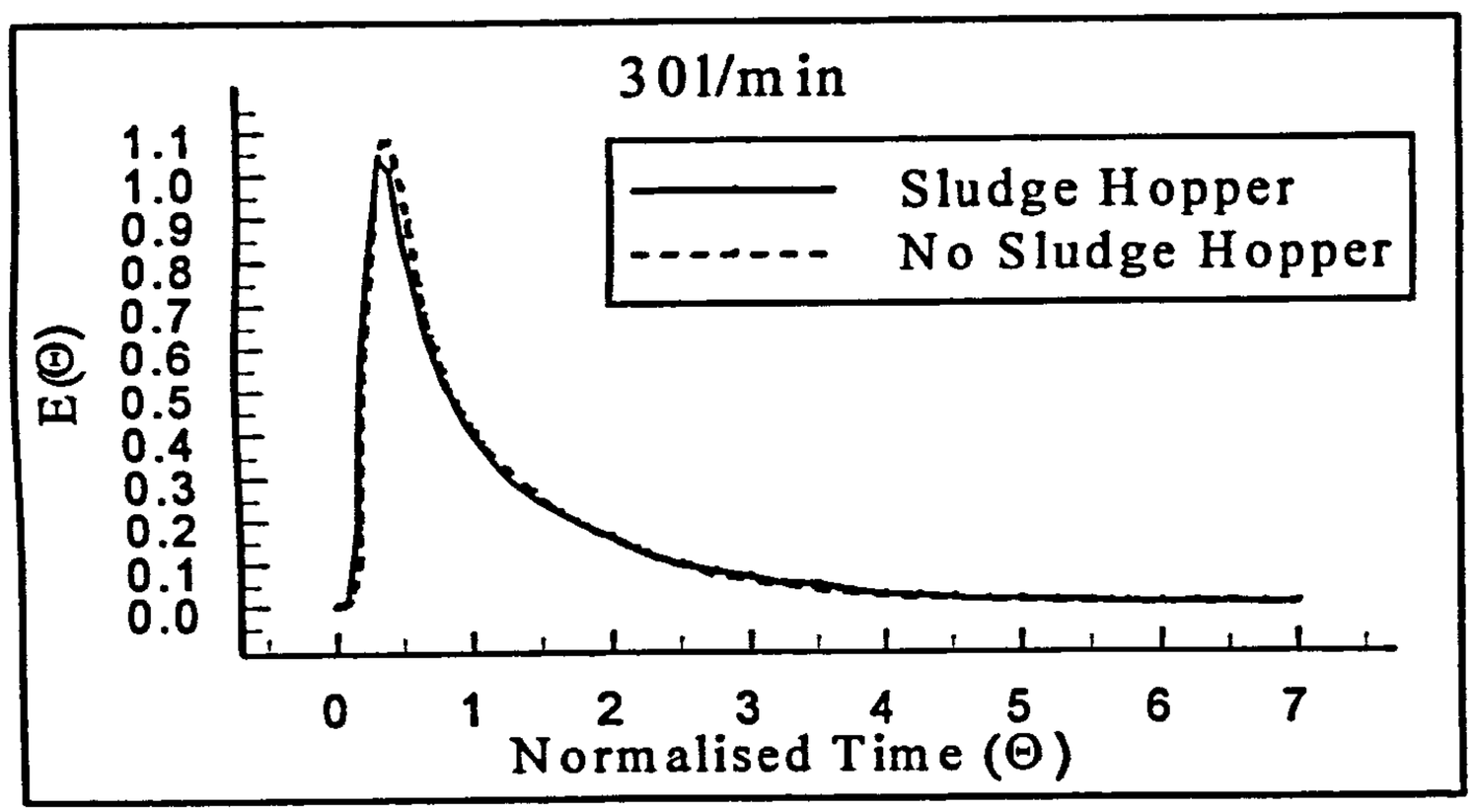

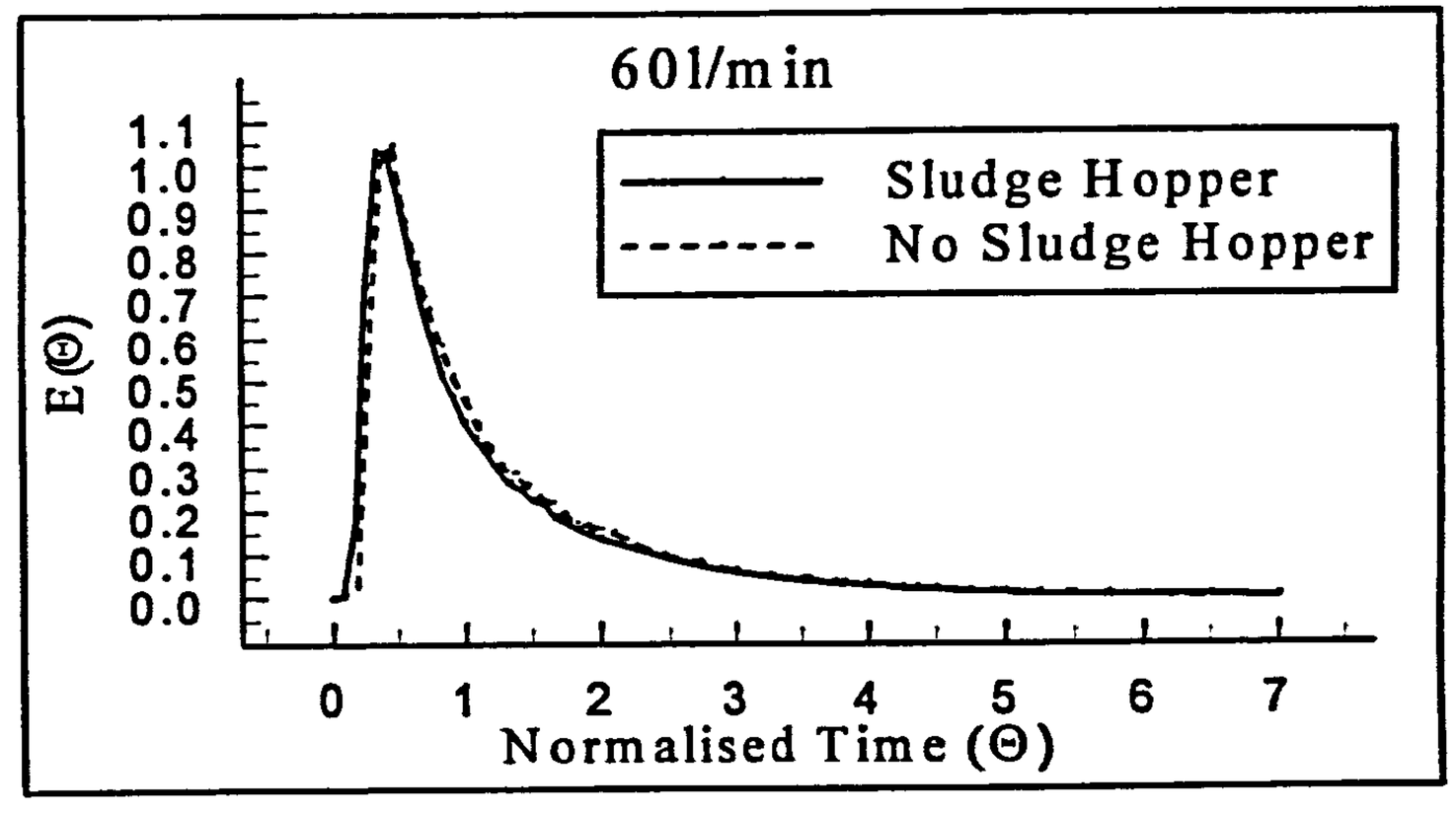

Fig. 4.32 Model HDVS No Baseflow - Comparison of Normalised Exit-Age Distribution Curves E(Θ) with and without the Sludge Hopper for Selected Flow Rates

Table 4.25 Model HDVS No Baseflow - Comparison of the Experimental Mean Residence Time Error and Tracer Mass Balance Results Calculated using the Method of Moments Operating with and without the Sludge Hopper

	Sludge Hopper		No Sludge Hopper	
Flow Rate (l/min)	Experimental Mean Residence Time % Error	Tracer Mass Balance (%)	Experimental Mean Residence Time % Error	Tracer Mass Balance (%)
4	+92.23	87.100	/	/
6	+81.41	78.000	+56.714	102.000
8	+57.81	93.650	/	/
10	+43.50	92.170	+40.727	99.8000
15	+35.05	109.00	+25.170	102.200
20	+27.07	106.50	+22.727	99.4000
30	+26.75	104.40	+21.004	104.933
40	+11.67	106.00	+19.709	107.333
45	+24.53	100.50	/	/
60	+23.10	108.00	+24.864	106.000
90	+22.64	110.50	/	/

Table 4.26 Model HDVS No Baseflow - Comparison of the Experimental Mean Residence Time Error Calculated using Non-Linear Regression Operating with and without the Sludge Hopper

	Sludge Hopper		No Sludge Hopper	
	ADM	TISM	ADM	TISM
Flow Rate (l/min)	Experimental Mean Residence Time % Error	Experimental Mean Residence Time % Error	Experimental Mean Residence Time % Error	Experimental Mean Residence Time % Error
4	+103.36	+90.093	/	/
6	+82.210	+27.410	+68.284	+68.076
8	+64.587	+24.560	/	/
10	+56.200	+22.000	+54.618	+33.891
15	+52.325	+8.2250	+33.800	+10.809
20	+26.400	-17.800	+12.582	+0.9820
30	+10.100	-7.5500	+3.0910	-6.4000
40	-2.2000	-16.933	+4.5090	-3.7090
45	+10.977	-9.0230	/	/
60	+6.0000	-10.300	+7.8910	-0.7270
90	+9.8510	-6.1190	/	/

The tracer recovery (mass balance) and error between the theoretical and experimental mean residence time calculated using the method of moments, clearly show an improvement for the model HDVS operating without the sludge hopper at low flow rates (Table 4.25). A reduction in the mean residence time error is associated with

an error value either approaching zero or a negative error. The latter indicates that the theoretical mean residence time is greater than the experimental mean residence time, which is generally the expected outcome for RTD investigations (Fogler, 1992) (section 4.4.1.1). This supports initial observations (section 4.4.1), which acted as a catalyst to investigate the HDVS operating without the sludge hopper, that the sludge hopper contributes to the stagnant volume within the HDVS. Stagnant volumes, refer to the tail section of the RTD curve, and have extended residence times compared to the theoretical mean residence time (eqn. 4.2), due to the presence of low velocities relative to the remaining system volume. Subsequently a stagnant volume will create tracer-hold-up resulting in a poor tracer recovery (mass balance). This was found to occur, even for RTD experimental duration's of 6 times the theoretical mean residence time, for the model HDVS operating with the sludge hopper (section 4.4.1.1).

The presence of stagnant volumes effects the method of moments RTD parameter estimation technique. The method of moments, calculates the mean residence time i.e. first moment (n), by using a time weighting factor i.e. E(t)t (eqn. 4.4). Hence this will have it greatest effect at low flow rates due to the shape of the HDVS RTD curve i.e. greater volumes E(t) at longer residence times (t). Therefore the combined effect of the RTD curves shape and method of moments data analysis technique, results in the error between the theoretical and experimental mean residence time. However as shown above, this error decreases for the model HDVS operating without the sludge hopper, due to a reduction in the stagnant volume and therefore weighting created at low flow rates.

The error between the theoretical and experimental mean residence time calculated using non-linear regression and the ADM also follows a similar relationship as the method of moments as discussed above (Table 4.26). However, for the error between the theoretical and experimental mean residence time calculated using non-linear

regression and the TISM, it is difficult to distinguish any difference between the model HDVS operating with and without the sludge hopper. This implies that the TISM and non-linear regression technique combination is less effected by the presence of stagnant volumes and therefore the tailing section of the RTD curve. This is in agreement with the non-linear regression RTD curve truncation investigation (section 4.4.1.2) and further supports previous conclusions suggesting that this RTD data analysis combination is superior for describing the HDVS mixing regime compared to other techniques (section 4.4.3).

Due to this reduction in the stagnant volume and subsequently an improved tracer recovery (mass balance) and reduced error between the experimental and theoretical mean residence time, the conflict (1) identified in section 4.4.1.1, does not equally apply to the model HDVS operating without the sludge hopper. However the error between the theoretical and experimental mean residence time for all flow rates and both HDVS operating conditions, is not always completely eliminated i.e. a positive error still occurs. Therefore, the stagnant volume or non-active flow behaviour in the HDVS is not only confined to the sludge hopper region. Coloured dye observations within the model HDVS also suggested that the inactive flow behaviour is not only confined to sludge hopper region (section 4.4.10). Chapter 5 presents a RTD combined model specifically configured to investigate the dead volume within the HDVS.

Appendix C.5.4 shows the estimated volume of the model HDVS operating with and without the sludge hopper. The volume is calculated from the experimental mean residence time, determined using the method of moments and the ADM and TISM using non-linear regression and equation 4.2. The difference in the estimated volume between the model HDVS operating with and without the sludge hopper should be equal to approximately 5 litres i.e. the volume of the sludge hopper. All flow rates above the lowest flow rate of 6l/min provide a good estimate of the sludge hopper volume. The

lowest flow rate shows the largest volume difference and this is due to the volume calculation for the model HDVS operating with the sludge hopper, as the sludge hopper has its greatest effect at low flow rates i.e. behaving as a stagnant volume (section 4.4.1.1). The method of moments estimated volume of the model HDVS operating with the sludge hopper at 6l/min is 82% greater than the actual volume and similarly operating without the sludge hopper is 44%. The non-linear regression ADM experimental mean residence time volume estimation provides a similar trend as the method of moments. However, the TISM for some flow rates shows a minus volume, indicating that the model HDVS operating without the sludge hopper volume estimation, is greater than the model HDVS operating with the sludge hopper. The sludge hopper occupies 8.3% of the total volume of the model HDVS. This is approximately equal to the experimental error in calculating the mean residence time (section 6.2.3). Hence, this prevents an accurate estimation of the volume difference between the model HDVS operating with and without the sludge hopper.

Comparing the model HDVS operating with and without the sludge hopper truncated RTD parameters (section 4.4.1.1 and 4.4.5.1) does not provide any more information regarding the contribution of the sludge hopper to the HDVS's mixing regime. This is due to the truncation time increments at which the RTD parameters were calculated and it is recommended for any future RTD truncation investigations that the truncation time should be investigated at a greater frequency and therefore normalised time (Θ) fractions as opposed to integers. This may possibly show that the model HDVS operating without the sludge hopper, can be operated for a longer RTD experimental duration and still provide an experimental mean residence time closer to the theoretical mean residence time, compared to the model HDVS operating with the sludge hopper, for the same flow rate. This would occur due to a reduction in the volume, associated with long residence times within the sludge hopper, which create a biased estimate of

the experimental mean residence time, when using the method of moments, as discussed above and in section 4.4.1.1. The ADM and TISM parameters calculated from the model HDVS operating with and without the sludge hopper truncated RTD curves do not show any significant difference with respect to the truncation time.

Table 4.27 Model HDVS No Baseflow - Comparison of ADM and TISM Parameters Calculated from RTD Experimental Data using the Method of Moments Operating with and without the Sludge Hopper

	Sludge Hopper		No Sludge Hopper	
Flow Rate (l/min)	Peclet Number (P_e)	N-Tanks	Peclet Number (P_e)	N-Tanks
4	3.48	2.410	/	/
6	2.48	1.965	4.57	2.919
8	2.60	2.020	/	/
10	2.48	1.969	2.73	2.076
15	1.96	1.745	1.93	1.731
20	1.63	1.608	1.67	1.624
30	0.80	1.284	0.99	1.357
40	0.87	1.311	0.72	1.254
45	0.79	1.280	/	/
60	0.57	1.198	1.18	1.428
90	0.70	1.248	/	/

Table 4.28 Model HDVS No Baseflow - Comparison of ADM and TISM Parameters Calculated from RTD Experimental Data using Non-Linear Regression Operating with and without the Sludge Hopper

	Sludge Hopper		No Sludge Hopper	
Flow Rate (l/min)	Peclet Number (P_e)	N-Tanks	Peclet Number (P_e)	N-Tanks
4	1.74	2.195	/	/
6	1.41	2.134	3.50	2.261
8	1.56	2.165	/	/
10	1.21	2.126	0.70	2.175
15	0.01	1.952	0.40	2.042
20	0.28	1.959	0.97	2.162
30	0.60	2.014	1.27	2.077
40	0.88	1.996	1.54	2.075
45	0.64	1.964	/	/
60	0.88	1.991	1.62	2.067
90	0.91	2.005	/	/

The model HDVS operating without the sludge hopper ADM and TISM parameters, calculated using the method of moments, are greater than the parameters for the model HDVS operating with the sludge hopper at the same flow rate (Table 4.27). The non-linear regression ADM and TISM parameter estimation technique also supports the method of moments results (Table 4.28). The Peclet number (P_e) is the ratio of the flow by convection to the flow by dispersion (section 4.3.3). The Peclet numbers (P_e) for the model HDVS operating without the sludge hopper show that the flow due to convection is generally greater than the flow due to dispersion, compared to the HDVS operating with the sludge hopper (Table 4.27 and 4.28). This is shown by several of the model HDVS operating without the sludge hopper Peclet numbers (P_e) approaching or increasing above a value of 1, compared to the HDVS operating with the sludge hopper at the same flow rate. Hence, the removal of the sludge hopper improves the plug-flow mixing characteristics of the HDVS by reducing the stagnant volume, which is associated with dispersion and mixing effects.

The difference between the ADM and TISM parameters, for the two HDVS operating conditions, is generally greater at low flow rates. This supports previous observations that the sludge hopper has a greater effect at low flow rates (section 4.4.1.1). The ADM and TISM parameters are not significantly different so as to change the classification of mixing. The Peclet number (P_e) still describes a device with an imperfect plug-flow mixing regime and high dispersion, $P_e<10$ (section 4.3.3) and is equivalent to approximately 2-3 tanks-in-series (N). The ADM and TISM parameters, calculated using the method of moments and non-linear regression, show the same decreasing trend as the flow rate increases. Therefore the model HDVS mixing regime, for both operating conditions, has improved plug-flow mixing characteristics at low flow rates and dispersion and mixing effects decrease.

The method of moments correlation parameters (R^2 and ESS) show that the ADM

provides the best-fit at all flow rates for the model HDVS operating with the sludge hopper. However for the model HDVS operating without the sludge hopper, the ADM only provides the best-fit at flow rates above the transition flow rate (15l/min) and the TISM provides the best-fit for flow rates below the transition flow rate. The TISM parameter N=2 provided the best fit to all flow rates for the model HDVS operating with the sludge hopper. However for the model HDVS operating without the sludge hopper, the TISM parameter N=3 provides the best-fit at low flow rates and N=2 still provides the best fit at high flow rates. Therefore, the TISM correlation parameters support previous observations, that the model HDVS operating without the sludge hopper has marginally improved plug-flow mixing characteristics and particularly at low flow rates, compared to operating with the sludge hopper (appendix C.1.6 and C.3.6). The non-linear regression analysis ADM and TISM correlation parameters show that for both operating conditions, the ADM provides the best-fit at all flow rates (appendix C.1.11 and C.3.12). The relationship between the ADM and TISM correlation parameters and the HDVS's non-ideal flow behaviour for both the method of moments and non-linear regression parameter estimation techniques is discussed in section 4.4.3.

It is interesting to observe previous research comparing the disinfection performance of a completely mixed tank, with a TISM parameter (N) equal to one and the HDVS (Boner *et al.*, 1994). This work concluded that the HDVS provides equivalent treatment in a volume of approximately one-third of the tank with mixer (section 2.1.5). This equates to the TISM parameters (N) obtained for the model and prototype HDVS (section 4.4.9.2) investigated in this project, which are generally in the vicinity of 2-4 tanks-in-series (N). Additionally, the ADM and TISM parameters for the model and prototype HDVS operating with and without the sludge hopper (section 4.4.9.2) fall in the range where any variation could effect the HDVS's disinfection efficiency, based on the work presented by Johnson *et al.*, (1997 and 1998) (section

2.2.3). Hence, there is scope for the HDVS to be modified and its mixing regime improved to provide a greater element of plug-flow mixing. This could be investigated using specific RTD and chemical reaction computer software (section 2.2.4) and applied in a similar manner, as previously undertaken to investigate the effect of internal modifications on the performance of the HDVS for solids-liquid separation (Harwood and Saul, 1996b and Faram and Andoh, 2000).

4.4.9.2 Prototype Hydrodynamic Vortex Separator (HDVS)

Fig. 4.33 and appendix C.5.5 compares the prototype HDVS operating with and without the sludge hopper RTD normalised exit-age distribution E(Θ) function curves. The RTD curves have a very similar distribution and therefore, imply a similar mixing regime is present, for both operating conditions at the same flow rate. The general observations obtained for the model HDVS apply to the prototype HDVS operating with and without the sludge hopper (section 4.4.9.1). However the tailing section of the prototype HDVS RTD curves, at the lowest flow rate (45l/min) for both operating conditions, have a very similar distribution and therefore, there is only a small reduction in the stagnant volume within the prototype HDVS by removing the sludge hopper. Whereas the model HDVS operating with and without the sludge hopper RTD curves, at the lowest flow rate investigated (6l/min), clearly show a reduction in the stagnant volume when the sludge hopper is removed (Fig. 4.32).

The prototype HDVS operating without the sludge hopper t_{90}/t_{10} index (section 4.3.4) is smaller compared to the prototype HDVS operating with the sludge hopper and therefore, implies a smaller extent of mixing and dispersion is present (section 4.4.4 and 4.4.8). This is also illustrated by the prototype HDVS ADM and TISM parameters calculated for both operating conditions discussed below. The difference between the

t_{90}/t_{10} index for the model HDVS operating with and without the sludge hopper, at the same flow rate, is greater than the prototype HDVS operating with and without the sludge hopper (section 4.4.4 and 4.4.8). This observation also suggests that removing the sludge hopper from the model HDVS improves the active volume and the plug-flow mixing characteristics (section 4.4.9.1). Whereas the prototype HDVS operating with and without the sludge hopper has very similar mixing characteristics and therefore, removing the sludge hopper has less effect on the total mixing regime, compared to the model HDVS (section 4.4.9.1).

Due to the similarities between the RTD normalised curves $E(\Theta)$ for the prototype HDVS operating with and without the sludge hopper, the resulting intensity function $\lambda(\Theta)$ (section 4.4.2.1 and 4.4.6.1) and the remaining RTD indices (section 4.4.4 and 4.4.8) follow a similar trend and magnitude. Subsequently these RTD data analysis techniques do not provide any further insight into the different mixing characteristics between the two HDVS operating conditions.

Table 4.29 Prototype HDVS No Baseflow - Comparison of the Experimental Mean Residence Time Error and Tracer Mass Balance Results Calculated using the Method of Moments Operating with and without the Sludge Hopper

	Sludge Hopper		No Sludge Hopper	
Flow Rate (l/min)	Experimental Mean Residence Time % Error	Tracer Mass Balance (%)	Experimental Mean Residence Time % Error	Tracer Mass Balance (%)
15	+118.05	67.3500	/	/
30	+71.500	70.5600	+58.411	91.067
45	+53.610	81.5600	+42.748	99.533
60	+37.880	96.1200	+33.222	99.467
90	+53.340	106.663	/	/
120	+21.520	90.6800	+23.723	103.20
240	+17.230	91.3600	+17.411	98.000
360	+16.910	100.133	+19.263	99.550
480	+24.820	99.0670	/	/

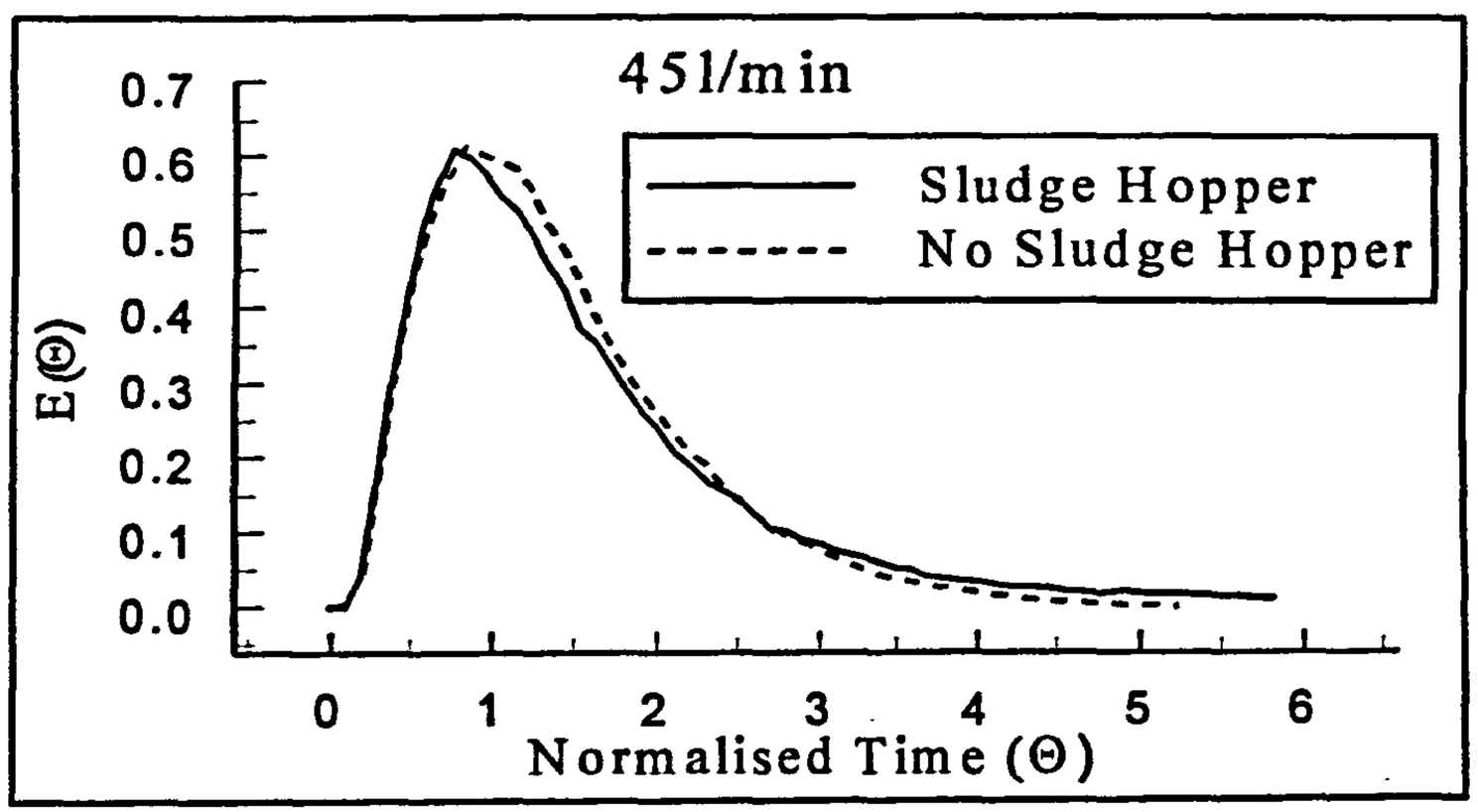

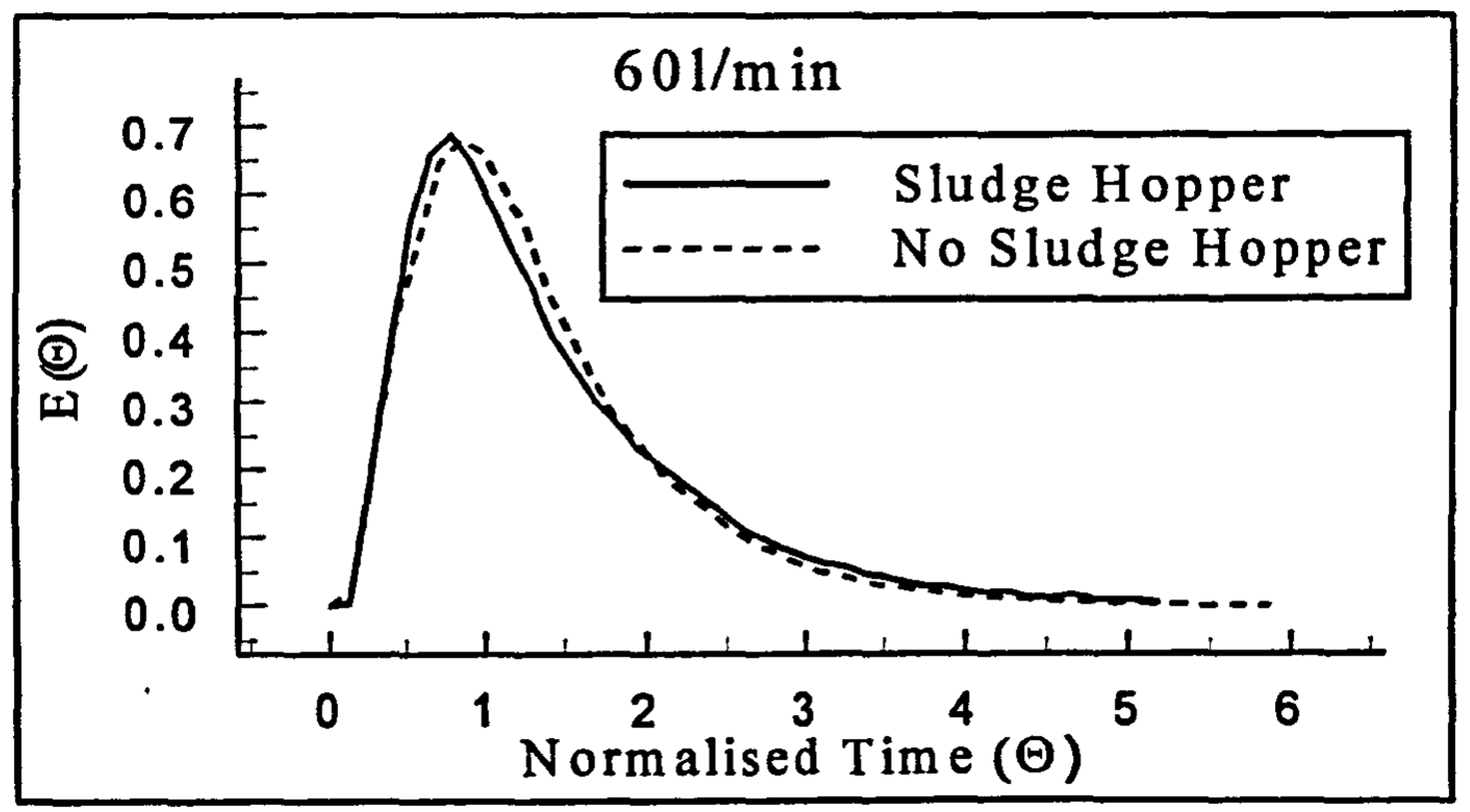

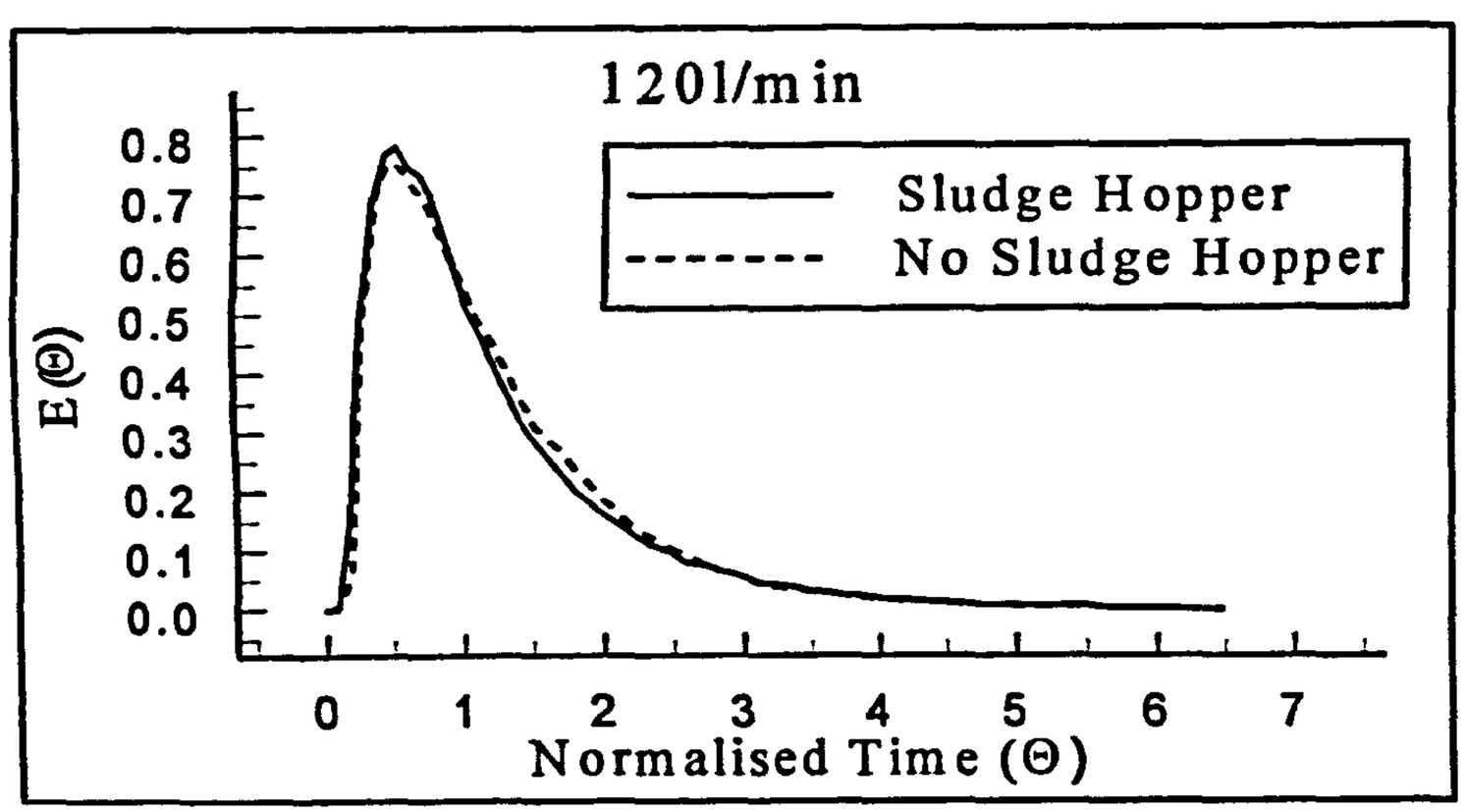

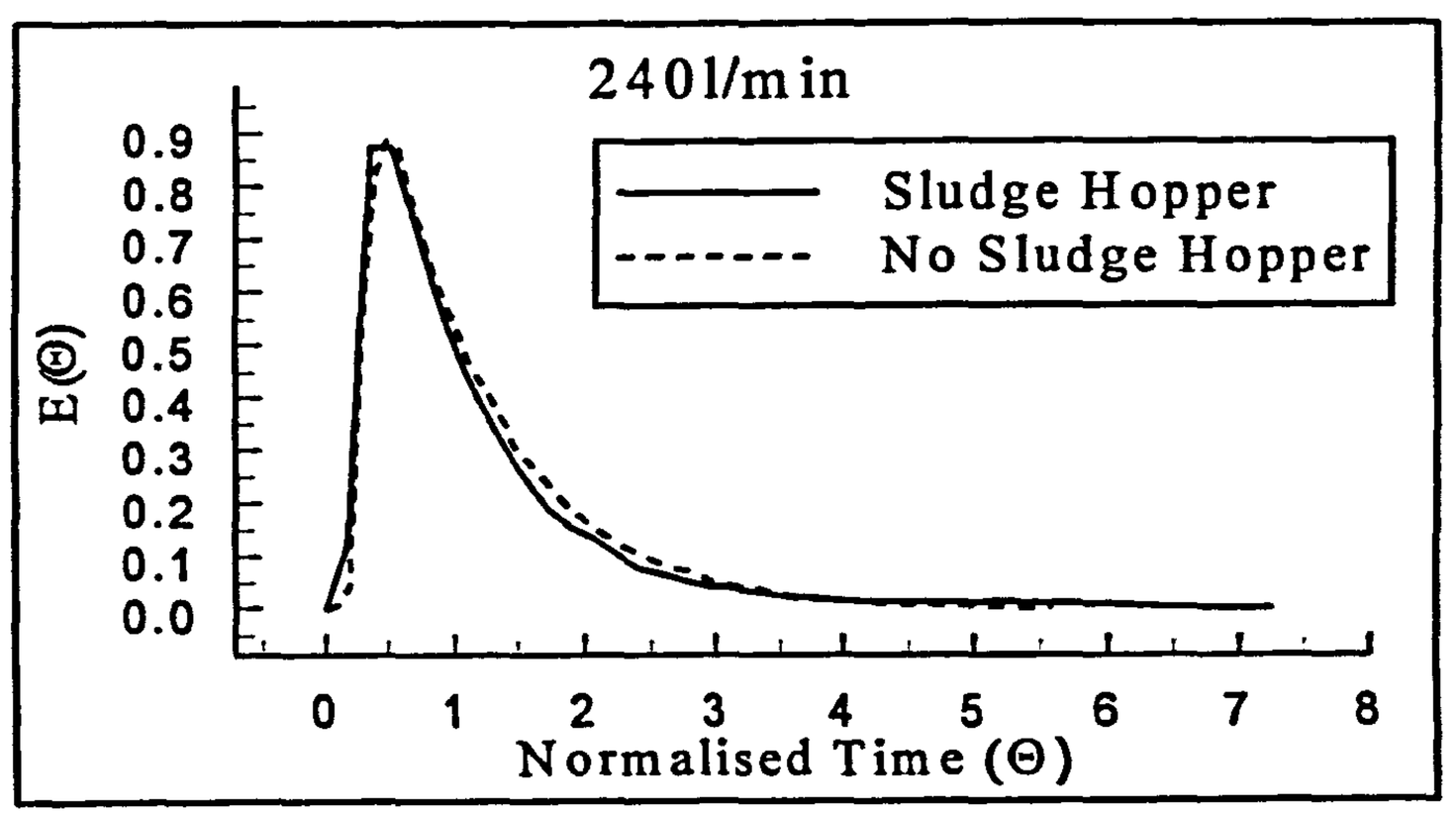

Fig. 4.33 Prototype HDVS No Baseflow - Comparison of Normalised Exit-Age Distribution Curves E(Θ) with and without the Sludge Hopper for Selected Flow Rates

Table 4.30 Prototype HDVS No Baseflow - Comparison of the Experimental Mean Residence Time Error Calculated using Non-Linear Regression Operating with and without the Sludge Hopper

	Sludge Hopper		No Sludge Hopper	
	ADM	TISM	ADM	TISM
Flow Rate (l/min)	Experimental Mean Residence Time % Error	Experimental Mean Residence Time % Error	Experimental Mean Residence Time % Error	Experimental Mean Residence Time % Error
15	+142.414	+137.022	/	/
30	+83.1450	+80.8560	+70.812	+78.033
45	+59.2570	+54.3590	+54.057	+55.145
60	+43.9160	+39.9460	+41.293	+40.484
90	+31.0120	+25.3690	/	/
120	+22.4720	+11.3520	+26.558	+17.991
240	+9.36400	+0.31000	+12.521	+9.1720
360	+10.0850	+4.26700	+10.847	+6.5770
480	+16.3390	+10.1340	/	/

The tracer recovery (mass balance) and error between the theoretical and experimental mean residence time calculated using the method of moments, clearly show an improvement for the prototype HDVS operating without the sludge hopper at low flow rates (Table 4.29). These observations are the same as the model HDVS operating without the sludge hopper (section 4.4.9.1). The error between the prototype HDVS operating with and without the sludge hopper theoretical and experimental mean residence time, calculated using the ADM and TISM non-linear regression technique, are very similar for the same flow rate (Table 4.30). This is the same relationship as achieved for the model HDVS TISM experimental mean residence time, calculated using non-linear regression and is further discussed in section 4.4.9.1. In addition, this also implies that removing the sludge hopper from the prototype HDVS has less effect on the stagnant volume compared to the model HDVS (section 4.4.9.1).

Appendix C.5.6 shows the estimated volume of the prototype HDVS operating with and without the sludge hopper. The volume is calculated from the experimental mean residence time, determined using the method of moments and the ADM and TISM using non-linear regression and equation 4.2. The difference in the estimated volume between

the prototype HDVS operating with and without the sludge hopper should be equal to approximately 35 litres i.e. the volume of the sludge hopper. All flow rates above the transition flow rate of 90l/min provide a good estimate of the sludge hopper volume. The lowest flow rate shows the largest volume difference and this is due to the volume calculation for the prototype HDVS operating with the sludge hopper, as the sludge hopper has its greatest effect at low flow rates i.e. behaving as a stagnant volume (section 4.4.1.1). The method of moments estimated volume of the prototype HDVS operating with the sludge hopper at 30l/min is 72% greater than the actual volume and similarly operating without the sludge hopper is 47%. The non-linear regression ADM experimental mean residence time volume estimation provides a similar trend as the method of moments. However, the TISM for some flow rates shows a minus volume, indicating that the prototype HDVS operating without the sludge hopper volume estimation, is greater than the prototype HDVS operating with the sludge hopper. The sludge hopper occupies 7.5% of the total volume of the prototype HDVS. This is approximately equal to the experimental error in calculating the mean residence time (section 6.2.3). Comparing the prototype HDVS operating with and without the sludge hopper truncated RTD parameters (section 4.4.2.1 and 4.4.6.1), does not provide any more information regarding the contribution of the sludge hopper to the HDVS's mixing regime. This is discussed in more detail for the model HDVS in section 4.4.9.1.

The prototype HDVS operating without the sludge hopper ADM and TISM parameters, calculated using the method of moments and non-linear regression, are greater than the parameters for the prototype HDVS operating with the sludge hopper, at the same flow rate (Table 4.31 and 4.32). The Peclet numbers (P_e) for the prototype HDVS operating without the sludge hopper show that the flow due to convection is greater than the flow due to dispersion, compared to the HDVS operating with the sludge hopper (section 4.3.3). This occurs as the prototype HDVS operating without the

sludge hopper Peclet numbers (P_e) are all greater than a value of 1, compared to the HDVS operating with the sludge hopper at the same flow rate. This change in flow characteristics between the HDVS operating conditions is greater for the model HDVS (section 4.4.9.1). Hence, the removal of the sludge hopper improves the plug-flow mixing characteristics of the HDVS by reducing the stagnant volume, which is associated with dispersion and mixing effects. Additionally, removing the sludge hopper from the model HDVS appears to further increase the plug-flow mixing characteristics compared to removing the sludge hopper from the prototype HDVS.

Table 4.31 Prototype HDVS No Baseflow - Comparison of ADM and TISM Parameters Calculated from RTD Experimental Data using the Method of Moments Operating with and without the Sludge Hopper

	Sludge Hopper		No Sludge Hopper	
Flow Rate (l/min)	Peclet Number (P_e)	N-Tanks	Peclet Number (P_e)	N-Tanks
15	4.24	2.762	/	/
30	4.42	2.849	5.65	3.425
45	3.25	2.309	5.10	3.165
60	3.63	2.481	4.20	2.740
90	2.72	2.070	/	/
120	1.98	1.754	2.67	2.049
240	0.93	1.333	2.58	2.008
360	1.91	1.724	2.48	1.965
480	1.84	1.695	/	/

Table 4.32 Prototype HDVS No Baseflow - Comparison of ADM and TISM Parameters Calculated from RTD Experimental Data using Non-Linear Regression Operating with and without the Sludge Hopper

	Sludge Hopper		No Sludge Hopper	
Flow Rate (l/min)	Peclet Number (P_e)	N-Tanks	Peclet Number (P_e)	N-Tanks
15	1.99	2.237	/	/
30	2.33	2.285	3.400	2.351
45	2.60	2.207	3.480	2.282
60	2.57	2.211	3.280	2.257
90	1.74	2.229	/	/
120	1.43	2.144	1.570	2.172
240	1.53	2.092	1.930	2.199
360	1.83	2.152	2.040	2.169
480	1.93	2.146	/	/

The difference between the ADM and TISM parameters, for the two HDVS operating conditions, is generally greater at low flow rates. This supports previous observations that the sludge hopper has a greater effect at low flow rates (section 4.4.1.1). The ADM and TISM parameters are not significantly different so as to change the classification of mixing. The Peclet number (P_e) still describes a device with an imperfect plug-flow mixing regime and high dispersion, P_e<10 (section 4.3.3) and is equivalent to approximately 2-3 tanks-in-series (N). The ADM and TISM parameters, calculated using the method of moments and non-linear regression, show the same decreasing trend as the flow rate increases. Therefore the prototype HDVS mixing regime, for both operating conditions, has improved plug-flow mixing characteristics at low flow rates and dispersion and mixing effects decrease. The increase in the model HDVS ADM and TISM parameters between the device operating with and without sludge hopper (section 4.4.9.1) is generally greater at low flow rates compared to the prototype HDVS. This provides further evidence that removing the sludge hopper from the model HDVS greater improves the plug-flow mixing characteristics compared to removing the sludge hopper from the prototype HDVS.

The prototype HDVS operating with and without the sludge hopper method of moments correlation parameters (R^2 and ESS), show that the TISM generally provides the best-fit for all flow rates below the transition flow rate (90l/min) and the ADM for all higher flow rates. The TISM provides the best-fit to the prototype HDVS operating with and without the sludge hopper for a parameter value of N=3, at flow rates below the transition flow rate and N=2 for higher flow rates (appendix C.2.5 and C.4.5). The non-linear regression analysis ADM and TISM correlation parameters show that for both prototype HDVS operating conditions, the ADM provides the best-fit for all flow rates (appendix C.2.10 and C.4.11). The relationship between the ADM and TISM correlation parameters and the HDVS's non-ideal flow behaviour for both the method of

moments and non-linear regression parameter estimation techniques is discussed in section 4.4.3.

The model HDVS TISM correlation parameters, suggested that at low flow rates, the model HDVS operating without the sludge hopper has improved plug-flow mixing characteristics compared to the model HDVS operating with the sludge hopper (section 4.4.9.1). However the TISM parameters (N) providing the best-fit to the prototype HDVS operating with and without the sludge hopper, are the same across the range of flow rates, as discussed above. Therefore, this also supports previous observations that removing the sludge hopper from the model HDVS greater improves the plug-flow mixing characteristics compared to removing the sludge hopper from the prototype HDVS.

The RTD parameters obtained for the prototype HDVS operating with and without the sludge hopper have shown that removing the sludge hopper does reduce the stagnant volume within the HDVS, although not to the same extent as the model HDVS (section 4.4.9.1). The sludge hopper occupies 8.3% of the total model HDVS volume and similarly for the prototype HDVS 7.5%. This may account for the relative effects of removing the sludge hopper, although neglecting any experimental errors. The RTD has been used to investigate the influence of the sludge hopper on the HDVS's mixing regime. However, the volume within the HDVS located above the inlet pipe and adjacent to the overflow spillway (Fig. 3.1) is typically designed as a quiescent area for the collection of floatable material when the HDVS is used for solids-liquid separation. Subsequently, observations using coloured dye clearly showed that this volume in the model HDVS contains fluid elements with residence times longer than the mean and therefore, contributes to the stagnant volume within the HDVS (section 4.4.10).

Chapter 5 presents and discusses the results obtained from a RTD combined mathematical model, specifically developed to estimate the inactive volume within the

model and prototype HDVS operating with and without the sludge hopper. This will aid in quantifying the stagnant volume present within the HDVS, for a given flow rate and show if it is only limited to a volume in the vicinity of the sludge hopper i.e. 5 litres for the model HDVS and similarly 35 litres for the prototype HDVS. Additionally the results obtained for the model and prototype HDVS operating with and without the sludge hopper can be directly compared and used to support the observations and conclusions presented in this chapter. Regardless of the estimated stagnant volume calculated by the mathematical model, it is not possible to precisely locate its position within the HDVS. This could possibly be accomplished using CFD and in situ velocity measurements and has partially been addressed by other workers (section 2.1.4).

The HDVS's mixing regime has evolved due to the internal configuration i.e. inclusion of a floatables trap and sludge hopper etc (Fig. 3.1), providing the required performance during extensive solids-liquid separation investigations (chapter 2). However, the advent of CFD and other techniques capable of simulating the hydrodynamic characteristics of a mixing device enable the hydraulic characteristics of the HDVS to be modified with consideration to its potential application i.e. kinetic processes, which may require different optimum mixing regimes (section 2.1.4 and 2.2.4).

4.4.9.3 Comparison with Existing RTD Investigations on a Swirl-Flo™ HDVS Operating without a Baseflow Component

The RTD investigations undertaken by Dudley and Marks, (1993) provide the only existing data on the Swirl-Flo™ HDVS (Table 1.1) in addition to the work presented in this project. These RTD tests were conducted on the coagulation and flocculation Swirl-Flo™ HDVS at Totnes WWTW and the experimental arrangement and procedure and

general conclusions are discussed in chapter 2 (section 2.2.2). The method of moments and the ADM (P_e) and TISM (N) parameters were used to describe the RTD (section 4.3).

The coagulation tank plug-flow mixing characteristics improve as the flow rate increases and the flocculation tank shows the opposite trend using the ADM and TISM. However, only two inlet flow rates were investigated and therefore, the results are far from comprehensive and representative of the mixing regime within the Swirl-Flo™ HDVS across the potential range of flow rates, as investigated in this project (section 4.4.1 and 4.4.2). Subsequently, comparing the coagulation and flocculation HDVS ADM and TISM parameters is also not representative of any difference in the mixing regime between two different size HDVS's.

The coagulation and flocculation Swirl-Flo™ HDVS RTD describes a device with high dispersion, resulting in a Peclet number (P_e) = 3.9-6.3 and is equivalent to 2.5–3.7 tanks-in-series (N), depending on the inlet flow rate as discussed above. The Totnes HDVS RTD tests were terminated at approximately 3-4 times the theoretical mean residence time (eqn. 4.2) and it is evident from the results presented in this project, that truncation effects should be taken into account, particularly when comparing data sets generated using the method of moments (section 4.4.1).

The model HDVS Peclet numbers (P_e) range from 1.56–5.40 and the equivalent number of tanks-in-series (N) from 1.576–3.308, for an experimental truncation time of 4 times the theoretical mean residence time (appendix C.1.7). Similarly, the prototype HDVS ADM parameters range from 2.6-6.76 and the TISM parameters from 2.020–3.968 (appendix C.2.6). The RTD tests undertaken by Dudley and Marks, (1993) were conducted on the two Swirl-Flo™ HDVS's operating with a mean residence time ranging from 13–300 minutes. Therefore, based on a similar mean residence time, the highest ADM and TISM parameters presented in this project above, should only be

compared to the coagulation and flocculation Swirl-Flo™ HDVS parameters. These ADM and TISM parameters correspond to a mean residence time of approximately 15 minutes and are very similar for both the model and prototype HDVS and the parameters previously reported for the coagulation and flocculation Swirl-Flo™ HDVS (Dudley and Marks, 1993). This shows that the flow regime remains stable for any size of HDVS and hence, the scale-up of the RTD for this particular HDVS (Table 1.1).

4.4.9.4 Comparison with Existing RTD Investigations on a Grit King™ HDVS Operating without a Baseflow Component

The results from RTD investigations conducted on a Grit King™ HDVS (Table 1.1) (Tyack and Fenner, 1997 and 1998b) are discussed below and the experimental procedure and general conclusions are presented in chapter 2 (section 2.2.2). The method of moments and the ADM (P_e) parameter were used to describe the RTD (section 4.3).

The RTD experimental curves presented for the Grit King™ HDVS i.e. low, moderate and high flow rates with respect to the range of flow rates investigated, were not normalised using either the theoretical or experimental mean residence time (section 4.3.1). However, their distribution follow a similar trend as the RTD data presented in this project across the range of flow rates, assuming the same concentration of tracer was injected for each flow rate e.g. Fig. 4.8. Therefore, the Grit King™ HDVS RTD curves also suggest that there may be a transition flow rate at which point the RTD curve changes shape. Subsequently the Grit King™ HDVS will have different mixing characteristics at flow rates above and below the transition flow rate (section 4.4.1).

The Grit King™ HDVS RTD experimental duration ranges from approximately 3-6 times the theoretical mean residence time with the truncation time decreasing i.e. shorter

experiment as the flow rate decreases. Therefore, the RTD experimental procedure is not consistent for all inlet flow rates. At low flow rates the experimental mean residence time is smaller than the theoretical mean residence time (small truncation time) as expected with RTD studies (section 4.4.1.1) whereas, at high flow rates (large truncation time) the opposite occurs and is not commented upon. The latter outcome occurs for the majority of flow rates investigated in this project, using the same RTD experimental truncation time for all experiments and is discussed in detail in section 4.4.1. Additionally, no tracer recovery (mass balance) data is provided, which may support the presence of stagnant regions, resulting in a fraction of the total volume residing in the Grit King™ HDVS for extended residence times and a long tail on the RTD curve (section 4.4.1.1).

The Grit King™ HDVS RTD investigations highlight the effect of the RTD experimental duration on the calculation of the RTD parameters e.g. mean residence time and ADM parameters. If the RTD experimental truncation times are not constant, they should preferably show the opposite trend as the flow rate increases, as illustrated by the results in this project due to the shape of the RTD with respect to the inlet flow rate (section 4.4.1.1). At low flow rates a greater stagnant volume is present within the HDVS. This contributes to a substantial error between the theoretical and experimental mean residence time calculated using the method of moments and a poor tracer recovery (mass balance). These RTD experimental problems are reduced at high flow rates when the same RTD truncation time is adopted for all inlet flow rates (section 4.4.1.1). Hence, a short experimental duration and particularly at low flow rates, will not comprehensively describe the RTD within the Grit King™ HDVS.

The Grit King™ HDVS ADM parameters were calculated using the method of moments and presented as the dispersion number (D). Subsequently the dispersion numbers (D) were converted into Peclet numbers (P_e) (section 4.3.3) to enable

comparison with the ADM parameters presented in this project (section 4.4.1 and 4.4.2). The Grit King™ HDVS Peclet numbers (P_e) describe a mixing regime with high dispersion (section 4.3.3) and is the same as achieved for the model and prototype Swirl-Flo™ HDVS investigated in this project. The Grit King™ and Swirl-Flo™ HDVS Peclet numbers (P_e) are not too dissimilar considering the different RTD truncation times used in the two projects and its effect on the ADM parameter calculation (section 4.4.1.1). The Grit King™ HDVS Peclet numbers (P_e) fluctuate across the range of flow rates and this possibly occurs due to the inconsistent RTD truncation times as discussed above. Subsequently, this relationship compares better with the model and prototype Swirl-Flo™ HDVS Peclet numbers (P_e) calculated using non-linear regression (section 4.4.1.2) as opposed to the method of moments (section 4.4.1.1). This is because the non-linear regression technique is less effected by the tail part of the RTD curve and therefore, the RTD experimental truncation time compared to the method of moments (section 4.4.1.2) (Haas *et al.*, 1997). This supports previous conclusions promoting the use of non-linear regression to calculate the ADM parameter as opposed to the method of moments (section 4.4.3).

4.4.10 Hydrodynamic Vortex Separator (HDVS) No Baseflow - Residence Time Distribution (RTD) Continuous Feed (Step) Experiments

This section presents and discusses the RTD results obtained using a continuous feed (step) injection technique (section 3.4.2). These experiments were undertaken to support the pulse injection technique RTD data presented above. The step RTD experiments were conducted on both the model and prototype HDVS operating with no baseflow component and with the sludge hopper (Fig. 3.1). The model and prototype HDVS cumulative distribution function F(t) values (section 4.3.2) are provided in

appendix C.6.2 and C.6.3. The model HDVS RTD curves and the ADM and TISM parameters calculated using the method of moments are presented below however, the same discussion applies to the prototype HDVS results presented in appendix C.6. The first and second moments (n) of the RTD curves were calculated using equation 4.8 (section 4.3.2) and the TISM and ADM parameters obtained from equation 4.10 and 4.12 respectively (section 4.3.3).

Fig. 4.34 shows the model HDVS cumulative distribution function F(t) for the range of flow rates investigated. The RTD curves support the observations obtained using the pulse injection method with regards to the type of mixing regime and that the model HDVS has a greater active volume at low flow rates (section 4.4.1.1). However, it is not possible to identify a transition flow rate and therefore, the high flow rates at which the mixing regime is very stable with the same clarity as using the pulse RTD data e.g. Fig. 4.8 (section 4.4.1.1).

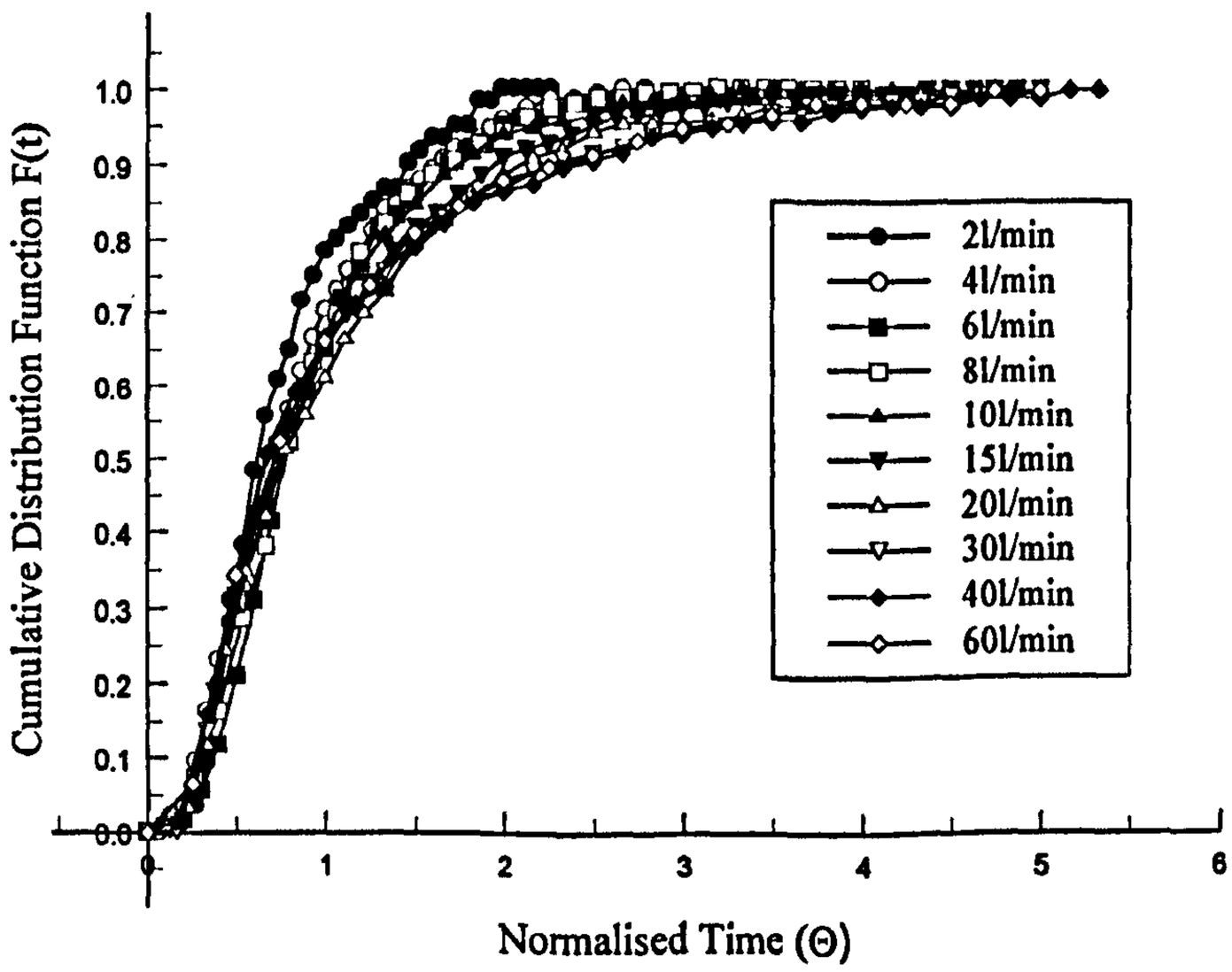

Fig. 4.34 Model HDVS No Baseflow - Comparison of Cumulative Distribution Function Curves F(t)

The experimental mean residence time calculated using the method of moments is smaller than theoretical mean residence time (eqn. 4.2) at low flow rates and at high flow rates the opposite occurs. However, the RTD experimental truncation time for the step experiments varied depending on the flow rate and generally increased as the flow rate increased (appendix C.6.5). The ADM and TISM parameters calculated using the method of moments decrease as the flow rate increases (Fig. 4.35) and is the same relationship as achieved for the pulse RTD data (section 4.4.1.1). Additionally the mixing regime classification is the same with high dispersion (section 4.3.3). However, the ADM and TISM parameters are smaller for the same flow rate and decrease over a smaller range as the flow rate is increased, compared to those obtained using the pulse RTD technique. The step RTD ADM and TISM parameters compare better to the pulse RTD ADM and TISM parameters calculated using non-linear regression (section 4.4.3). These observations regarding the experimental mean residence time and the ADM and TISM parameters are the same as obtained when comparing the model and prototype HDVS investigated in this project to existing Grit King™ HDVS RTD investigations (Tyack and Fenner, 1997 and 1998b). Hence, as previously suggested these observations possibly occur due to the inconsistent RTD experimental truncation time and the non-linear regression technique being less sensitive to the RTD truncation time compared to the method of moments (section 4.4.9.4). Additionally, the washout function W(t) (eqn. 4.8) used to calculate the first and second moments (n) is also less effected by the tail part of the RTD curve compared to the exit-age distribution function E(t) used for the pulse RTD data analysis (section 4.3.2) (Nauman, 1981).

During the step RTD experiments it was observed that there is coloured dye tracer hold-up around the sludge hopper and cone region and at the top water level in the outer zone (Fig. 3.1). Therefore, these regions may contribute to the inactive flow behaviour within the model HDVS in addition to the sludge hopper (section 4.4.1.1) and is

supported by previous workers who identified an active region (Tyack and Fenner, 1998b) (section 2.2.2). Chapter 5 presents a RTD combined model specifically configured to investigate the dead volume within the HDVS and will therefore aid in determining the extent of any dead or inactive flow behaviour within the HDVS.

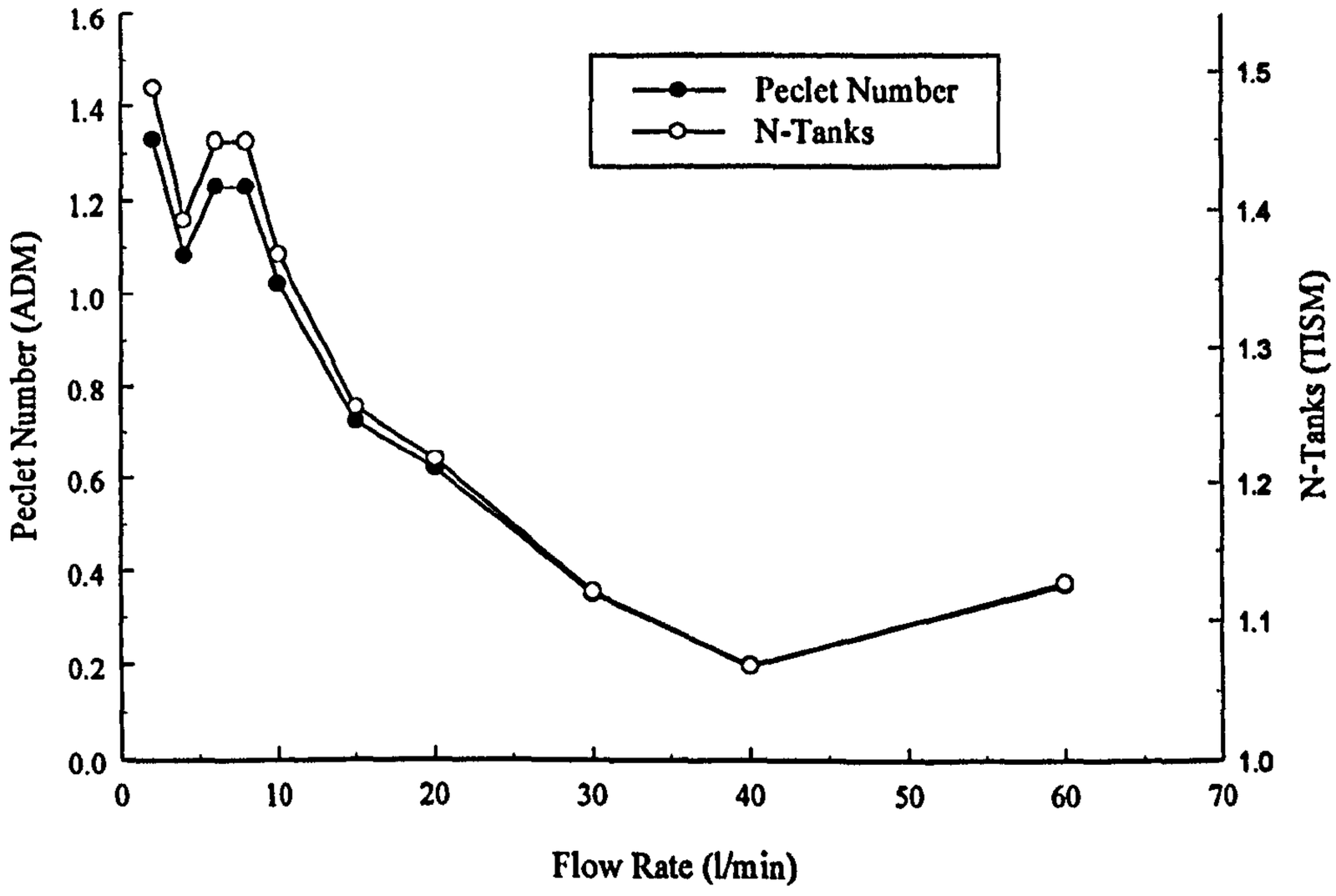

Fig. 4.35 Model HDVS No Baseflow - Comparison of ADM and TISM Parameters Calculated using the Method of Moments

If further step RTD data analysis investigations are to be conducted as part of future research, the author recommends the work presented by Wolf and Resnick, (1963). This work presents the solution to several simple RTD combined mathematical models (chapter 5), which describe a completely mixed tank with dead space or short-circuiting or the volume of plug-flow mixing. Additionally the individual combined models are presented in a generic form and therefore, simultaneously describe all possible non-ideal flow behaviour combinations within a completely mixed tank.

4.5 Chapter Overview

This chapter has characterised the mixing regime within a model and prototype HDVS operating without a baseflow component and with and without the sludge hopper using RTD analysis (Fig. 3.1). The model and prototype HDVS pulse injection RTD results describe a system with a complex mixing regime, which depends on the inlet flow rate. The HDVS has an imperfect plug-flow mixing regime and the non-ideal flow behaviour is associated with both dispersion and dead volumes, which result in short-circuiting.

The RTD curves show that short-circuiting occurs at high flow rates and fluid elements with residence times greater than the theoretical mean residence time are present at low flow rates within the HDVS. The flow rate that identifies this change in the HDVS mixing characteristics is termed the transition flow rate and is approximately 15l/min and 90l/min for the model and prototype HDVS operating with no baseflow and with and without the sludge hopper respectively. At all flow rates above the transition flow rate the RTD curves have a very similar shape and therefore, the HDVS has a very stable mixing regime at high flow rates. Hence, the mixing regime within any size of HDVS above its transition flow rate is likely to be stable and therefore, provide the same plug-flow mixing and inactive flow behaviour irrespective of the flow rate. At flow rates below the transition flow rate the RTD curve shape depends on the flow rate and implies that the HDVS has a greater active volume as the flow rate decreases. This is shown by the peak of the RTD curve, as it shifts away from the origin and towards a normalised time (Θ) value equal to 1 as the flow rate decreases. The prototype HDVS RTD curves at low flow rates peak closer to a normalised time (Θ) value of 1 compared to the model HDVS. Therefore, at low flow rates the prototype HDVS has a greater active volume compared to the model HDVS. This study shows the importance of

investigating the mixing regime within a system for a range of flow rates. This has been achieved for the HDVS by obtaining the RTD at flow rates, which cover and exceed existing design flow rates for a variety of applications.

The model and prototype HDVS ADM (P_e) and TISM (N) parameters (section 4.3) calculated using both the method of moments and non-linear regression, show that the plug-flow mixing characteristics increase and dispersion and mixing effects decrease, as the flow rate decreases. The mixing regime is classified as high dispersion and equal to approximately 2-4 completely mixed tanks-in-series. The evidence of a transition flow rate i.e. a change in HDVS mixing characteristics, is also provided by the ADM and TISM parameters as they are stable at high flow rates. Therefore, the stable mixing regime within the HDVS at high flow rates is associated with both the inactive flow behaviour and the plug-flow mixing characteristics.

The model and prototype HDVS ADM and TISM parameters are of a similar order of magnitude and therefore, they operate with a very similar mixing regime. However, the prototype HDVS ADM and TISM parameters are generally greater than the model HDVS at a flow rate providing a similar theoretical mean residence time within each device. Therefore, the prototype HDVS has marginally improved plug-flow mixing characteristics compared to the model HDVS. Additionally, at low flow rates the prototype HDVS also has less inactive flow behaviour as mentioned above. Hence, as the HDVS is scaled-up the plug-flow mixing and active volume characteristics are improved.

Existing HDVS disinfection trials have observed that the HDVS provides equivalent treatment in a volume of approximately one-third of a tank with mixer (Boner *et al.*, 1994). This equates to the TISM parameter (N) obtained for the HDVS investigated in this project i.e. 2-4 completely mixed tanks-in-series. Additionally, the HDVS ADM and TISM parameters fall in the range where any variation could effect

the performance of the HDVS for disinfection processes (Johnson *et al.*, 1997 and 1998). Hence, there is scope for the HDVS to be modified and its mixing regime improved to provide a greater element of plug-flow mixing. This could be investigated using specific RTD and chemical reaction computer software (section 2.2.4). This software enables the hydraulic characteristics of a system to be modified with consideration to the potential application, which may require different optimum mixing regimes e.g. kinetic processes.

The HDVS RTD curve has a long tail with tracer detection occurring at a time up to 6 times the theoretical mean residence time. Subsequently, the RTD experimental duration is an important parameter in calculating the experimental mean residence time and the ADM and TISM parameters. This is also exaggerated due to the shape of the HDVS RTD curve at low flow rates, as a greater fraction of the flow resides in the HDVS for long residence times and increases the tail section of the RTD curve compared to high flow rates. This significantly effects the method of moments and non-linear regression experimental mean residence calculation due the biased weighting created at high time values (section 4.4.1.1). Subsequently, the calculated HDVS experimental mean residence time is generally greater than the theoretical mean residence time for the same flow rate. The difference between the experimental and theoretical mean residence time is greater at low flow rates and combined with poor tracer recoveries (mass balance) implies the presence of inactive flow behaviour. This is largely associated with sludge hopper due to its isolated position relative to the remainder of the system (Fig. 3.1). Therefore, the combined effect of the HDVS RTD curves shape and the data analysis technique results in the error between the theoretical and experimental mean residence time. These observations acted as a catalyst to investigate the effects of the RTD experimental duration i.e. truncation analysis and the contribution of the sludge hopper to the HDVS's mixing regime.

The HDVS operating with the sludge hopper RTD curve truncation investigation using the method of moments showed that at low flow rates a greater truncation time (shorter experiment) is required to provide an experimental mean residence time in the vicinity of the theoretical mean residence time compared to high flow rates. Therefore, the inactive flow behaviour at low flow rates has a greater effect on the RTD data analysis techniques. At flow rates greater than the transition flow rate, a truncation time of approximately 3-4 times the theoretical mean residence time provides a better experimental estimation of the theoretical mean residence time. This is the recommended truncation time for when using the method of moments RTD data analysis technique (Nauman, 1981). The HDVS operating at the lowest flow rate and a RTD curve truncation time of 2-3 times the theoretical mean residence time provides a Peclet number (P_e) suggesting moderate dispersion as opposed to high dispersion for all other flow rates. Similarly the TISM parameter implies that the HDVS is equal to approximately 6 tanks-in-series (N). Therefore, the RTD experimental duration is a critical parameter in characterising the HDVS's mixing regime and the author encourages the use of the entire RTD, as opposed to individual RTD parameters, to estimate the HDVS's efficiency for specific kinetic process applications (chapter 7). Additionally, it is preferable to conduct the RTD experiment for a significant duration to obtain a comprehensive description of the mixing regime across the range of flow rates investigated. This will also provide an improved correlation between the experimental RTD curve and the ADM and TISM.

The RTD curve truncation investigation using non-linear regression provided similar results as the method of moments discussed above. However, the non-linear regression technique clearly showed a reduction in sensitivity to the tail part of the RTD curve and hence, the weighting created by the fraction of flow with long residence times at low flow rates compared to the method of moments. This is shown by a smaller

change in the estimated RTD parameters across the range of truncation times for the same flow rate. Additionally, the TISM appears to be superior to the ADM, as its parameters are relatively constant for all truncation times at the same inlet flow. Subsequently the non-linear regression technique reduces the magnitude of the ADM and TISM parameters across the range of inlet flow rates compared to the method of moments for the complete RTD data.

In the traditional design of kinetic process applications the theoretical mean residence time is an important parameter and the presence of non-ideal flow behaviour can result in a significantly under or overestimated value. However, obtaining the residence time of individual volumes i.e. RTD, eliminates the need to use either the theoretical or experimental mean residence time, as a kinetic processes efficiency can be determined as a function of each volume and the contact time it provides (section 7.5). Additionally, by obtaining the RTD there is no need to assume an active volume for the design process.

The RTD investigations undertaken on the HDVS operating with no baseflow and without the sludge hopper confirmed that the sludge hopper contributes to the inactive flow behaviour within the HDVS. The HDVS operating with and without the sludge hopper RTD curves have very similar characteristics as discussed above. However, at flow rates below the transition flow rate the RTD curves characteristics do marginally change and predominantly for the model HDVS. The RTD curve peak is slightly higher for the HDVS operating without the sludge hopper and therefore, a greater volume passes through the HDVS at the same time interval at which the peak occurs, compared to HDVS operating with the sludge hopper. This suggests a reduction in the stagnant volume, as a greater volume of the HDVS is conducted closer to the mean velocity. The model HDVS operating without the sludge hopper RTD curve peak is closer to a normalised time (Θ) value of 1 and the RTD curves also show a reduction in the

fraction of the total volume with long residence times at the lowest flow rate investigated (6l/min). This is shown by a reduction in the tail part of the RTD curve for the HDVS operating without the sludge hopper compared to with the sludge hopper. These observations provide further evidence of a reduction in the stagnant volume and therefore, a greater active volume within the HDVS operating without the sludge hopper. Hence, the sludge hopper does contribute to the inactive flow behaviour within the HDVS. However, the prototype HDVS operating with and without the sludge hopper RTD curve tail section, at the lowest flow rate investigated (45l/min), does not show this change in characteristics with the same clarity as the model HDVS. Subsequently, the removal of the sludge hopper from the model HDVS appears to greater effect the mixing regime compared to the prototype HDVS.

The error between the theoretical and experimental mean residence time decreases when the HDVS is operated without the sludge hopper due to a reduction in the stagnant volume which subsequently, reduces the method of moments and non-linear regression biased RTD parameter estimation at low flow rates. This is supported by a better tracer recovery (mass balance), particularly at low flow rates, for the HDVS operating without the sludge hopper compared to with the sludge hopper. Hence, this provides further evidence that the sludge hopper contributes to the stagnant volume within the HDVS and particularly at low flow rates. Comparing the HDVS operating with and without the sludge hopper truncated RTD parameters does not provide any more information regarding the contribution of the sludge hopper to the HDVS's mixing regime. This is due to the truncation time increments at which the RTD parameters were calculated and it is recommended for any future RTD truncation investigations that the truncation time should be investigated at a greater frequency.

The HDVS operating without the sludge hopper ADM and TISM parameters, calculated using the method of moments and non-linear regression, are greater than the

parameters obtained for the HDVS operating with the sludge hopper at the same flow rate. The HDVS operating without the sludge hopper Peclet numbers (P_e) show that the flow due to convection is generally greater than the flow due to dispersion, compared to the HDVS operating with the sludge hopper. This is shown by several of the HDVS operating without the sludge hopper Peclet numbers (P_e) approaching or increasing above a value of 1, compared to the HDVS operating with the sludge hopper, at the same flow rate. Hence, the removal of the sludge hopper improves the plug-flow mixing characteristics of the HDVS by reducing the stagnant volume, which is associated with dispersion and mixing effects. This change in flow characteristics between the HDVS operating conditions is greater for the model HDVS. Subsequently, removing the sludge hopper from the model HDVS appears to further increase the plug-flow mixing characteristics compared to removing the sludge hopper from the prototype HDVS.

The ADM and TISM parameter estimation using the indirect method of moments and direct non-linear regression techniques provide a very good fit to the experimental RTD data. Hence, both the ADM and TISM description of the mixing regime is suitable for further investigations to predict the HDVS's performance for kinetic processes. The ADM and TISM parameters obtained using non-linear regression provide a better correlation between the experimental and model generated RTD curve i.e. higher coefficient of correlation (R^2). This is due to the flexibility provided by the non-linear regression technique, as it directly fits the ADM and TISM curve to the experimental curve. Whereas, the method of moments is an indirect parameter estimation technique, as it relies on only two parameters i.e. first and second moments (n) to describe the shape of the RTD curve, from which the ADM and TISM parameters are calculated. The ADM generally provides the best-fit to the experimental data for both the model and prototype HDVS operating conditions and parameter estimation techniques.

The method of moments ADM correlation parameters generally improve as the

flow rate is increased and the TISM correlation parameters improve as the flow rate decreases. It should be noted that the ADM used throughout this project and commonly employed by other workers conducting RTD studies is an analytical solution obtained from the ADM first principles and will therefore contain mathematical errors (section 4.3.3). The ADM parameter is also approaching a value describing a system with high dispersion and confidence in its accuracy and true description of the HDVS's mixing regime reduces as it is approaching its lower confidence limits. Whereas the TISM is not subject to such confidence limits (Levenspiel, 1972). The non-linear regression ADM and TISM correlation parameters improve as the flow rate decreases. The trend in the method of moments TISM correlation parameters and non-linear regression ADM and TISM correlation parameters is expected due to the limitations of these models. The ADM and TISM do not account for the fraction of dead volume and subsequently short-circuiting within the HDVS, which is evidently present due to the shape of the RTD curves and increases as the flow rate increases as discussed above. Hence, the experimental data and the ADM and TISM goodness of fit should improve as the flow rate decreases. Therefore, based on the above discussion and the sensitivity of the method of moments and non-linear regression techniques to the RTD truncation time, the non-linear regression TISM parameter estimation technique is superior for describing the HDVS's mixing regime. Haas *et al.*, (1997) also concluded that the non-linear regression parameter estimation technique should be used to characterise the RTD.

Additional RTD data analysis techniques used to characterise the mixing regime within the HDVS include the intensity function (λ) and the RTD indices (section 4.3). The intensity function $\lambda(\Theta)$ describes a mixing regime with dead volumes, short-circuiting and dispersion and therefore, supports the conclusions obtained from the RTD curves and the ADM and TISM parameters discussed above. However, the intensity

function $\lambda(\Theta)$ does not illustrate the relationship between the non-ideal flow behaviour and the flow rate and therefore, identify a transition flow rate at which point the HDVS's mixing characteristics change as discussed above.

The RTD indices either increase or decrease at low flow rates, depending on their individual properties and then remain stable as the flow rate increases. This supports previous conclusions that a transition flow rate exists, above and below which the HDVS mixing regime has different characteristics and that the HDVS has a stable mixing regime at high flow rates. Additionally, the RTD indices also show that the prototype HDVS has greater plug-flow mixing characteristics and improved active flow behaviour compared to the model HDVS. The model and prototype HDVS t_{10} parameter values have a similar relationship with the mean residence time and therefore, when using this parameter for the design of the HDVS for kinetic processes i.e. the time element of the CT product, it is independent of the size of the HDVS. The RTD indices support the improvement in the HDVS's mixing regime when the sludge hopper is removed and that it has less effect on the total mixing regime within the prototype HDVS compared to the model HDVS. Limited RTD experiments conducted using a step tracer injection technique for the model and prototype HDVS operating with no baseflow and with sludge hopper also supported the detailed RTD pulse tracer injection results.

The RTD results presented in this chapter and limited RTD data on different styles of HDVS (Table 1.1) both provide similar descriptions of the mixing regime within the HDVS using the RTD curves and the ADM and TISM parameters. However, the existing HDVS RTD investigations are not consistent or comprehensive in their characterisation of the HDVS's mixing regime and prevents a reliable comparison. Subsequently, the author proposes that a RTD investigation protocol should be established, based on the approach undertaken in this project, to provide an accurate

characterisation of the mixing regime within the different styles of HDVS (Table 1.1) (chapter 8).

The RTD results presented in this project identify a conflict (1) between the mixing regime described by the RTD curves and the ADM and TISM parameters and the RTD experimental parameters (section 4.4.1.1). This is due to extended residence times and subsequently an experimental mean residence time greater than the theoretical mean residence time and a poor tracer recovery (mass balance) at low flow rates, which are largely associated with inactive flow behaviour. Whereas the RTD curve peak concentration occurs closer to a normalised time (Θ) value of 1 at low flow rates suggesting the total volume is active. Additionally, a possible conflict (2) also arises due to the RTD curves at high flow rates having significant plug-flow mixing characteristics combined with short-circuiting and therefore dead volumes, which cannot be adequately described using the ADM or TISM due to their limitations discussed above (section 4.4.1.1). The first conflict (1) does not equally apply to the HDVS operating without the sludge hopper, due to a reduction in the stagnant volume and subsequently an improved tracer recovery (mass balance) and reduced error between the experimental and theoretical mean residence time. However, the error between the theoretical and experimental mean residence time for both HDVS operating conditions and all flow rates is not always eliminated i.e. a positive error still occurs. Therefore, the inactive flow behaviour within the HDVS is possibly not only confined to the sludge hopper region. The second conflict (2) also identified for the HDVS operating with the sludge hopper does equally apply to the HDVS operating without the sludge hopper.

The RTD has been used to investigate the influence of the sludge hopper on the HDVS's mixing regime. However, the volume within the HDVS located above the inlet pipe and adjacent to the overflow spillway (Fig. 3.1) is typically designed as a quiescent zone for the collection of floatable material when the HDVS is used for solids-liquid

separation. Subsequently, observations using coloured dye clearly showed that this volume in the model HDVS contains fluid elements with residence times longer than the mean residence time and therefore, contributes to the inactive flow behaviour within the HDVS.

The RTD parameter conflicts, ADM and TISM limitations and the potential extent of the inactive flow behaviour within the HDVS are the main reason for developing a RTD combined mathematical model (chapter 5). The RTD combined mathematical model is specifically developed to provide physical realism of the mixing regime within the HDVS. The combined model describes the non-ideal flow behaviour associated with both the plug-flow mixing characteristics i.e. dispersion and the inactive volume within the HDVS, whereas the generic ADM and TISM only describe non-ideal flow behaviour associated with dispersion. This will aid in quantifying the inactive flow behaviour within the HDVS and show if it is only limited to a volume in the vicinity of the sludge hopper. Additionally, the model and prototype HDVS operating with and without the sludge hopper RTD combined model results can be directly compared and used to support the observations and conclusions presented in this chapter, obtained using different RTD data analysis techniques. Regardless of the estimated inactive flow behaviour calculated using the combined model, it is not possible to precisely locate its position within the HDVS. This could possibly be accomplished using CFD and in situ velocity measurements and has partially been addressed by other workers (section 2.1.4). The RTD combined mathematical model is presented and the results discussed in chapter 5.

5.0 Residence Time Distribution (RTD) Combined Mathematical Model

This chapter presents the first RTD combined mathematical model specifically developed to describe and provide physical realism of the mixing regime within the HDVS. The combined model (Fig. 5.1) is configured to quantify the dead volume within the HDVS as a function of an exchange flow rate between the active and non-active volumes. The ADM and TISM RTD data analysis techniques do not account for the presence of any inactive flow behaviour in their description of the mixing regime (Morgan-Sagastume *et al.*, 1999). The RTD combined model data analysis technique is applied to the model and prototype HDVS operating with no baseflow and with and without the sludge hopper RTD experimental data (chapter 4). This was undertaken to address the conflicts (1 and 2) first identified in chapter 4 (section 4.4.1.1) and repeated below, between visual characteristics of the RTD normalised curves E(Θ) and the RTD ADM, TISM and method of moments data analysis parameters. Additionally the combined model results should also aid in supporting previous descriptions of the HDVS mixing regime provided in chapter 4.

The combined model parameters and experimental RTD data investigated will show if the dead volume is only limited to the sludge hopper region (Fig. 3.1) and the inclusion of a bypass flow rate (Fig. 5.1) will aid in accessing the HDVS's dead volume relationship with the inlet flow rate. The combined model parameter sensitivity and true physical realism is also discussed. The combined model is an alternative method of describing the mixing regime within the HDVS and is not necessarily superior to previous descriptions obtained using the ADM and TISM (chapter 4). The combined model configuration (Fig. 5.1) can be applied to RTD investigations undertaken on any size HDVS i.e. diameter and therefore, used to aid in developing scaling relationships based on the mixing regime (section 8.6). Several workers have used the RTD

combined model data analysis method to describe the mixing regime in a number of different systems (section 2.2.1).

5.1 General Characteristics

The combined model is designed to provide physical realism of the model and prototype HDVS and is so named as it considers that a flow pattern may be composed of three basic elements: effective volume of mixing, short-circuiting and plug-flow mixing (Wen and Fan, 1975). The combined model corresponds to the second RTD data analysis technique i.e. the use of mathematical models in order to assess the flow pattern by fitting to the RTD experimental curve (section 4.3). The combined model was only applied to the RTD pulse injection data for the model and prototype HDVS operating with no baseflow with and without the sludge hopper (Fig. 3.1) (chapter 4). The RTD experimental duration for all inlet flow rates and operating configurations was approximately 6 times the theoretical mean residence time and therefore, provides consistent data describing the HDVS's mixing regime and eliminates the need to consider any RTD truncation effects (section 4.4.1).

The ADM and TISM are one parameter models, which can be used to suitably investigate and describe the RTD when there is a small amount of non-ideal flow behaviour (section 4.3.3). However, the standard ADM and TISM do not always adequately account for any stagnant regions, which result in dead volumes and short-circuiting (Morgan-Sagastume *et al.*, 1999) and are evidently present within the HDVS (section 4.4). Additionally with increased dispersion it becomes increasingly unlikely that the assumptions of the ADM will be satisfied by the real system (section 4.3.3). Similarly the method of moments technique for determining the RTD is also subject to errors when the RTD is not of a normal distribution i.e. symmetrical about the mean.

This is illustrated by other workers who have shown that as the ADM Peclet number (P_e) decreases, indicating greater mixing, the RTD parameters need to be measured to a greater accuracy i.e. first and second moments (Haas *et al.*, 1997).

The ADM and TISM parameters calculated using the method of moments and non-linear regression provide a good fit to the experimental RTD data i.e. model validation. However, the ADM and TISM may still not provide physical realism of the true mixing regime within the HDVS i.e. model verification. This is due to the limitations of the method of moments, ADM and TISM and combined with the internal geometry of the HDVS i.e. sludge hopper region, contribute to errors between the experimental and theoretical pulse tracer recovery (mass balance) and mean residence time values (section 4.4). Additionally, visual observations of the RTD normalised curves $E(\Theta)$ and the results obtained and implied by the ADM, TISM and RTD parameters, created two possible conflicts (1 and 2) (section 4.4.1.1):

1 - At low flow rates poor tracer recovery, a greater fraction of the volume with extended residence times and a substantially large experimental mean residence time calculation, are all attributed to dead volumes within the model HDVS i.e. sludge hopper region (Fig. 3.1). However the RTD normalised curves $E(\Theta)$ (Fig. 4.8) suggest that a greater fraction of the total volume of the model HDVS is active at low flow rates. This is due to the peak of the RTD curves occurring in the vicinity of a normalised time (Θ) value of 1 (eqn. 4.2).

2 - At high flow rates there is a more defined peak of the RTD curves, implying that the majority of the flow leaves the HDVS in the vicinity of certain contact time, although before a normalised time (Θ) value of 1 and therefore, short-circuiting and dead spaces are present. The former RTD characteristics, are representative of plug-flow mixing

however, the ADM and TISM parameters do not account for any short-circuiting or stagnant zones (Morgan-Sagastume *et al.*, 1999). Subsequently this could account for the ADM and TISM parameters decreasing as the flow rate is increased and create a possible conflict with visual observations. Hence, it is possible for the HDVS to have a greater element of plug-flow mixing at high flow rates, compared to low flow rates, in a volume smaller than the total volume of the HDVS. This conflict is purely visual and not supported by any other experimental or RTD parameters e.g. RTD indices (section 4.4.4).

The combined model configuration, considering the previously mentioned basic mixing elements, selected to describe both the model and prototype HDVS, is 3 completely mixed tanks (V_1-V_3) with a dead volume (V_4) and an exchange flow rate (Q_2) between the dead and active volumes (Fig. 5.1). A bypass flow (Q_3) has also been included to investigate the presence of short-circuiting. Therefore, the combined model configuration is effectively a modification of the TISM, limited to 3 tanks-in-series (N) as opposed to infinity (eqn. 4.9) and incorporating non-ideal flow behaviour associated with dead volumes, which the basic TISM does not describe (section 4.3.3). The combined model is illustrated schematically in Fig. 5.1. This arrangement was selected to represent the mixing regime in the model and prototype HDVS from the RTD experimental results and data analysis investigations presented in chapter 4.

The combined model is considered to provide physical realism of the HDVS's mixing regime, as it's plug-flow mixing characteristics are fixed equal to 3 tanks-in-series (N) (section 4.3.3). The TISM parameters (N) calculated using the method of moments and non-linear regression, for the model and prototype HDVS operating with and without the sludge hopper, are all generally between N=1 and N=3, across the range of flow rates (section 4.4). Therefore the combined model configuration (Fig. 5.1)

should not be limited by its ability to describe the plug-flow mixing characteristics of both the model and prototype HDVS for their different operating conditions.

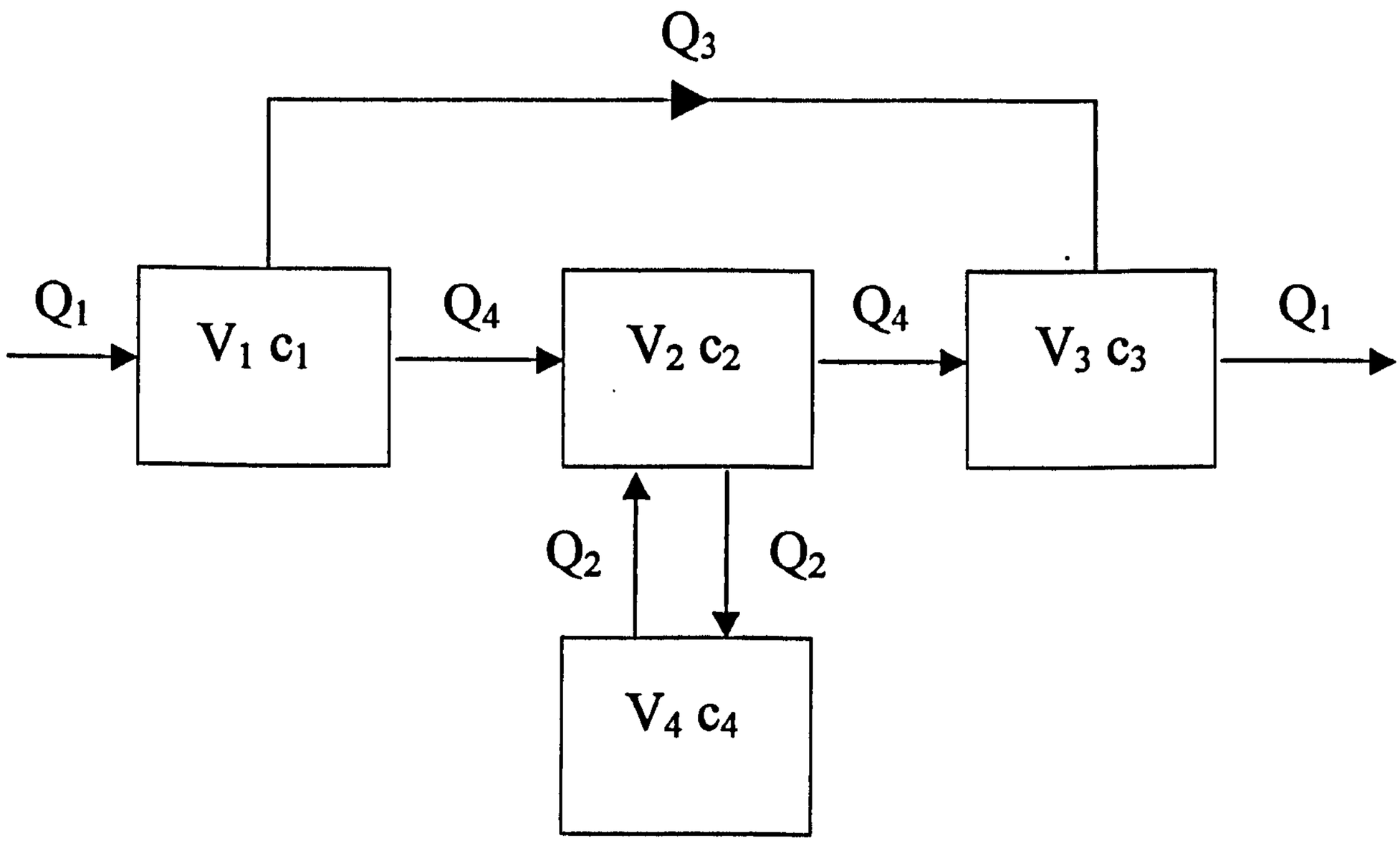

Fig. 5.1 RTD Combined Mathematical Model Schematic Configuration

Where: Q_1 = Inlet Flow Rate (l/min)

Q_2 = Exchange Flow Rate (l/min)

Q_3 = Bypass Flow Rate (l/min)

$Q_4 = Q_1 - Q_3$ (l/min)

V_1, V_2 and V_3 = (HDVS volume – V_4)/3 (l)

V_4 = Dead volume (l)

C_1-C_4 = RTD Pulse Tracer Injection Concentration (mg/l)

Since many combined model configurations of varying complexity are available and with a large number of parameters, which make the model flexible in fitting to a wide variety of situations, the combined model adopted is not necessarily unique to the

HDVS or vice versa. The selected combined model configuration (Fig. 5.1) has three adjustable parameters: a dead volume (V_4), exchange flow rate (Q_2) between the dead volume and remaining active volume and a bypass flow rate (Q_3) i.e. short-circuiting. However, the combined model was predominantly investigated with only two adjustable parameters, the dead volume (V_4) and exchange flow rate (Q_2) and therefore the bypass flow rate (Q_3) was set to zero (section 5.2). This situation makes the model much more tractable (Fogler, 1992). The combined model dead volume parameter (V_4) will provide an indication as to whether the stagnant volumes are only confined to the sludge hopper (Fig. 3.1). Observations with coloured dye in the model HDVS (section 4.4.10) suggested that such regions may also exist around the cone area and at the top water level in the outer zone, which is used for the collection of floatable material during solid-liquid separation applications (Fig. 3.1).

5.2 Development and Analysis

The combined model is classified as a physically-based deterministic model (appendix D.1) where, "one combination of input data will always give the same output, randomness is not accounted for" (Butler and Davies, 2000). The combined model development procedure consisted of establishing mass balance relationships (eqn. D.1.1-D.1.4) and subsequently, differential equations for the concentration of tracer through each tank of the combined model with respect to time (eqn. D.1.5-D.1.8). The resulting second order differential equations were solved analytically and therefore a mathematical solution is obtained directly from the differential equations, as opposed to numerically, which requires further analysis to obtain a solution, generally using finite difference methods. The combined mathematical model equations are described along with the complete derivation and solution in appendix D.1.

The combined model provides either a modelled concentration C(t) or exit-age distribution function E(t) curve (section 4.3) and the experimental data is presented in appendix C for the model and prototype HDVS operating with no baseflow with and without sludge hopper. The best-fit criteria for the modelled data, compared to the experimental data, was based on the correlation parameters previously discussed in section 4.3.3 i.e. coefficient of correlation (R^2) and sum of the errors squared (ESS). A combined model solution was obtained using an EXCEL spreadsheet and the SOLVER function, as used for the RTD non-linear regression ADM and TISM parameter estimation technique (section 4.3.3) and by trial and error. The combined model solution obtained using the latter method, was achieved by creating a parameter matrix and employed, as the SOLVER function is an iterative process and therefore, depends on the initial parameter values selected, which may not provide the true maximum correlation. The author is aware of more complex computational iterative parameter optimisation techniques available in Mathcad and Matlab computer packages and Monte Carlo simulations (Haas *et al.*, 1997). However, using the EXCEL SOLVER function and a trial and error parameter matrix to obtain a best-fit combined model solution was considered adequate for comparing and supporting conclusions obtained from the RTD curves and the ADM and TISM parameters (chapter 4). The advanced parameter optimisation techniques may require consideration if the RTD combined model is used to investigate the HDVS operating with a baseflow component RTD data (chapter 6) and to develop scaling relationships between the model and prototype HDVS (section 8.6). This is due to the large number of RTD experiments and also to provide greater confidence in obtaining the best-fit solution.

The model and prototype HDVS operating conditions i.e. flow rate, volume and therefore theoretical mean residence time, are incorporated into the combined model solution by using simplification constants (appendix D.1). These are represented by the

'k' values and aid in simplifying the mass balance equations (eqn. D.1.1-D.1.4) into differential equations (eqn. D.1.5-D.1.8) to obtain an analytical solution. The initial experimental tracer concentration (C_o) calculation method for a pulse injection is described in appendix D.1 and assumes the injected tracer is only diluted with one complete volume of the HDVS. However, as the RTD experimental duration was maintained at approximately 6 times the theoretical mean residence time for all HDVS operating conditions, this assumption is unlikely to be representative of the true tracer concentration within the HDVS. Subsequently the initial experimental tracer concentration (C_o) was also treated as an adjustable combined model parameter.

The combined model was configured to represent the individual 'active' volumes i.e. V_1, V_2 and V_3 as equal volumes, once the dead volume (V_4) has been subtracted from the total HDVS volume (Fig. 5.1). This volume distribution was adopted, as the dead volume (V_4) is considered unlikely to be confined to one specific area within the HDVS. Alternatively, if this is not a true representation of the dead volume (V_4), it could be removed from the volume of either one or two tanks only.

The combined model solution (appendix D.1) assumes the model and prototype HDVS mean residence time is equal to the theoretical mean residence time for each individual flow rate (eqn. 4.2). This is achieved using the 'k' constants as discussed above and presented in appendix D.1. The theoretical mean residence time for the total system is maintained by modelling the dead volume (V_4) as a function of the exchange flow rate (Q_2). If the dead volume (V_4) was independent of the exchange flow rate (Q_2), the theoretical mean residence time would need to be treated as an adjustable parameter. This is because a change in the dead volume (V_4) would increase or decrease the active volume and therefore, result in the remaining flow having a different theoretical mean residence time. The bypass flow rate (Q_3) parameter was only investigated independently of the dead volume (V_4) and exchange flow rate (Q_2) parameters and

hence, the combined model solution obtained for one variable parameter i.e. (Q_3). This was undertaken to support conclusions obtained from the combined model best-fit dead volume (V_4) and exchange flow rate (Q_2) parameters for zero bypass (Q_3) operating conditions (Fig. 5.11).

5.3 Results and Discussion

The combined model results for both the model and prototype HDVS operating with no baseflow and with and without the sludge hopper are all presented in this section. The combined model results have the same general trend, irrespective of the HDVS size and operating configuration and therefore, the same discussion and conclusions apply.

This project only presents in detail the combined model results generated independently of the initial tracer concentration (C_o), as opposed to also investigating a fixed-dependent value, for reasons discussed below. A combined model solution, independent of the initial tracer concentration (C_o), was achieved by comparing the exit-age distribution function E(t) calculated by the combined model, generated from the concentration-time data, to the experimental exit-age distribution function E(t) data. The exit-age distribution function E(t) (eqn. 4.1) is independent of the initial tracer concentration (C_o) when comparing two different RTD data sets. Subsequently the combined model exit-age distribution function E(t) presented, provides the best-fit based on the criteria discussed below however, it does not necessarily provide the best-fit concentration-time curve.

The best-fit combined model curve was first based on a visual observation and once approaching an optimum fit then using the best-fit criteria (section 4.3.3). The correlation parameters (R^2 and ESS) are presented in appendix D.2. This approach was

taken, as it was found that the combined model parameters providing the best-fit depended on the correlation parameter selected i.e. R^2 or ESS. Additionally, it is difficult to compare the ESS correlation parameter across the range of inlet flow rates, as the magnitude of the exit-age distribution function E(t) for each corresponding time interval reduces as the flow rate decreases and therefore the ESS values naturally follow the same trend. Hence, the ESS values do not necessarily indicate that the goodness of fit is improving or reducing. Selecting the RTD combined model and experimental curve best-fit criteria is recommended as part of future studies using the combined model (section 8.6).

Fig. 5.2-5.5 compares the model and prototype HDVS experimental and combined model exit-age distribution function E(t) curves for selected flow rates. The remaining flow rates are presented in appendix D.3-D.6. A reduction in the combined model dead volume (V_4) and exchange flow rate (Q_2) parameters sensitivity and therefore model fitting flexibility, occurs as the inlet flow rate decreases. This coincides with the transition flow rates previously identified for both the model and prototype HDVS i.e. 15l/min and 90l/min respectively (section 4.4). This is illustrated in Fig. 5.6, for the model HDVS operating with the sludge hopper, for flow rates of 6 and 60l/min and an increase in the best-fit dead volume (V_4) and exchange flow rate (Q_2) parameters of 20, 40 and 60%. These curves clearly show that the shape of the combined model RTD curve is significantly altered at high flow rates. Whereas at low flow rates there is little change in the shape of the combined model curve generated by the different parameter values. Fig. 5.2-5.5 show from visual inspection that the modelled data adequately describes the experimental data for flow rates greater than the transition flow rate and as the flow rate decreases, the combined model and experimental curves goodness of fit reduces. This is supported by the R^2 correlation parameter, which show that the combined model and experimental RTD curves goodness of fit generally improves as

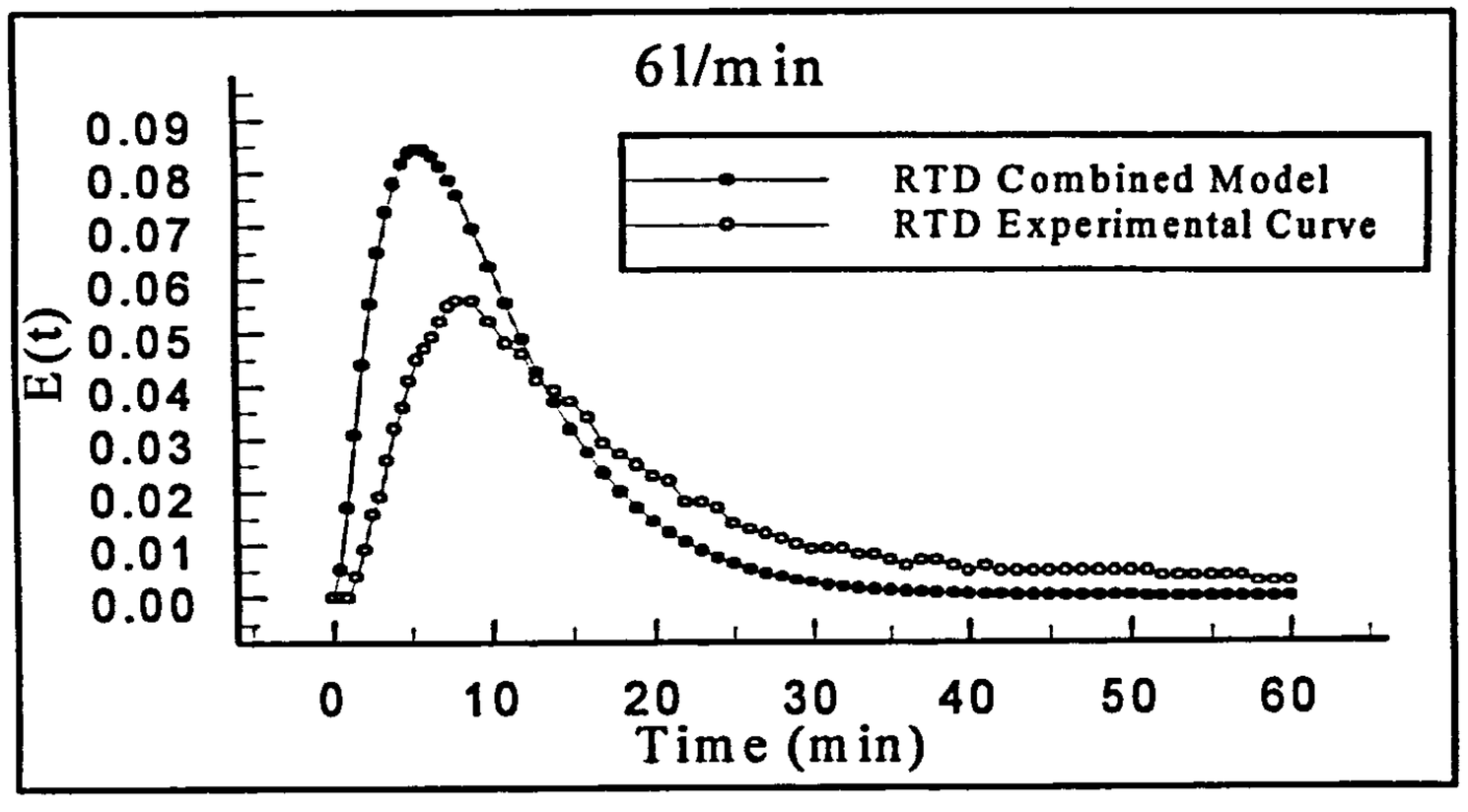

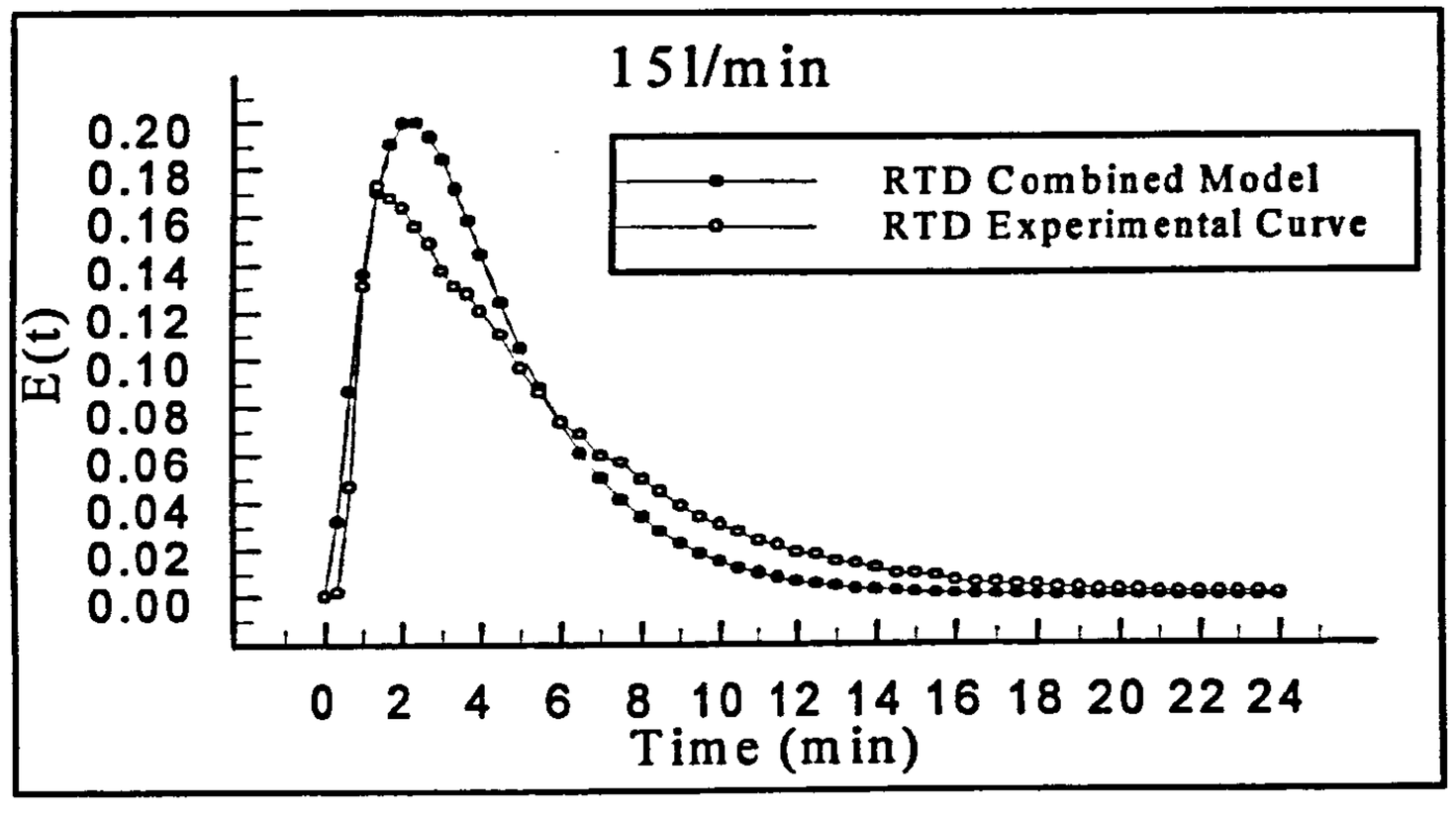

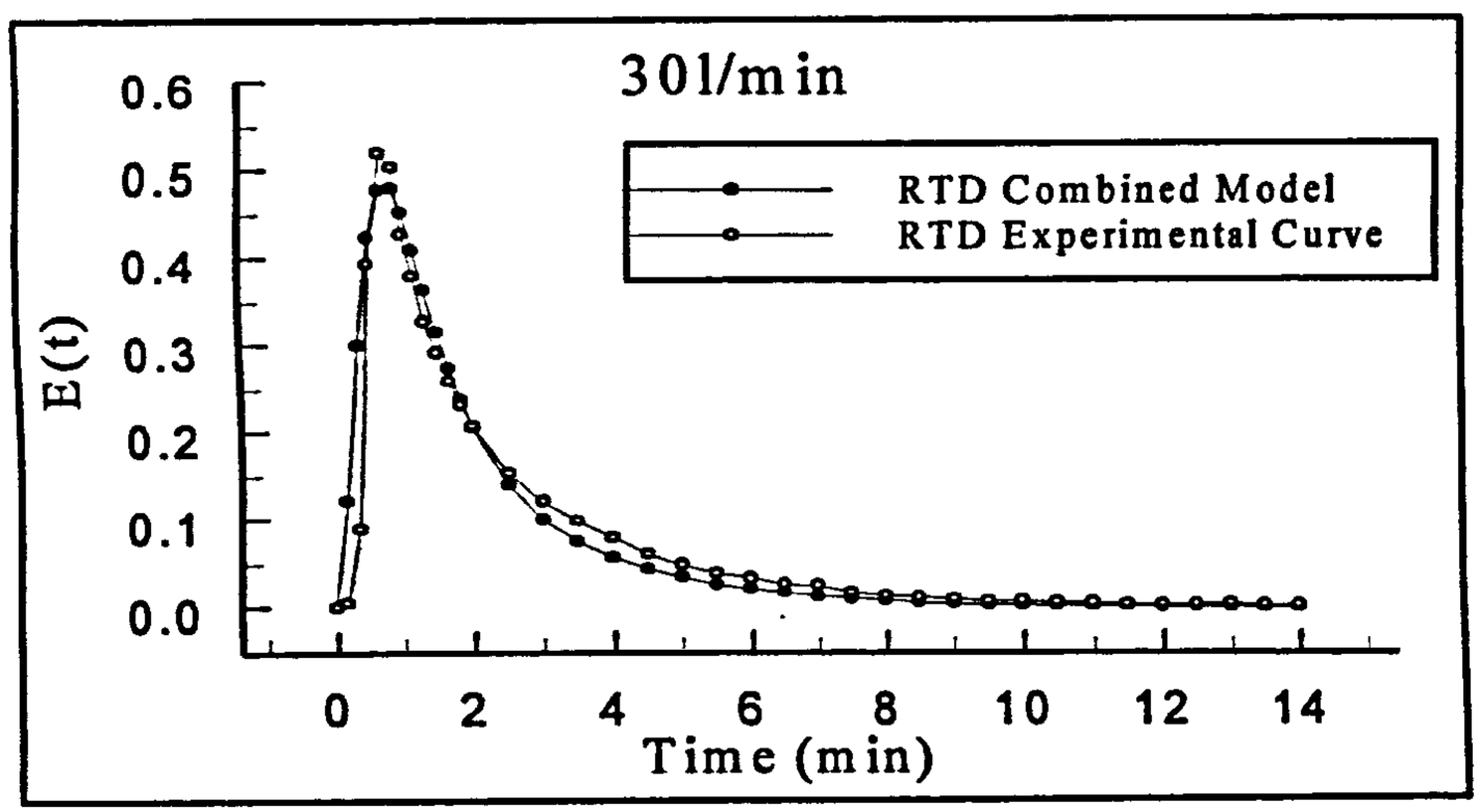

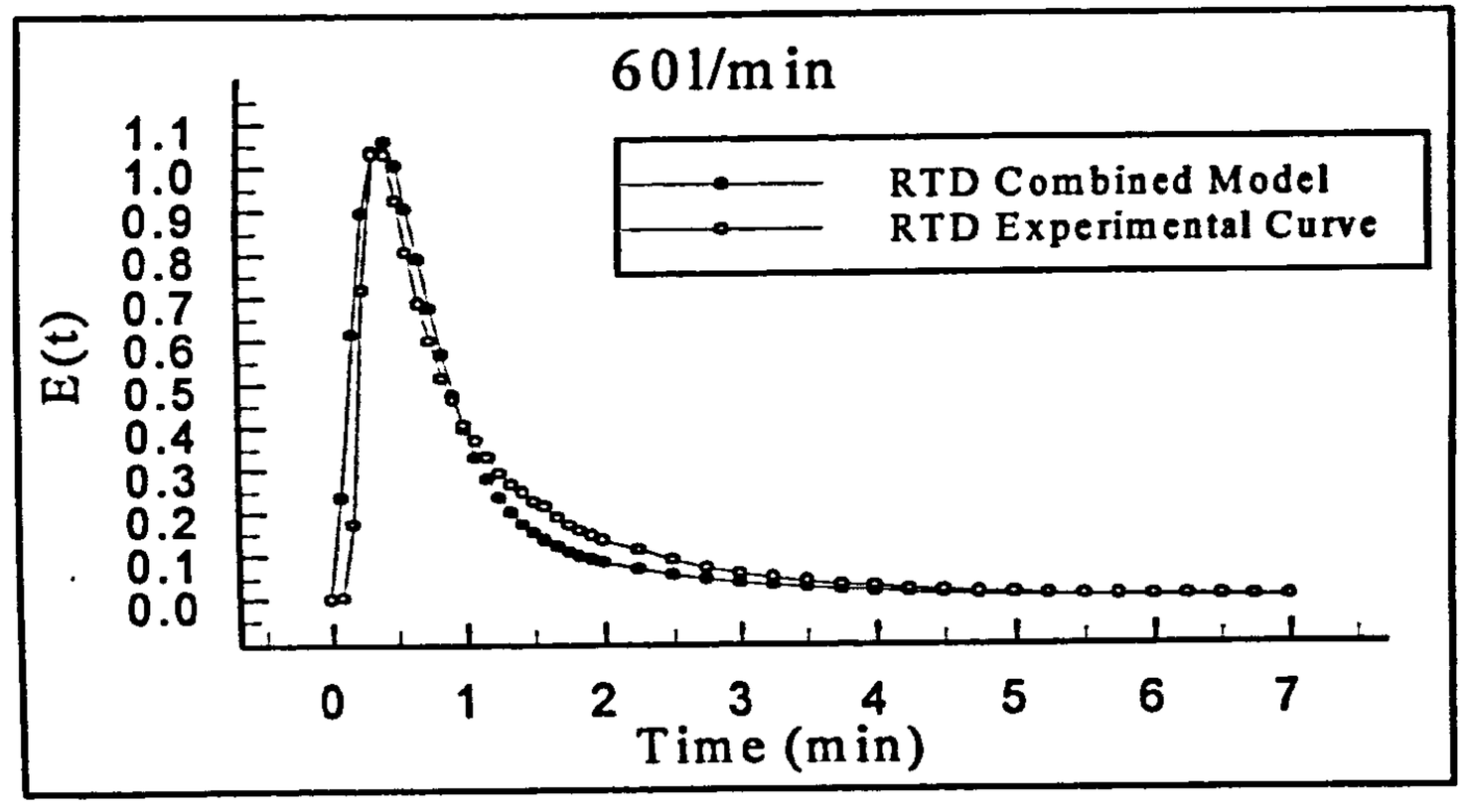

Fig. 5.2 Model HDVS No Baseflow - Comparison of RTD Combined Model and Experimental E(t) Curves for Selected Flow Rates

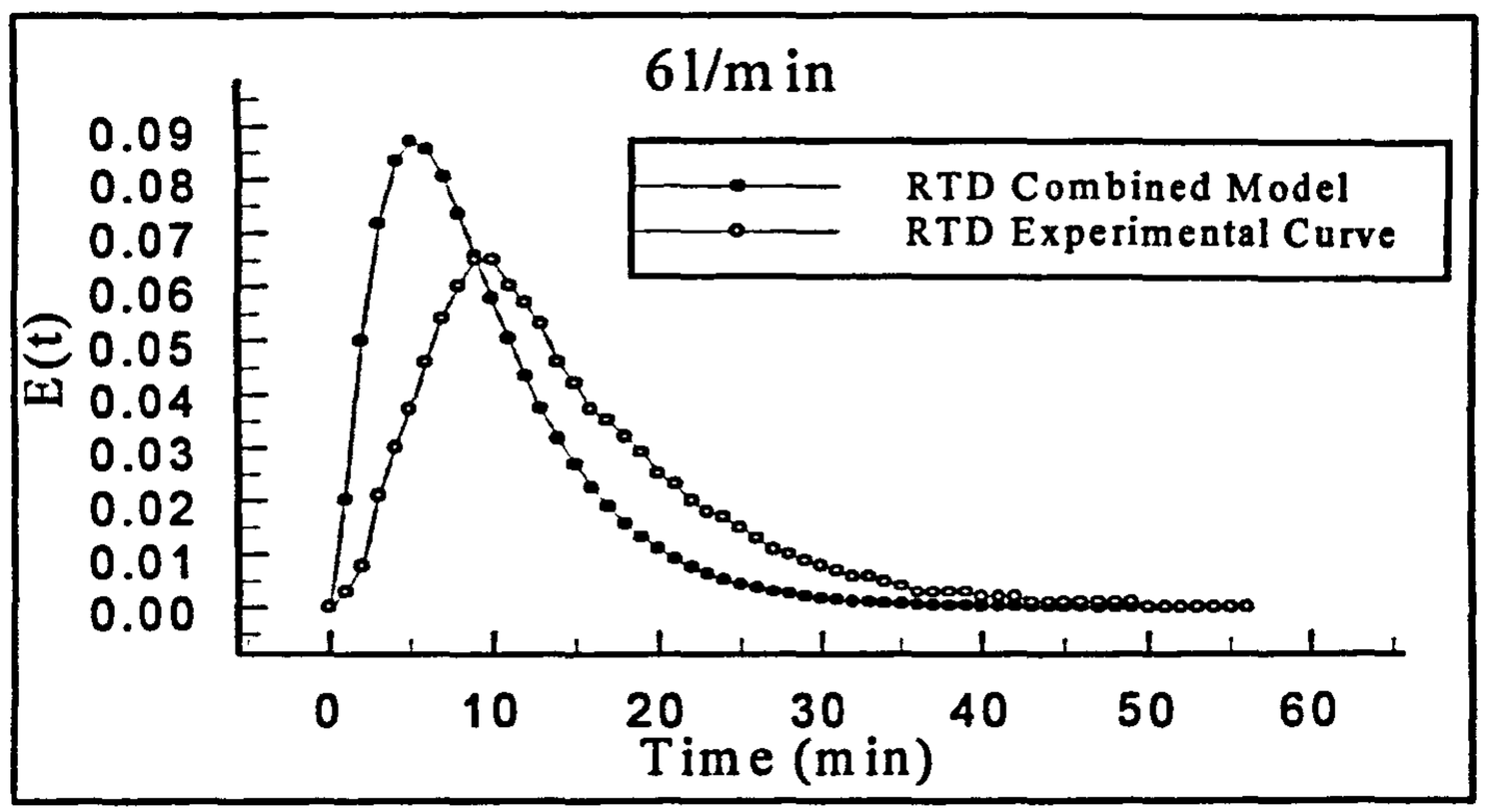

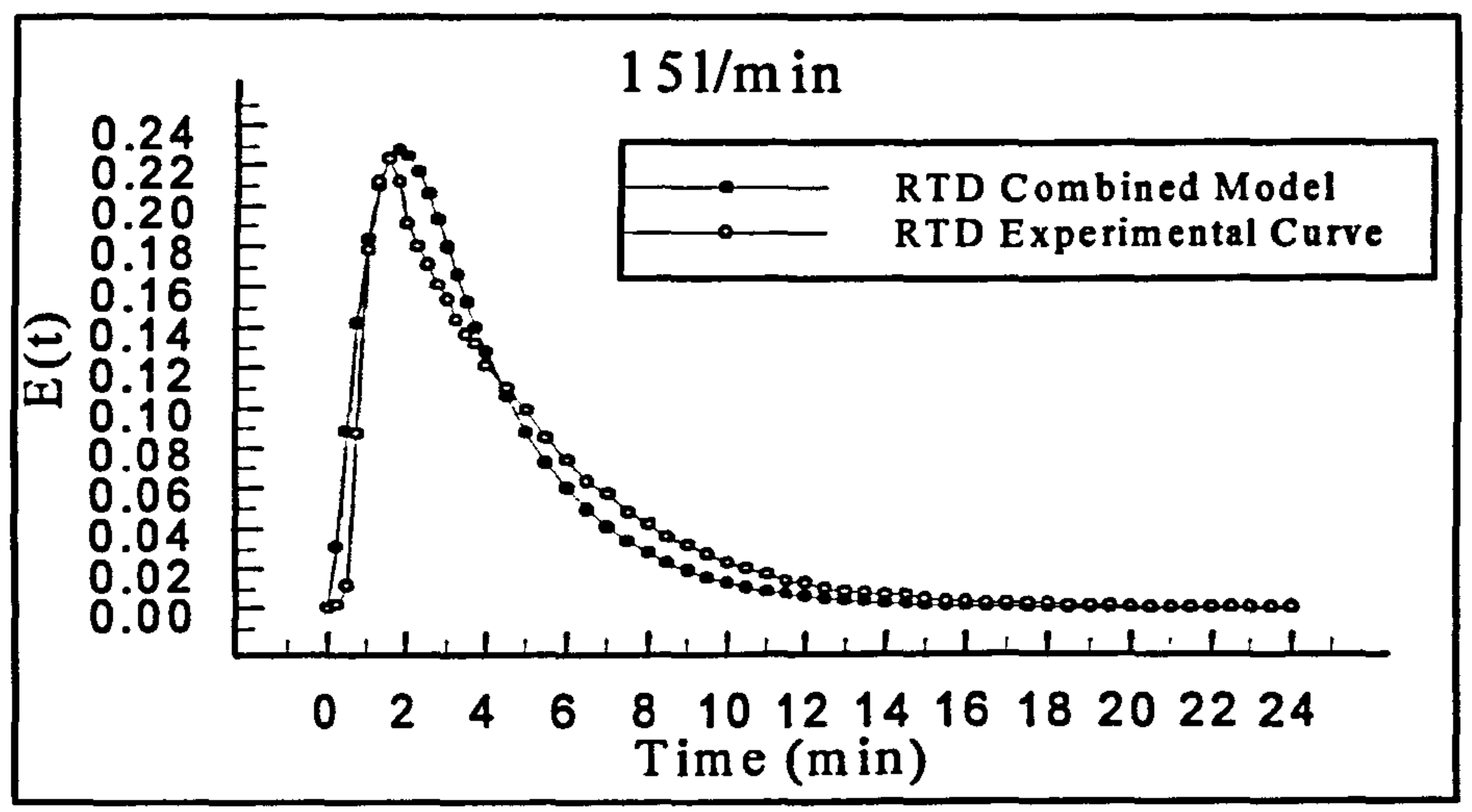

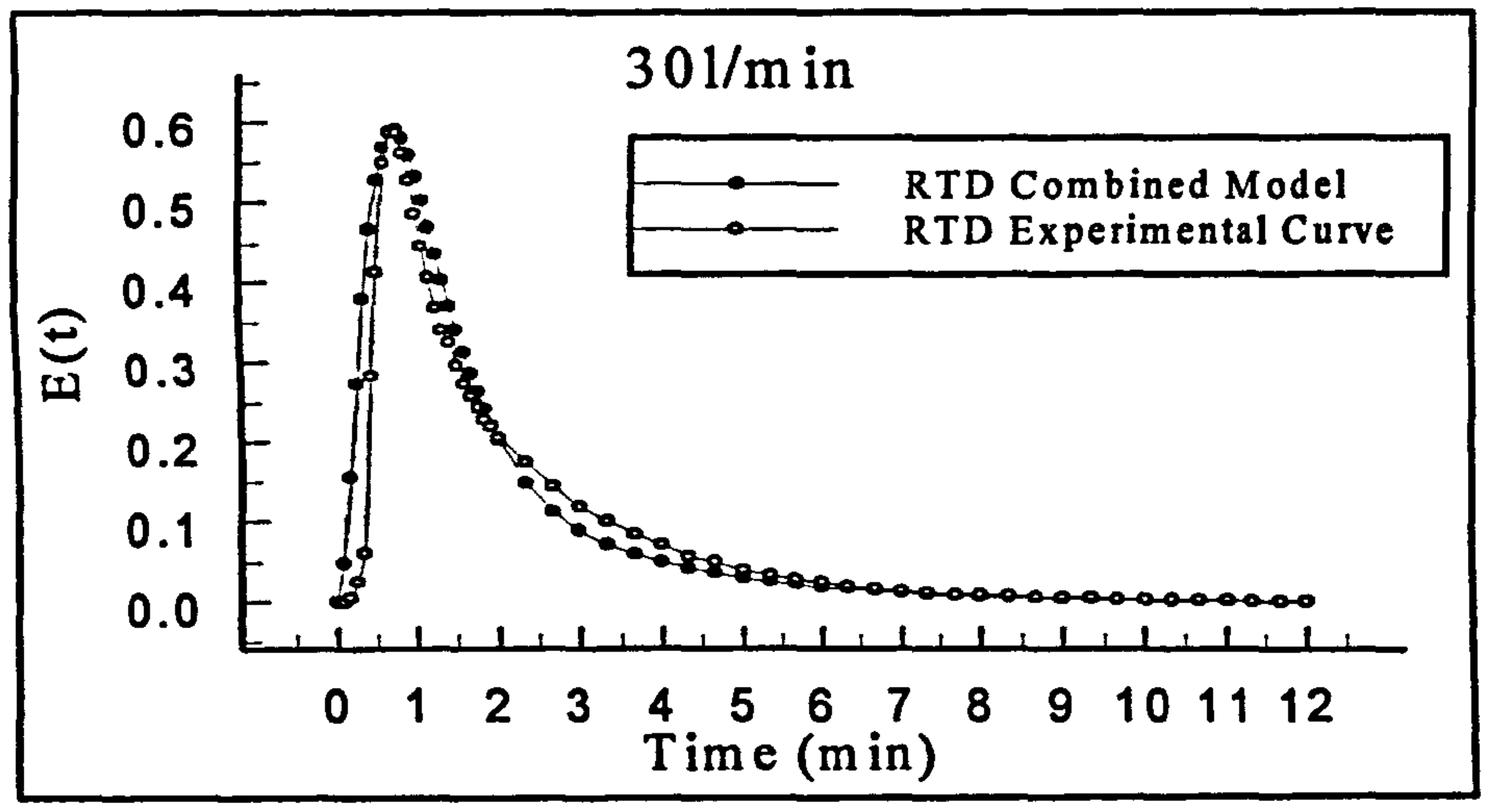

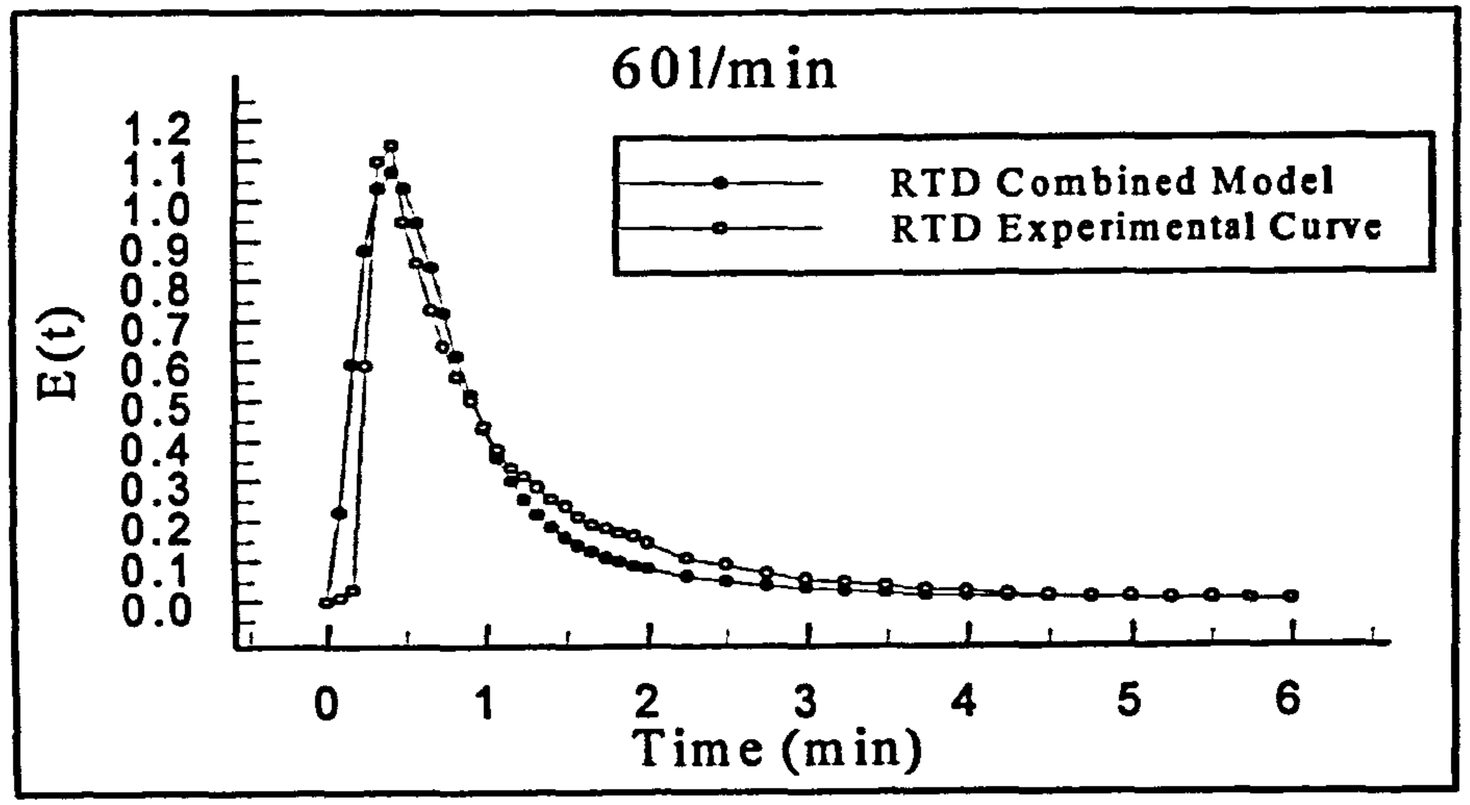

Fig. 5.3 Model HDVS No Sludge Hopper - Comparison of RTD Combined Model and Experimental E(t) Curves for Selected Flow Rates

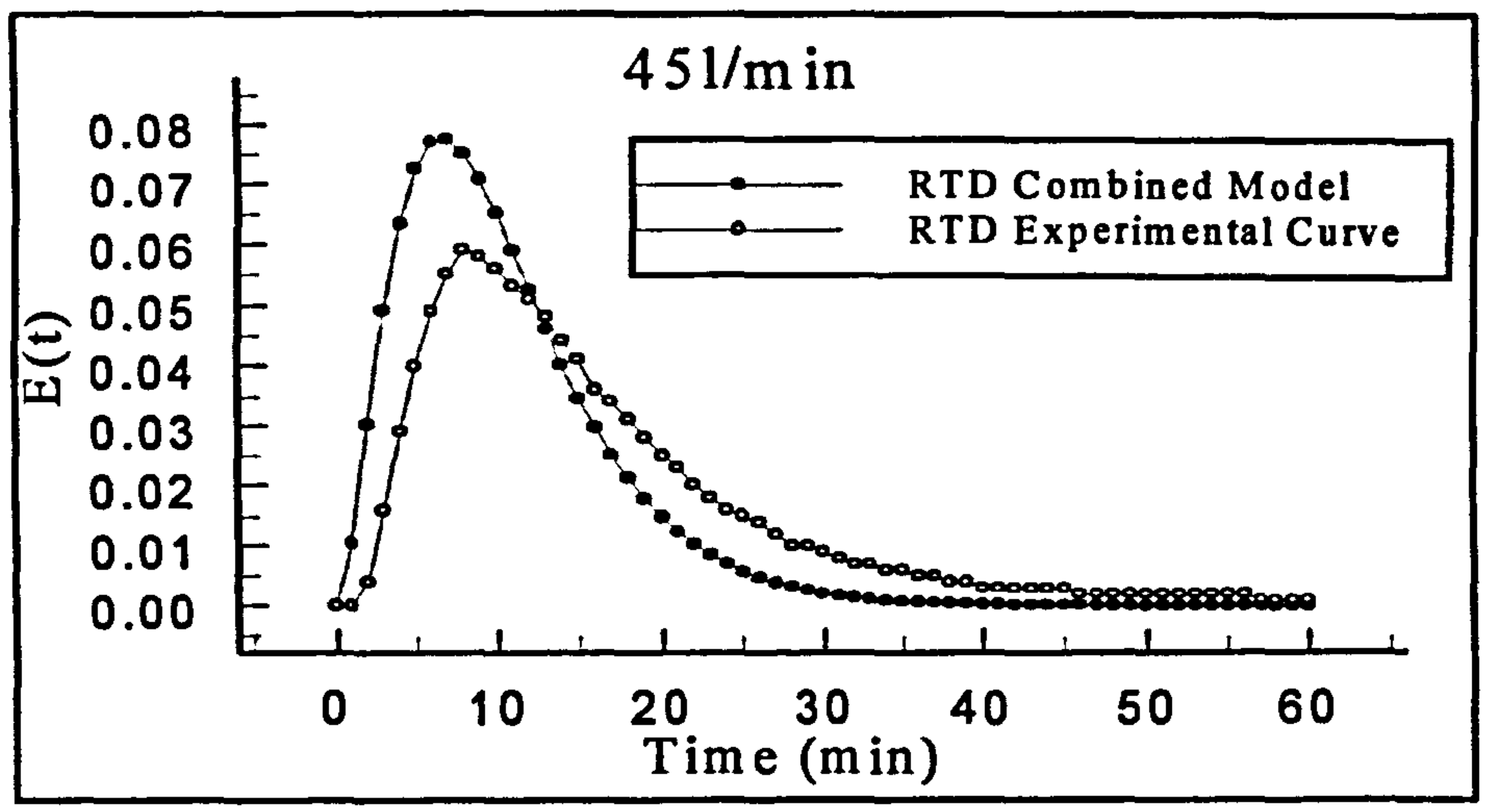

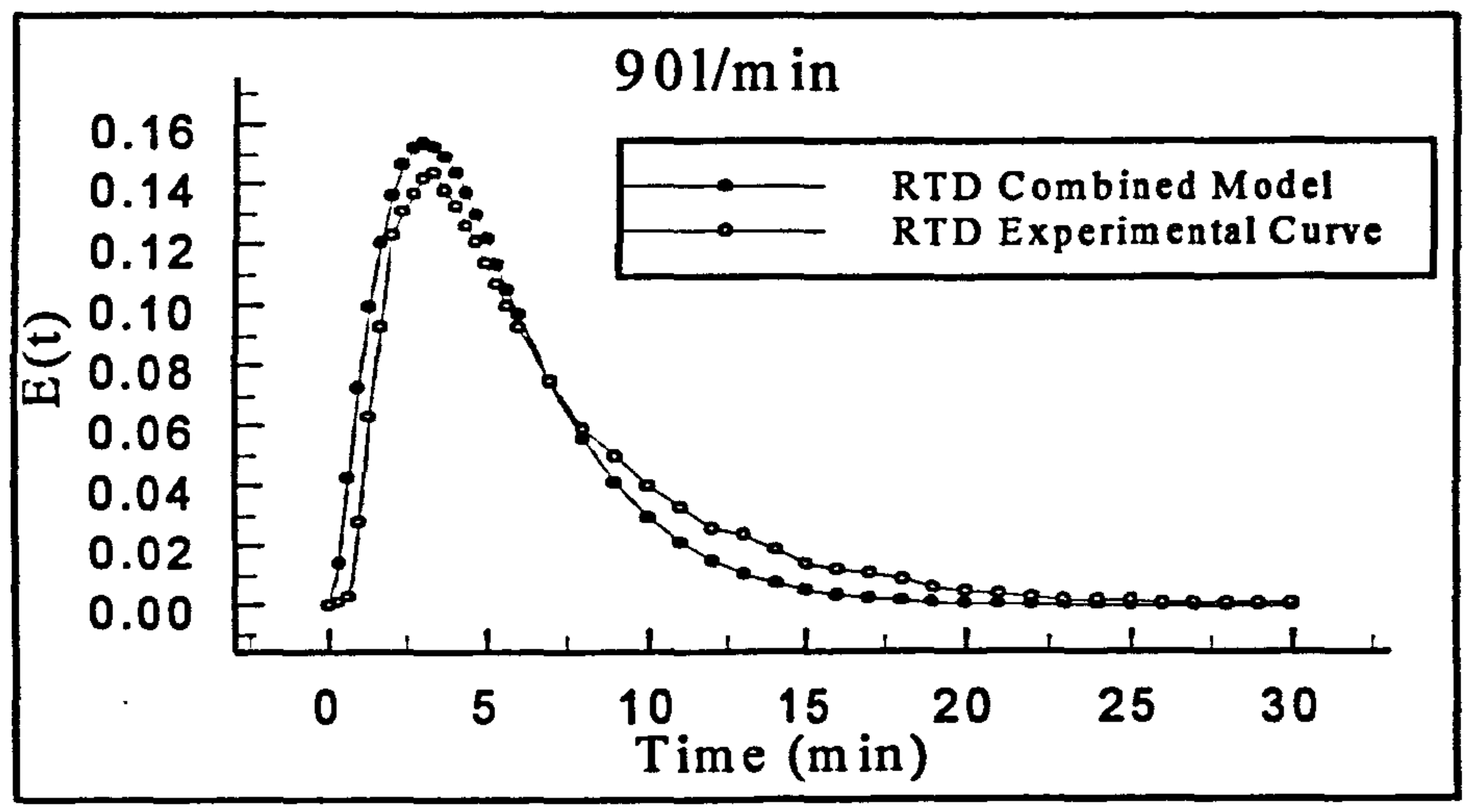

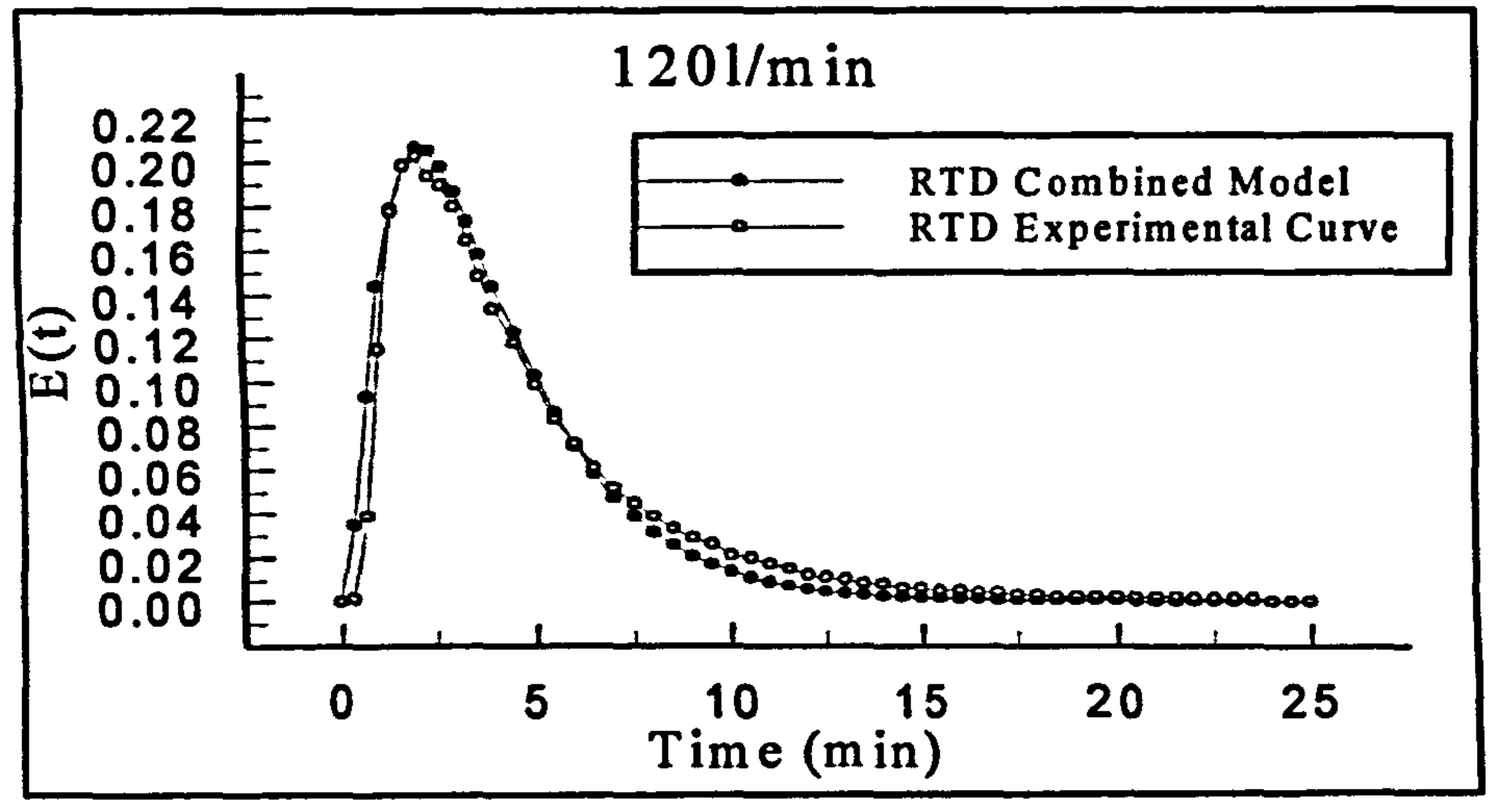

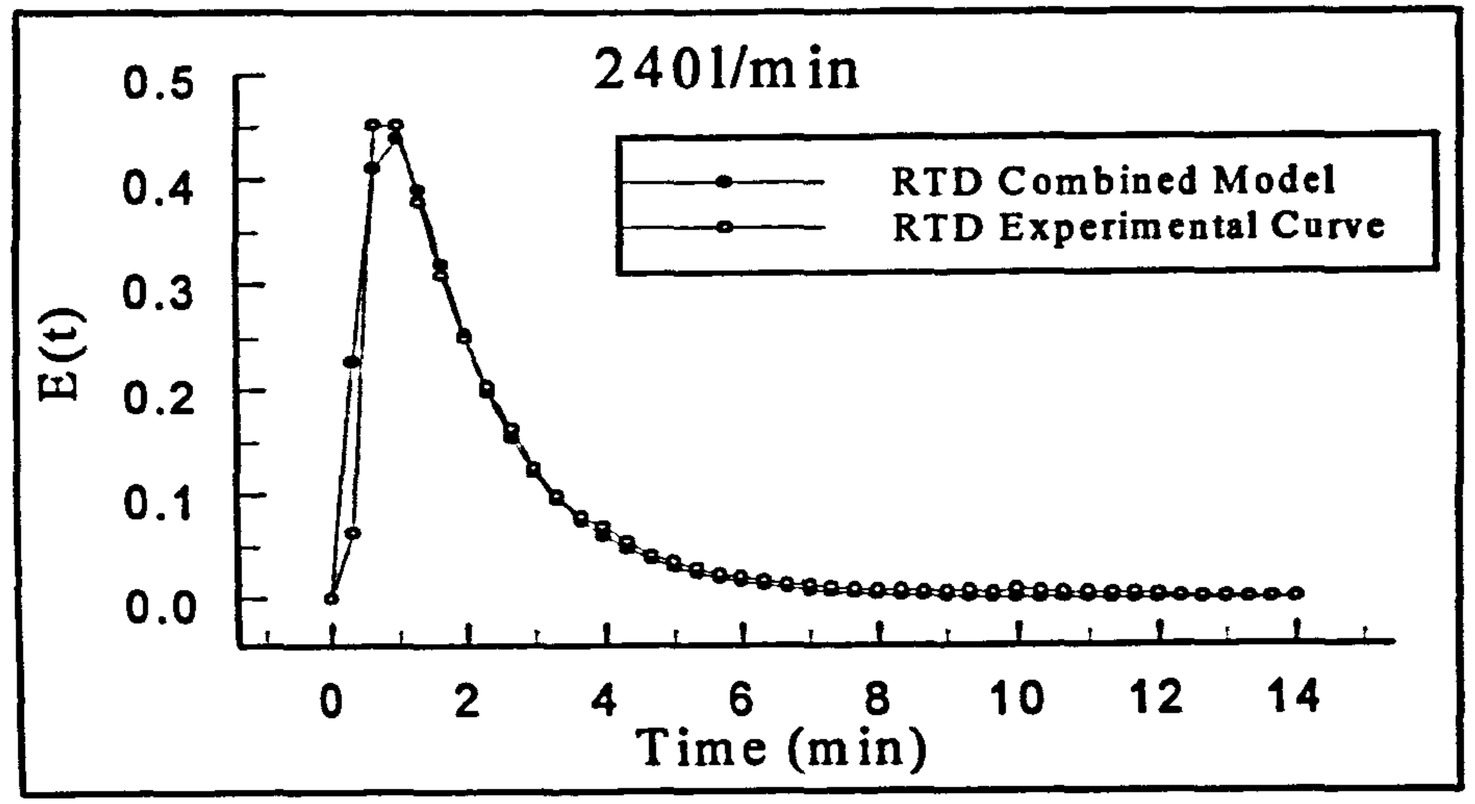

Fig. 5.4 Prototype HDVS No Baseflow - Comparison of RTD Combined Model and Experimental E(t) Curves for Selected Flow Rates

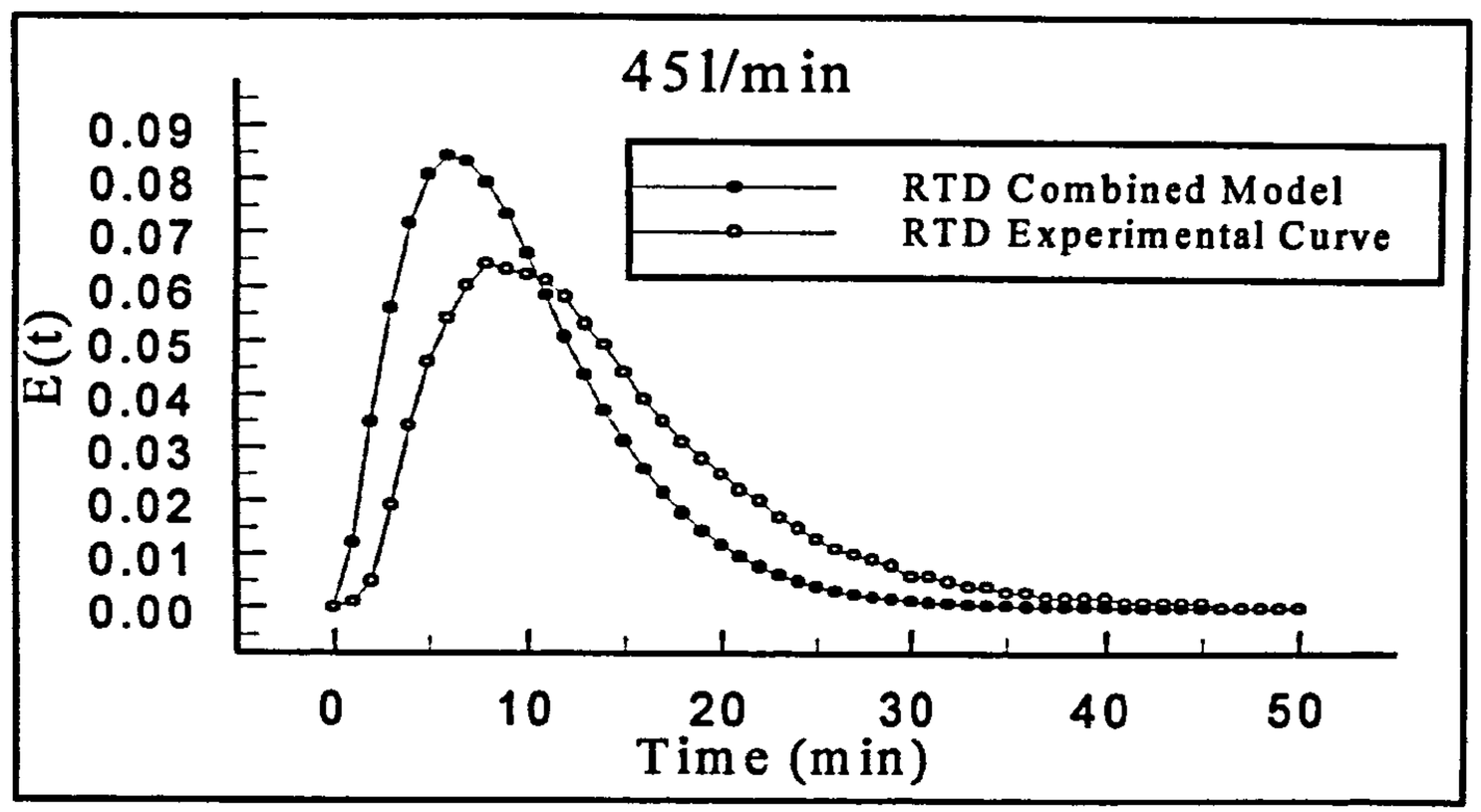

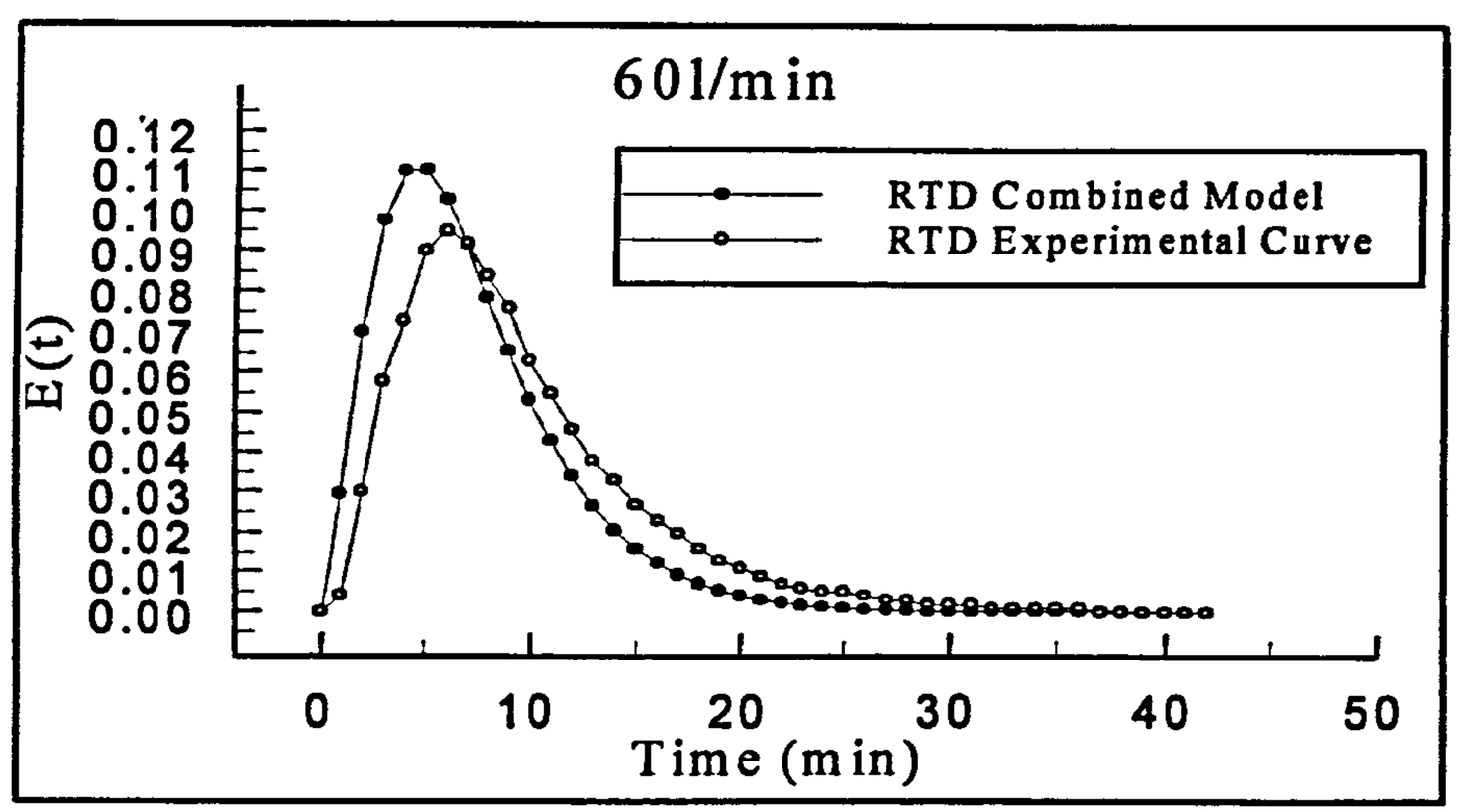

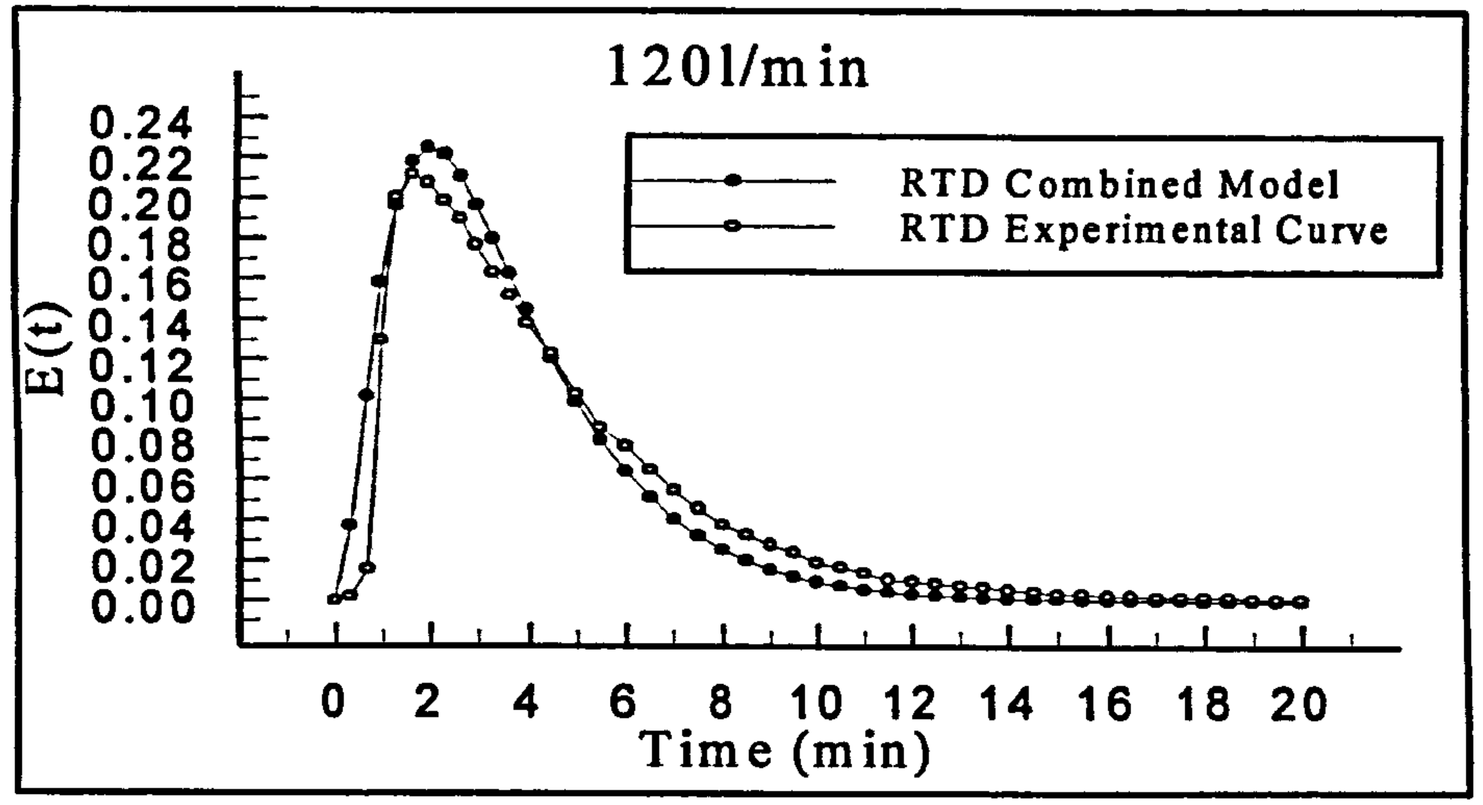

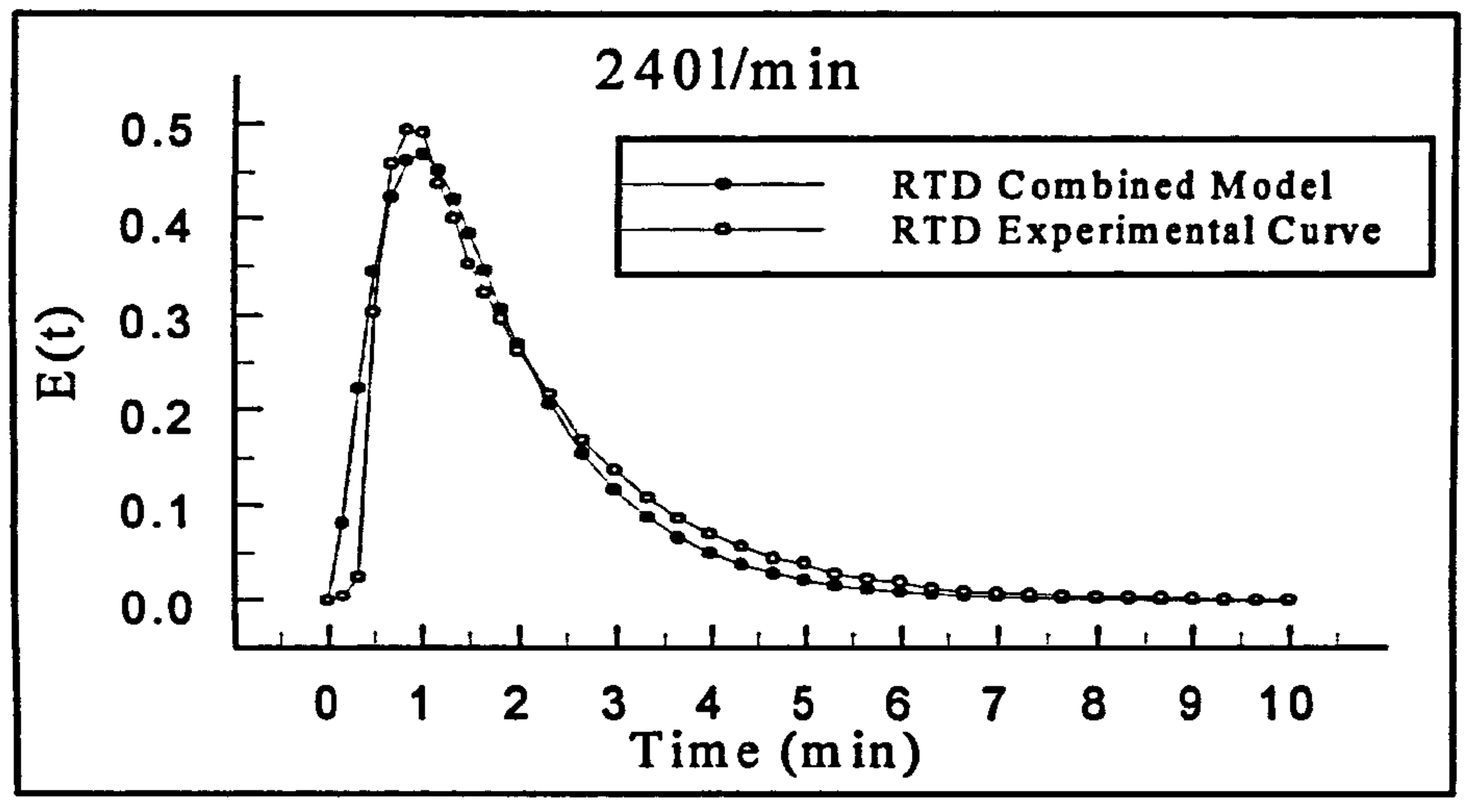

Fig. 5.5 Prototype HDVS No Sludge Hopper - Comparison of RTD Combined Model and Experimental E(t) Curves for Selected Flow Rates

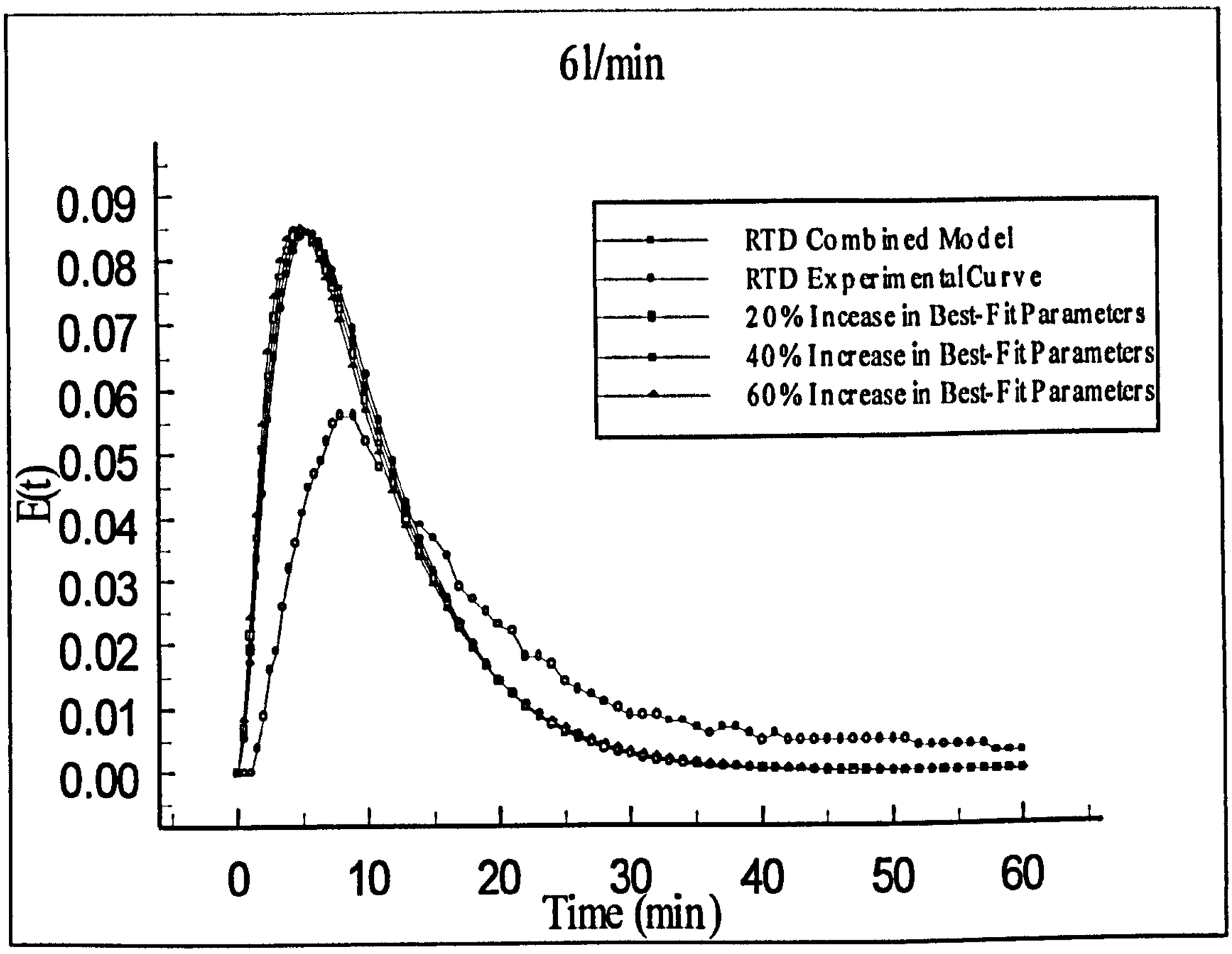

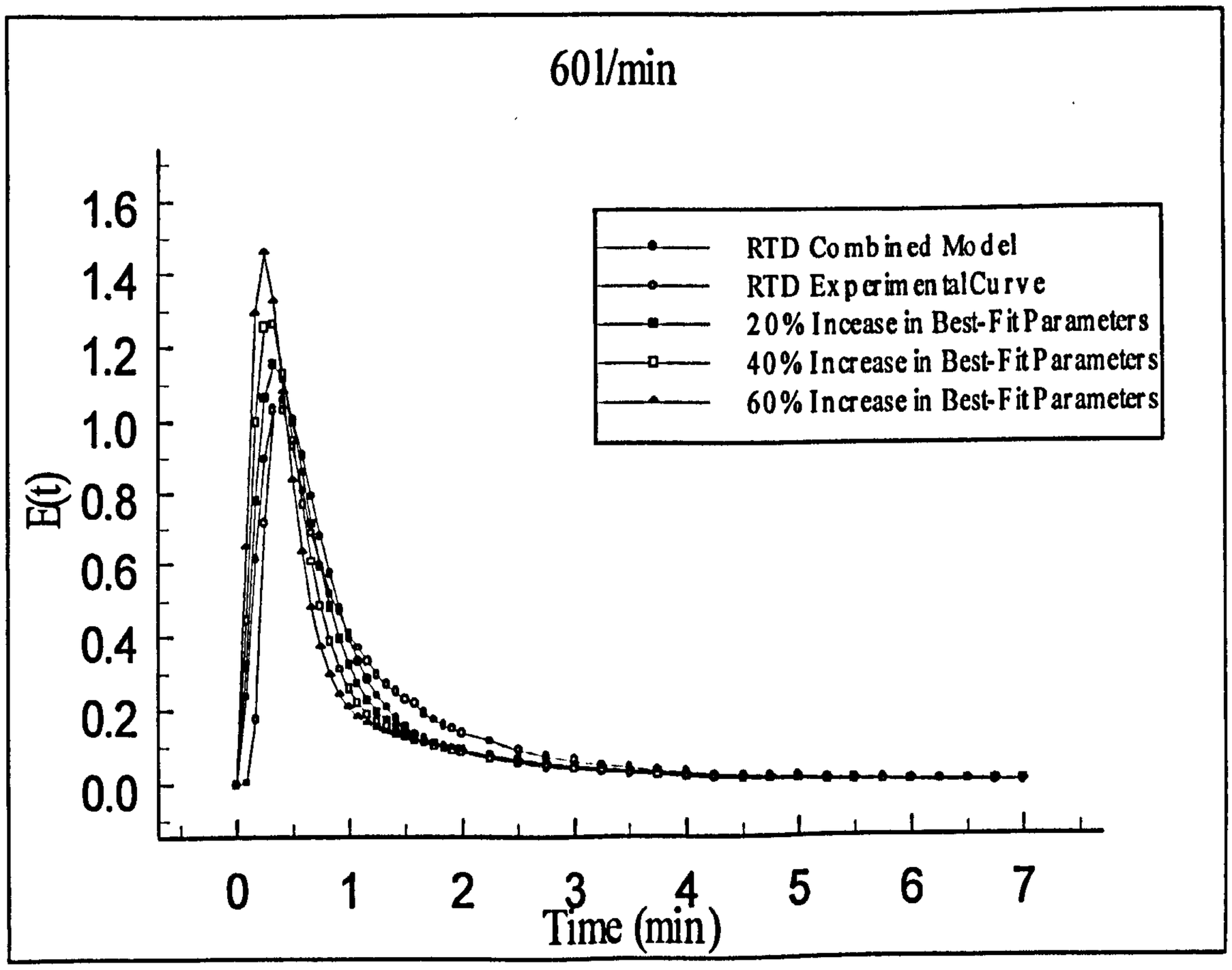

Fig. 5.6 Model HDVS No Baseflow – Relationship of Combined Model Parameter Sensitivity with Flow Rate

the inlet flow rate is increased (appendix D.2). Therefore, this trend in the correlation parameters is related to the reduction in parameter sensitivity (V_4 and Q_2) and subsequently, the flexibility in fitting the combined model curve to the experimental data at low flow rates.

At low flow rates the peak of the combined model curve occurs before the experimental curve (Fig. 5.2-5.5). This is possibly due to the combined model being limited to 3 tanks-in-series (N) (Fig. 5.1). Whereas if additional tanks (N) were incorporated, the combined model will describe a greater element of plug-flow mixing, which appears to be a characteristic of the RTD curves at low flow rates and the peak would occur closer to the theoretical mean residence time and therefore further away from the origin. This is shown in Fig. 4.3 by the relationship between the number of tanks-in-series (N) and the shape of the RTD curve using the standard TISM (section 4.3.3). Hence, the combined model does not provide complete physical realism of the HDVS. This supports the reduction in the goodness of fit, illustrated by the correlation parameters (R^2) (appendix D.2), provided by the combined model and similarly, in the sensitivity and flexibility of the model parameters (V_4 and Q_2) as the flow rate decreases. Therefore the combined model at low flow rates is approaching the upper limit of its ability to describe any greater degree of plug-flow mixing. Subsequently the RTD curve obtained after the first (V_1) or second (V_2) tank (Fig. 5.1) has not been investigated or presented, as they will not provide any better description of the mixing regime within the HDVS. These observations, regarding the physical realism provided by the combined model of the HDVS's mixing regime, suggest the need for a different combined model configuration including additional tanks-in-series (N), to better describe the RTD and model the dead volume (V_4) within the HDVS at low flow rates.

Investigations using the combined model and a fixed-dependent experimental initial tracer concentration (C_o) provided a very poor correlation between the modelled and

experimental data across the range of inlet flow rates. The term 'fixed-dependent' refers to comparisons made between the combined model and experimental concentration-time data, which is dependent on the fixed initial tracer concentration (C_o), set in the combined model solution (appendix D.1). The experimental injected tracer concentration values (C_o) are provided in appendix D.2 and were obtained using the methodology presented in appendix D.1. The combined model curves all have a smaller 'peak height' compared to the experimental curve. This is illustrated in Fig. 5.7, for the model HDVS operating with the sludge hopper and a combined model fixed-dependent initial tracer concentration (C_o) and the best-fit dead volume (V_4) and exchange flow rate (Q_2) parameters. Fig. 5.2 shows the same experimental results as Fig. 5.7 and a combined model solution obtained for an independent initial tracer concentration (C_o) and the best-fit dead volume (V_4) and exchange flow rate (Q_2) parameters i.e. E(t) as opposed to C(t) and an improved visual correlation between the combined model and experimental curves is clearly evident.

The initial tracer concentration value (C_o) is the dominant parameter in determining the peak height of the combined model curve. The dead volume parameter (V_4) also alters the peak height of the combined model curve and in addition, the position of the rising and falling limbs and therefore changes the spread of the curve and peak position relative to the time axis. The combined model curve 'peak time' occurs closer to the origin as the dead volume (V_4) is increased. This is expected, as an increase in the dead volume (V_4) reduces the active volume and therefore shifts the peak of the RTD curve towards the origin (Westerterp *et al.*, 1984). The exchange flow rate (Q_2) parameter appears to have the same combined effects as the initial tracer concentration value (C_o) and dead volume (V_4) parameter, although to a lesser extent. Fig. 5.7 shows the combined model curves response to a range of percentage increases in the initial tracer concentration (C_o), maintaining the original best-fit parameters (V_4 and Q_2), using the

concentration-time data. Fig. 5.8 shows the response of the combined model curves shape, as the dead volume (V_4) and exchange flow rate (Q_2) parameters are individually changed, for a fixed inlet flow rate. The range of combined model parameters (V_4 and Q_2) illustrated in Fig. 5.8, cover the best-fit parameters for the model HDVS operating with the sludge hopper for a flow rate of 30l/min.

The method of calculating the initial tracer concentration (C_o), provided by a pulse injection, is based on the tracer being mixed with one volume of the HDVS (appendix D.1). However, it is clear from the RTD experiments presented in chapter 4, that the tracer is mixed with a volume ranging from less than 1-6 times the volume of the HDVS, depending on the time that different fluid elements remain in the system. This occurs as the RTD experimental duration is approximately 6 times the theoretical mean residence time. Therefore, a true representation of the tracer concentration within the HDVS at time t can only be achieved by weighting the initial tracer concentration (C_o) according to each time step, which cannot be accomplished using the present combined model configuration. The RTD combined model curve initial tracer concentration (C_o) value for time steps before a normalised time (Θ) value equal to 1, require dilution by less than one complete volume of the HDVS and for greater normalised time (Θ) values, dilution by more than one complete volume. As a significant fraction of the injected tracer leaves the system before being diluted with one complete volume, this causes the initial tracer concentration (C_o) to be significantly underestimated. This is shown in Fig. 5.7, as the combined model concentration-time curves response to an increase in the initial tracer concentration (C_o) clearly improves the goodness of fit, particularly in the peak region of the curves. Additionally, the percentage increase in the initial tracer concentration (C_o) required to improve the visual goodness of fit, is significantly greater at high flow rates compared to low flow rates. This supports the above theory that a smaller dilution is required for time steps before a normalised time (Θ) value equal to 1

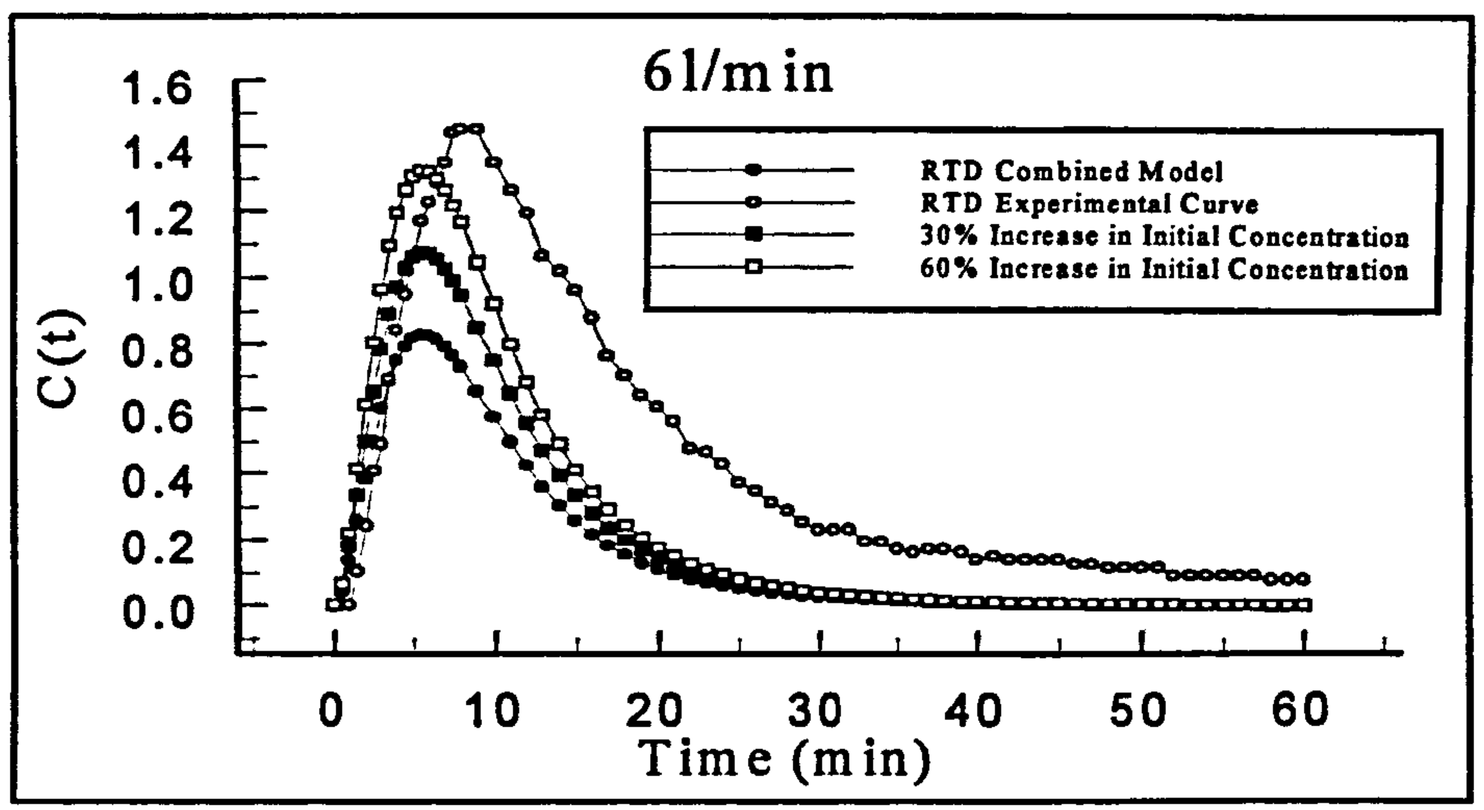

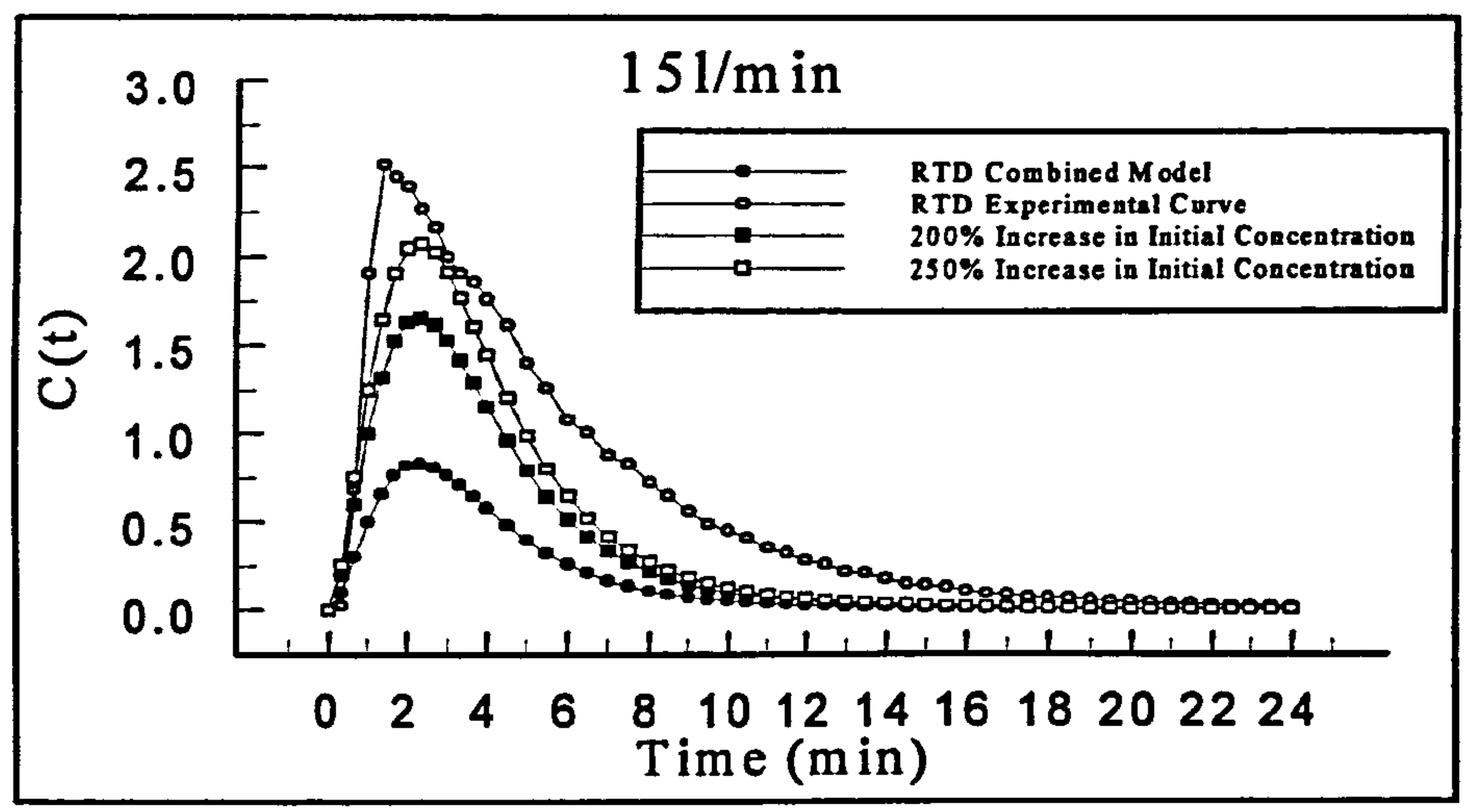

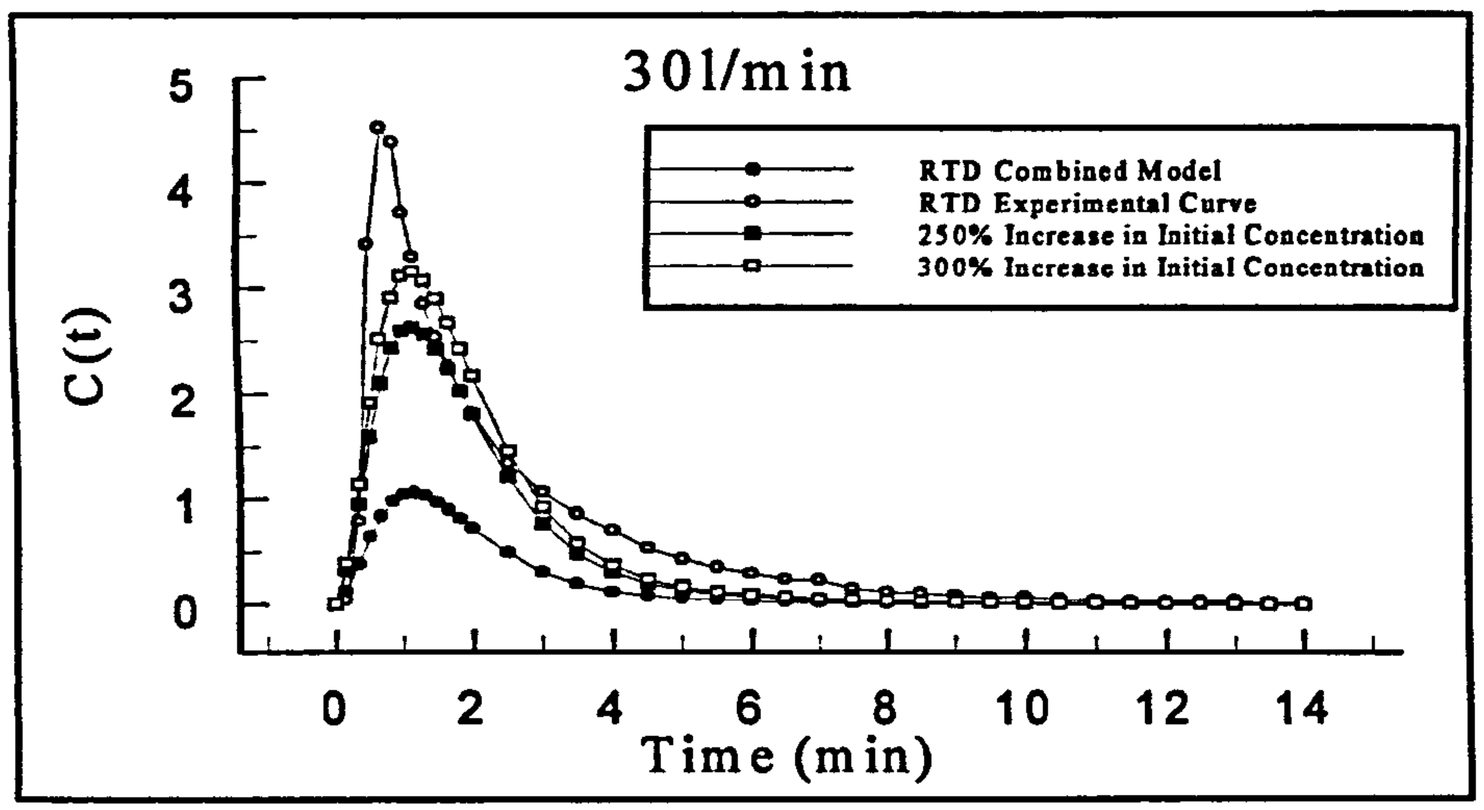

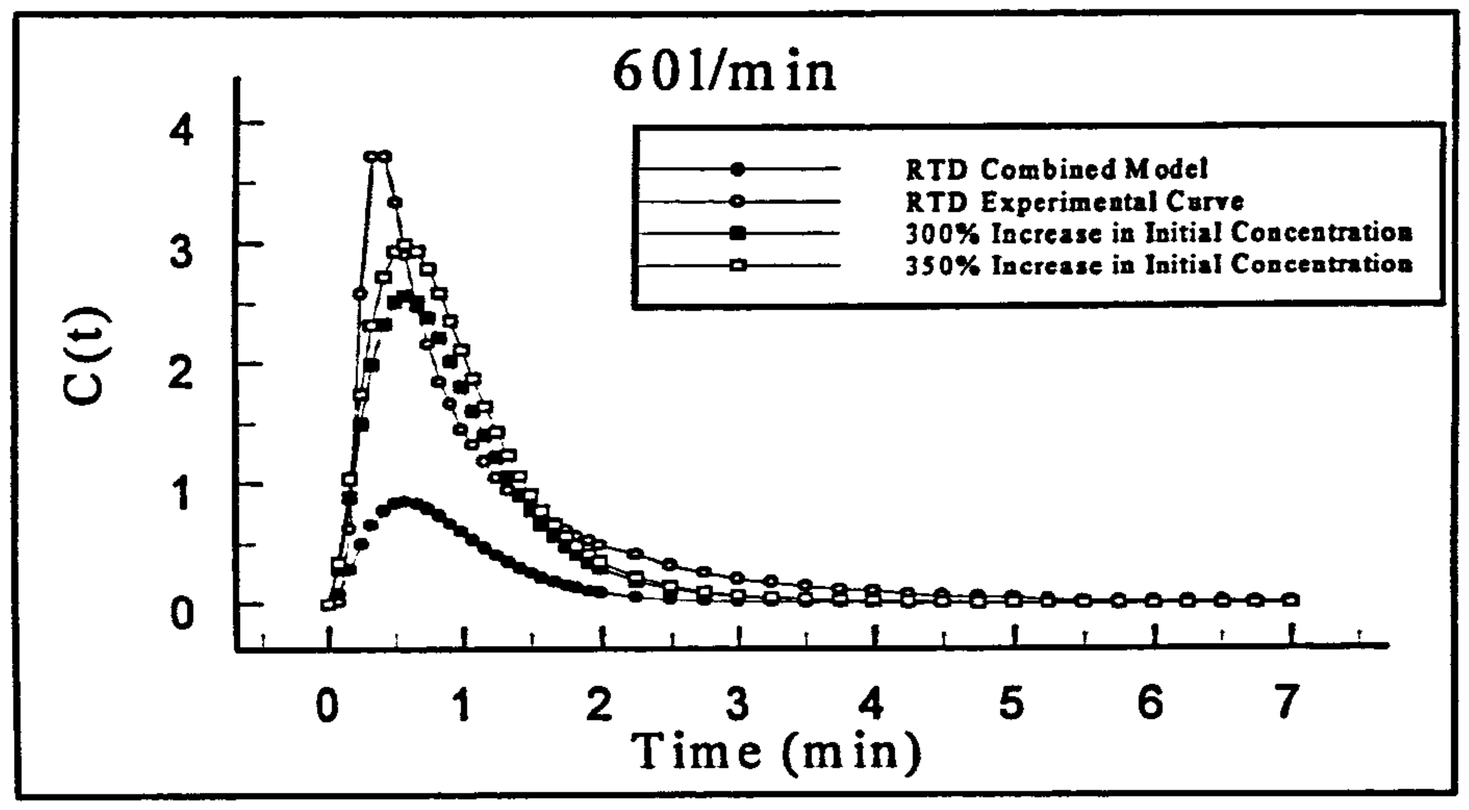

Fig. 5.7 Model HDVS No Baseflow - Comparison of RTD Combined Model and Experimental C(t) Curves using a Fixed Initial Concentration (C_o) for Selected Flow Rates

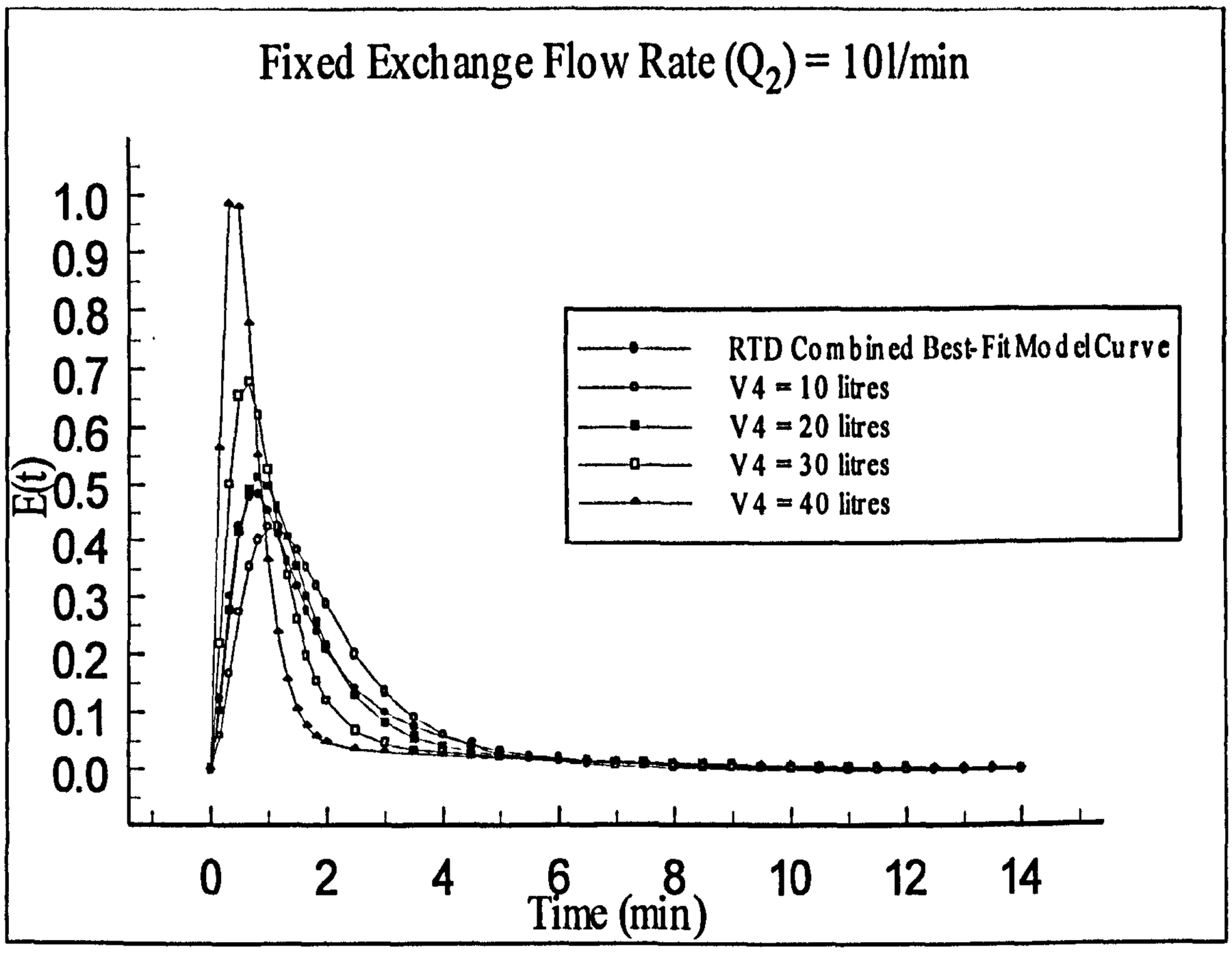

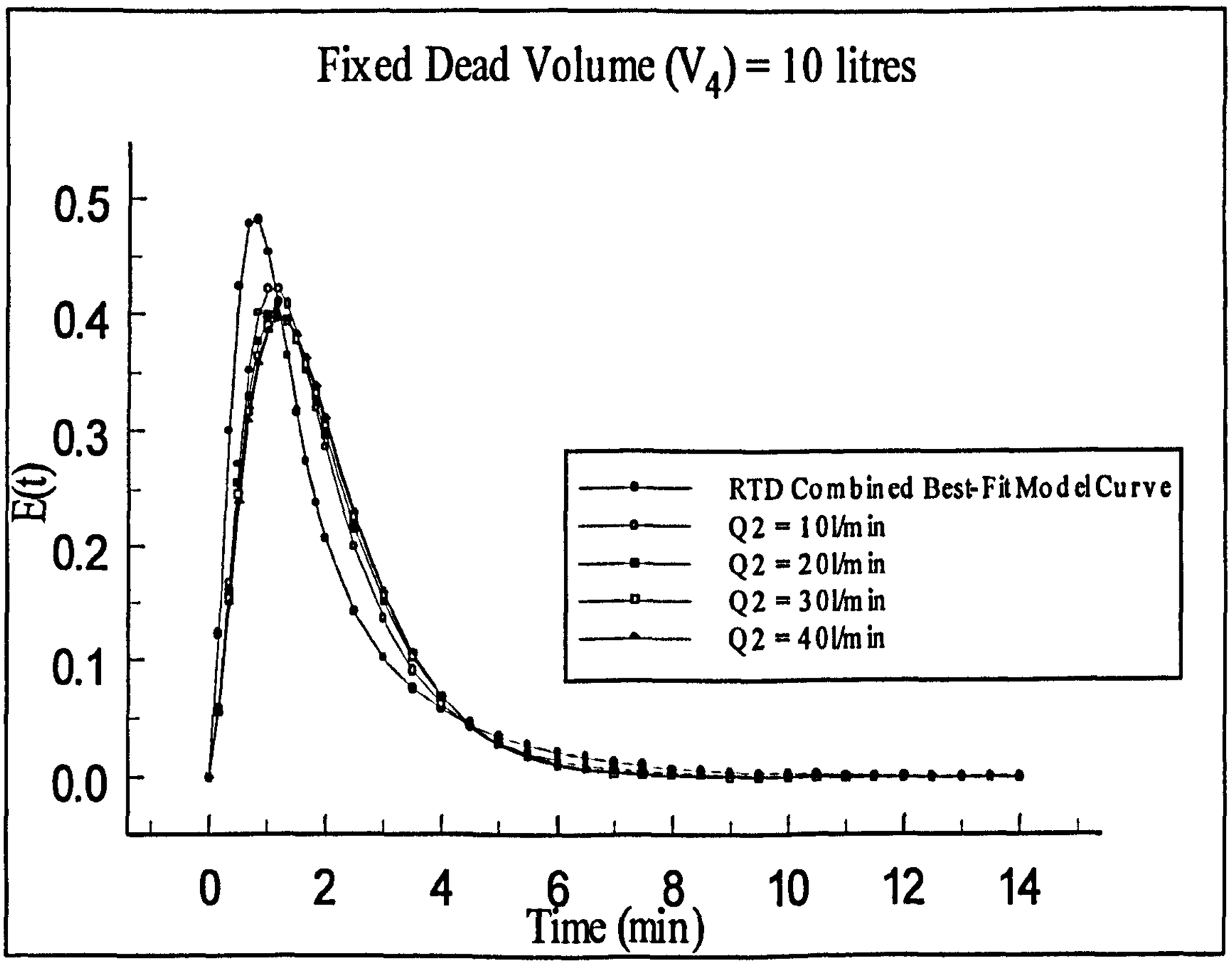

Fig. 5.8 Model HDVS No Baseflow – Combined Model Curve Response to Parameter Changes for a Fixed Flow Rate of 30l/min

and particularly at high flow rates, where a greater fraction of the HDVS volume passes through the system in this period due to short-circuiting (section 4.4). Therefore based on the approach in appendix D.1, the initial tracer concentration (C_o) is significantly underestimated i.e. the initial tracer concentration (C_o) should be diluted with less than one volume of the HDVS at high flow rates. Due to these problems, no further results are presented or discussed using a fixed-dependent initial tracer concentration (C_o) and therefore the concentration-time data. Hence the following results were obtained by comparing the combined model and experimental RTD exit-age distribution function E(t) curves, which are independent of the initial tracer concentration (C_o) (section 4.3.1).

The combined model dead volume (V_4) parameter generally increases as the inlet flow rate increases and subsequently there is greater short-circuiting of the flow within the HDVS, due to a reduction in the active volume (Fig. 5.9 and 5.10). However, the dead volume (V_4) remains relatively stable at high flow rates. These results are supported by the type of mixing regime identified within the HDVS using the RTD normalised curves E(Θ) e.g. Fig. 4.8. Tyack and Fenner, (1998b) also reported short-circuiting in a Grit King™ HDVS (section 2.2.2).

At low flow rates, below the transition flow rate for each device, the exchange flow rate (Q_2) approximates the inlet flow rate (Q_1) (appendix D.2). This may be a limitation of the combined model i.e. physical realism, however it supports previous observations (section 4.4) that the majority of the HDVS's volume is active at low flow rates and therefore, also supports the presence of a conflict (1) between the RTD curves and parameters as discussed above (section 5.1). However, this conflict (1) can be explained, as the dead volume (V_4) calculated using the RTD combined model is also a function of the exchange flow rate (Q_2). Applying the terminology presented by Robinson and Tester, (1986), the dead volume (V_4) for a high exchange flow rate (Q_2),

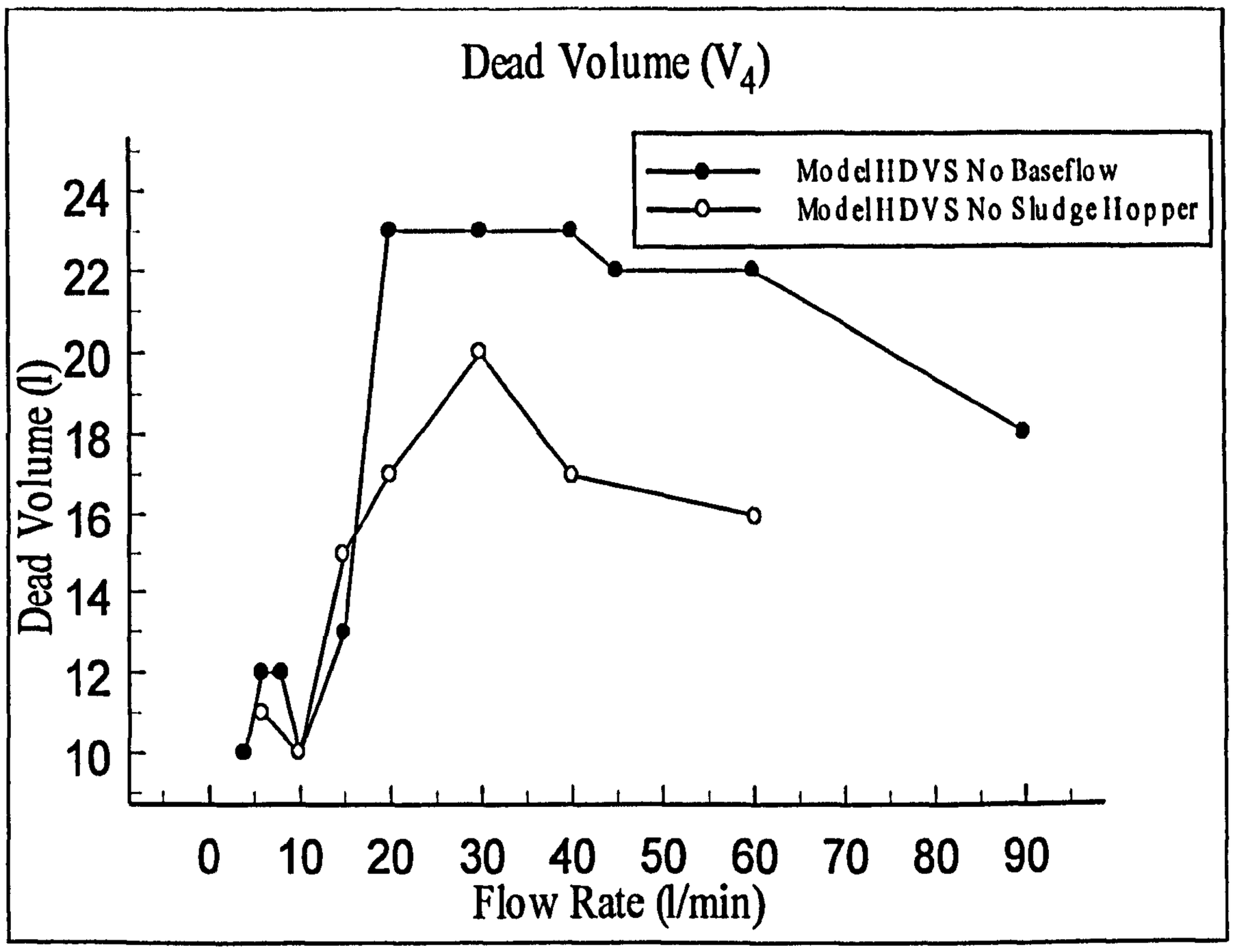

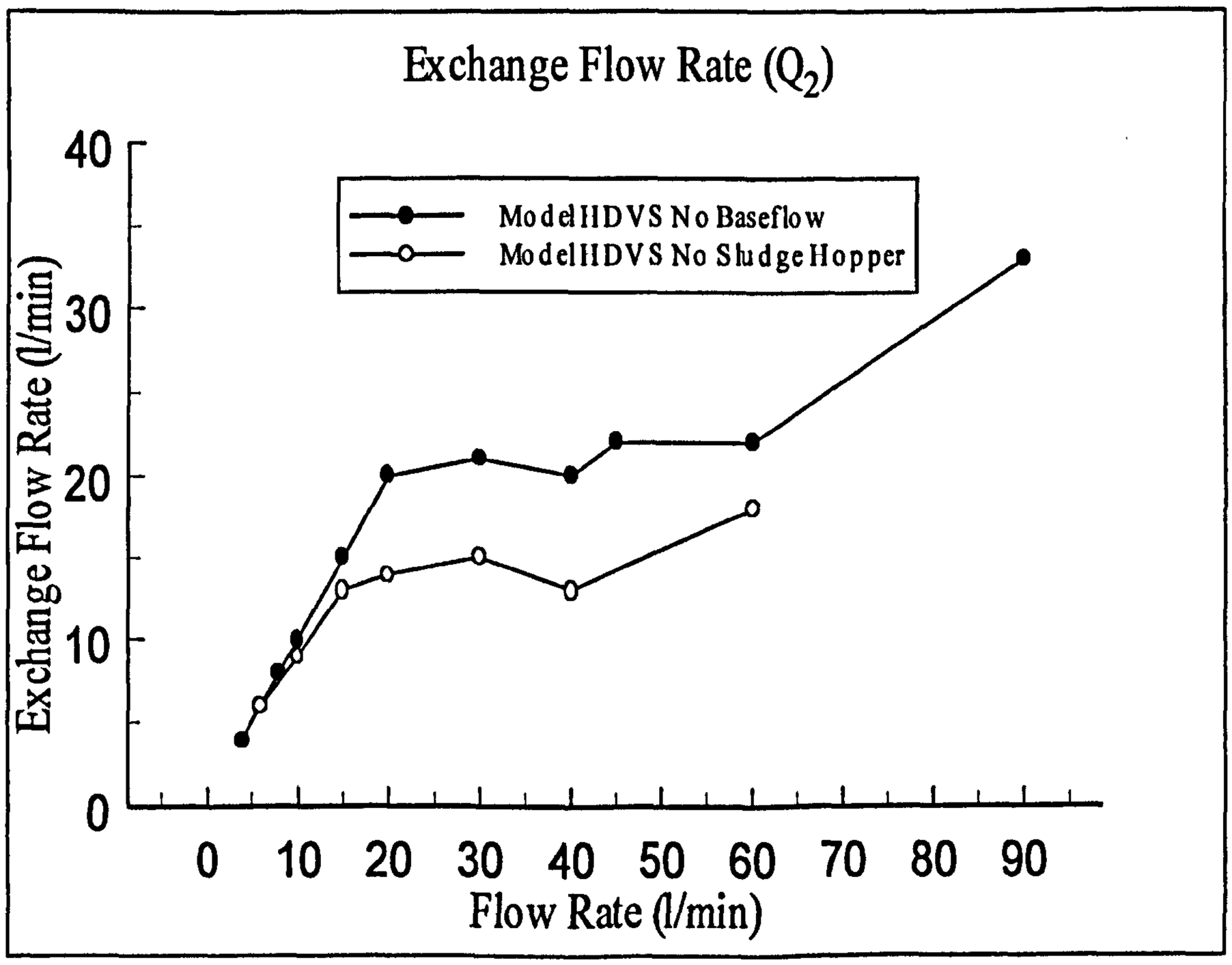

Fig. 5.9 Model HDVS – RTD Combined Model Parameter Relationship with Flow Rate

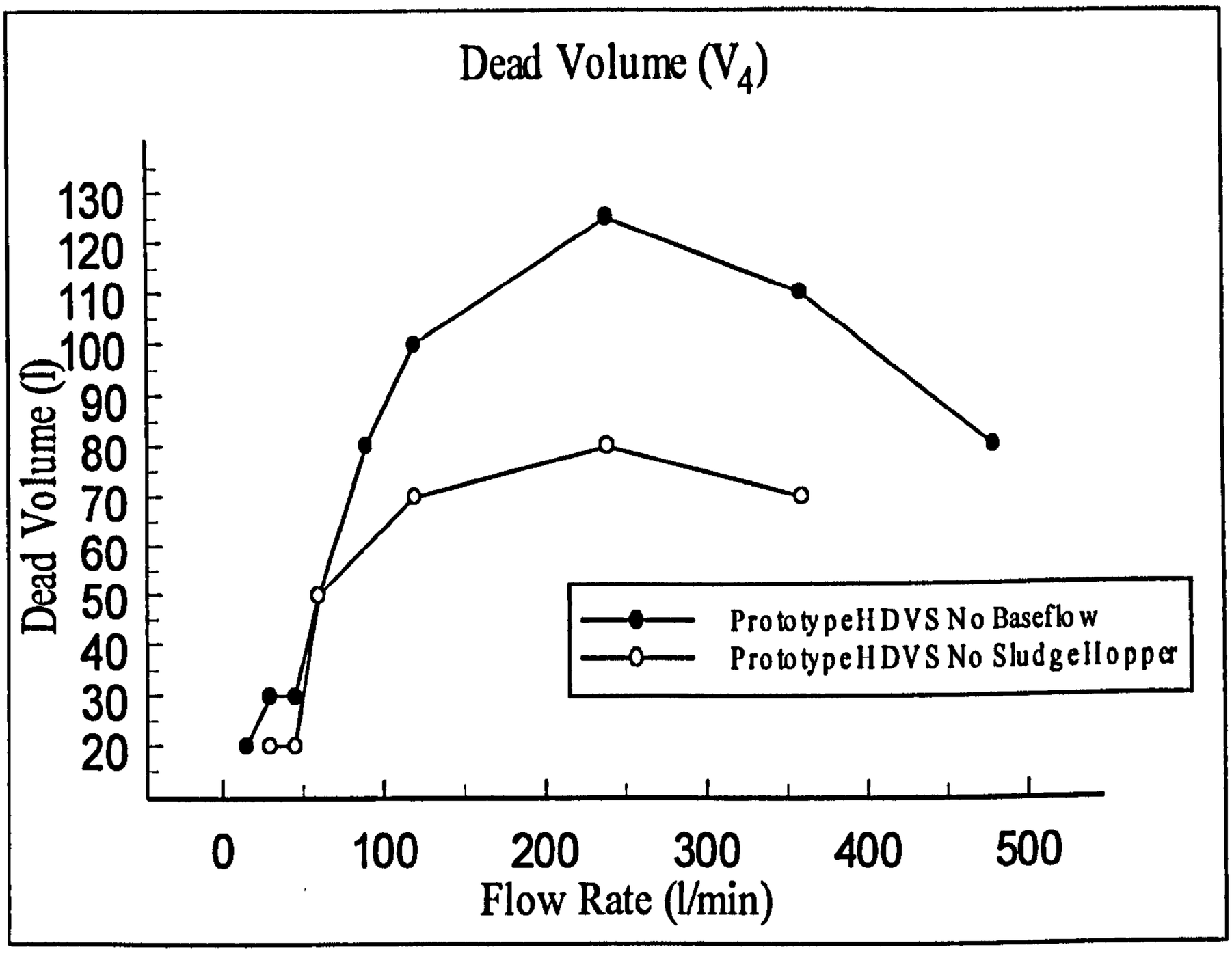

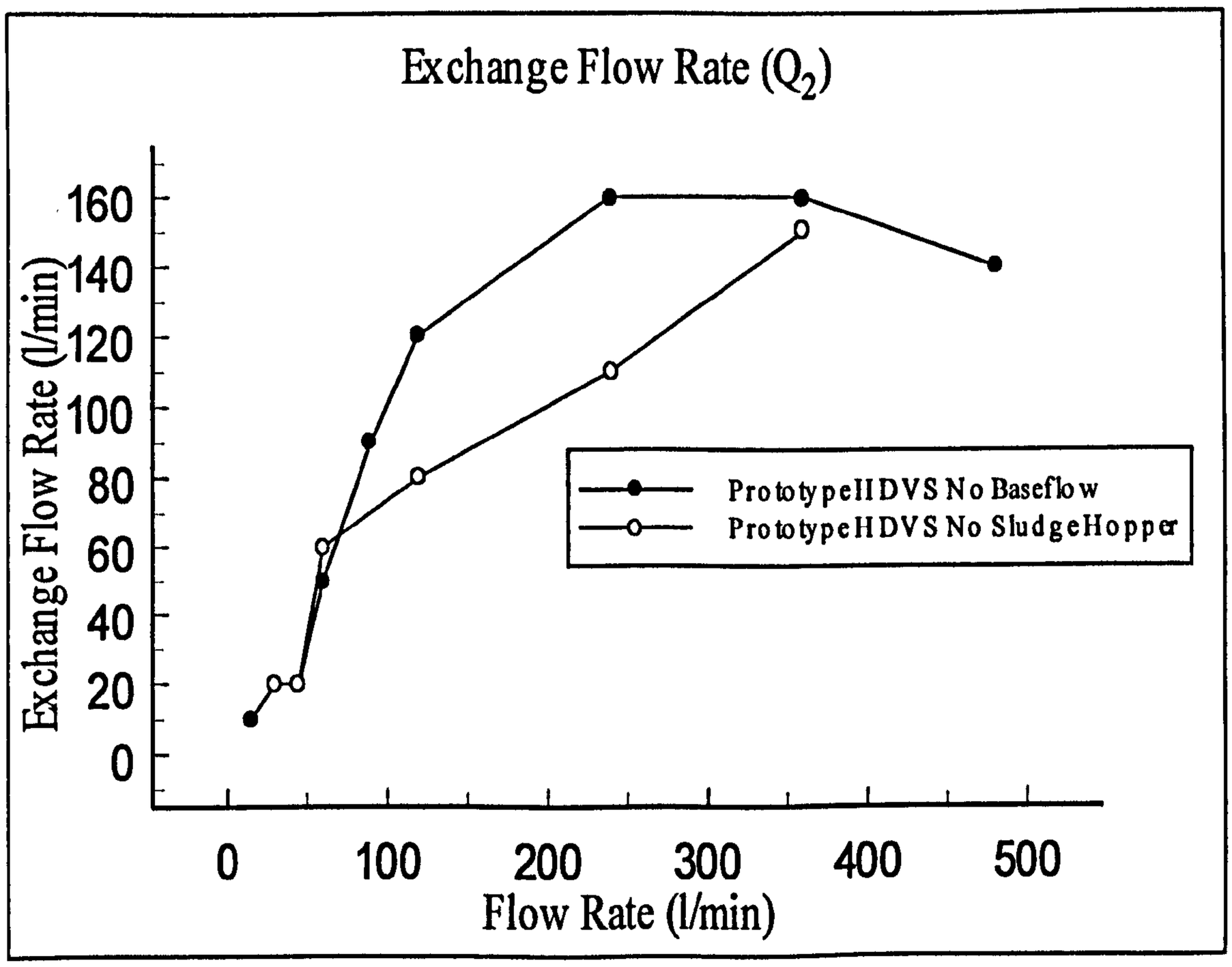

Fig. 5.10 Prototype HDVS – RTD Combined Model Parameter Relationship with Flow Rate

relative to the inlet flow rate, acts or is modelled as a stagnant or 'sluggish-flow' region, as opposed to a dead volume. A stagnant region has smaller velocities relative to the rest of the system and the majority of the flow is due to molecular diffusion whereas, a 'sluggish-flow' region conducts flow but at a rate much slower than the mean. A dead volume is completely isolated from the rest of the system and therefore reduces its 'true' volume. As it is not possible to distinguish between a stagnant and 'sluggish-flow' region, the latter is preferred and considered representative of the type of inactive flow behaviour within the HDVS. This is due to the magnitude of the exchange flow rate (Q_2) relative to the inlet flow rate (Q_1) (appendix D.2) i.e. reduced convection as opposed to molecular dispersion. Therefore in the following discussion the term 'sluggish-flow' and dead volume are used to describe the relationship between the HDVS's inactive flow behaviour and the flow rate. However, the term 'dead volume' is used when generally discussing and comparing the combined model dead volume parameter (V_4). This will provide consistent terminology with all previous discussions and references in other chapters.

The mean residence time of the dead volume (V_4) i.e. dead volume/exchange flow rate generally decreases as the inlet flow rate increases (appendix D.2). This justifies previous observations that a greater fraction of the flow resides in the HDVS for a period greater than the theoretical mean residence time at low flow rates compared to high flow rates i.e. partial or temporary accumulation (section 4.4.1.1). Hence, at low flow rates there appears to be greater 'sluggish-flow' regions and at high flow rates, dead volumes predominate within the HDVS. This different inactive flow behaviour across the range of inlet flow rates, explains and accounts for the conflict (1) discussed above (section 5.1) and first observed in chapter 4 (section 4.4.1.1).

The average residence time of the 'sluggish-flow' region does not completely account for the difference between the experimental and theoretical mean residence

time and particularly at low flow rates (chapter 4). The experimental RTD curve compared to the combined model curve is the complete data i.e. the experiment duration is approximately 6 times the theoretical mean residence time. Therefore, considering a truncated RTD curve may provide improved results (section 4.4).

The bypass flow rate parameter (Q_3) was set to zero for all comparisons of the modelled and experimental data (Fig. 5.1). However, it was observed that introducing a bypass flow rate (Q_3) at low inlet flow rates (6l/min) reduced the combined model goodness of fit and at high flow rates (60l/min) it was marginally improved. This is illustrated in Fig. 5.11 and is only observed by comparing the correlation parameters presented for the combined model curve generated with and without a bypass flow rate (Q_3). The bypass flow rate (Q_3) was introduced into the combined model solution as 20% of the inlet flow rate and maintaining the same best-fit dead volume (V_4) and exchange flow rate (Q_2) parameters as obtained for the no bypass conditions (appendix D.2). This supports the conclusions presented above, for the combined model operating with a zero bypass flow rate (Q_3), as there is less short-circuiting at low flow rates.

The magnitude of the dead volume (V_4), within the HDVS operating with the sludge hopper, suggests that it is not only confined to the sludge hopper region and particularly at high flow rates (Fig. 5.9 and 5.10). The sludge hopper volume is 5 litres for the model HDVS (8.3% of the total volume) and 35 litres for the prototype HDVS (7.5% of the total volume). The dead volume (V_4) within the model HDVS operating with and without the sludge hopper occupies approximately 20-40% of the total volume and similarly for the prototype HDVS 5-25% and generally increases as the inlet flow rate increases (appendix D.2). These results show that the prototype HDVS has less dead volume and therefore short-circuiting compared to the model HDVS (section 4.4.3 and 4.4.7). Hence, the model and prototype HDVS combined model results imply that the dead volume (V_4) reduces as the HDVS volume increases. This was identified using

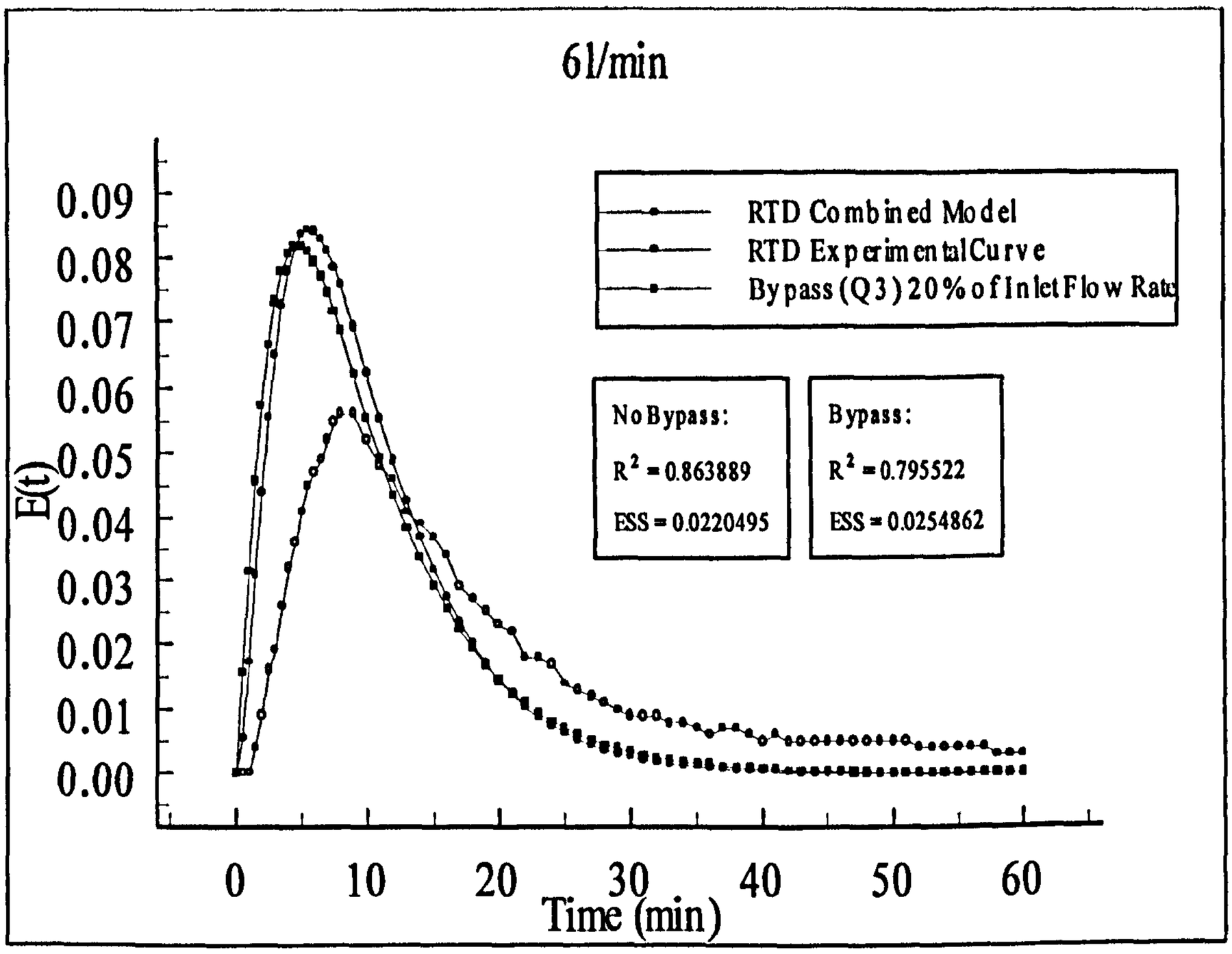

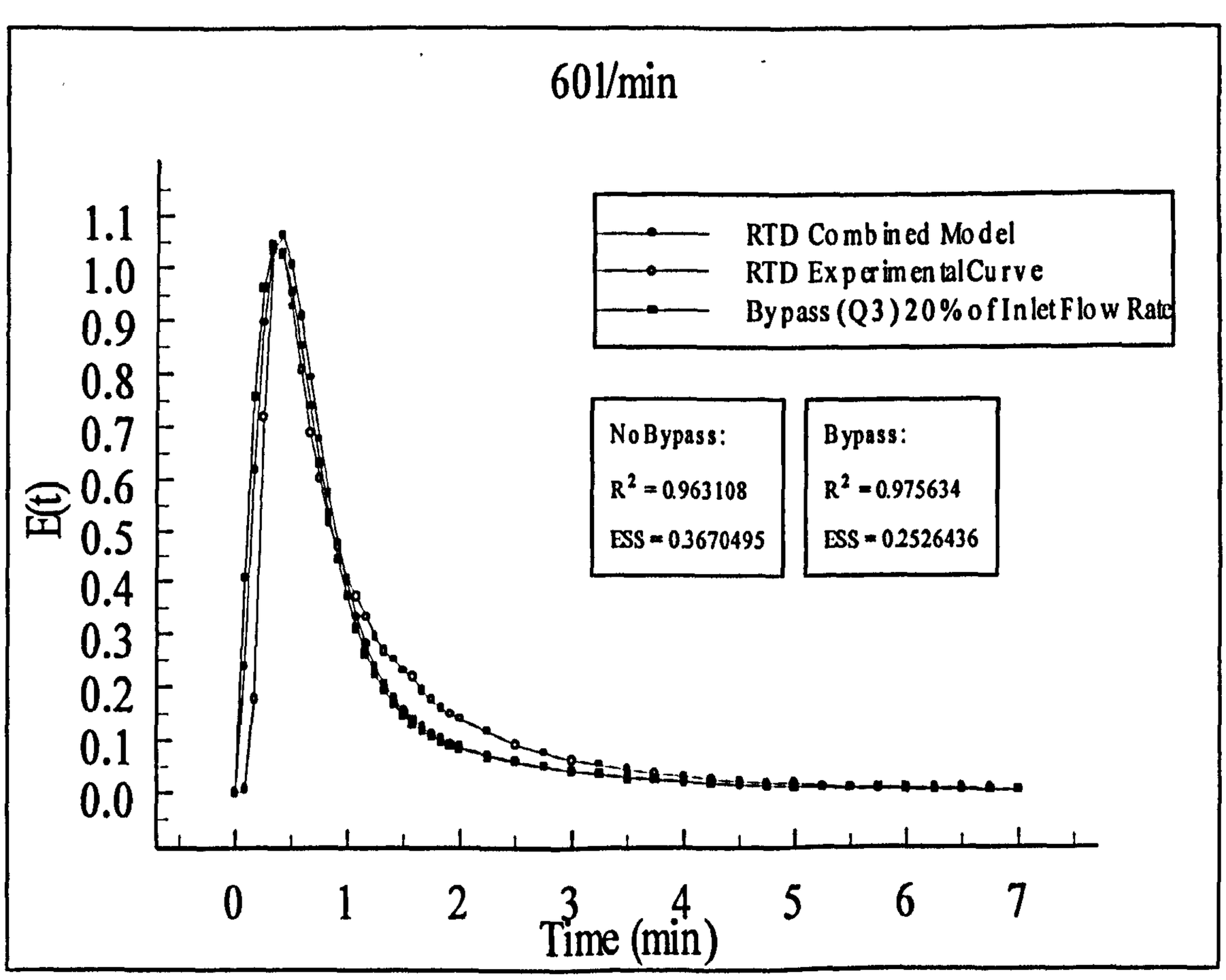

Fig. 5.11 Model HDVS No Baseflow – Combined Model Curve Response to the Introduction of a Bypass Flow Rate (Q_3)

different RTD data analysis techniques, although the dead volume was not quantified (section 4.4.3 and 4.4.7). The prototype HDVS also has marginally better plug-flow mixing characteristics compared to the model HDVS, which is shown by the ADM and TISM parameters presented in chapter 4 (section 4.4.3 and 4.4.7). Hence, the scale-up of the HDVS will provide a mixing regime with less short-circuiting and improved plug-flow mixing characteristics and therefore, more conducive for certain kinetic processes and particularly chemical disinfection processes (section 2.2.3).

The dead volume (V_4) within the prototype HDVS operating with the sludge hopper is less than the volume of the sludge hopper at low flow rates. This scenario never occurs for the model HDVS operating with the sludge hopper and therefore, removing the sludge hopper from the model HDVS will have a greater effect on the mixing regime i.e. a reduction in stagnant volume, compared to removing the sludge hopper from the prototype HDVS. This was also observed using different RTD data analysis techniques in chapter 4 (section 4.4.9.2).

The dead volume (V_4) within the model and prototype HDVS is generally smaller when operated without the sludge hopper and at the same flow rate (appendix D.2). This observation neglects any combined model parameter estimation errors, which cannot be quantified due to no comparative experimental or theoretical data and the reduction in parameter sensitivity discussed above. Hence, the sludge hopper contributes to the inactive flow behaviour within the HDVS. The difference in dead volume (V_4), between the two HDVS operating conditions, is generally greater than the volume of the sludge hopper at high flow rates. However, at low flow rates the difference is generally less than the sludge hopper volume. It should be noted that the above observations hold better for the prototype HDVS compared to the model HDVS combined model results (appendix D.2). Therefore, there appears to be greater dead volumes within the HDVS operating with the sludge hopper at high flow rates, which are not only confined to the

sludge hopper region, compared to 'sluggish-flow' volumes at low flow rates, which are predominantly associated with the sludge hopper region. Subsequently, removing the sludge hopper will reduce the 'sluggish-flow' volume within the HDVS and the remaining non-active flow behaviour is more likely to be associated with dead volumes. A reduction in the 'sluggish-flow' volume by removing the sludge hopper (Fig. 3.1) is shown by comparing the RTD normalised curves E(Θ) for the HDVS operating with and without the sludge hopper (Fig. 4.32 and 4.33). The low velocities in the sludge hopper region relative to the rest of the system is also supported by CFD investigations undertaken by Faram and Andoh, (2000) on the same style of HDVS (chapter 2). The model and prototype HDVS dead volume (V_4) also remains relatively stable for all flow rates greater than the transition flow rate (section 4.4) and therefore, implies that the mixing regime is also stable at high flow rates. This is also shown by the RTD normalised curves E(Θ) e.g. Fig. 4.8 and the ADM and TISM parameters presented in chapter 4 (section 4.4.3 and 4.4.7) and has also been reported by Andoh and Harper, (1994).

In addition to the sludge hopper, the volume in the outer zone above the soffit level of the inlet pipe (Fig. 3.1) also has the potential to contribute to the dead volume within the HDVS. This is due its preferred isolated and quiescent mixing characteristics, as it is used for the collection of floatable material during solids-liquid separation applications (section 5.1). Tyack and Fenner, (1998b) identified an active zone in a Grit King™ HDVS (Table 1.1) (section 2.2.2). This was located between the soffit level of the inlet pipe and the position at which the flow regime reverts from a high velocity downward motion to a slower velocity upward motion i.e. shear zone (section 3.2). Hence, the Grit King™ HDVS active zone also indirectly identifies the floatables collection area within the outer zone as an inactive volume (Fig. 3.1).

The presence of 'sluggish-flow' regions at low flow rates will contribute to the solids removal efficiency of the HDVS by providing quiescent conditions and for kinetic processes, by providing a greater volume with long residence times and therefore contact times. The presence of dead volumes in any mixing device is detrimental to it's performance, although by conducting detailed RTD investigations as presented in this project, it can be accounted for in the design process. Additionally, the high inlet flow rates at which dead volumes appear, are far greater than employed in the HDVS's current applications (Andoh, 2000).

The dead volume parameter (V_4) cannot be presented as a true dead volume, by allowing the exchange flow rate (Q_2) to equal zero, as this results in several combined model equations approaching infinity, which is not permitted in producing a solution. Subsequently the combined model cannot accurately differentiate between 'sluggish-flow' and dead volumes, which may provide a better insight into the different inactive flow behaviour at low and high flow rates respectively. This requires consideration when directly comparing the combined model and other RTD data analysis techniques estimation of the HDVS's dead volume.

During the development of the combined model and initial investigations, it was observed that at low flow rates if the overall theoretical mean residence time was increased in the combined model solution, the fit between the combined model and experimental curve was improved (Fig. 5.12). This was achieved by either increasing the total system volume i.e. 60 litres for the model HDVS and 464 litres for the prototype HDVS or decreasing the flow rate in the combined model solution. This implies the possibility of the existence of errors in the HDVS's volume and flow rate measurement techniques. However, this is strongly dismissed by the author due to several experimental methods being employed to calculate both the HDVS volume and flow rate and will therefore minimise any potential errors (section 3.3).

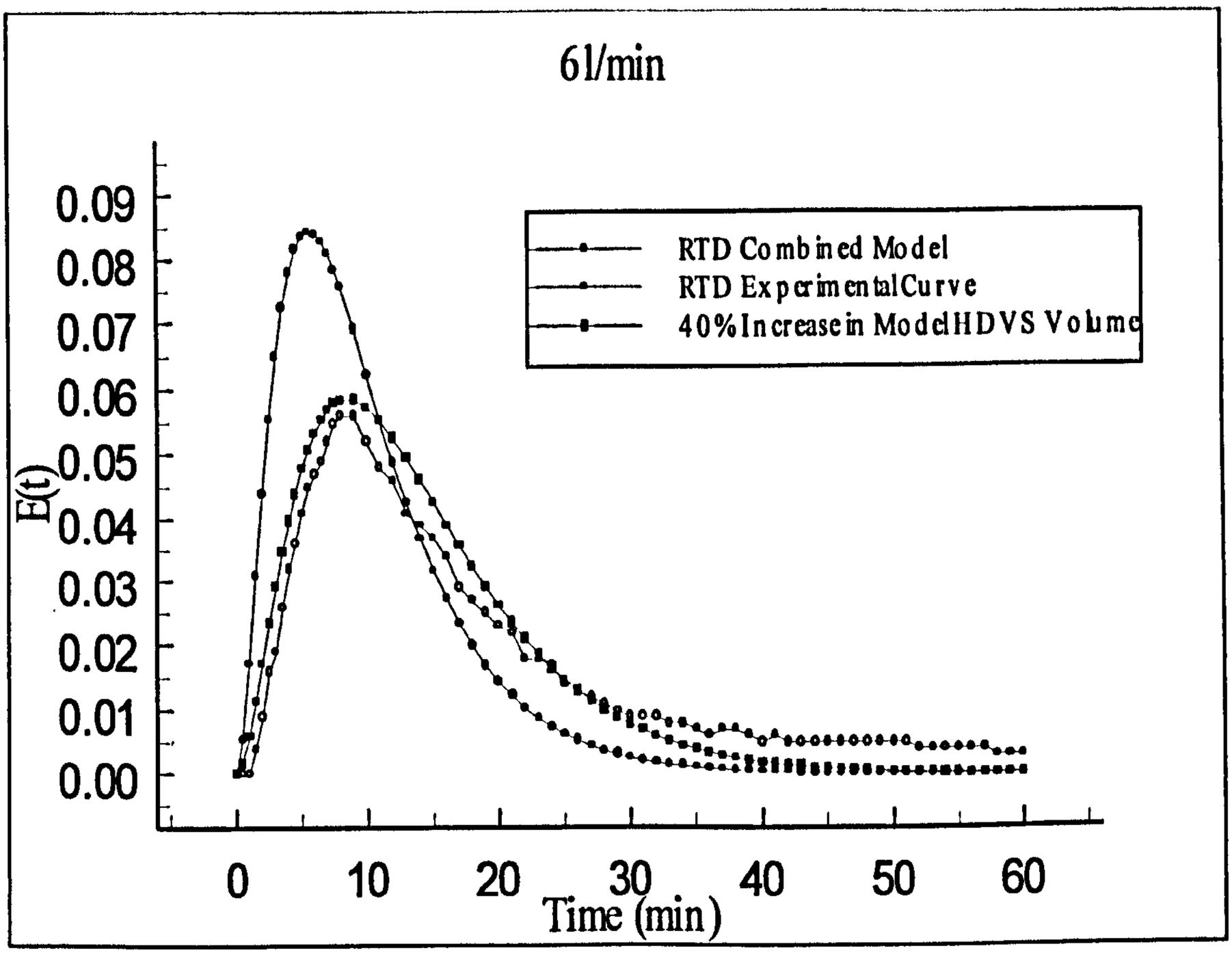

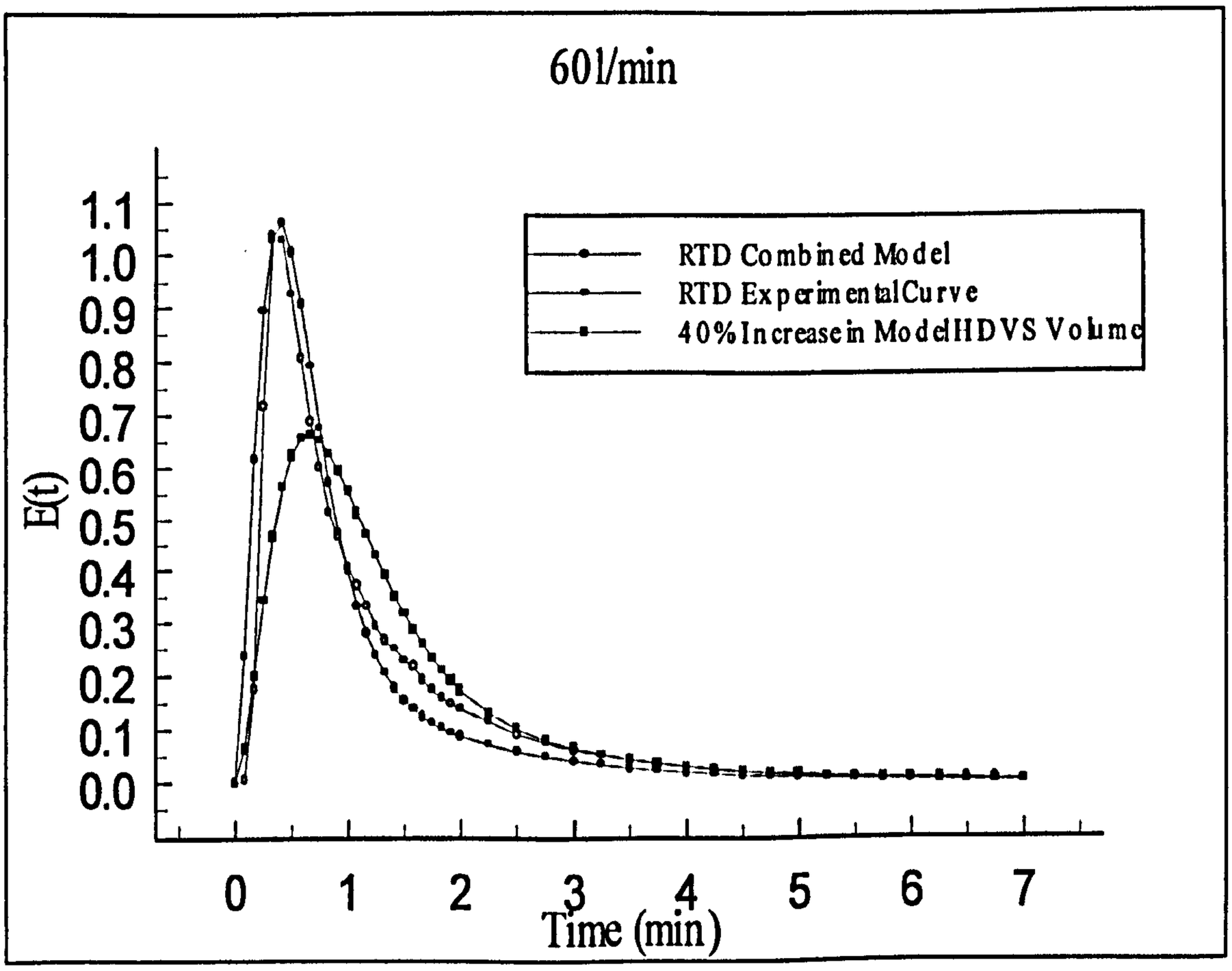

Fig. 5.12 Model HDVS No Baseflow – Combined Model Curve Response to an Increase in the Total HDVS volume

It is therefore proposed, that the fit between the combined model and experimental curve is significantly improved, as an increase in the theoretical mean residence time results in a shifting of the peak away from the origin of the modified modelled RTD curve compared to the same RTD experimental curve. This change in the modified combined model curve is a characteristic of the RTD experimental curves at low flow rates i.e. greater plug-flow mixing and fluid elements with long residence times, compared to high flow rates (section 4.4). This anomaly is due to the limited physical realism of the HDVS provided by the combined model solution. As commented above, it appears that at low flow rates the combined model's ability to reproduce the plug-flow mixing characteristics present in the HDVS reduces. This is supported by the response of the modified combined model curve at high flow rates and a significant reduction in the goodness of fit (Fig. 5.12). Therefore, the true combined model solution and HDVS operating parameters i.e. volume and flow rate provide physical realism of the HDVS mixing regime at high flow rates.

An increase in the system's theoretical mean residence time is equivalent to artificially increasing the number of tanks-in-series (N) in the combined model solution. This reduces the probability that a fraction of the system volume that will leave before the theoretical mean residence time (Fig. 4.3) and therefore improves the combined model's ability to describe a system with greater plug-flow mixing characteristics (section 4.1). This supports previous observations, suggesting the need for a different combined model configuration including additional tanks-in-series (N), to better describe the RTD and model the dead volume within the HDVS at low flow rates.

The conflict (2) initially identified in chapter 4 (section 4.4.1.1) and repeated above (section 5.1), regarding the plug-flow mixing characteristics of the HDVS RTD curves at high flow rates, is indirectly disproved by the combined model results. This is due to the combined model's ability to accurately describe the HDVS RTD curves at high flow

rates using a fixed plug-flow mixing regime i.e. N=3 (Fig. 5.1). Whereas at low flow rates the combined model is approaching it's upper limit of describing the plug-flow mixing characteristics within the HDVS, as discussed above. Therefore it follows that the HDVS RTD at high flow rates will not have greater plug-flow mixing characteristics compared to low flow rates. Hence the HDVS's mixing regime at low flow rates does have improved plug-flow mixing characteristics, occupying a larger volume of the HDVS, compared to high flow rates and the possible conflict (2) is disproved. The ADM and TISM parameters and RTD indices calculated for the model and prototype HDVS operating with and without the sludge hopper also do not support this conflict (2) (section 4.4). However, as stated previously conflict (2) was based purely on visual observations (section 4.4.1.1).

This conflict (2) could only be directly disproved by using a combined model solution including a variable plug-flow mixing parameter i.e. dispersion and maintaining a dead volume parameter. This could possibly be achieved using IMPULSE RTD computer software (section 2.2.4). The use of such software may permit the development of a more complex combined model capable of describing non-ideal flow behaviour due to both dead volumes and dispersion. This would provide information regarding the amount of dispersion in the active volume, as the latter may decrease due to the presence of dead volumes but the plug-flow mixing characteristics could increase and therefore dispersion reduce. The ADM and TISM cannot accurately describe this combination of non-ideal flow behaviour, as they do not account for any dead volumes and subsequently short-circuiting (section 5.1). Additionally, this RTD computer software could be used to investigate the same combined model configuration presented in this project (Fig. 5.1) and the results compared. This would provide a check on the mathematical solution (appendix D.1) and other workers mathematical interpretation of the theoretical mixing regimes.

The trend in the combined model correlation parameters (R^2 and ESS) discussed above, is generally the opposite to that achieved for the ADM and TISM correlation parameters, with respect to the inlet flow rate (section 4.4.3). However, the limitations of the generic ADM and TISM (section 5.1) and particularly their ability to represent the 'true' mixing regime for systems with high dispersion and dead volumes, as occurs at high flow rates for the HDVS, creates doubt as to their verification (section 4.3.3). Whereas the application of a bespoke RTD combined model will increase confidence and therefore verification of the modelled curve. This is due to the combined model solution using the theoretical mean residence time (eqn. 4.2) as a constant (appendix D.1), as opposed to the ADM and TISM using the experimental mean residence time as a variable parameter (section 4.3.3). The theoretical mean residence time is more likely to represent the true mean residence time particularly due to the errors present in the experimental mean residence time results (section 4.4). However, the combined model is also limited by the physical realism it provides in describing the HDVS RTD at low flow rates and this will affect the goodness of fit as discussed above. Hence, the correlation parameters for the combined model, ADM and TISM are subject to the limitations of each model relative to the HDVS's non-ideal flow behaviour across the range of inlet flow rates. Therefore, in future HDVS RTD-kinetic process optimisation investigations, it maybe better to use the ADM or TISM non-linear regression relationship with the experimental data at low flow rates and the RTD combined model at high flow rates. Experimental observations of the dead volume within the HDVS will provide greater confidence in the combined model results (section 8.6) and also provide comparable data to assess possible combined model parameter errors.

The combined model can also be developed to include a reaction rate constant (k) (section 7.2). This enables the combined model solution to estimate the performance of a kinetic process within the HDVS accounting for the degree of non-ideal flow

behaviour associated with both dispersion and dead volumes. This is achieved by making the initial mass of material in the system i.e. kinetic reactants, a function of the reaction rate constant (k) and therefore decaying with time, as opposed to maintaining a constant value for generating the RTD (appendix D.1). The best-fit dead volume (V_4) and exchange flow rate (Q_2) parameters, obtained by comparing the original combined model curve to the experimental RTD, are maintained in the combined model solution including the reaction rate constant (k) to account for the degree of non-ideal flow behaviour. The introduction of a rate constant (k) (section 7.2) into the combined model solution would allow the performance of kinetic processes, such as a chemical reactions and coagulation/flocculation and disinfection processes, to be investigated and optimised within the HDVS i.e. conversion, dosing rate and biological inactivation respectively. In this form, the combined model can equally be applied to physical determinants and in particularly the BOD concentration of the effluent. Recommendations for future research using the RTD combined mathematical model are discussed in section 8.6.

5.4 Chapter Overview

This chapter presented the results and conclusions obtained from the first RTD combined mathematical model specifically developed to describe and provide physical realism of the mixing regime within the HDVS. This is in addition to the generic ADM and TISM also used to describe the HDVS's mixing regime (chapter 4). The combined model configuration enables the HDVS's dead volume to be estimated, as a function of an exchange flow rate between the active and non-active volumes. This RTD data analysis technique is generally avoided by many other workers to describe the mixing regime within a system due to the lack of reliable experimental data, complex

mathematical solutions and time constraints. However, developing a combined model has ensured that the HDVS's mixing regime has been characterised in this project using the complete range of available RTD data analysis techniques (section 4.3.1). Additionally, all RTD data analysis techniques have individual limitations and the approach adopted in this project allows these limitations to be compared and therefore indirectly eliminated, to provide a comprehensive and consistent description of the HDVS's mixing regime using RTD analysis.

The combined model results show that at low flow rates 'sluggish-flow' regions are dominant i.e. slow moving fluid elements and at high flow rates dead volumes are present, which do not contribute to the mixing regime and effectively reduce the total active volume. This is concluded as the dead volume calculated using the RTD combined model is a function of the exchange flow rate and it's mean residence time i.e. dead volume/exchange flow rate generally decreases as the inlet flow rate increases. Additionally, at low flow rates the exchange flow rate is approaching values close to the inlet flow rate, implying that a greater fraction of the total volume is active and has a velocity closer to the mean. This different inactive flow behaviour, across the range of flow rates, explains and accounts for the conflict (1) identified between the RTD curves and parameters (section 5.1). The combined model results also indirectly prove that the HDVS's mixing regime at low flow rates does have improved plug-flow mixing characteristics, occupying a larger volume of the HDVS, compared to high flow rates. Hence, the possible conflict (2) between the visual plug-flow mixing characteristics of the RTD curves at high flow rates and the ADM and TISM parameters which decrease at high flow rates, is disproved (section 5.1).

The presence of 'sluggish-flow' regions at low flow rates will contribute to the solids removal efficiency of the HDVS by providing quiescent conditions and for kinetic processes, by providing a greater volume with long residence times and

therefore contact times. The presence of dead volumes in any mixing device is detrimental to it's performance, although by conducting detailed RTD investigations as presented in this project, it can be accounted for in the design process.

The dead volume within the model HDVS operating with and without the sludge hopper occupies approximately 20-40% of the total volume and similarly for the prototype HDVS 5-25%. These results support previous observations, using different RTD data analysis techniques, that the prototype HDVS has less dead volume and therefore short-circuiting compared to the model HDVS (chapter 4). Subsequently the model and prototype HDVS combined model results show that the dead volume occupies a smaller fraction of the total volume as the HDVS is increased in size (diameter). The prototype HDVS also has marginally better plug-flow mixing characteristics compared to the model HDVS, which is shown by the ADM and TISM parameters (chapter 4). Hence, the scale-up of the HDVS will provide a mixing regime with less short-circuiting and improved plug-flow mixing characteristics and therefore, more conducive for certain kinetic processes and particularly chemical disinfection processes (section 2.2.3).

The dead volume within the model and prototype HDVS generally increases up to the transition flow rate (15l/min – model HDVS and 90l/min – prototype HDVS) and then remains relatively stable for all higher flow rates. This implies that the mixing regime is also stable at high flow rates and is illustrated by the model and prototype HDVS RTD normalised curves $E(\Theta)$ (chapter 4) and therefore, the RTD combined model also supports the change in the RTD curve shape at the transition flow rate (section 4.4). The introduction of a bypass flow rate i.e. short-circuiting into the combined model solution also supports these observations, by providing a better fit combined model curve at high flow rates and reducing the goodness of fit at low flow rates.

The dead volume within the prototype HDVS operating with the sludge hopper is less than the volume of the sludge hopper at low flow rates. This scenario never occurs for the model HDVS operating with the sludge hopper. Therefore, removing the sludge hopper from the model HDVS will have a greater effect on the mixing regime i.e. a reduction in stagnant volume, compared to removing the sludge hopper from the prototype HDVS, as observed in chapter 4 (section 4.4.9.2). The model and prototype HDVS dead volume is generally smaller when the HDVS is operated without the sludge hopper for the same flow rate. Hence, the sludge hopper contributes to the inactive flow behaviour within the HDVS. The combined model results also suggest that there are greater dead volumes within the HDVS at high flow rates, which are not only confined to the sludge hopper region, compared to 'sluggish-flow' volumes at low flow rates, which are predominantly associated with the sludge hopper region. Therefore removing the sludge hopper reduces the 'sluggish-flow' volume within the HDVS and any remaining non-active flow behaviour is more likely to be associated with dead volumes.

A reduction in the stagnant volume associated with the sludge hopper was also shown by comparing the RTD normalised curves $E(\Theta)$ for the HDVS operating with and without the sludge hopper (section 4.4.9). Additionally, observations with coloured dye in the model HDVS (section 4.4.10) suggested that inactive volumes could also exist around the cone area and at the top water level in the outer zone (Fig. 3.1). This volume in the outer zone, above the soffit level of the inlet pipe, will naturally contribute to the inactive flow within the HDVS due its preferred isolated and quiescent mixing characteristics, as it is used for the collection of floatable material during solids-liquid separation applications.

The combined model correlation parameters (R^2 and ESS) improve as the flow rate increases and therefore as the dead volume increases. This is the opposite relationship generally achieved for the ADM and TISM (chapter 4) and is related to the limited

physical realism of the combined model i.e. 3 tanks-in-series (N), whereas at low flow rates the RTD curves appear to have greater plug-flow mixing characteristics. The decrease in the goodness of fit coincides with a reduction in the combined model parameters sensitivity and therefore flexibility in describing the RTD experimental curve. The correlation parameters for the combined model, ADM and TISM are subject to the limitations of each model relative to the HDVS's non-ideal flow behaviour across the range of inlet flow rates (chapter 4). Therefore, in future HDVS RTD-kinetic process optimisation investigations, it may be better to use the ADM or TISM non-linear regression relationship with the experimental data at low flow rates and the RTD combined model at high flow rates.

A reduction in the physical realism and subsequently the combined model parameters flexibility and sensitivity at low flow rates is shown by artificially increasing the theoretical mean residence time in the combined model solution, for the same experimental RTD curve. This increases the combined model's ability to describe a system with greater plug-flow mixing characteristics and provided a better fit between the combined model and experimental RTD curve at low flow rates. These observations, regarding the physical realism provided by the combined model of the HDVS's mixing regime, suggest the need for a different combined model configuration, including additional tanks-in-series (N) to better describe the RTD and model the dead volume within the HDVS at low flow rates.

It is difficult to explicitly say that the results generated by the combined model are 'absolute' but the results are most definitely useful and warrant further investigation. This statement could be improved by comparing the combined model results with RTD experimental observations of the dead volume within the HDVS. However, the combined model results do generally support the observations obtained using different RTD data analysis techniques (chapter 4) and therefore provides confidence in the

characterisation of the HDVS's mixing regime. The combined model solution can be further developed to estimate the performance of a kinetic process within the HDVS accounting for the degree of non-ideal flow behaviour. This would provide a design methodology to optimise the HDVS for kinetic process applications, in addition to other methodologies cited in chapter 4 and 7. The combined model is currently being used as part of an ongoing project at LJMU to investigate scaling of the HDVS, based on the RTD and therefore the mixing regime (section 8.6). The results presented in this chapter and in chapter 4 will aid this scaling investigation.

The second stage in characterising the HDVS's mixing regime using RTD analysis investigates the effect of introducing a baseflow component (chapter 6). This will provide information regarding the mixing regime characteristics associated with both the overflow and baseflow component. Additionally, the mixing characteristics of the total flow (overflow + baseflow) can be compared to the HDVS operating with no baseflow i.e. overflow only and the effect of the baseflow component on the total mixing regime assessed. The HDVS operating with a baseflow component will provide a continuous flow through the sludge hopper and therefore a further insight into its mixing behaviour.

6.0 Hydrodynamic Vortex Separator (HDVS) Operating with a Baseflow Component Residence Time Distribution (RTD) Analysis

The second stage in characterising the mixing regime of the HDVS using RTD analysis investigates the effect of introducing a baseflow component, while maintaining an overflow component and therefore, operating the HDVS with multiple outlets (Fig. 6.1). This HDVS operating configuration has not previously been extensively characterised using RTD analysis.

It can be argued that the mixing characteristics of most typical mixing devices will be the same throughout the complete volume and therefore, the RTD is very similar regardless of its sampled location i.e. overflow or baseflow component (Fig. 6.1). However, the first HDVS RTD characterisation stage investigating the model and prototype HDVS operating without a baseflow component (chapter 4 and 5) showed that the HDVS has a complex mixing regime and it is not uniform throughout the complete volume. The HDVS operating without a baseflow has improved plug-flow mixing characteristics and a greater volume is active in the mixing process as the flow rate decreases. At low flow rates, the inactive flow behaviour within the HDVS is associated with 'sluggish-flow' regions, which conduct flow slower than the mean velocity and at high flow rates it is due to dead volumes, which reduce the effective volume of the HDVS. Therefore there is greater short-circuiting of the flow within the HDVS at high flow rates. The sludge hopper region (Fig. 6.1) contributes to the 'sluggish-flow' volume particularly at low flow rates. Subsequently, when the sludge hopper is removed from the HDVS configuration, the plug-flow mixing and active flow behaviour characteristics are improved. Additionally, the prototype HDVS has marginally better plug-flow mixing and active flow behaviour characteristics compared to the model HDVS for all no baseflow operating conditions (chapter 4 and 5).

The introduction of a baseflow component will provide additional information to support the observations and conclusions obtained from the first HDVS RTD characterisation stage (chapter 4 and 5). This will be achieved by comparing and relating the mixing characteristics of the overflow component to the baseflow component considering existing knowledge of the flow paths within the HDVS (Andoh and Smisson, 1993). Additionally, introducing a baseflow component will aid in identifying different mixing regimes within the HDVS associated with the overflow and baseflow component. The individual contribution of each flow component and their summation will also illustrate the effect of introducing a baseflow component on the total HDVS mixing regime compared to the HDVS operating without a baseflow component. The RTD sampling arrangement (Fig. 6.1) enables the mixing behaviour of the sludge hopper and its contribution to the baseflow component to be investigated and subsequently this is compared to the sludge hopper mixing characteristics for the HDVS operating with no baseflow (chapter 4 and 5). Measuring the RTD at several points will also possibly identify different mixing regimes and their locations within the HDVS.

The same RTD data analysis techniques used for the HDVS operating with no baseflow were also employed to describe the overflow and baseflow component mixing regime (section 4.3). This includes the ADM and TISM parameters solved indirectly and directly using the method of moments and non-linear regression techniques respectively and the RTD indices. The RTD experimental curve, ADM and TISM goodness of fit is assessed using typical RTD correlation parameters i.e. coefficient of correlation (R^2) and sum of the errors squared (ESS) (section 4.3.3). The introduction of a second outlet does not change the RTD data analysis procedure. The overflow and baseflow RTD curves were treated as totally separate RTD curves and analysed in this manner. A sample calculation and the experimental tracer concentration C(t) and exit-age

distribution function E(t) values for both the model and prototype HDVS, obtained at both baseflow sample points, are presented in appendix E.1-E.4.

This project presents the RTD within the model and prototype HDVS operating with and without a baseflow component and with and without the sludge hopper (Fig. 6.1) in a consistent and comprehensive manner. This approach provides suitable data for future HDVS kinetic process investigations (chapter 7), RTD scaling investigations (section 8.6) and comparisons to other systems subject to RTD analysis. The model and prototype HDVS RTD results are also compared with existing limited RTD data on different styles of HDVS operating with a baseflow component (Table 1.1) (section 2.2.2).

6.1 General Characteristics of the Hydrodynamic Vortex Separator (HDVS) Operating with a Baseflow Component

The HDVS operating with a baseflow component has a range of potential operating conditions. This relates to the ratio of the baseflow component (Qb) and the inlet flow rate (Qi), which is termed the flow split i.e. Qb/Qi x 100 (%) (Fig. 6.1). The HDVS's performance as a solids-liquid separation process is directly related to the flow split (section 2.1.2). Fig. 6.1 is a schematic illustration of the flow components and sampling arrangement used for the HDVS operating with a baseflow component in this project.

The RTD experimental investigations undertaken for the model and prototype HDVS operating with a baseflow were approached so that the influence of the sludge hopper could be further investigated. This was achieved by locating 2 sampling points on the baseflow outlet. These were positioned above (SP2) and below (SP3) the sludge hopper (Fig. 6.1). Therefore comparing the RTD data for the HDVS operating with and

without a baseflow component, SP2 relates to the HDVS without the sludge hopper (section 4.4.5 and 4.4.6) and SP3 to the HDVS with the sludge hopper (section 4.4.1 and 4.4.2). The model and prototype HDVS operating with no baseflow and with and without the sludge hopper RTD results are presented and discussed in chapter 4.

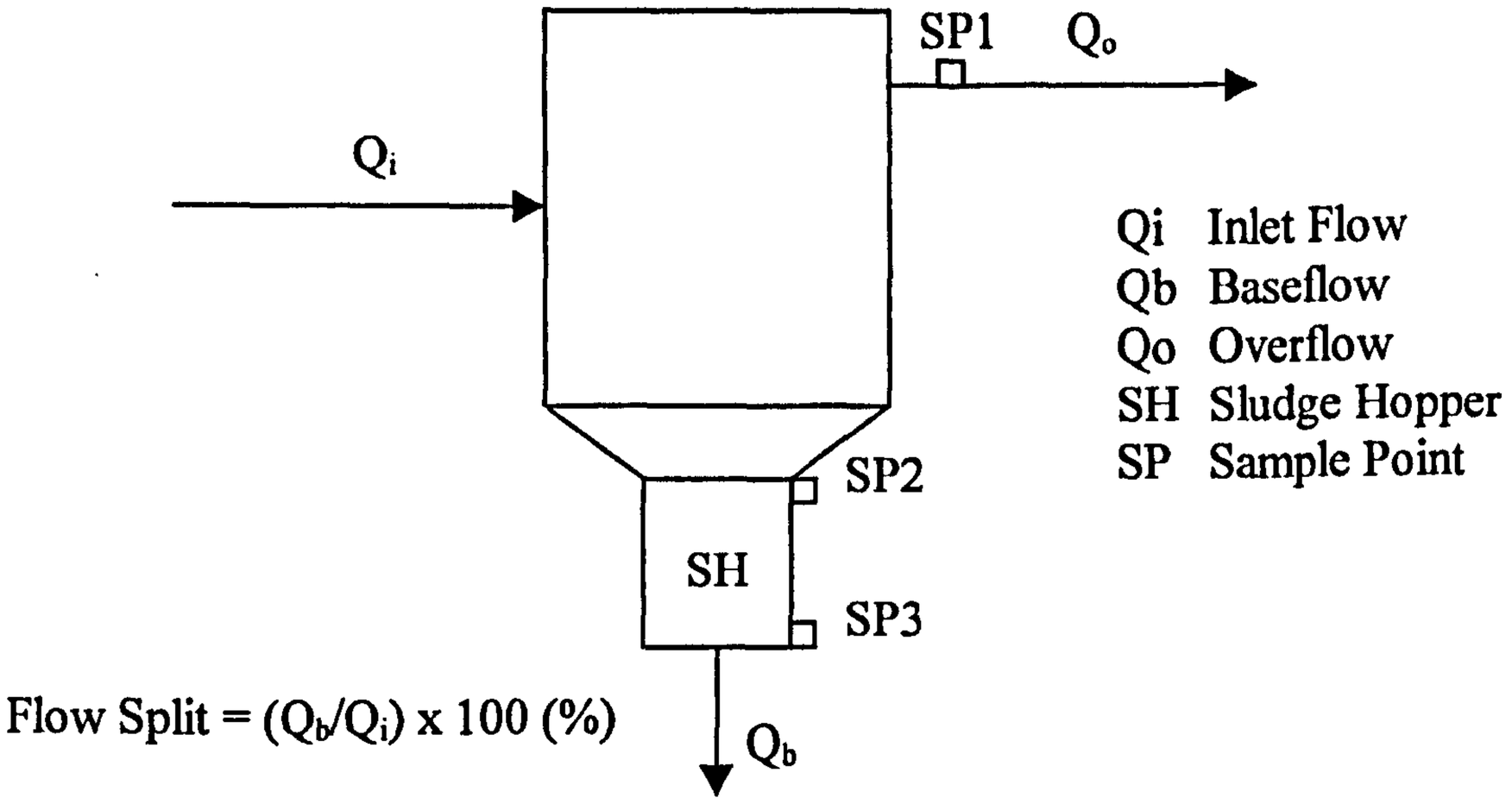

Fig. 6.1 HDVS Flow Component and Baseflow Sample Point Arrangement

This project investigated the Swirl-Flo™ HDVS and by operating it with a baseflow component with and without the sludge hopper provided a similar configuration to the Storm King™ and Grit King™ HDVS (Table 1.1). The former operates without a sludge hopper and the latter has a grit pot and therefore a similar collection area for solids as the Swirl-Flo™ HDVS (Fig. 6.1).

Preliminary RTD baseflow investigations undertaken on the prototype HDVS sampled the baseflow tracer concentration from a location downstream of the baseflow exit point i.e. on the baseflow pipe downstream of the sludge hopper (Fig. 6.1). These results clearly included the transit time of the flow through the baseflow pipe and increased the amount of plug-flow mixing associated with the baseflow component as the

pipe behaves as a tubular reactor (section 4.1). Subsequently, this sampling arrangement was deemed not to be representative of the mixing regime within the HDVS and the results are not presented or further discussed in this project. Therefore, the location of SP2 and SP3 used throughout this project are considered to accurately represent the baseflow component RTD from the HDVS operating with and without the sludge hopper (Fig. 6.1).

Due to the large number of experiments investigated for the HDVS operating with a baseflow component, as a result of investigating a model and prototype HDVS at two sample points and for various flow split combinations, only the RTD pulse injection technique using the lithium chloride (LiCl) tracer was employed. The RTD experimental procedure was the same as the HDVS operating without a baseflow component, except for taking two sets of samples i.e. one set from both the overflow and baseflow outlets (chapter 3). A selection of the model and prototype HDVS operating without a baseflow component inlet flow rates were investigated for the HDVS operating with a baseflow component. The baseflow flow splits (Qb/Qi) investigated were 10, 20, 30 and 40%.

6.2 Results and Discussion

6.2.1 Model Hydrodynamic Vortex Separator (HDVS) Baseflow - Residence Time Distribution (RTD) Pulse Experiments Sample Point 2 (SP2)

6.2.1.1 Method of Moments Data Analysis

This section describes the RTD analysis undertaken on the model HDVS operating with a baseflow component measured at sample point 2 (SP2), which is located above

the sludge hopper (Fig. 6.1).

To directly compare the RTD curves for different flow splits, the RTD needs to be normalised with respect to the mean residence time (section 4.3.1). The RTD normalised curves E(Θ) were obtained by using both the theoretical and experimental mean residence time calculated using the method of moments. This normalisation approach is different to that used for the HDVS operating without a baseflow, as operating with only one outlet i.e. overflow component, the true HDVS theoretical mean residence time is known (section 4.4.1).

The theoretical mean residence time for both the overflow and baseflow components were estimated using equation 4.2 and setting the volume (V) and flow rate (Q) according to the flow split. Subsequently, a 10% flow split results in 10% of the total volume and inlet flow rate passing through the baseflow and therefore 90% through the overflow. Hence, the theoretical mean residence time for both the overflow and baseflow component will be equal to the model HDVS operating with no baseflow and without the sludge hopper for the same inlet flow rate (section 4.4.5). The theoretical mean residence time values are based on there being no interaction between the two flow components and the associated volumes are directly proportional to the flow split (appendix E.1.4). This normalisation procedure was adopted for all model and prototype HDVS operating with a baseflow component RTD experiments.

Fig. 6.2 and 6.3 show the RTD normalised curves E(Θ) obtained using the theoretical mean residence time and experimental mean residence time calculated using the method of moments, for the model HDVS operating with an inlet flow rate of 20l/min and for the range of flow splits investigated i.e. 10-40%. The remaining flow rates are shown in appendix E.1.5 and E.1.6 respectively.

The overflow and baseflow RTD curves illustrate a plug-flow mixing device with a degree of non-ideal flow behaviour. This is evident, as there is a significant peak on the RTD curves which, occurs before a normalised time (Θ) value of 1 (section 4.3.1) and there is also tailing of the RTD curves (section 4.4.1.1). This demonstrates that there is short-circuiting within the HDVS and subsequently stagnant regions are present. The RTD curves show similar characteristics as the RTD curves for the model HDVS operating without the sludge hopper (section 4.4.5). The normalised exit-age distribution function E(Θ) values are greater when using the method of moments experimental mean residence time compared to the theoretical mean residence time. This is due to the error between the experimental and theoretical mean residence time results, which are discussed below and presented in appendix E.1.4.

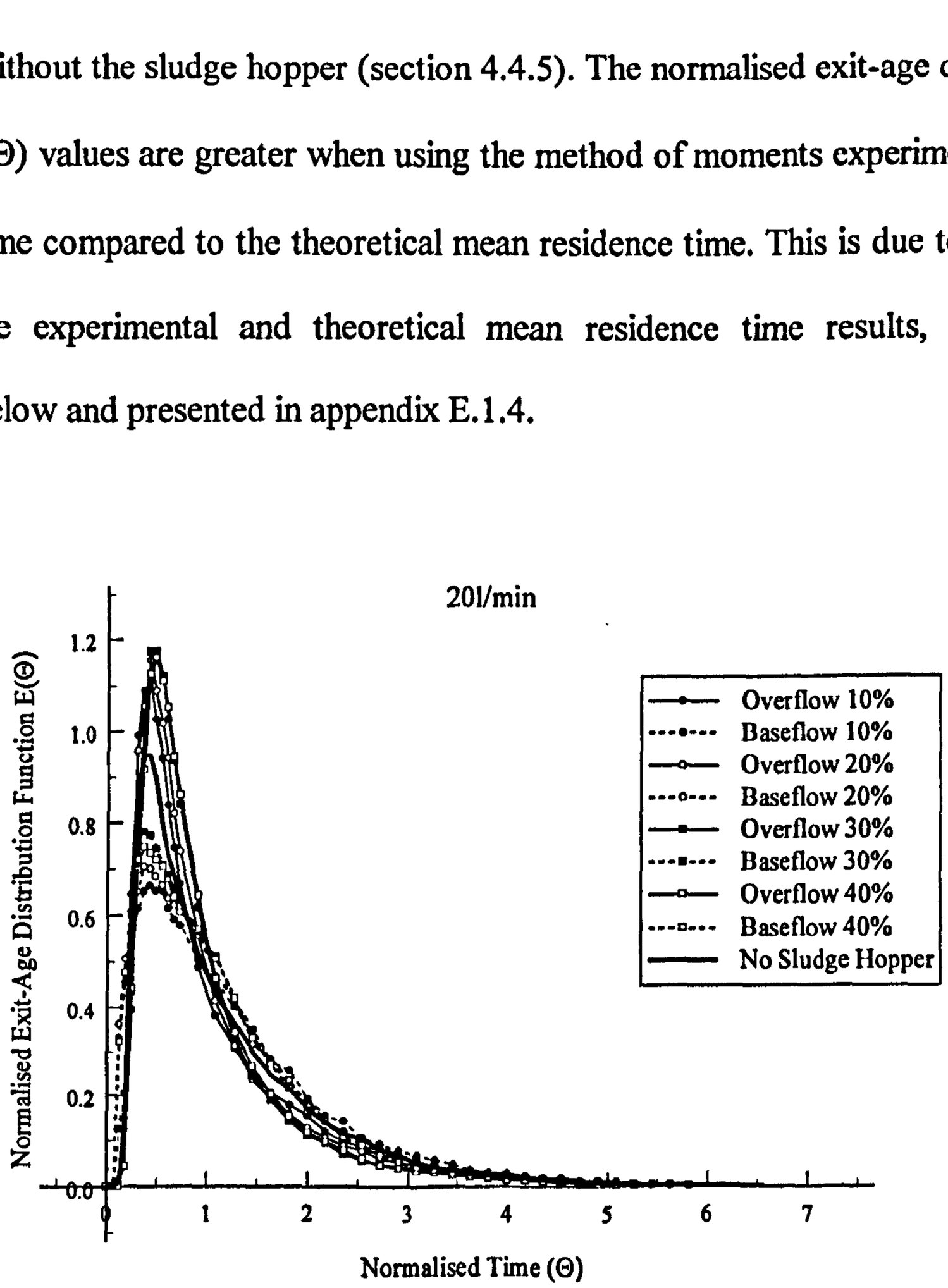

Fig. 6.2 Model HDVS Baseflow (SP2) - Comparison of Normalised Exit-Age Distribution Curves E(Θ) using the Theoretical Mean Residence Time

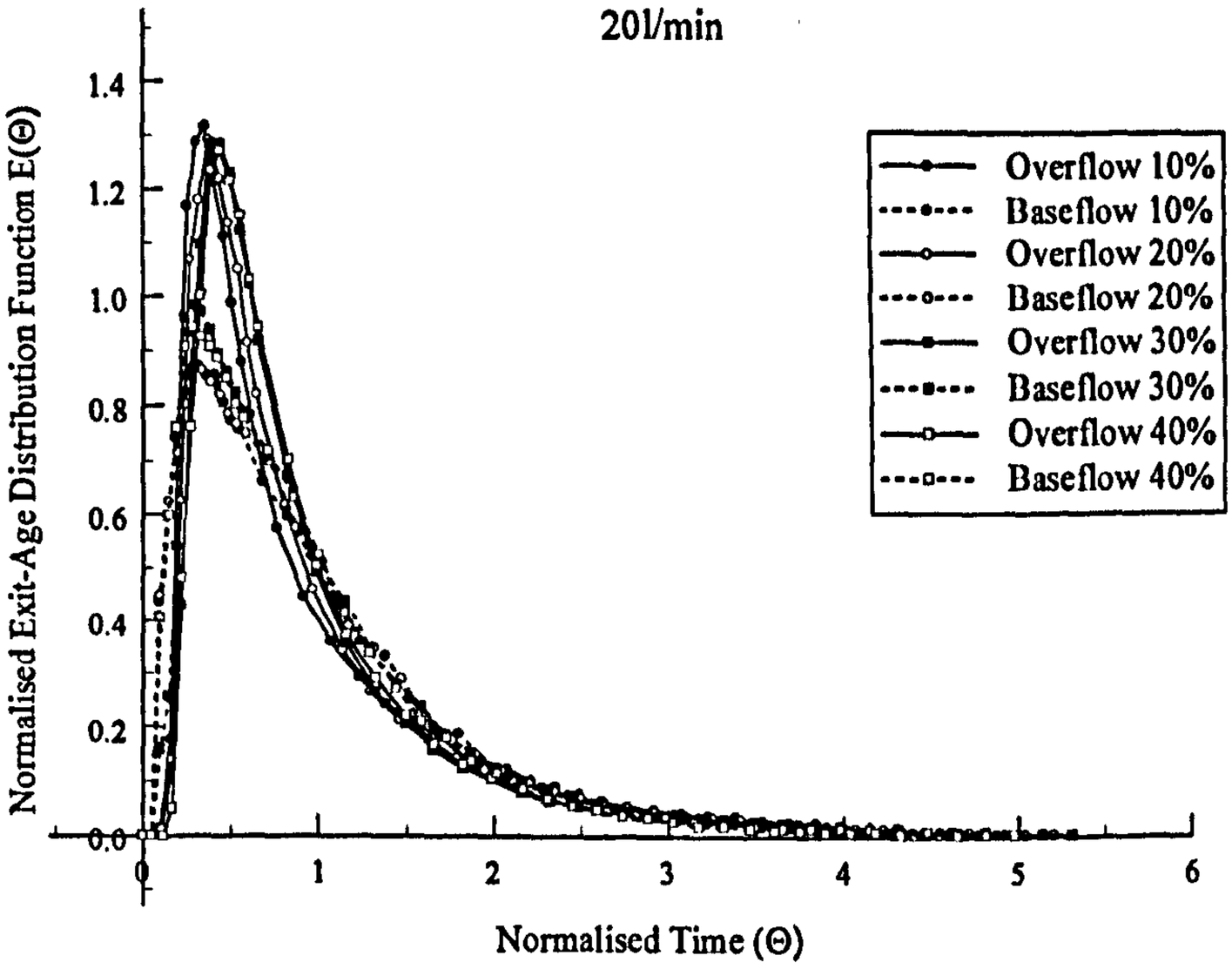

Fig. 6.3 Model HDVS Baseflow (SP2) - Comparison of Normalised Exit-Age Distribution Curves E(Θ) using the Method of Moments

The theoretical mean residence time is the same for both the overflow and baseflow component at the same inlet flow rate, across the range of flow splits investigated (appendix E.1.4). Therefore, neglecting any non-ideal mixing associated with dispersion (back-mixing), the RTD curves should peak at a very similar normalised time (Θ) and height value. However, the overflow component RTD curves significantly increase in height and the baseflow curves decrease relative to each other as the inlet flow rate increases. Hence, at low flow rates the baseflow peak height is greater than the overflow and at high flow rates the opposite relationship is observed (appendix E.1.5 and E.1.6). This implies that the overflow component has a greater volume element, which short-circuits at high flow rates and the baseflow component at low flow rates. This interpretation can be used as the overflow and baseflow RTD curves time to peak concentration generally occurs before a normalised time (Θ) value of 1, implying that short-circuiting is definitely present. The above observations are supported by the

baseflow component RTD curves, which peak closer to a normalised time value (Θ) of 1 as the inlet flow rate is increased. The relationship between the overflow and baseflow RTD curves using the time to peak concentration, as opposed to the peak height, is discussed below. There is no significant difference in the relative height of the overflow and baseflow RTD curve peaks across the range of flow splits for a given inlet flow rate.

Appendix E.1.7 shows the time taken for the peak tracer (LiCl) concentration to occur for the overflow and baseflow RTD curves. The RTD curve time to peak concentration for the model HDVS operating with a baseflow component measured at SP2 and SP3 (Fig. 6.1) are compared and also presented in section 6.2.3 (Table 6.9). The peak concentration corresponds to the time at which the maximum volume passes through the HDVS. These values show that for inlet flow rates less than 30l/min the baseflow RTD curve peaks before the overflow and for high flow rates the opposite occurs. The baseflow flow path (SP2) is considered to be shorter than the overflow flow path from the geometry of the HDVS (Fig. 3.1) and therefore, the baseflow component time to peak should be less than the overflow, as is achieved at low inlet flow rates. Luyckx *et al.*, (1998a) also commented on the assumed flow path of the baseflow relative to the overflow and that the former is likely to produce an RTD peak before the latter. This was based on previous descriptions of the flow patterns within a Storm King™ HDVS (Table 1.1) (Andoh and Smisson, 1993). Therefore the results suggest that short-circuiting of the overflow component occurs in the model HDVS at high flow rates. The overflow component short-circuiting at high flow rates was also observed for the HDVS operating with no baseflow component. This is shown by the RTD normalised curves E(Θ) (section 4.4.5.1) and the RTD combined mathematical model results (chapter 5). The model HDVS operating with a baseflow component time to peak concentration is also illustrated by the exit-age distribution function E(t) curves (Fig.

6.7).

The short-circuiting of the overflow component at high flow rates and the baseflow component at low flow rates is possibly related to the strength of the vortex generated within the HDVS and the internal configuration of the HDVS (Fig. 3.1). At low flow rates, a weak vortex could allow the baseflow component to take a shorter flow path, whereas at high flow rates a stronger induced vortex would force the flow path around the perimeter of the HDVS prior to leaving the baseflow outlet. Hence, at high flow rates the forced longer flow path would reduce short-circuiting. This contrasts with the overflow component, as a weak vortex would be confined between the outer wall and vertical dip plate i.e. outer zone and would leave the HDVS as it is displaced by the incoming flow in a time equal to approximately the mean residence time. Whereas a stronger vortex creating turbulent conditions at the inlet, could possibly direct the flow beneath the inlet deflector plate and vertical dip plate, which provides an easier flow path to the overflow outlet and hence short-circuiting of the overflow component (Fig. 3.1) (section 6.2.3).

The model HDVS operating without a baseflow component RTD data was also presented using the intensity function (λ) (section 4.3.5). This has not been presented for the HDVS operating with a baseflow component as the RTD curves have a very similar distribution and therefore characteristics as the model HDVS operating without a baseflow component (section 4.4.1.1 and 4.4.5.1). Hence, the intensity function (λ) will not provide any further significant discussion.

The RTD experimental duration was approximately 5-6 times the theoretical mean residence time (appendix E.1.4). The RTD investigations previously conducted with the HDVS operating with no baseflow highlighted the effect of the sludge hopper region (Fig. 6.1) by acting as a stagnant region (section 4.4.1). These stagnant volumes can

significantly affect the overall tracer recovery (mass balance) by creating tracer hold-up for times greater than the experimental duration. However, in the baseflow mode of operation, the sludge hopper and remaining HDVS volume is considered to be completely active. The concentration C(t) curves also converge to zero tracer concentrations (mg/l), implying that there is complete washing out of the tracer from the HDVS. The experimental tracer recoveries (mass balance) for all flow rates are shown in appendix E.1.8. These values show that near 100% tracer recovery was obtained for all inlet flow rates and flow splits. The overflow values decrease and the baseflow increase as the flow split increases and are approximately proportional to the flow split. The average error is +/- 5% with the largest error approximately 10%. The errors do not show any particular trend with respect to the inlet flow rate or flow split and therefore, are attributed to experimental errors rather than the HDVS configuration and internal localised mixing patterns i.e. sludge hopper (section 4.4.1.1).

The overflow and baseflow component experimental mean residence time calculated using the method of moments cannot be greater than the theoretical mean residence time calculated from first principles (eqn. 4.2) (appendix E.1.4), as discussed in section 4.4.1.1 (Fogler, 1992). However, the RTD is used to investigate the non-ideal mixing behaviour of a device, which results in discrepancies between the theoretical and actual mean residence time. This is illustrated by comparing the theoretical mean residence time in appendix E.1.4 to the experimental mean residence time in Table 6.1.

Table 6.1 Model HDVS Baseflow (SP2) – Comparison of First and Second Moments Calculated from RTD Experimental Data

Flow Rate (l/min)	Flow Split (%)	Experimental Mean Residence Time (min)		Variance (min^2)		Normalised Variance (σ_0^2)	
		O	B	O	B	O	B
10	10	7.284	6.368	27.629	23.692	0.521	0.584
	20	6.830	5.835	25.402	24.180	0.544	0.710
	30	6.755	5.897	26.149	22.738	0.573	0.654
	40	6.680	5.531	23.940	22.272	0.536	0.728
15	10	4.647	4.717	15.757	14.742	0.730	0.663
	20	4.478	4.147	12.238	10.705	0.610	0.622
	30	4.240	4.427	10.726	11.949	0.597	0.610
	40	4.334	4.003	9.7230	9.6620	0.518	0.603
20	10	3.252	3.620	7.264	7.459	0.687	0.569
	20	3.075	3.407	6.199	6.546	0.656	0.564
	30	3.013	3.467	5.655	6.474	0.623	0.539
	40	2.963	3.227	4.828	5.655	0.550	0.543
30	10	2.286	2.877	3.652	4.296	0.699	0.519
	20	2.015	2.520	3.386	3.935	0.834	0.620
	30	2.020	2.509	2.714	3.175	0.665	0.504
	40	1.996	2.306	2.517	2.902	0.632	0.546
45	10	1.449	1.899	1.634	1.925	0.778	0.534
	20	1.340	1.697	1.117	1.244	0.622	0.432
	30	1.068	1.612	0.867	1.230	0.759	0.473
	40	1.302	1.536	0.964	1.005	0.569	0.426
60	10	0.993	1.232	0.616	0.653	0.624	0.430
	20	0.996	1.185	0.618	0.612	0.623	0.436
	30	1.010	1.352	0.701	0.815	0.687	0.446
	40	0.998	1.137	0.619	0.566	0.622	0.438

Fig. 6.4 shows the experimental mean residence time for all inlet flow rates plotted against the flow split. The values are relatively constant for the individual overflow and baseflow components across the range of flow splits for each inlet flow rate. The magnitude of the overflow mean residence time, relative to the baseflow, follows a similar trend as the time to peak concentration, which were discussed above. This is expected as the mean residence time calculation (RTD centroid – first moment) is strongly influenced by the time at which the peak tracer concentration occurs (eqn. 4.4). The experimental mean residence time values are similar to the theoretical mean

residence time calculated for the model HDVS operating with no baseflow and without the sludge hopper (Table 4.13).

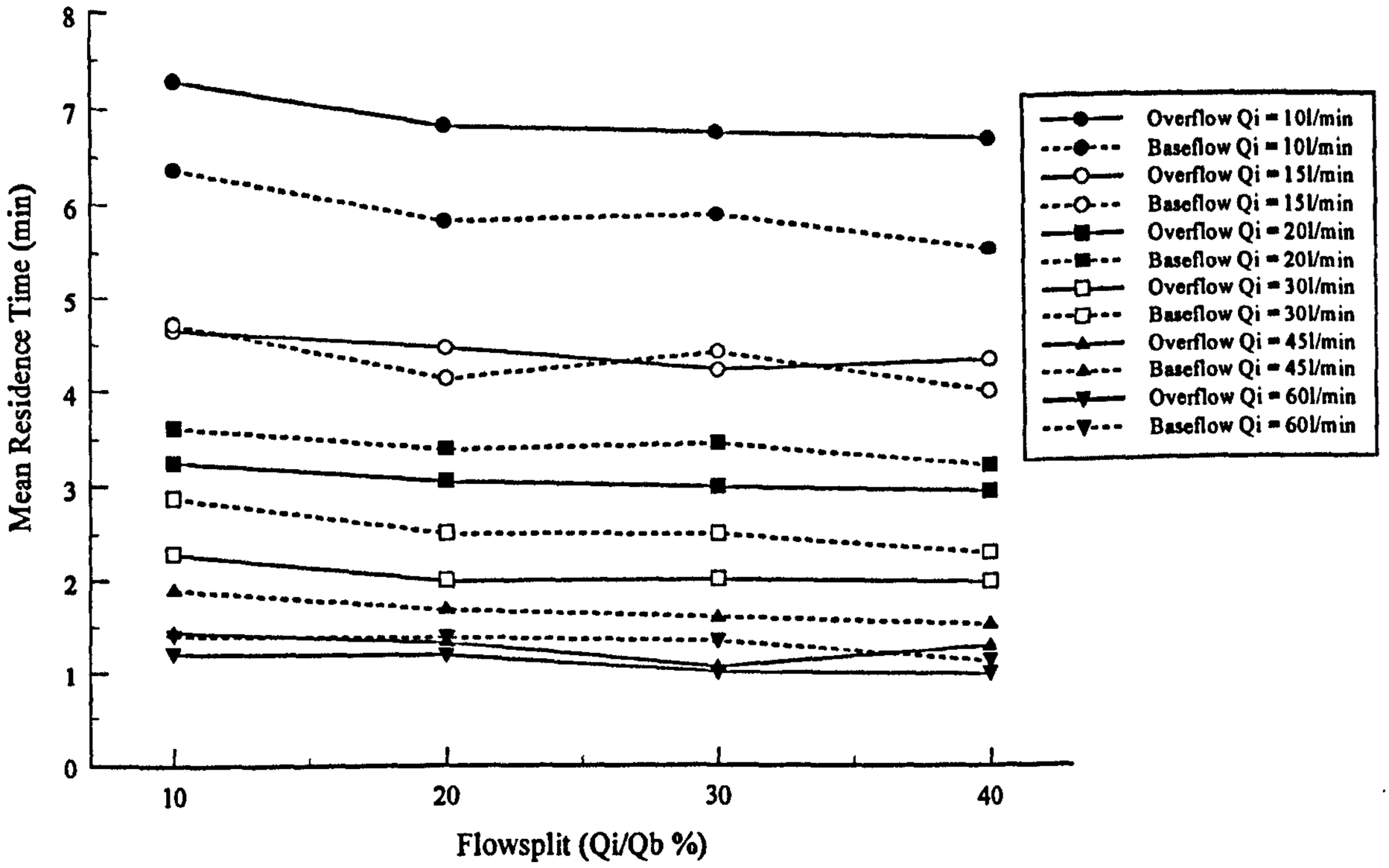

Fig. 6.4 Model HDVS Baseflow (SP2) - Experimental Mean Residence Time using the Method of Moments

SP2 is located such that the sample is effectively being withdrawn from within the main volume of the HDVS (Fig. 6.1). Therefore, as the overflow and baseflow experimental mean residence time values are very similar for a given inlet flow rate, this suggests that the HDVS is behaving very much nearer a completely mixed system rather than a plug-flow mixing system i.e. the mean residence time in a completely mixed tank will be the same anywhere in the system (section 4.1).

Appendix E.1.4 also shows the error between the theoretical (Table 6.1) and the experimental mean residence time calculated using the method of moments. The experimental mean residence time values are all generally greater than the theoretical mean residence time values and therefore, all have positive errors. This trend was also observed for the RTD investigations undertaken on the model HDVS operating with no

baseflow and without the sludge hopper (section 4.4.5). This error is associated with the RTD curves characteristics and the data analysis technique (section 4.4.1.1).

The average error for the overflow component experimental mean residence time values compared with the theoretical mean residence time is +14% and similarly for the baseflow is +25%. This error generally decreases for the overflow component and increases for the baseflow component as the inlet flow rate is increased. Based on the discussion in section 4.4.1.1, this implies that a greater fraction of the volume associated with the baseflow component has a residence time greater than the theoretical mean residence time. Subsequently, there are greater stagnant volumes within the baseflow component as the flow rate increases and the overflow component has the opposite trend, which is the same as the model HDVS operating with no baseflow and without the sludge hopper (section 4.4.5.1). This also suggests that the baseflow component has a greater volume, which passes through the HDVS closer to a normalised time (Θ) value of 1, as the flow rate increases and therefore there is less short-circuiting. Additionally, the baseflow component also has improved plug-flow mixing characteristics at high flow rates and the overflow component at low flow rates. This is supported by the overflow and baseflow RTD curves relative time to peak concentration and peak height discussed above and the plug-flow mixing characteristics of both flow components is discussed below using the ADM and TISM parameters.

Chapter 4 showed the influence of the RTD experimental duration by truncating the RTD curves (section 4.4.1.1). This has not been investigated for any of the model or prototype HDVS baseflow RTD data and will influence the mean residence time and HDVS volume estimations. The errors between the theoretical and experimental mean residence time are significantly less than the errors obtained for the model HDVS operating with no baseflow and without the sludge hopper (section 4.4.5.1). Hence,

although stagnant regions are possibly present as discussed above, the majority of the total volume is completely active when the HDVS is operated with a baseflow component. Therefore, a RTD curve truncation analysis is expected to provide an experimental mean residence time in the vicinity of the theoretical mean residence time for the recommended truncation time of 3-4 times the theoretical mean residence time (section 4.4.1.1) (Nauman, 1981). A truncation analysis is largely dependent on the shape of the RTD curve, which is very similar for the model HDVS operating with and without a baseflow component and therefore, the same general observations and conclusions will apply (section 4.4.1.1).

Table 6.2 Model HDVS Baseflow (SP2) – Estimated Model HDVS Volume using the Experimental Mean Residence Time Calculated from the Method of Moments

Flow Rate (l/min)	Flow Split (%)	Volume (l)		Percentage of Experimental Volume (%)		Total Volume (l)
		O	B	O	B	
10	10	65.556	6.3680	91.146	8.8540	71.924
	20	54.640	11.670	82.401	17.599	66.310
	30	47.285	17.691	72.773	27.227	64.976
	40	40.080	22.124	64.433	35.567	62.204
15	10	62.735	7.0760	89.865	10.135	69.810
	20	53.736	12.441	81.200	18.800	66.177
	30	44.520	19.922	69.086	30.914	64.442
	40	39.006	24.018	61.891	38.109	63.024
20	10	58.536	7.2400	88.993	11.007	65.776
	20	49.200	13.628	78.309	21.691	62.828
	30	42.182	20.802	66.973	33.027	62.984
	40	35.556	25.816	57.935	42.065	61.372
30	10	61.722	8.6310	87.732	12.268	70.353
	20	48.360	15.120	76.181	23.819	63.480
	30	42.420	22.581	65.261	34.739	65.001
	40	35.928	27.672	56.491	43.509	63.600
45	10	58.685	8.5460	87.289	12.711	67.230
	20	48.240	15.273	75.953	24.047	63.513
	30	33.642	21.762	60.721	39.279	55.404
	40	35.154	27.648	55.976	44.024	62.802
60	10	53.622	7.3920	87.885	12.115	61.014
	20	47.808	14.220	77.075	22.925	62.028
	30	42.420	24.336	63.545	36.455	66.756
	40	35.928	27.288	56.834	43.166	63.216

Table 6.2 shows the estimated model HDVS volume obtained from the experimental mean residence time calculated using the method of moments. The model HDVS operating without the sludge hopper (Fig. 6.1) has a volume of approximately 55 litres and the estimated experimental volumes have an average error of +15%. The HDVS volume estimations measured at SP2 are compared to the SP3 results in section 6.2.3. The percentage of the experimental volume associated with the overflow and baseflow components is also presented in Table 6.2. These values show that the volume split is approximately proportional to the flow split i.e. a 10% flow split results in 10% of the total HDVS volume being associated with the baseflow and 90% with the overflow component.

Fig. 6.5 and 6.6 illustrate the ADM (P_e) and TISM (N) parameters for all flow splits and inlet flow rates calculated using the method of moments. The numerical values are provided in appendix E.1.9. The overflow and baseflow component Peclet numbers (P_e) remain relatively stable across the flow splits investigated. However comparing the Peclet number (P_e) across the range of inlet flow rates, the overflow Peclet number (P_e) increases as the inlet flow rate is decreased. This is the same relationship as achieved for the model HDVS operating with no baseflow and without the sludge hopper (section 4.4.5). The baseflow component shows the opposite trend with higher Peclet numbers (P_e) at high inlet flow rates.

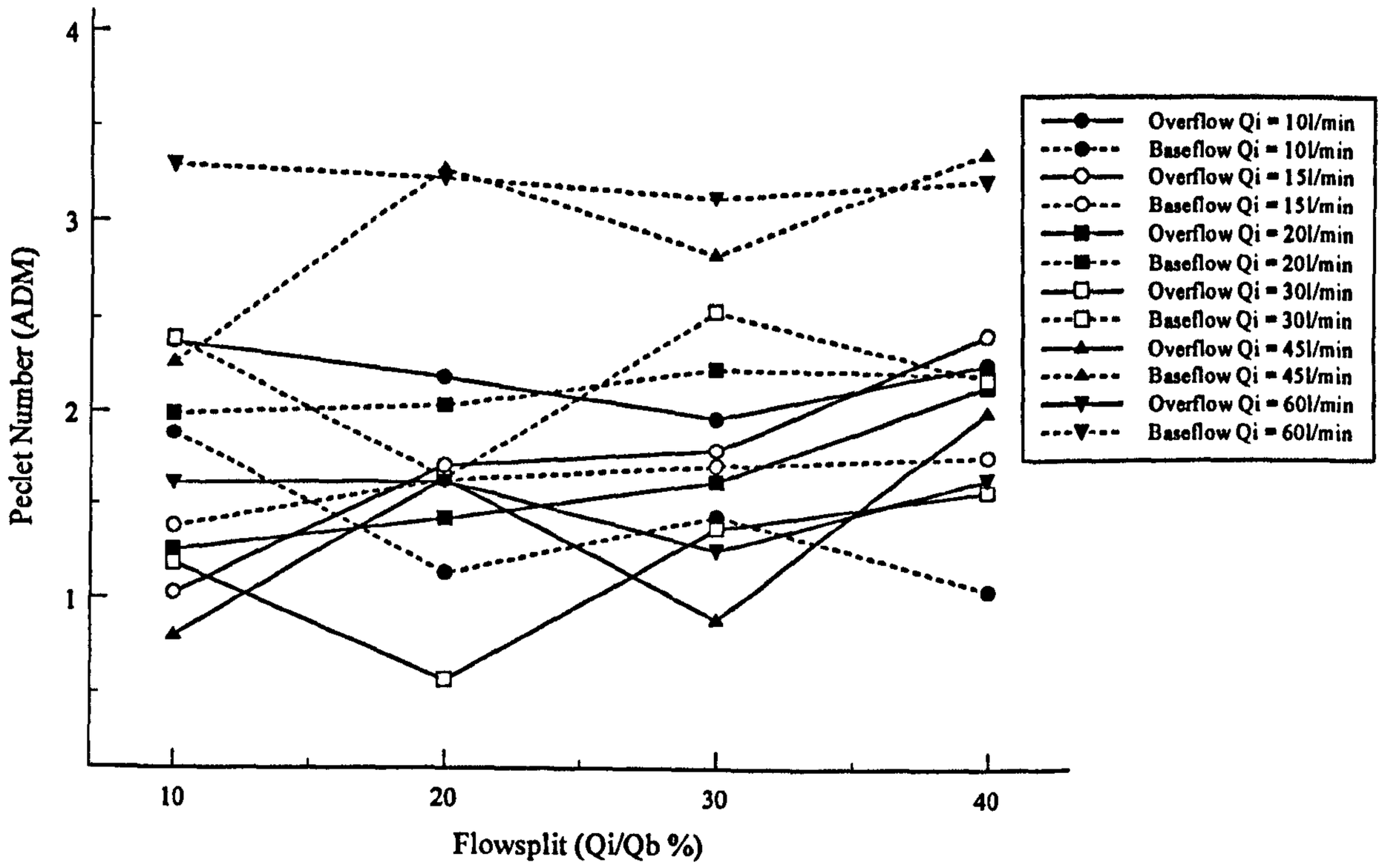

Fig. 6.5 Model HDVS Baseflow (SP2) - Comparison of the ADM Parameters Calculated using the Method of Moments

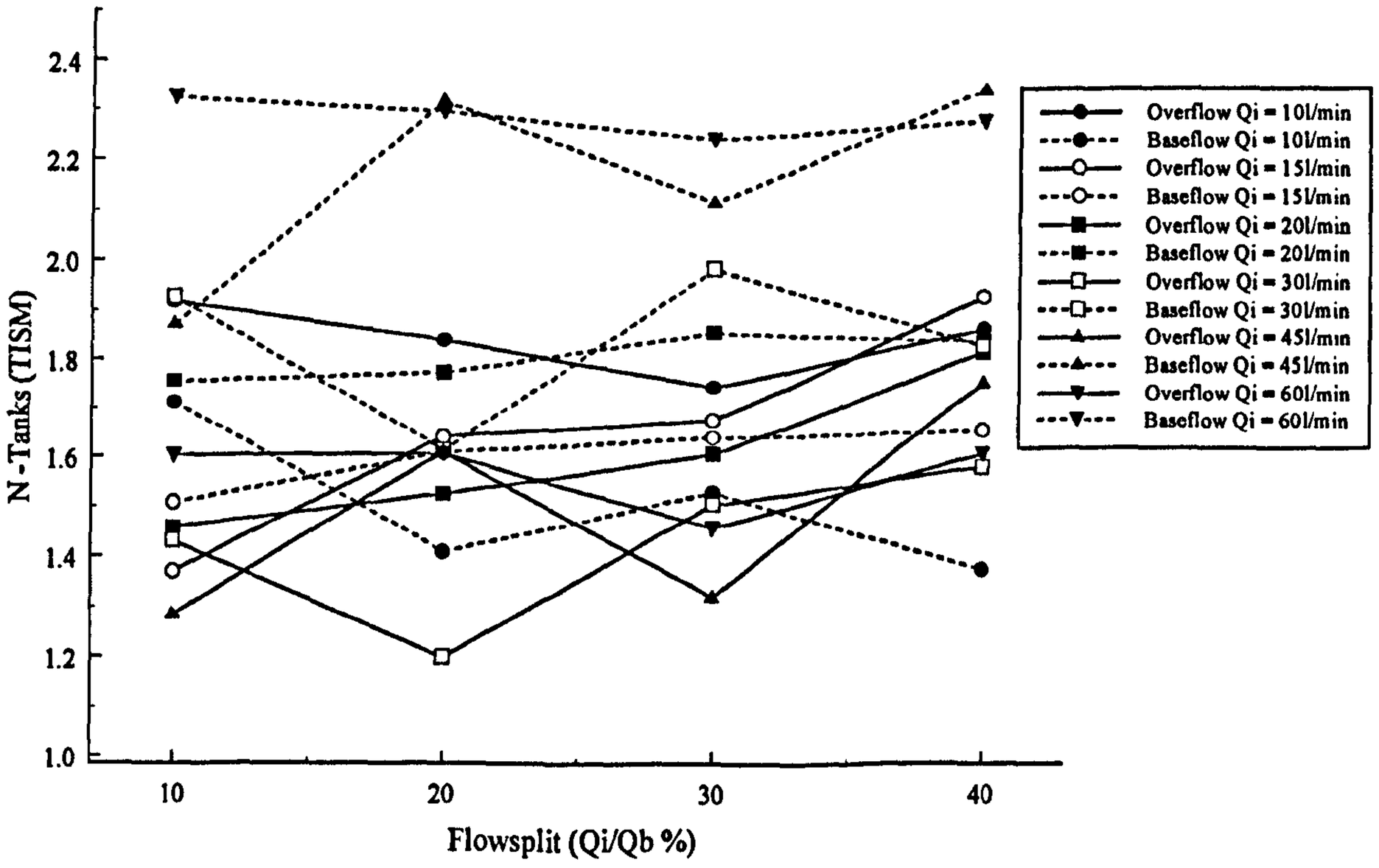

Fig. 6.6 Model HDVS Baseflow (SP2) - Comparison of the TISM Parameters Calculated using the Method of Moments

The ADM and TISM parameters show the same trend as they are both calculated directly from the normalised variance (σ_θ^2) (eqn. 4.6) i.e. the RTD curve first and second moments (n) and there are no other influencing parameters. The performance of the HDVS for kinetic process applications can be directly obtained using the ADM and TISM (section 7.5) (Levenspiel, 1972). Hence, Fig. 6.5 and 6.6 enables the optimisation of both the overflow and baseflow effluents to provide a specific kinetic process efficiency i.e. the inlet flow rate and flow split can be set accordingly depending on the process and mixing regime requirements e.g. chemical conversion, microorganisms kill curves and disinfectant residue.

Appendix E.1.9 also details the summation of the individual overflow and baseflow component ADM and TISM parameters for the range of inlet flow rates at each flow split. This is shown as it describes the mixing regime of the total flow (overflow + baseflow) within the model HDVS operating with a baseflow component. Subsequently, comparing the total flow ADM and TISM parameters obtained for the HDVS operating without a baseflow component (chapter 4) will provide some indication as to whether the overall mixing regime changes between the two operating conditions. The total flow ADM and TISM parameters for the model HDVS operating with a baseflow component measured at SP2 and SP3 are compared and also presented in section 6.2.3 (Table 6.10). The model HDVS operating with and without a baseflow component RTD experimental duration was approximately 5-6 times the theoretical mean residence time. Therefore, this provides comparable total flow data and is not subject to interpretation accounting for different truncation times, which significantly effects the RTD parameters calculated using the method of moments (section 4.4.1.1) and to a lesser extent using non-linear regression (section 4.4.1.2). The ADM and TISM total flow parameters calculated using non-linear regression are presented in section 6.2.1.2. The model HDVS operating with

no baseflow and without the sludge hopper ADM and TISM parameters for an inlet flow rate of 40l/min are compared to an inlet flow rate of 45l/min for the HDVS operating with a baseflow. All other inlet flow rate comparisons are at the same inlet flow rate. It must be reiterated that the RTD SP2 baseflow results do not include the sludge hopper (Fig. 6.1).

The results for both the ADM and TISM parameters clearly show that the total mixing regime within the model HDVS operating with a baseflow has a greater element of plug-flow mixing compared to the model HDVS operating with no baseflow and without the sludge hopper (section 4.4.5.1). The total flow ADM and TISM parameters are relatively consistent across the range of inlet flow rates and all flow splits. Whereas the model HDVS operating with no baseflow and without the sludge hopper total flow ADM and TISM parameters decrease as the inlet flow rate increases. The overflow component ADM and TISM parameters for the model HDVS operating with a baseflow are in the same order of magnitude as obtained for the HDVS operating with no baseflow component and without the sludge hopper i.e. overflow component only (section 4.4.5.1). The model HDVS baseflow component ADM and TISM parameters increase and the overflow parameters decrease as the inlet flow rate increases however, they are relatively stable across the range of flow splits as discussed above. Hence, the introduction of a baseflow component maintains the same degree of plug-flow mixing at low flow rates and increases it at high flow rates for the total flow within the model HDVS.

Fenner and Tyack, (1997 and 1998) investigated scaling relationships for a Grit King™ HDVS operating with and without a baseflow component (section 2.1.3) and showed that different scaling protocols are dominant depending on the operating conditions. The inclusion of a baseflow component improved the solids removal

efficiency of the Grit King™ HDVS and ensured that once the particles have become trapped in the central core and the grit pot (Table 1.1) they are not likely to be removed back to the main body of flow i.e. scour resulting in resuspension. This was considered due to a visibly stronger vortex in this region when the HDVS is operated with a baseflow component compared to no baseflow conditions. Therefore, it follows that the total mixing regime within the HDVS is different depending on the operating conditions i.e. with or without a baseflow component.

There appears to be two marginally different types of mixing regimes within the model HDVS, which is observed by comparing the difference between the individual overflow and baseflow components RTD normalised curves $E(\Theta)$ and the ADM and TISM parameters discussed above. The RTD investigations undertaken in this project on a Swirl-Flo™ HDVS (Table 1.1) support previous studies undertaken on a prototype Grit King™ HDVS operating with a baseflow component (Tyack and Fenner, 1998b) (section 6.2.7.1) by observing different flow regimes within the HDVS associated with the overflow and baseflow components.

The total flow ADM and TISM parameters presented in this project for the model HDVS operating with no baseflow and without the sludge hopper (section 4.4.5.1) were compared to the overflow component ADM and TISM parameters for the HDVS operating with a baseflow for flow splits of 10% and 40%. If the overflow mixing regime differs with the introduction of a baseflow component these flow splits should provide an insight into the smallest and greatest deviation respectively from the overflow component ADM and TISM parameters for the HDVS operating with no baseflow and without the sludge hopper. However, there is no significant difference between the overflow component ADM and TISM parameters for both model HDVS operating conditions across the range of flow splits. Hence, the overflow component plug-flow mixing regime

remains stable for the two HDVS operating conditions and therefore, the introduction of a baseflow component is dominant in introducing a greater element of plug-flow mixing.

Fig. 6.7 compares the experimental exit-age distribution function E(t) curve to the TISM (eqn. 4.9) and ADM (eqn. 4.11) curves obtained using the method of moments for an inlet flow rate of 20l/min and flow splits ranging from 10-40%. The remaining flow rates and all correlation parameters (R^2 and ESS) are presented in appendix E.1.10 and E.1.11 respectively. The correlation parameters show the results for the TISM parameter N=1 and N=3. However, the former is omitted from Fig. 6.7 for clarity and the latter, as it provides a poor fit and greatly effects the graphs scaling. The TISM parameter N=3 correlation parameters also highlight the importance of using more than one correlation parameter to assess the best-fit criteria. The coefficient of correlation (R^2) for a TISM parameter N=3 provides a value suggesting an equally as good-fit as the TISM parameter N=2. However, the ESS is significantly greater and this is also shown by visual inspection. This implies that the experimental and modelled data have a large dependency on each other i.e. high R^2 however, their magnitude at corresponding time intervals differs greatly i.e. high ESS. Subsequently, the highest R^2 value does not necessarily result in the smallest ESS and therefore it is important to assess the goodness of fit using more than one correlation parameter and visually.

The ADM generally provides the best-fit to the overflow component for all inlet flow rates and flow splits and similarly the TISM provides the best-fit for the baseflow component (section 6.2.3). The overflow component (ADM) correlation parameters do not show any significant trend across the range of inlet flow rates or flow splits. However, the baseflow component (TISM) correlation parameters improve as the inlet flow rate increases and this is the expected relationship due to the limitations of both models. The ADM and TISM do not account for short-circuiting within the HDVS and

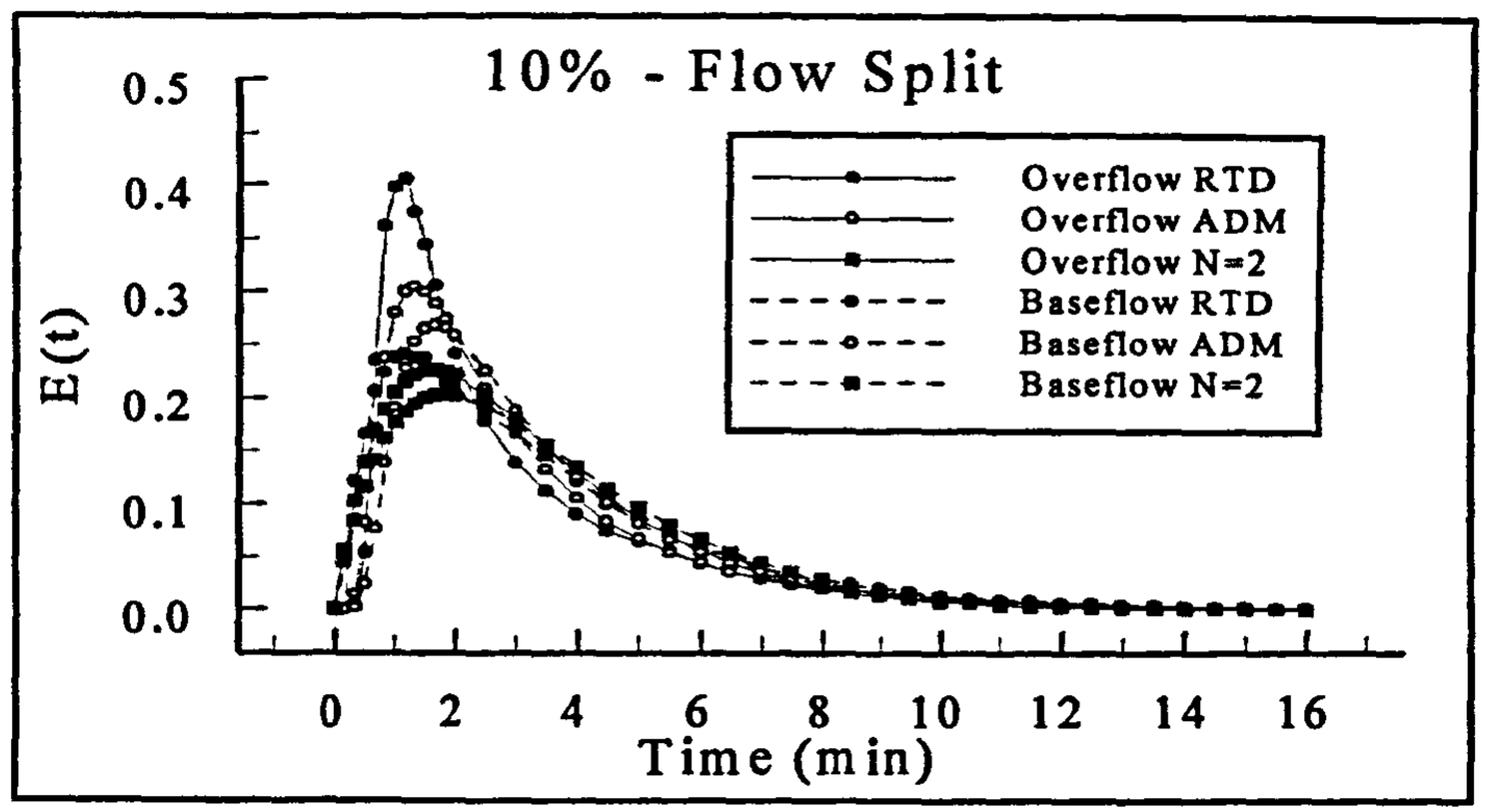

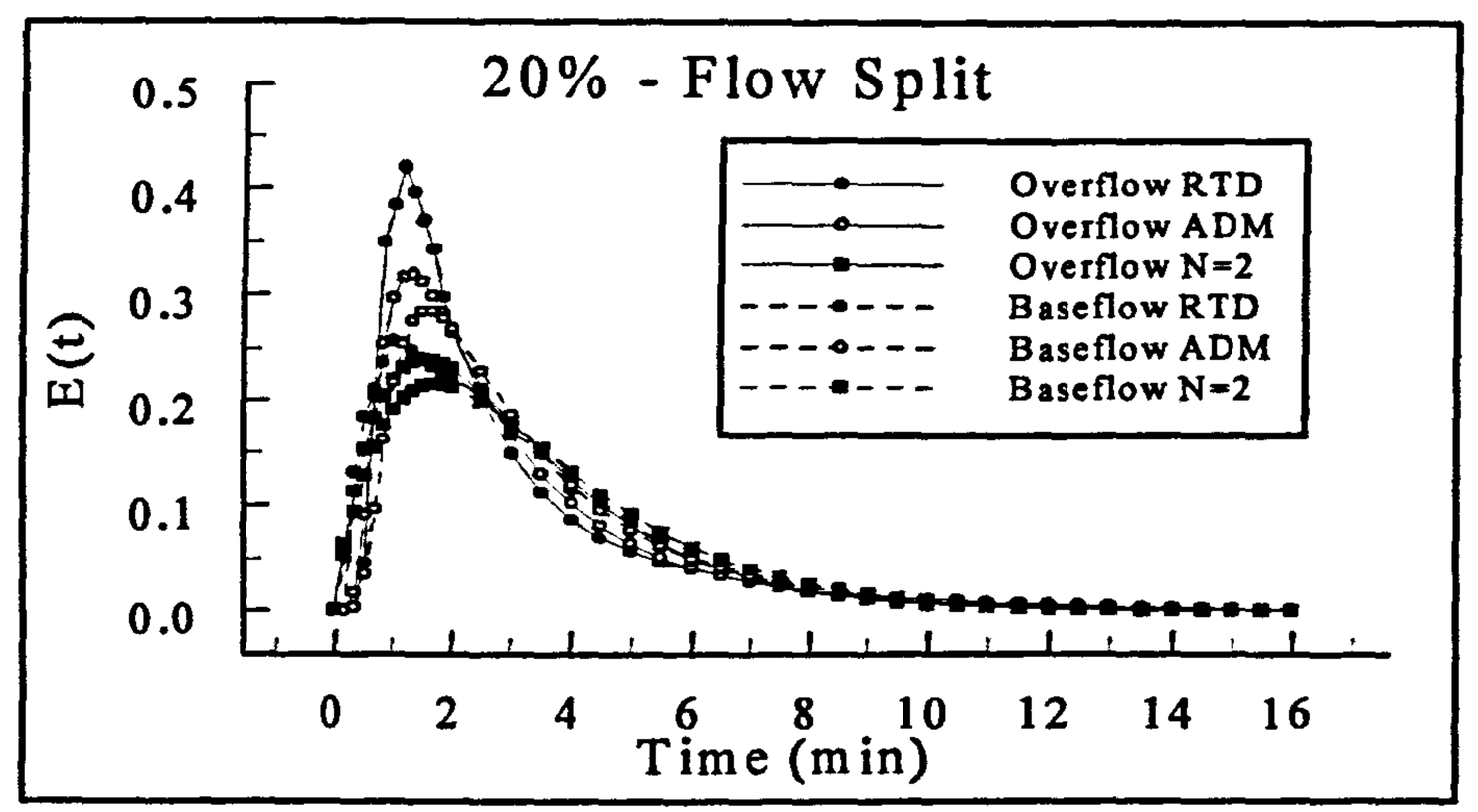

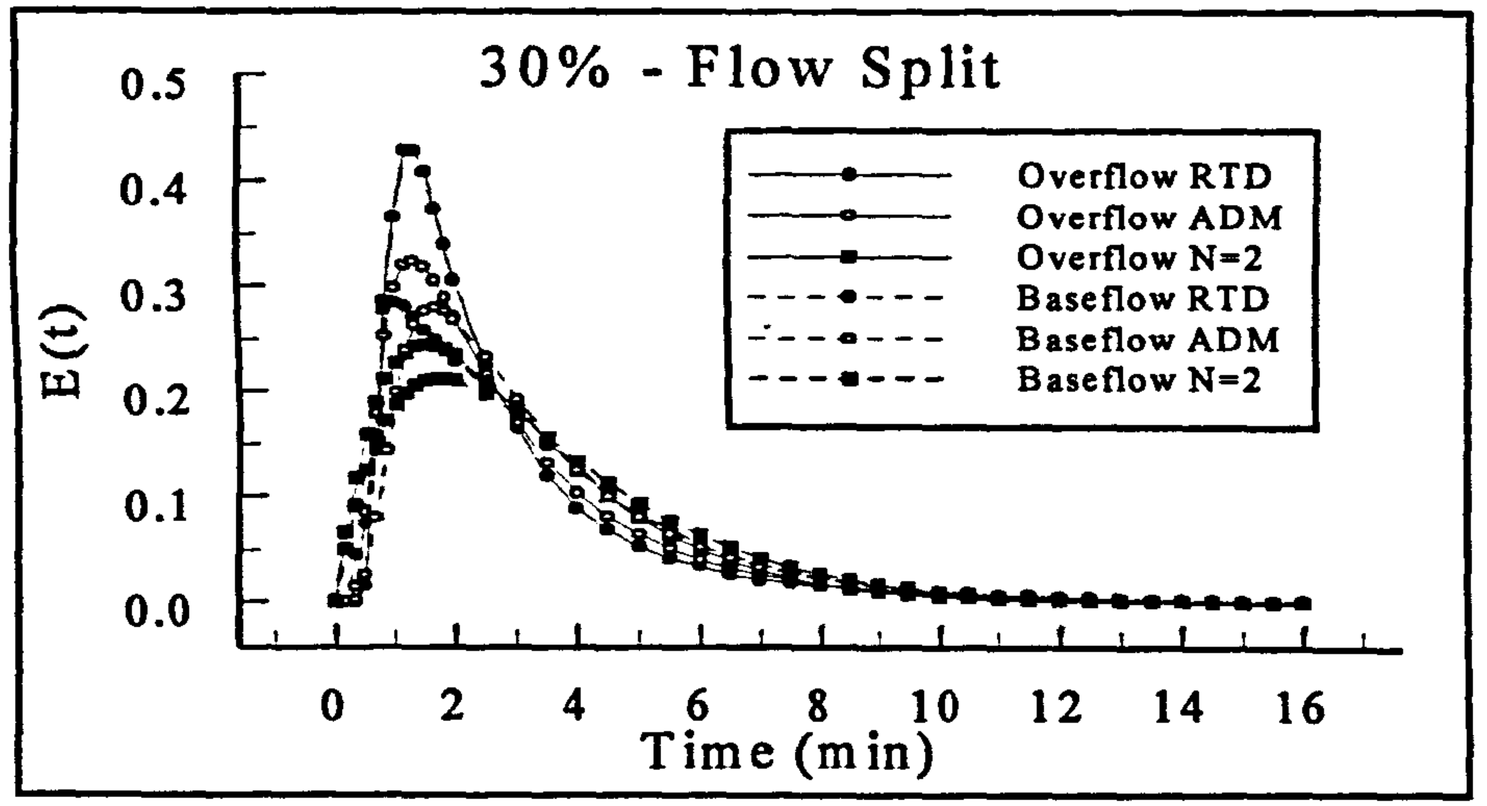

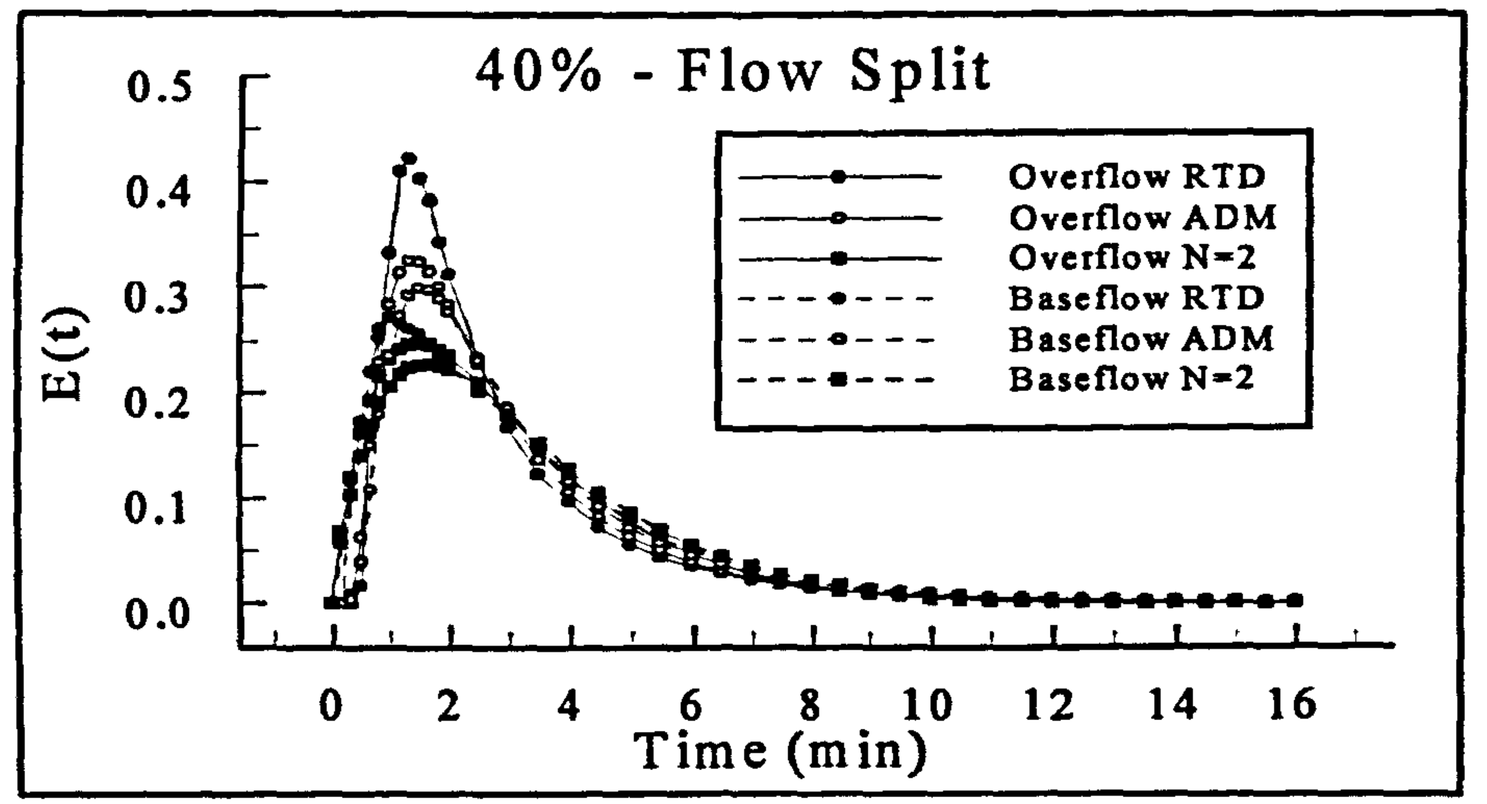

Fig. 6.7 - Model HDVS Baseflow (SP2) - Comparison of E(t), ADM and TISM Curves Calculated using the Method of Moments for an Inlet Flow Rate of 20l/min

therefore, as the baseflow component appears to short-circuit less at high flow rates as discussed above, the TISM correlation parameter and inlet flow rate relationship is anticipated. The relationship between the ADM and TISM correlation parameters and the HDVS's non-ideal flow behaviour is also discussed in chapter 4 (section 4.4.3).

6.2.1.2 Non-Linear Regression Data Analysis

Fig. 6.8 and 6.9 show the RTD normalised curves E(Θ) for an inlet flow rate of 20l/min. The RTD curves were normalised (section 4.3.1) using the experimental mean residence time calculated from the ADM (eqn. 4.11) and TISM (eqn. 4.9) non-linear regression technique (section 4.3.3). The remaining flow rates are shown in appendix E.1.12 and E.1.13. The RTD curves show the same characteristics and therefore, the same conclusions are obtained as for Fig. 6.3 and 6.4 using the method of moments (section 6.2.1.1). The ADM RTD normalised curves E(Θ) (Fig. 6.8) using non-linear regression estimate a significantly higher baseflow mean residence time compared to the theoretical mean residence time (appendix E.1.4). Subsequently, the ADM normalisation procedure results in the overflow and baseflow RTD curve peak height occurring at a similar normalised exit-age distribution E(Θ) value. Hence, the RTD normalisation procedure using the method of moments (Fig. 6.3) and TISM-non-linear regression (Fig. 6.9) only provide similar RTD normalised curves E(Θ) as the theoretical mean residence time RTD normalised curves E(Θ) (Fig. 6.2).

Tables 6.3 and 6.4 show the ADM and TISM parameters calculated using non-linear regression. The experimental mean residence time values calculated using non-linear regression are of a similar order of magnitude as calculated directly from the method of moments (section 6.2.1.1). However, as mentioned above the ADM estimates a larger

mean residence time for the baseflow component compared to the method of moments and TISM using non-linear regression. Appendix E.1.14 shows the experimental mean residence time calculated using the ADM and TISM for all inlet flow rates. The ADM baseflow experimental mean residence time values are all generally greater than the overflow values. This is the opposite trend expected due to the relative flow paths of each flow component and the location of the sampling point (SP2) (Fig. 6.1) (section 6.2.1.1). However, the ADM non-linear regression iteration technique was subject to a constraint on the normalised variance parameter (eqn. 4.11), which is discussed below and therefore, reduces confidence in the estimated ADM mean residence time and parameter (P_e). The average error between the overflow ADM experimental mean residence time values and the theoretical mean residence time is -2% and similarly for the baseflow is +34% (appendix E.1.4). The relationship between this error and the HDVS's non-ideal flow behaviour and the inlet flow rate is discussed in section 6.2.1.1.

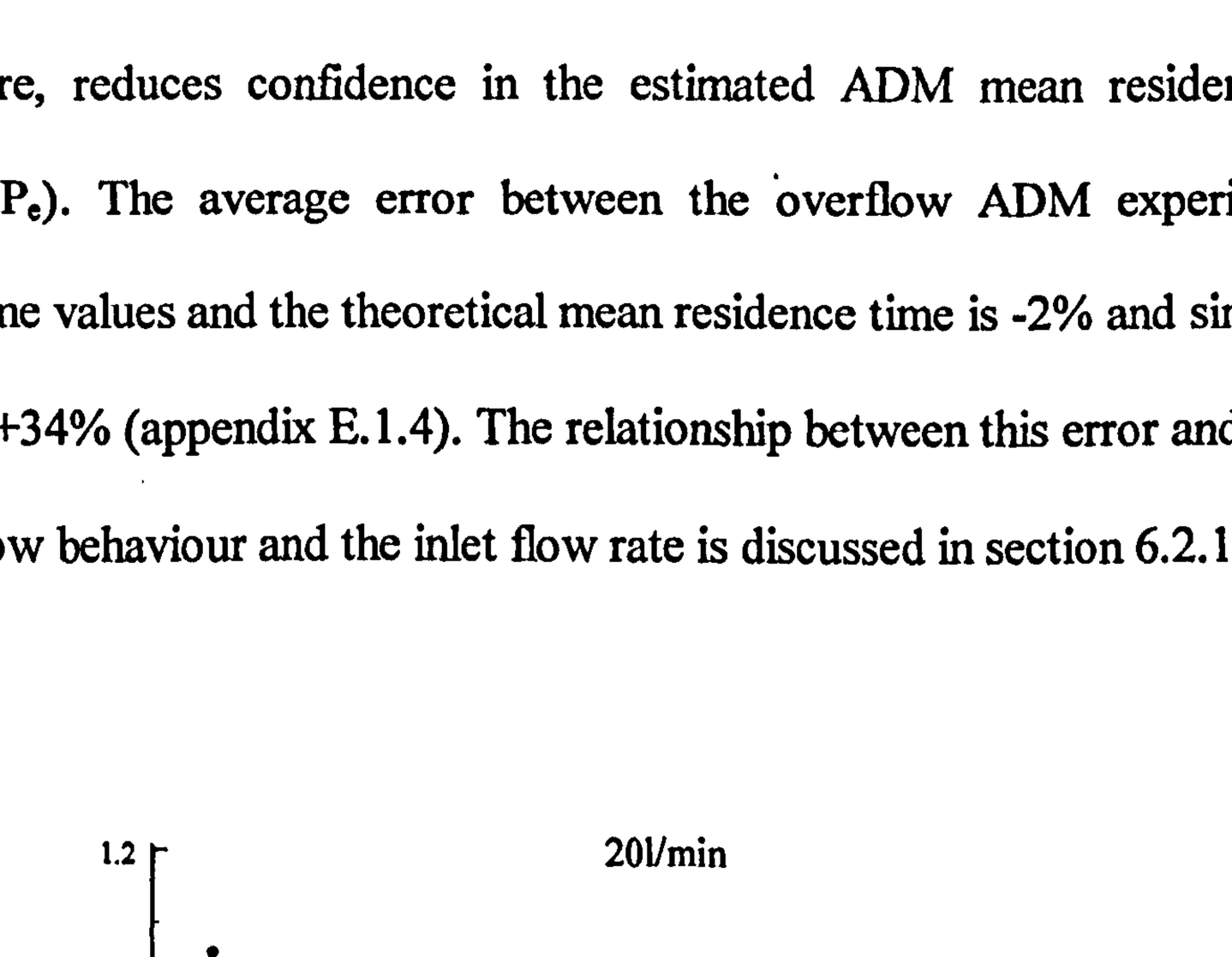

Fig. 6.8 Model HDVS Baseflow (SP2) - Comparison of Normalised Exit-Age Distribution Curves E(Θ) using Non-Linear Regression and the ADM

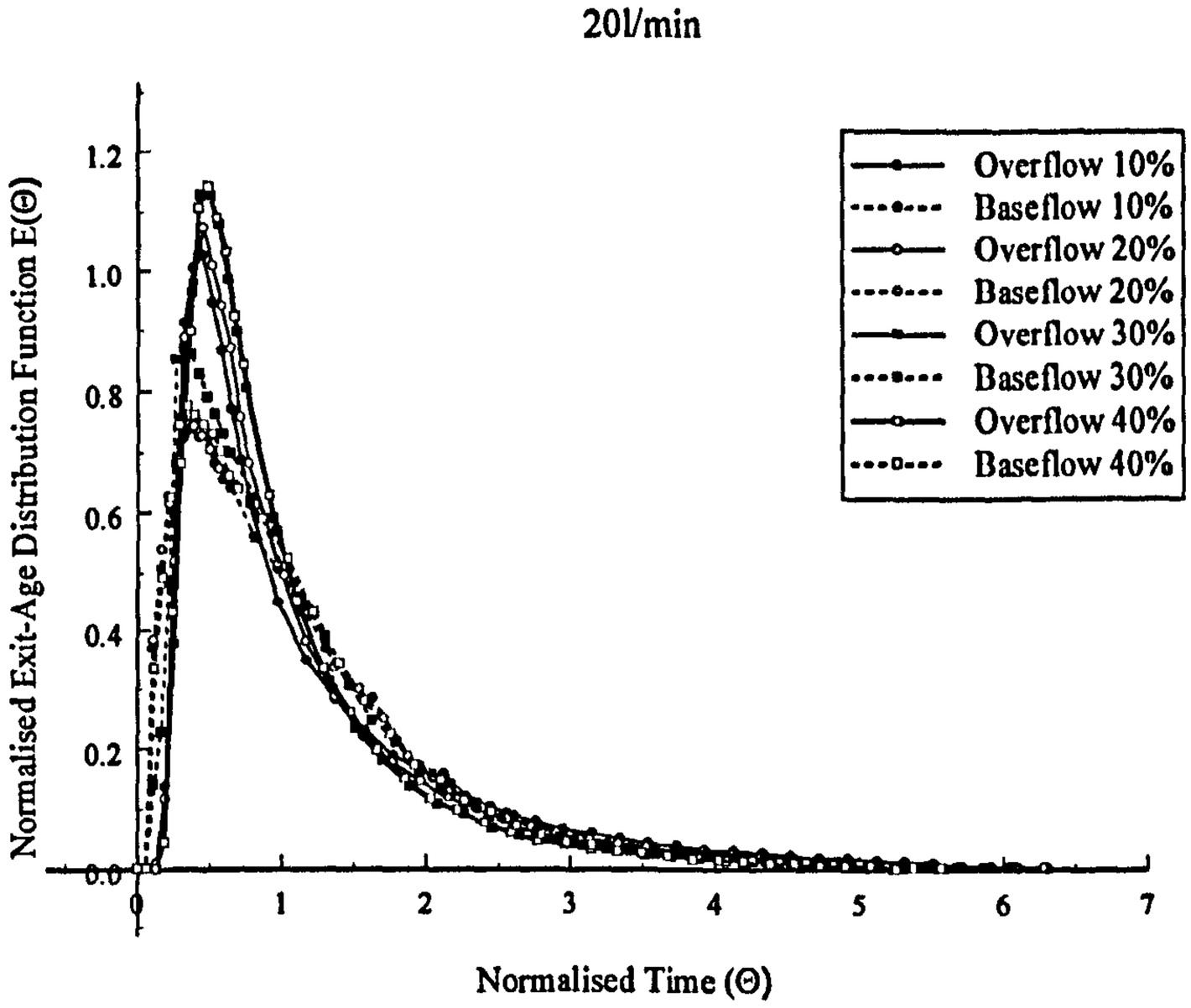

Fig. 6.9 Model HDVS Baseflow (SP2) - Comparison of Normalised Exit-Age Distribution Curves E(Θ) using Non-Linear Regression and the TISM

The overflow and baseflow component TISM mean residence time values follow the same trend as the RTD curves time to peak concentration, as described above for the method of moments (section 6.2.1.1). The average error between the overflow TISM experimental mean residence time values and the theoretical mean residence time is -2% and similarly for the baseflow is +11% (appendix E.1.4). The TISM using non-linear regression provides a more accurate mean residence time estimation compared to the other techniques i.e. method of moments and ADM using non-linear regression (section 4.4.3) and subsequently provides a better model HDVS volume estimation, which is discussed below.

Appendix E.1.15 shows the estimated volume of the model HDVS using the mean residence time calculated from the ADM and TISM. As stated above the model HDVS operating without the sludge hopper has a volume of 55 litres (Fig. 6.1). Both the ADM and TISM using non-linear regression provide a better estimation of the model HDVS

volume compared to the method of moments (section 6.2.1.1). The ADM estimated experimental volumes have an average error of +7% and the TISM has a negligible error. The percentage of the experimental volume associated with the overflow and baseflow components is also presented in appendix E.1.15. These values show that the volume split is approximately proportional to the flow split i.e. a 10% flow split results in 10% of the total HDVS volume being associated with the baseflow and 90% with the overflow component. The theoretical mean residence time (appendix E.1.4) of both the overflow and baseflow components is not necessarily a true representation, as implied by Tyack and Fenner, (1998b) who stated it was "not possible to determine with any meaning". However, RTD tracer studies are a recognised technique to calculate such unknowns and the HDVS volume estimation results, combining the overflow and baseflow components, provide confidence in the presented experimental mean residence time values.

Initial ADM non-linear regression simulations (eqn. 4.11) resulted in the baseflow component normalised variance being greater than 1, particularly at low inlet flow rates, which is not permitted as it is out of the permissible parameter range (section 4.3.1). Therefore, a constraint was applied to the baseflow component ADM normalised variance for it not to be greater than 0.999 in the EXCEL SOLVER toolbar. Subsequently, the following normalised variance values for the baseflow component at low inlet flow rates approximate a value of 1 (Table 6.3) and therefore produce an ADM parameter (P_e) approximately equal to 0, suggesting perfect complete mixing conditions are present (section 4.1).

Table 6.3 Model HDVS Baseflow (SP2) – Comparison of ADM Parameters using Non-Linear Regression

Flow Rate (l/min)	Flow Split (%)	Experimental Mean Residence Time (min)		Normalised Variance (σ_0^2)		Peclet Number (P_e)	
		O	B	O	B	O	B
10	10	7.322	6.809	0.813	0.979	0.655	0.065
	20	5.964	5.322	0.564	0.885	2.025	0.380
	30	5.854	5.644	0.538	0.871	2.230	0.430
	40	5.730	5.341	0.466	0.999	2.885	0.010
15	10	3.927	4.715	0.746	0.999	0.950	0.010
	20	3.875	4.239	0.679	0.999	1.290	0.010
	30	3.531	4.445	0.492	0.999	2.635	0.010
	40	3.650	4.075	0.435	0.999	3.230	0.010
20	10	2.614	3.969	0.593	0.999	1.820	0.010
	20	2.470	3.789	0.499	0.999	2.565	0.010
	30	2.382	3.643	0.395	0.843	3.740	0.535
	40	2.434	3.674	0.394	0.999	3.755	0.010
30	10	1.860	3.014	0.590	0.844	1.840	0.530
	20	1.577	2.801	0.549	0.999	2.140	0.010
	30	1.637	2.652	0.431	0.834	3.275	0.570
	40	1.613	2.539	0.396	0.999	3.725	0.010
45	10	1.193	2.214	0.559	0.817	2.065	0.640
	20	1.153	1.827	0.472	0.599	2.825	1.780
	30	1.092	1.897	0.841	0.661	0.545	1.395
	40	1.140	1.690	0.408	0.648	3.565	1.470
60	10	0.864	1.357	0.486	0.603	2.690	1.755
	20	0.869	1.332	0.492	0.628	2.635	1.590
	30	0.858	1.412	0.478	0.567	2.765	2.005
	40	0.874	1.307	0.499	0.658	2.565	1.410

Fig. 6.10 shows the ADM parameter (P_e) for all inlet flow rates and flow splits investigated. The overflow Peclet number (P_e) increases as the flow split is increased for each individual inlet flow rate. However, the baseflow Peclet number (P_e) remains stable across the range of flow splits. The overflow component Peclet numbers (P_e) generally increase as the inlet flow rate is increased. This is the opposite relationship achieved for the method of moments results (section 6.2.1.1) and the model HDVS operating with no baseflow and without the sludge hopper (section 4.4.5). The baseflow component shows the same trend as the overflow component with higher Peclet numbers (P_e) at high inlet

flow rates. This relationship was also achieved for the method of moments analysis (section 6.2.1.1). At low flow rates the baseflow component Peclet number (P_e) is approximately equal to zero for some flow rates and flow splits. This is due to the constraint applied to the non-linear regression ADM (eqn. 4.11) simulation procedure described above and implies a large degree of mixing is present around the top of the sludge hopper and cone region (Fig. 3.1).

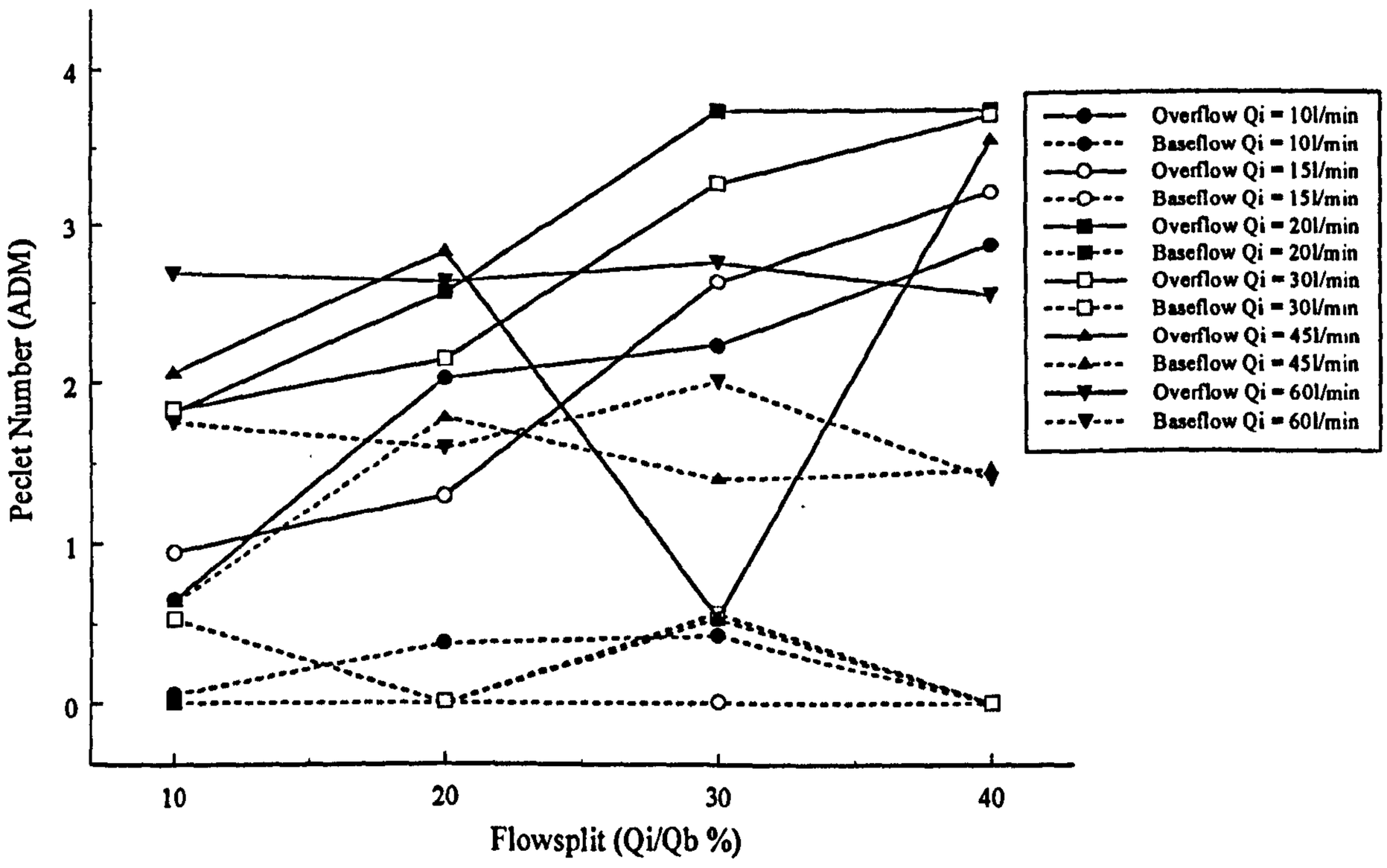

Fig. 6.10 Model HDVS Baseflow (SP2) - Comparison of the ADM Parameters Calculated using Non-Linear Regression

Fig. 6.11 illustrates the TISM parameter (N) for all flow splits and the range of inlet flow rates and unlike the method of moments, has a different independent trend to the ADM parameters. The TISM parameters calculated using non-linear regression are obtained directly from the TISM (eqn. 4.9) and therefore not from intermediate related parameters i.e. the normalised variance, as in the method of moments data analysis technique (section 6.2.1.1).

Table 6.4 Model HDVS Baseflow (SP2) – Comparison of TISM Parameters using Non-Linear Regression

Flow Rate (l/min)	Flow Split (%)	Experimental Mean Residence Time (min)		N-Tanks	
		O	B	O	B
10	10	6.284	5.338	2.159	2.066
	20	5.908	4.364	2.273	2.016
	30	5.867	4.650	2.292	2.045
	40	6.013	4.161	2.341	1.967
15	10	3.440	3.643	2.060	1.918
	20	3.555	3.280	2.109	1.987
	30	3.656	3.483	2.267	1.948
	40	3.998	3.214	2.358	1.915
20	10	2.539	3.065	2.212	1.951
	20	2.549	2.929	2.290	1.980
	30	2.643	3.072	2.386	2.146
	40	2.699	2.856	2.398	2.033
30	10	1.791	2.548	2.136	2.140
	20	1.532	2.094	2.143	1.828
	30	1.749	2.272	2.279	2.138
	40	1.771	2.013	2.309	2.015
45	10	1.138	1.797	2.102	2.031
	20	1.158	1.701	2.173	2.177
	30	0.879	1.625	1.970	2.083
	40	1.191	1.548	2.232	2.182
60	10	0.869	1.248	2.165	2.171
	20	0.870	1.205	2.160	2.157
	30	0.869	1.341	2.169	2.195
	40	0.871	1.163	2.155	2.144

The overflow TISM parameter increases as the flow split increases for the same inlet flow rate. However, the baseflow TISM parameter shows no significant trend as the flow split increases and stays relatively constant across the range of flow splits. The overflow component TISM parameter increases as the inlet flow rate is decreased and the baseflow has the opposite trend. This is the same relationship as achieved for both the overflow and baseflow component TISM parameters calculated using the method of moments (section 6.2.1.1). The overflow TISM parameter values are still in the same order of magnitude as calculated for the model HDVS operating with no baseflow and

without the sludge hopper (section 4.4.5.2).

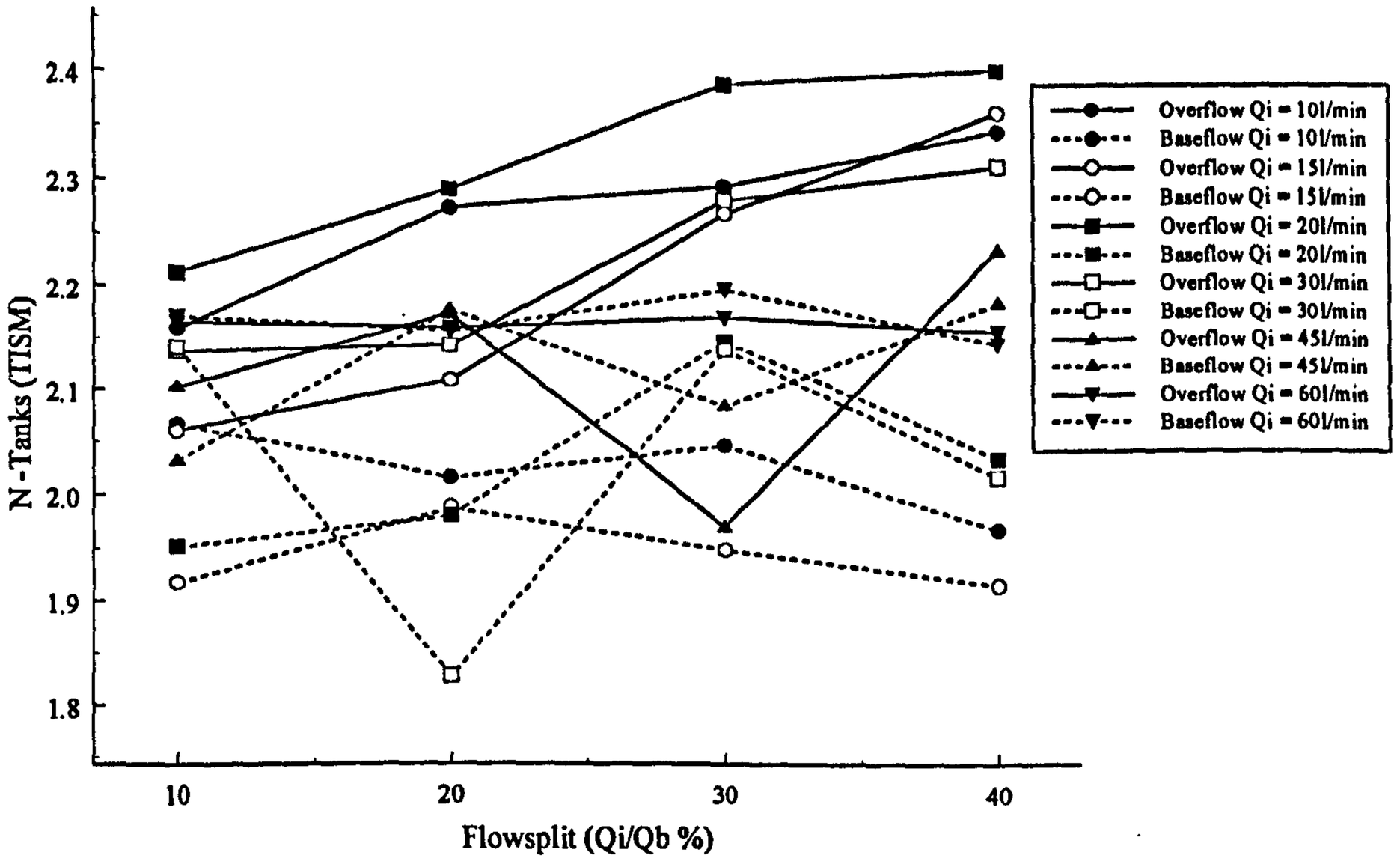

Fig. 6.11 Model HDVS Baseflow (SP2) - Comparison of the TISM Parameters Calculated using Non-Linear Regression

It is difficult to accurately compare the ADM total flow (overflow + baseflow) parameters for the model HDVS operating with a baseflow component to the HDVS operating with no baseflow and without the sludge hopper (section 4.4.5.2). This is due to the constraint applied to the baseflow component normalised variance term (σ_θ^2) in the ADM solution (eqn. 4.11). This resulted in a negligible baseflow ADM parameter (P_e) as discussed above (appendix E.1.9). This constraint was applied to the baseflow component RTD experimental curve mainly at low inlet flow rates and flow splits and therefore, produces a trend suggesting that the total flow plug-flow mixing increases as the inlet flow rate and flow split increases. This may be true and is similar to the total flow method of moments results (appendix E.1.9) and therefore, the same general discussion applies (section 6.2.1.1). However, the data needs to be treated with caution

due to the constraint. The TISM non-linear regression curve fitting technique did not require a constraint and therefore allows direct comparison.

The total flow TISM parameters for all inlet flow rates and flow splits are very stable (appendix E.1.9). The introduction of a baseflow component appears to increase the total flow TISM parameter of the model HDVS operating with a baseflow by a factor of 2 compared to the model HDVS operating with no baseflow and without the sludge hopper (section 4.4.5.2). Hence, as the overflow component TISM parameter values are very similar for both modes of operation, the baseflow component also has a similar TISM parameter.

The TISM parameters estimated using non-linear regression is the superior RTD data analysis technique. This is based on the error between the theoretical and experimental mean residence time and subsequently the model HDVS experimental volume estimations. Additionally, the ADM parameters calculated using non-linear regression are subject to a mathematical constraint and therefore, this reduces confidence in their description of the HDVS's mixing regime. The TISM parameters estimated using non-linear regression were also shown to be superior to other RTD data analysis combinations for the HDVS operating without a baseflow component (section 4.4.3). This was observed, mainly due to the non-linear regression techniques reduced biased estimation of the TISM parameters, compared to other RTD data analysis techniques. Hence, the TISM-non-linear regression combination is less sensitive to the RTD experimental duration and the HDVS's non-ideal flow behaviour relative to the flow rate.

Fig. 6.12 compares the experimental exit-age distribution function E(t) curves to the TISM (eqn. 4.9) and ADM (eqn. 4.11) curves, for an inlet flow rate of 20l/min and all flow splits, using the non-linear regression analysis technique. The remaining flow rates

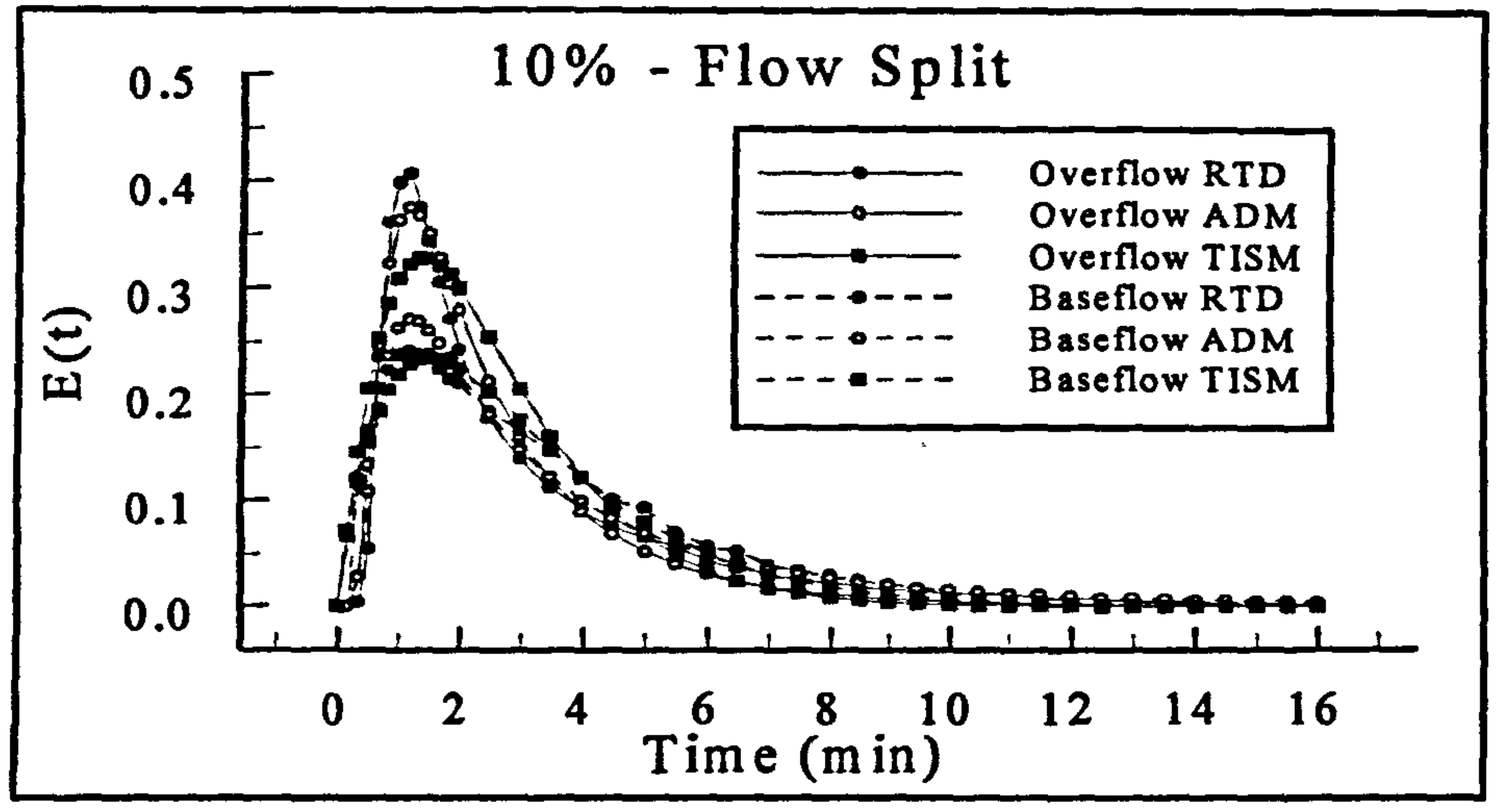

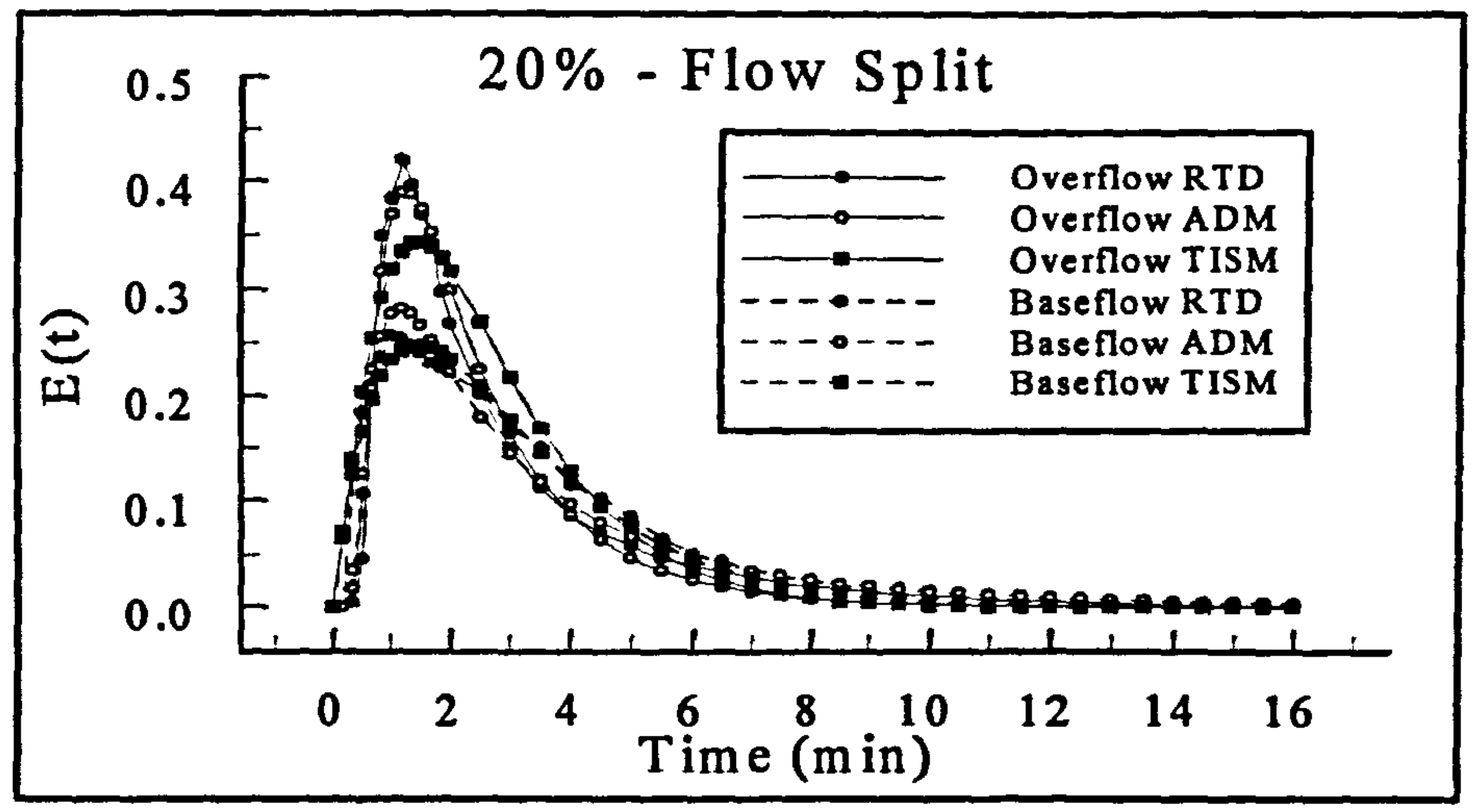

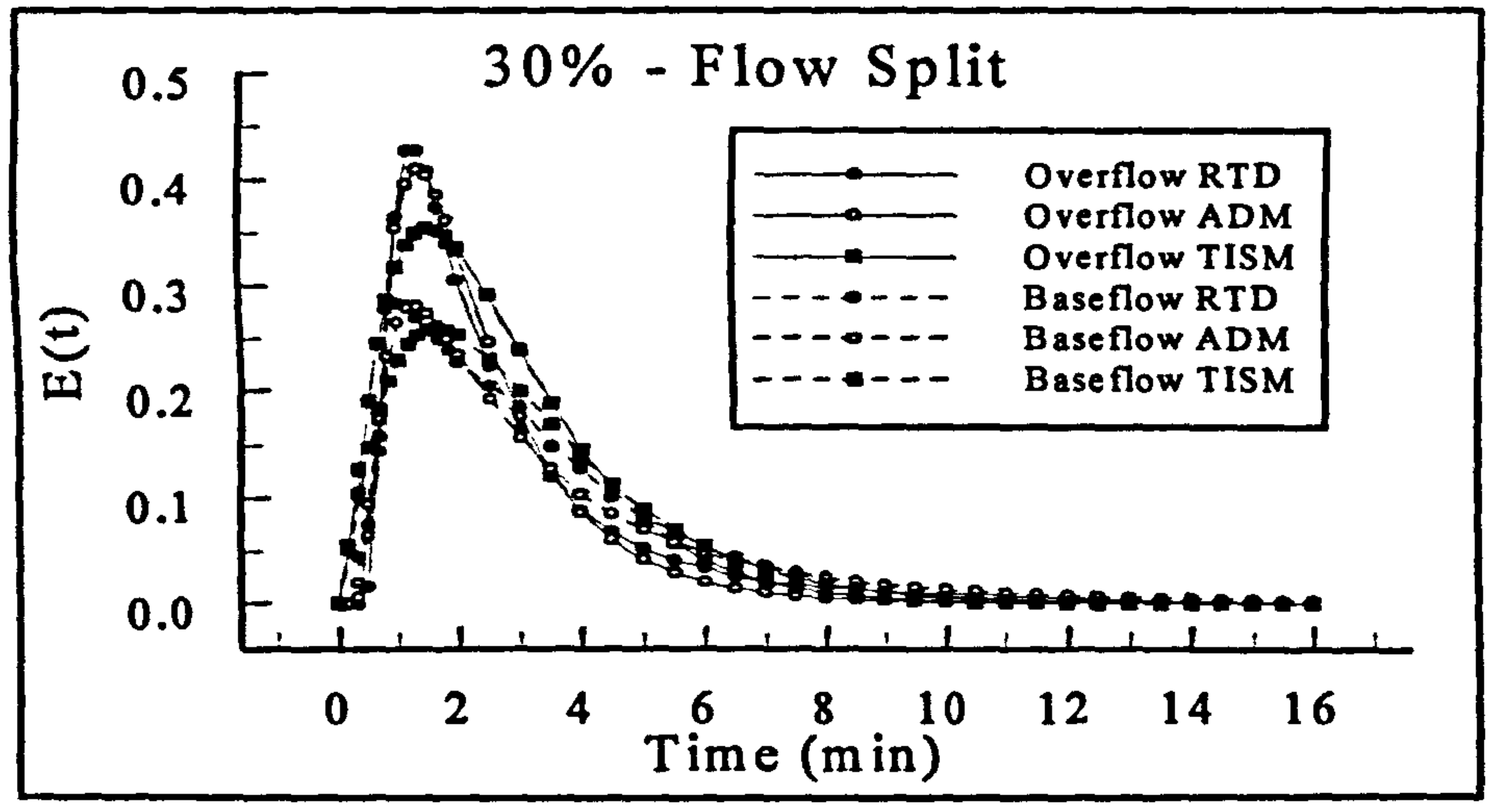

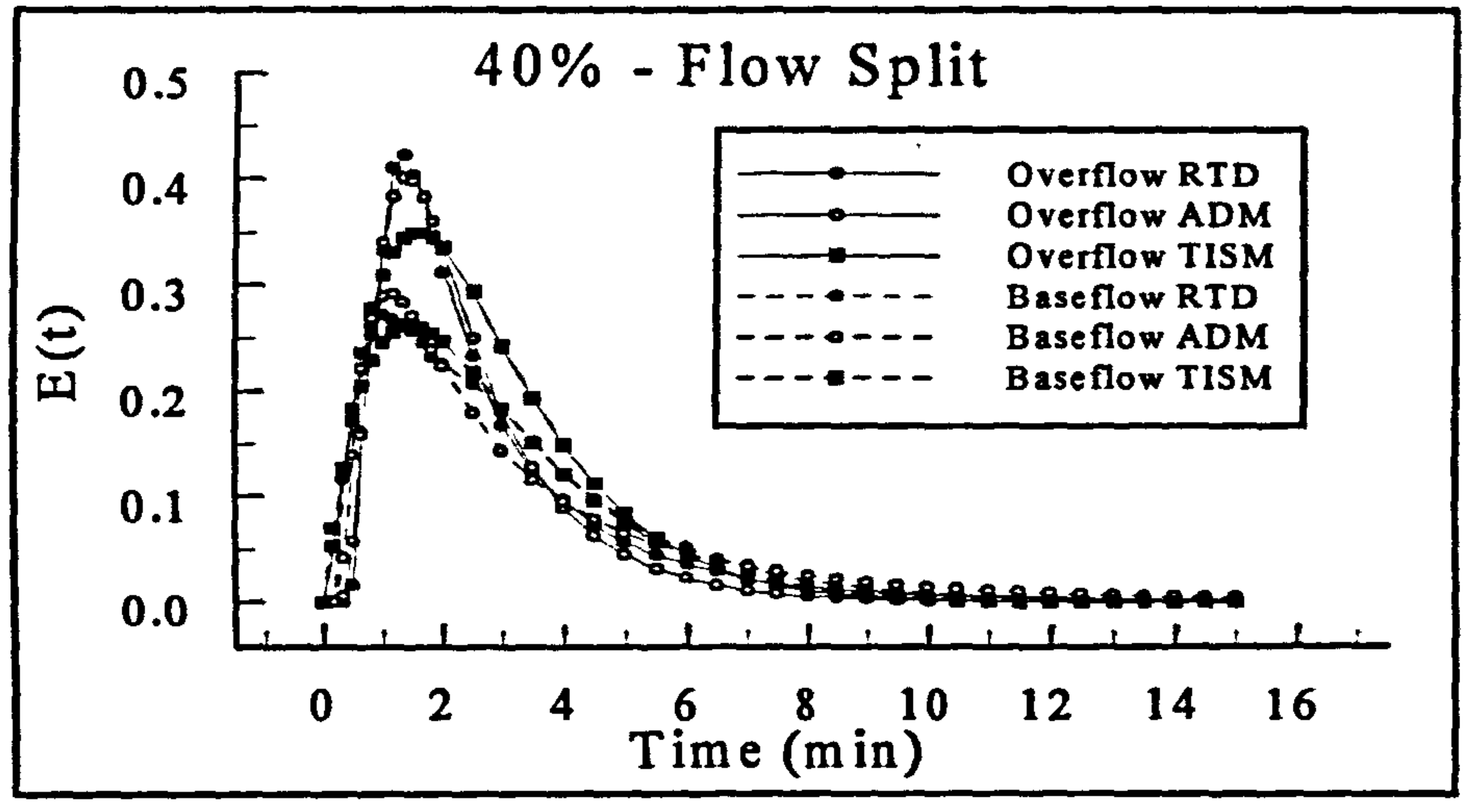

Fig. 6.12 - Model HDVS Baseflow (SP2) - Comparison of E(t), ADM and TISM Curves Calculated using Non-Linear Regression for an Inlet Flow Rate of 20l/min

and all correlation parameters (R^2 and ESS) are presented in appendix E.1.16 and E.1.17 respectively. The ADM provides a better fit to the overflow component for all inlet flow rates and flow splits. However, it is not possible to distinguish any significant difference between the ADM and TISM correlation parameters for the baseflow component and therefore, both provide an equal goodness of fit. The overflow component TISM correlation parameters improve as the flow rate decreases and therefore, only provide the expected relationship due to the HDVS's non-ideal flow behaviour and limitations of the ADM and TISM (section 4.4.3). The non-linear regression correlation parameters are generally better than obtained for the method of moments (section 6.2.1.1). This is due to the flexibility provided by the non-linear regression direct curve fitting procedure (section 4.4.3).

The initial data analysis procedure adopted to calculate the exit-age distribution function E(t) (section 4.3.1) was found to effect the experimental, ADM and TISM correlation results using both the method of moments and non-linear regression techniques. The initial exit-age distribution function E(t) data analysis calculation involved combining the overflow and baseflow RTD curves by using the total tracer recovered (mass balance) from both flow components as the denominator in equation 4.1. The first and second moments (n) were calculated by accounting for the fraction of tracer recovered (mass balance) through the overflow and baseflow component and used as the denominator in equation 4.4 and 4.5 i.e. proportional to the flow split. This resulted in the overflow and baseflow component exit-age distribution function E(t) being underestimated and the ADM and TISM curve fitting procedures providing a very poor correlation with the experimental data. The poor correlation was found to occur due to the denominator in equation 4.1 not approximating a value of 1 for the individual overflow and baseflow components, as a result of previously using the total tracer

recovered (mass balance) i.e. overflow + baseflow. This denominator approximating a value of 1 is a condition applied in the derivation of the ADM and TISM, as the exit-age distribution function E(t) is a normalised parameter i.e. ranging from 0-1 with respect to the initial pulse tracer concentration and therefore, its summation for the experimental duration for both the overflow and baseflow component should equal 1. It was found that the correct approach to calculate the overflow and baseflow component exit-age distribution function E(t) was to investigate the baseflow and overflow RTD as separate curves, with their individual tracer recoveries (mass balance) used as the dominator in equation 4.1. The first and second moments (n) were then calculated by treating the RTD curves independently and as if they were from two separate RTD experiments. Hence, the denominator in equations 4.4 and 4.5 was set to approximately 1 as opposed to proportional to the flow split.

This resulted in the experimental exit-age distribution function E(t) providing a good correlation with the ADM and TISM curves discussed previously. It should be noted that both the above methods used to calculate the RTD curves first and second moments (n) provided similar results. Therefore, the first exit-age distribution function E(t) calculation technique only effected the ADM and TISM, using the method of moments and non-linear regression, experimental curve fitting results.

6.2.2 Model Hydrodynamic Vortex Separator (HDVS) Baseflow - Residence Time Distribution (RTD) Pulse Experiments Sample Point 3 (SP3)

6.2.2.1 Method of Moments Data Analysis

This section describes the RTD analysis undertaken on the model HDVS operating with a baseflow component measured at sample point 3 (SP3), which is located below the sludge hopper (Fig. 6.1).

The RTD normalisation procedure is the same as that used for the model HDVS operating with a baseflow measured at SP2 (section 6.2.1.1). The theoretical mean residence time for both the overflow and baseflow components are presented in appendix E.2.3. Fig. 6.13 and 6.14 show the normalised exit-age distribution function E(Θ) curves calculated using the theoretical mean residence time and experimental mean residence time for the model HDVS operating with an inlet flow rate of 20l/min and the range of flow splits investigated i.e. 10-40%. The remaining flow rates are shown in appendix E.2.4 and E.2.5 respectively.

The overflow and baseflow RTD curves illustrate a plug-flow mixing device with a degree of non-ideal flow behaviour. The RTD normalised curves E(Θ) show similar characteristics as for the baseflow RTD investigated at SP2 (section 6.2.1.1) and the model HDVS operating without a baseflow and with the sludge hopper (section 4.4.1). The overflow RTD normalised curves E(Θ) show a very similar distribution for both the theoretical and experimental mean residence time curves (section 6.2.1.1). However, the baseflow RTD curves show a significant difference depending on which mean residence time values are used for the normalisation procedure (section 4.3.1). The baseflow RTD curves using the theoretical mean residence time peak closer to a normalised time (Θ)

value of 1 as the flow split is decreased. Hence, for a small baseflow component flow rate and the same inlet flow rate the baseflow RTD curve has improved plug-flow mixing characteristics and less short-circuiting. Additionally, the baseflow component RTD curve has the same mixing characteristics as the inlet flow rate is increased. This is in agreement with the previous observations regarding the strength of the vortex generated within the HDVS and its effect on the flow path and subsequently short-circuiting (section 6.2.1.1). As the flow split increases the baseflow is less likely to be forced around the perimeter of the HDVS prior to leaving the baseflow outlet and hence, will take a shorter flow path and therefore short-circuit. The difference between the baseflow RTD normalised curves E(Θ) using the theoretical and experimental mean residence time is due to the former remaining constant and the latter decreasing for all flow splits at the same inlet flow rate (Table 6.5). This effects the normalised time (Θ) axis (section 4.3.1) and subsequently the shape of the baseflow RTD normalised curves E(Θ).

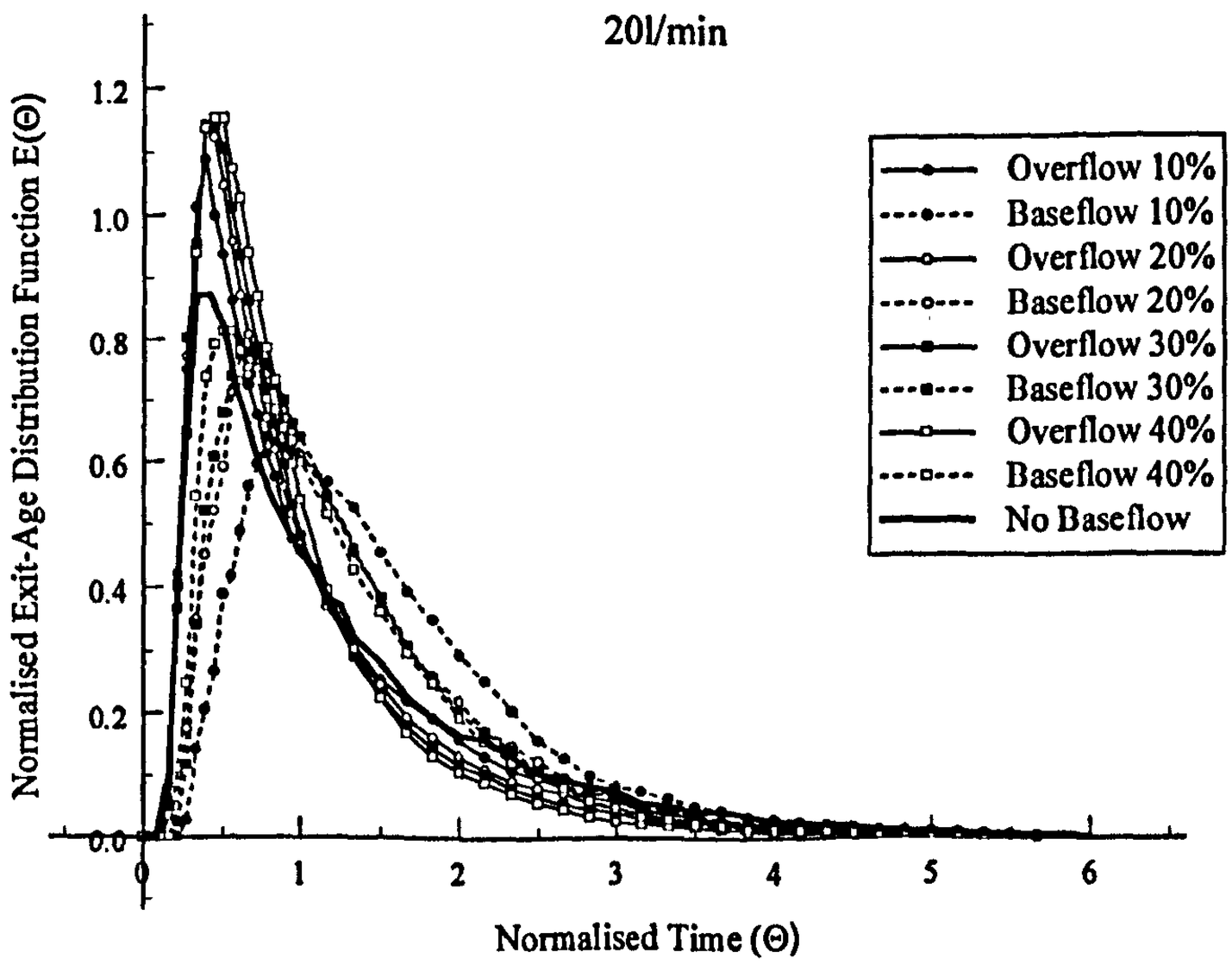

Fig. 6.13 Model HDVS Baseflow (SP3) - Comparison of Normalised Exit-Age Distribution Curves E(Θ) using the Theoretical Mean Residence Time

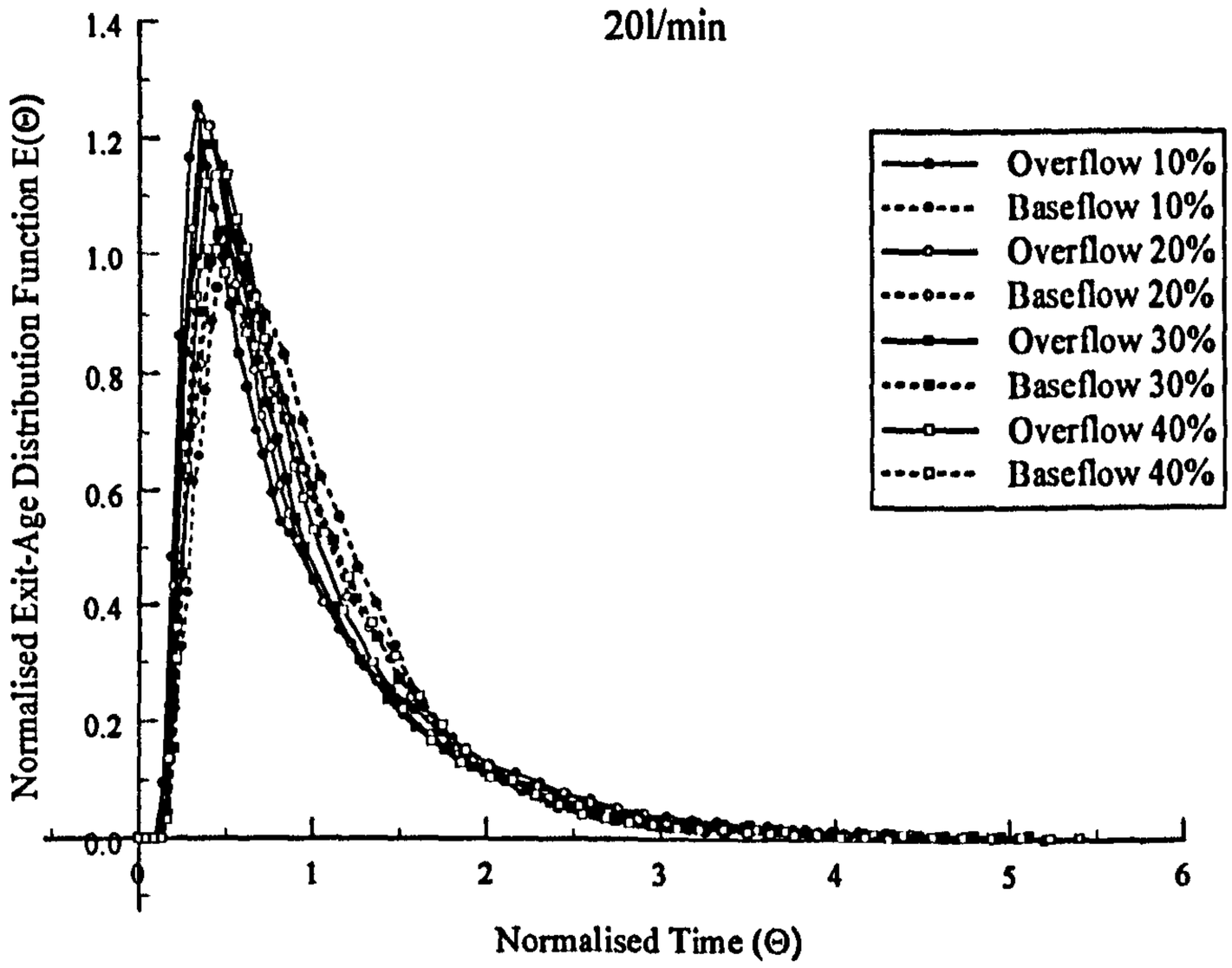

Fig. 6.14 Model HDVS Baseflow (SP3) - Comparison of Normalised Exit-Age Distribution Curves E(Θ) using the Method of Moments

Appendix E.2.6 shows the time taken for the peak tracer (LiCl) concentration to occur for the overflow and baseflow RTD curves. The RTD curve time to peak concentration for the model HDVS operating with a baseflow component measured at SP2 and SP3 (Fig. 6.1) are compared and also presented in section 6.2.3 (Table 6.9). These values show that for all inlet flow rates the baseflow RTD curve peaks after the overflow component. Therefore, the sludge hopper appears to have slower internal velocities relative to the main volume of the HDVS and acts as a quiescent zone based on the relative flow paths of each flow component (section 6.2.1.1). However, short-circuiting of the overflow component at high inlet flow rates will still occur as discussed in section 6.2.1.1. The time to peak concentration is also illustrated by the exit-age distribution function E(t) curves (Fig. 6.18).

The experimental tracer recovery (mass balance) is shown in appendix E.2.7 and discussed in detail in section 6.2.1.1 with respect to the RTD experimental duration and

previous RTD investigation tracer recovery observations. These values show that near 100% tracer recovery (mass balance) is obtained for all inlet flow rates and flow splits. The overflow values decrease and the baseflow increase as the flow split increases and are generally proportional to the flow split. The average error is +/- 5%.

Fig. 6.15 shows the experimental mean residence time plotted against the flow split for all inlet flow rates. The overflow and baseflow component values are relatively constant across the range of flow splits for the same inlet flow rate. The relative magnitude of the overflow and baseflow mean residence time follows a similar trend as the time to peak concentration i.e. baseflow > overflow, as discussed in section 6.2.1.1.

Table 6.5 Model HDVS Baseflow (SP3) – Comparison of First and Second Moments Calculated from RTD Experimental Data

Flow Rate (l/min)	Flow Split (%)	Experimental Mean Residence Time (min)		Variance (min^2)		Normalised Variance (σ_θ^2)	
		O	B	O	B	O	B
10	10	7.471	7.589	27.864	22.119	0.499	0.384
	20	6.983	7.155	28.090	23.500	0.576	0.459
	30	6.489	6.605	25.445	21.690	0.604	0.497
	40	6.032	6.075	18.818	18.746	0.517	0.508
15	10	4.587	5.979	13.187	12.172	0.627	0.341
	20	4.319	5.652	12.960	12.552	0.695	0.393
	30	3.944	5.339	8.6960	10.561	0.559	0.370
	40	4.005	5.005	8.1570	10.996	0.509	0.439
20	10	3.455	4.755	7.140	7.171	0.598	0.317
	20	3.268	4.146	6.574	6.972	0.615	0.406
	30	3.131	4.004	6.004	6.260	0.612	0.391
	40	2.961	3.719	4.667	5.681	0.532	0.411
30	10	2.315	3.536	3.760	4.115	0.701	0.329
	20	2.121	2.954	3.088	3.274	0.686	0.375
	30	2.146	2.789	2.372	3.321	0.515	0.427
	40	2.498	3.233	3.442	3.968	0.551	0.380
45	10	1.470	2.553	1.591	1.832	0.736	0.281
	20	1.396	2.263	1.416	1.756	0.727	0.343
	30	1.336	2.277	1.007	1.359	0.564	0.262
	40	1.388	2.014	1.228	1.397	0.637	0.345
60	10	1.054	2.147	0.870	1.053	0.783	0.229
	20	1.025	1.785	0.719	0.901	0.685	0.283
	30	1.023	1.720	0.711	0.812	0.680	0.275
	40	0.971	1.490	0.463	0.557	0.492	0.251

Appendix E.2.3 shows the errors between the theoretical and experimental mean residence time calculated using the method of moments (Table 6.5). The experimental values are all greater than the theoretical values and therefore have positive errors. This trend was also observed for the RTD investigations undertaken on the model HDVS operating with no baseflow and with the sludge hopper and is discussed in section 4.4.1. The average error for the overflow experimental mean residence time values compared with the theoretical is +7% and similarly for the baseflow is +50%. The relative trend in the baseflow and overflow component theoretical and mean residence time errors as the flow rate increases and the associated HDVS mixing regime characteristics are discussed in section 6.2.1.1. The overflow component errors are significantly less than the errors obtained for the model HDVS operating with no baseflow and with the sludge hopper (section 4.4.1.1).

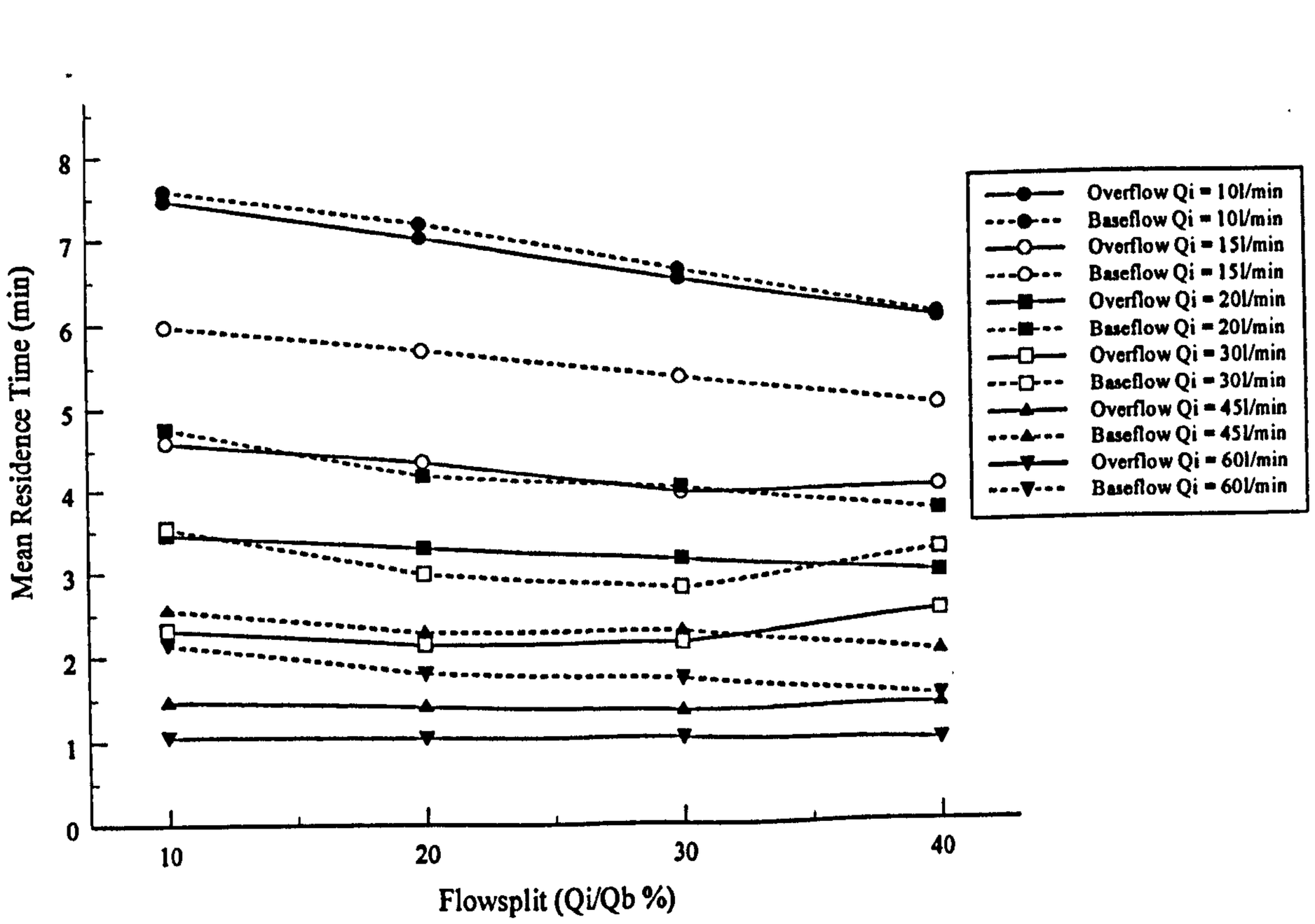

Fig. 6.15 Model HDVS Baseflow (SP3) - Experimental Mean Residence Time using the Method of Moments

SP3 is located such that the sample is effectively being withdrawn from outside the main volume of the HDVS (Fig. 6.1). Therefore, as the overflow and baseflow experimental mean residence time values are very similar for a given inlet flow rate this suggests that the sludge hopper is increasing the baseflow transit time and introduces an element of plug-flow mixing. This contrasts with the completely mixed characteristics observed for the baseflow component measured at SP2 (section 6.2.1.1) and is shown by the ADM and TISM parameters discussed below.

Table 6.6 shows the estimated model HDVS volume calculated using the method of moments experimental mean residence time. The model HDVS operating with the sludge hopper (Fig. 6.1) has a volume of approximately 60 litres and the estimated experimental volumes have an average error of +15% (section 6.2.1.1). The percentage of the experimental volume associated with the overflow and baseflow components is also presented in Table 6.6. These values show that the volume split is approximately proportional to the flow split i.e. a 10% flow split results in 10% of the total HDVS volume being associated with the baseflow and 90% with the overflow component.

Fig. 6.16 and 6.17 illustrate the ADM (P_e) and TISM (N) parameters for all flow splits and inlet flow rates respectively. The numerical values are provided in appendix E.2.8. The overflow Peclet numbers (P_e) gradually increase as the flow split increases for the same inlet flow rate. The baseflow Peclet number (P_e) significantly decreases as the flow split increases and is supported by the RTD normalised curves $E(\Theta)$, which peak closer to the origin as the flow split is increased (appendix E.2.4). Therefore, using the method of moments, improved plug-flow mixing characteristics are achieved at the lowest individual flow rates for the overflow and baseflow components. The overflow Peclet number (P_e) marginally increases as the inlet flow rate is decreased and the baseflow shows the opposite trend with higher Peclet numbers (P_e) at high inlet flow

rates. The ADM and TISM parameters show the same trend, as they are both determined directly from the normalised variance (eqn. 4.6) (section 6.2.1.1).

Table 6.6 Model HDVS Baseflow (SP3) – Estimated Model HDVS Volume using the Experimental Mean Residence Time Calculated from the Method of Moments

Flow Rate (l/min)	Flow Split (%)	Volume (l)		Percentage of Experimental Volume (%)		Total Volume (l)
		O	B	O	B	
10	10	67.239	7.5890	89.858	10.142	74.828
	20	55.864	14.310	79.608	20.392	70.174
	30	45.423	19.815	69.627	30.373	65.238
	40	36.192	24.300	59.829	40.171	60.492
15	10	61.925	8.9690	87.349	12.651	70.893
	20	51.828	16.956	75.349	24.651	68.784
	30	41.412	24.026	63.285	36.715	65.438
	40	36.045	30.030	54.552	45.448	66.075
20	10	62.190	9.5100	86.736	13.264	71.700
	20	52.288	16.584	75.921	24.079	68.872
	30	43.834	24.024	64.597	35.403	67.858
	40	35.532	29.752	54.427	45.573	65.284
30	10	62.505	10.608	85.491	14.509	73.113
	20	50.904	17.724	74.174	25.826	68.628
	30	45.066	25.101	64.227	35.773	70.167
	40	44.964	38.796	53.682	46.318	83.760
45	10	59.535	11.489	83.824	16.176	71.024
	20	50.256	20.367	71.161	28.839	70.623
	30	42.084	30.740	57.789	42.211	72.824
	40	37.476	36.252	50.830	49.170	73.728
60	10	56.916	12.882	81.544	18.456	69.798
	20	49.200	21.420	69.669	30.331	70.620
	30	42.966	30.960	58.120	41.880	73.926
	40	34.956	35.760	49.432	50.568	70.716

Appendix E.2.8 also details the summation of the individual overflow and baseflow component ADM and TISM parameters at each flow split for all inlet flow rates. The total flow ADM and TISM parameters for the model HDVS operating with a baseflow component measured at SP2 and SP3 are compared and also presented in section 6.2.3 (Table 6.10). All observations and conclusions identified for the model HDVS operating with a baseflow measured at SP2 (section 6.2.1.1) apply to the results for the baseflow

component measured at SP3. However, the baseflow measured at SP3 total flow ADM and TISM parameters also show an increase in the total flow plug-flow mixing element at low flow rates compared to the model HDVS operating with no baseflow (section 4.4.1.1) and it gradually increases as the inlet flow rate increases. This is due to the weighting created by the baseflow component ADM and TISM parameters measured at SP3, which significantly increase as the inlet flow rate increases, whereas the overflow component remains relatively stable. Hence, the introduction of a baseflow component, including the sludge hopper, significantly increases the degree of plug-flow mixing within the total flow from the HDVS.

Fig. 6.18 compares the experimental exit-age distribution function E(t) curves to the TISM (eqn. 4.9) and ADM (eqn. 4.11) curves obtained using the method of moments for an inlet flow rate of 20l/min and flow splits ranging from 10-40%. The remaining flow rates and all correlation parameters (R^2 and ESS) are presented in appendix E.2.9 and E.2.10 respectively. The ADM provides the best-fit to the overflow and baseflow component RTD curves for all inlet flow rates and flow splits. The ADM correlation parameters show no significant trend across the range of inlet flow rates or flow splits and therefore, provides a similar goodness of fit independent of the HDVS operating conditions.

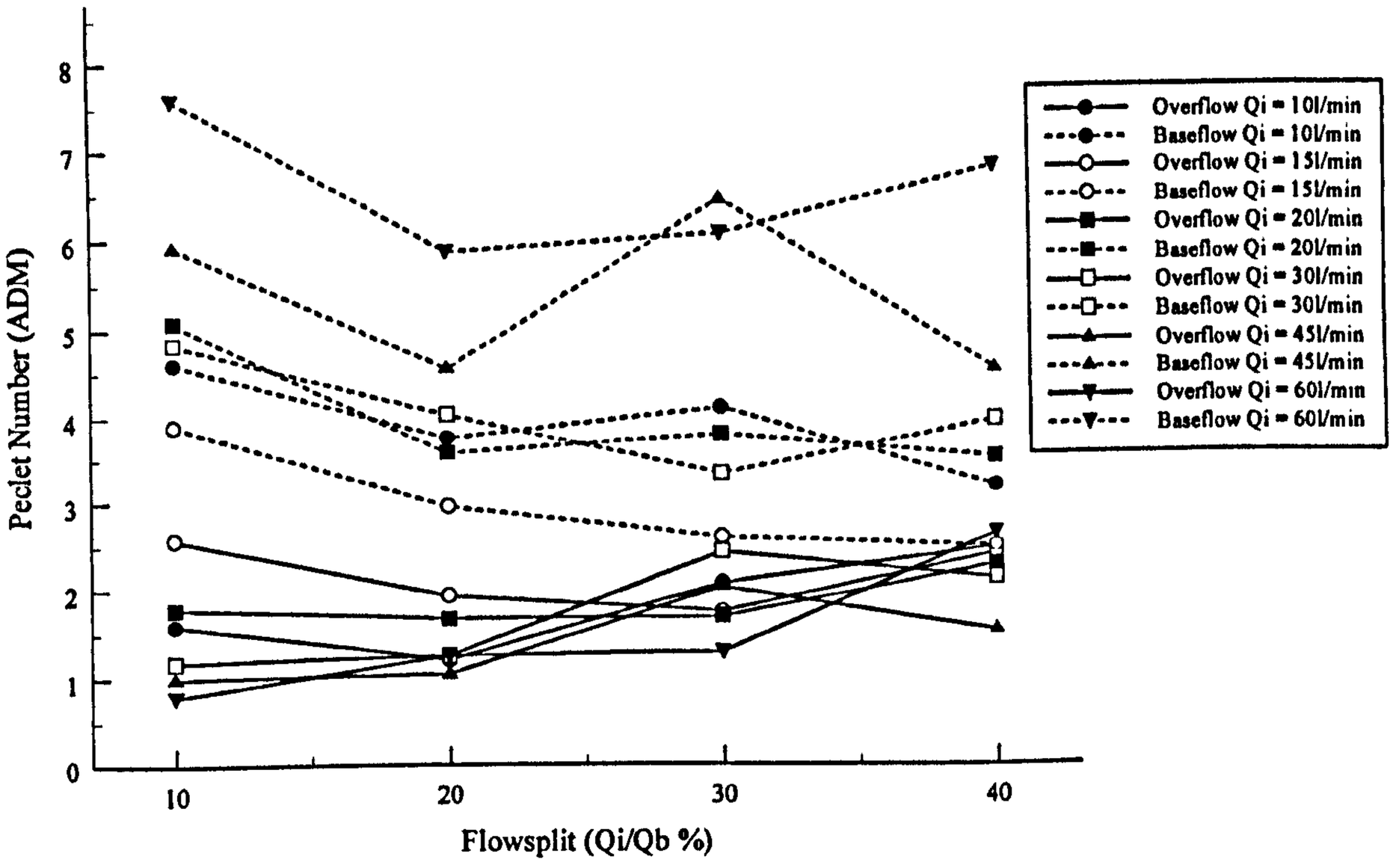

Fig. 6.16 Model HDVS Baseflow (SP3) - Comparison of the ADM Parameters Calculated using the Method of Moments

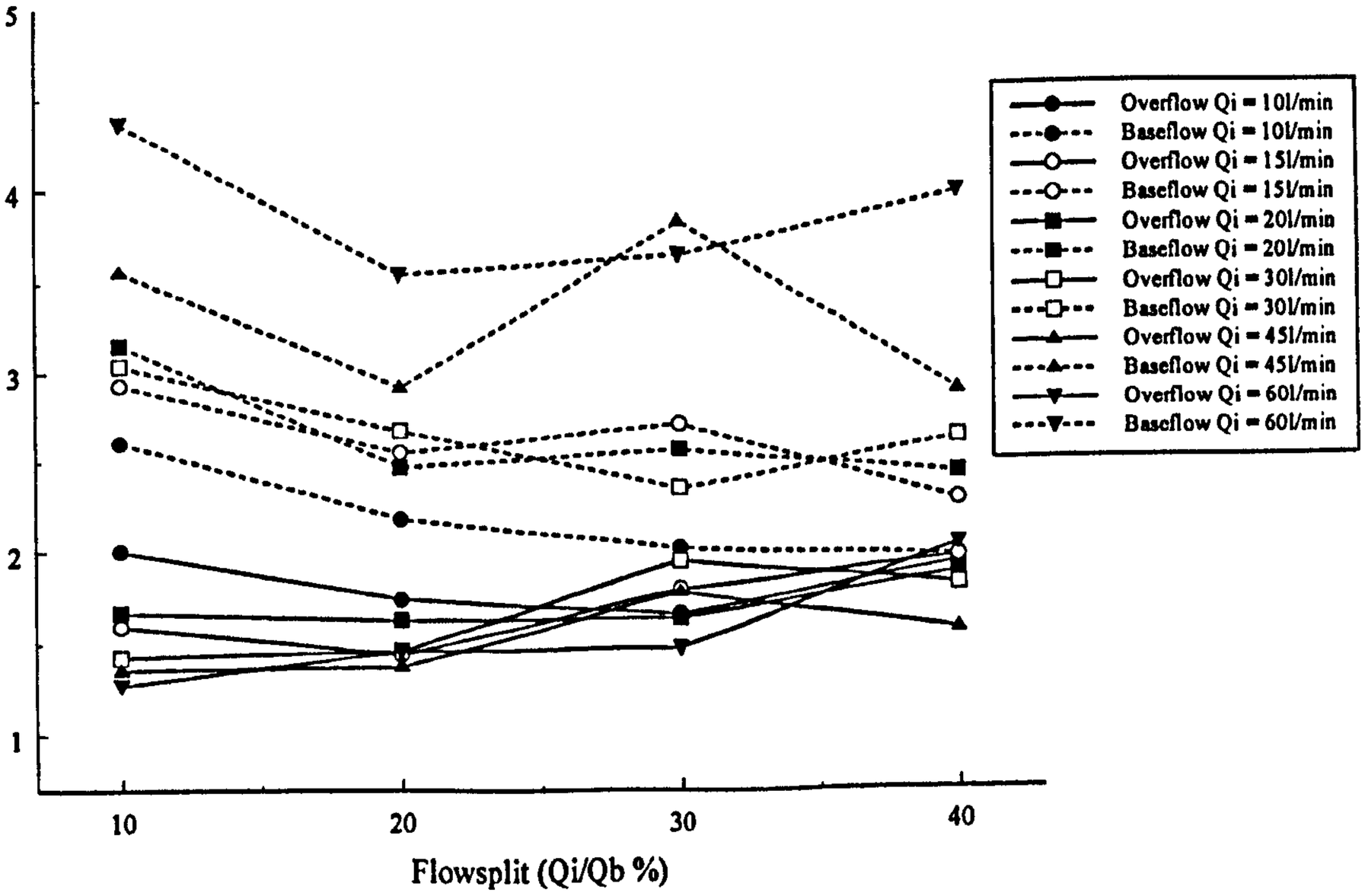

Fig. 6.17 Model HDVS Baseflow (SP3) - Comparison of the TISM Parameters Calculated using the Method of Moments

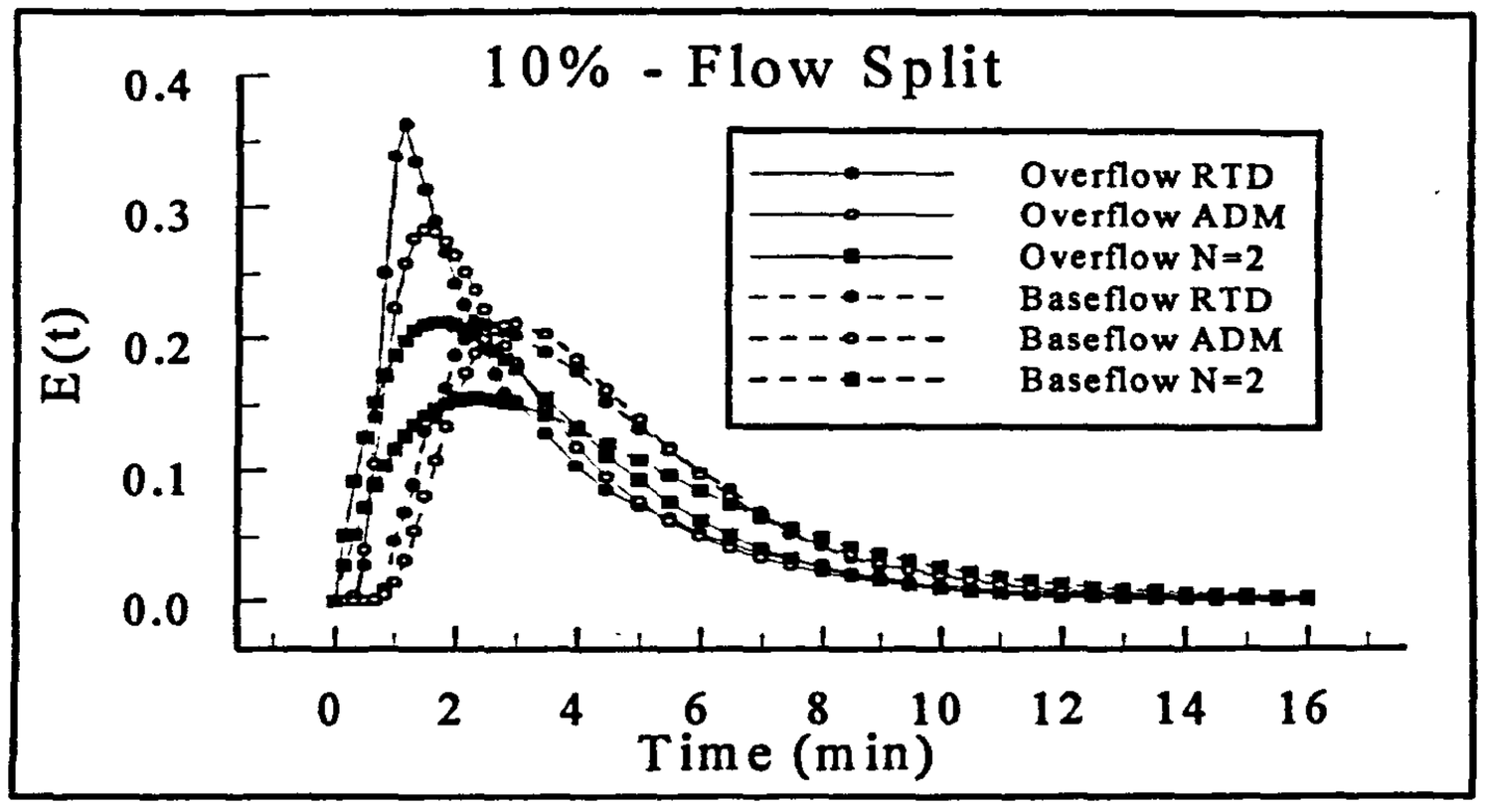

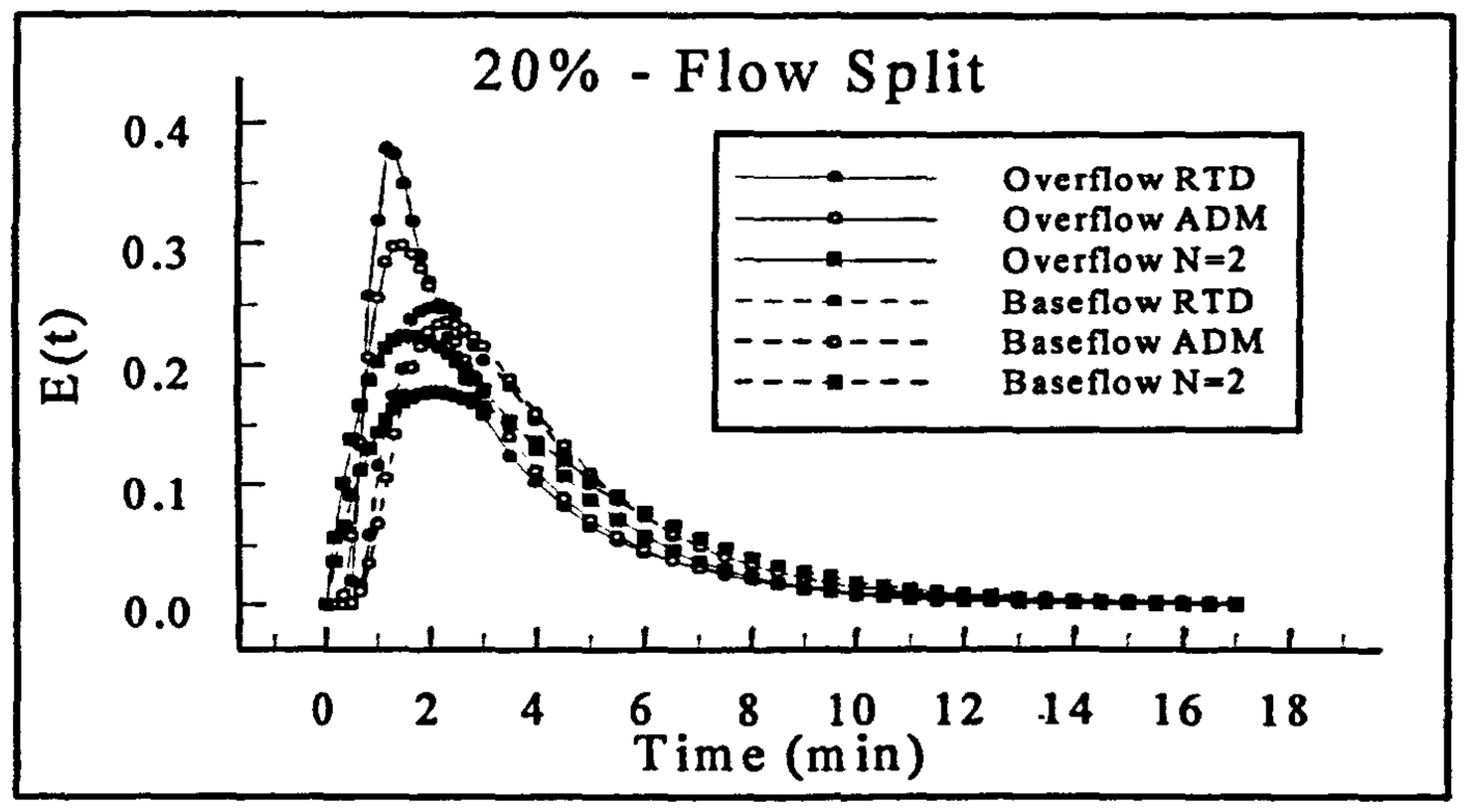

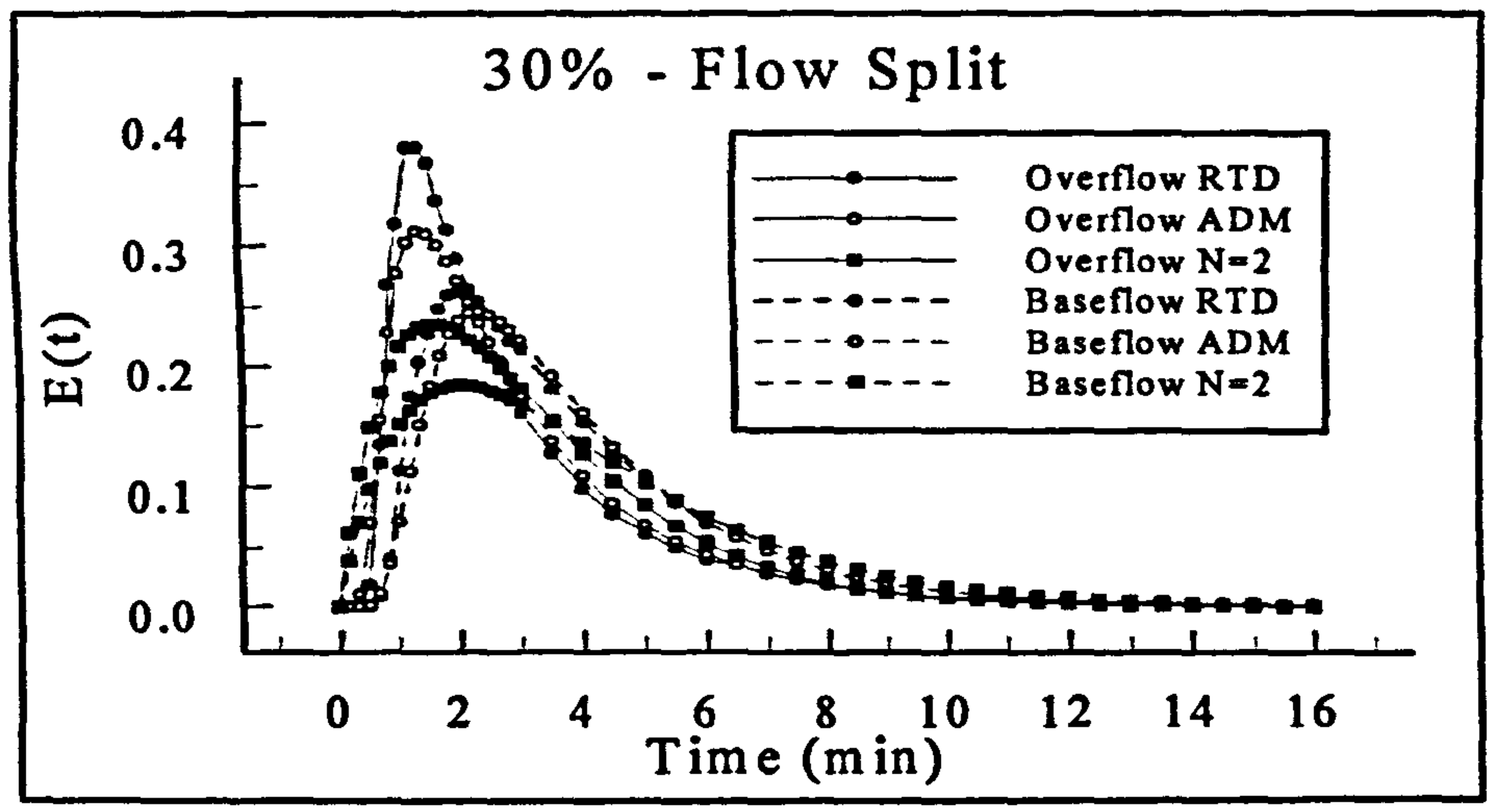

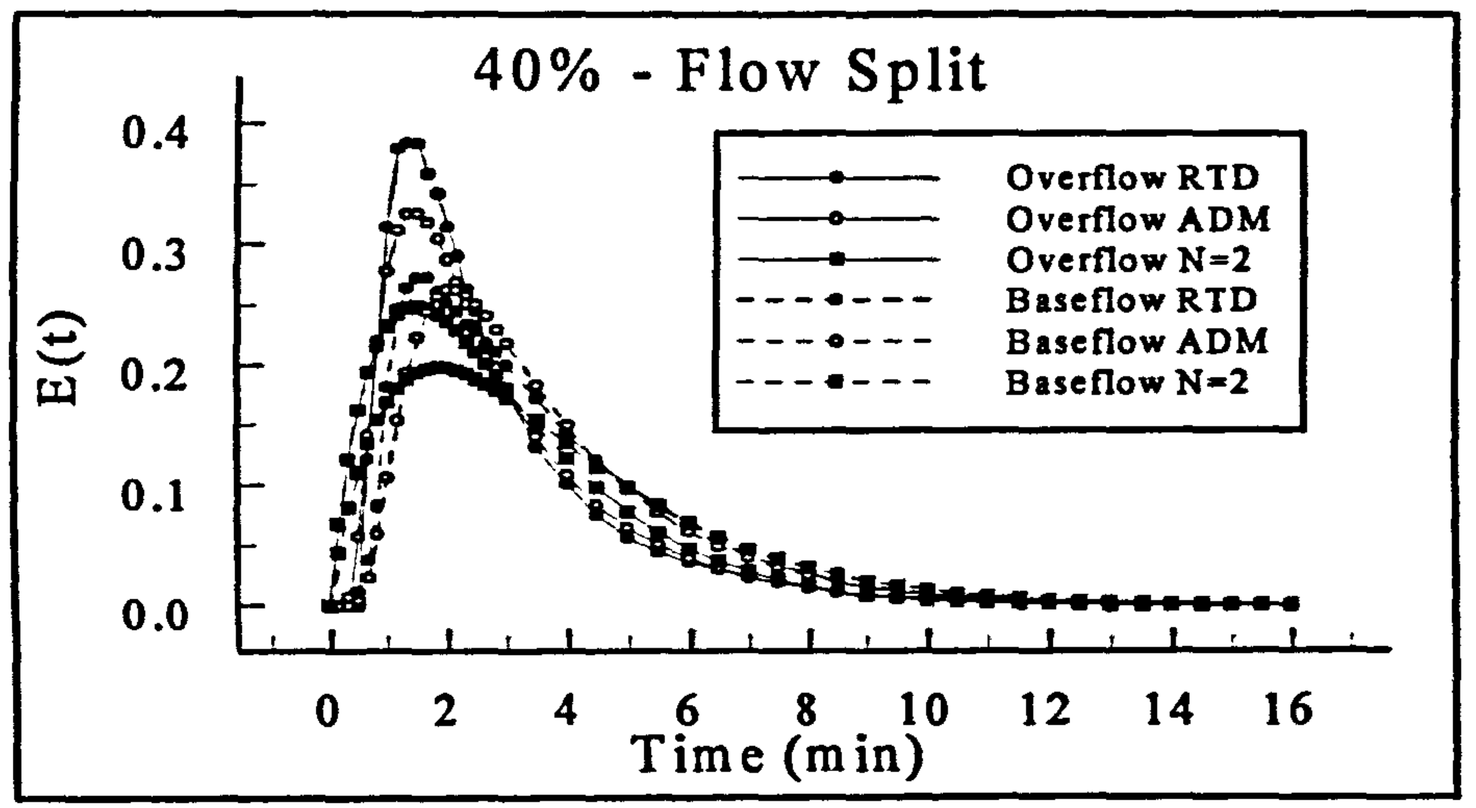

Fig. 6.18 - Model HDVS Baseflow (SP3) - Comparison of E(t), ADM and TISM Curves Calculated using the Method of Moments for an Inlet Flow Rate of 20l/min

6.2.2.2 Non-Linear Regression Data Analysis

Fig. 6.19 and 6.20 show the RTD normalised curves E(Θ) for an inlet flow rate of 20l/min. The RTD curves were normalised (section 4.3.1) using the experimental mean residence time calculated from the ADM (eqn. 4.11) and TISM (eqn. 4.9). The remaining flow rates are shown in appendix E.2.11 and E.2.12. The RTD curves show the same characteristics and therefore, the same observations and conclusions apply as the RTD normalised curves E(Θ) obtained using the method of moments (section 6.2.2.1). The RTD normalised curves E(Θ) using the ADM (Fig. 6.19) and TISM (Fig. 6.20) show that the non-linear regression technique estimates a higher baseflow mean residence time, compared to the theoretical mean residence time (appendix E.2.3), as both the overflow and baseflow RTD curves peaks occur at a similar normalised exit-age distribution E(Θ) value. Subsequently, the RTD normalisation procedure using the method of moments (Fig. 6.14) and ADM (Fig. 6.19) and TISM (Fig. 6.20) using non-linear regression, do not provide the same trend in the RTD normalised curves E(Θ) as the theoretical RTD normalised curves E(Θ) and particularly for the baseflow component (Fig. 6.13).

Tables 6.7 and 6.8 show the ADM and TISM parameters calculated using non-linear regression. The experimental mean residence time values calculated using non-linear regression are of a similar order of magnitude as calculated directly from the method of moments (section 6.2.2.1). Appendix E.2.13 shows the experimental mean residence time for all inlet flow rates plotted against the flow split calculated using the ADM and TISM. These curves show the same trend as the experimental mean residence time calculated using the method of moments (Fig. 6.15). The overflow and baseflow experimental mean residence time values and therefore, the RTD normalised curves E(Θ)

are very similar regardless of the flow model used for the non-linear regression iteration i.e. TISM (eqn. 4.9) and ADM (eqn. 4.11).

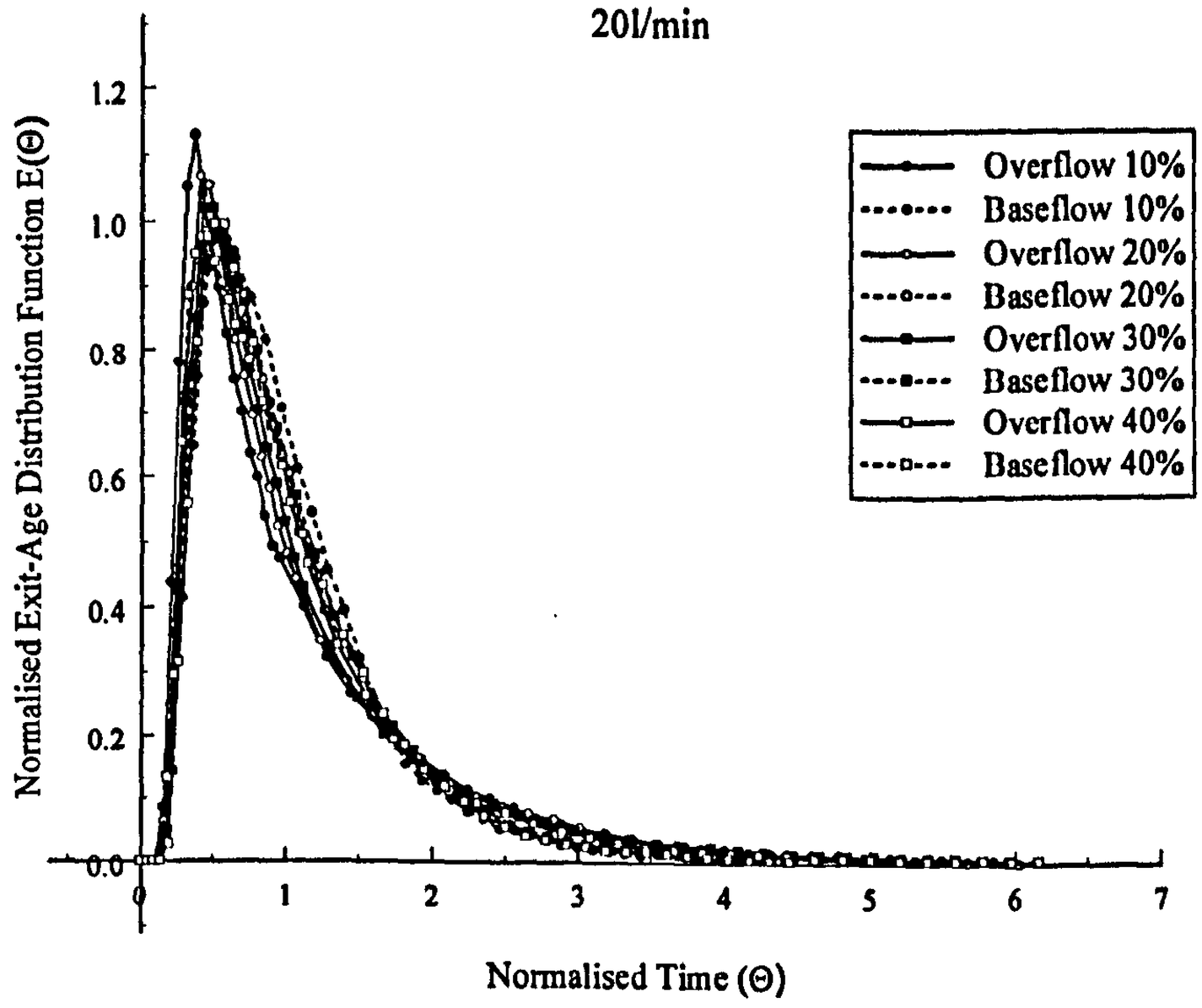

Fig. 6.19 Model HDVS Baseflow (SP3) - Comparison of Normalised Exit-Age Distribution Curves E(Θ) using Non-Linear Regression and the ADM

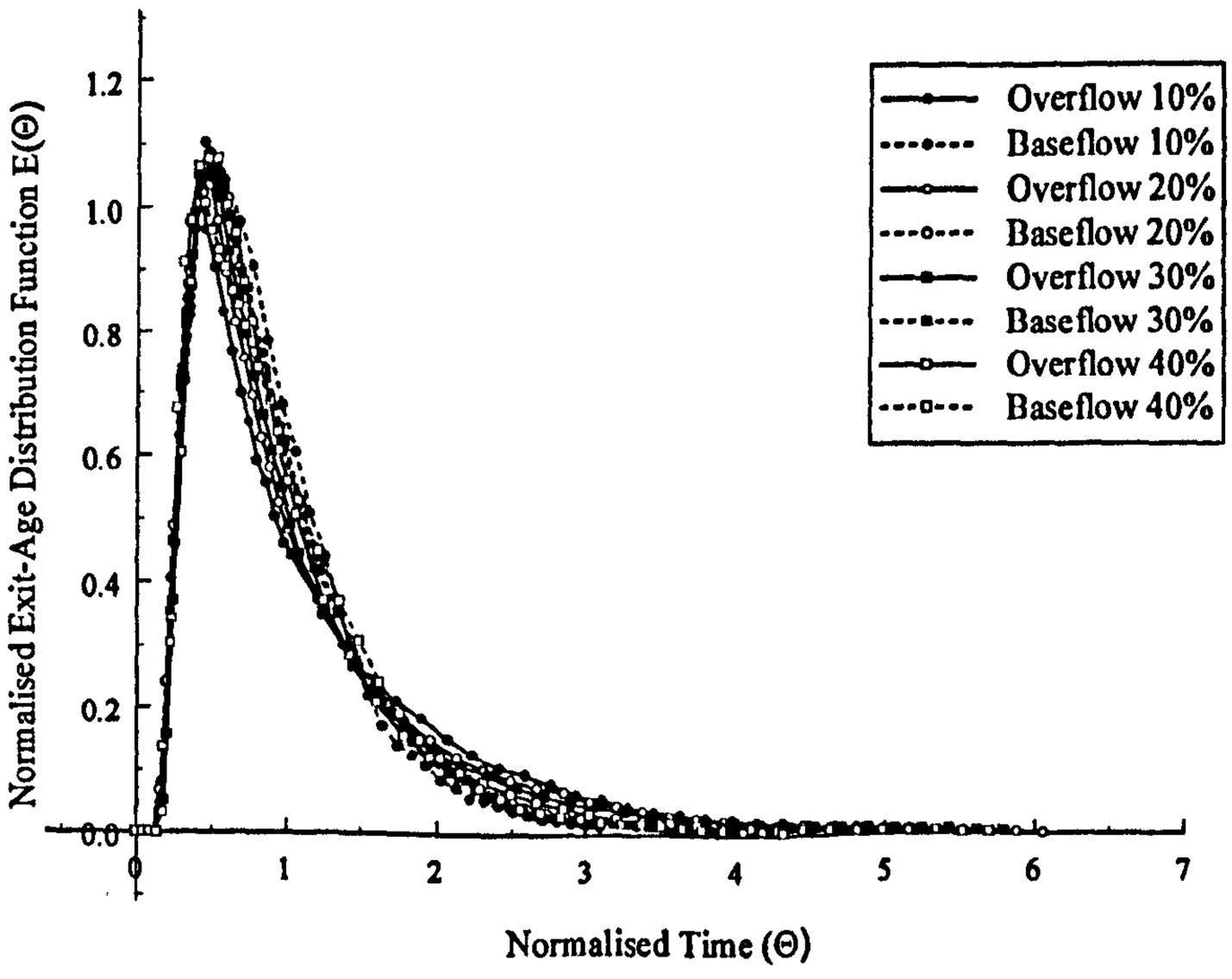

Fig. 6.20 Model HDVS Baseflow (SP3) - Comparison of Normalised Exit-Age Distribution Curves E(Θ) using Non-Linear Regression and the TISM

The ADM and TISM baseflow experimental mean residence time values are all greater than the overflow values and both follow the same trend as the RTD curves time to peak concentration as described above (section 6.2.2.1). This is the expected trend, particularly due to the location of the sampling point (SP3) (Fig. 6.1) and introduction of the sludge hopper (section 6.2.3). The ADM non-linear regression iteration technique was not subject to a constraint on the normalised variance parameter (eqn. 4.11), which is discussed below and in section 6.2.1.2. The average error using the ADM for the overflow experimental mean residence time values compared with the theoretical is -6% and similarly for the baseflow is +43%. Similarly, the average error using the TISM for the overflow is -7% and for the baseflow is +55% (appendix E.2.3). The ADM using non-linear regression provides a better estimation of the theoretical mean residence time compared to other techniques i.e. method of moments and TISM using non-linear regression and subsequently provides a better model HDVS volume estimation discussed below. The relative trend in the baseflow and overflow component theoretical and mean residence time errors as the flow rate increases and the associated HDVS mixing regime characteristics are discussed in section 6.2.1.1.

Appendix E.2.14 shows the estimated model HDVS volume calculated using the ADM and TISM mean residence time. As stated above the model HDVS operating with the sludge hopper (Fig. 6.1) has a volume of 60 litres. Both the ADM and TISM provide a better estimation of the model HDVS volume compared to the method of moments. The ADM estimated model HDVS volume has an average error of +5% and the TISM +6%. The percentage of the experimental volume estimate associated with the overflow and baseflow components is also presented in appendix E.2.14. These values show that the volume split is approximately proportional to the flow split i.e. a 10% flow split results in 10% of the total HDVS volume being associated with the baseflow and 90%

with the overflow component. The normalised variance values for the baseflow component (SP3) were all less than 1 (Table 6.7) and therefore, the constraint applied to this parameter for the baseflow component measured at SP2 was not required in the non-linear regression simulation of the ADM (section 6.2.1.2).

Table 6.7 Model HDVS Baseflow (SP3) – Comparison of ADM Parameters using Non-Linear Regression

Flow Rate (l/min)	Flow Split (%)	Experimental Mean Residence Time (min)		Normalised Variance (σ_θ^2)		Peclet Number (P_e)	
		O	B	O	B	O	B
10	10	8.380	7.256	0.948	0.447	0.165	3.095
	20	6.695	6.690	0.736	0.490	1.000	2.655
	30	5.715	5.910	0.544	0.503	2.185	2.530
	40	5.340	5.761	0.437	0.631	3.210	1.570
15	10	4.108	5.757	0.707	0.430	1.145	3.285
	20	3.491	5.115	0.513	0.408	2.440	3.565
	30	3.338	4.983	0.445	0.463	3.100	2.920
	40	3.382	4.846	0.398	0.565	3.700	2.020
20	10	3.120	4.664	0.662	0.389	1.390	3.830
	20	2.820	3.932	0.542	0.446	2.200	3.100
	30	2.684	3.757	0.488	0.427	2.670	3.330
	40	2.595	3.597	0.415	0.512	3.475	2.450
30	10	2.024	3.411	0.658	0.395	1.410	3.745
	20	1.830	2.847	0.564	0.437	2.030	3.210
	30	1.863	2.729	0.441	0.548	3.165	2.150
	40	1.810	2.759	0.455	0.480	3.005	2.745
45	10	1.217	2.596	0.538	0.350	2.230	4.445
	20	1.139	2.239	0.459	0.368	2.965	4.145
	30	1.174	2.231	0.431	0.288	3.280	5.740
	40	1.181	1.992	0.405	0.360	3.610	4.275
60	10	0.927	2.061	0.661	0.264	1.395	6.405
	20	0.834	1.737	0.450	0.296	3.065	5.550
	30	0.876	1.652	0.469	0.264	2.860	6.405
	40	0.875	1.480	0.397	0.267	3.715	6.315

Fig. 6.21 illustrates the ADM parameter (P_e) for all flow splits and the range of inlet flow rates investigated. The overflow Peclet number (P_e) increases and the baseflow Peclet number (P_e) marginally decreases as the flow split is increased for the same inlet flow rate. The overflow Peclet numbers (P_e) increase as the inlet flow rate is increased.

This is the opposite relationship as achieved for the model HDVS operating with no baseflow and with the sludge hopper (section 4.4.1). The overflow Peclet numbers (P_e) are still in the same order of magnitude as calculated for the model HDVS operating with no baseflow and with the sludge hopper (section 4.4.1.2). The baseflow component Peclet numbers (P_e) have the same trend as the overflow, with higher Peclet numbers (P_e) at high inlet flow rates and is the same relationship as obtained using the method of moments (section 6.2.2.1).

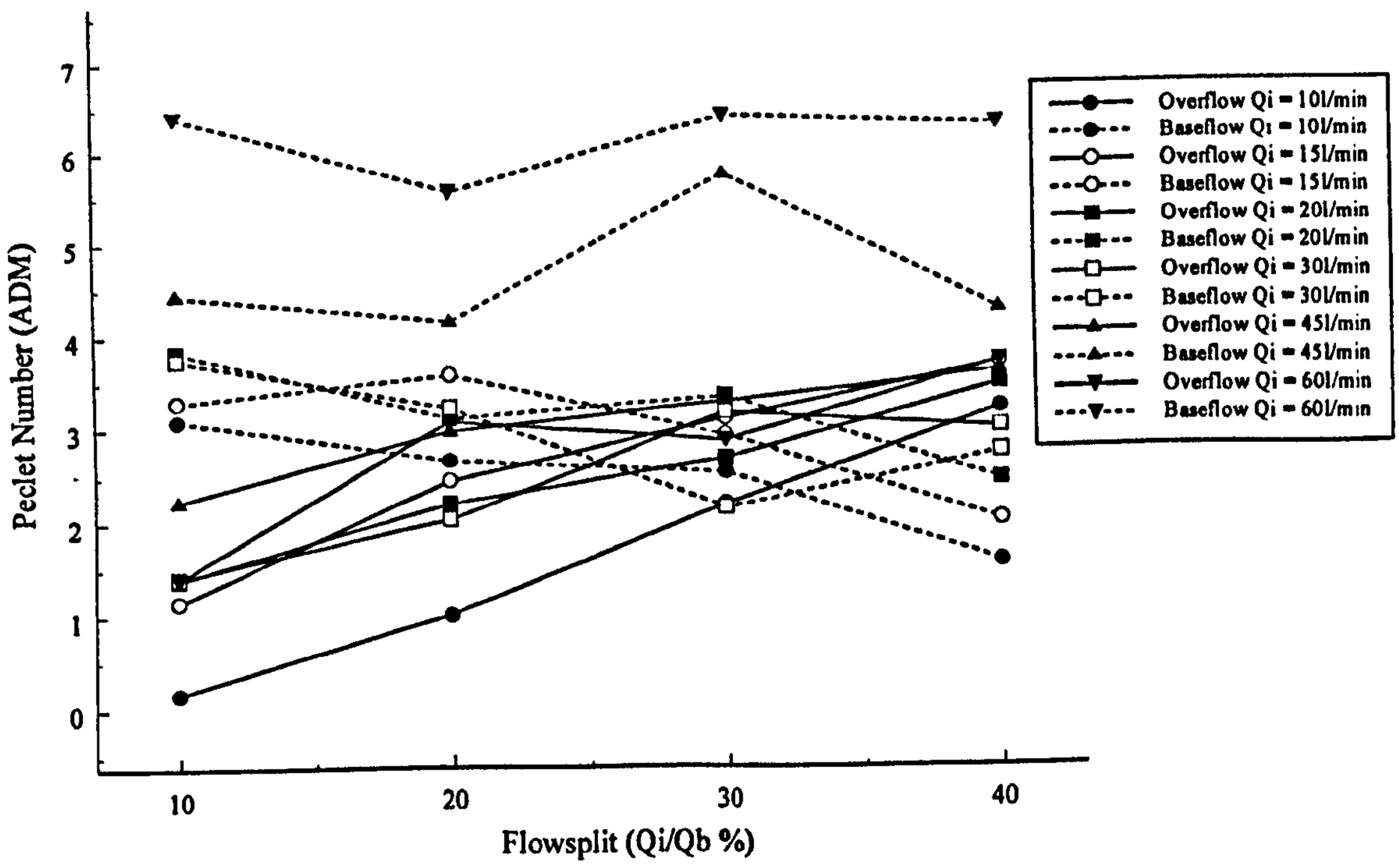

Fig. 6.21 Model HDVS Baseflow (SP3) - Comparison of the ADM Parameters Calculated using Non-Linear Regression

Table 6.8 Model HDVS Baseflow (SP3) – Comparison of TISM Parameters using Non-Linear Regression

Flow Rate (l/min)	Flow Split (%)	Experimental Mean Residence Time (min)		N-Tanks	
		O	B	O	B
10	10	6.759	7.761	2.066	2.383
	20	5.941	6.924	2.112	2.317
	30	5.651	6.137	2.210	2.264
	40	5.687	5.462	2.309	2.166
15	10	3.701	6.207	2.097	2.416
	20	3.516	5.626	2.202	2.418
	30	3.532	5.317	2.278	2.380
	40	3.708	4.829	2.331	2.303
20	10	2.894	5.167	2.126	2.419
	20	2.807	4.188	2.203	2.375
	30	2.761	4.078	2.248	2.393
	40	2.808	3.708	2.326	2.322
30	10	1.828	3.769	2.062	2.425
	20	1.745	3.039	2.126	2.353
	30	1.993	2.736	2.324	2.332
	40	1.907	2.889	2.264	2.367
45	10	1.177	2.811	2.113	2.376
	20	1.151	2.401	2.164	2.354
	30	1.208	2.531	2.213	2.430
	40	1.238	2.147	2.227	2.364
60	10	0.818	2.440	2.018	2.509
	20	0.863	1.962	2.177	2.416
	30	0.893	1.904	2.182	2.442
	40	0.924	1.689	2.253	2.441

Fig. 6.22 illustrates the TISM parameter (N) for all flow splits and inlet flow rates and unlike the method of moments technique has a different independent trend to the ADM parameters (section 6.2.1.2). However, the overflow and baseflow TISM parameters obtained using non-linear regression show the same trend with respect to the flow split and inlet flow rate as the TISM parameters obtained using the method of moments (section 6.2.2.1). The overflow TISM parameter values are in the same order of magnitude as calculated for the model HDVS operating with no baseflow and with the sludge hopper (section 4.4.1.2).

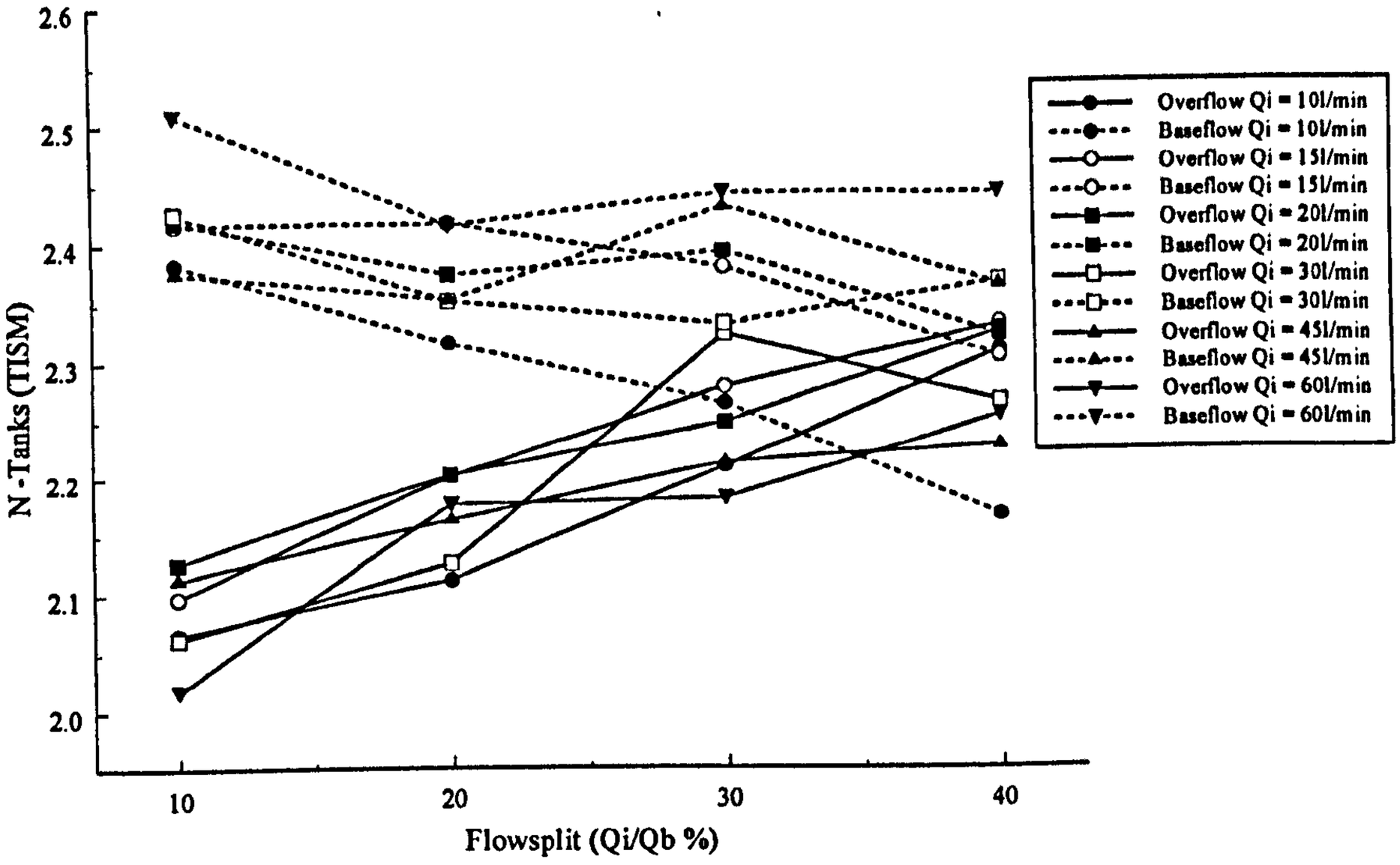

Fig. 6.22 Model HDVS Baseflow (SP3) - Comparison of the TISM Parameters Calculated using Non-Linear Regression

Appendix E.2.8 also details the summation of the individual overflow and baseflow component ADM and TISM parameters for the range of inlet flow rates at each flow split. The ADM total flow results show the same trend as the ADM total flow parameters calculated using the method of moments, as no constraint is applied to the ADM non-linear regression analysis for the baseflow component measured at SP3 (section 6.2.2.1). The TISM total flow results show the same relationship as the baseflow component measured at SP2 using non-linear regression (section 6.2.1.2).

Fig. 6.23 compares the experimental exit-age distribution function E(t) curves to the TISM (eqn. 4.9) and ADM (eqn. 4.11) curves obtained using non-linear regression for an inlet flow rate of 20l/min and all flow splits. The remaining flow rates and all correlation parameters (R^2 and ESS) are presented in appendix E.2.15 and E.2.16 respectively. The ADM provides the better fit to both the overflow and baseflow

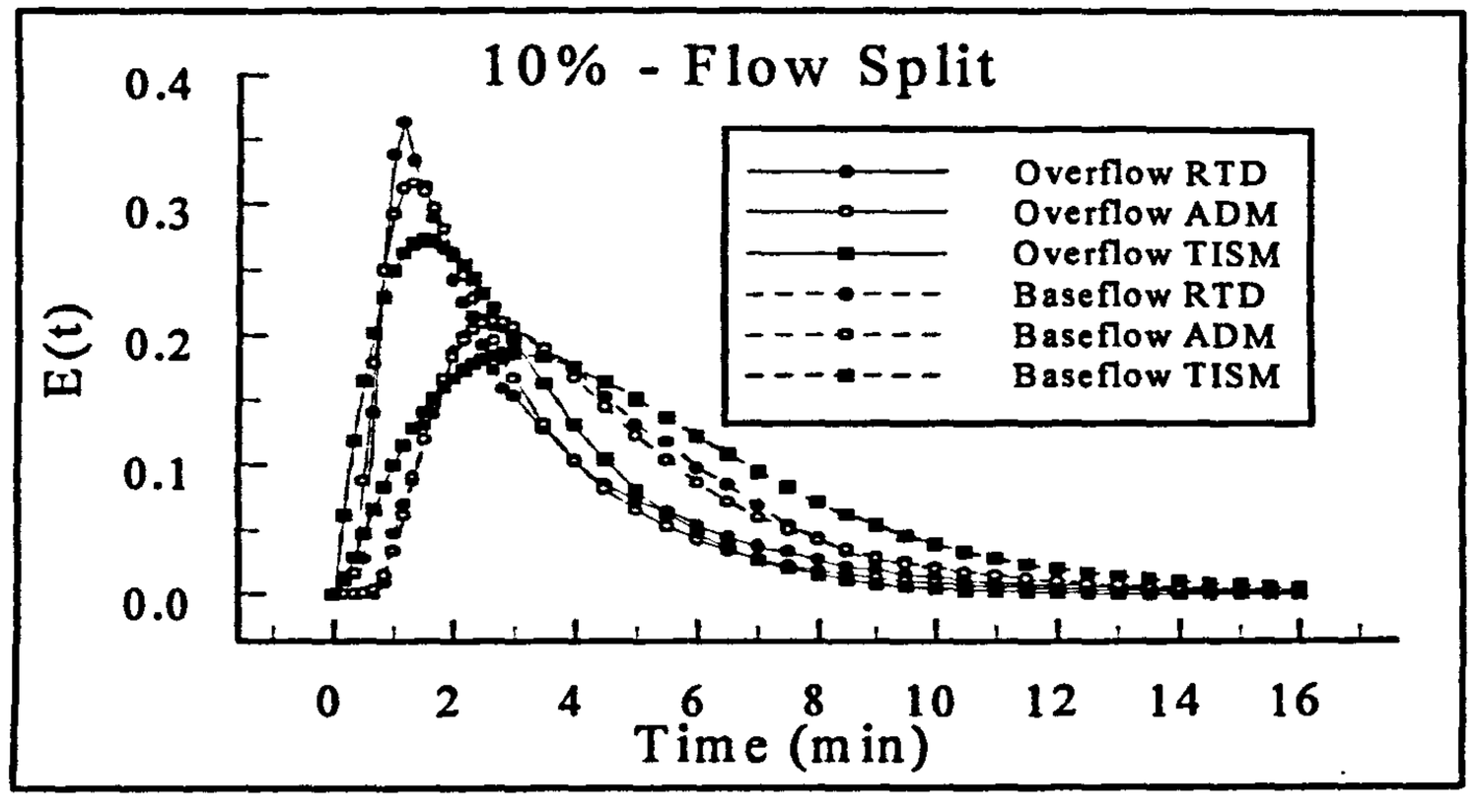

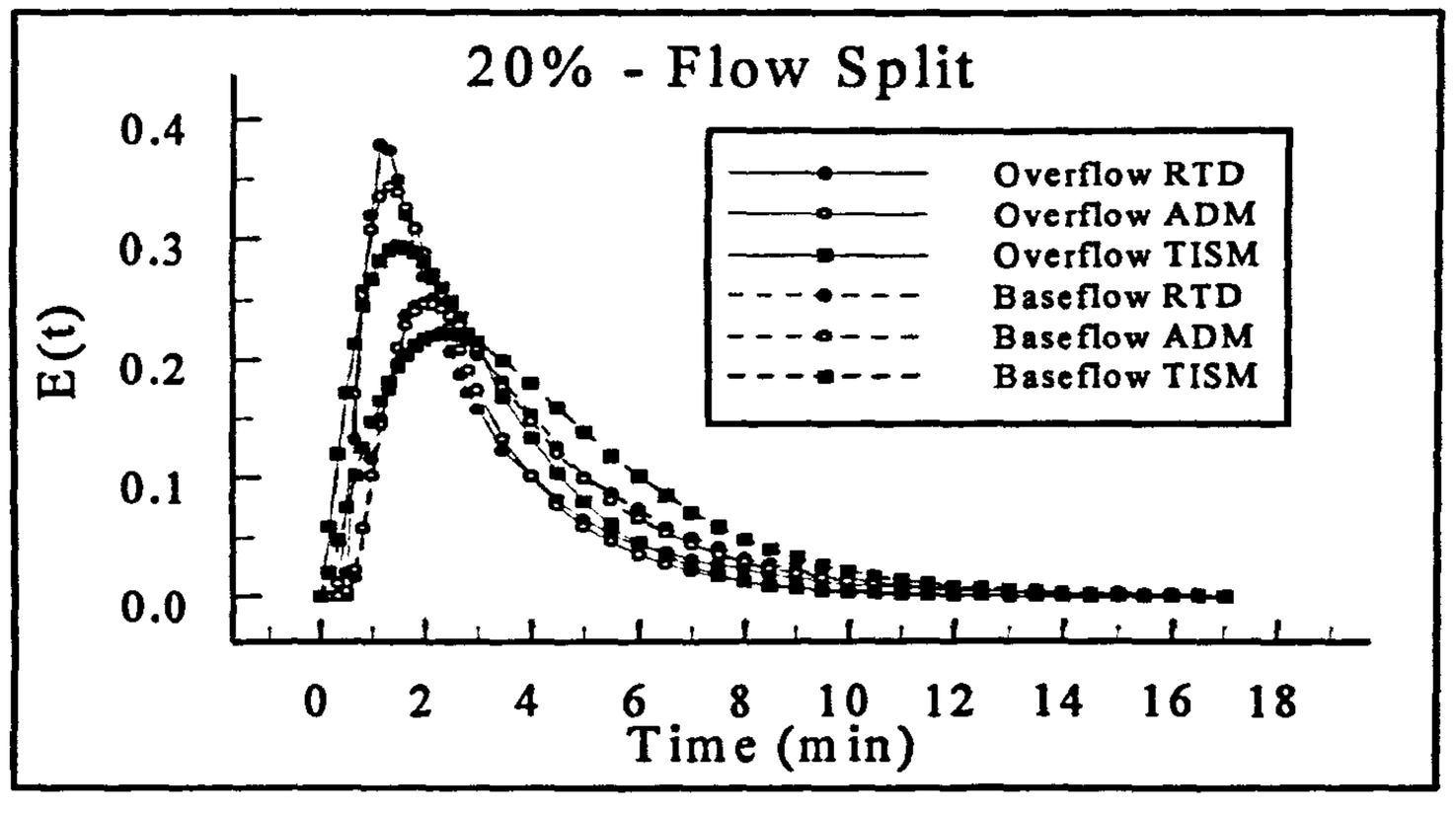

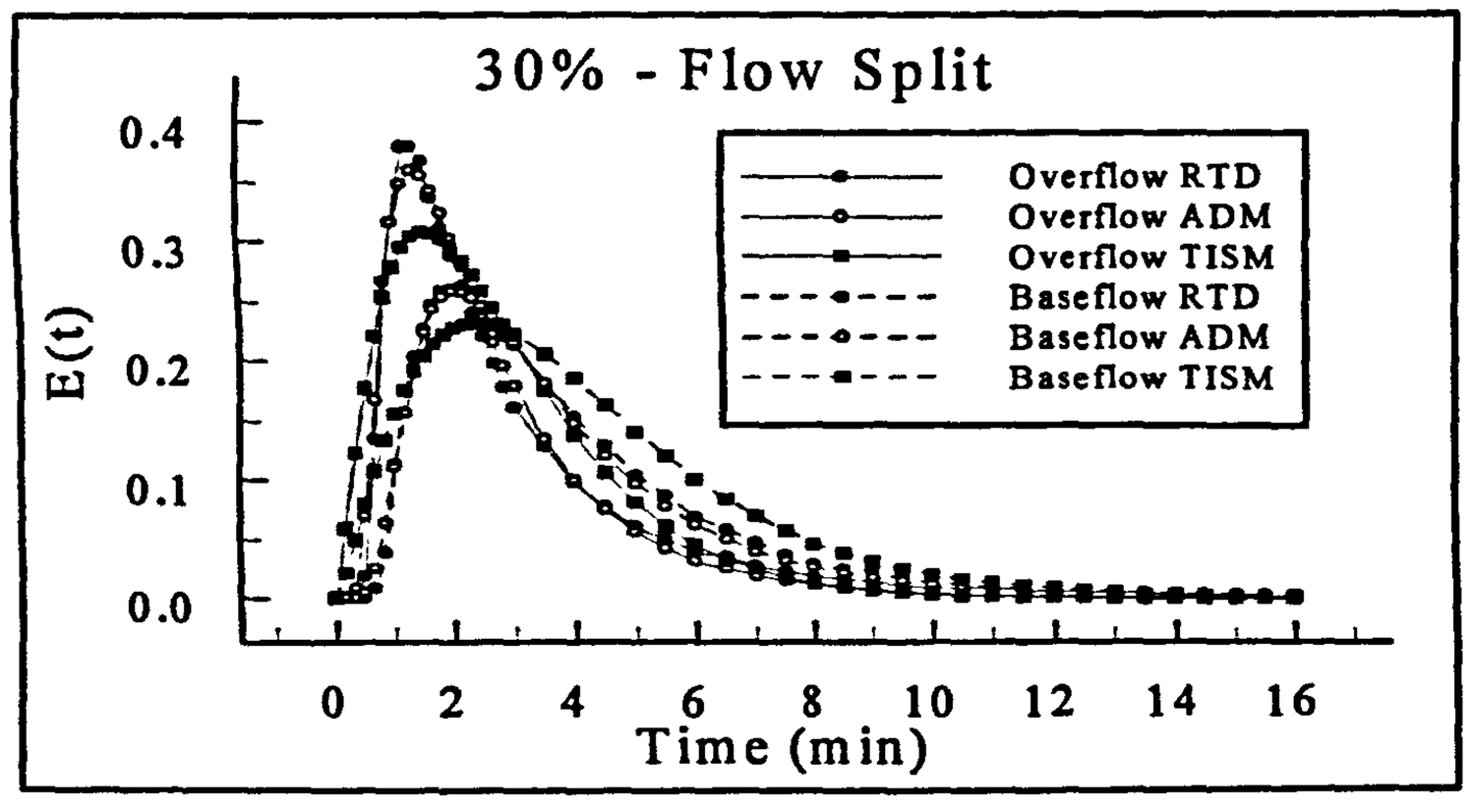

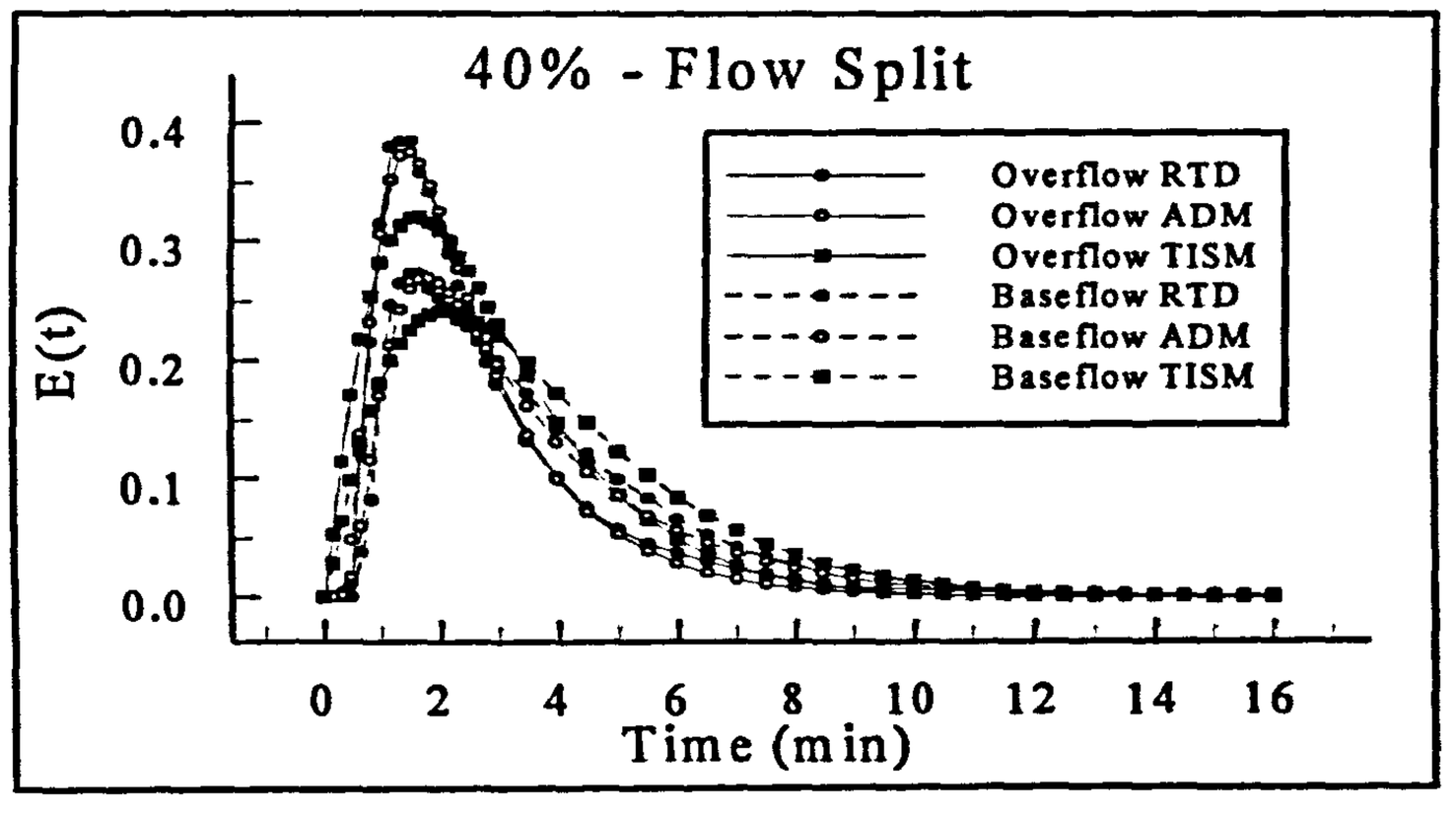

Fig. 6.23 - Model HDVS Baseflow (SP3) - Comparison of E(t), ADM and TISM Curves Calculated using Non-Linear Regression for an Inlet Flow Rate of 20l/min

experimental RTD curves for all inlet flow rates and flow splits compared to the TISM. The ADM and TISM correlation parameters remain very stable for the range of inlet flow rates and flow splits. The correlation parameters are very similar regardless of the ADM and TISM parameter estimation technique i.e. method of moments or non-linear regression. However, the non-linear regression correlation parameters are generally better compared to the method of moments (section 4.4.3).

6.2.3 Comparison of the Model Hydrodynamic Vortex Separator (HDVS) Baseflow RTD Pulse Injection Results for Sample Point 2 (SP2) and Sample Point 3 (SP3)

It was first assumed that the baseflow RTD curve would peak before the overflow RTD curve. This assumption was based on the physical characteristics i.e. internal configuration of the HDVS (Fig. 3.1) and the 'assumed' relative flow paths of the overflow and baseflow component. The flow is likely to leave the HDVS through the baseflow before the overflow as higher velocities are located in the outer zone of the HDVS compared to the inner zone. The inner zone is located between the baseflow and overflow outlet (Fig. 3.1) and therefore, slows the flow prior to leaving through the overflow. The practical significance of the inner zone is that it allows more time, by providing quiescent conditions, to allow settling of solids (Andoh, 1994). However, the baseflow RTD curves peak concentration occurs at different times depending on the sample point (SP2 or SP3) used to measure the RTD tracer concentration (Table 6.9).

The baseflow RTD curves measured at SP2 (Fig. 6.1) peak before the overflow curves at low inlet flow rates as expected however, at high inlet flow rates (>20l/min) the opposite occurs and implies that short-circuiting of the overflow component occurs (section 6.2.1.1). The relative height of the overflow and baseflow RTD curves also

support the time to peak concentration observations however, it also suggests that short-circuiting of the baseflow component occurs at low inlet flow rates. Short-circuiting of the overflow and baseflow component at high and low inlet flow rates respectively is considered to occur due to the strength of the vortex generated within the HDVS at these flow rates and the HDVS internal configuration (Fig. 3.1) (section 6.2.1.1).

The baseflow RTD curves measured at SP3 (Fig. 6.1) all peak after the overflow curve (section 6.2.2.1). This is due to the buffering capacity of the sludge hopper, which is included in the SP3 RTD analysis (Fig. 6.1) and increases the transit time of the baseflow component. The sludge hopper acts as a stagnant volume when the HDVS is operated without a baseflow (section 4.4.1). However, with the introduction of a baseflow component, the sludge hopper does not behave as a stagnant volume but as a controlled quiescent zone with slower velocities relative to the main volume of the HDVS. The sludge hopper is used for the collection of solids in the HDVS's typical application of solids-liquid separation and by operating as a quiescent zone it will provide controlled settlement and prevent resuspension of the solids (Andoh, 1994). The baseflow measured at SP3 RTD normalised curves E(Θ) support the baseflow measured at SP2 observations that the baseflow component short-circuits at low flow rates (section 6.2.2.1). This is shown by the SP3 baseflow RTD curves peak concentration occurring closer to a normalised time (Θ) value of 1 as the inlet flow rate increases (section 4.3.1). Additionally, the baseflow measured at SP3 RTD normalised curves E(Θ) also show that as the flow split is increased for the same inlet flow rate short-circuiting of the baseflow component increases (section 6.2.2.1).

The RTD curves times to peak concentration observations are also illustrated by comparing the overflow and baseflow experimental mean residence times. The overflow mean residence time is generally greater than the baseflow component when the latter is

measured at SP2 (except at high inlet flow rates due to short-circuiting) and at SP3 the mean residence time shows the opposite trend for all flow rates and flow splits. This also implies that the sludge hopper significantly extends the mean residence time of the baseflow component.

Table 6.9 Model HDVS – Comparison of SP2 and SP3 Residence Time Distribution (RTD) Time To Peak Concentration

Flow Rate (l/min)	Flow Split (%)	SP2 Time To Peak Concentration (min)		SP3 Time To Peak Concentration (min)	
		O	B	O	B
10	10	2.333	1.667	2.333	4.000
	20	2.667	1.667	2.333	3.333
	30	2.667	1.667	2.667	2.333
	40	3.000	1.333	2.667	2.333
15	10	1.500	1.333	1.667	3.333
	20	1.667	1.333	1.667	3.000
	30	1.833	1.333	1.667	2.667
	40	1.667	1.333	1.667	2.000
20	10	1.167	1.167	1.667	2.333
	20	1.167	1.000	1.667	2.167
	30	1.167	1.000	1.667	2.000
	40	1.333	1.000	1.333	1.667
30	10	0.833	1.000	0.833	2.000
	20	0.667	1.000	0.833	1.500
	30	0.833	0.833	1.000	1.667
	40	0.833	0.667	0.833	1.500
45	10	0.500	0.833	0.500	1.667
	20	0.500	0.667	0.500	1.333
	30	0.500	0.833	0.667	1.500
	40	0.667	0.667	0.667	1.333
60	10	0.500	0.667	0.333	1.500
	20	0.500	0.667	0.500	1.167
	30	0.500	0.833	0.500	1.167
	40	0.500	0.667	0.500	1.000

Tyack and Fenner, (1998b) observed that part of the flow is immediately swept up and out of the overflow under the vertical dip plate (Fig. 3.1), resulting in an immediate tracer response in a Grit King™ HDVS (Table 1.1). Luyckx *et al.*, (1998a) observed at

low flow splits (10%) and therefore the overflow flow rate is at it's greatest compared to the baseflow flow rate, that the Storm King™ HDVS (Table 1.1) overflow component RTD curve peaks before the baseflow, implying that short-circuiting of the overflow component occurs. This project also supports these results by comparing the RTD time to peak concentration of both flow components and their likely flow paths as discussed above. The short-circuiting of the overflow component observed in this project is with respect to the inlet flow rate and not the flow split as observed by Luyckx *et al.*, (1998a). However, at the high inlet flow rates at which short-circuiting of the overflow component occurs, it is predominantly at low flow splits (Table 6.9). The Storm King™ HDVS results compare favourable with the baseflow RTD measured at SP2 presented in this project as the Storm King™ HDVS operates without a sludge hopper (Table 1.1). Existing research has shown that increasing the depth of the vertical dip plate (Fig. 3.1), to potentially minimise short-circuiting of the overflow component, is detrimental to the solids retention efficiency of the HDVS (Harwood and Saul, 1996b). However, the RTD provides the necessary information to address this non-ideal flow behaviour for the design of kinetic processes within the HDVS.

The model HDVS volume estimations, using the method of moments experimental mean residence time for both the SP2 and SP3 RTD results, have an average error of +15%. The average estimated volume difference between the SP2 and SP3 RTD results is approximately 5 litres, which is equal to the measured volume of the sludge hopper (section 3.3.2). This provides confidence in the experimental mean residence time results, particularly as a long RTD experimental duration has been used for all RTD tests and truncation effects have not been considered (section 4.4.1). The non-linear regression technique using the ADM has an average model HDVS volume error of +5% and +7% for the SP2 and SP3 RTD results respectively. Similarly, the TISM has a negligible error

for SP2 and +6% for SP3. The average estimated volume difference between the SP2 and SP3 RTD results is approximately 8 litres for the ADM and 13 litres for the TISM, which are slightly greater than the measured volume of the sludge hopper. Therefore the average difference between the SP2 and SP3 baseflow component experimental mean residence time is approximately equal to the flow transit time through the sludge hopper (Fig. 6.1). The increase in volume between the baseflow component RTD measured at SP2 and SP3 is expected as the latter sample point (SP3) includes the volume of the sludge hopper (Fig. 6.1). Subsequently, the baseflow component experimental mean residence time should be greater when measured at SP3 (Table 6.5) compared to SP2 (Table 6.1).

The overflow RTD curves and characteristics are very similar irrespective of where the baseflow component is sampled i.e. SP2 or SP3 (Fig. 6.1) for a given inlet flow rate. The error between the average overflow component experimental mean residence time, calculated from the SP2 and SP3 RTD data using both the method of moments and non-linear regression and the measured experimental mean residence time is 0.02% and ranges from -7% to +10%. As the overflow RTD parameters should be the same for the SP2 and SP3 RTD experiments, these errors correspond to experimental errors in calculating the experimental mean residence time. However, it is evident that the baseflow theoretical and experimental mean residence time error is significantly greater at SP3 compared to SP2 and is due to the mixing characteristics of the baseflow component and the influence of the sludge hopper as the flow rate increases (section 6.2.1.1). The error between the theoretical and experimental mean residence time for both the SP2 and SP3 baseflow component RTD results is reduced when the non-linear regression technique is adopted (appendix E.1.4 and E.2.3). Additionally the TISM mean residence time values calculated using non-linear regression are superior compared to the

ADM mean residence time values as discussed in section 6.2.1.2. The advantages of the non-linear regression ADM and TISM parameter estimation technique compared to the method of moments are discussed in section 4.4.3.

Tyack and Fenner, (1998b) commented that the delayed response observed in the baseflow compared to the overflow component is due to a number of combinations. This includes the longer flow path the fluid must take to pass into the baseflow region, the lower velocities nearer to the inner region (Fig. 3.1) and the throttling effect that the vortex core and exit pipe have on the baseflow flow rate i.e. limiting the rate of flow into this region. These observations were obtained using a Grit King™ HDVS (Table 1.1), which operates with a grit pot and therefore, is similar to the Swirl-Flo™ HDVS investigated in this project operating with the sludge hopper (SP3) (Fig. 6.1).

The overflow component ADM (P_e) and TISM (N) parameters calculated using the method of moments, for both the SP2 (section 6.2.1.1) and SP3 (section 6.2.2.1) RTD experiments, produce very similar results both in their magnitude and trend with respect to the inlet flow rate and flow split (Fig. 6.5 and Fig. 6.16). This is anticipated as the overflow component is unaffected by changing the baseflow sample point location (Fig. 6.1). The following discussion only refers to the ADM parameter (P_e), as the TISM parameter (N) follows the same trend, due to the method of moments ADM and TISM parameter estimation technique (section 6.2.1.1). The overflow Peclet number (P_e), for both sample points, generally remains stable as the flow split increases i.e. as the overflow component flow rate decreases. The baseflow component Peclet number (P_e) does show different characteristics with respect to the flow split, depending on the sample point location (Fig. 6.1). At SP2 the baseflow component Peclet number (P_e) remains relatively stable, whereas at SP3 the Peclet number (P_e) significantly decreases as the flow split increases for the same inlet flow rate. The baseflow component mixing

regime sampled at SP2 is considered to have a large element of mixed flow and therefore, increasing the flow rate of the baseflow component i.e. increasing the flow split, will have little effect in changing the plug-flow mixing characteristics. Whereas the flow path from SP2 to SP3 i.e. through the sludge hopper has significant plug-flow mixing characteristics and this will be affected by increasing the flow rate i.e. increasing the flow split. The Peclet numbers (P_e) for the baseflow component measured at SP3 (appendix E.2.8) are also significantly higher than at SP2 (appendix E.1.9) for the same inlet flow rate. Therefore the sludge hopper behaves as a quiescent zone and improves the plug-flow mixing characteristics of the baseflow component. The above and following observations obtained using the ADM and TISM parameters are also illustrated by the position of the baseflow component RTD normalised curves $E(\Theta)$ peak concentration for SP2 (Fig. 6.2) and SP3 (Fig. 6.13) relative to a normalised time (Θ) value of 1 (section 4.3.1).

The overflow component ADM and TISM parameters calculated using non-linear regression also show similar trends for the SP2 (section 6.2.1.2) and SP3 (section 6.2.2.2) RTD experiments. The overflow parameters gradually increase as the flow split increases i.e. as the overflow component flow rate decreases for the same inlet flow rate. The baseflow component measured at SP3 ADM and TISM parameters generally decrease and at SP2 they remain stable as the flow split is increased for the same inlet flow rate. The ADM non-linear regression simulation constraint applied to the normalised variance for SP2 was not required for the SP3 RTD data (section 6.2.1.2). The requirement of a mathematical constraint to solve the ADM using non-linear regression, for the baseflow component measured at SP2 only, suggests that the assumptions of the ADM are not satisfied by the real system (section 4.3.3). Subsequently the mixing regime is approaching complete mixing at the SP2 location (Fig.

6.1). Additionally, as the constraint is not required for the baseflow component measured at SP3 this implies that the mixing regime has improved plug-flow mixing characteristics due to the introduction of the sludge hopper. The influence of the sludge hopper at SP3 on the ADM and TISM parameters calculated using the method of moments also applies to the non-linear regression analysis.

The overflow and baseflow ADM and TISM parameters calculated using the method of moments and non-linear regression generally decrease and increase respectively as the inlet flow rate is increased for both sample points (Fig. 6.1). Therefore the overflow component ADM and TISM parameters generally follow the same trend as achieved for the model HDVS operating with no baseflow and without the sludge hopper (SP2) and with the sludge hopper (SP3) (chapter 4). This project is the first comprehensive characterisation of the HDVS operating with an overflow and baseflow component simultaneously using RTD analysis and interestingly shows that there is a greater element of plug-flow mixing for the baseflow component as the inlet flow rate increases. Therefore, depending on the desired performance of a specific kinetic process, a compromise is required between the overflow and baseflow component mixing regime, based on the inlet flow rate and the required properties of the overflow and baseflow effluent. However, this is only true with respect to the inlet flow rate and not the baseflow flow rate i.e. flow split. As the flow split increases for the same inlet flow rate the baseflow component mixing regime has a greater element of mixing and therefore less plug-flow mixing (section 4.1).

The improvement in the baseflow component plug-flow mixing characteristics as the inlet flow rate is increased is greater for the baseflow component measured at SP3 compared to SP2 and is due to the inclusion of the sludge hopper as discussed above. Hence, the difference between the mixing regimes associated with the overflow and

baseflow component is greater when the baseflow is measured at SP3 (Fig. 6.1). This is also shown by comparing the total flow (overflow + baseflow) ADM and TISM parameters calculated using the method of moments and non-linear regression (appendix E.1.9 and E.2.8). Table 6.10 compares the total flow ADM and TISM parameters calculated using the method of moments for the baseflow component measured at SP2 and SP3. The total flow ADM and TISM parameters calculated using non-linear regression also follow a similar trend as the method of moments total flow results (section 6.2.1.2 and 6.2.2.2).

Table 6.10 Model HDVS - Comparison of SP2 and SP3 Total Flow ADM and TISM Parameters Calculated using the Method of Moments

		SP2	SP3	SP2	SP3
Flow Rate (l/min)	Flow Split (%)	Total Flow Peclet Number (P_e)	Total Flow Peclet Number (P_e)	Total Flow N-Tanks	Total Flow N-Tanks
10	10	4.255	6.200	3.631	4.608
	20	3.310	4.975	3.246	3.915
	30	3.395	6.170	3.274	3.668
	40	3.285	5.660	3.240	3.903
15	10	2.410	6.465	2.878	4.528
	20	3.335	4.900	3.247	3.984
	30	3.495	4.330	3.314	4.492
	40	4.150	4.890	3.589	4.243
20	10	3.240	6.860	3.213	4.827
	20	3.450	5.265	3.297	4.089
	30	3.840	5.495	3.460	4.192
	40	4.320	5.810	3.660	4.313
30	10	3.570	6.005	3.358	4.467
	20	2.210	5.290	2.812	4.125
	30	3.890	5.750	3.488	4.284
	40	3.730	6.085	3.414	4.447
45	10	3.065	6.920	3.158	4.918
	20	4.895	5.615	3.923	4.291
	30	3.705	8.475	3.432	5.590
	40	5.330	6.070	4.104	4.469
60	10	4.905	8.375	3.929	5.644
	20	4.840	7.145	3.899	4.994
	30	4.355	7.355	3.698	5.107
	40	4.825	9.445	3.891	6.017

The largest plug-flow mixing element within the model HDVS operating with a baseflow component exists at the highest inlet flow rate (Table 6.10). This is due to the relationship between the overflow and baseflow component ADM and TISM parameters and the inlet flow rate as discussed above. This has significant advantages for providing effective high-rate chemical treatment particularly as the HDVS has the ability to operate at very high inlet flow rates for a small footprint compared to conventional treatment processes (Boner *et al.*, 1994). However, if the HDVS is to provide combined solids removal and chemical treatment, a compromise in the operating conditions will be required. This is because the HDVS solids removal efficiency generally improves at low flow rates and high flow splits (chapter 2) and this combination of operating conditions provides the smallest element of plug-flow mixing based on the RTD results presented in this chapter. Therefore it maybe beneficial to operate the HDVS in series to achieve the desired overflow and baseflow component composition. The inclusion of the sludge hopper in the HDVS configuration provides optimum conditions for solids separation (Andoh, 1994) and also increases the contact time and the plug-flow mixing characteristics of the baseflow component. Subsequently the baseflow component will provide better mixing characteristics for disinfection processes compared to the overflow e.g. greater microbial kill and less residual disinfectant (section 2.2.3).

It appears that the high internal velocities in the outer zone and velocity gradients in the cone region (Fig. 3.1), which are a feature of the HDVS and advantageous for solids-liquid separation (Andoh, 1994), create a large degree of mixing and subsequently short-circuiting. This is detected in the baseflow RTD measured at SP2 and due to the influence of the sludge hopper at SP3 is subsequently reduced. The relative trend and magnitude of the overflow and baseflow component (SP2 and SP3) ADM and TISM parameters suggests that there are three different mixing regimes within the HDVS.

These are the outer zone, inner zone and sludge hopper (section 3.2) (Fig. 3.1). The former provides a mixing regime closer to complete mixing and the remaining two regions have improved plug-flow mixing (section 4.1). The sludge hopper region also provides a greater degree of quiescent flow behaviour and therefore, plug-flow mixing conditions compared to the inner zone. This is shown by the baseflow component measured at SP3 ADM and TISM parameters, which are greater than the overflow component (section 6.2.2) and for the baseflow component measured at SP2 (section 6.2.1) either the opposite occurs or it is not possible to distinguish any significant difference between the overflow and baseflow ADM and TISM parameters. Additionally, as previously stated, the ADM and TISM parameters are greater for the baseflow component measured at SP3 compared to SP2 and the overflow ADM and TISM parameters are very similar regardless of the baseflow component sample location. The implications of requiring a mathematical constraint to solve the ADM using non-linear regression for the baseflow component measured at SP2 only as discussed above, also supports these different mixing regimes within the HDVS.

The ADM and TISM correlation parameters (R^2 and ESS) for the SP2 and SP3 RTD experiments are presented in appendix E.1 and E.2 for both the method of moments and non-linear regression ADM and TISM parameter estimation techniques. The method of moments and non-linear regression correlation parameters generally show that the ADM provides the best-fit to the experimental overflow and baseflow RTD curves for all SP3 RTD experiments and the overflow component only for the SP2 RTD baseflow experiments. The TISM generally provides the best-fit to the baseflow component measured at SP2 using both the method of moments and non-linear regression parameter estimation techniques. The baseflow RTD measured at SP3 has improved plug-flow mixing characteristics compared to the baseflow RTD measured at

SP2, as shown by the ADM and TISM parameters discussed above. The ADM describes the deviation from plug-flow mixing and hence, is more likely to provide a better fit when less dispersion is present (SP3) (section 4.3.3). This occurs for the ADM and TISM correlation parameters discussed above and therefore, the correlation parameters are a function of the individual flow models and the model HDVS non-ideal flow behaviour. The ADM and TISM correlation parameters calculated using the non-linear regression parameter estimation technique are generally better compared to the method of moments (section 4.4.3).

6.2.3.1 Model Hydrodynamic Vortex Separator (HDVS) Baseflow (SP2) and (SP3) – Residence Time Distribution (RTD) Indices

The RTD indices have been calculated to further investigate the different mixing characteristics of the baseflow RTD curves measured at SP2 and SP3 (Fig. 6.1) (appendix E.1.18 and E.2.17). The RTD indices predominantly describe the shape of the RTD i.e. time of start, peak and finish relative to each other (section 4.3.4). The overflow component RTD indices are not presented or discussed in this section, as the overflow RTD curves obtained for the model HDVS operating with and without the baseflow component have very similar mixing characteristics (section 6.2.3). Therefore, for the model HDVS overflow component RTD indices the reader is referred to section 4.4.4. Table 6.11 compares selected RTD indices to illustrate the different characteristics of the baseflow component RTD curve obtained at SP2 and SP3 (Fig. 6.1).

Table 6.11 Model HDVS - Comparison of Selected SP2 and SP3 Baseflow Component RTD Indices

Flow Rate (l/min)	Flow Split (%)	SP2 t_f/τ	SP3 t_f/τ	SP2 t_p/τ	SP3 t_p/τ	SP2 t_{90}/t_{10}	SP3 t_{90}/t_{10}	SP2 t_{50}/t_m	SP3 t_{50}/t_m
10	10	0.121	0.278	0.303	0.667	8.667	4.667	0.864	0.857
	20	0.121	0.167	0.303	0.556	7.798	5.249	0.686	0.792
	30	0.121	0.278	0.303	0.389	7.798	5.572	0.848	0.757
	40	0.121	0.167	0.242	0.389	8.000	6.000	0.723	0.768
15	10	0.091	0.333	0.364	0.833	8.569	4.715	0.707	0.962
	20	0.091	0.250	0.364	0.750	7.712	4.572	0.723	0.885
	30	0.136	0.250	0.364	0.667	8.141	5.000	0.715	0.937
	40	0.091	0.250	0.364	0.500	8.500	5.799	0.749	0.799
20	10	0.121	0.278	0.424	0.778	7.500	4.250	0.898	0.946
	20	0.121	0.222	0.364	0.722	7.000	5.333	0.881	0.904
	30	0.121	0.222	0.364	0.667	7.000	5.000	0.865	0.874
	40	0.121	0.222	0.364	0.556	6.500	5.251	0.930	0.807
30	10	0.182	0.250	0.546	1.000	7.203	4.333	0.869	0.848
	20	0.091	0.167	0.546	0.750	8.246	4.713	0.794	0.846
	30	0.182	0.250	0.454	0.834	6.002	5.250	0.797	0.896
	40	0.091	0.250	0.364	0.750	7.121	4.713	0.795	0.851
45	10	0.137	0.375	0.682	1.251	5.997	3.856	0.878	0.930
	20	0.137	0.375	0.546	1.000	4.873	4.250	0.884	0.884
	30	0.137	0.375	0.682	1.125	6.500	3.428	0.827	0.878
	40	0.137	0.375	0.546	1.000	5.000	4.000	0.911	0.894
60	10	0.182	0.667	0.727	1.500	5.000	3.334	0.947	0.885
	20	0.182	0.500	0.727	1.167	5.000	3.824	0.928	0.896
	30	0.182	0.500	0.908	1.167	5.000	3.529	0.863	0.901
	40	0.182	0.333	0.727	1.000	4.500	3.250	1.026	0.940

The following observations were obtained from the baseflow component measured at SP3 and SP2 RTD indices:

- The t_f/τ index measures the most severe short-circuiting and a value approaching 1 implies plug-flow mixing (section 4.1). The baseflow component measured at SP3 values are all greater than those calculated at SP2 for the same inlet flow rate and flow split.

- The t_p/τ follows the same trend as the t_f/τ index and illustrates that the effective baseflow component volume is greater for the baseflow component measured at SP3 compared to SP2 for the same inlet flow rate and flow split.

- The t_{90}/t_{10} index (Morrill Dispersion Index) implies that the baseflow component RTD measured at SP3 has improved plug-flow mixing characteristics compared to the baseflow component RTD measured at SP2 for the same inlet flow rate and flow split. The t_{90}/t_{10} index obtained for the baseflow component measured at SP3 approaches values adequate for efficient reactor design (section 4.3.4).

- The t_{50}/t_m index measures the skew of the RTD curve towards the origin and therefore away from a normalised time (Θ) value = 1 (section 4.3.1). The values are very similar for the baseflow component measured at SP2 and SP3. However, this is because the experimental mean residence time, as opposed to the theoretical mean residence time, is used as the denominator for this index. If the theoretical mean residence time is used to calculate this index its trend will follow the RTD normalised curves E(Θ) time to peak concentration for SP2 (Fig. 6.2) and SP3 (Fig. 6.13).

- The t_{10} parameter is occasionally used as the time element (T) in the CT disinfection design methodology (section 4.3.4). The t_{10} parameter calculated at SP3 (appendix E.2.17) are all greater than at SP2 (appendix E.1.18) for the same inlet flow rate and flow split. Therefore, including the sludge hopper (SP3) reduces the C component required to achieve a specified CT value, compared to the baseflow component without the sludge hopper (SP2). This has practical, environmental and financial implications by reducing the quantity of the reactant required e.g. disinfectant.

The baseflow component including the sludge hopper (SP3) has less short-circuiting compared to the baseflow component measured at SP2 and subsequently has a greater active volume at the same inlet flow rate and flow split. Additionally the baseflow component including the sludge hopper (SP3) has better plug-flow mixing characteristics. Therefore, the sludge hopper acts a tubular reactor and provides plug-flow mixing when the model HDVS is operated with a baseflow component (section 4.1) compared to a stagnant volume when the model HDVS is operated without a baseflow component (section 4.4.1.1).

The baseflow component RTD indices (SP2 and SP3) relationship with the inlet flow rate shows that the baseflow component has improved plug-flow mixing characteristics as the inlet flow rate is increased. Additionally, the baseflow component has less short-circuiting at high flow rates compared to low flow rates and therefore, a greater volume is active in the mixing process. The baseflow component RTD indices support previous observations obtained from the RTD normalised curves E(Θ) and the ADM and TISM parameters (section 6.2.3). It is not possible to distinguish any noticeable trend in the RTD indices across the range of flow splits investigated for the same inlet flow rate.

6.2.4 Prototype Hydrodynamic Vortex Separator (HDVS) Baseflow - Residence Time Distribution (RTD) Pulse Experiments Sample Point 2 (SP2)

6.2.4.1 Method of Moments Data Analysis

This section describes the RTD analysis undertaken on the prototype HDVS operating with a baseflow component measured at sample point 2 (SP2), which is located above the sludge hopper (Fig. 6.1).

The RTD normalisation procedure is the same as used for the model HDVS operating with a baseflow component (section 6.2.1.1). The theoretical mean residence time for both the overflow and baseflow components are presented in appendix E.3.3. Fig. 6.24 and 6.25 show the normalised exit-age distribution function E(Θ) curves obtained using the theoretical mean residence time and experimental mean residence time calculated using the method of moments at an inlet flow rate of 120l/min and the range of flow splits investigated i.e. 10-40%. The remaining flow rates are shown in appendix E.3.4 and E.3.5.

The overflow and baseflow RTD curves illustrate a plug-flow mixing device with a degree of non-ideal flow behaviour. The prototype HDVS overflow and baseflow RTD normalised curves E(Θ) have a very similar distribution as the model HDVS and therefore the same observations apply (section 6.2.1.1). Appendix E.3.6 shows the time taken for the peak tracer (LiCl) concentration to occur for the RTD curves. The RTD curve time to peak concentration for the prototype HDVS operating with a baseflow component measured at SP2 and SP3 (Fig. 6.1) are compared and also presented in section 6.2.6 (Table 6.20). The peak concentration corresponds to the time at which the maximum volume passes through the HDVS. These values show that for flow rates less

than 240l/min the baseflow RTD curve peaks before the overflow and for high flow rates the opposite occurs. Therefore, based on the assumed relative flow path of each flow component, this implies that short-circuiting of the overflow component occurs at high flow rates and was also observed for the model HDVS operating with a baseflow component (section 6.2.3). The overflow RTD normalised curves E(Θ) also suggest that short-circuiting occurs at high flow rates, as the peak concentration shifts towards the origin as the flow rate increases and therefore, a smaller volume of the overflow component is active in the mixing process. However, the baseflow RTD normalised curves E(Θ) peak concentration shows the opposite trend as the flow rate increases and therefore, occurs closer to a normalised time (Θ) value of 1. Subsequently the baseflow component short-circuits at low flow rates (appendix E.3.4). The baseflow component short-circuiting at low flow rates was also observed for the model HDVS operating with a baseflow component (section 6.2.1.1). The overflow and baseflow component short-circuiting as the flow rate is increased and decreased respectively is possibly related to the strength of the vortex generated within the HDVS at these flow rates (section 6.2.1.1). The time to peak concentration is also illustrated by the exit-age distribution function E(t) curves in Fig. 6.28.

The experimental tracer recovery i.e. mass balance is shown in appendix E.3.7 and discussed in greater detail in section 6.2.1.1. These values show that near 100% tracer recovery was obtained for all inlet flow rates and flow splits. The overflow values decrease and the baseflow increase as the flow split increases and are approximately proportional to the flow split. The average error is +/- 2% with the largest error approximately 10%.

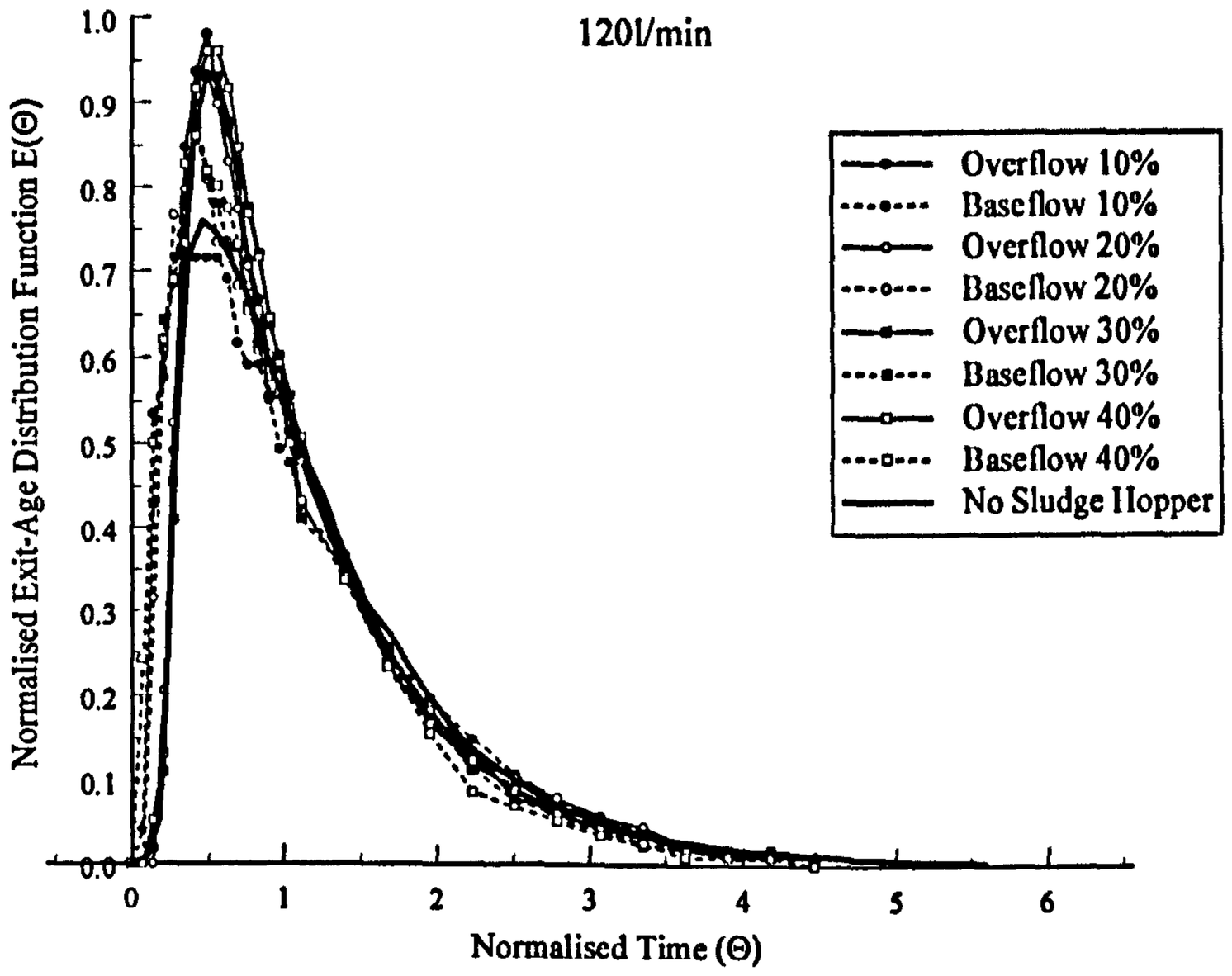

Fig. 6.24 Prototype HDVS Baseflow (SP2) - Comparison of Normalised Exit-Age Distribution Curves E(Θ) using the Theoretical Mean Residence Time

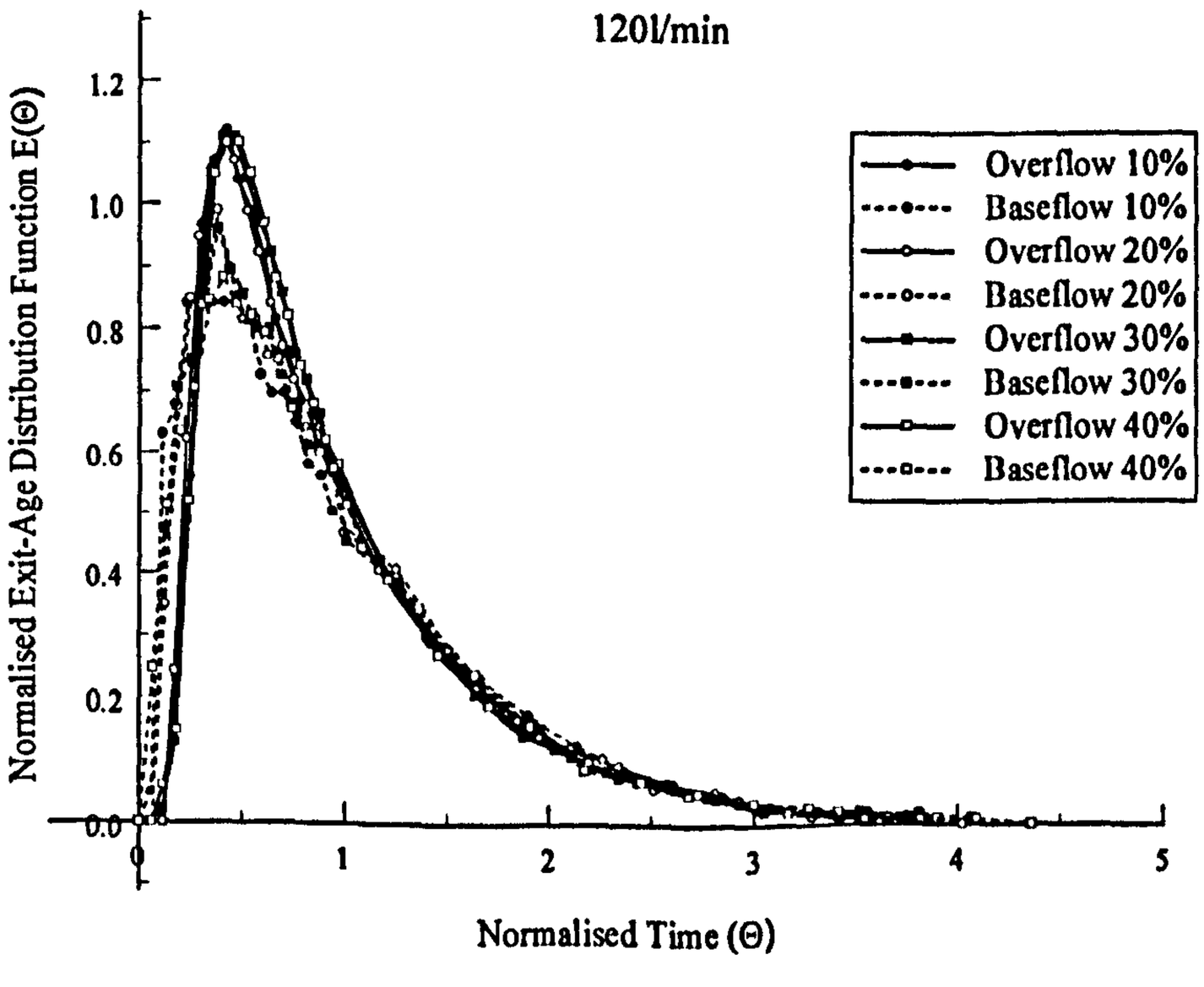

Fig. 6.25 Prototype HDVS Baseflow (SP2) - Comparison of Normalised Exit-Age Distribution Curves E(Θ) using the Method of Moments

Fig. 6.26 shows the experimental mean residence time for all inlet flow rates plotted against the flow split. The overflow and baseflow component values are relatively constant across the range of flow splits for each inlet flow rate. The magnitude of the overflow mean residence time relative to the baseflow generally follows a similar trend as the RTD curves time to peak concentration (section 6.2.1.1). The experimental mean residence time values are similar to the theoretical mean residence time calculated for the prototype HDVS operating with no baseflow and without the sludge hopper for the same inlet flow rate (Table 4.17).

Table 6.12 Prototype HDVS Baseflow (SP2) – Comparison of First and Second Moments Calculated from RTD Experimental Data

Flow Rate (l/min)	Flow Split (%)	Experimental Mean Residence Time (min)		Variance (min^2)		Normalised Variance (σ_θ^2)	
		O	B	O	B	O	B
45	10	13.431	9.367	71.791	67.280	0.398	0.767
	20	13.227	8.340	67.543	52.140	0.386	0.750
	30	12.581	8.644	64.922	61.471	0.410	0.823
	40	12.418	7.326	54.420	42.415	0.353	0.790
60	10	9.785	6.704	41.961	33.943	0.438	0.755
	20	9.264	6.634	35.739	31.025	0.416	0.705
	30	9.027	6.171	35.928	26.041	0.441	0.684
	40	8.802	6.503	31.027	26.247	0.400	0.621
120	10	4.092	4.211	7.353	9.192	0.439	0.518
	20	4.263	3.975	8.292	7.636	0.456	0.483
	30	4.258	3.934	8.002	8.037	0.441	0.519
	40	4.098	3.667	7.346	6.933	0.437	0.516
240	10	1.985	2.239	1.803	2.518	0.457	0.502
	20	2.159	2.244	2.297	2.488	0.493	0.494
	30	2.116	2.307	2.152	2.212	0.481	0.416
	40	2.033	2.062	1.780	1.727	0.431	0.406
360	10	1.651	1.961	1.354	1.770	0.497	0.460
	20	1.721	1.869	1.282	1.390	0.433	0.398
	30	1.733	1.564	1.300	1.168	0.433	0.478
	40	1.827	1.606	1.433	1.247	0.429	0.484

Appendix E.3.3 shows the errors between the theoretical and experimental mean residence time calculated using the method of moments (Table 6.12). The experimental

values are all greater than the theoretical values and therefore, all the errors are positive. This trend was also observed for the RTD investigation undertaken on the prototype HDVS operating with no baseflow and without the sludge hopper (section 4.4.6). The average error between the overflow experimental mean residence time values and the theoretical is +28% and similarly for the baseflow is +11%. However, the errors are significantly less than the errors obtained for the prototype HDVS operating with no baseflow and without the sludge hopper (section 4.4.6.1).

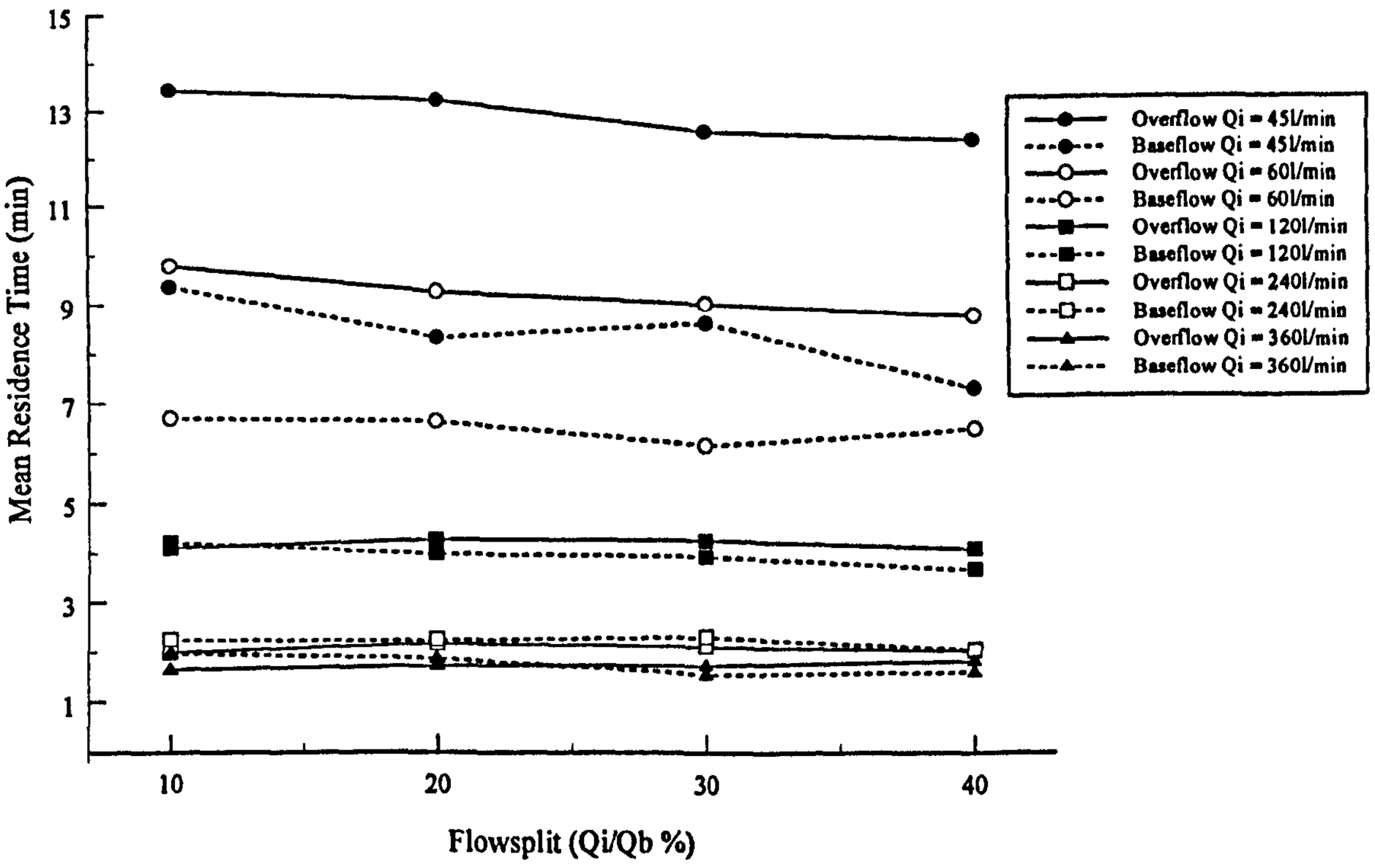

Fig. 6.26 Prototype HDVS Baseflow (SP2) - Experimental Mean Residence Time using the Method of Moments

Table 6.13 shows the estimated prototype HDVS volume calculated using the experimental mean residence time. The prototype HDVS operating without the sludge hopper (Fig. 6.1) has a volume of approximately 430 litres and the estimated experimental volumes have an average error of +18%. Chapter 4 showed the influence of the RTD experimental duration and the effect of the truncation time on the experimental

mean residence time however, this has not been investigated for any of the model or prototype HDVS baseflow RTD data (section 6.2.1.1). The percentage of the experimental volume estimation associated with the overflow and baseflow components is also presented in Table 6.13. These values show that the volume split is approximately proportional to the flow split.

Table 6.13 Prototype HDVS Baseflow (SP2) – Estimated Prototype HDVS Volume using the Experimental Mean Residence Time Calculated from the Method of Moments

Flow Rate (l/min)	Flow Split (%)	Volume (l)		Percentage of Experimental Volume (%)		Total Volume (l)
		O	B	O	B	
45	10	543.956	42.1520	92.808	7.1920	586.107
	20	476.172	75.0600	86.383	13.617	551.232
	30	396.302	116.694	77.252	22.748	512.996
	40	335.286	131.868	71.772	28.228	467.154
60	10	528.390	40.2240	92.926	7.0740	568.614
	20	444.672	79.6080	84.816	15.184	524.280
	30	379.134	111.078	77.341	22.659	490.212
	40	316.872	156.072	67.000	33.000	472.944
120	10	441.936	50.5320	89.739	10.261	492.468
	20	409.248	95.4000	81.096	18.904	504.648
	30	357.672	141.624	71.635	28.365	499.296
	40	295.056	176.016	62.635	37.365	471.072
240	10	428.760	53.7360	88.863	11.137	482.496
	20	414.528	107.712	79.375	20.625	522.240
	30	355.488	166.104	68.154	31.846	521.592
	40	292.752	197.952	59.660	40.340	490.704
360	10	534.924	70.5960	88.341	11.659	605.520
	20	495.648	134.568	78.647	21.353	630.216
	30	436.716	168.912	72.110	27.890	605.628
	40	394.632	231.264	63.051	36.949	625.896

Fig. 6.27 shows the ADM parameters (P_e) calculated using the method of moments for all flow splits and inlet flow rates. The TISM parameters (N) show the same trend as the ADM parameters as they are both calculated directly from the normalised variance (eqn. 4.6) and this is illustrated for the model HDVS (section 6.2.1.1 and 6.2.2.1). Therefore the TISM parameter curves are presented in appendix E.3.8 and all numerical

values are provided in appendix E.3.9. The Peclet number (P_e) for both the overflow and baseflow components remain relatively stable across the range of flow splits investigated for the same inlet flow rate. The overflow Peclet number (P_e) increases as the inlet flow rate decreases and is the same relationship achieved for the prototype HDVS operating with no baseflow and without the sludge hopper (section 4.4.6). However, the baseflow component shows the opposite trend with higher Peclet numbers (P_e) at high inlet flow rates. The Peclet numbers (P_e) suggest that the mixing regime is fairly uniform throughout the volume of the HDVS for the same inlet flow rate and is therefore, implying a well-mixed system rather than a perfect plug-flow mixing regime (section 4.1). The overflow ADM and TISM parameters are in the same order of magnitude as calculated for the prototype HDVS operating without a baseflow component and without the sludge hopper (section 4.4.6.1).

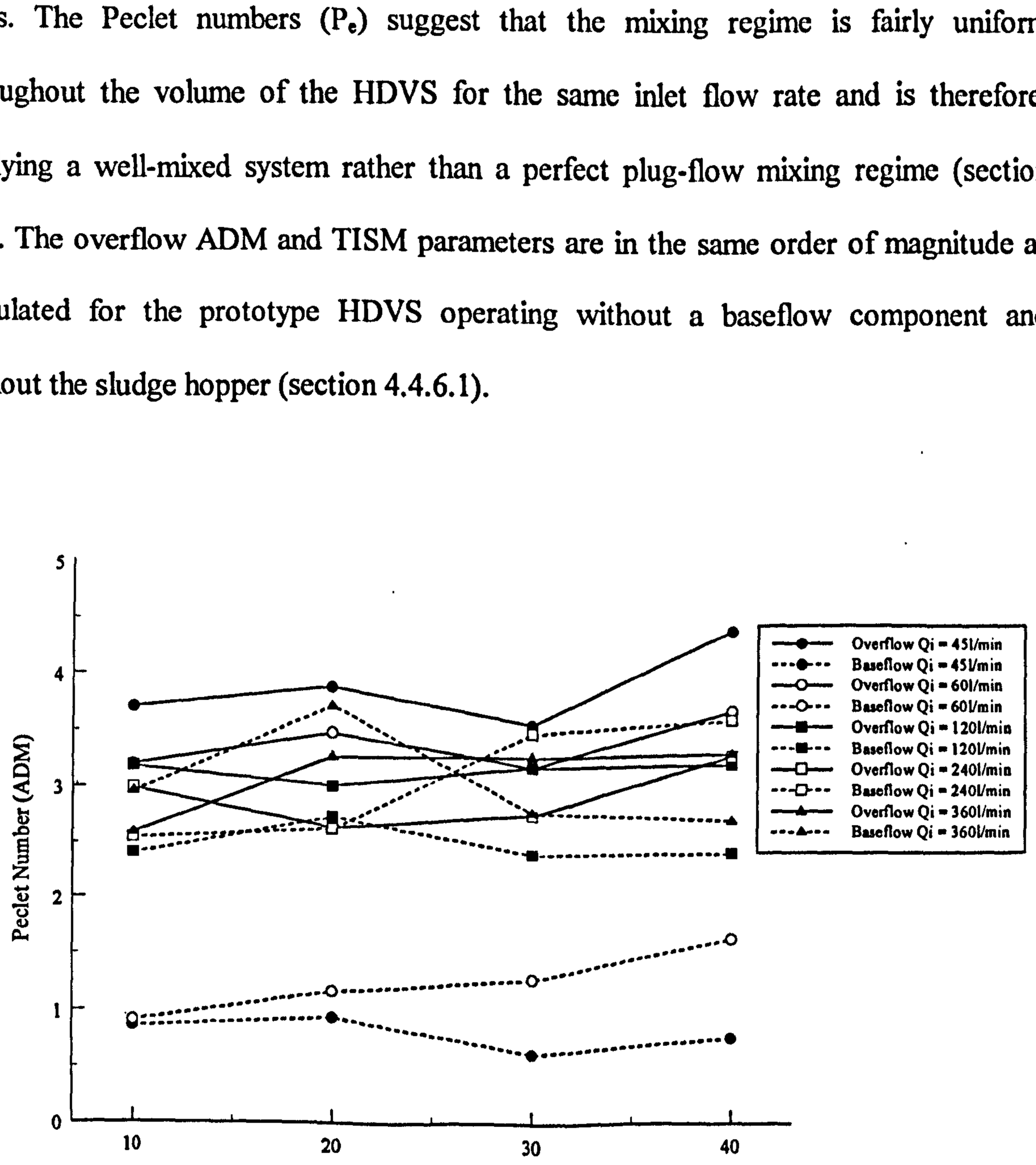

Fig. 6.27 Prototype HDVS Baseflow (SP2) - Comparison of the ADM Parameters Calculated using the Method of Moments

Appendix E.3.9 also details the summation of the individual overflow and baseflow component ADM and TISM parameters at each flow split for all inlet flow rates. This describes the mixing regime of the total flow within the prototype HDVS operating with a baseflow component. The reader is referred to the results and conclusions presented for the model HDVS operating with a baseflow component measured at SP2, as the same trend in the ADM and TISM total flow parameters is observed (section 6.2.1.1). The total flow ADM and TISM parameters for the prototype HDVS operating with a baseflow component measured at SP2 and SP3 are compared and also presented in section 6.2.6 (Table 6.21).

Fig. 6.28 compares the experimental exit-age distribution function E(t) curves to the TISM (eqn. 4.9) and ADM (eqn. 4.11) curves obtained using the method of moments for an inlet flow rate of 120l/min. The remaining flow rates and all correlation parameters (R^2 and ESS) are presented in appendix E.3.10 and E.3.11 respectively. The ADM provides the best-fit to the overflow component for all inlet flow rates and flow splits and also to the baseflow component for the lowest inlet flow rate of 45l/min. The TISM for a parameter N=2 provides the best-fit to the baseflow component for all inlet flow rates greater than 45l/min. The TISM parameter N=2 is only presented for reasons discussed in section 6.2.1.1. The best-fit overflow ADM correlation parameters generally decrease and the baseflow TISM correlation parameters increase as the flow rate increases. This is the expected relationship due to the limitations of both models and the non-ideal flow behaviour associated with each flow component as the flow rate increases (section 6.2.1.1). The relationship between the ADM and TISM correlation parameters and the HDVS's non-ideal flow behaviour is also discussed in chapter 4 (section 4.4.3).

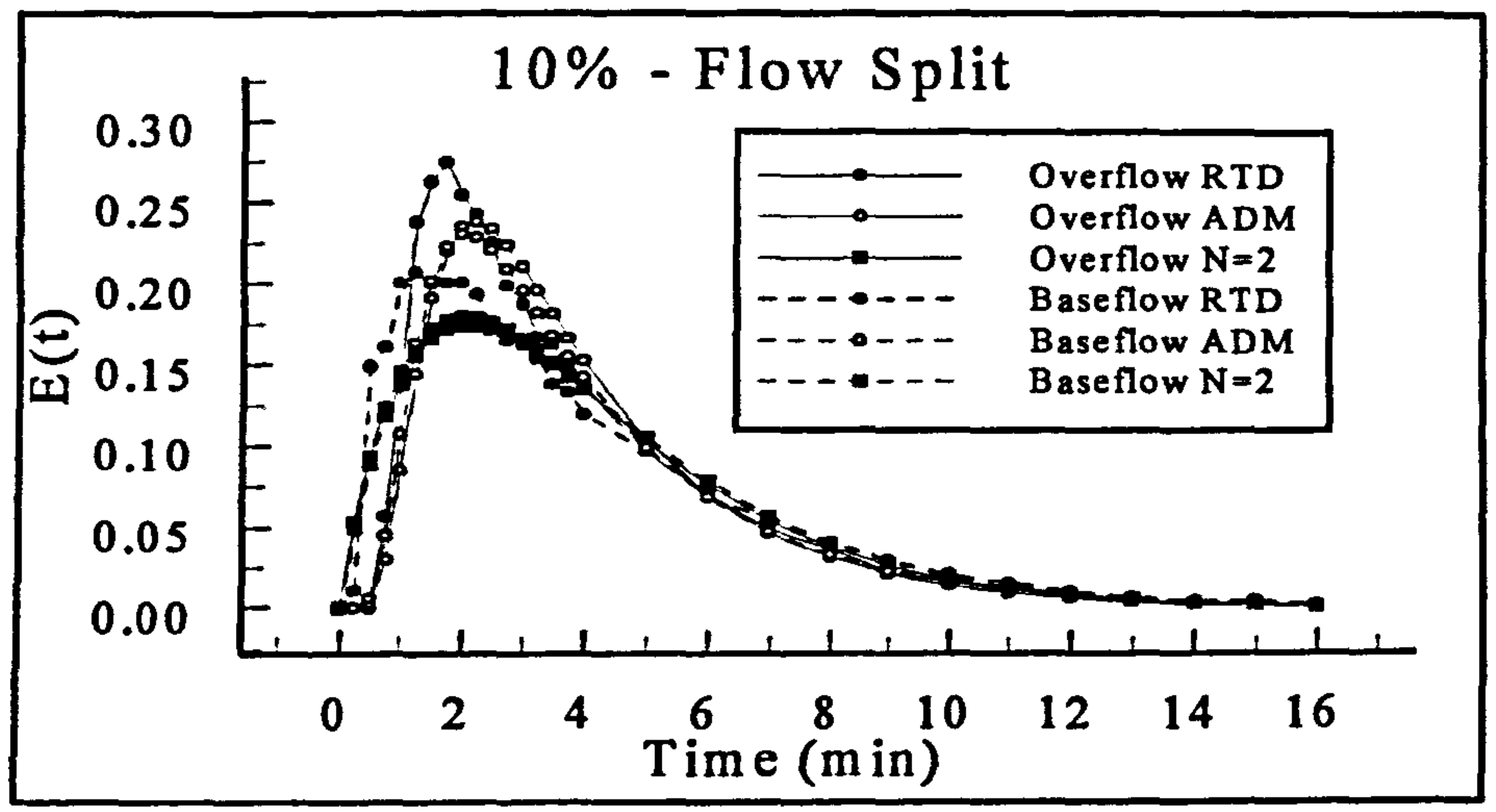

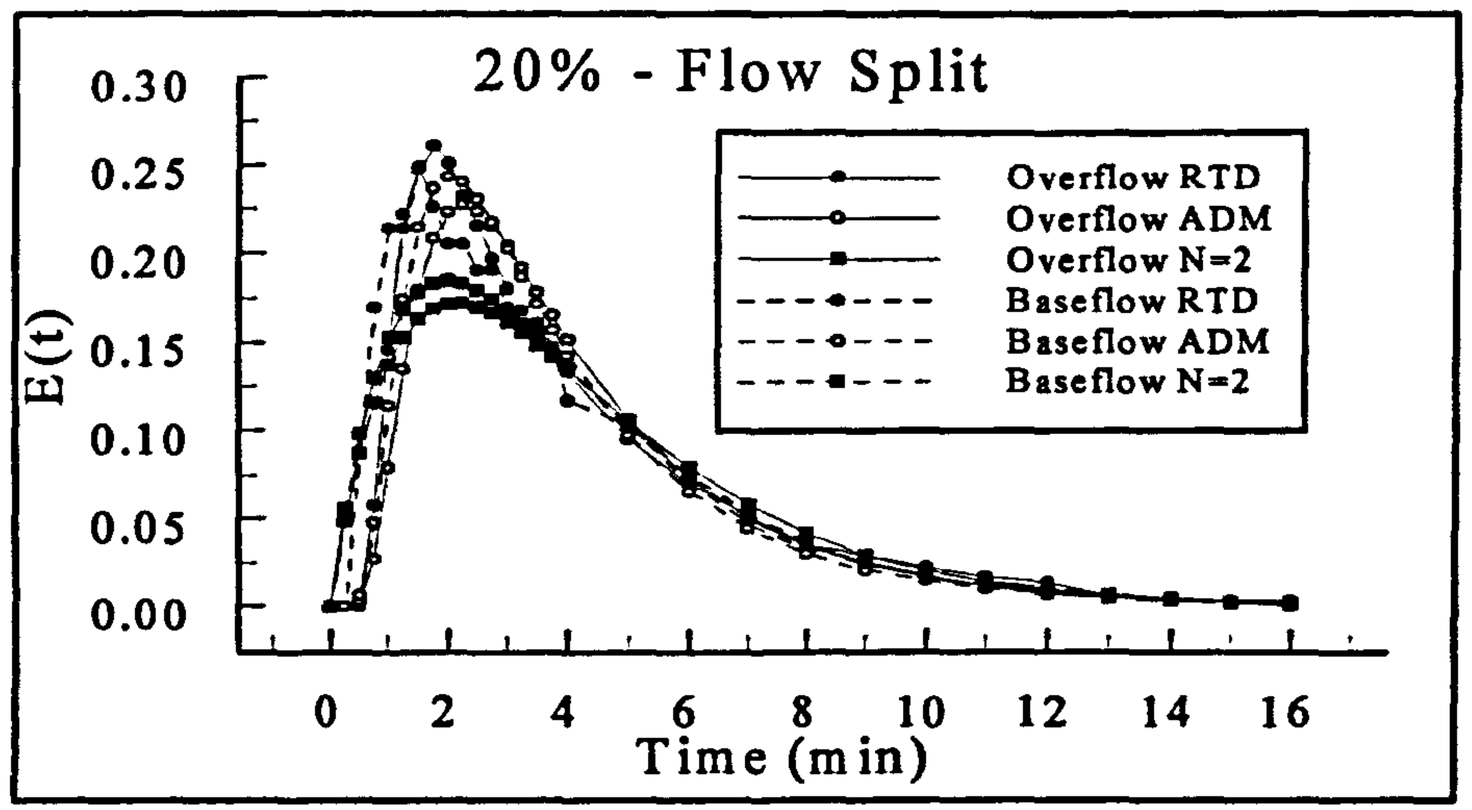

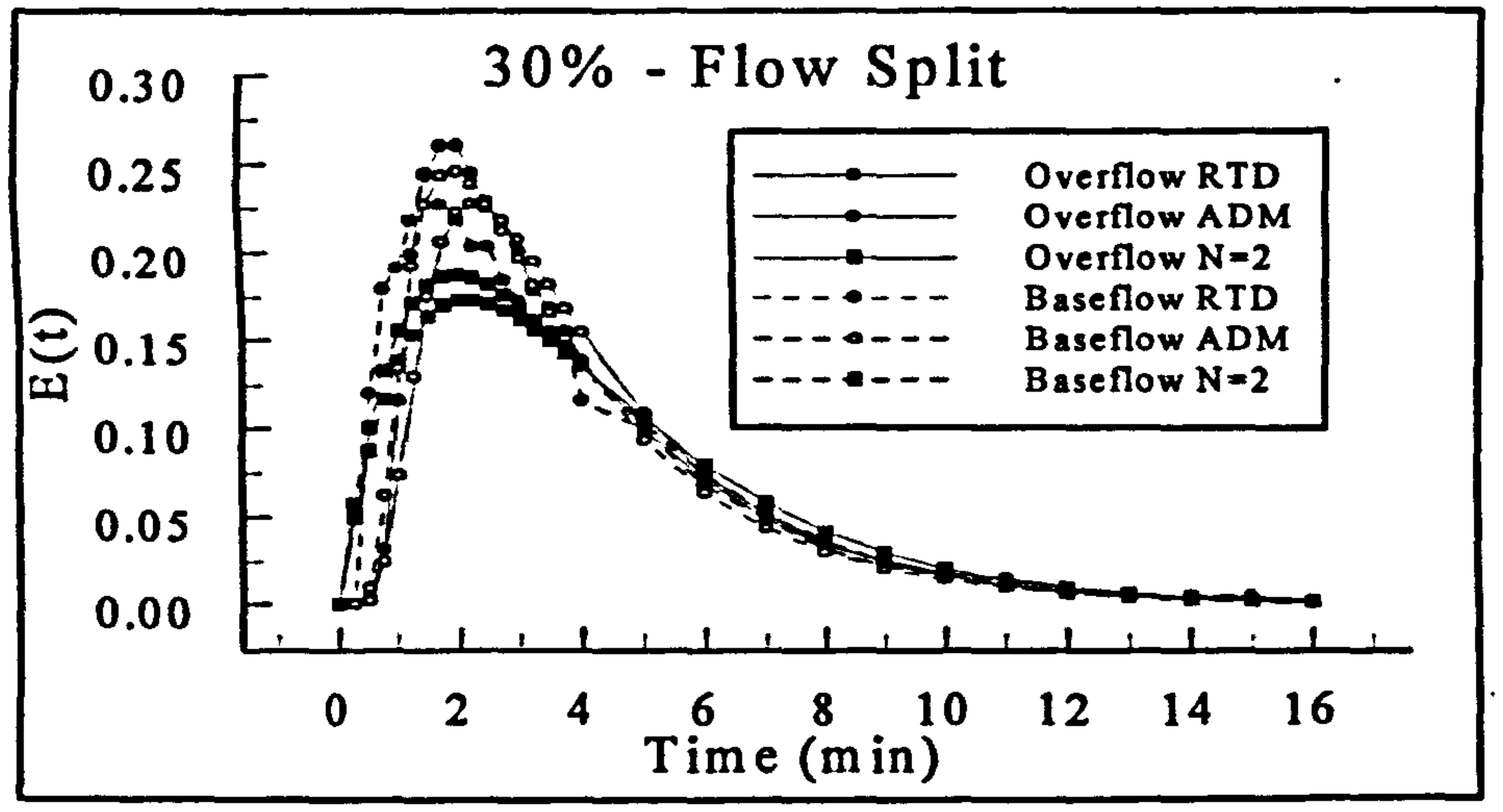

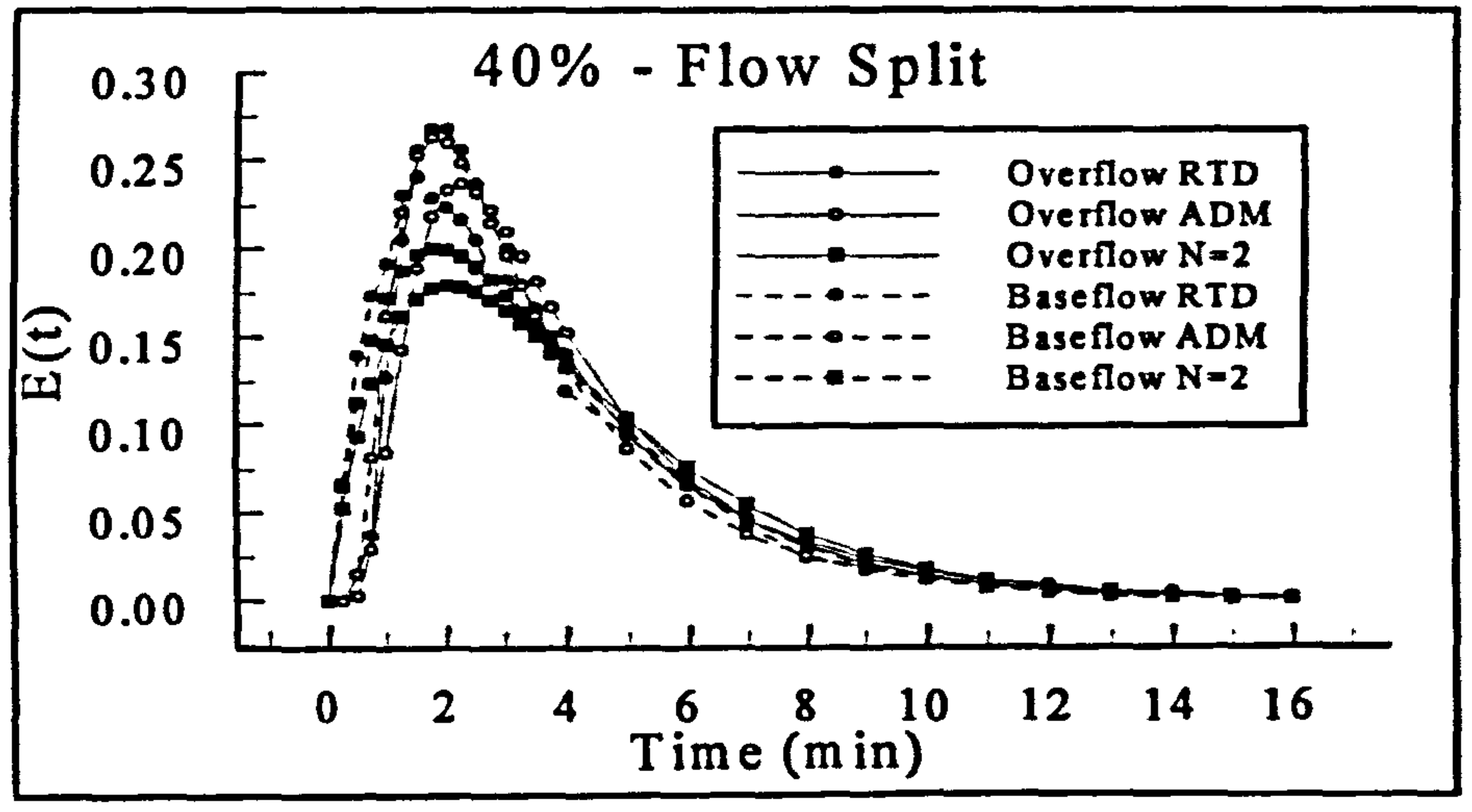

Fig. 6.28 - Prototype HDVS Baseflow (SP2) - Comparison of E(t), ADM and TISM Curves Calculated using the Method of Moments for an Inlet Flow Rate of 120l/min

6.2.4.2 Non-Linear Regression Data Analysis

Fig. 6.29 and 6.30 show the RTD normalised curves E(Θ) for an inlet flow rate of 120l/min. The RTD curves were normalised using the experimental mean residence time calculated from the ADM (eqn. 4.11) and TISM (eqn. 4.9) non-linear regression technique (section 4.3.3). The remaining flow rates are shown in appendix E.3.12 and E.3.13. The RTD normalisation procedure using the method of moments (Fig. 6.25) and TISM-non-linear regression (Fig. 6.30) experimental mean residence time provide similar RTD normalised curves E(Θ) as the theoretical mean residence time (Fig. 6.24). This trend in the prototype HDVS RTD normalised curves E(Θ) measured at SP2 is also provided by the model HDVS (section 6.2.1.2).

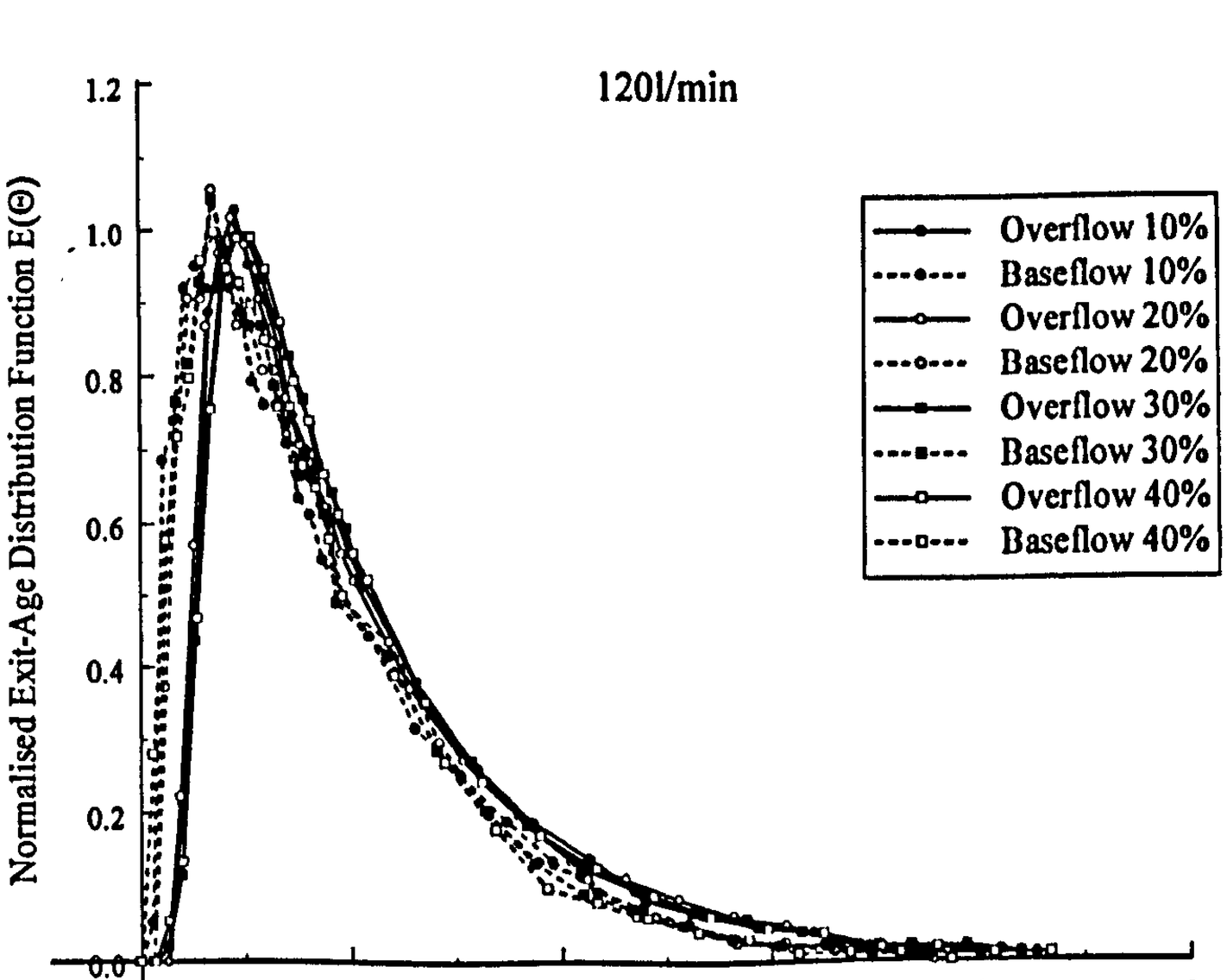

Fig. 6.29 Prototype HDVS Baseflow (SP2) - Comparison of Normalised Exit-Age Distribution Curves E(Θ) using Non-Linear Regression and the ADM

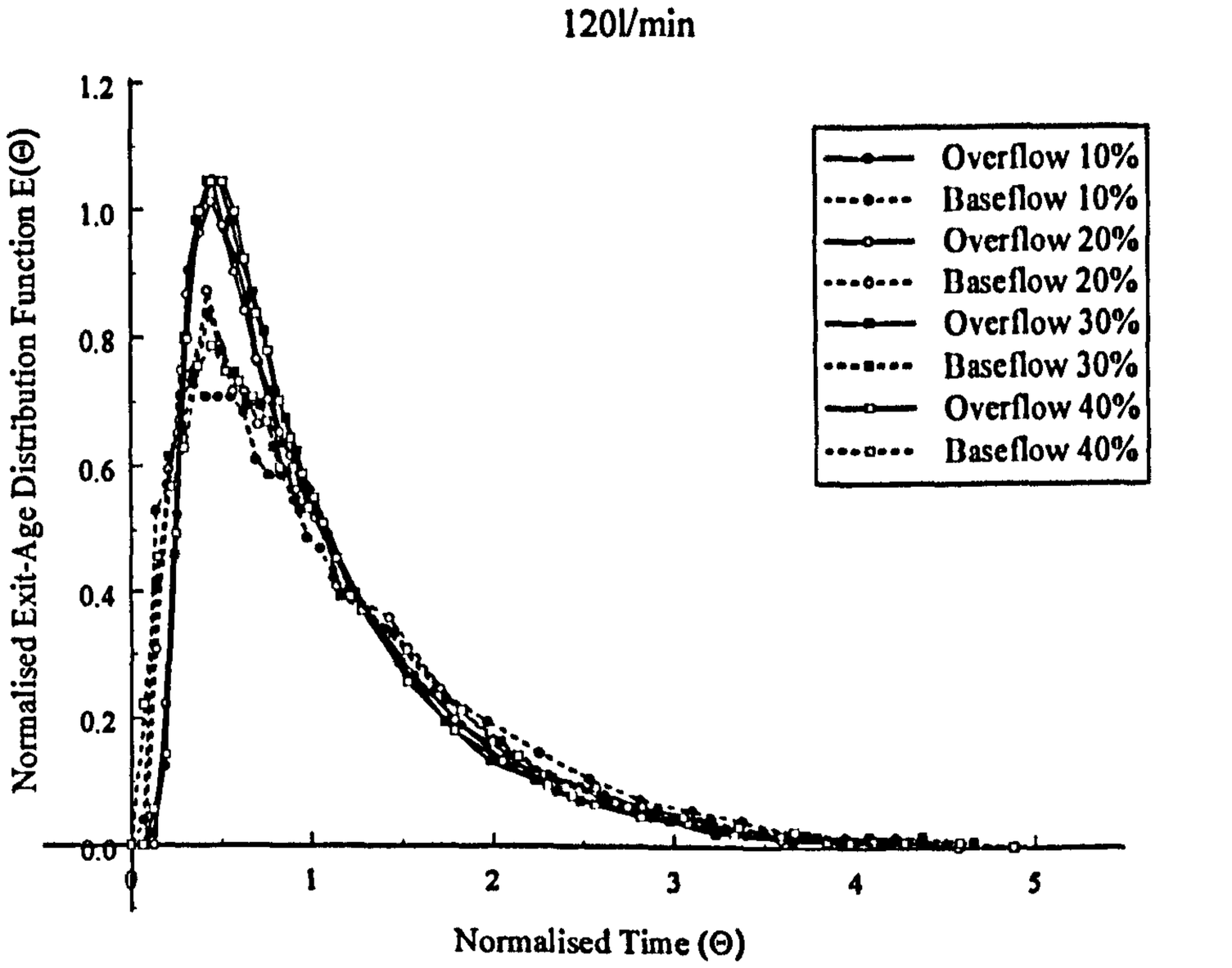

Fig. 6.30 Prototype HDVS Baseflow (SP2) - Comparison of Normalised Exit-Age Distribution Curves E(Θ) using Non-Linear Regression and the TISM

Tables 6.14 and 6.15 show the ADM and TISM parameters calculated using non-linear regression. The experimental mean residence time values calculated using non-linear regression are of a similar order of magnitude as calculated using the method of moments (section 6.2.4.1). The ADM estimates a larger mean residence time for the baseflow component compared the TISM using non-linear regression. Appendix E.3.14 shows the ADM and TISM experimental mean residence time for all inlet flow rates plotted against the flow split. The curves show a similar trend as the experimental mean residence time values calculated using the method of moments (Fig. 6.26). The ADM and TISM baseflow experimental mean residence time values are greater than the overflow at inlet flow rates above 120-240l/min (Table 6.14 and 6.15) and is due to the overflow and baseflow components short-circuiting at high and low flow rates respectively (section 6.4.2.1). Additionally, the ADM non-linear regression iteration technique was subject to a constraint on the baseflow component normalised variance

parameter (eqn. 4.11) and therefore, reduces confidence in the estimated mean residence time and the ADM parameter (P_e) discussed below. The ADM and TISM mean residence time values for the overflow and baseflow component generally follows the same trend as the RTD curves time to peak concentration (section 6.2.4.1). The average error between the ADM overflow experimental mean residence time and the theoretical mean residence time is +15% and for the baseflow is +8%. Similarly the average error between the TISM overflow experimental mean residence time values and the theoretical mean residence time is +18% and for the baseflow is -9% (section 6.2.1.1).

Table 6.14 Prototype HDVS Baseflow (SP2) – Comparison of ADM Parameters using Non-Linear Regression

Flow Rate (l/min)	Flow Split (%)	Experimental Mean Residence Time (min)		Normalised Variance (σ_θ^2)		Peclet Number (P_e)	
		O	B	O	B	O	B
45	10	12.989	8.453	0.545	0.999	2.175	0.010
	20	12.377	7.876	0.473	0.999	2.815	0.010
	30	11.633	7.788	0.484	0.999	2.710	0.010
	40	11.551	6.721	0.403	0.917	3.635	0.265
60	10	9.790	5.536	0.580	0.999	1.910	0.010
	20	9.183	6.467	0.546	0.999	2.165	0.010
	30	8.878	6.372	0.514	0.999	2.435	0.010
	40	8.770	6.869	0.467	0.923	2.880	0.245
120	10	3.746	4.600	0.521	0.999	2.370	0.010
	20	3.903	4.234	0.557	0.873	2.080	0.420
	30	3.810	4.266	0.473	0.910	2.820	0.290
	40	3.688	4.143	0.464	0.887	2.910	0.370
240	10	1.857	2.392	0.525	0.999	2.340	0.010
	20	1.982	2.302	0.558	0.810	2.075	0.670
	30	1.905	2.275	0.504	0.559	2.520	2.065
	40	1.835	1.989	0.449	0.518	3.075	2.400
360	10	1.275	1.703	0.551	0.830	2.130	0.585
	20	1.342	1.653	0.520	0.729	2.380	1.035
	30	1.360	1.334	0.462	0.610	2.930	1.705
	40	1.408	1.441	0.469	0.661	2.860	1.395

Table 6.15 Prototype HDVS Baseflow (SP2) – Comparison of TISM Parameters using Non-Linear Regression

Flow Rate (l/min)	Flow Split (%)	Experimental Mean Residence Time (min)		N-Tanks	
		O	B	O	B
45	10	13.371	6.511	2.372	1.883
	20	13.371	6.041	2.427	1.914
	30	12.483	6.009	2.397	1.884
	40	13.093	5.284	2.481	1.954
60	10	9.554	4.776	2.286	1.536
	20	9.159	5.126	2.304	1.907
	30	8.828	4.896	2.255	1.925
	40	8.983	5.480	2.299	1.987
120	10	3.828	3.549	2.269	1.931
	20	3.894	3.498	2.244	2.072
	30	4.024	3.432	2.318	2.050
	40	3.898	3.274	2.315	2.022
240	10	1.876	1.906	2.265	1.952
	20	1.957	1.995	2.239	2.121
	30	1.960	2.233	2.270	2.282
	40	1.949	2.007	2.322	2.296
360	10	1.232	1.424	2.167	2.060
	20	1.321	1.471	2.194	2.148
	30	1.382	1.242	2.244	2.165
	40	1.430	1.273	2.236	2.115

Appendix E.3.15 shows the estimated prototype HDVS volume calculated using the ADM and TISM experimental mean residence time. As stated above the prototype HDVS operating without the sludge hopper (Fig. 6.1) has a volume of 430 litres. The ADM and TISM estimated prototype HDVS volume have an average error of +10%. The ADM and TISM provide a better estimation of the prototype HDVS volume compared to the method of moments (section 6.4.1.1) for reasons discussed in section 4.4.3. The percentage of the estimated experimental volume associated with the overflow and baseflow components is also presented in appendix E.3.15. These values show that the volume split is approximately proportional to the flow split.

The baseflow component ADM normalised variance parameter (eqn. 4.11) is approximately equal to 1 at low flow rates and therefore implies that the mixing regime is approaching complete mixing (Table 6.14) (section 6.2.3). This occurred as initial ADM non-linear regression simulations resulted in a normalised variance greater than 1 and is not permitted, as it is out of the permissible parameter range (section 4.3.1). Subsequently a constraint was applied to the ADM normalised variance parameter in the EXCEL SOLVER toolbar for it not to be greater than 0.999 to estimate the mean residence time and ADM parameter (P_e) (section 4.3.3). This constraint was also required for the model HDVS baseflow component measured at SP2 (section 6.2.1.2).

Fig. 6.31 illustrates the ADM parameter (P_e) for all inlet flow rates and flow splits. The overflow and baseflow component Peclet number (P_e) increases as the flow split increases for the same inlet flow rate. The overflow Peclet number (P_e) show no significant trend across the range of inlet flow rates. However, the baseflow Peclet number (P_e) is greater at high inlet flow rates and is the same relationship as obtained using the method of moments (section 6.2.4.1). At low flow rates the baseflow component Peclet number (P_e) is approximately equal to zero for some flow splits. This is due to the constraint applied in the ADM non-linear regression simulation procedure described above and implies that there is a large degree of mixing around the cone region within the HDVS (Fig. 3.1) (section 6.2.3).

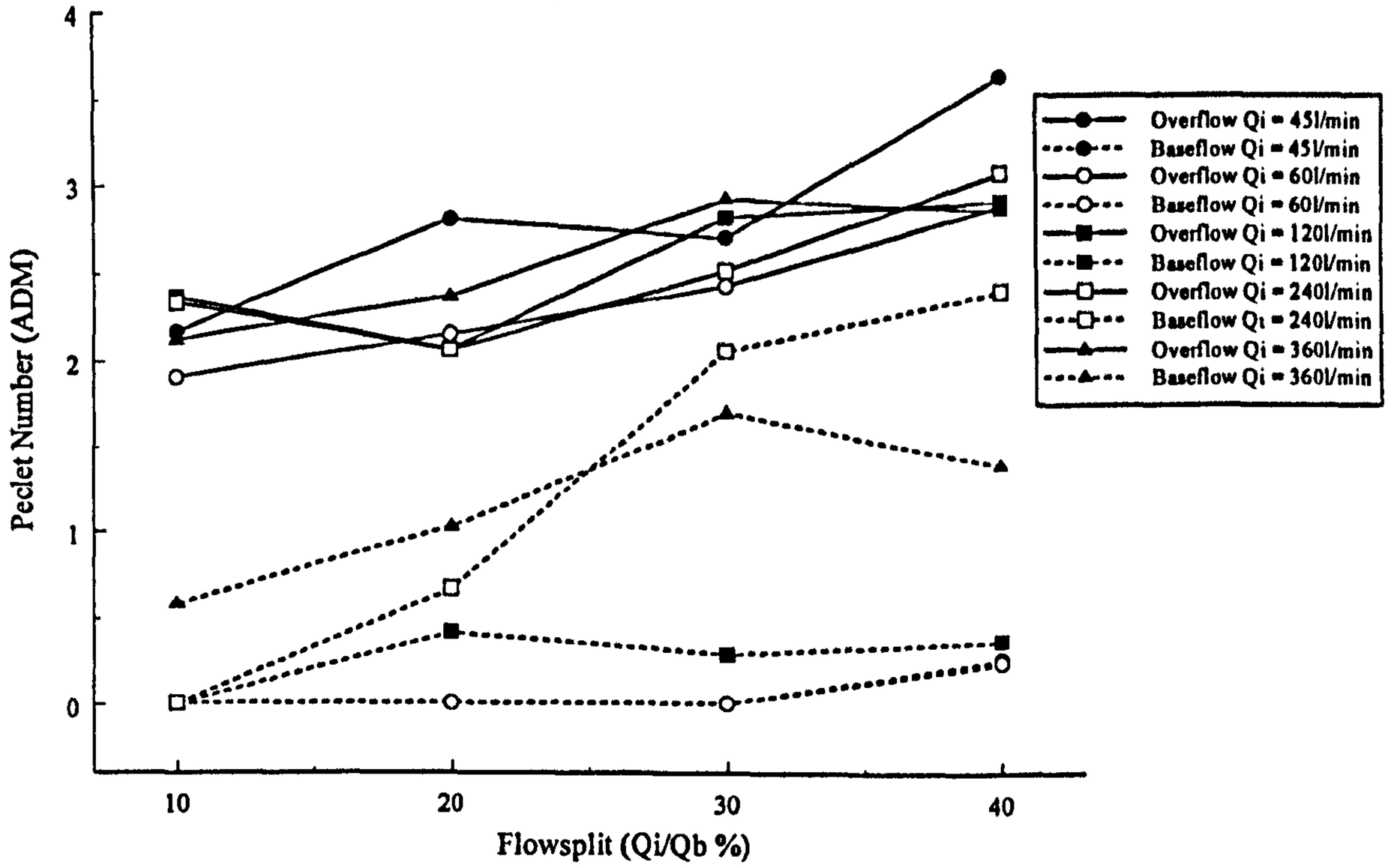

Fig. 6.31 Prototype HDVS Baseflow (SP2) - Comparison of the ADM Parameters Calculated using Non-Linear Regression

Fig. 6.32 illustrates the TISM parameter (N) for all inlet flow rates and flow splits. The overflow and baseflow component TISM parameters are relatively constant across the range of flow splits for the same inlet flow rate. The overflow TISM parameter increases as the inlet flow rate decreases and the baseflow shows the opposite trend with higher TISM parameters at high inlet flow rates. This is the same trend, for both the overflow and baseflow, as obtained using the method of moments (section 6.2.4.1). The TISM parameters suggest that the mixing regime is fairly uniform throughout the volume of the HDVS for the same inlet flow rate and is therefore, implying a well-mixed system rather than a perfect plug-flow mixing regime (section 4.1).

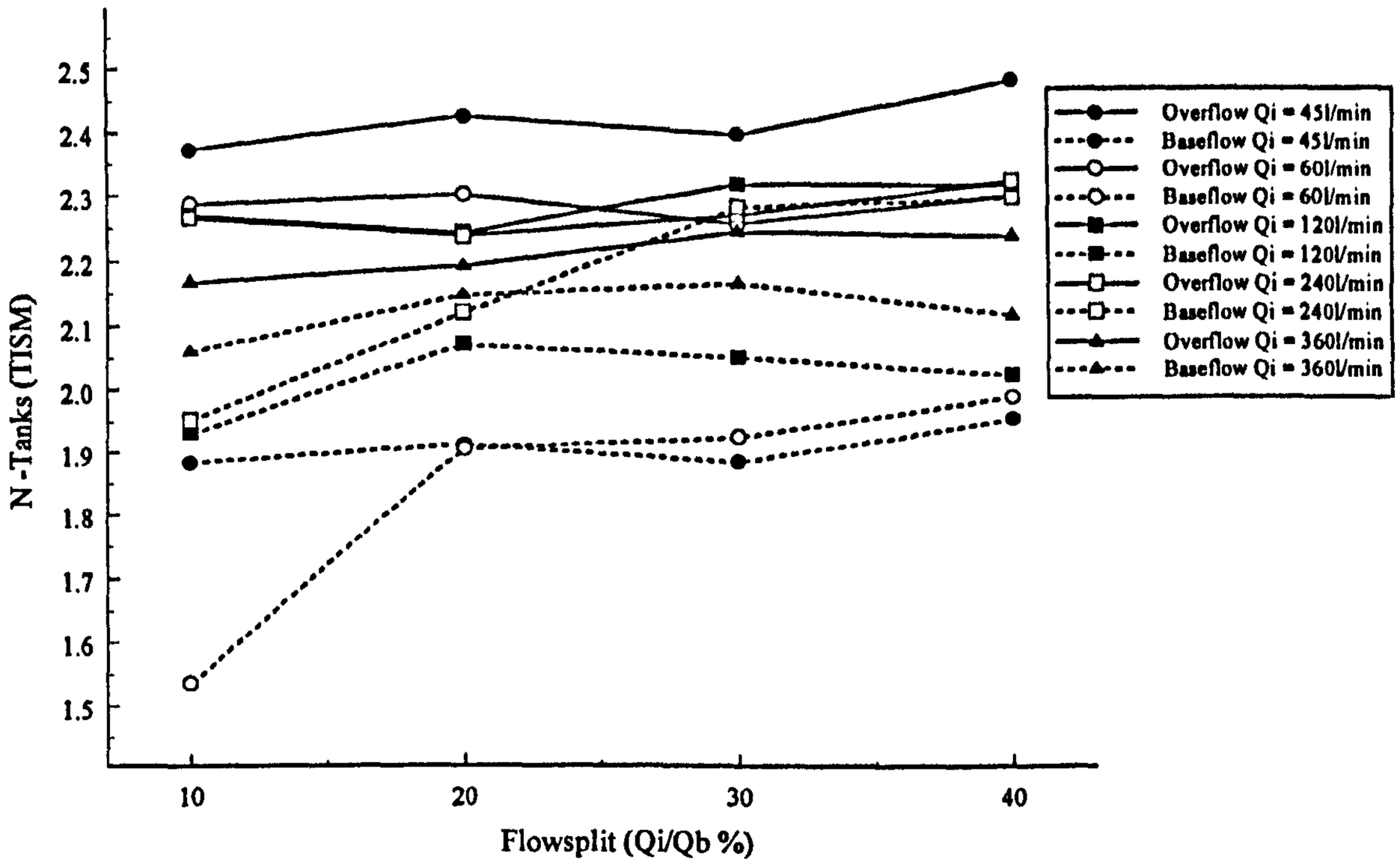

Fig. 6.32 Prototype HDVS Baseflow (SP2) - Comparison of the TISM Parameters Calculated using Non-Linear Regression

Appendix E.3.9 also details the summation of the individual overflow and baseflow component ADM and TISM parameters at each flow split for all inlet flow rates. The ADM total flow results show the same trend as the ADM total flow results obtained using the method of moments (section 6.2.4.1). Although a constraint was applied to the ADM non-linear regression technique, it appears not to significantly effect the total flow results as occurred for the model HDVS (SP2) (section 6.2.1.2). The TISM total flow results show the same relationship as the model HDVS (SP2) (section 6.2.1.2).

Fig. 6.33 compares the experimental exit-age distribution function E(t) curves to the TISM (eqn. 4.9) and ADM (eqn. 4.11) curves for an inlet flow rate of 120l/min and all flow splits. The remaining flow rates and all correlation parameters (R^2 and ESS) are presented in appendix E.3.16 and E.3.17 respectively. The ADM provides the best-fit to both the overflow and baseflow components for all inlet flow rates compared to the

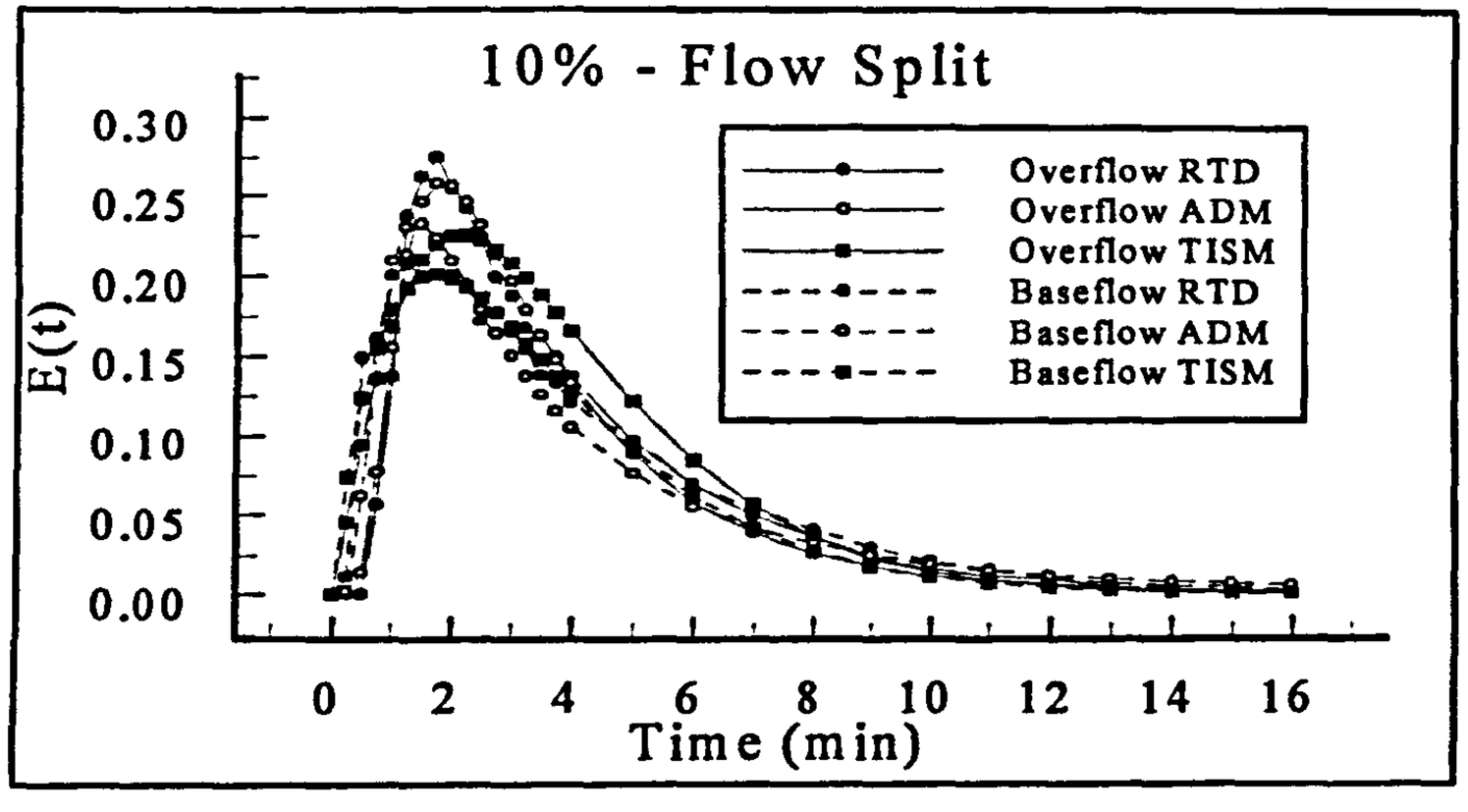

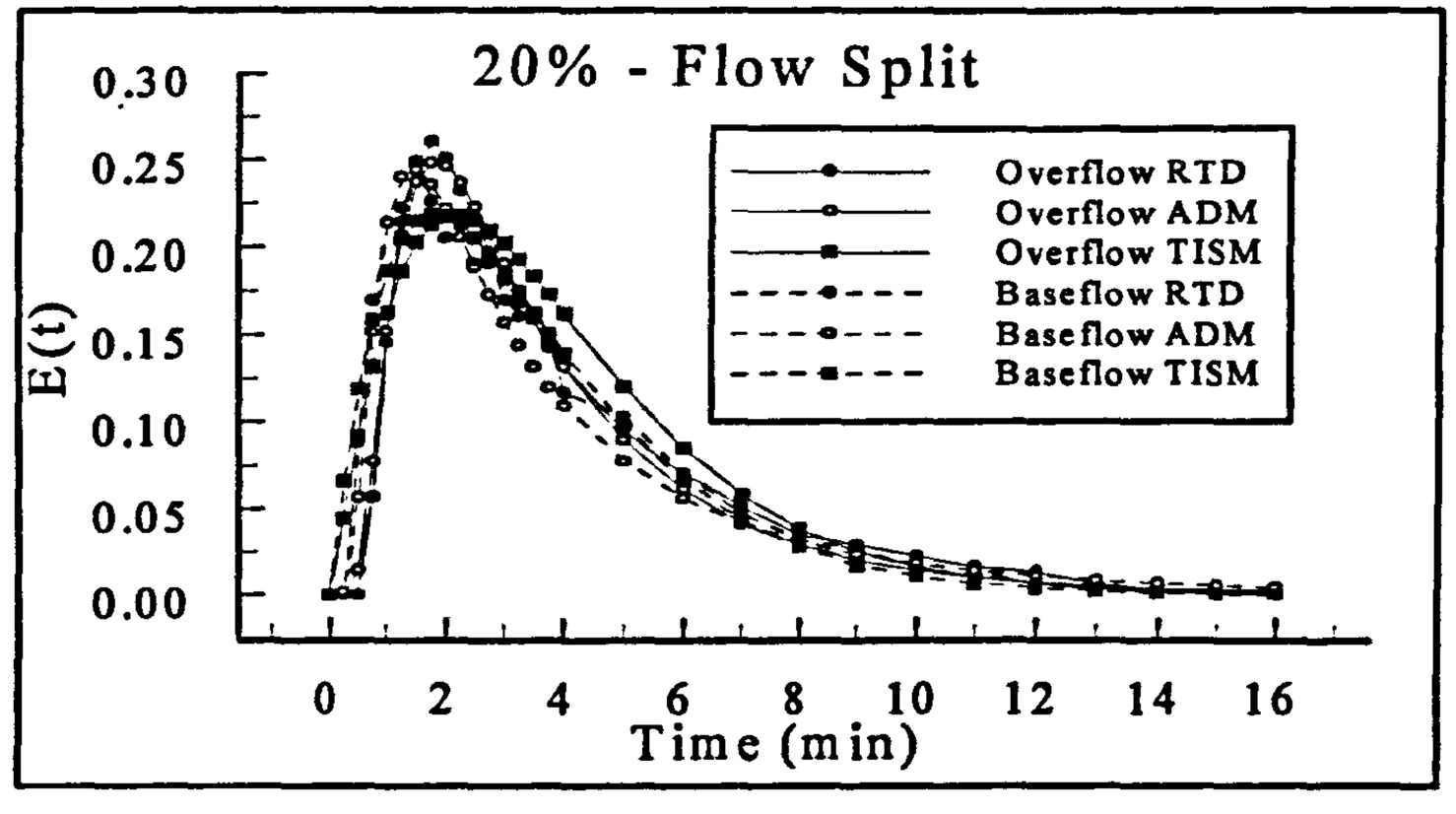

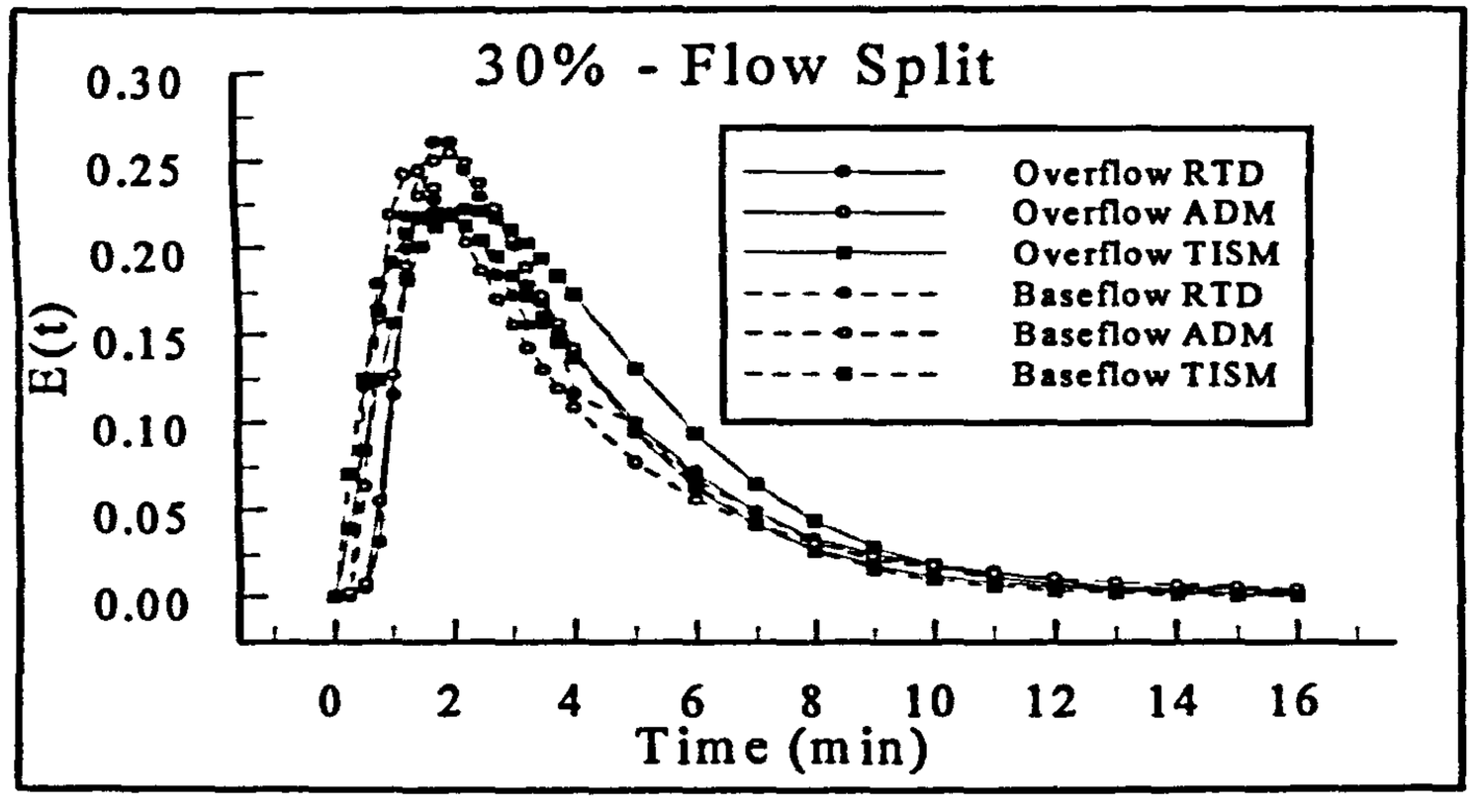

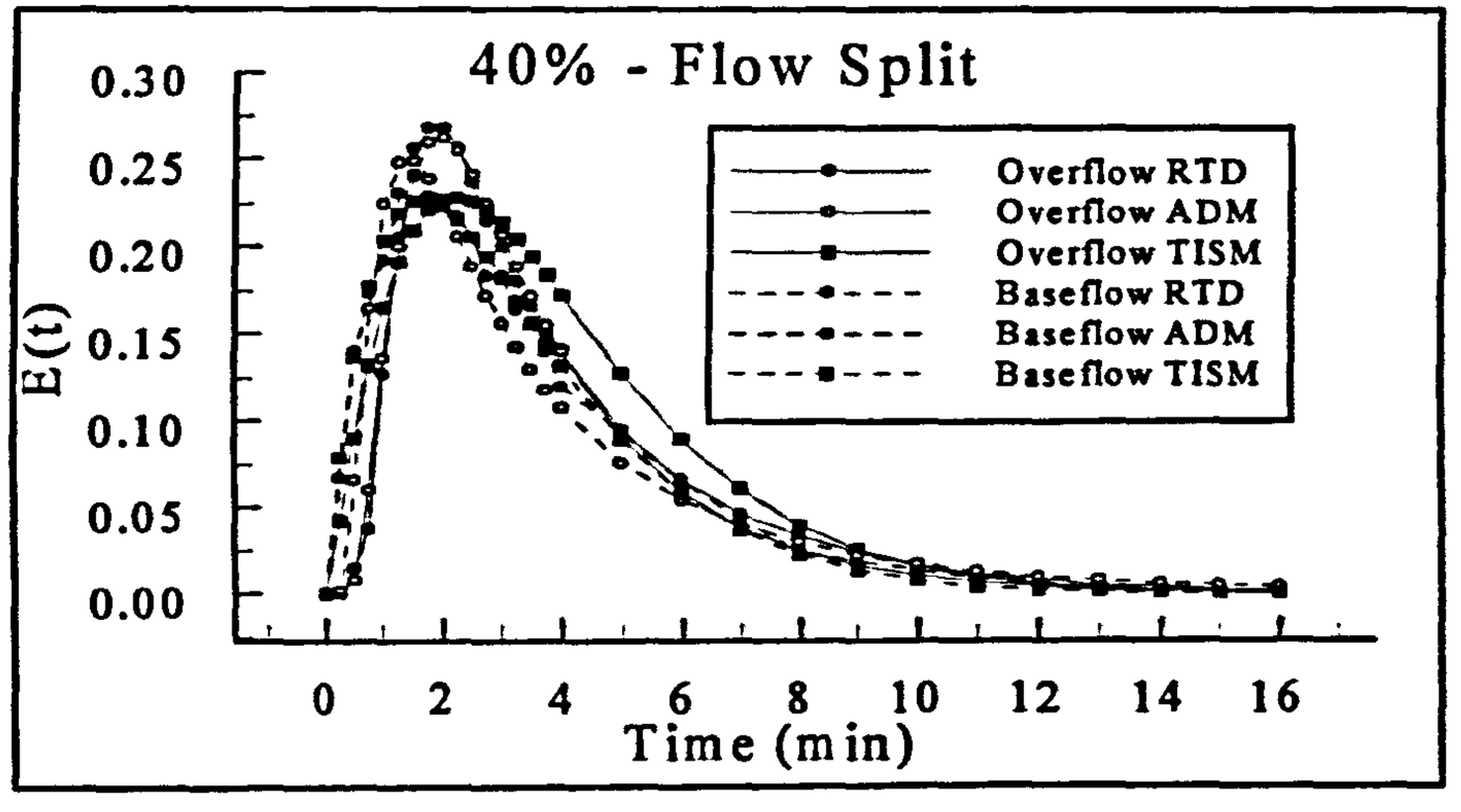

Fig. 6.33 - Prototype HDVS Baseflow (SP2) - Comparison of E(t), ADM and TISM Curves Calculated using Non-Linear Regression for an Inlet Flow Rate of 120l/min

TISM. The ADM correlation parameters for both the overflow and baseflow component are of a similar order of magnitude and also remain stable for the range of inlet flow rates and flow splits investigated. However, even though the TISM does not provide the best-fit, the correlation parameters do follow the expected trend for reasons discussed in section 6.2.1.1. The non-linear regression correlation parameters are generally better than those obtained for the method of moments. This is due to the flexibility provided by the direct non-linear regression curve fitting procedure (section 4.4.3).

6.2.5 Prototype Hydrodynamic Vortex Separator (HDVS) Baseflow - Residence Time Distribution (RTD) Pulse Experiments Sample Point 3 (SP3)

6.2.5.1 Method of Moments Data Analysis

This section describes the RTD analysis undertaken on the prototype HDVS operating with a baseflow component measured at sample point 3 (SP3), which is located below the sludge hopper (Fig. 6.1).

The RTD normalisation procedure is the same as used for the model HDVS (SP2) (section 6.2.1.1). The theoretical mean residence time for both the overflow and baseflow components are presented in appendix E.4.3. Fig. 6.34 and 6.35 illustrate the normalised exit-age distribution function E(Θ) curves calculated using the theoretical mean residence time and experimental mean residence time for an inlet flow rate of 120l/min. The remaining flow rates are shown in appendix E.4.4 and E.4.5 respectively. The overflow and baseflow RTD curves illustrate a plug-flow mixing device with a degree of non-ideal flow behaviour. The overflow and baseflow component RTD curves clearly show that short-circuiting is present at high and low flow rates respectively. This

is shown by the position of the RTD curve peak concentration relative to a normalised time (Θ) value of 1 (section 4.3.1). Additionally, the baseflow RTD curves using the theoretical mean residence time peak closer to a normalised time (Θ) value of 1 as the flow split is decreased. Hence, for a small baseflow component flow rate and the same inlet flow rate the baseflow RTD curve has improved plug-flow mixing characteristics and less short-circuiting. The same conclusions were also obtained for the model HDVS RTD normalised curves E(Θ) (SP3) (section 6.2.2.1).

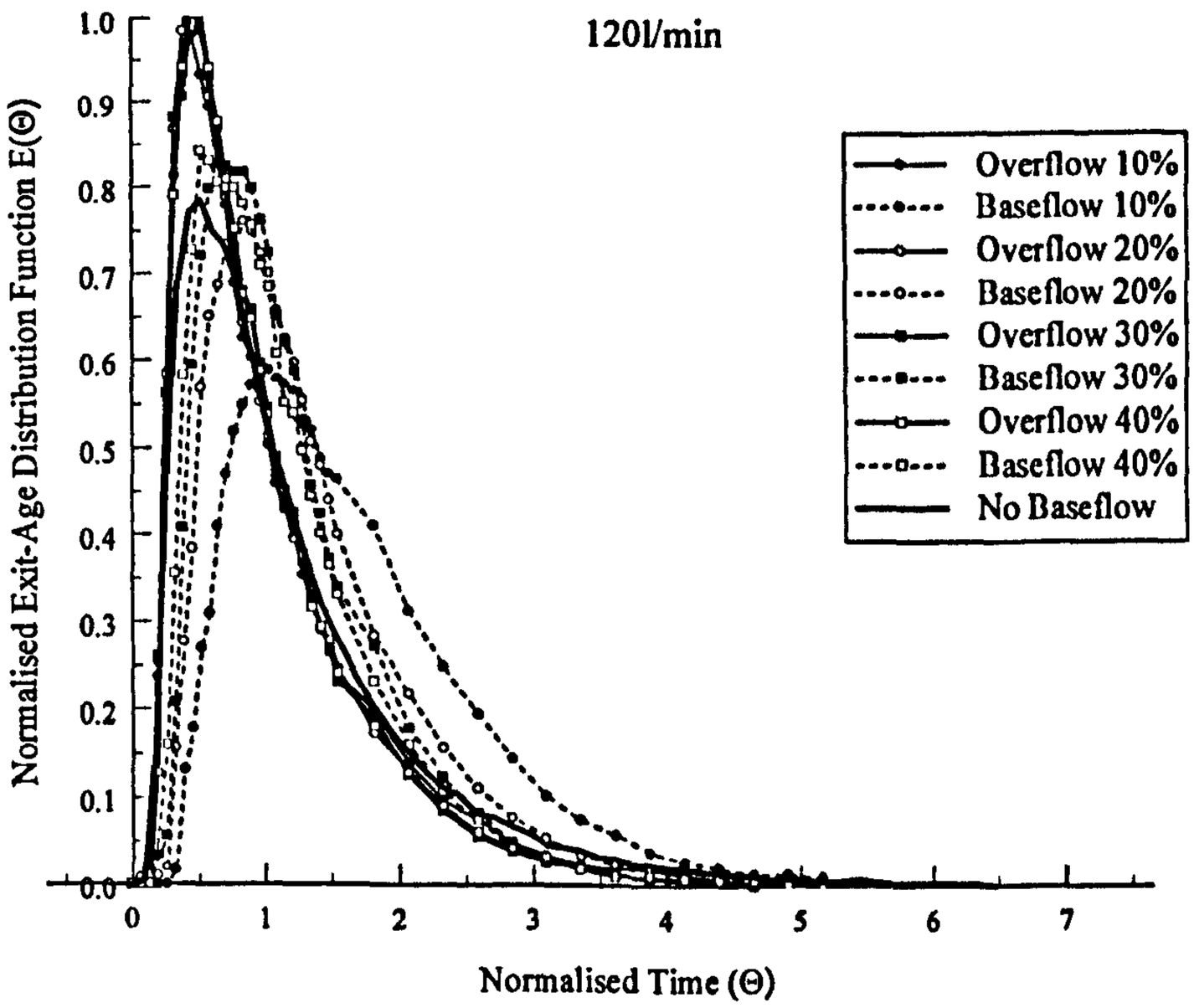

Fig. 6.34 Prototype HDVS Baseflow (SP3) - Comparison of Normalised Exit-Age Distribution Curves E(Θ) using the Theoretical Mean Residence Time

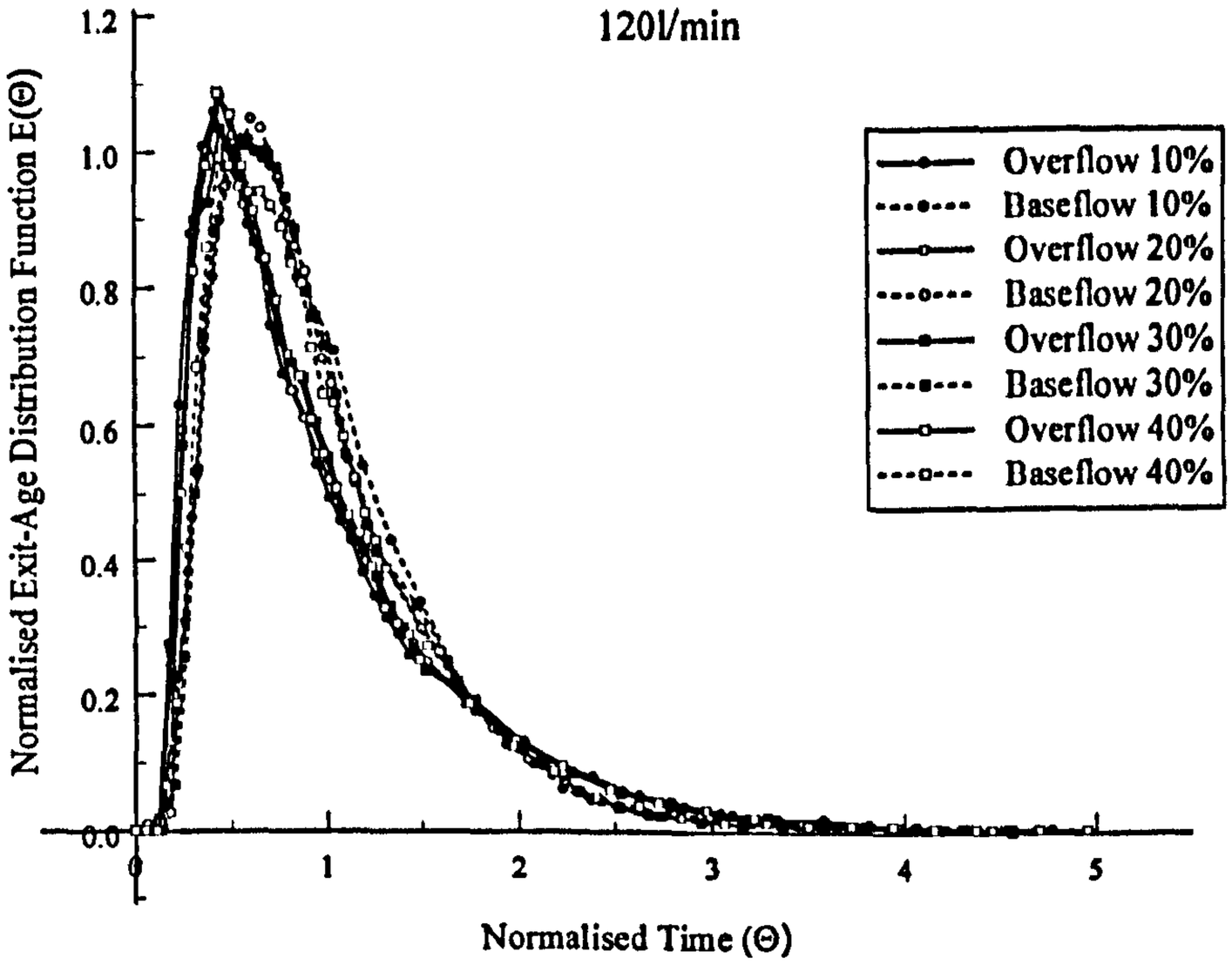

Fig. 6.35 Prototype HDVS Baseflow (SP3) - Comparison of Normalised Exit-Age Distribution Curves E(Θ) using the Method of Moments

Appendix E.4.6 show the time taken for the peak tracer (LiCl) concentration to occur for the RTD curves. The RTD curve time to peak concentration for the prototype HDVS operating with a baseflow component measured at SP2 and SP3 (Fig. 6.1) are compared and also presented in section 6.2.6 (Table 6.20). These values show that for all inlet flow rates greater than 60l/min the baseflow RTD curve peaks after the overflow component and therefore, short-circuiting of the baseflow component occurs at low inlet flow rates as discussed above. The introduction of the sludge hopper greatly increases the transit time of the flow through the baseflow component. Therefore, the sludge hopper appears have slower internal velocities relative to the main volume of the HDVS and acts as a quiescent zone. This was also observed for the model HDVS baseflow component measured at SP3 (section 6.2.2.1). The time to peak concentration is also illustrated by the exit-age distribution function E(t) curves in Fig. 6.38.

The experimental tracer recovery (mass balance) is shown in appendix E.4.7 and

discussed in greater detail in section 6.2.1.1. These values show that near 100% tracer recovery was obtained for all inlet flow rates and flow splits. The overflow values decrease and the baseflow increase as the flow split increases and are approximately proportional to the flow split. The average error is +/- 2%.

Table 6.16 Prototype HDVS Baseflow (SP3) – Comparison of First and Second Moments Calculated from RTD Experimental Data

Flow Rate (l/min)	Flow Split (%)	Experimental Mean Residence Time (min)		Variance (min^2)		Normalised Variance (σ_θ^2)	
		O	B	O	B	O	B
45	10	14.176	12.895	84.031	74.103	0.418	0.446
	20	13.374	12.005	80.846	65.211	0.452	0.452
	30	12.999	10.867	69.666	62.093	0.412	0.526
	40	12.481	9.0190	59.035	45.644	0.379	0.561
60	10	9.564	11.245	38.811	44.099	0.424	0.349
	20	9.070	8.8560	32.070	31.914	0.390	0.407
	30	8.920	8.3820	34.934	28.845	0.439	0.411
	40	9.069	7.9020	32.923	29.206	0.400	0.468
120	10	4.190	6.720	9.020	11.970	0.514	0.265
	20	3.938	5.348	7.340	8.890	0.473	0.311
	30	3.947	4.750	7.073	6.733	0.454	0.298
	40	4.036	4.570	7.560	7.558	0.464	0.362
240	10	2.290	3.646	2.649	3.718	0.505	0.280
	20	2.116	2.849	2.358	2.633	0.527	0.324
	30	1.945	2.577	1.862	2.134	0.492	0.321
	40	2.128	2.522	2.203	2.218	0.487	0.349
360	10	1.270	2.046	0.851	1.311	0.528	0.313
	20	1.433	2.032	1.077	1.152	0.525	0.279
	30	1.455	1.741	1.026	1.060	0.485	0.350
	40	1.472	1.611	0.923	0.920	0.426	0.355

Fig. 6.36 shows the experimental mean residence time for all inlet flow rates plotted against the flow split. The overflow and baseflow component values are relatively constant across the range of flow splits for the same inlet flow rate. The magnitude of the overflow mean residence time relative to the baseflow component follows a similar trend as the RTD curves time to peak concentration i.e. baseflow greater than overflow (section 6.2.1.1). The experimental mean residence time values are similar to the

theoretical mean residence time calculated for the prototype HDVS operating with no baseflow and with the sludge hopper (Table 4.5).

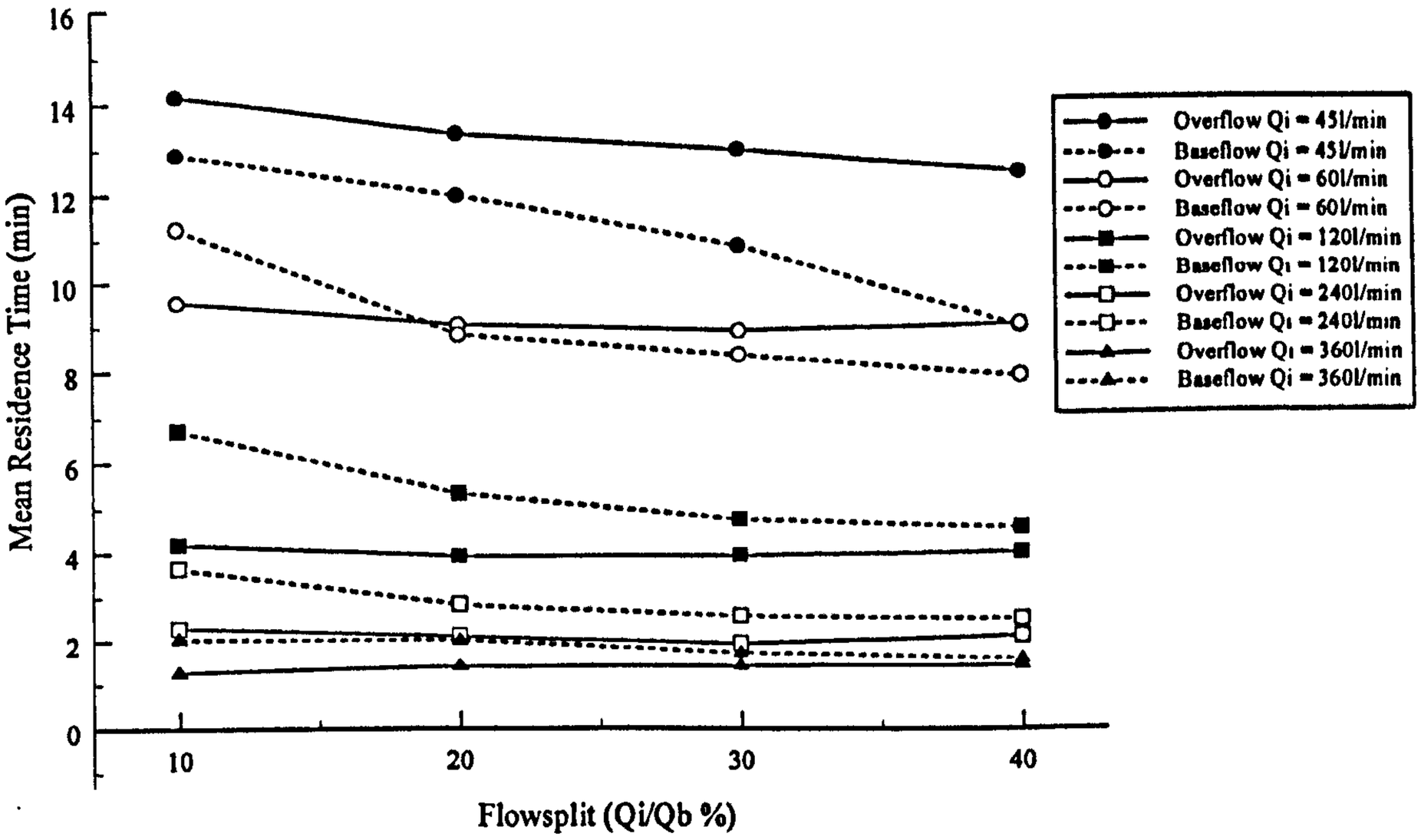

Fig. 6.36 Prototype HDVS Baseflow (SP3) - Experimental Mean Residence Time using the Method of Moments

Appendix E.4.3 shows the error between the theoretical and experimental mean residence time calculated using the method of moments (Table 6.16). The experimental values are all greater than the theoretical values and therefore, the errors are positive. This trend was also observed for the RTD investigations undertaken on the prototype HDVS operating with no baseflow and with the sludge hopper and is discussed in section 4.4.2. The average error between the overflow experimental mean residence time values and the theoretical is +14% and similarly for the baseflow is +32%. The overflow component errors are significantly less than the errors obtained for the prototype HDVS operating with no baseflow (section 4.4.2.1). The relative trend in the baseflow and overflow component experimental mean residence time errors as the flow rate increases and the associated HDVS mixing regime characteristics are discussed in section 6.2.1.1.

Table 6.17 shows the estimated prototype HDVS volume calculated using the method of moments experimental mean residence time (Table 6.16). The prototype HDVS operating with the sludge hopper (Fig. 6.1) has a volume of approximately 464 litres and the estimated experimental volumes have an average error of +17%. Chapter 4 showed the influence of the RTD experimental duration and the effect of the truncation time on the experimental mean residence time however, this has not been investigated for any of the model or prototype HDVS baseflow RTD data (section 6.2.1.1). The percentage of the experimental volume associated with the overflow and baseflow components is also presented in Table 6.17. These values show that the volume split is approximately proportional to the flow split.

Table 6.17 Prototype HDVS Baseflow (SP3) – Estimated Prototype HDVS Volume using the Experimental Mean Residence Time Calculated from the Method of Moments

Flow Rate (l/min)	Flow Split (%)	Volume (l)		Percentage of Experimental Volume (%)		Total Volume (l)
		O	B	O	B	
45	10	574.128	58.0280	90.821	9.1790	632.156
	20	481.464	108.045	81.672	18.328	589.509
	30	409.469	146.705	73.623	26.378	556.173
	40	336.987	162.342	67.488	32.512	499.329
60	10	516.456	67.4700	88.445	11.555	583.926
	20	435.360	106.272	80.379	19.621	541.632
	30	374.640	150.876	71.290	28.710	525.516
	40	326.484	189.648	63.256	36.744	516.132
120	10	452.520	80.6400	84.875	15.125	533.160
	20	378.048	128.352	74.654	25.346	506.400
	30	331.548	171.000	65.973	34.027	502.548
	40	290.592	219.360	56.984	43.016	509.952
240	10	494.640	87.5040	84.969	15.031	582.144
	20	406.272	136.752	74.817	25.183	543.024
	30	326.760	185.544	63.782	36.218	512.304
	40	306.432	242.112	55.863	44.137	548.544
360	10	411.480	73.6560	84.817	15.183	485.136
	20	412.704	146.304	73.828	26.172	559.008
	30	366.660	188.028	66.102	33.898	554.688
	40	317.952	231.984	57.816	42.184	549.936

Fig. 6.37 shows the ADM parameters (P_e) calculated using the method of moments for all flow splits and inlet flow rates. The TISM parameter (N) will show the same trend as the ADM parameters when both are calculated using the method of moments (section 6.2.4.1). Therefore the TISM parameter curves are presented in appendix E.4.8 and all numerical values are provided in appendix E.4.9. The overflow component Peclet numbers (P_e) are relatively stable across the flow splits for the same inlet flow rate. The baseflow Peclet number (P_e) decreases as the flow split is increased and therefore, as the baseflow component flow rate decreases the mixing regime has improved plug-flow mixing characteristics. The overflow Peclet number (P_e) increases as the inlet flow rate decreases and is the same relationship as achieved for the prototype HDVS operating with no baseflow and with the sludge hopper (section 4.4.2). However, the baseflow Peclet numbers (P_e) increase as the inlet flow rate increases and this is the same relationship as the model HDVS baseflow component measured at SP3 (section 6.2.2.1).

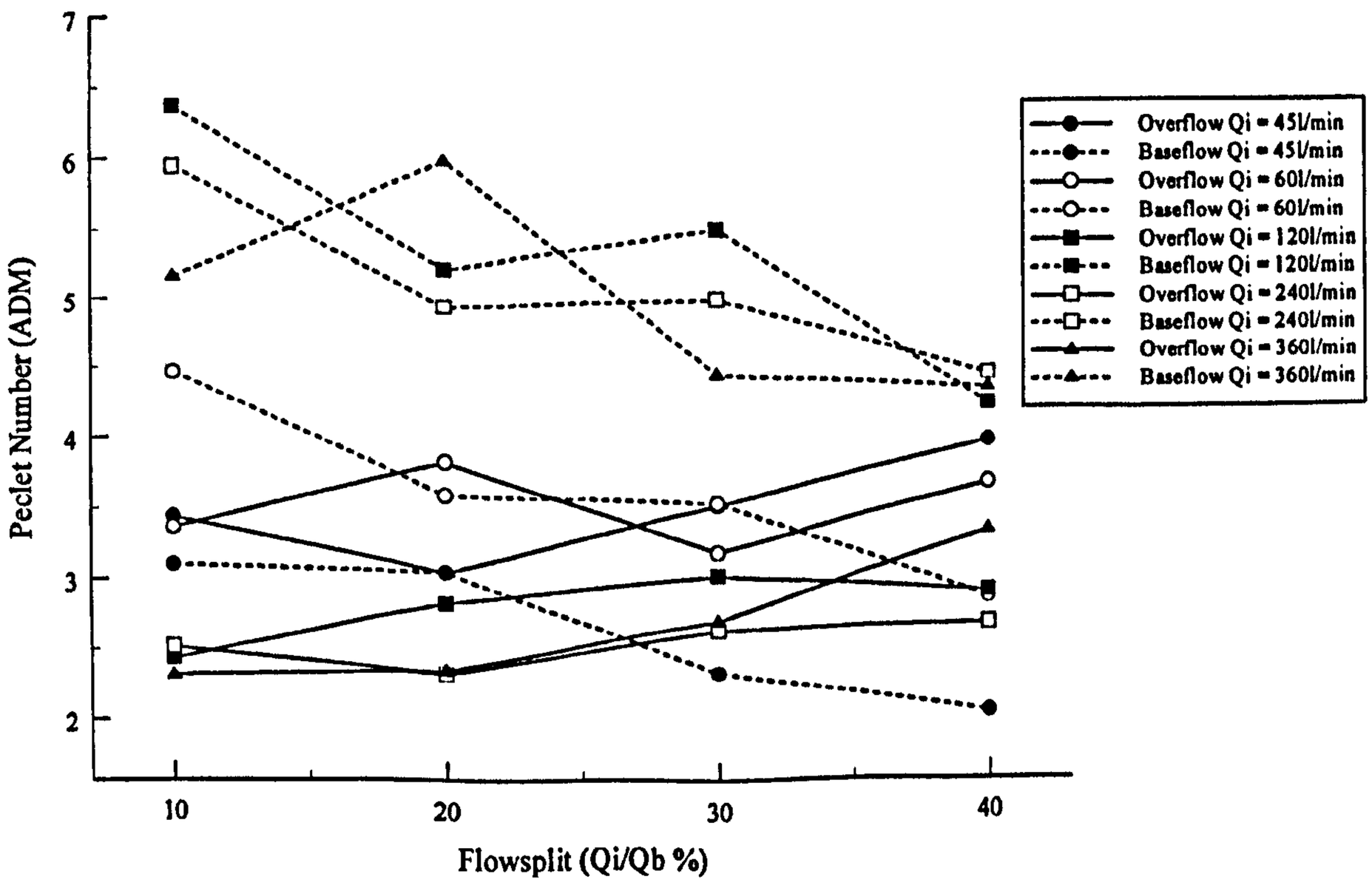

Fig. 6.37 Prototype HDVS Baseflow (SP3) - Comparison of the ADM Parameters Calculated using the Method of Moments

Appendix E.4.9 also details the summation of the individual overflow and baseflow component ADM and TISM parameters at each flow split for all inlet flow rates. The results clearly show that the baseflow component introduces an element of plug-flow mixing compared to the prototype HDVS operating without a baseflow component (section 4.4.2). The reader is referred to the total flow ADM and TISM parameter results and conclusions presented for the model HDVS (SP3) as the same trend in the data is observed (section 6.2.2.1). The total flow ADM and TISM parameters for the prototype HDVS operating with a baseflow component measured at SP2 and SP3 are compared and also presented in section 6.2.6 (Table 6.21).

Fig. 6.38 compares the experimental exit-age distribution function E(t) curve to the TISM (eqn. 4.9) and ADM (eqn. 4.11) curves obtained using the method of moments for an inlet flow rate of 120l/min. The remaining flow rates and all correlation parameters (R^2 and ESS) are presented in appendix E.4.10 and E.4.11 respectively. The ADM provides the best-fit for both the overflow and baseflow components at all inlet flow rates and flow splits compared to the TISM. The ADM and TISM correlation parameters do not show any significant trend for the range of inlet flow rates or flow splits. The expected relationship between the correlation parameters and the inlet flow rate is discussed in section 6.2.4.1.

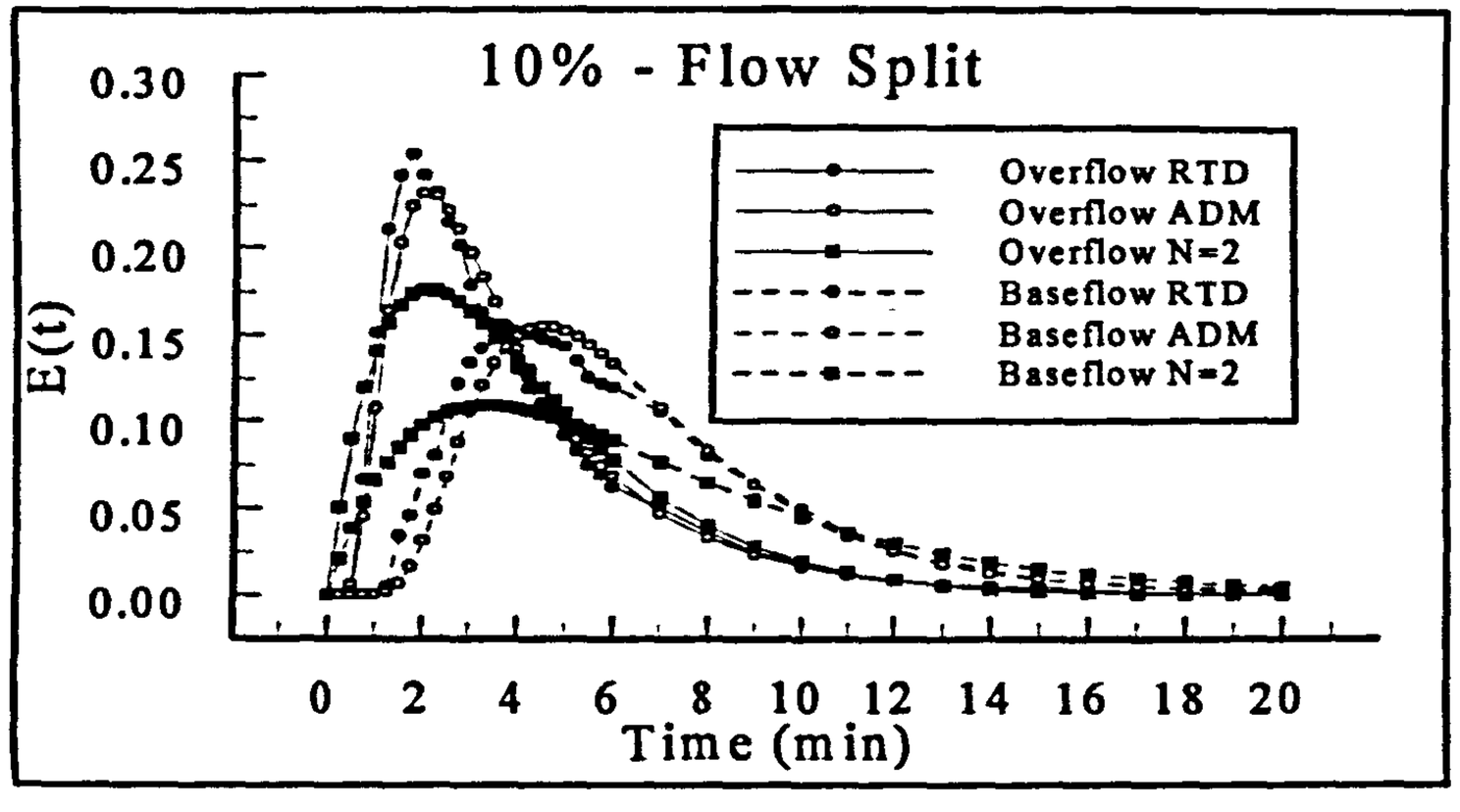

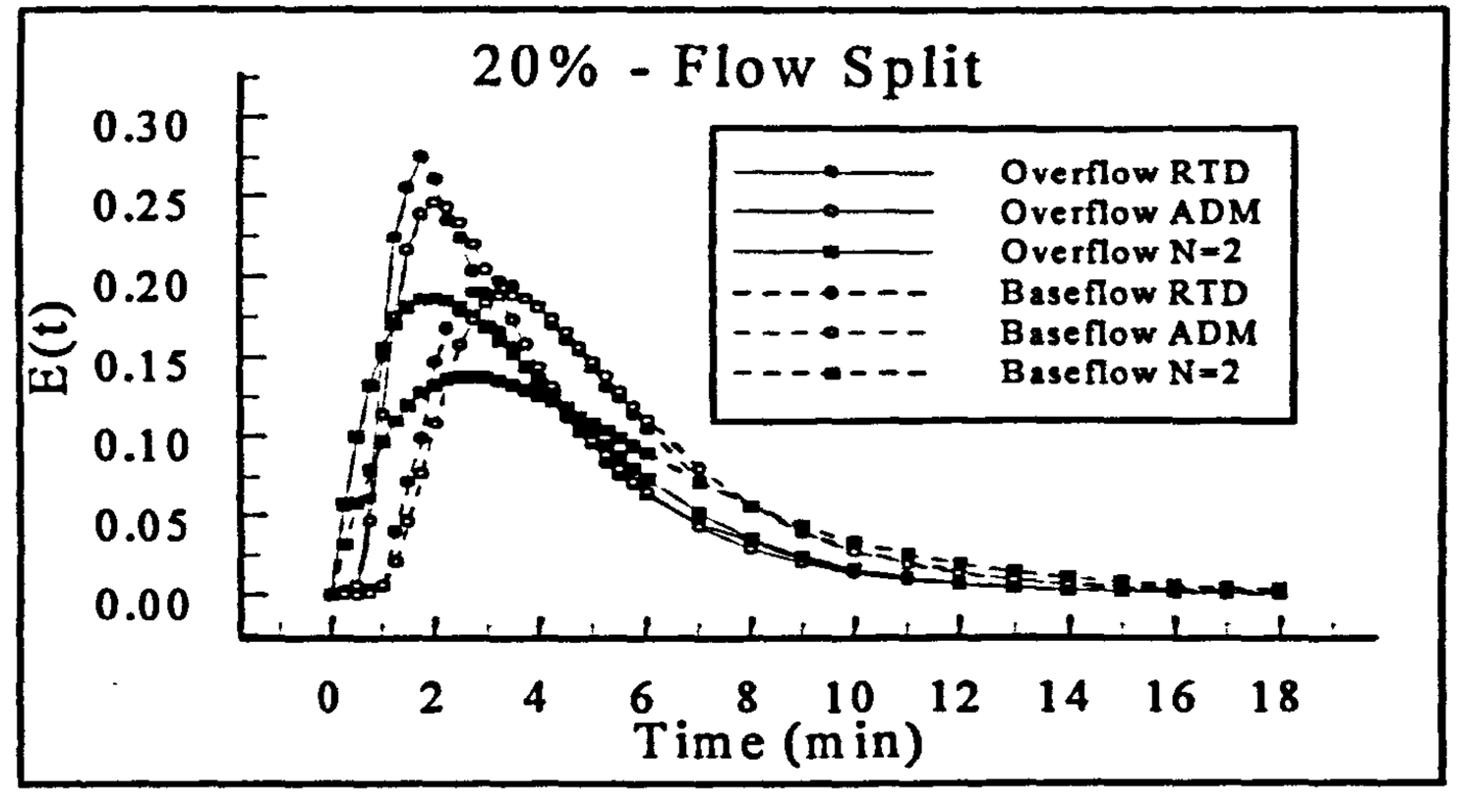

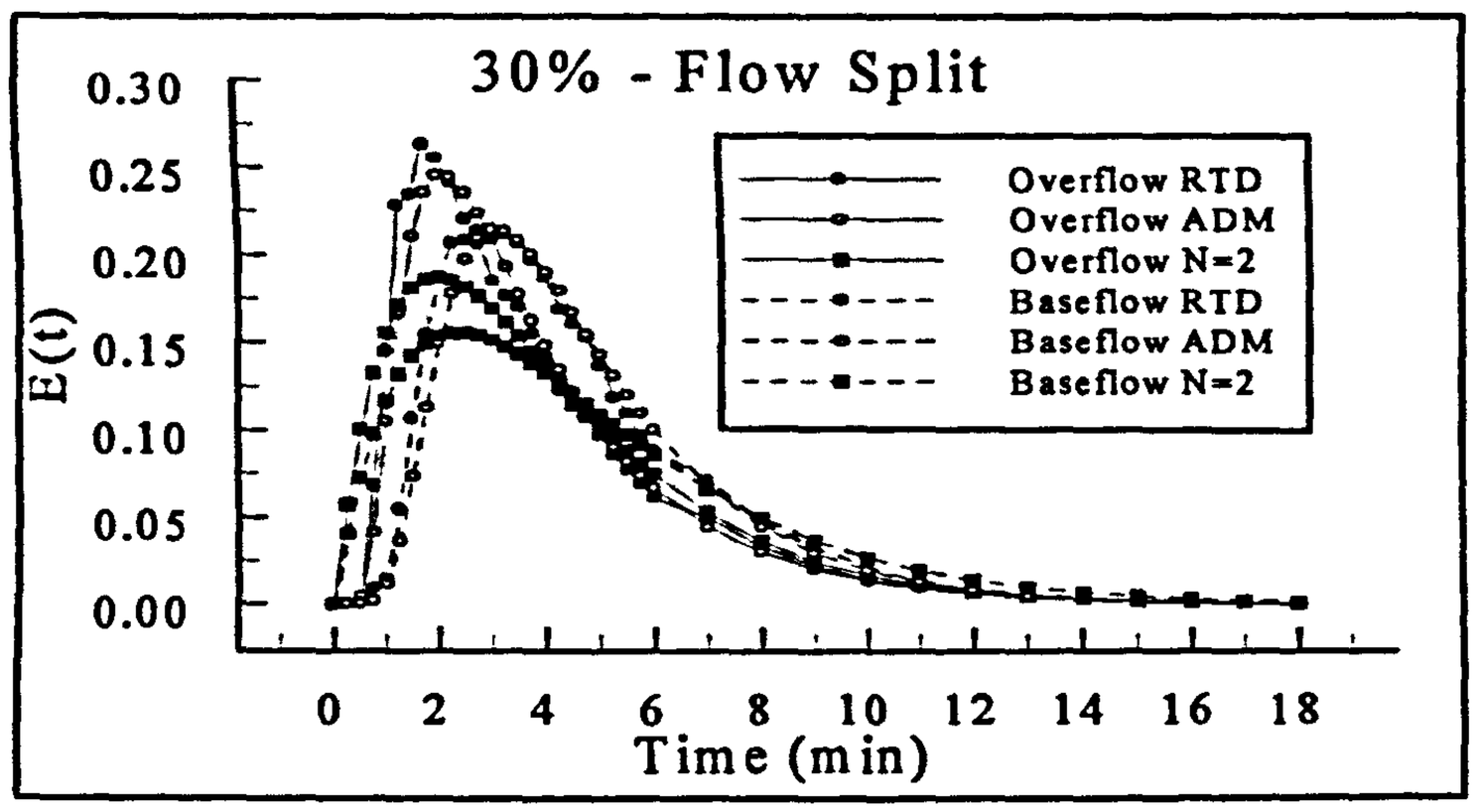

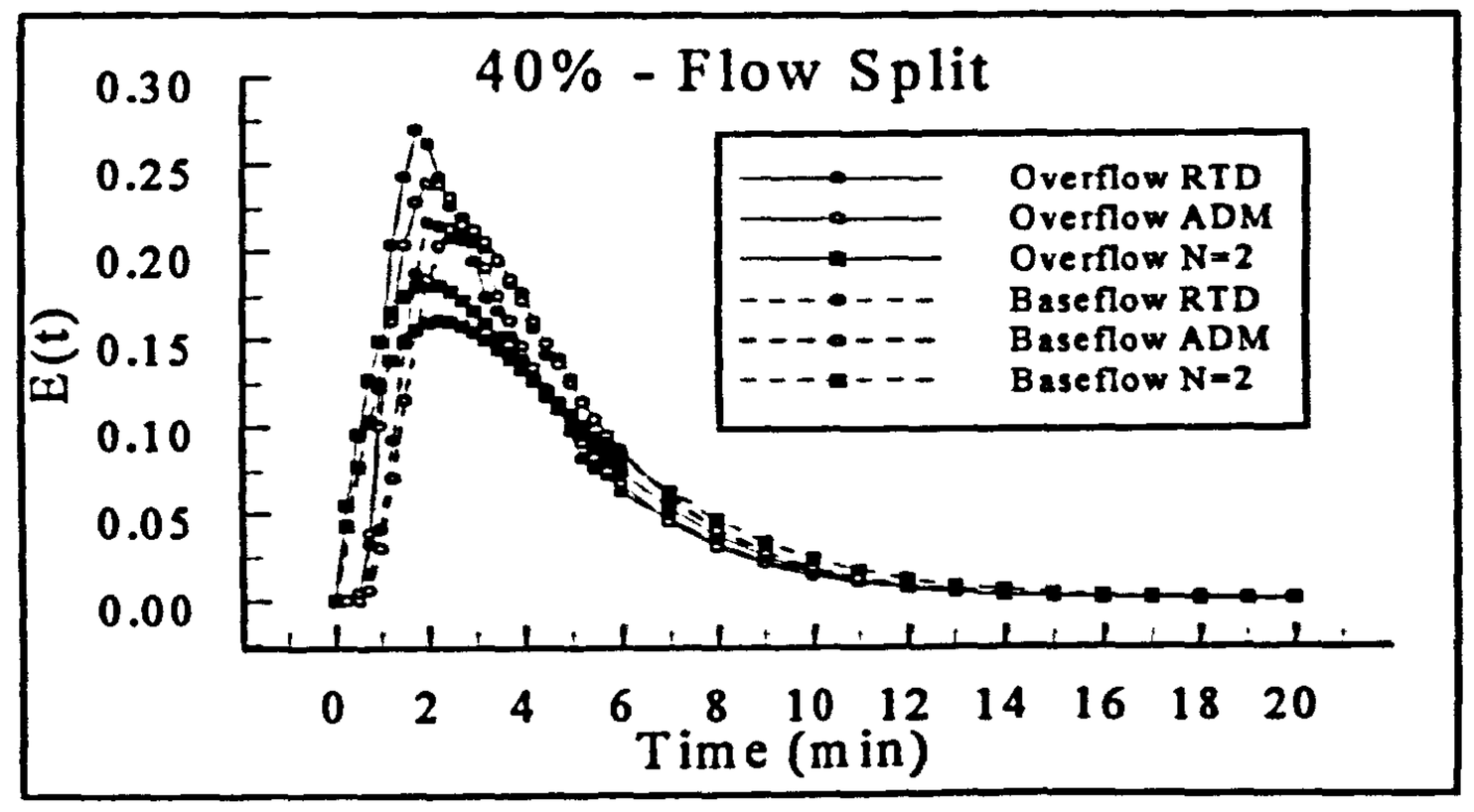

Fig. 6.38 - Prototype HDVS Baseflow (SP3) - Comparison of E(t), ADM and TISM Curves Calculated using the Method of Moments for an Inlet Flow Rate of 120l/min

6.2.5.2 Non-Linear Regression Data Analysis

Fig. 6.39 and 6.40 show the RTD normalised curves E(Θ) calculated using the experimental mean residence time, estimated from the ADM and TISM non-linear regression curve fitting technique, for an inlet flow rate of 120l/min. The remaining flow rates are shown in appendix E.4.12 and E.4.13. The RTD normalised curves E(Θ) show the same characteristics as the model HDVS (SP3) and therefore, the same observations apply (section 6.2.2.2).

Tables 6.18 and 6.19 show the ADM and TISM parameters calculated using non-linear regression. The experimental mean residence time values calculated using non-linear regression are of a similar order of magnitude as calculated using the method of moments (section 6.2.5.1). Appendix E.4.14 shows the ADM and TISM experimental mean residence time plotted against the flow split for all inlet flow rates. The curves have the same characteristics as the experimental mean residence time calculated using the method of moments (Fig. 6.36). The ADM and TISM mean residence time values for the overflow and baseflow component generally follow the same trend as the RTD curves time to peak concentration (section 6.2.5.1). The average error between the overflow ADM experimental mean residence time and the theoretical mean residence time is +9% and for the baseflow is +26%. Similarly the average error using the TISM for the overflow is +10% and for the baseflow is +39% (section 6.2.1.1).

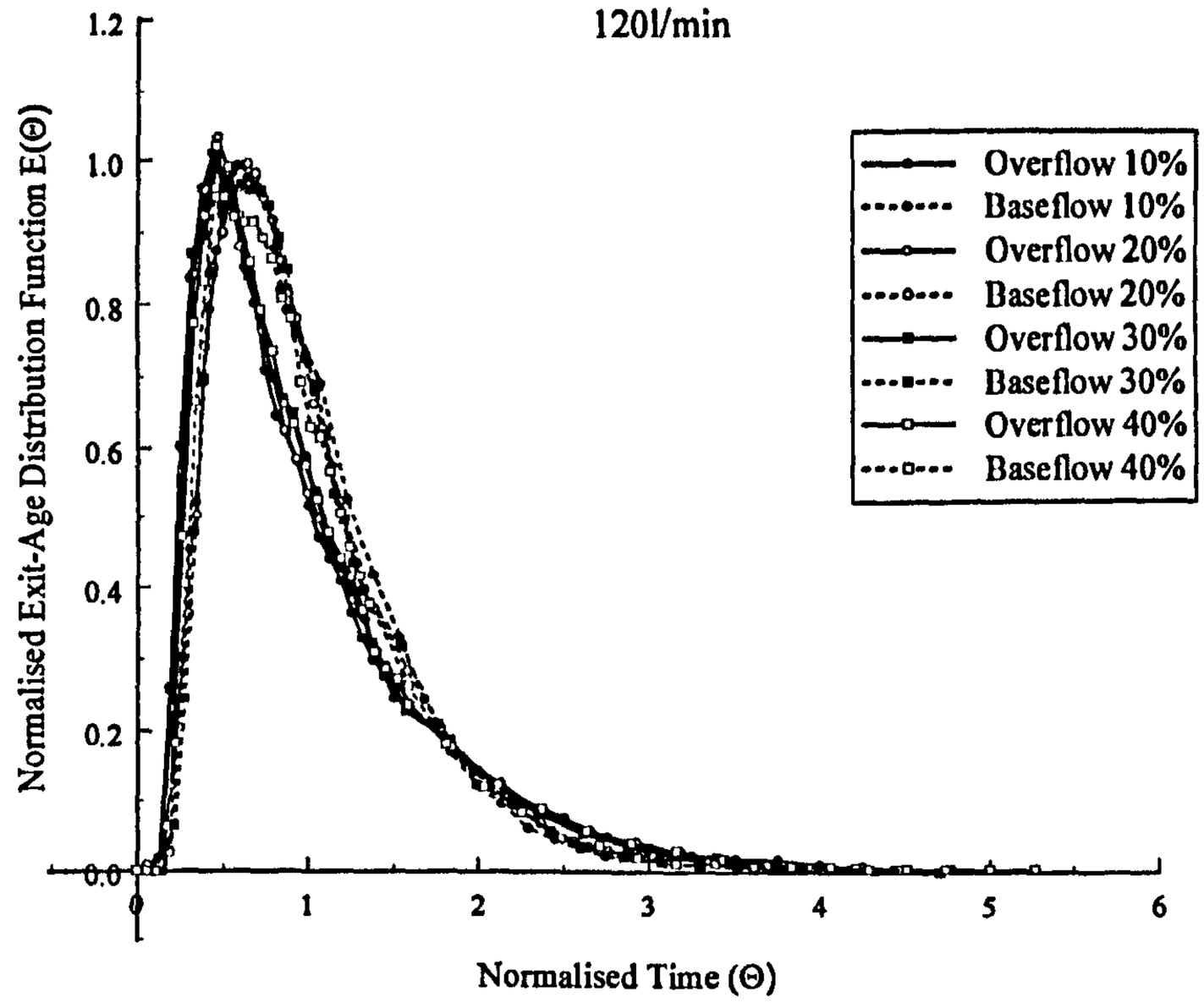

Fig. 6.39 Prototype HDVS Baseflow (SP3) - Comparison of Normalised Exit-Age Distribution Curves E(Θ) using Non-Linear Regression and the ADM

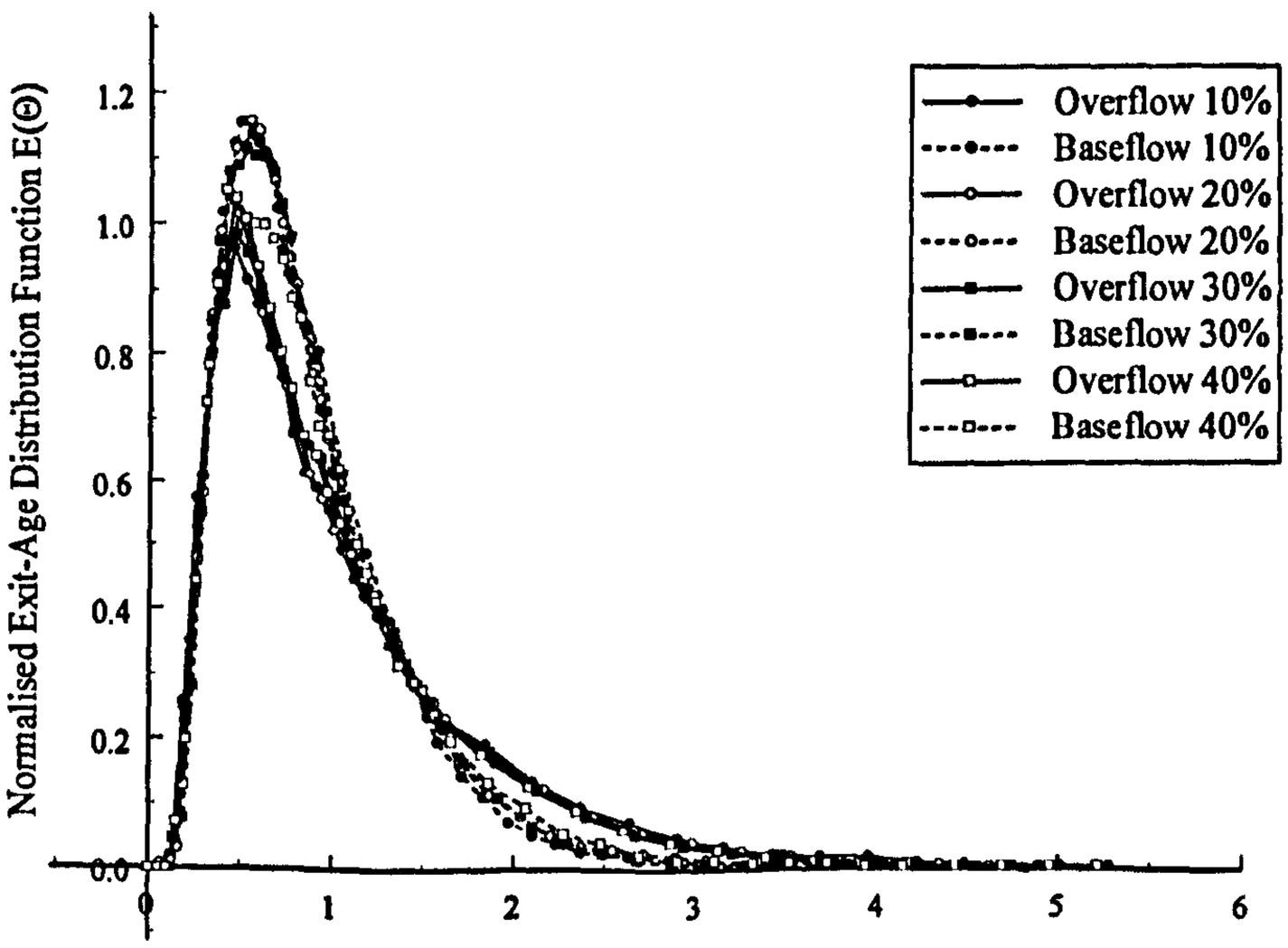

Fig. 6.40 Prototype HDVS Baseflow (SP3) - Comparison of Normalised Exit-Age Distribution Curves E(Θ) using Non-Linear Regression and the TISM

Appendix E.4.15 shows the estimated prototype HDVS volume calculated using the ADM and TISM experimental mean residence time. As stated above the prototype HDVS operating with the sludge hopper (Fig. 6.1) has a volume of 464 litres. The ADM and TISM estimated experimental volumes have an average error of +11% and +15% respectively. The ADM and TISM provide a better estimation of the prototype HDVS volume compared to the method of moments for reasons discussed in section 4.4.3. The percentage of the experimental volume associated with the overflow and baseflow components is also presented in Appendix E.4.15. These values show that the volume split is approximately proportional to the flow split.

Table 6.18 Prototype HDVS Baseflow (SP3) – Comparison of ADM Parameters using Non-Linear Regression

Flow Rate (l/min)	Flow Split (%)	Experimental Mean Residence Time (min)		Normalised Variance (σ_θ^2)		Peclet Number (P_e)	
		O	B	O	B	O	B
45	10	13.526	13.038	0.473	0.612	2.820	1.695
	20	12.579	10.573	0.495	0.394	2.605	3.755
	30	11.987	9.4570	0.427	0.447	3.330	3.095
	40	11.491	7.8440	0.379	0.513	3.975	2.440
60	10	9.770	11.130	0.560	0.438	2.060	3.195
	20	9.082	8.3280	0.477	0.400	2.780	3.675
	30	8.524	7.8310	0.479	0.423	2.760	3.380
	40	8.785	7.3240	0.436	0.486	3.220	2.690
120	10	3.991	6.538	0.580	0.348	1.910	4.480
	20	3.762	5.071	0.530	0.333	2.295	4.755
	30	3.820	4.546	0.529	0.330	2.305	4.810
	40	3.795	4.427	0.483	0.391	2.720	3.800
240	10	2.228	3.528	0.612	0.349	1.695	4.460
	20	1.937	2.662	0.511	0.308	2.460	5.265
	30	1.833	2.473	0.508	0.341	2.485	4.605
	40	1.967	2.395	0.463	0.336	2.925	4.700
360	10	1.241	2.120	0.558	0.368	2.075	4.145
	20	1.418	2.046	0.599	0.314	1.780	5.140
	30	1.422	1.701	0.503	0.323	2.530	4.950
	40	1.411	1.599	0.418	0.360	3.440	4.275

The ADM normalised variance values (eqn. 4.11) for the baseflow component measured at SP3 were all less than 1 and therefore, the constraint applied to this parameter for the prototype HDVS baseflow component measured at SP2 (section 6.2.4.2) was not required in the ADM non-linear regression simulation (section 6.2.1.2). Fig. 6.41 illustrates the ADM parameter (P_e) for all inlet flow rates and flow splits. The overflow component Peclet number (P_e) increases and the baseflow component decreases as the flow split is increased for the same inlet flow rate. The overflow component Peclet numbers (P_e) decrease and the baseflow increase as the inlet flow rate is increased. This is the same relationship as obtained using the method of moments (section 6.2.5.1).

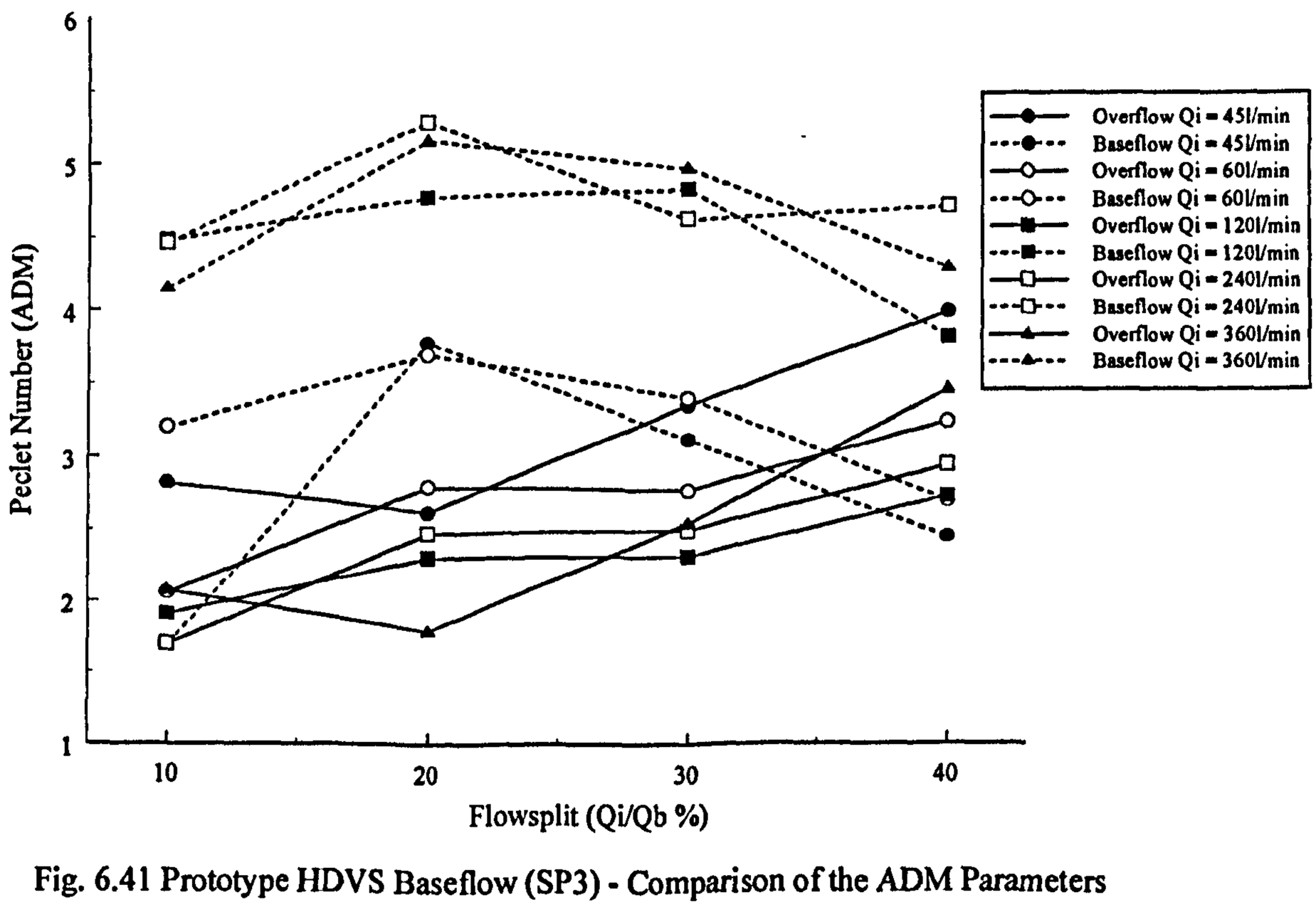

Fig. 6.41 Prototype HDVS Baseflow (SP3) - Comparison of the ADM Parameters Calculated using Non-Linear Regression

Fig. 6.42 illustrates the TISM parameter (N) for all inlet flow rates and flow splits. The overflow and baseflow component TISM parameters increase and decrease

respectively across the range of flow splits for the same inlet flow rate. The overflow component TISM parameters decrease and the baseflow increase as the inlet flow rate is increased. This is the same trend for both the overflow and baseflow component as obtained for the TISM parameter calculated using the method of moments (section 6.2.5.1).

Table 6.19 Prototype HDVS Baseflow (SP3) – Comparison of TISM Parameters using Non-Linear Regression

Flow Rate (l/min)	Flow Split (%)	Experimental Mean Residence Time (min)		N-Tanks	
		O	B	O	B
45	10	14.251	12.595	2.393	2.295
	20	13.098	11.905	2.363	2.427
	30	13.115	10.187	2.420	2.338
	40	12.961	7.9060	2.464	2.204
60	10	9.576	11.930	2.248	2.367
	20	9.372	9.0730	2.303	2.342
	30	8.775	8.3750	2.264	2.295
	40	9.306	7.4980	2.322	2.224
120	10	3.789	7.584	2.162	2.504
	20	3.680	5.873	2.194	2.462
	30	3.738	5.216	2.208	2.434
	40	3.835	4.826	2.231	2.367
240	10	2.105	4.033	2.169	2.469
	20	1.920	3.095	2.193	2.475
	30	1.813	2.788	2.207	2.424
	40	2.104	2.703	2.248	2.419
360	10	1.193	2.250	2.167	2.359
	20	1.323	2.278	2.142	2.401
	30	1.395	1.857	2.201	2.353
	40	1.461	1.700	2.259	2.321

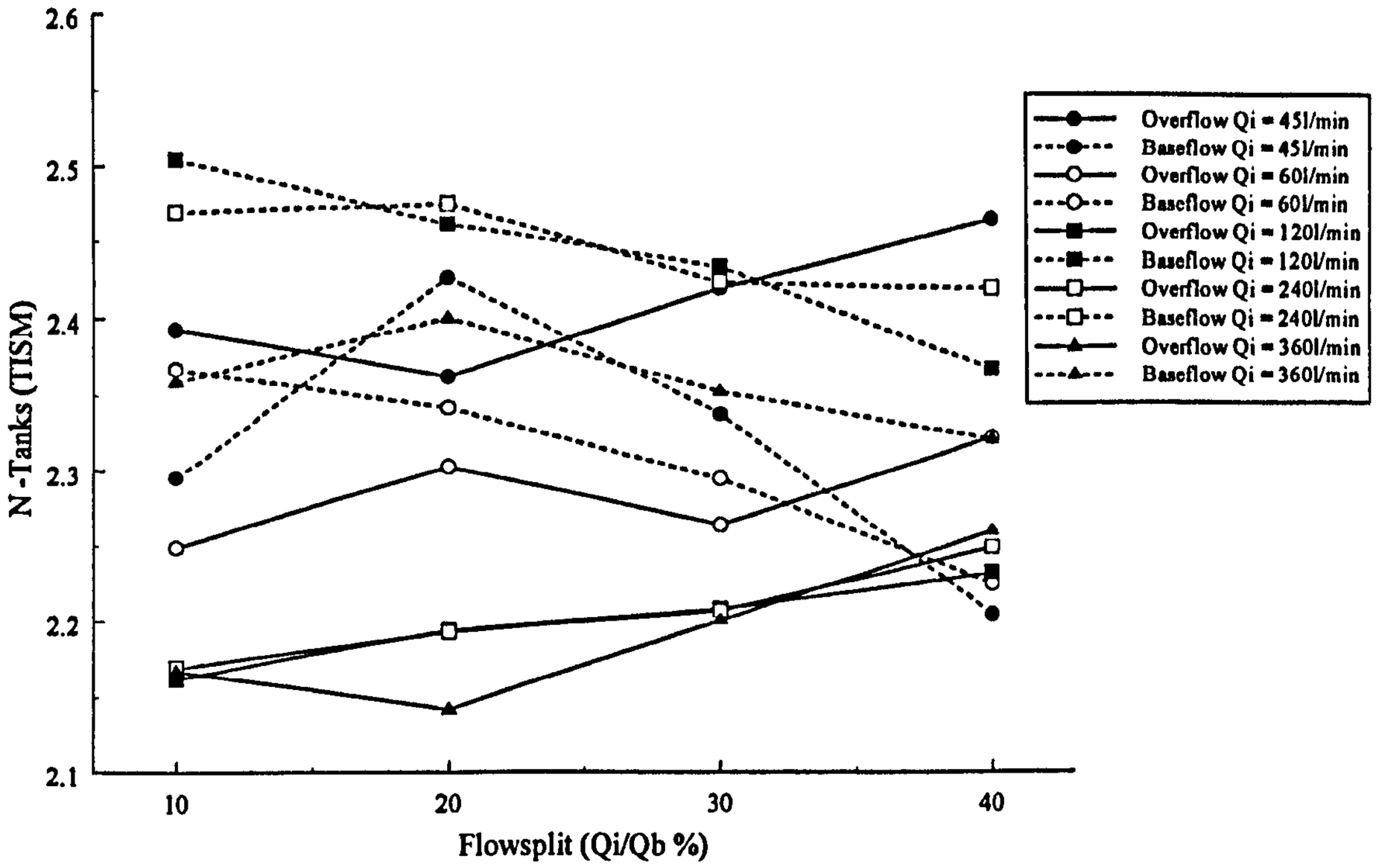

Fig. 6.42 Prototype HDVS Baseflow (SP3) - Comparison of the TISM Parameters Calculated using Non-Linear Regression

Appendix E.4.9 also details the summation of the individual overflow and baseflow component ADM and TISM parameters at each flow split for all inlet flow rates. The ADM results show the same trend as the ADM total flow results obtained using the method of moments (section 6.2.5.1). The TISM total flow results show the same trend as the model HDVS (SP2) (section 6.2.1.2).

Fig. 6.43 compares the experimental exit-age distribution function E(t) curve to the TISM (eqn. 4.9) and ADM (eqn. 4.11) curves obtained using non-linear regression for an inlet flow rate of 120l/min and all flow splits investigated. The remaining flow rates and all correlation parameters (R^2 and ESS) are presented in appendix E.4.16 and E.4.17 respectively. The ADM provides the best-fit to both the overflow and baseflow components for all inlet flow rates compared to the TISM. The overflow and baseflow component ADM and TISM correlation parameters remain stable for the range of inlet flow rates and flow splits investigated (section 6.2.1.1).

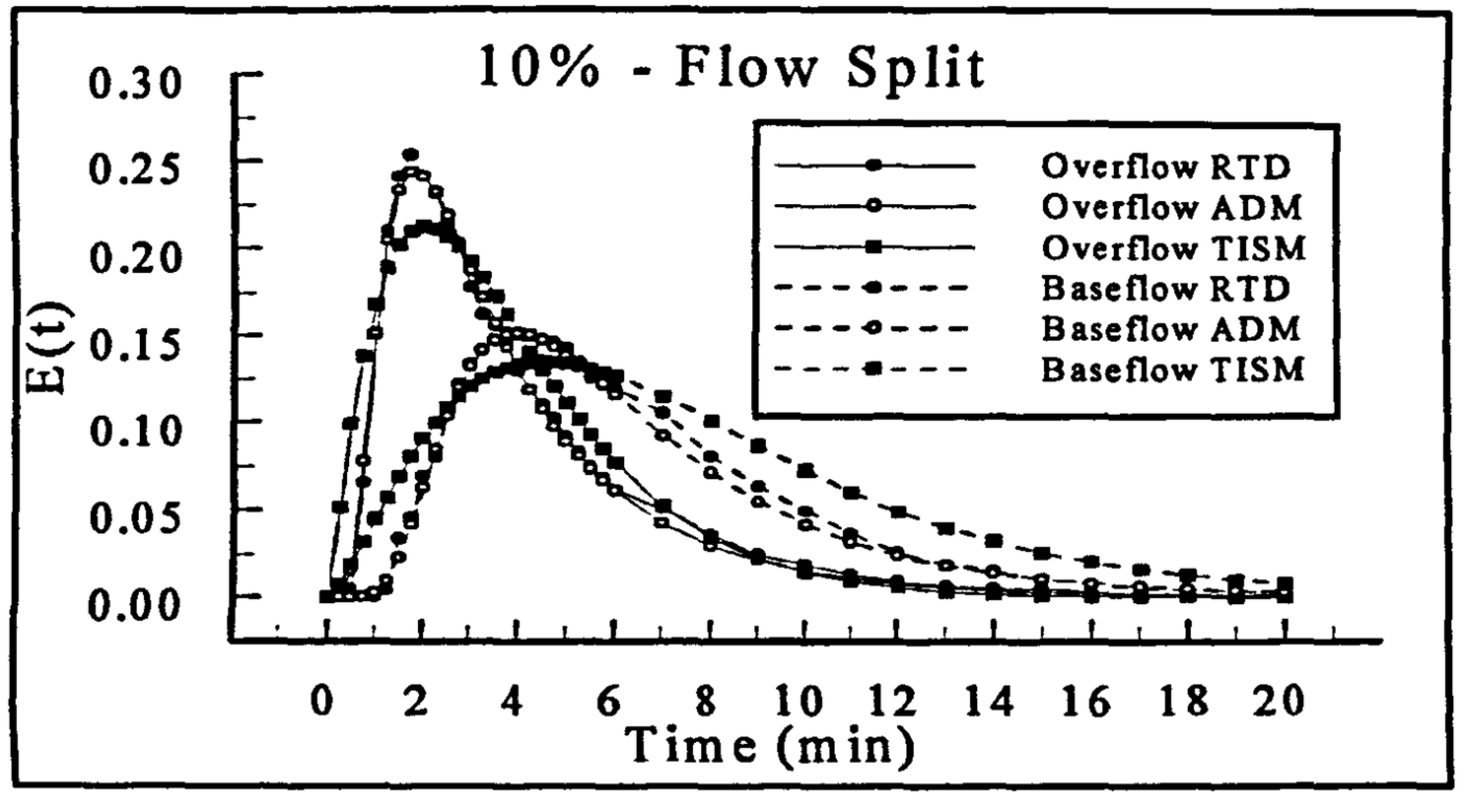

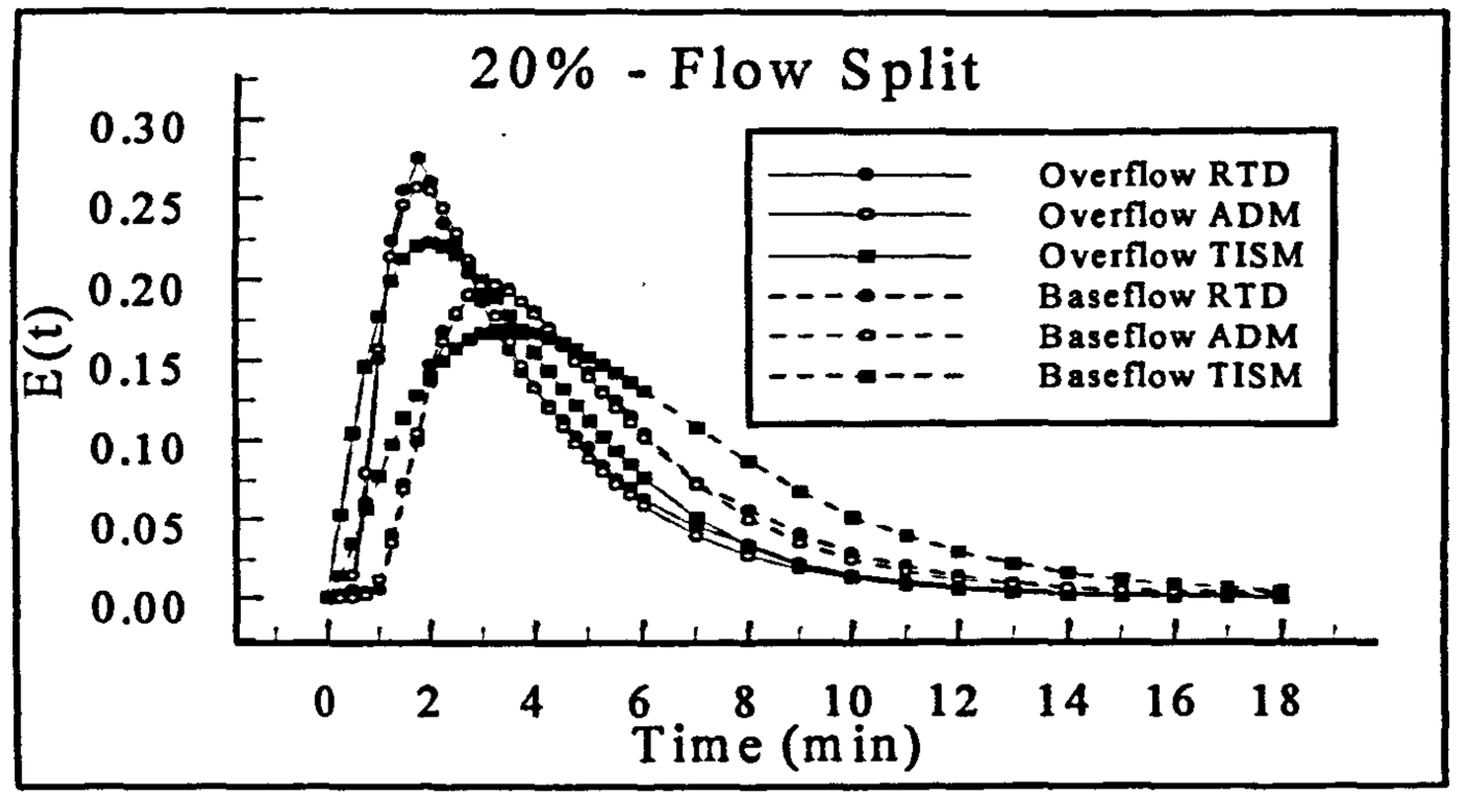

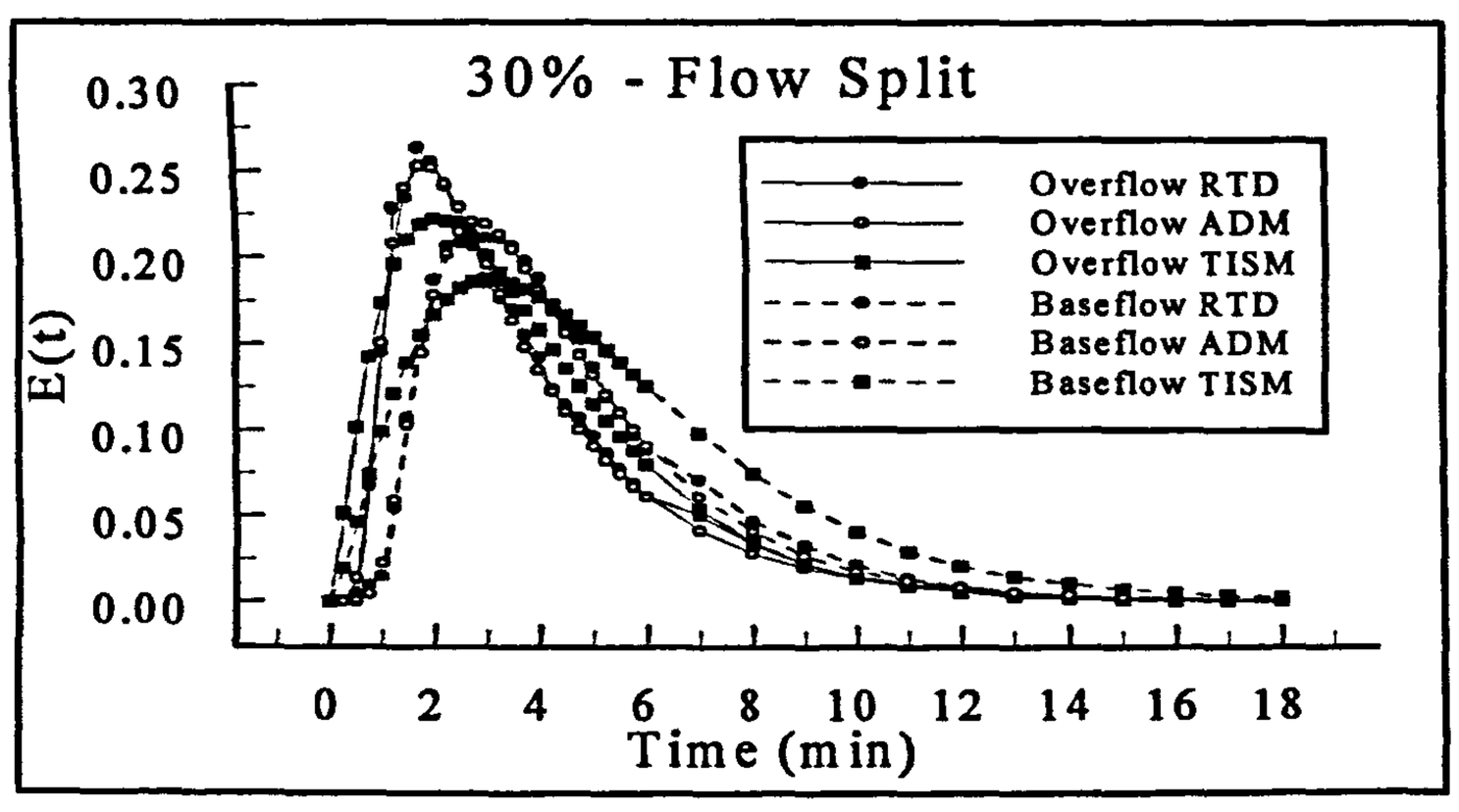

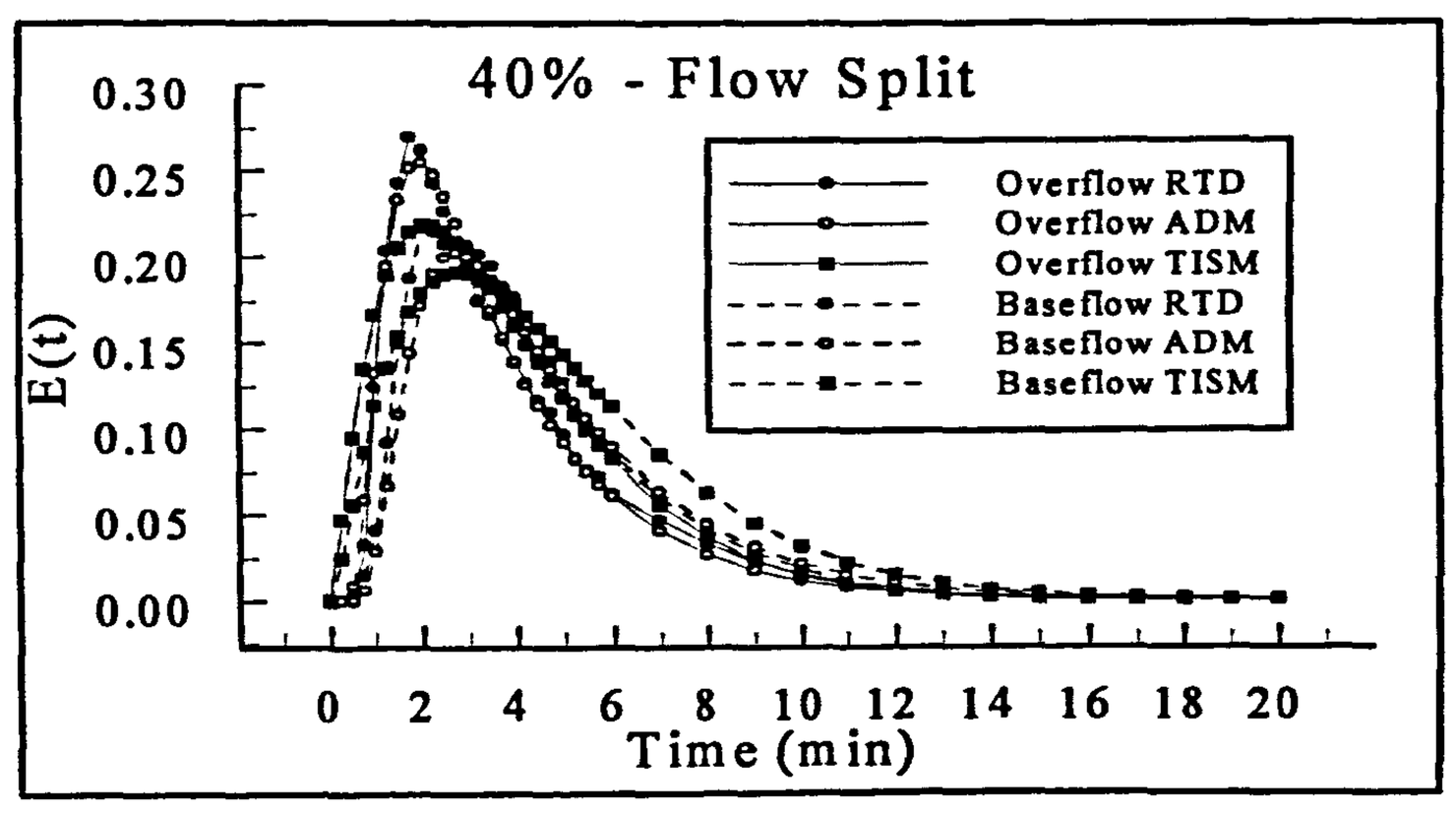

Fig. 6.43 - Prototype HDVS Baseflow (SP3) - Comparison of E(t), ADM and TISM Curves Calculated using Non-Linear Regression for an Inlet Flow Rate of 120l/min

6.2.6 Comparison of the Prototype Hydrodynamic Vortex Separator (HDVS) Baseflow RTD Pulse Injection Results for Sample Point 2 (SP2) and Sample Point 3 (SP3)

The model and prototype HDVS operating with a baseflow component measured at SP2 and SP3 RTD results are very similar and therefore, to prevent excessive repetition the detailed comparison of the baseflow component results measured at SP2 and SP3 is provided for the model HDVS in section 6.2.3.

The RTD normalised curve E(Θ) show that the overflow component short-circuits at high flow rates and the baseflow component at low flow rates. Additionally the baseflow component short-circuits at high flow splits for the same inlet flow rate. Subsequently the plug-flow mixing characteristics of each flow component has the same trend with respect to the inlet flow rates and is illustrated by the ADM and TISM parameters discussed below. The short-circuiting of the overflow and baseflow component at high and low flow rates respectively is associated with the strength of the vortex generated within the HDVS at these flow rates and the internal configuration of the HDVS (Fig. 3.1) (section 6.2.1.1).

The baseflow component exit-age distribution function E(t) curves have different times to peak concentration depending on the sample point (SP2 and SP3) used to measure the RTD tracer concentration (Fig. 6.1) (Table 6.20). The baseflow (SP2) RTD curves peak before the overflow curves at low inlet flow rates and at high inlet flow rates (>120l/min) the opposite generally occurs. This implies that short-circuiting of the overflow component occurs at high flow rates based on the assumed relative flow path of each flow component (section 6.2.3). The baseflow (SP3) RTD curves all peak after the overflow curve for inlet flow rates greater than 60l/min (section 6.2.5.1) and therefore

also suggests that short-circuiting of the baseflow component occurs at low flow rates based on the assumed relative flow path of each flow component (section 6.2.3). The baseflow component peak occurring after the overflow for the baseflow component measured at SP3 compared to SP2 is due to the buffering capacity of the sludge hopper, which is included in the baseflow component measured at SP3 (Fig. 6.1). The sludge hopper increases the baseflow component transit time and introduces an element of plug-flow mixing particularly at high flow rates (section 6.2.3).

Table 6.20 Prototype HDVS – Comparison of SP2 and SP3 Residence Time Distribution (RTD) Time To Peak Concentration

		SP2		SP3	
Flow Rate (l/min)	Flow Split (%)	Time To Peak Concentration (min)		Time To Peak Concentration (min)	
		O	B	O	B
45	10	5.333	2.000	7.500	6.500
	20	6.000	2.333	6.500	6.500
	30	5.333	1.667	7.000	5.000
	40	6.667	1.667	6.500	4.000
60	10	4.000	1.333	5.000	6.667
	20	4.000	1.667	4.333	5.000
	30	4.000	2.000	4.333	4.000
	40	4.500	2.000	4.667	3.000
120	10	1.750	1.250	1.750	4.000
	20	1.750	1.500	1.750	3.250
	30	2.000	1.500	1.750	2.750
	40	2.000	1.500	1.750	2.000
240	10	0.833	0.667	1.000	2.167
	20	0.833	0.667	0.833	1.833
	30	0.833	1.167	0.833	1.500
	40	0.833	1.167	0.833	1.500
360	10	0.500	0.500	0.500	1.500
	20	0.667	0.833	0.667	1.333
	30	0.667	0.500	0.667	1.167
	40	0.667	0.667	0.667	1.000

The experimental prototype HDVS volume estimation using the method of moments for the baseflow component measured at SP2 and SP3 (Fig. 6.1) have an average error

of +18% and +17% respectively. The average estimated volume difference between the baseflow component measured at SP2 and SP3 is approximately 43 litres and the measured volume of the sludge hopper is 35 litres. This provides confidence in the experimental mean residence time estimated values (section 6.2.3). The ADM non-linear regression analysis technique has an average volume error of +10% and +11% for the baseflow component measured at SP2 and SP3 respectively. Similarly, the TISM has a 10% error for SP2 and +15% for SP3. The average estimated volume difference between SP2 and SP3 is approximately 30 litres for the ADM and 55 litres for the TISM.

The overflow RTD curves and characteristics are very similar irrespective of where the baseflow component is sampled i.e. SP2 or SP3 (Fig. 6.1) for a given inlet flow rate. The error between the average overflow component experimental mean residence time, calculated from the SP2 and SP3 RTD data using both the method of moments and non-linear regression and the measured experimental mean residence time is negligible and ranges from -4% to +5%. As the overflow RTD parameters should be the same for the SP2 and SP3 RTD experiments, these errors correspond to experimental errors in calculating the experimental mean residence time. The error between the theoretical and experimental mean residence time for both the SP2 and SP3 baseflow component RTD results is reduced when the non-linear regression technique is adopted (appendix E.3.3 and E.4.3). The advantages of the non-linear regression ADM and TISM parameter estimation technique compared to the method of moments are discussed in section 4.4.3.

The overflow ADM (P_e) and TISM (N) parameters for both the SP2 (section 6.2.4.1) and SP3 RTD experiments (section 6.2.5.1) calculated using the method of moments produce very similar results both in the magnitude and trend with respect to inlet flow rate and flow split (Fig. 6.27 and Fig. 6.37). This is anticipated as the overflow component is unaffected by changing the baseflow sample point location (Fig. 6.1). The

overflow component Peclet numbers (P_e) remain relatively stable as the flow split increases i.e. as the overflow component flow rate decreases for the same inlet flow rate. The baseflow component Peclet number (P_e) does show different characteristics with respect to the flow split, depending on the sample point used to measure the RTD. At SP2 the baseflow component Peclet number (P_e) also remains relatively stable as the flow split increases however, at SP3 the Peclet number (P_e) decreases as the flow split increases. This was also observed for the model HDVS operating with a baseflow component and is discussed in section 6.2.3. The Peclet number (P_e) obtained for the baseflow measured at SP3 (Fig. 6.37) are also all significantly higher than at SP2 (Fig. 6.27) for the same inlet flow rate. This is illustrated by the position of the baseflow component RTD normalised curves E(Θ) peak concentration for SP2 (Fig. 6.24) and SP3 (Fig. 6.34) relative to a normalised time (Θ) value of 1 (section 4.3.1). The prototype HDVS total flow ADM and TISM parameters (overflow + baseflow) calculated using the method of moments and non-linear regression (Table 6.21) also support the increase in plug-flow mixing due to the introduction of the sludge hopper and the same discussion applies as for the model HDVS (section 6.2.3).

The overflow component ADM and TISM parameters calculated using non-linear regression show similar a trend for the SP2 (section 6.2.4.2) and SP3 (section 6.2.5.2) RTD experiments. The overflow parameters gradually increase as the flow split increases i.e. as the overflow component flow rate decreases for the same inlet flow rate. The baseflow ADM and TISM parameters obtained at SP3 generally decrease and at SP2 they are relatively stable as the flow split increases for the same inlet flow rate. The ADM non-linear regression simulation constraint applied to the baseflow component measured at SP2 normalised variance parameter was not required for the SP3 RTD data. The implications of requiring a mathematical constraint on the baseflow component

mixing regime characteristics is discussed in section 6.2.3. The ADM and TISM parameters calculated using non-linear regression also support the mixing characteristics introduced by the sludge hopper for the baseflow component measured at SP3.

Table 6.21 Prototype HDVS - Comparison of SP2 and SP3 Total Flow ADM and TISM Parameters Calculated using the Method of Moments

		SP2	SP3	SP2	SP3
Flow Rate (l/min)	Flow Split (%)	Total Flow Peclet Number (P_e)	Total Flow Peclet Number (P_e)	Total Flow N-Tanks	Total Flow N-Tanks
45	10	4.555	6.545	3.817	4.634
	20	4.800	6.080	3.924	4.424
	30	4.155	5.845	3.654	4.328
	40	5.145	6.025	4.099	4.422
60	10	4.105	7.825	3.608	5.223
	20	4.620	7.390	3.822	5.021
	30	4.430	6.715	3.730	4.711
	40	5.310	6.545	4.110	4.637
120	10	5.580	8.800	4.209	5.720
	20	5.715	8.020	4.263	5.329
	30	5.555	8.515	4.195	5.559
	40	5.625	7.150	4.226	4.917
240	10	5.525	8.460	4.180	5.551
	20	5.240	7.250	4.052	4.984
	30	6.205	7.630	4.483	5.148
	40	6.875	7.140	4.783	4.918
360	10	5.540	7.475	4.186	5.089
	20	6.955	8.310	4.822	5.489
	30	6.020	7.145	4.401	4.919
	40	6.010	7.700	4.397	5.164

The ADM and TISM parameters calculated using the method of moments and non-linear regression decrease for the overflow and increase for the baseflow component as the inlet flow rate is increased. This is the same trend as achieved for the model HDVS (section 6.2.3). The relationship between the overflow and baseflow component (SP2 and SP3) ADM and TISM parameters suggests that there are different mixing regimes associated with different volumes within the HDVS. This was also observed for the model HDVS and is discussed in detail in section 6.2.3. The overflow component and the

baseflow component measured at SP2 and SP3 ADM and TISM correlation parameters obtained using the method of moments and non-linear regression are presented in appendix E3 and E4. The correlation parameters generally show the same trend as achieved for the model HDVS (section 6.2.3).

6.2.6.1 Prototype Hydrodynamic Vortex Separator (HDVS) Baseflow (SP2) and (SP3) – Residence Time Distribution (RTD) Indices

The RTD indices have been calculated to further investigate the different mixing characteristics of the baseflow RTD curves measured at SP2 and SP3 (Fig. 6.1) (appendix E.3.18 and E.4.18). The RTD indices predominantly describe the shape of the RTD i.e. time of start, peak and finish relative to each other (section 4.3.4). The overflow component RTD indices are not presented or discussed in this section, as the overflow RTD curves obtained for the prototype HDVS operating with and without the baseflow component have very similar mixing characteristics (section 6.2.6). Therefore, for the prototype HDVS overflow component RTD indices the reader is referred to section 4.4.4. Table 6.22 compares selected RTD indices to illustrate the different characteristics of the baseflow component RTD curve obtained at SP2 and SP3 (Fig. 6.1).

The same conclusions obtained from the model HDVS operating with a baseflow component RTD indices apply to the prototype HDVS (section 6.2.3.1). The individual RTD indices for the baseflow component measured at SP2 and SP3 are compared in section 6.2.3.1 and the general observations are presented below.

Table 6.22 Prototype HDVS - Comparison of Selected SP2 and SP3 Baseflow Component RTD Indices

		SP2	SP3	SP2	SP3	SP2	SP3	SP2	SP3
Flow Rate (l/min)	Flow Split (%)	t_f/τ	t_f/τ	t_p/τ	t_p/τ	t_{90}/t_{10}	t_{90}/t_{10}	t_{50}/t_m	t_{50}/t_m
45	10	0.105	0.194	0.209	0.630	9.430	5.647	0.676	0.775
	20	0.105	0.242	0.244	0.630	9.048	5.111	0.679	0.750
	30	0.105	0.194	0.174	0.485	10.000	5.500	0.656	0.736
	40	0.070	0.194	0.174	0.388	8.947	5.938	0.683	0.732
60	10	0.093	0.216	0.186	0.862	11.253	4.847	0.696	0.830
	20	0.046	0.216	0.233	0.647	8.398	4.636	0.716	0.828
	30	0.140	0.216	0.279	0.517	7.778	4.800	0.729	0.795
	40	0.140	0.172	0.279	0.388	7.000	5.333	0.769	0.801
120	10	0.070	0.323	0.349	1.034	8.182	4.000	0.772	0.856
	20	0.140	0.194	0.419	0.840	6.667	4.444	0.780	0.841
	30	0.140	0.194	0.419	0.711	6.957	4.286	0.763	0.842
	40	0.070	0.194	0.419	0.517	7.500	4.730	0.777	0.832
240	10	0.186	0.345	0.372	1.121	7.917	4.063	0.782	0.960
	20	0.186	0.259	0.372	0.948	6.429	4.200	0.780	0.842
	30	0.186	0.172	0.651	0.776	5.402	4.070	0.795	0.841
	40	0.186	0.172	0.651	0.776	5.000	3.856	0.808	0.859
360	10	0.140	0.258	0.419	1.164	6.060	4.074	0.663	0.896
	20	0.279	0.258	0.698	1.034	5.455	3.667	0.713	0.902
	30	0.140	0.258	0.419	0.905	5.334	3.601	0.703	0.890
	40	0.140	0.258	0.559	0.776	5.334	4.119	0.727	0.869

The baseflow component including the sludge hopper (SP3) has less short-circuiting compared to the baseflow component measured at SP2 and subsequently has a greater active volume at the same inlet flow rate and flow split. Additionally the baseflow component including the sludge hopper (SP3) has better plug-flow mixing characteristics (section 6.2.3.1). The baseflow component RTD indices (SP2 and SP3) relationship with the inlet flow rate shows that the baseflow component has improved plug-flow mixing characteristics as the inlet flow rate is increased. Additionally, the baseflow component has less short-circuiting at high flow rates compared to low flow rates and therefore, a greater volume is active in the mixing process. The baseflow component RTD indices support previous observations obtained from the RTD normalised curves $E(\Theta)$ and the

ADM and TISM parameters (section 6.2.6). It is not possible to distinguish any noticeable trend in the RTD indices across the range of flow splits investigated for the same inlet flow rate.

6.2.7 Comparison of the Model and Prototype Hydrodynamic Vortex Separator (HDVS) Baseflow RTD Pulse Injection Results for Sample Point 2 (SP2) and Sample Point 3 (SP3)

A detailed comparison of the model and prototype HDVS operating with a baseflow component RTD data has not been presented. The RTD and the ADM and TISM parameters calculated using the method of moments and non-linear regression have very similar relationships with the inlet flow rate and flow split are of a similar order of magnitude for both the model and prototype HDVS at the same sample point. This also applies to the correlation parameters for both RTD data analysis techniques. However, this does imply that the HDVS operating with a baseflow component individual and total flow component mixing characteristics are very similar for any size of HDVS. A better insight into the HDVS mixing regime is provided by individually comparing either the model or prototype HDVS SP2 and SP3 RTD data (section 6.2.3 and 6.2.6).

6.2.7.1 Comparison with Existing RTD Investigations on a Grit King™ HDVS Operating with a Baseflow Component

The Grit King™ HDVS operating with a baseflow component RTD investigation was undertaken by Tyack and Fenner, (1998b). This style of HDVS (Table 1.1) operates with a grit pot and therefore the Swirl-Flo™ HDVS baseflow component RTD measured

at SP3 (Fig. 6.1) presented in this project is used for comparable data (section 6.2.3 and 6.2.6). The method of moments and the ADM (P_e) parameter were used to describe the RTD (section 4.3). The same Grit King™ HDVS operating with no baseflow was also investigated using RTD analysis as discussed in chapter 2 (section 2.2.2) and chapter 4 (section 4.4.9.4).

The Grit King™ HDVS baseflow RTD experiments were not conducted over a range of flow splits for the same inlet flow rate. Therefore, the relationship between the RTD and ADM parameters (P_e) and the flow split cannot be investigated. However, the results for all four inlet flow rates and the single flow split do suggest that the baseflow component has a greater element of plug-flow mixing compared to the overflow. Additionally, for the limited number of inlet flow rates investigated on the Grit King™ HDVS the baseflow component plug-flow mixing element appears to increase as the inlet flow rate increases. These observations are supported by the results presented in this project for the Swirl-Flo™ HDVS operating with a baseflow component measured at SP2 and to a greater extent at SP3 i.e. including the sludge hopper (Fig. 6.1) (section 6.2.3 and 6.2.6).

The overflow component RTD for the Grit King™ HDVS operating with a baseflow has a similar shape to the no baseflow operating conditions (section 4.4.9.4). However the overflow and baseflow components have a different RTD and therefore the results imply that there maybe more than one flow regime within the Grit King™ HDVS. The summation of the individual flow component ADM parameters provide a very similar value as the no baseflow operating conditions (section 4.4.9.4), although the spread of the results i.e. variance is far greater. The overflow and baseflow component ADM parameters reported for the Grit King™ HDVS are slightly greater than the Swirl-Flo™ HDVS ADM parameters presented in this project. However, this does not necessarily

represent or confirm a significant difference in the mixing regime of the two styles of HDVS (Table 1.1), due to the different and limited operating conditions investigated on the Grit King™ HDVS.

The RTD investigations undertaken in this project on a Swirl-Flo™ HDVS operating with a baseflow component support the previous study undertaken on the Grit King™ HDVS by observing different flow regimes within the HDVS associated with the overflow and baseflow components. However, the Grit King™ HDVS operating with a baseflow component total flow (overflow + baseflow) mixing regime characteristics i.e. backmixing and recirculation, are very similar to that achieved for the no baseflow operating conditions. This is not supported by the Swirl-Flo™ HDVS total flow results, as a greater element of plug-flow mixing is present in the total flow when a baseflow component is introduced (SP2) and the difference is further increased by introducing the sludge hopper (SP3) (section 6.2.3 and 6.2.6).

The overflow component ADM and TISM parameters for the Swirl-Flo™ HDVS investigated in this project operating with a baseflow component are very similar to the overflow component values for the HDVS operating with no baseflow. Hence, there is no significant difference in the overflow component mixing regime for the two HDVS operating conditions. This again differs from the Grit King™ HDVS, as the overflow component had a higher Peclet number (P_e) when the device is operated with a baseflow component. However, the workers compared the no baseflow operating conditions overflow component results to the overflow component obtained for only one flow split at the same inlet flow rate for the device operating with a baseflow component.

Tyack and Fenner, (1998b) commented on the delayed response of the baseflow RTD curve compared to the overflow (section 6.2.3). This was also observed in this project for the baseflow component measured at SP3 i.e. including the sludge hopper

(Fig. 6.1) and is anticipated due to the likely flow paths of the overflow and baseflow components (section 6.2.3). This project has shown the importance of the sample point location on the RTD curves characteristics however, its location on the baseflow pipe has not been detailed in the Grit King™ HDVS study which may also account for an exaggerated delay (section 6.1 and 6.2.7.2).

The Grit King™ HDVS operating with a baseflow component RTD investigations did not present the theoretical mean residence time for either the overflow or baseflow component (chapter 2). The RTD baseflow investigations were conducted for a limited number of inlet flow rates and one flow split only. This approach does not provide the relationship between the overflow and baseflow component experimental mean residence time and the flow split. This is provided by the RTD baseflow investigations conducted in this project by operating the Swirl-Flo™ HDVS at four flow splits for each inlet flow rate. The experimental mean residence time results presented in this project showed that the assumptions made in determining the theoretical mean residence time are generally supported by the experimental mean residence time (section 6.2.1.1). This is shown by the overflow and baseflow component experimental mean residence time remaining relatively constant across the range of flow splits for the same inlet flow rate (Fig. 6.4). However, the overflow and baseflow component experimental mean residence time values differ in magnitude and this does not hold with the theoretical assumptions (section 6.2.1.1). This is associated with the overflow and baseflow components short-circuiting at high and low flow rates respectively (section 6.2.3 and 6.2.6). These observations neglect the errors between the experimental and theoretical mean residence time, which are associated with the HDVS's non-ideal flow behaviour and the RTD data analysis techniques used to calculated the experimental mean residence time (section 4.4.1.1 and 4.4.3).

6.2.7.2 Comparison with Existing RTD Investigations on a Storm King™ HDVS Operating with a Baseflow Component

The Storm King™ HDVS operating with a baseflow component RTD investigations were undertaken by Luyckx *et al.*, (1998a). This style of HDVS operates without a sludge hopper (Table 1.1) and therefore the Swirl-Flo™ HDVS baseflow component RTD measured at SP2 (Fig. 6.1) presented in this project is used for comparable data (section 6.2.3 and 6.2.6). The t_{50}/τ index was used to describe the RTD (section 4.3.4).

There are certain anomalies with the method used to interpret and calculate the t_{50}/τ index presented by Luyckx *et al.*, (1998a) (section 2.2.2). This is due to the theoretical (τ) as opposed to the experimental (t_m) mean residence time being used as the denominator. Neglecting this problem and directly comparing the Swirl-Flo™ HDVS t_{50}/t_m index (Table 6.11 and 6.22) to the Storm King™ HDVS t_{50}/τ index provides very similar results for both the overflow and baseflow components. The Swirl-Flo™ and Storm King™ HDVS both have a dead volume of approximately 25% of the total volume based on the approach adopted by Luyckx *et al.*, (1998a). Additionally it is not clear if the t_{50}/τ index presented by Luyckx *et al.*, (1998a) relates to the overflow or baseflow component and the t_{50}/t_m index presented in this project shows that this information is required. The overflow t_{50}/t_m index for the Swirl-Flo™ HDVS operating with no baseflow and without the sludge hopper (section 4.4.8) decreases and the baseflow t_{50}/t_m index increases as inlet flow rate increases (Table 6.11 and 6.22). However, the Swirl-Flo™ HDVS investigated in this project, based on the approach adopted by Luyckx *et al.*, (1998a), has a greater fraction of the overflow component short-circuiting at high flow rates and the baseflow component at low flow rates. This is supported by the Swirl-Flo™ HDVS overflow and baseflow RTD curves (section 6.2.3

and 6.2.6).

The USEPA RTD parameter guidelines (Stover *et al.*, 1986) state that the t_{50}/t_m index only measures the skew of the RTD curve and a value less than one is detrimental (section 4.3.4). Therefore, the t_{50}/τ index used by Luyckx *et al.*, (1998a) is not only incorrect as mentioned above, it is also not truly representative of the short-circuiting within the HDVS. This index can provide a value equal to one and therefore, perfect plug-flow mixing is present however, short-circuiting can still occur (section 4.3.4). Additionally, this RTD index is only designed to provide an indication of the non-ideal flow behaviour within a device for comparative purposes and not to provide quantitative information. The RTD indices, which identify short-circuiting are t_f/τ (severe) and t_p/τ (average) (section 4.3.4). The Storm King™ and Swirl-Flo™ HDVS inactive flow behaviour could be quantified and compared using the RTD combined model (chapter 5).

The Storm King™ HDVS RTD normalised curves E(Θ) presented for the same inlet flow rate and the maximum (50%) and minimum (10%) flow splits investigated, show that as the flow split increases the baseflow component plug-flow mixing characteristics reduce, as the peak of the RTD curve is closer to the origin. This is supported by the RTD normalised curves E(Θ) and the ADM and TISM parameters obtained for the Swirl-Flo™ HDVS baseflow component measured at SP2 and to a greater extent at SP3 (section 6.2.3 and 6.2.6). The Storm King™ HDVS RTD baseflow experiments operating with a 50% flow split also showed that the tracer was equally split between the two flow components. This is in agreement with the RTD tracer recovery (mass balance) and flow split relationship presented in this project (appendix E.1-E.4).

The Swirl-Flo™ HDVS operating with a baseflow component and measured at SP3 i.e. including the sludge hopper also provides similar results to the Storm King™ HDVS baseflow component. This is surprising as the Storm King™ HDVS operates without a

sludge hopper (Table 1.1) and this project has shown that the sludge hopper significantly effects the mixing characteristics of the baseflow component (section 6.2.3 and 6.2.6). However, as neither the Grit King™ (6.2.7.1) or Storm King™ HDVS RTD baseflow investigations detail the exact location of the baseflow sampling point, it is difficult to be entirely confident as to which data generated in this project is directly comparable. A RTD sample location downstream of the baseflow exit point will detect the mixing characteristics of the length of pipe between the exit and sampling point and it will behave in a similar manner as the sludge hopper. This was observed during preliminary prototype HDVS RTD investigations undertaken in this project (section 6.1).

6.3 Chapter Overview

This chapter has characterised the mixing regime within a model and prototype HDVS operating with a baseflow component using RTD analysis. This HDVS operating configuration enables the mixing regime associated with the overflow and baseflow component to be individually characterised. Additionally the total flow (overflow + baseflow) mixing regime characteristics are also obtained and compared to the total flow mixing characteristics for the HDVS operating without a baseflow component i.e. overflow only (chapter 4). The sludge hopper mixing regime is also investigated by obtaining the baseflow component RTD from a location above (SP2) and below (SP3) the sludge hopper. The overflow and baseflow components have a different and complex mixing regime, which depends on the inlet flow rate. The individual flow components and the total HDVS volume has an imperfect plug-flow mixing regime and the non-ideal flow behaviour is associated with both dispersion and dead volumes, which result in short-circuiting.

It was first assumed that the baseflow RTD curve peak concentration would occur before the overflow RTD curve. This assumption was based on the physical characteristics i.e. internal configuration of the HDVS (Fig. 3.1) and the 'assumed' relative flow paths of the overflow and baseflow component. The flow is likely to leave the HDVS through the baseflow before the overflow as higher velocities are located in the outer zone of the HDVS compared to the inner zone. The inner zone is located between the baseflow and overflow outlet and therefore, slows the flow prior to leaving through the overflow. However, the baseflow RTD curves peak concentration occurs at different times depending on the sample point (SP2 or SP3) used to measure the RTD tracer concentration. This highlights the importance of the sample point location on the measured RTD within a system.

The baseflow RTD curves measured at SP2 peak before the overflow curves at low inlet flow rates as expected however, at high inlet flow rates the opposite occurs and implies that short-circuiting of the overflow component occurs. This was also observed for the HDVS operating with no baseflow component (chapter 4) and supported by the RTD combined model analysis (chapter 5). The baseflow RTD curves measured at SP3 generally peak after the overflow curve. This is due to the buffering capacity of the sludge hopper, which is included in the SP3 RTD analysis and increases the transit time of the baseflow component. The RTD curves times to peak concentration observations are also illustrated by comparing the overflow and baseflow experimental mean residence times. This is expected as the mean residence time calculation (RTD centroid – first moment) is strongly influenced by the time at which the peak tracer concentration occurs (section 4.3). The sludge hopper acted as a stagnant or 'sluggish-flow' volume when the HDVS is operated without a baseflow (chapter 4 and 5). However, with the introduction of a baseflow component, the sludge hopper acts as a controlled quiescent zone.

Subsequently, the majority of the HDVS volume is active when a baseflow component is introduced. This is shown by the excellent tracer recovery (mass balance) results obtained at all flow rates investigated and the reduced tailing of the RTD curves and therefore, fraction of the total volume with long residence times.

The RTD curves also show that the overflow component short-circuits at high flow rates, as the overflow component time to peak concentration occurs closer to the origin at high flow rates and therefore, further away from a normalised time (Θ) value of 1. A normalised time (Θ) value of 1 corresponds to one complete volume of the HDVS and a peak concentration occurring at this time, would suggest that a greater volume of the overflow component is active in the mixing process. Additionally, using this criteria the RTD curves also clearly show that the baseflow component short-circuits at low flow rates and is greater for the baseflow component measured at SP2 compared to SP3. The baseflow measured at SP3 RTD curves also show that as the flow split is increased for the same inlet flow rate, short-circuiting of the baseflow component increases and at SP2 the short-circuiting remains constant for all flow splits.

The model HDVS volume estimations calculated using the experimental mean residence time for both the SP2 and SP3 RTD results have an average error of +5-+15%. The average estimated volume difference between the SP2 and SP3 RTD results is approximately 8.5 litres and the measured volume of the sludge hopper is 5 litres (section 3.3.2). The theoretical mean residence time of both the overflow and baseflow components is not necessarily a true representation, as implied by Tyack and Fenner, (1998b) who stated it was "not possible to determine with any meaning". However, RTD tracer studies are a recognised technique to calculate such unknowns and the model HDVS volume estimation results, combining the overflow and baseflow components, provide confidence in the presented experimental mean residence time values and

particularly as a long RTD experimental duration and truncation effects have not been considered (section 4.4.1.1). The prototype HDVS volume estimation results also provided similar conclusions.

The short-circuiting of the overflow component at high flow rates and the baseflow component at low flow rates is possibly related to the strength of the vortex generated within the HDVS and the internal configuration of the HDVS (Fig. 3.1). At low flow rates, a weak vortex could allow the baseflow component to take a shorter flow path, whereas at high flow rates a stronger induced vortex would force the flow path around the perimeter of the HDVS prior to leaving the baseflow outlet. Hence, at high flow rates the forced longer flow path would reduce short-circuiting. Additionally as the flow split increases the baseflow is less likely to be forced around the perimeter of the HDVS prior to leaving the baseflow outlet and hence, will take a shorter flow path and therefore short-circuit. This contrasts with the overflow component, as a weak vortex would be confined between the outer wall and vertical dip plate i.e. outer zone and would leave the HDVS as it is displaced by the incoming flow in a time equal to approximately the mean residence time. Whereas a stronger vortex creating turbulent conditions at the inlet, could possibly direct the flow beneath the inlet deflector plate and vertical dip plate and provide an easier flow path to the overflow outlet and hence, short-circuiting of the overflow component. Existing research has shown that increasing the depth of the vertical dip plate (Fig. 3.1), which may potentially minimise short-circuiting of the overflow component, is detrimental to the solids retention efficiency of the HDVS (Harwood and Saul, 1996b). However, the RTD provides the necessary information to account for this non-ideal flow behaviour in the design of the HDVS for kinetic process applications.

The overflow component ADM (P_e) and TISM (N) parameters are very similar for

the baseflow component measured at SP2 and SP3 RTD experiments. This is anticipated as the overflow component is unaffected by changing the baseflow sample point location (Fig. 6.1). The overflow component ADM and TISM parameters calculated using the method of moments and non-linear regression generally remain stable or marginally increase as the flow split increases i.e. as the overflow component flow rate decreases. However, the baseflow component ADM and TISM parameters have different characteristics with respect to the flow split, depending on the sample point location (Fig. 6.1). At SP2 the baseflow component ADM and TISM parameters are relatively stable and at SP3 they significantly decrease as the flow split increases for the same inlet flow rate. Therefore, for a fixed inlet flow rate the baseflow component measured at SP3 plug-flow mixing characteristics decrease and greater short-circuiting occurs as the flow split increases. However the baseflow component measured at SP2 mixing characteristics are the same across the range of flow splits for the same inlet flow rate.

The baseflow component measured at SP2 ADM and TISM parameters suggest that the mixing regime is fairly uniform for the same inlet flow rate and all flow splits and therefore, imply a well-mixed system rather than a perfect plug-flow mixing regime (section 4.1). Subsequently, increasing the flow rate of the baseflow component i.e. increasing the flow split, will have little effect in changing the plug-flow mixing characteristics. Whereas the flow path from SP2 to SP3 i.e. through the sludge hopper has significant plug-flow mixing characteristics and this will be affected by increasing the flow rate i.e. increasing the flow split. The Peclet numbers (P_e) for the baseflow component measured at SP3 are also significantly higher than at SP2 for the same inlet flow rate. Therefore, the sludge hopper behaves as a quiescent zone and improves the plug-flow mixing characteristics of the baseflow component. The sludge hopper appears to act a tubular reactor and provide plug-flow mixing when the HDVS is operated with a

baseflow component. However, the sludge hopper behaves as a stagnant or 'sluggish-flow' volume when the HDVS is operated without a baseflow component and contributes to dispersion and mixing effects (chapter 4 and 5).

At low flow rates the baseflow component measured at SP2 Peclet number (P_e) is approximately equal to zero for some flow splits. This is due the constraint applied to the normalised variance parameter in the ADM non-linear regression simulation and is required to obtain a meaningful solution (section 6.2.1.2). The requirement of a mathematical constraint to solve the ADM using non-linear regression, for the baseflow component measured at SP2 only, suggests that the assumptions of the ADM are not satisfied by the real system (section 4.3.3). Subsequently, the mixing regime is approaching complete mixing at the SP2 location i.e. around the cone region within the HDVS (Fig. 3.1). Additionally, as the constraint is not required for the baseflow component measured at SP3, this implies that the mixing regime has improved plug-flow mixing characteristics due to the introduction of the sludge hopper.

The overflow and baseflow ADM and TISM parameters calculated using the method of moments and non-linear regression generally decrease and increase respectively as the inlet flow rate is increased. The overflow component ADM and TISM parameters generally follow the same trend as achieved for the HDVS operating with no baseflow and therefore show that the plug-flow mixing characteristics improve as the flow rate decreases (chapter 4). This project is the first comprehensive characterisation of the HDVS operating with an overflow and baseflow component simultaneously using RTD analysis and interestingly shows that the baseflow component has a greater element of plug-flow mixing as the inlet flow rate increases. The relationship between the overflow and baseflow component ADM and TISM parameters and the inlet flow rate is possibly a function of the vortex generated within the HDVS and the internal configuration as

discussed above (Fig. 3.1). Subsequently, from the previous discussion there are two different mixing regimes within the HDVS which are associated with the overflow and baseflow component. The difference between the overflow and baseflow component mixing regimes is greater when the baseflow is measured at SP3 (Fig. 6.1).

It appears that the high internal velocities in the outer zone and velocity gradients in the cone region (Fig. 3.1), which are a feature of the HDVS and advantageous for solids-liquid separation (Andoh, 1994), create a large degree of mixing and subsequently short-circuiting. This is detected in the baseflow RTD measured at SP2 and due to the influence of the sludge hopper at SP3 is subsequently reduced. The HDVS RTD sampling configuration operating with a baseflow component provides a measured RTD from 3 locations within the HDVS i.e. SP1, SP2 and SP3 (Fig. 6.1). Comparing the magnitude of the ADM and TISM parameters, calculated from the RTD measured at each location, suggests that there are three different mixing regimes within the HDVS. These are the outer zone, inner zone and sludge hopper (section 3.2) (Fig. 3.1). The former provides a mixing regime closer to complete mixing and the remaining two regions have improved plug-flow mixing characteristics. The sludge hopper region also provides a greater degree of quiescent flow behaviour and therefore, plug-flow mixing conditions compared to the inner zone. This is shown by the baseflow component measured at SP3 ADM and TISM parameters, which are greater than the overflow component and for the baseflow component measured at SP2, either the opposite occurs or it is not possible to distinguish any significant difference between the overflow and baseflow ADM and TISM parameters. Additionally, as previously stated, the ADM and TISM parameters are greater for the baseflow component measured at SP3 compared to SP2 and the overflow ADM and TISM parameters are very similar regardless of the baseflow component sample location.

The different mixing characteristics identified for the overflow and baseflow component supports introductory comments to this chapter that the HDVS has a complex mixing regime and it is not the same throughout the complete volume. Subsequently, conducting RTD experiments for the HDVS operating with a baseflow component are justified, whereas measuring the RTD at different locations within a perfect plug-flow or complete mixing reactor will provide the same mixing characteristics and is therefore a futile exercise.

The improvement in the baseflow component plug-flow mixing characteristics measured at SP3 compared to SP2 is also shown by comparing the total flow (overflow + baseflow) ADM and TISM parameters calculated using the method of moments and non-linear regression. The individual flow components are still classified as high dispersion, as achieved for the overflow component when the HDVS is operated with no baseflow (chapter 4). However, the total flow plug-flow mixing characteristics describe a system with moderate dispersion at high flow rates. The overflow component ADM and TISM parameters are very similar for the HDVS operating with and without a baseflow component. Hence, the introduction of a baseflow component, including the sludge hopper, significantly increases the degree of plug-flow mixing within the total flow from the HDVS. The introduction of a baseflow component maintains the same degree of total flow plug-flow mixing at low flow rates and increases it at high flow rates compared to the HDVS operating without a baseflow component (chapter 4). This statement is improved by including the sludge hopper in the baseflow component RTD (SP3), as this increases the total flow plug-flow mixing at low flow rates and therefore, further increases it at high flow rates. This is due to the weighting created by the baseflow component ADM and TISM parameters measured at SP3, which significantly increase as the inlet flow rate increases, whereas the overflow component remains relatively stable.

As stated above, the sludge hopper appears to act as a tubular reactor i.e. pipe when the HDVS is operated with a baseflow component.

The largest plug-flow mixing element within the HDVS operating with a baseflow component exists at the highest inlet flow rate. This has significant advantages for providing effective high-rate chemical treatment and particularly as the HDVS has the ability to operate at very high inlet flow rates for a small footprint compared to conventional treatment processes (Boner *et al.*, 1994). However, if the HDVS is to provide combined solids removal and chemical treatment, a compromise in the operating conditions will be required. This is because the HDVS solids removal efficiency generally improves at low flow rates and high flow splits (chapter 2). This combination of operating conditions provides the smallest element of plug-flow mixing based on the RTD results presented in this chapter. However, the inclusion of the sludge hopper in the HDVS configuration provides optimum conditions for solids separation (Andoh, 1994) and also increases the contact time and the plug-flow mixing characteristics of the baseflow component. Subsequently the baseflow component will provide better mixing characteristics for disinfection processes compared to the overflow e.g. greater microbial kill and less residual disinfectant (section 2.2.3). Additionally, depending on the desired performance of a specific kinetic process, a compromise is also required between the overflow and baseflow component mixing regime, based on the inlet flow rate and the required properties of the overflow and baseflow effluent. This is because the overflow and baseflow component plug-flow mixing characteristics decrease and increase respectively as the flow rate increases. Therefore, considering kinetic process applications within the HDVS, largely dependent on the mixing characteristics (chapter 7), it maybe beneficial to operate the HDVS in series to achieve the desired overflow and baseflow component composition.

The method of moments and non-linear regression correlation parameters (R^2 and ESS) generally show that the ADM provides the best-fit to the experimental overflow and baseflow RTD curves for all SP3 RTD experiments and the overflow component only for the SP2 RTD baseflow experiments. The TISM generally provides the best-fit to the baseflow component measured at SP2. The baseflow RTD measured at SP3 has improved plug-flow mixing characteristics compared to the baseflow RTD measured at SP2, as shown by the ADM and TISM parameters discussed above. The ADM describes the deviation from plug-flow mixing and hence, is more likely to provide a better fit when less dispersion is present (SP3) (section 4.3.3). This occurs for the ADM and TISM correlation parameters discussed above and therefore, the correlation parameters are a function of the individual flow models and the HDVS's non-ideal flow behaviour. The ADM and TISM correlation parameters calculated using the non-linear regression parameter estimation technique are generally better compared to the method of moments (section 4.4.3). The ADM and TISM do not account for short-circuiting within the HDVS and therefore, as the overflow and baseflow component short-circuit at high and low flow rates respectively, the correlation parameters should follow same trend. However, only the TISM correlation parameters generally provide this relationship with the inlet flow rate. The relationship between the ADM and TISM correlation parameters and the HDVS's non-ideal flow behaviour is discussed in detail in chapter 4 (section 4.4.3).

The TISM parameters estimated using non-linear regression were shown to be superior to other RTD data analysis combinations for the HDVS operating without a baseflow component (section 4.4.3). This was observed, mainly due to the non-linear regression techniques reduced biased estimation of the TISM parameters as a result of being less sensitive to the RTD experimental duration and the HDVS's non-ideal flow

behaviour compared to other RTD data analysis techniques. This is supported for the HDVS operating with a baseflow component RTD results based on the error between the theoretical and experimental mean residence time and subsequently the HDVS experimental volume estimations. Additionally, the ADM parameters calculated using non-linear regression are subject to a mathematical constraint and therefore, this reduces confidence in their description of the HDVS's mixing regime.

The RTD indices were also calculated to investigate the different mixing characteristics of the baseflow component measured at SP2 and SP3 (section 4.3.4). The baseflow component RTD indices support previous observations obtained from the RTD curves and the ADM and TISM parameters. Subsequently, the RTD indices show that the baseflow component including the sludge hopper (SP3) has less short-circuiting compared to the baseflow component without the sludge hopper (SP2) (Fig. 6.1). Additionally the baseflow component including the sludge hopper (SP3) has better plug-flow mixing characteristics. The baseflow component RTD indices (SP2 and SP3) relationship with the inlet flow rate shows that the baseflow component has improved plug-flow mixing characteristics as the inlet flow rate is increased. The baseflow component also has less short-circuiting at high flow rates compared to low flow rates and therefore, a greater volume is active in the mixing process. It is not possible to distinguish any noticeable trend in the RTD indices across the range of flow splits investigated for the same inlet flow rate.

The t_{10} parameter is occasionally used as the time element (T) in the CT disinfection design methodology (section 4.3.4) and significantly, the t_{10} parameter calculated for the baseflow component measured at SP3 are all greater than at SP2 for the same inlet flow rate and flow split. Subsequently, including the sludge hopper (SP3) reduces the C component required to achieve a specified CT value, compared to the baseflow

component without the sludge hopper (SP2). This has practical, environmental and financial implications by reducing the quantity of the reactant required e.g. disinfectant.

The RTD results presented in this chapter and limited RTD data on different styles of HDVS (Table 1.1) both provide similar descriptions of the mixing regime within the HDVS using the RTD curves and the ADM and TISM parameters. However the existing HDVS RTD investigations are not consistent or comprehensive in their characterisation of the HDVS's mixing regime and prevents a reliable comparison. Subsequently, the author proposes a RTD investigation protocol, based on the approach undertaken in this project, to provide an accurate characterisation of the mixing regime within the different styles of HDVS (Table 1.1) (chapter 8).

The characterisation of the mixing regime within the model and prototype HDVS operating with and without a baseflow component and with and without the sludge hopper (Fig. 6.1) has now been achieved in a consistent and comprehensive manner using RTD analysis (chapter 4-6). This has been accomplished using a variety of RTD data analysis techniques to eliminate any associated limitations and to obtain a clear understanding of the HDVS's mixing regime. Subsequently, the RTD data exists in a number of different of formats suitable for future investigations. This includes: HDVS kinetic process efficiency investigations, HDVS RTD scaling investigations and comparisons to other systems subject to RTD analysis. The RTD data is presented in the appendices in electronic format and therefore, allows future workers to easily and readily gain access to apply the data to investigate any of the recommendations for future research (section 8.6).

The following chapter addresses the first recommendation above, by investigating the first-order decomposition of hydrogen peroxide (H_2O_2) using a biological enzyme – catalase (chapter 7). This kinetic process was investigated to support the RTD

investigations by showing that combining the RTD with batch reactor data can provide a reasonable prediction of the efficiency of a kinetic process within the HDVS.

7.0 Hydrogen Peroxide (H_2O_2) Decomposition Investigation – Kinetic Analysis

This project has extensively characterised the mixing regime within a HDVS using RTD analysis (chapter 4-6). However RTD analysis can be further developed to estimate the efficiency of a system for kinetic process applications. Typical kinetic process applications include chemical reactions, coagulation/flocculation and disinfection processes. This is investigated in this chapter.

The main objective for conducting a kinetic investigation is to measure the efficiency e.g. conversion, microbial inactivation etc and then to compare this to the efficiency estimated from RTD and batch reactor first-order principles. Hence, if the experimental and estimated (RTD modelled) kinetic process efficiency data provides similar results, it will be possible to model the HDVS using only RTD data and batch reactor investigations. This approach accounts for the non-ideal flow behaviour within the continuously operated HDVS and therefore, provides an optimum design as opposed to that obtained assuming a theoretical mixing regime (section 4.1). The kinetic process investigated in this study is the first-order decomposition of hydrogen peroxide (H_2O_2) by an enzyme - catalase.

The H_2O_2 concentration was measured for the model and prototype HDVS operating without a baseflow component (SP1) and with a baseflow component (SP3) (Fig. 6.1). Subsequently the corresponding pulse RTD results were used in the RTD - batch reactor H_2O_2 conversion estimation (chapter 4-6). The batch reactor and HDVS H_2O_2 decomposition experimental procedures and the H_2O_2 sample analysis technique are presented in chapter 3 (section 3.5). Recommendations for future research combining the RTD with kinetic process principles are provided in chapter 8 (section 8.6).

7.1 Hydrogen Peroxide (H_2O_2) and Catalase – A Natural Reaction

Hydrogen peroxide (H_2O_2) is produced naturally by both animal and plant cells and is formed as a by-product during the growth of bacteria to which it is toxic. However, the protein catalase, which is also naturally present, decomposes the H_2O_2 in to water and oxygen i.e.

$$H_2O_2\ (aq) \rightarrow H_2O\ (l) + O_2\ (g) \qquad (7.1)$$

H_2O_2 is one of the most versatile, dependable and environmentally desirable oxidising agents available today. It is relatively safe and simple to use for the treatment of organic and inorganic municipal and industrial wastewater, chemical processing and the bleaching of textiles, pulp and paper (Aldershof *et al.*, 1997). H_2O_2 is considered a poor disinfectant compared to chlorine, bromine and ozone and consequently H_2O_2 is generally not employed as a stand-alone treatment. However, there are a number of technologies, which use H_2O_2 as part of the treatment programme and include combined UV disinfection and H_2O_2 or ozone and H_2O_2. H_2O_2 is also combined with acetic acid (vinegar) to produce peracetic acid, which is commonly used for disinfection and sterilisation. Disinfection trials in the UK have combined the HDVS with peracetic acid (Realey, 1989) (section 2.1.5). Many metals improve the utility of H_2O_2 by acting as a catalyst for the H_2O_2 reaction. By far the most common of these is iron which, when used in a prescribed manner, results in the generation of highly reactive hydroxyl radicals (OH) and is termed Fenton's Reagent (Aldershof *et al.*, 1997). This combination is used to treat a variety of industrial wastes containing a range of toxic organic compounds e.g. wastewater and sludge. The primary reasons for investigating the decomposition of H_2O_2 by catalase are:

- Widely accepted that the decomposition of H_2O_2 using catalase rigorously follows first-order reaction kinetics (Dennis, 1984).
- H_2O_2 is an alternative disinfectant to methods currently employed i.e. concerns over chlorine due to the formation of trihalomethanes (THM) - carcinogenic.
- H_2O_2-catalase reaction considered to mimic behaviour of a disinfection mechanism.

7.2 Reaction Kinetics

The term first-order arises from the relationship between the reaction rate (r_A), rate constant (k) and the concentration of reacting species (C_A and C_B) thus:

$$-r_A = kC_A^{\alpha}C_B^{\beta} \qquad (7.2)$$

The individual reactant reaction order is α and β and the overall reaction order is the sum of the powers to which the individual reacting species are raised i.e. $\alpha + \beta$. The reaction rate constant (k) is only a constant for certain conditions e.g. temperature, pH etc. The reaction under investigation has only one reacting species i.e. H_2O_2, as catalase is an enzyme and assumed not to be consumed. Consequently, the last term on the right hand side of equation 7.2 is omitted and the reaction is termed pseudo first-order (Fogler, 1992) and equation 7.2 becomes:

$$-r_A = k'C_A^{\alpha} \qquad (7.3)$$

The reaction rate (r_A) is the rate of disappearance of a reactant or reactants i.e. H_2O_2 and for disinfection systems the inactivation rate of the target microorganisms. A first-order reaction can be defined as a process which proceeds at a rate proportional to the

concentration of the remaining reactants (Fogler, 1992). This is described by equation 7.5 and is obtained by combining equation 7.3 with the reaction rate (r_A) for a constant-volume batch reactor (eqn. 7.4).

$$r_A = \frac{dC_A}{dt} \tag{7.4}$$

and integrating with the limits $C_A = C_{AO}$ at t= 0.

$$C_A = C_{AO} \exp.(-kt) \tag{7.5}$$

Where: C_{AO} = Initial concentration of reactants (mg/l or mol/l)

C_A = Concentration at time t (mg/l or mol/l)

k = Reaction rate constant (min^{-1})

t = Time (min)

The reaction kinetics discussed above are analogous to disinfection processes. Disnfection kinetic relationships i.e. disinfectant and microorganism concentrations were first presented by Chick, (1908) and Watson, (1908). The former related the microorganism inactivation rate to the concentration of viable organisms and hence, the close similarity of microbial inactivation by chemical disinfectants to chemical reactions. The latter presented the relationship between the rate of inactivation (k) to the disinfectant concentration. The Chick-Watson method is a pseudo first-order relationship for microbial decay and assumes there is no disinfectant demand. More sophisticated and statistically accurate kinetic models exist, which are considered to better describe the disinfection process and include the Hom and Rational model (Haas

et al., 1995). These models account for the time lag until the onset of disnfection is often observed and a reduced rate of inactivation as time increases.

7.3 Residence Time Distribution (RTD) Conversion Theory

The characterisation of the mixing regime within the HDVS using RTD analysis has shown that it is non-ideal (chapters 4-6). This needs to be considered when predicting the performance of the HDVS, since a description of the true contact time of individual volumes is required. This could be achieved by using the single parameter flow models previously used to describe the RTD i.e. the ADM and TISM (section 4.3.3) and by considering micromixing effects discussed below i.e. the complete segregation model and the maximum mixedness model (section 7.5). In the experiments presented in this chapter the chemical conversion (X) is required i.e. H_2O_2 decomposition and is typically presented as a percentage of the initial concentration i.e. $X = (1- C_A / C_{AO}) \times 100$ (%).

If the reaction is first-order and proceeds in either a perfect plug-flow or complete mixing flow regime (section 4.1) the conversion (X) can be obtained using the following relationships (Levenspiel, 1972):

$$\text{Perfect Plug-Flow -} \quad X = 1 - e^{-\tau k} \tag{7.6}$$

$$\text{Complete Mixing -} \quad X = \frac{\tau k}{1 + \tau k} \tag{7.7}$$

Where: k = Reaction rate constant (min^{-1})

τ = Mean contact time (min)

τk = Damköhler number (Da) (dimensionless)

The plug-flow and complete mixing models provide the upper and lower limits of conversion (X) respectively. The conversion (X) for a first-order reaction using the ADM and TISM are determined using the following two equations respectively (Fogler, 1992):

ADM:
$$X = 1 - \frac{4\,q\,\exp(P_e/2)}{(1+q)^2\exp(P_e\,q/2) - (1-q)^2\exp(-P_e\,q/2)} \qquad (7.8)$$

Where:
$$q = \sqrt{1 + 4Da/P_e}$$

P_e = Peclet Number i.e. ADM parameter

TISM:
$$X = 1 - \frac{1}{(1+\tau\,k)^N} \qquad (7.9)$$

Where: N = Number of Tanks-in-Series i.e. TISM parameter

k = Reaction rate constant (min^{-1})

τ = Mean contact time (min)

τk = Damköhler Number (Da) (dimensionless)

The individual flow model conversion calculations (eqn. 7.6-7.9) require the relevant RTD parameters (chapter 4) and the reaction rate constant (k). The reaction rate constant (k) was obtained by conducting H_2O_2 – catalase conversion batch reactor experiments.

7.4 Batch Reactor Experiments

The batch reactor experiments were conducted to determine the reaction rate constant (k) (eqn. 7.10). Confidence in the actual reaction order (α) (Dennis, 1984) enables the integral method to be used to determine the rate constant (k), as opposed to other methods which obtain the rate constant (k) by an iterative process when the true reaction order (α) is unknown e.g. the differential method. The integral method is most often used when the reaction order (α) is known and it is desired to evaluate the reaction rate constant (k) at different temperatures to determine the activation energy (Fogler, 1992). Equation 7.10 is the equation commonly used to model a batch system if the reaction is first-order.

$$\ln \frac{C_{AO}}{C_A} = kt \qquad (7.10)$$

where: C_{AO} = Initial concentration (mg/l or mol/l)

C_A = Concentration at time t (mg/l or mol/l)

k = Reaction rate constant (min^{-1})

The rate constant (k) is the slope of the $\ln(C_{AO}/C_A)$ vs. time plot. If the reaction order assumed is correct i.e. α=1, the concentration vs. time data should provide a linear relationship (Fogler, 1992). The H_2O_2 – catalase conversion batch reactor results are discussed in section 7.6.1.

7.5 Micromixing Effects

The RTD describes how long different fluid elements have been in the system i.e. macromixing, but it does not provide information on the interaction of fluid elements with different residence times i.e. micromixing. Micromixing describes how molecules of different 'ages' encounter each other in the reactor. However, for first-order reactions all that is required to predict the conversion (X) is knowledge of the length of time each fluid element spends in the reacting environment i.e. first-order reaction conversion is independent of the concentration (Fogler, 1992). There are two zero parameter models which describe the theory of micromixing and as with macromixing, there are two extremes:

Complete Segregation - Fluid elements of the same 'age' remain together and only all mix once they have left the reactor i.e. late mixing (Fig. 7.1a) (Danckwerts, 1958).

$$\overline{X} = \int_0^\infty X(t)\,E(t)\,dt \qquad (7.11)$$

Where: $\overline{X}$ = mean conversion within the total volume spending between time t and t + dt in the reactor

X(t) = conversion achieved after spending time t in the reactor

E(t) = fraction of the total volume that spend between t and t + dt in the reactor (min^{-1})

Because each volume element between t and t + dt i.e. E(t) acts as a batch reactor of constant volume, the batch reactor design equation (eqn. 7.10) is used to calculate the conversion as a function of time i.e. X(t).

Maximum Mixedness - Fluid entering the reactor is completely mixed with the fluid already present i.e. early mixing (Fig. 7.1b) (Zwietering, 1959).

$$\frac{dX}{d\lambda} = \frac{r_A}{C_{AO}} + \frac{E(\lambda)}{1 - F(\lambda)}(X) \qquad (7.12)$$

The Euler method can be used for the numerical integration of the maximum mixedness model to obtain a solution (Fogler, 1992). The term on the right-hand side of equation 7.12 is the intensity function (λ), which is presented and discussed for the model and prototype HDVS (chapter 4). The maximum mixedness model is not investigated in this project, however the required RTD data is presented and available for any future studies into reaction kinetics and particularly for reactions other than first-order as discussed below.

These two extremes of micromixing will provide the upper and lower limits of conversion (X) respectively for a given RTD i.e. macromixing. Fig. 7.1a and 7.1b show the two theories of micromixing for a perfect plug-flow mixing reactor (section 4.1).

As the reaction between H_2O_2 and catalase is first-order it is irrelevant whether the complete segregation (eqn. 7.11) or maximum mixedness (eqn. 7.12) model is used to estimate the conversion within the HDVS. This is because the rate of change in conversion (X) for a first-order reaction does not depend on the concentration of the reacting molecules (Fogler, 1992). To follow current literature and particularly for disinfection systems, the complete segregation model (eqn. 7.11) is used to predict the experimental H_2O_2 conversion (Haas *et al.*, 1997). It should be noted that for any other reaction order e.g. second or third order, the degree of micromixing can significantly affect the predicted conversion. This was observed when predicting the microbiological load from a CSO discharge (Haas, 1988) (section 2.2.3). For reaction orders greater than one, the complete segregation model will give the highest conversion and for reaction

orders less than one, the maximum mixedness model will give the highest conversion (Fogler, 1992).

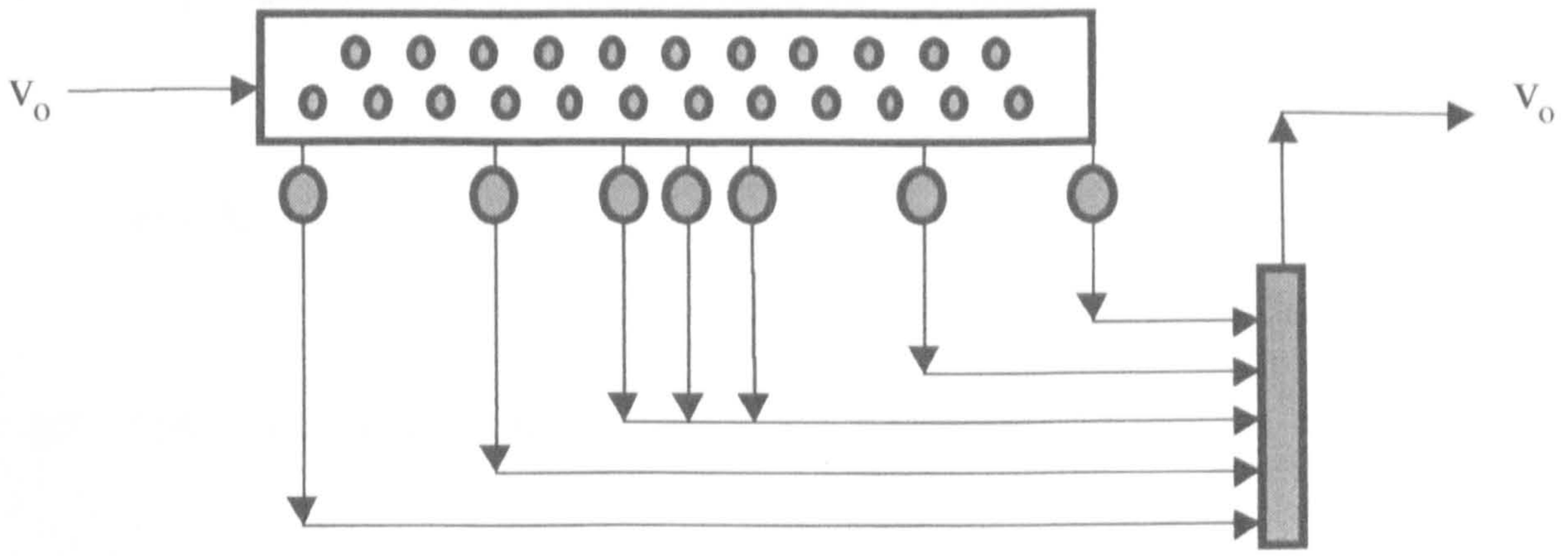

Fig. 7.1a Complete Segregation - Mixing at the Latest Possible Point

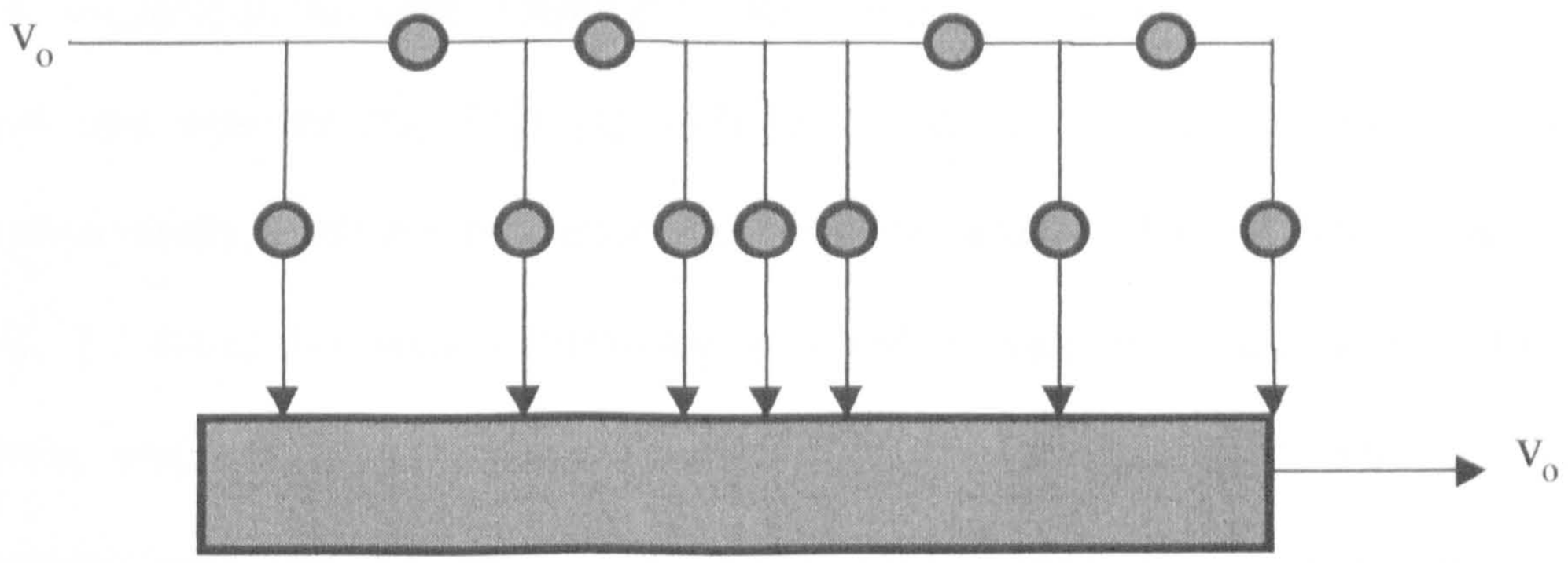

Fig. 7.1b Maximum Mixedness - Mixing at the Earliest Possible Point

The H_2O_2 and catalase experimental inlet feed arrangement consisted of a 'Y' shape connection located at DP2 (Fig. 3.1), which mixed both the H_2O_2 and catalase prior to entering the inlet pipe. This premixed feed arrangement was used in order to provide both reactants with the same mean residence time and ensures that they are completely mixed prior to entering the HDVS. This arrangement enables the outcome of the reaction using the RTD to be uniquely predicted (Treleaven and Tobgy, 1971). Therefore, the HDVS is not required to bring about mixing between the two reactants

but simply to provide sufficient volume to ensure that the necessary contact time is achieved at the flow rates investigated. A separate reactant feed arrangement would self-induce micromixing effects. This is a consideration for disinfection systems as they dose the incoming flow using a separate feed arrangement.

7.6 Results and Discussion

7.6.1 Batch Reactor Experiments

The same H_2O_2 and catalase concentrations were maintained for all model and prototype HDVS flow rates investigated (chapter 3). Subsequently, these H_2O_2 and catalase concentrations were subjected to batch reactor experiments to calculate the reaction rate constant (k). This approach allows the RTD – batch reactor H_2O_2 conversion results to be directly compared to the model and prototype HDVS results.

Fig. 7.2 shows the linear relationship achieved between the batch reactor H_2O_2 conversion and time using the integral method (R^2= 0.9945) (section 7.4). The reaction rate constant (k) obtained from the slope of this plot is 0.245min^{-1}. Hence, the original assumption that the reaction is first-order was correct (section 7.4). The rate constant value (k) is an average value obtained from 5 batch reactor experiments (appendix F.1.1). Evidence of the decomposition of H_2O_2 was provided by the formation of small oxygen bubbles (O_2) (eqn. 7.1) within the batch reactor as the experiment proceeded.

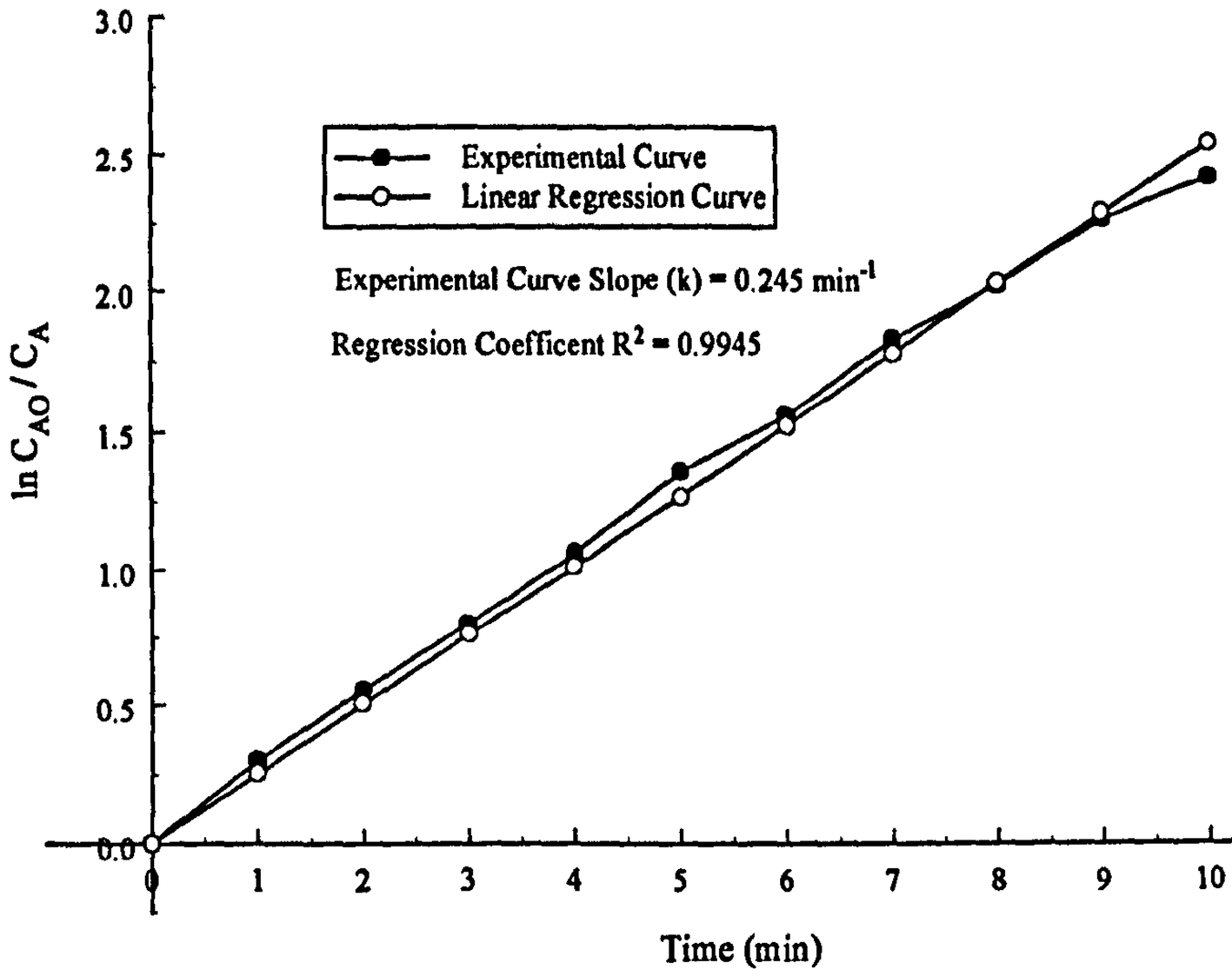

Fig. 7.2 Batch Reactor Experimental Data - Reaction Rate Constant (k)

Despite all experiments been conducted under nonadiabatic conditions i.e. heat is allowed to escape or be added to the system, it is apparent from the batch reactor H_2O_2 decomposition data (Fig. 7.2) that the reaction rate constant (k) describes a first-order decay i.e. linear relationship (section 7.4). The integral method assumes the experimental batch reactor was operated under isothermal conditions i.e. maintaining the same temperature and constant volume (Levenspiel, 1972). H_2O_2 can undergo spontaneous self oxidation-reduction but this decomposition is usually very slow (Hansen, 1996). The primary factors contributing to H_2O_2 decomposition include temperature, pH and contamination by metal ions. In most cases the pH and contamination work in tandem as the dominant factors. The change in temperature and pH on the decomposition rate of H_2O_2 has been documented by Aldershof *et al.*, (1997). The H_2O_2 decomposition rate is not effected by temperatures below 20°C however it increases approximately 2.2 times for each 10°C rise between 20°C and 100°C. The effect of pH is considered to be at a minimum between a pH of 4.5–6.8. All temperature

readings i.e. water supply and H_2O_2 samples ranged from 11-15°C and therefore, will have very little effect if any on the reaction rate constant (k) and measured experimental H_2O_2 conversion results based on the above critical temperature range. Mains tap water was used for all experiments and is considered to be free of any significant levels of contaminants and also provided a pH value in the range where its effects are considered to be a minimum. The water supply and H_2O_2 sample pH values ranged from 6.3-6.6.

Alternative data analysis techniques can be used to estimate the reaction rate constant (k) i.e. Weibull survival curve (Aldershof *et al.*, 1997) but the physical effects are relatively constant for all experiments and any potential errors can be ignored and the H_2O_2 conversion data from all experiments directly compared. Gustavsson *et al.*, (1998) showed that the catalase activity is independent of both the temperature and pH for the respective ranges achieved throughout this project.

7.6.2 Model Hydrodynamic Vortex Separator (HDVS) No Baseflow

Fig. 7.3 shows the experimental H_2O_2 conversion (X) plotted against the theoretical and experimental mean residence time calculated using the method of moments (Table 4.1) and non-linear regression (NLR) (Table 4.3 and 4.4). Appendix F.1.2 details the experimental results and provides the experimental H_2O_2 feed concentrations and overflow sample concentrations (SP1) from which the conversion is directly calculated. As expected, the conversion exponentially decreases as the mean residence time decreases i.e. as the flow rate increases.

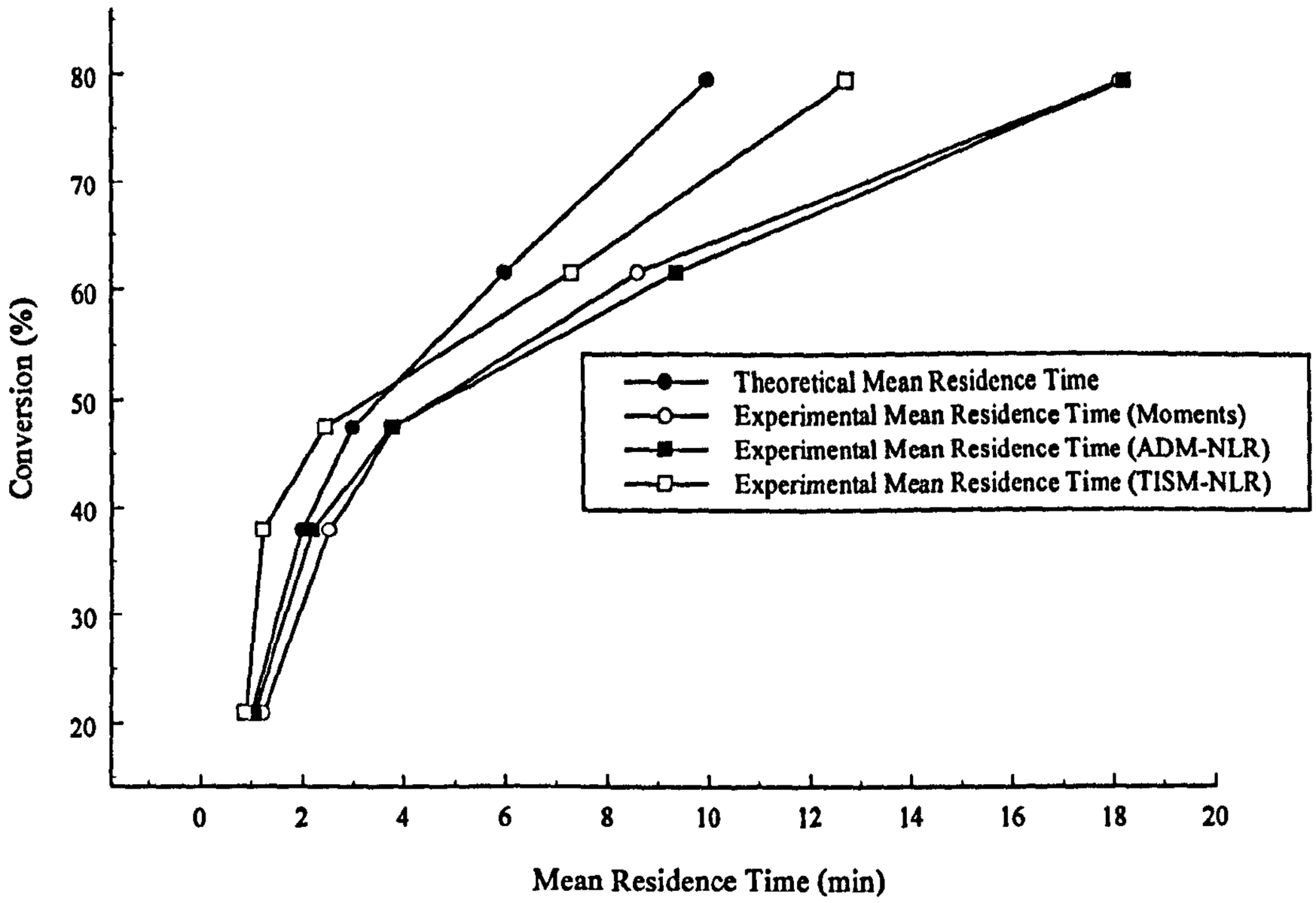

Fig. 7.3 Model HDVS No Baseflow - Experimental Conversion Results Plotted Against the Theoretical and Experimental Mean Residence Time

Figs. 7.4–7.6 compare the predicted and experimental H_2O_2 conversions. The different curves relate to the theoretical and experimental mean residence time, calculated using the method of moments or non-linear regression. The modelled conversion results for all combinations are presented in appendix F.1.3 and F.1.4.

The model HDVS results show that the experimental conversion is between the theoretical conversion boundaries i.e. plug-flow and complete mixing using the theoretical mean residence time (Fig. 7.4) (section 7.3). The experimental conversion tends to exceed these boundaries since the experimental mean residence time is greater than the theoretical mean residence time (section 4.4.1.1). The modelled conversion obtained from the ADM and TISM parameters calculated using non-linear regression provide a better estimation of the experimental conversion results as the experimental conversion is between the upper and lower limits (Fig. 7.6). These results provide confidence in the experimental data i.e. RTD curve, reaction rate constant (k) and the

H_2O_2 conversion and subsequently the use of the RTD and batch reactor data to predict the efficiency of the continuously operated HDVS. The H_2O_2 conversion results also support the RTD investigations by showing that the HDVS's mixing regime does not conform to a theoretical mixing regime and non-ideal flow behaviour is present (section 4.1).

The experimental conversion and flow model data correlation parameters (R^2 and ESS) (section 4.3.3) are presented in appendix F.1.5. These show for the method of moments ADM and TISM parameters and the theoretical mean residence time that the TISM provides the best-fit to the experimental data ($R^2 = 0.99232$, ESS = 46.143). The complete mixing model i.e. N=1 provides the best-fit using the method of moments experimental mean residence time ($R^2 = 0.99558$, ESS = 49.420). The theoretical mean residence time generally provides the better fit compared to the experimental mean residence time when used as the time element in the flow models.

The non-linear regression technique provides the best-fit using the complete mixing model and the ADM experimental mean residence time ($R^2 = 0.99073$, ESS = 78.497). The flow models that describe a well-mixed system (section 4.1) generally provide a better estimation of the experimental H_2O_2 conversion and this supports previous descriptions of the HDVS's mixing regime (chapter 4). Care needs to be taken when comparing the correlation parameters, due to the possibility of obtaining a good R^2 and poor ESS for the same data and therefore, a visual comparison of the goodness-of-fit is also recommended (section 6.2.1.1).

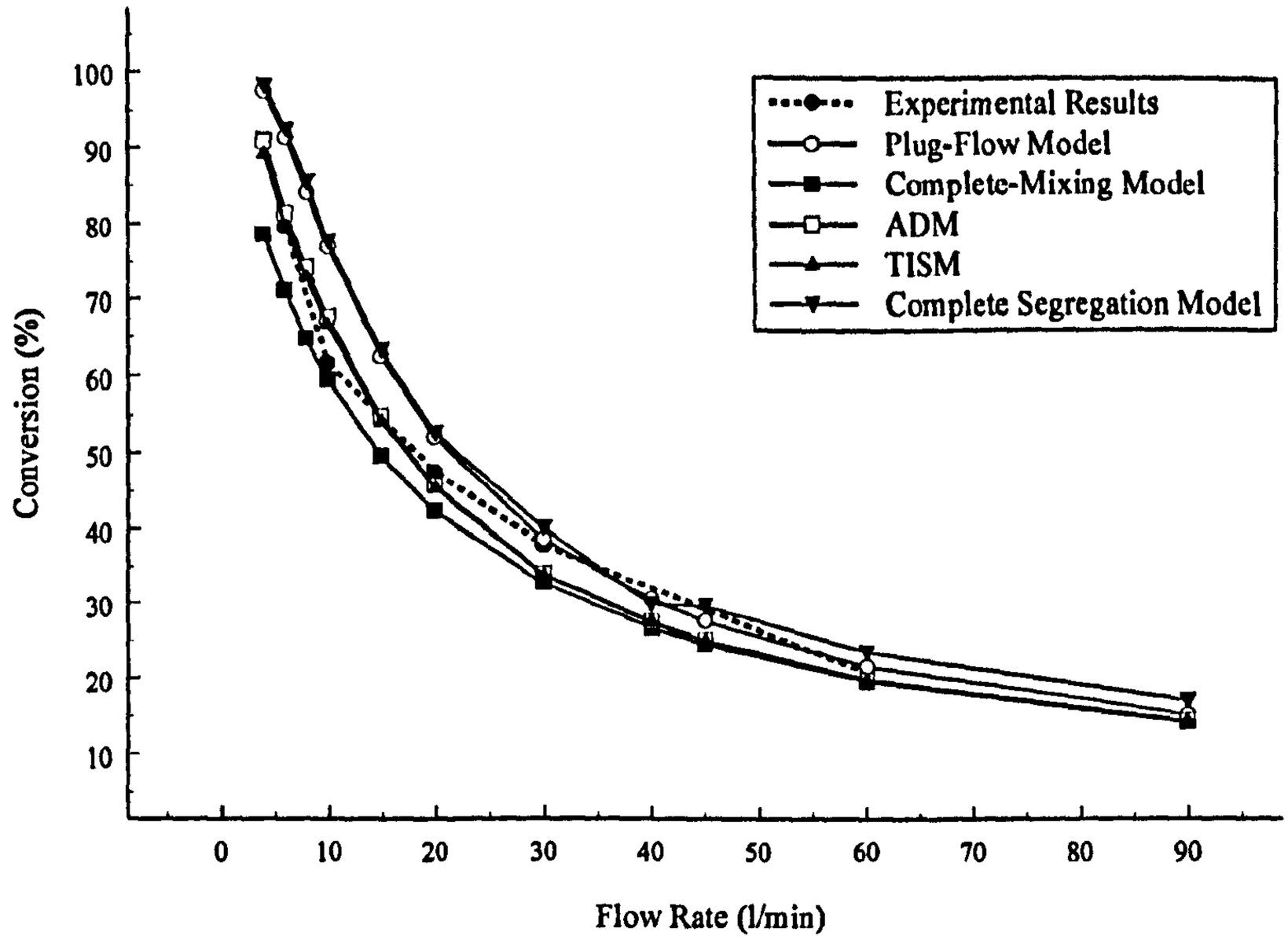

Fig. 7.4 Model HDVS No Baseflow - Comparison of Experimental and Flow Model Conversion Results using the Theoretical Mean Residence Time and Method of Moments ADM and TISM Parameters

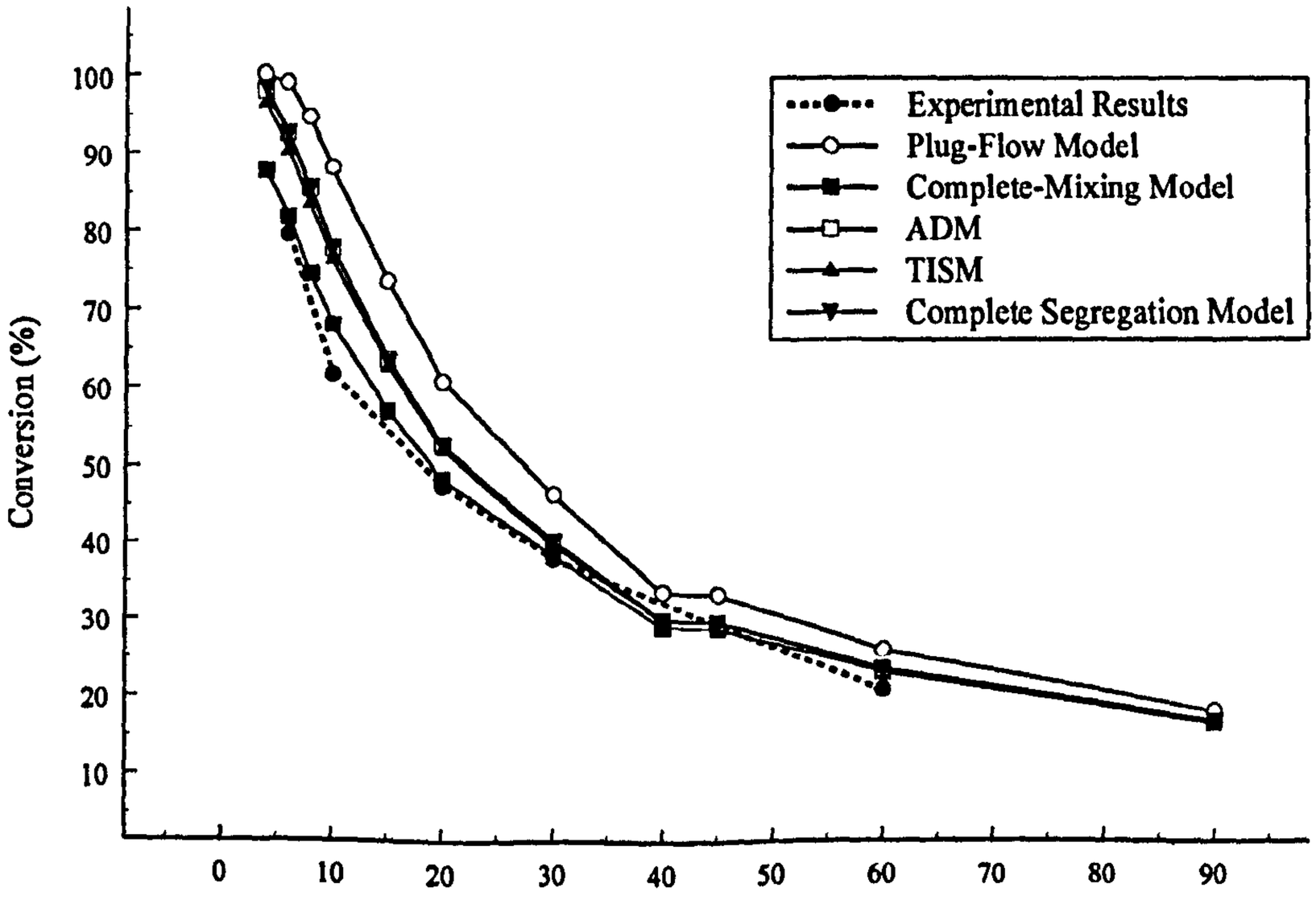

Fig. 7.5 Model HDVS No Baseflow - Comparison of Experimental and Flow Model Conversion Results using the Experimental Mean Residence Time, ADM and TISM Parameters Calculated using the Method of Moments

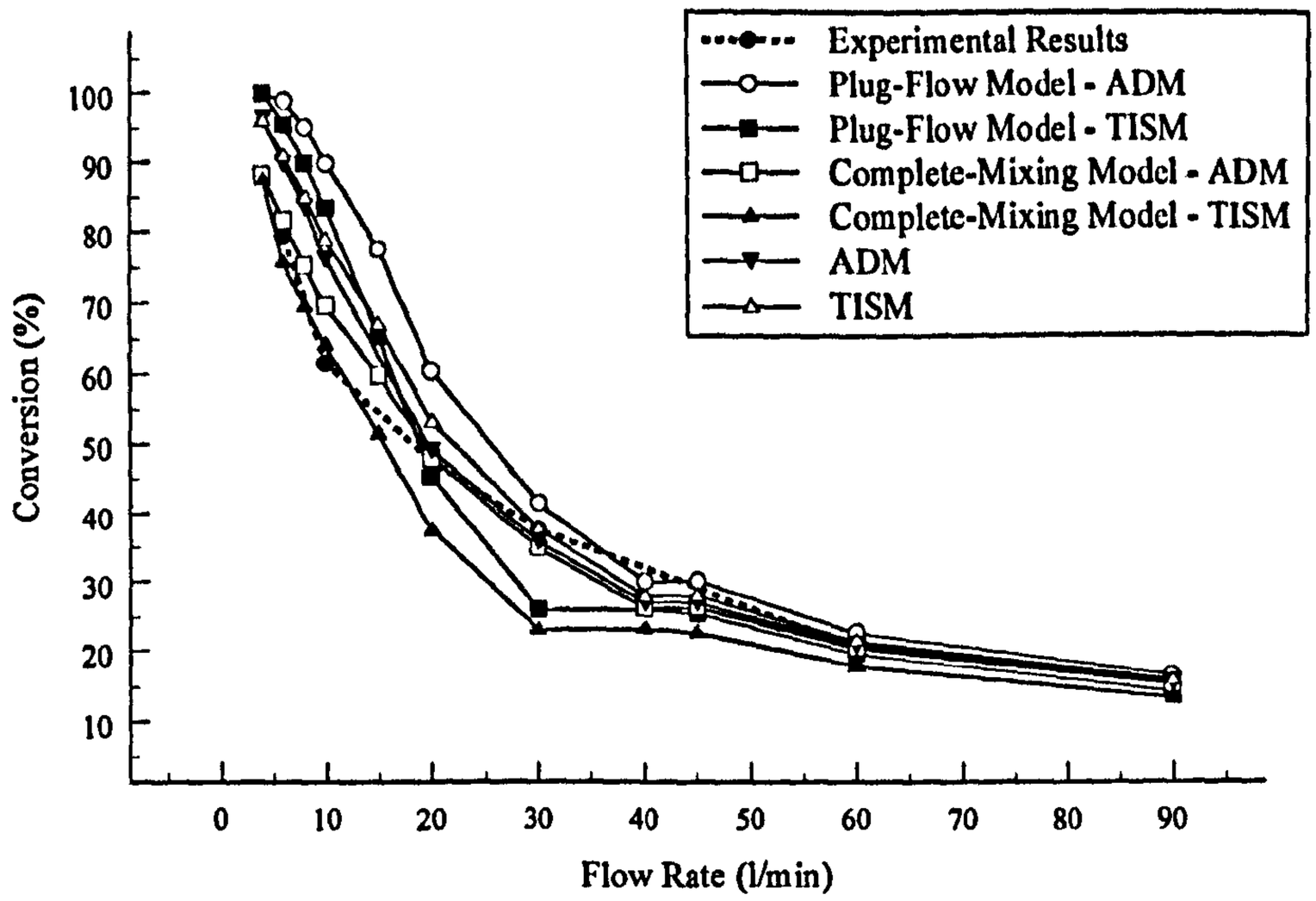

Fig. 7.6 Model HDVS No Baseflow - Comparison of Experimental and Flow Model Conversion Results using the Experimental Mean Residence Time, ADM and TISM Parameters Calculated using Non-Linear Regression

The complete experimental RTD data has been used to predict the flow model conversion however, truncating the RTD curve will influence the flow models conversion estimation. Consequently the duration of the RTD experiment is also an important parameter in calculating the performance of a system for kinetic processes. A truncated RTD curve will decrease the mean residence time and hence conversion. When the ADM and TISM parameters are included in the flow model, the conversion will increase as the parameters imply improved plug-flow mixing characteristics as the truncation time decreases (section 4.4.1.1). This statement discusses the experimental mean residence time and the ADM and TISM parameters as separate influences. Appendix F.1.6 shows the ADM and TISM flow model conversion values for various RTD truncation times (section 4.4.1.1). These results clearly show that the experimental mean residence time is the dominant parameter as opposed to the ADM and TISM parameters in estimating the experimental conversion. This is shown by the estimated

flow model conversion increasing as the truncation time is increased i.e. 2t → 6t and therefore, as the mean residence time increases. At the lowest truncation time (2t) i.e. smallest experimental mean residence time, the ADM and TISM parameters are at their highest however, the estimated conversion is still less than that obtained for the complete data.

The HDVS RTD investigations conducted in this project have shown that the characterisation of a mixing regime is subject to the limitations of the data analysis techniques used to describe the RTD (chapters 4 and 5). To minimise any possible errors due to these individual and combined limitations, the use of the complete segregation model (eqn 7.11) to estimate the kinetic process efficiency of a system is recommended (section 7.5). This is because the complete segregation model is a zero parameter model and a solution is obtained directly from the RTD curve. Hence the complete segregation model estimates the kinetic process efficiency directly as a function of the contact time provided by individual volumes as opposed to an average residence time for the complete system volume i.e. ADM and TISM. Subsequently the errors in the complete segregation model will only be associated with the experimental techniques used to obtain the RTD curve and batch reactor data (section 7.6.1). These errors can be more easily controlled and minimised by adopting the correct experimental procedures, compared to the errors associated with the mathematical interpretation of the RTD data analysis techniques. A truncated RTD curve will still affect the complete segregation model conversion estimation and therefore it is important to conduct the RTD experiment for a significant duration to ensure that a true description of the mixing regime is obtained across the range of flow rates (chapter 4).

The experimental H_2O_2 conversion results obtained at low flow rates provide a better indication of the flow model which best describes the mixing regime, as at high flow rates the predicted conversion range reduces and its interpretation is subject to

experimental errors. The experimental conversion calculation error based on the H_2O_2 concentration sample analysis technique is approximately +/-2% (section 3.5.3). Applying this to both the feed and sample concentrations provides a total experimental error of approximately +/-4%. At a flow rate of 60l/min the plug-flow mixing model (eqn. 7.6) conversion is only 10% greater than the conversion for a completely mixed tank (eqn. 7.7) compared to 30% at the lowest flow rate of 6l/min. The conversion difference at high flow rates (60l/min) is approaching experimental errors and hence, the data needs to treated with caution in this region. The above statement does not account for any experimental errors in the inlet flow rate and reactant feed flow rates. However, the inlet flow rate was measured using a calibrated rotameter and volumetrically during the experiment and the reactant feed flow rates were also fed into the HDVS using a calibrated rotameter (chapter 3). Additionally, experiments were conducted feeding only H_2O_2 through the model HDVS. The overflow H_2O_2 concentration results showed that there is no natural decomposition of the H_2O_2 and also proved that the inlet and reactant feed flow rates were correct. The Perspex used to construct the model HDVS is considered to be inert to any reactants used in this project. The results for these tests show that any potential experimental errors associated with the initial and sample concentration of H_2O_2 and the reactant and inlet flow rates are at a minimum (appendix F.1.7).

Fig. 7.7 shows the relationship between the experimental conversion and the ADM and TISM parameters calculated using the method of moments and non-linear regression. This shows that the conversion increases as both the model parameters increase. This supports RTD conversion theory, as maximum conversion will be achieved as the mixing regime approaches plug-flow mixing (section 7.3). As the flow rate decreases a greater contact time is provided however, the mixing regime is also closer to plug-flow mixing compared to high flow rates (section 4.4.1).

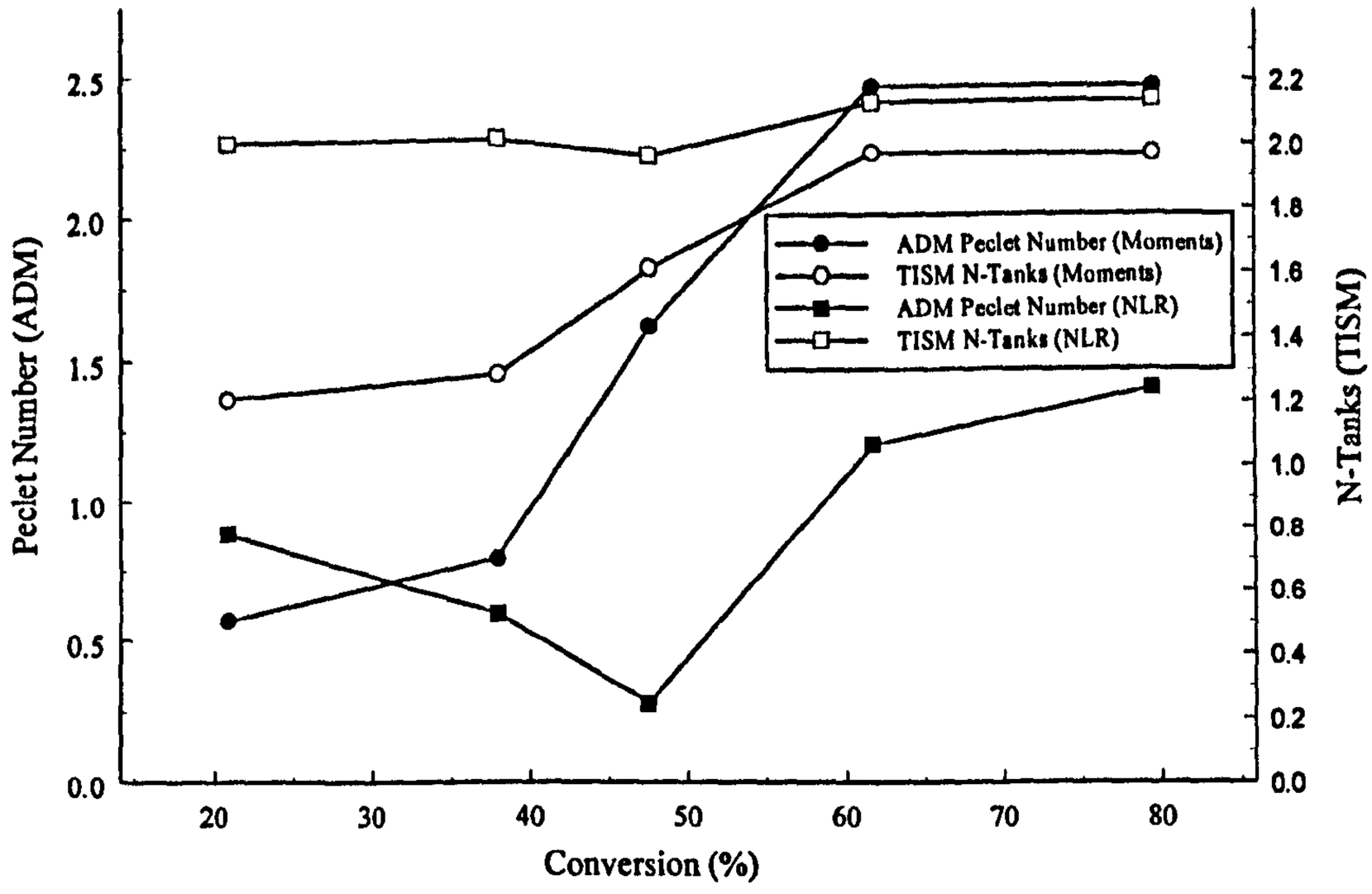

Fig. 7.7 Model HDVS No Baseflow - Comparison of Experimental Conversion and ADM and TISM Parameters Calculated using the Method of Moments and Non-Linear Regression

The RTD combined mathematical model previously used in this project to characterise the HDVS's mixing regime (chapter 5) can also be developed to include a reaction rate constant (k) (section 7.2). This enables the combined model solution to estimate the performance of a kinetic process within the HDVS accounting for the degree of non-ideal flow behaviour i.e. H_2O_2 decomposition. This could aid in determining which RTD data analysis combinations best describe the mixing regime and therefore, the HDVS's kinetic process efficiency.

Commercial grades of H_2O_2 contain stabilisers, which minimise its decomposition during transport and storage. The type and quantity of stabiliser varies depending on the manufacturer and have been shown to affect the rate of H_2O_2 decomposition (Aldershof *et al.*, 1997). Hence, this needs to be considered when comparing data sets obtained using different manufacturers or grades of H_2O_2 and for further work on the HDVS using the same procedure as adopted in this project.

7.6.3 Prototype Hydrodynamic Vortex Separator (HDVS) No Baseflow

Fig. 7.8 shows the experimental H_2O_2 conversion (X) plotted against the theoretical and experimental mean residence time calculated using the method of moments (Table 4.5) and non-linear regression (NLR) (Table 4.7 and 4.8). Appendix F.2.1 details the experimental results and provides the experimental H_2O_2 feed concentrations and overflow sample concentrations (SP1) from which the conversion is directly calculated. As expected, the conversion exponentially decreases as the mean residence time decreases i.e. as the flow rate increases.

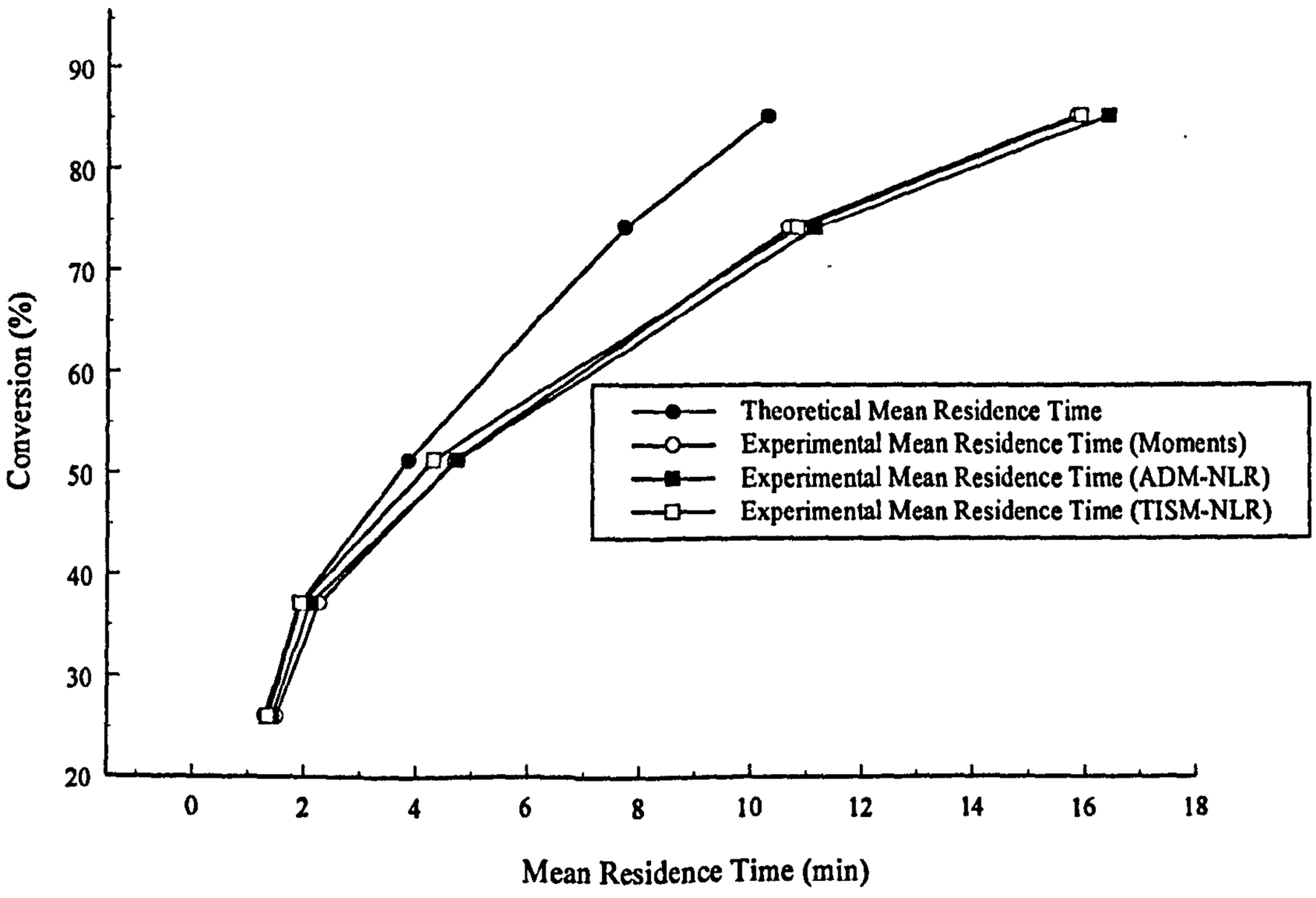

Fig. 7.8 Prototype HDVS No Baseflow - Experimental Conversion Results Plotted Against the Theoretical and Experimental Mean Residence Time

Figs. 7.9–7.11 compare the predicted and experimental H_2O_2 conversions. The different curves relate to the theoretical and experimental mean residence time, calculated using the method of moments or non-linear regression. The modelled conversion results for all combinations are presented in appendix F.2.2 and F.2.3.

The prototype HDVS results show that the experimental conversion is generally between the conversion boundaries of plug-flow and complete mixing (section 7.3). The relationship between the experimental conversion and the conversion boundaries is the same as obtained for the model HDVS (section 7.6.2).

The experimental conversion and flow model data correlation parameters (R^2 and ESS) (section 4.3.3) are presented in appendix F.2.4. These show for the method of moments ADM and TISM parameters and the theoretical mean residence time, the ADM provides the best-fit to the experimental conversion data. ($R^2 = 0.99477$, ESS = 29.800). The complete mixing model i.e. N=1, provides the best-fit using the method of moments experimental mean residence time ($R^2 = 0.99552$, ESS = 41.944).

The non-linear regression technique provides the best-fit using the complete mixing model and the ADM experimental mean residence time ($R^2 = 0.99389$, ESS = 40.476). The same observations for the model HDVS results apply to the prototype HDVS (section 7.6.2). Additionally, the influence of the RTD curve truncation time (appendix F.2.5) and the potential experimental errors are also the same as the model HDVS (section 7.6.2).

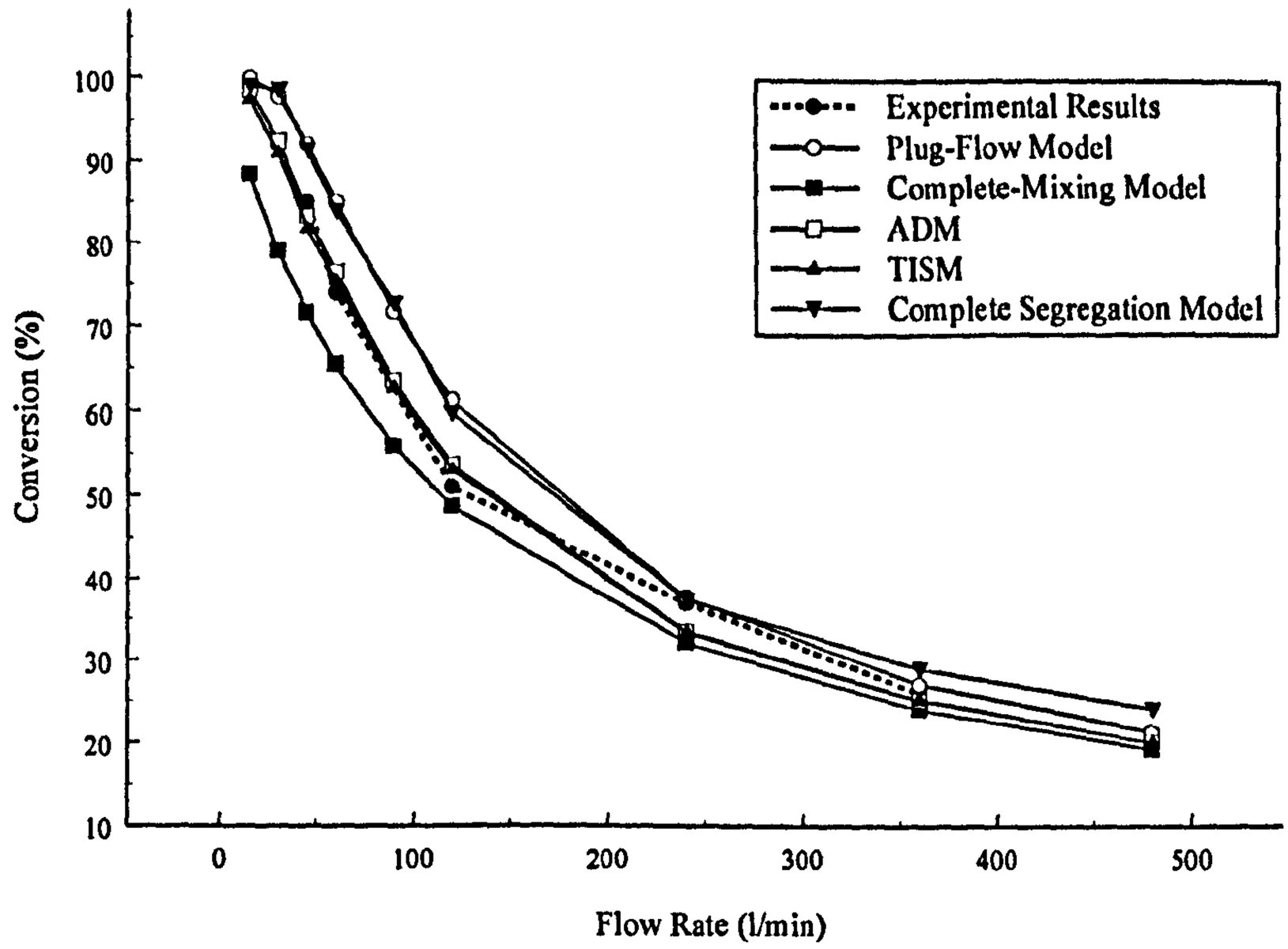

Fig. 7.9 Prototype HDVS No Baseflow - Comparison of Experimental and Flow Model Conversion Results using the Theoretical Mean Residence Time and Method of Moments ADM and TISM Parameters

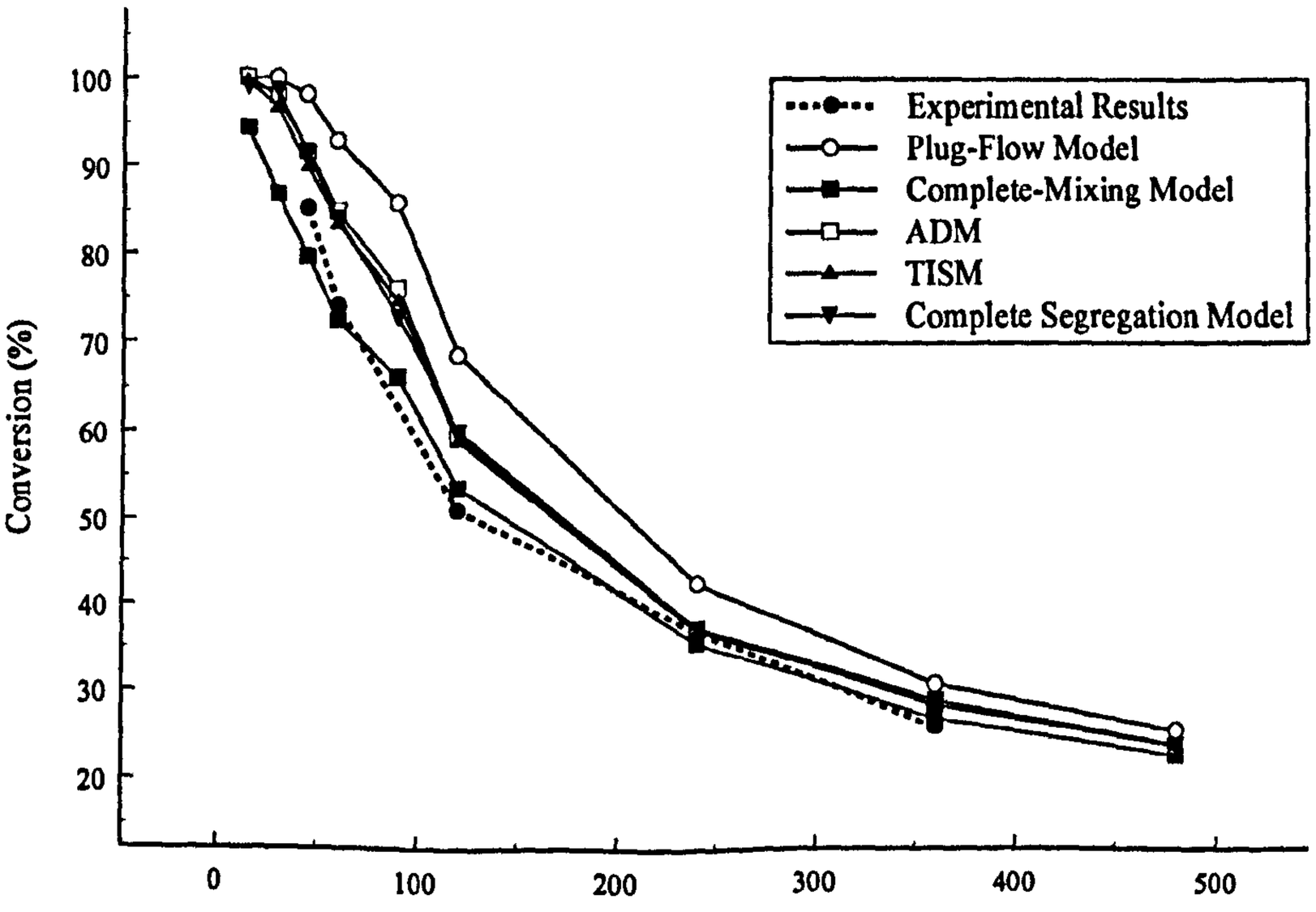

Fig. 7.10 Prototype HDVS No Baseflow - Comparison of Experimental and Flow Model Conversion Results using the Experimental Mean Residence Time, ADM and TISM Parameters Calculated using the Method of Moments

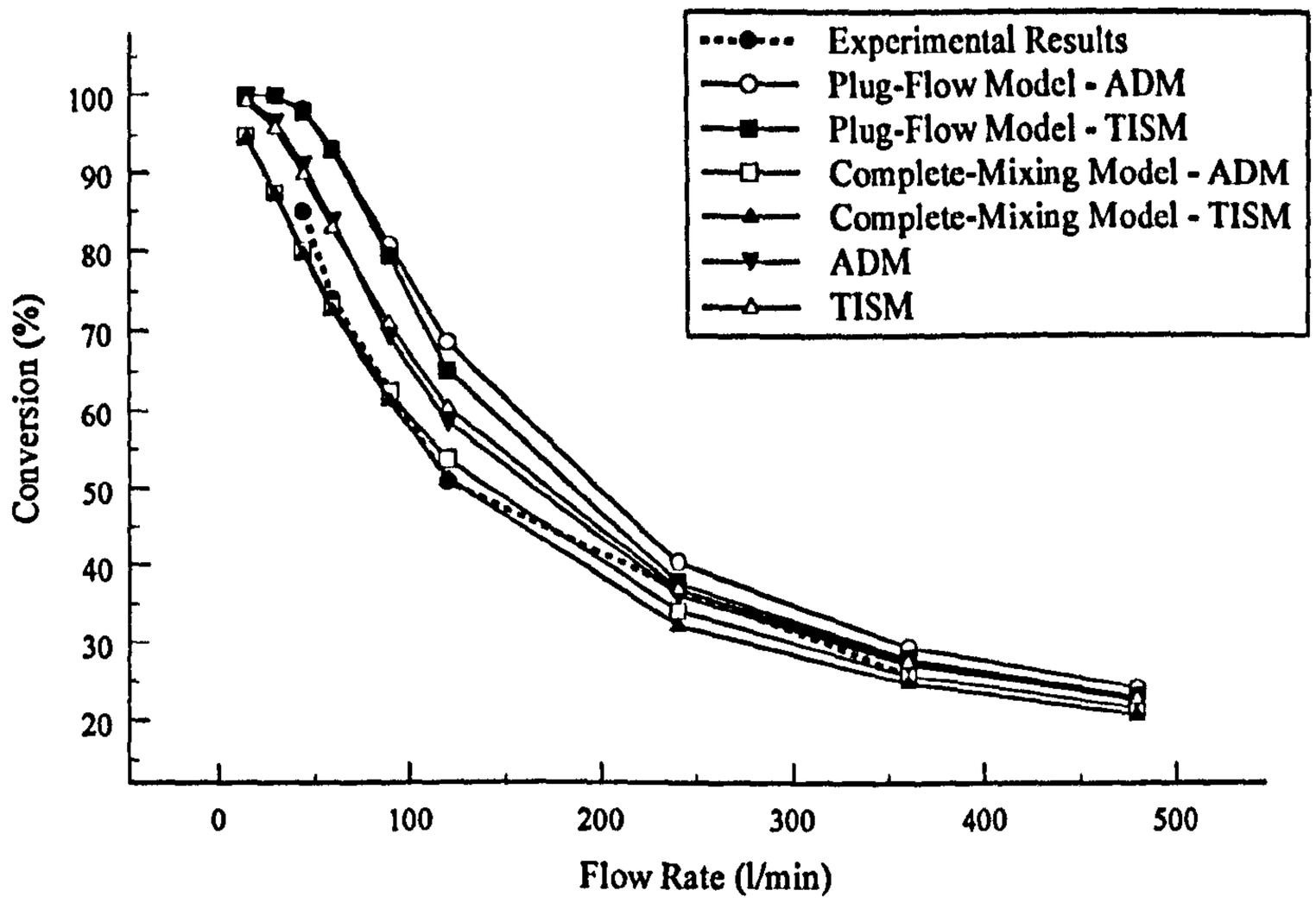

Fig. 7.11 Prototype HDVS No Baseflow - Comparison of Experimental and Flow Model Conversion Results using the Experimental Mean Residence Time, ADM and TISM Parameters Calculated using Non-Linear Regression

Fig. 7.12 shows the relationship between the experimental conversion and the ADM and TISM parameters calculated using the method of moments and non-linear regression. This shows that the conversion increases as the model parameters increase and therefore, as the HDVS plug-flow mixing characteristics improve (section 7.6.2).

Experiments conducted feeding only H_2O_2 through the prototype HDVS showed that there is no natural decomposition of the H_2O_2 and also proved that the inlet and reactants feed flow rates were correct. This test is considered more important for the prototype HDVS compared to the model HDVS (section 7.6.2) as it is constructed of mild steel, which may promote the decomposition of H_2O_2. The results for these tests are shown in appendix F.2.6 and their implications on the experimental errors are discussed in section 7.6.2.

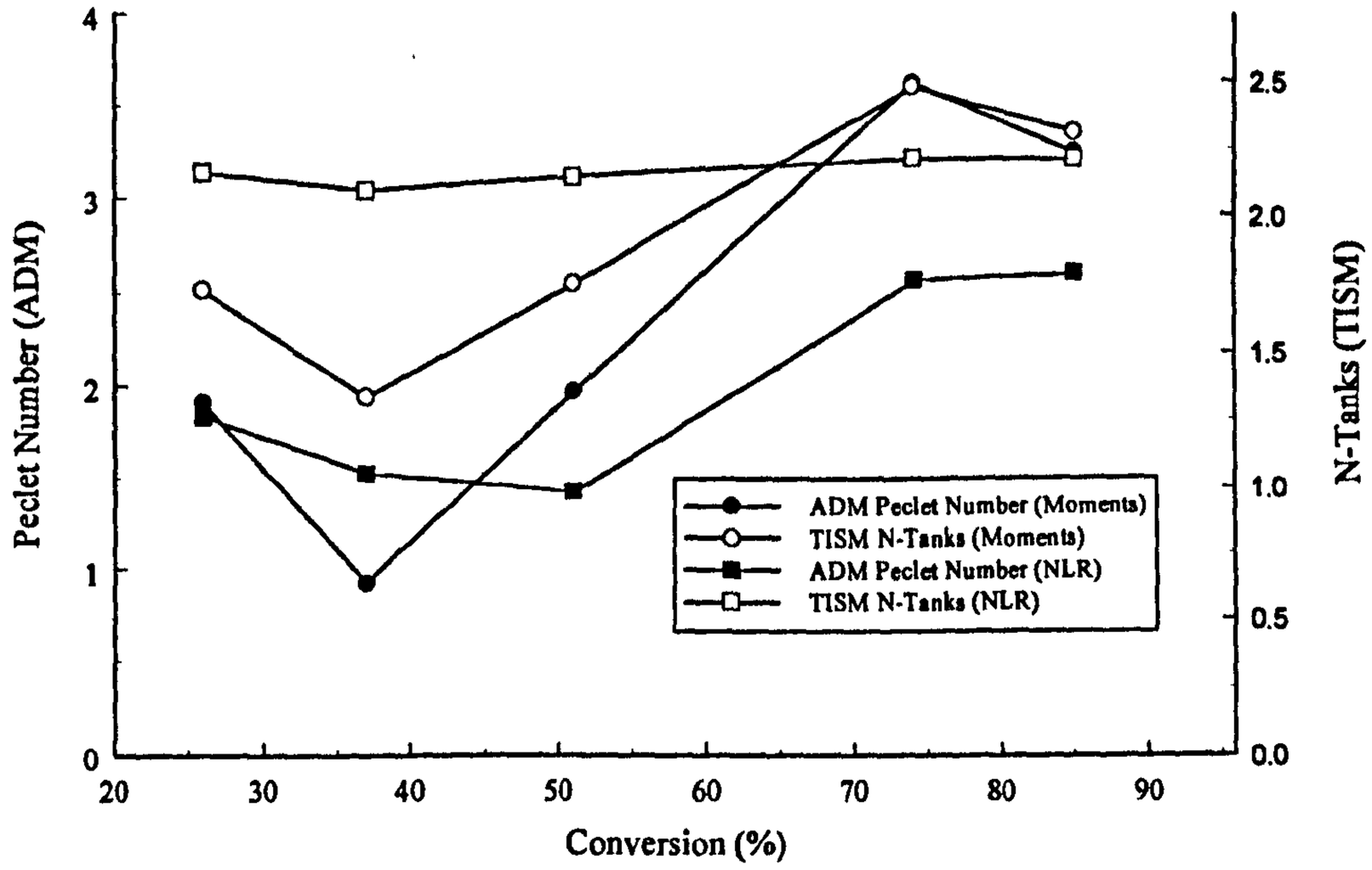

Fig. 7.12 Prototype HDVS No Baseflow - Comparison of Experimental Conversion and ADM and TISM Parameters Calculated using the Method of Moments and Non-Linear Regression

7.6.4 Model Hydrodynamic Vortex Separator (HDVS) Operating with a Baseflow Component (SP3)

For the model HDVS operating with a baseflow component, H_2O_2 samples were taken from sample point 3 (SP3) and therefore the sludge hopper is included in the HDVS configuration (Fig. 6.1). The experimental conversion was measured at selected inlet flow rates used for the RTD baseflow investigations (section 6.2.2). Experimental conversion data does not exist for certain flow rates but all possible flow rates have been modelled irrespectively. The model HDVS operating with a baseflow component theoretical mean residence time is calculated as described in section 6.2.1 and presented in appendix E.2.3. The flow splits used for the H_2O_2 experiments ranged from 10-60% (section 6.1). This is generally greater than typically used for the HDVS's current applications (chapter 2). However, experiments of this nature have not previously been

conducted on the HDVS and therefore, it was considered appropriate to investigate the HDVS outside its normal operating conditions.

The conversions as a function of the flow split for all inlet flow rates are presented in Fig. 7.13. The H_2O_2 sample analysis results and conversion calculations are presented in appendix F.3.1.

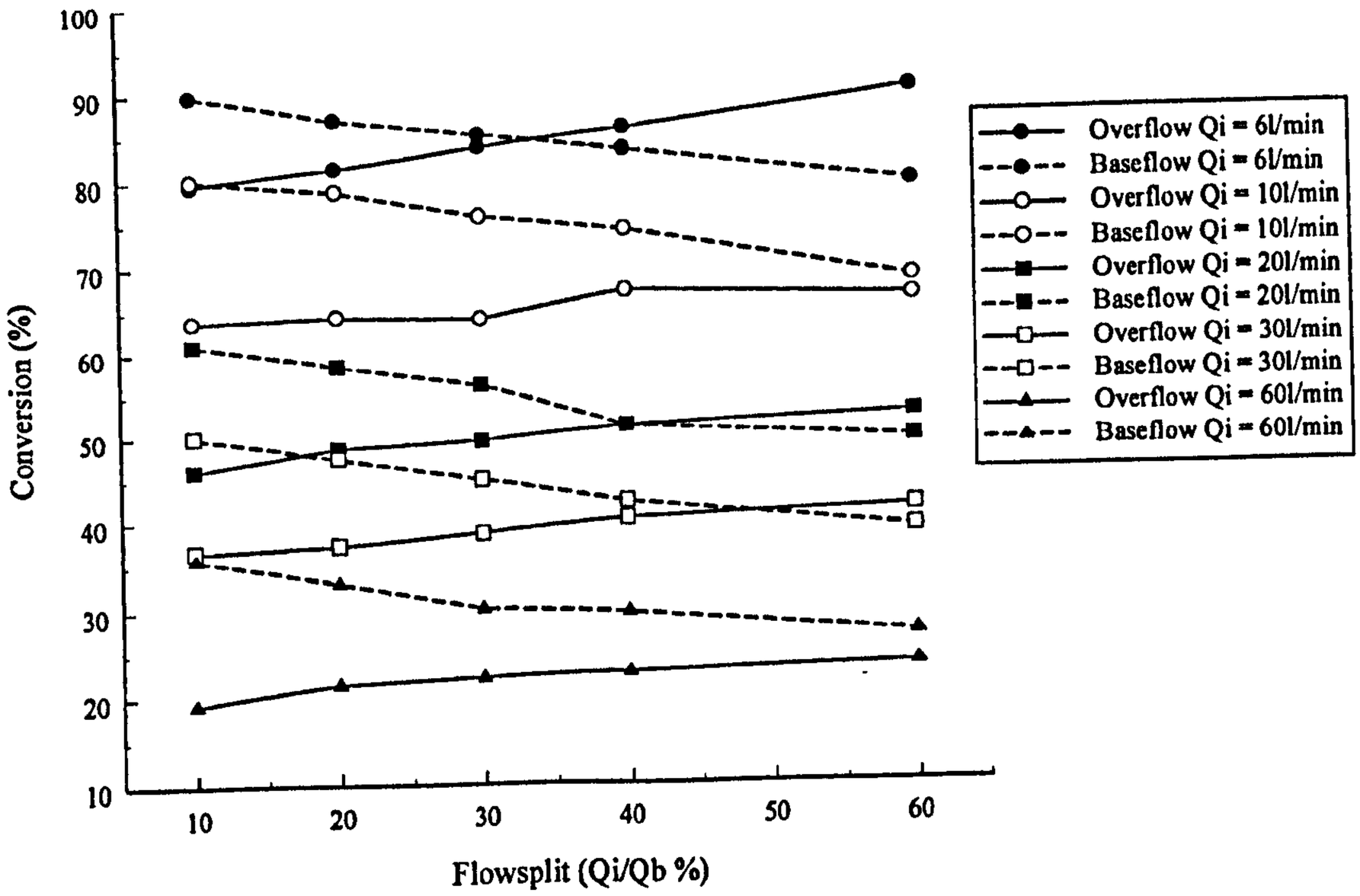

Fig. 7.13 Model HDVS Baseflow - Experimental Conversion Results

As expected the conversion at both the overflow and baseflow decreases as the inlet flow rate increases due to a smaller contact time. The baseflow component ADM and TISM parameters obtained at SP3 increase and the overflow parameters decrease as the inlet flow rate increases (section 6.2.3). Not surprisingly, this implies that the mean residence time is the dominant parameter in predicting the conversion as opposed to the ADM and TISM parameters.

The overflow and baseflow component H_2O_2 experimental conversion has a linear relationship with the flow split for a constant inlet flow rate. The baseflow conversion decreases and the overflow conversion gradually increases as the flow split is increased.

This trend is the same achieved for the overflow and baseflow ADM and TISM parameters (section 6.2.3). Therefore, the baseflow component has greater plug-flow mixing characteristics as the flow split decreases and the overflow component has the opposite relationship. The conversion will also follow the same trend as plug-flow mixing increases the conversion (section 7.3). The baseflow conversion is generally greater than the overflow conversion at the same inlet flow rate. This is because the baseflow component measured at SP3 also has a greater element of plug-flow mixing, due to the inclusion of the sludge hopper, compared to the overflow component (section 6.2.3). These observations support the overflow and baseflow component theoretical mean residence time calculations, which are constant for the same inlet flow rate irrespective of the flow split (section 6.2.1.1). Assuming the theoretical mean residence time is an accurate description of the contact time, this provides confidence in the experimental data i.e. RTD curve, reaction rate constant (k) and the H_2O_2 conversion and subsequently the use of the RTD and batch reactor data to predict the efficiency of the continuously operated HDVS for kinetic process applications.

Figs. 7.14–7.17 compares the experimental conversion and the estimated flow model conversion values for an inlet flow rate of 20l/min. The results are presented in appendix F.3.2-F.3.7 and the correlation parameters (R^2 and ESS) in appendix 3.8. The correlation parameters for the plug-flow (eqn. 7.6) and complete mixing (eqn. 7.7) models calculated using the theoretical mean residence time are not provided as this flow model data analysis combination produces a constant value for the range of flow splits and therefore provides a poor correlation.

As the inlet flow rate increases the difference between the overflow and baseflow component plug-flow and complete mixing models decrease (section 7.6.2). Additionally, the overflow and baseflow component experimental conversion results do not always fall between the plug-flow (upper limit) and complete mixing (lower limit)

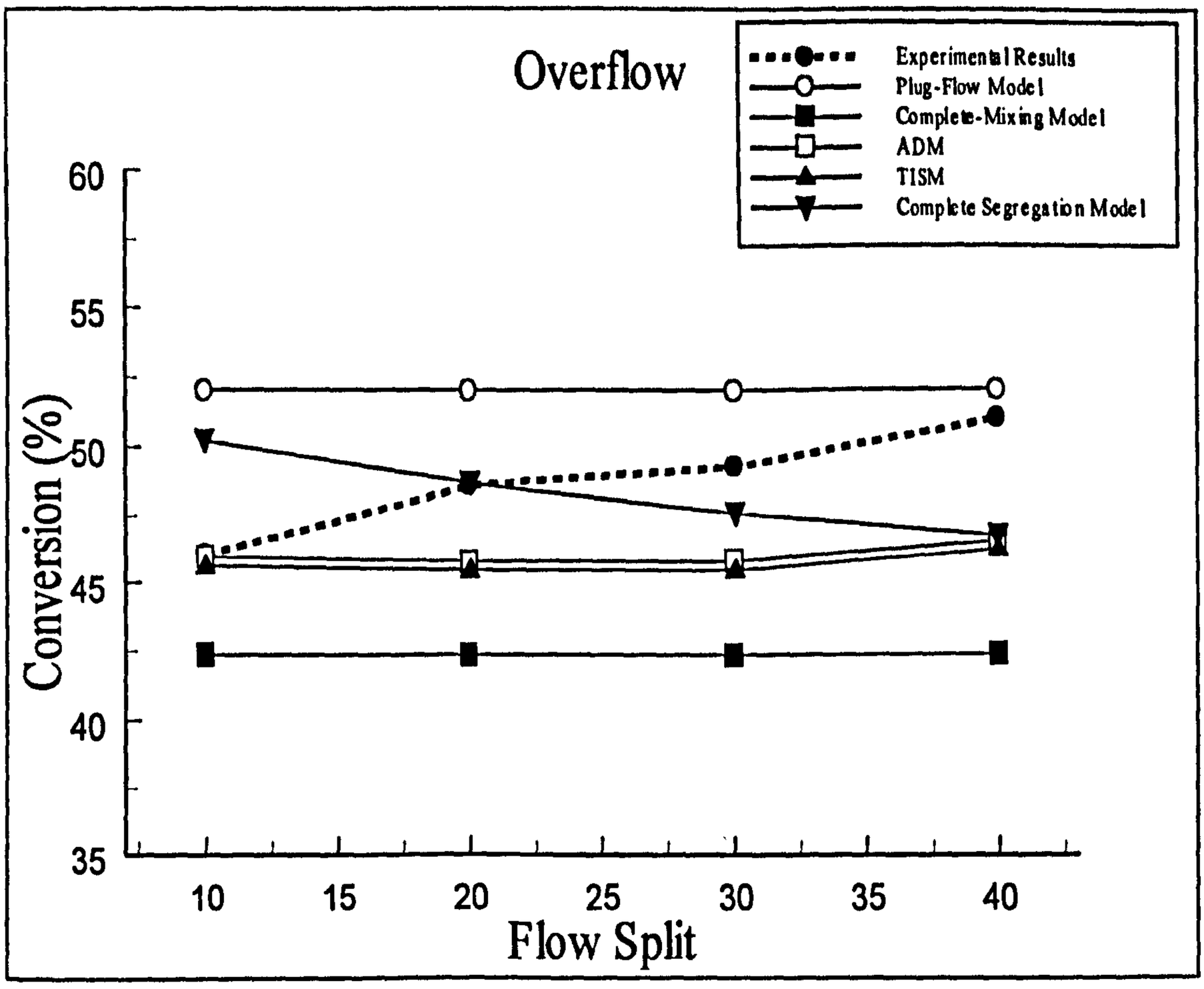

Fig. 7.14 Model HDVS Baseflow - Comparison of Experimental and Flow Model Conversion Results using the Theoretical Mean Residence Time and Method of Moments ADM and TISM Parameters for an Inlet Flow Rate of 20l/min

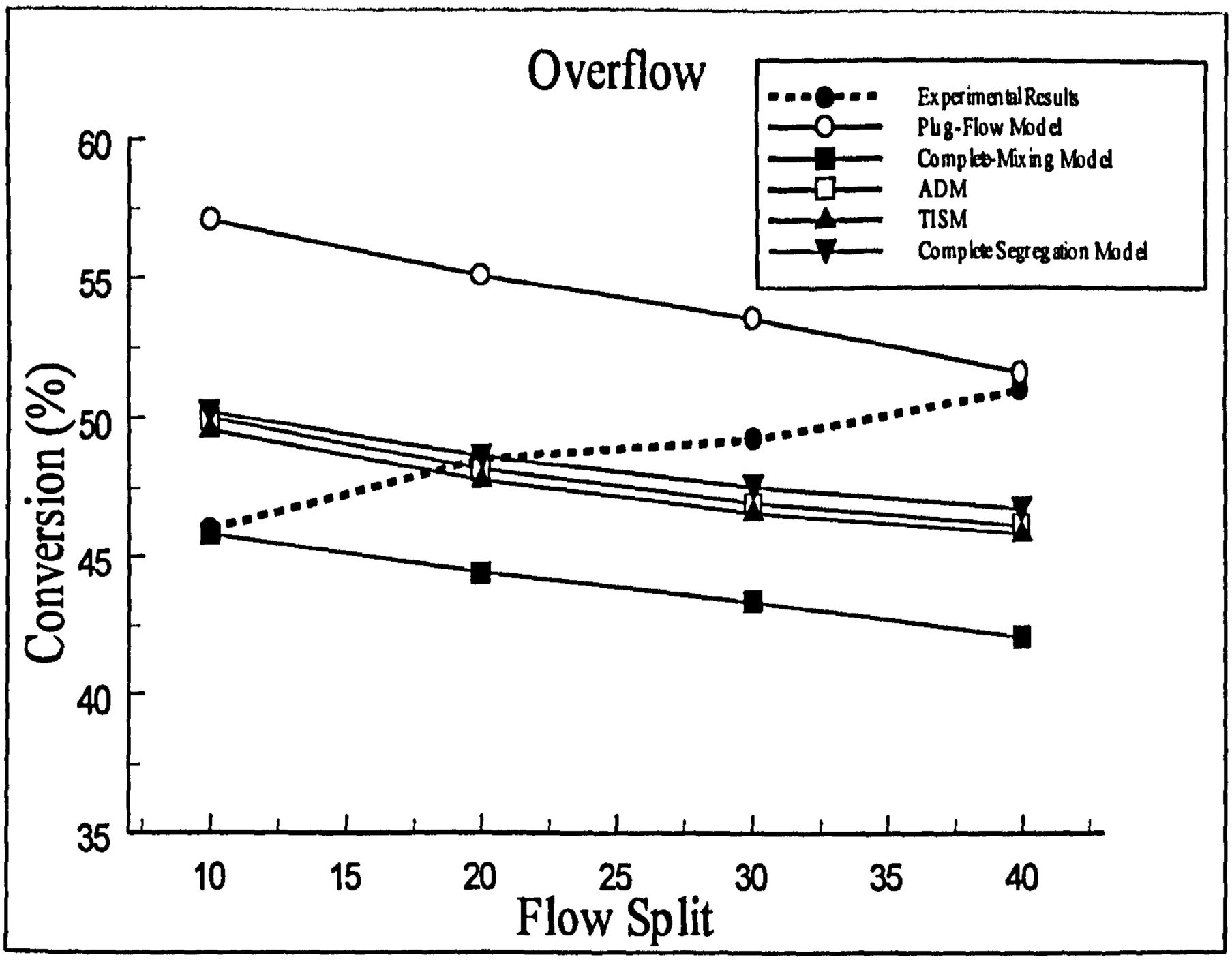

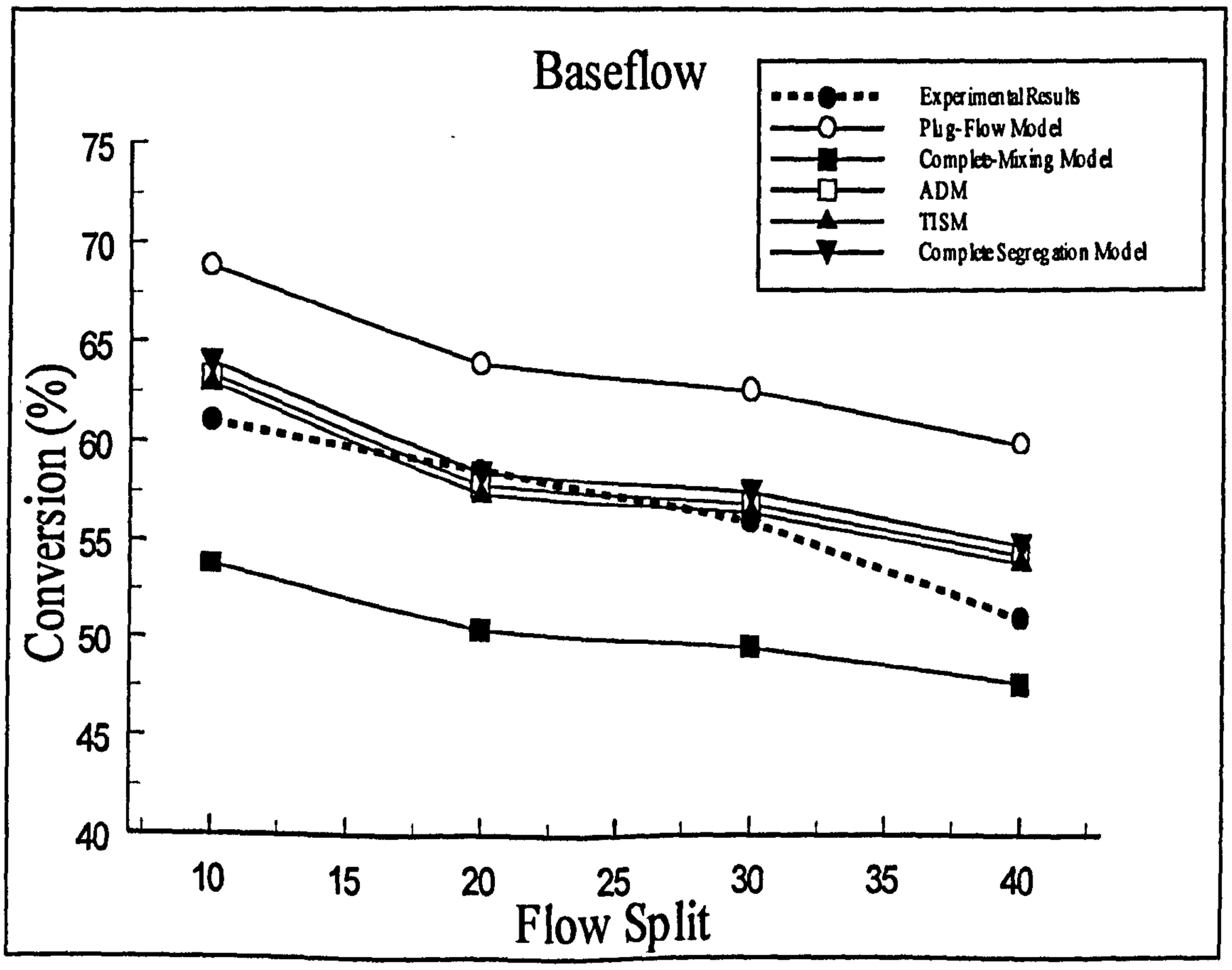

Fig. 7.15 Model HDVS Baseflow - Comparison of Experimental and Flow Model Conversion Results using the Experimental Mean Residence Time, ADM and TISM Parameters Calculated using the Method of Moments for an Inlet Flow Rate of 20l/min

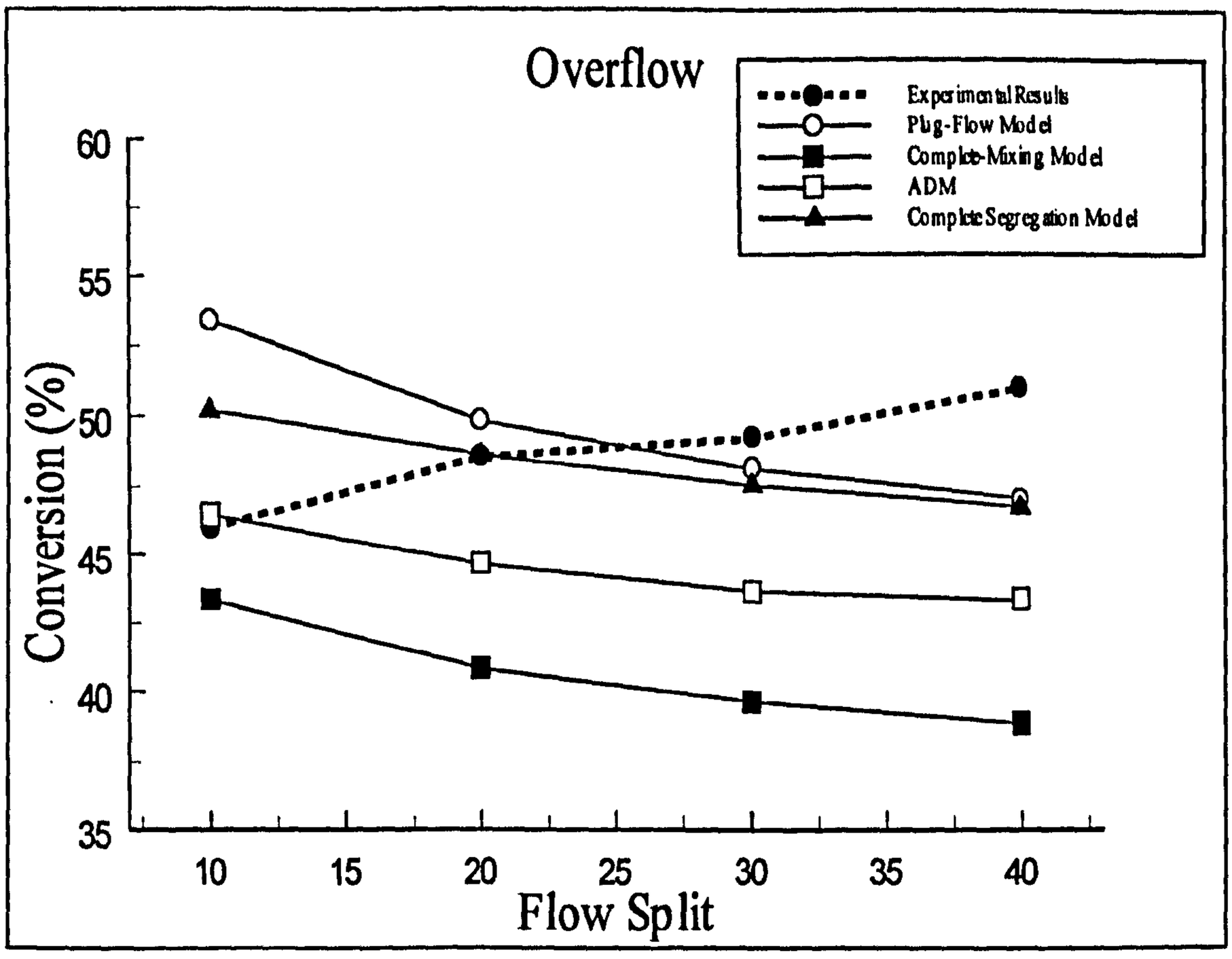

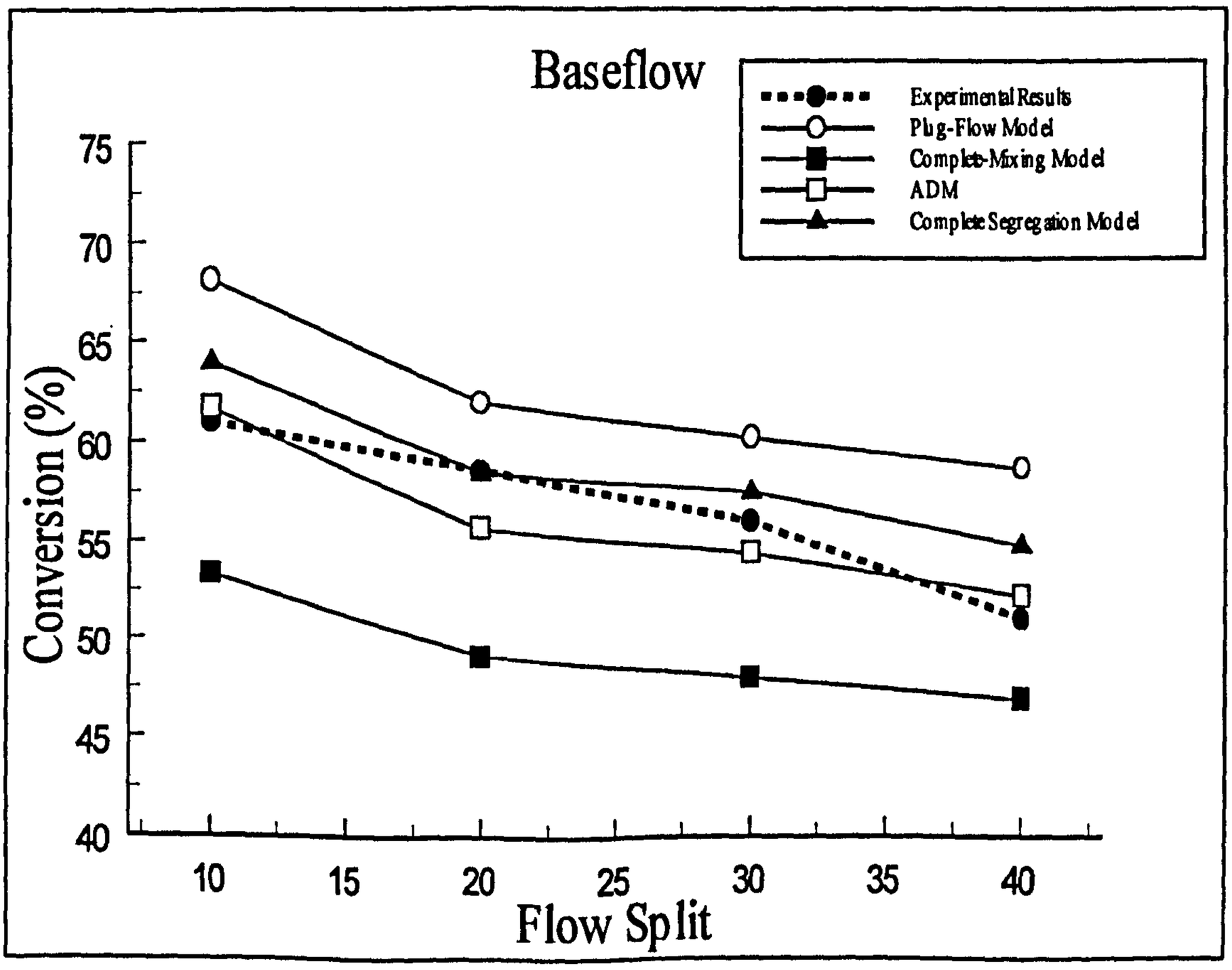

Fig. 7.16 Model HDVS Baseflow - Comparison of Experimental and Flow Model Conversion Results Calculated using the ADM and Non-Linear Regression for an Inlet Flow Rate of 20l/min

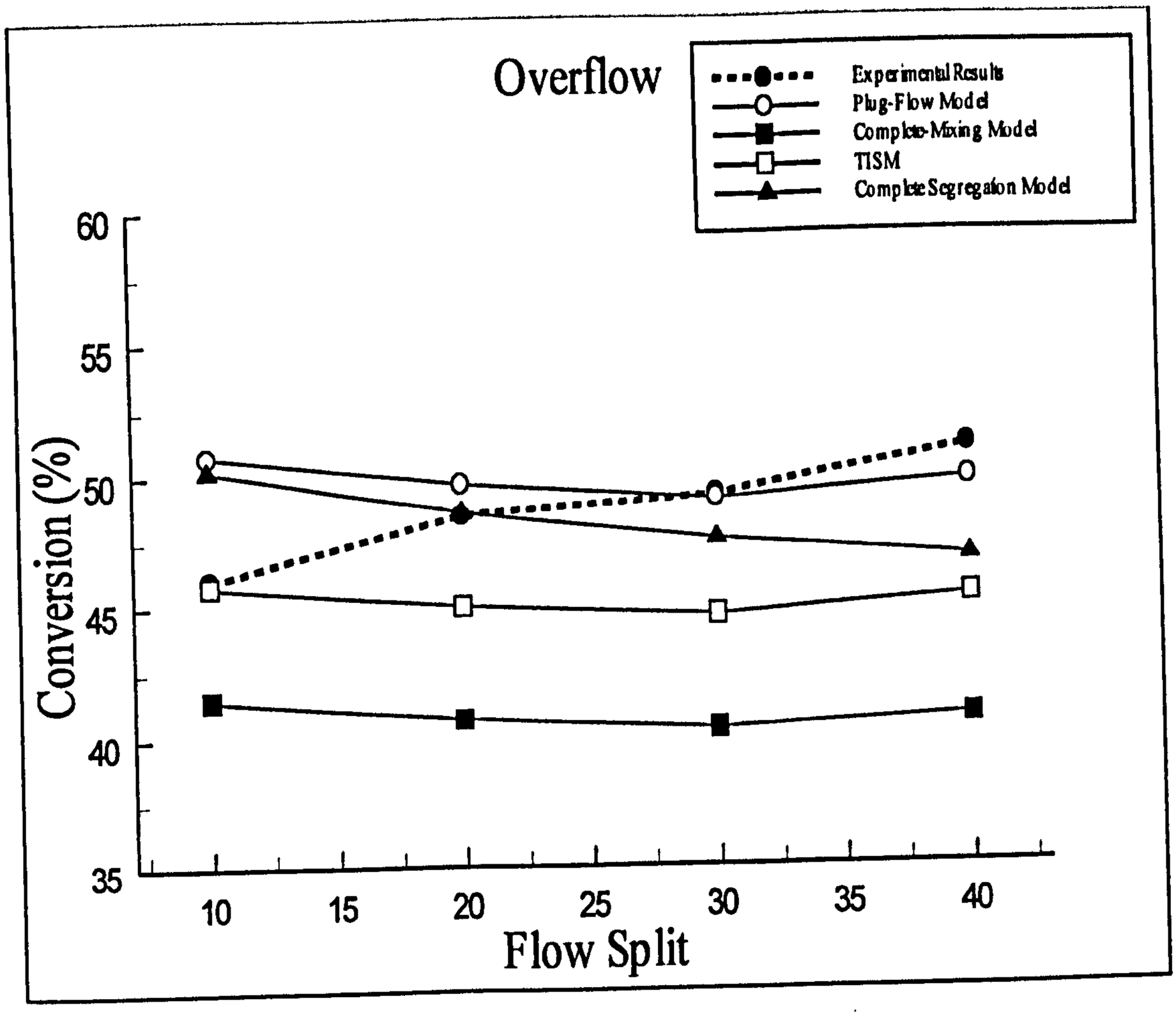

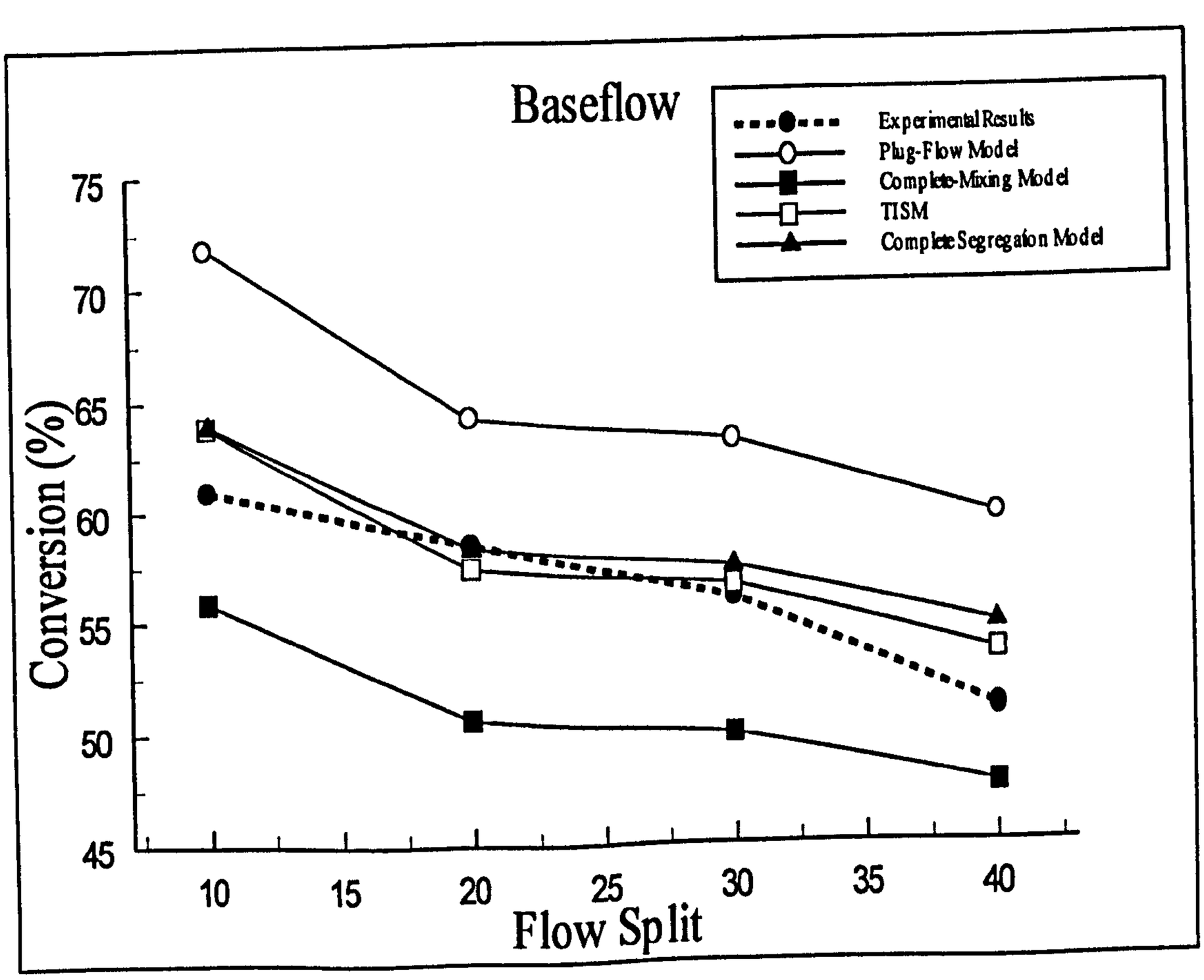

Fig. 7.17 Model HDVS Baseflow - Comparison of Experimental and Flow Model Conversion Results Calculated using the TISM and Non-Linear Regression for an Inlet Flow Rate of 20l/min

models (section 7.3). The complete segregation model appears to provide the closest estimation of the experimental conversion i.e. directly from the RTD curve when the experimental conversion does not fall between the upper and lower limits. The advantages of the complete segregation model over other flow models, to estimate the kinetic process efficiency of a system, are discussed in section 7.6.2. The ADM and TISM estimated conversion results provide a very similar trend (Figs. 7.14 and 7.15). This is due to the ADM and TISM parameter calculation method and their common relationship with the normalised variance (section 6.2.1.1). The experimental data does not always show the same trend as the flow model data across the range of flow splits for the same inlet flow rate. The difference in the experimental data and the predicted flow model data trends is highlighted by the correlation parameters (R^2 and ESS) in appendix F.3.8.

The overflow component experimental conversion results occasionally have a positive gradient and the modelled data a negative gradient with respect to the flow split and this relative trend produces a negative R^2 value. The baseflow component R^2 correlation parameters are positive, as the experimental and modelled data observe the same decreasing trend as the flow split increases. Subsequently, the baseflow correlation parameters are better than the overflow component. Due to the negative R^2 values obtained for the overflow component, the ESS correlation parameter is used to assess the goodness of fit for both the overflow and baseflow component (section 6.2.1.1). The correlation parameters were only obtained for a small number of samples (4) which reduces confidence in their representation of the best-fit.

Rather than discussing each flow model presented in Figs. 7.14-7.17 (appendix F.3.4-F.3.7) and its correlation parameters individually they have been summarised in Table 7.1. This shows the best-fit flow model and the data analysis technique used to calculate the mean residence time for the range of inlet flow rates. The best-fit

combination at each inlet flow rate for both the baseflow and overflow component is donated by an asterisk (*).

For each technique used to calculate the mean residence time the overflow component experimental conversion is generally described by a mixing regime that approaches plug-flow mixing as the inlet flow rate is increased. However, there is no significant trend in the best-fit flow model and mean residence time combination for the overflow component. The baseflow component at low flow rates is generally described by plug-flow mixing and as the inlet flow rate increases it is better described by a flow model indicating an intermediate mixing regime between plug-flow and complete mixing. This is also shown by the best-fit flow model and mean residence time combination. These trends in the best-fit flow model for both the overflow and baseflow components are the opposite of the ADM and TISM parameters (section 6.2.3). Therefore, the experimental mean residence time appears to be the dominant factor in predicting the conversion for a first-order reaction.

Table 7.1 Model HDVS Baseflow – Best-Fit Correlation Parameters for all Flow Model and Mean Residence Time Calculation Combinations

Data Analysis Technique used to Calculate the Mean Residence Time	Flow Rate (l/min)	O	B
Theoretical (eqn. 4.2)	10	ADM*	ADM
	20	ADM	ADM
	30	ADM	ADM
	60	ADM*	ADM
Method of Moments	10	CMM	PFM
	20	ADM	TISM
	30	TISM*	CSEG
	60	CSEG	CMM
Non-Linear Regression - ADM	10	ADM	PFM*
	20	PFM	ADM*
	30	PFM	ADM*
	60	PFM	ADM
Non-Linear Regression -TISM	10	TISM	PFM
	20	PFM*	TISM
	30	PFM	TISM
	60	PFM	CMM*

Where: PFM - Plug-Flow Model
CMM - Complete mixing Model
ADM - Axial Dispersion Model
TISM - Tanks-in-Series Model
CSEG - Complete Segregation Model

Fig. 7.18 compares the overflow and baseflow component measured at SP2 and SP3 estimated H_2O_2 conversion using the complete segregation model (eqn. 7.11). This is presented to illustrate how the different mixing characteristics of the baseflow component measured at SP2 and SP3 affect the estimated conversion (Fig. 6.1). Additionally, the overflow component results should provide the same estimated conversion whether the baseflow RTD is measured at SP2 or SP3 (section 6.2.3). The overflow component results provide confidence in replicating RTD experiments on the model HDVS and the baseflow component measured at SP3 results are significantly greater than at SP2 for the same inlet flow rate. The baseflow component results support previous observations, as the baseflow component measured at SP3 i.e. including the sludge hopper, has greater plug-flow mixing characteristics compared to at SP2 and hence, provides better kinetic process efficiency (section 6.2.3).

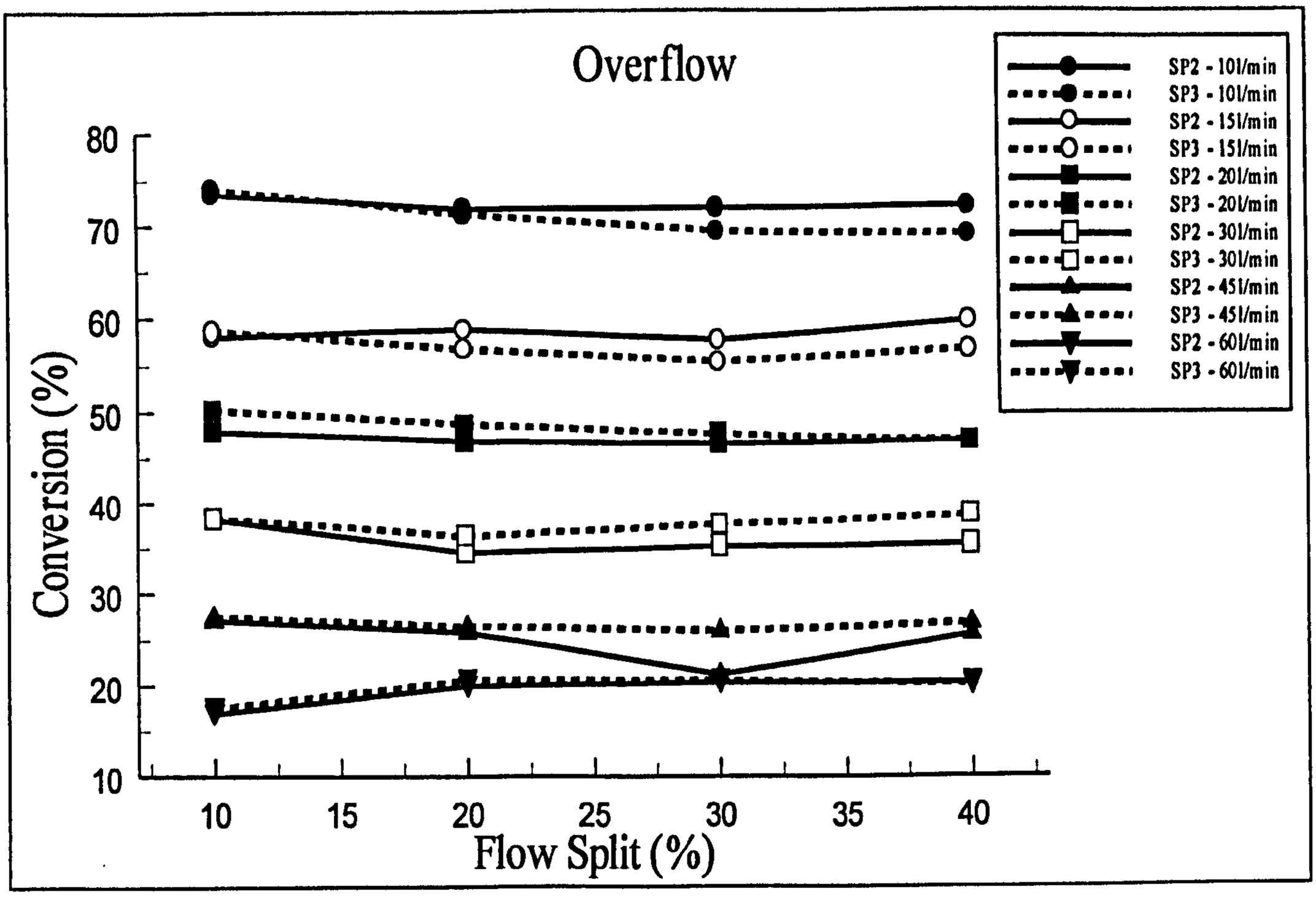

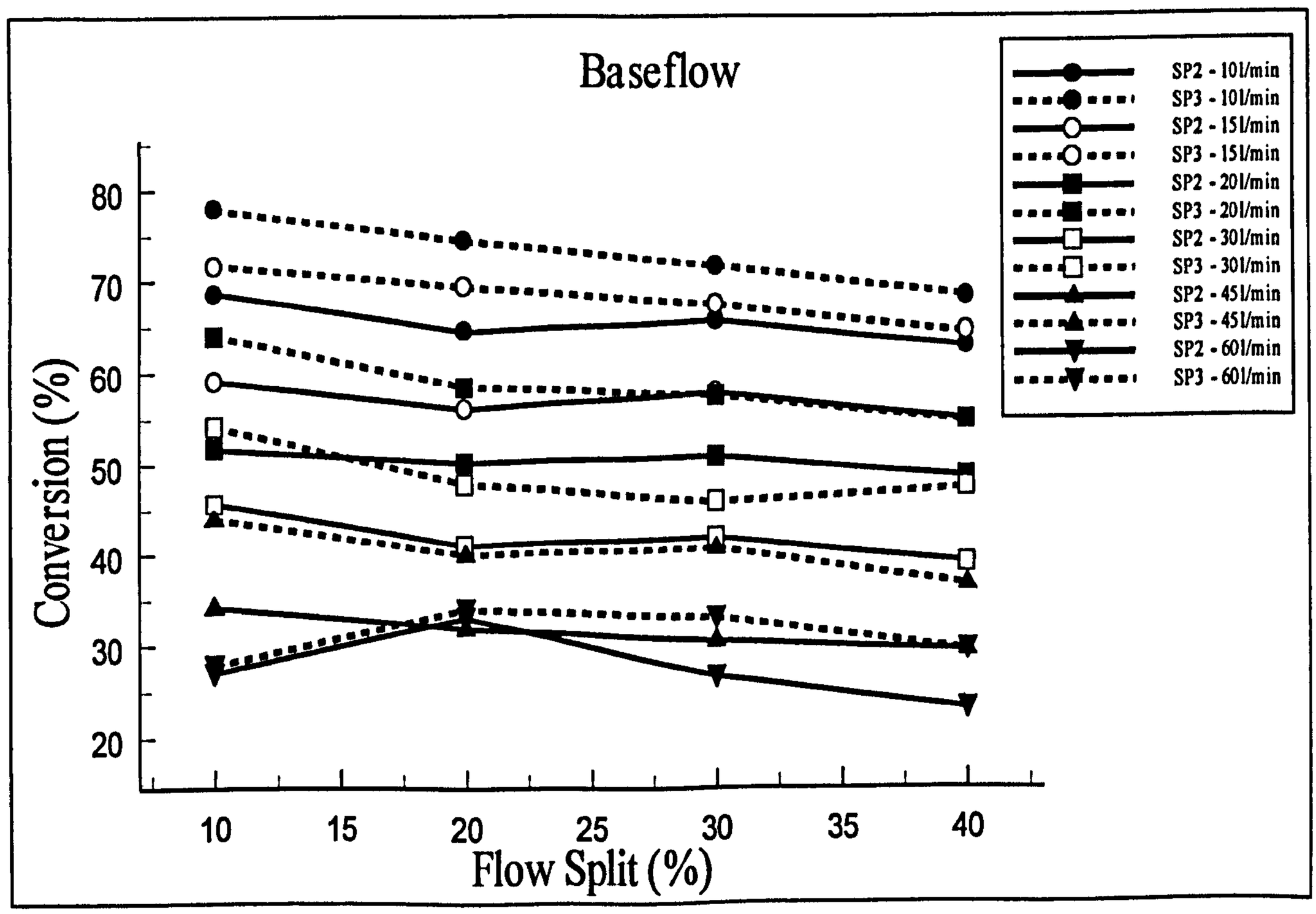

Fig. 7.18 Model HDVS Baseflow - Comparison of Complete Segregation Model Conversion Results for the Overflow and Baseflow Components using the SP2 and SP3 RTD Experimental Data

7.6.5 Prototype Hydrodynamic Vortex Separator (HDVS) Operating with a Baseflow Component (SP3)

For the prototype HDVS operating with a baseflow component, H_2O_2 samples were taken from sample point 3 (SP3) and therefore the sludge hopper is included in the HDVS configuration (Fig. 6.1). The prototype HDVS operating with a baseflow component theoretical mean residence time is calculated as described in section 6.2.1 and presented in appendix E.4.3. The same model HDVS experimental procedures and data analysis techniques were used for the prototype HDVS (section 7.6.4).

The conversions as a function of the flow split for all inlet flow rates are presented in Fig. 7.19. The H_2O_2 sample analysis results and conversion calculations are presented in appendix F.4.1. As expected, the prototype HDVS experimental conversion results for both the overflow and baseflow components decrease as the inlet flow rate increases. The overflow and baseflow component experimental conversion has a linear relationship with the flow split for a constant inlet flow rate. The baseflow conversion decreases and the overflow conversion marginally increases or remains very stable as the flow split is increased. The trend in the prototype HDVS H_2O_2 conversion results with respect to the flow rate and flow split is very similar to that achieved for the model HDVS (section 7.6.4).

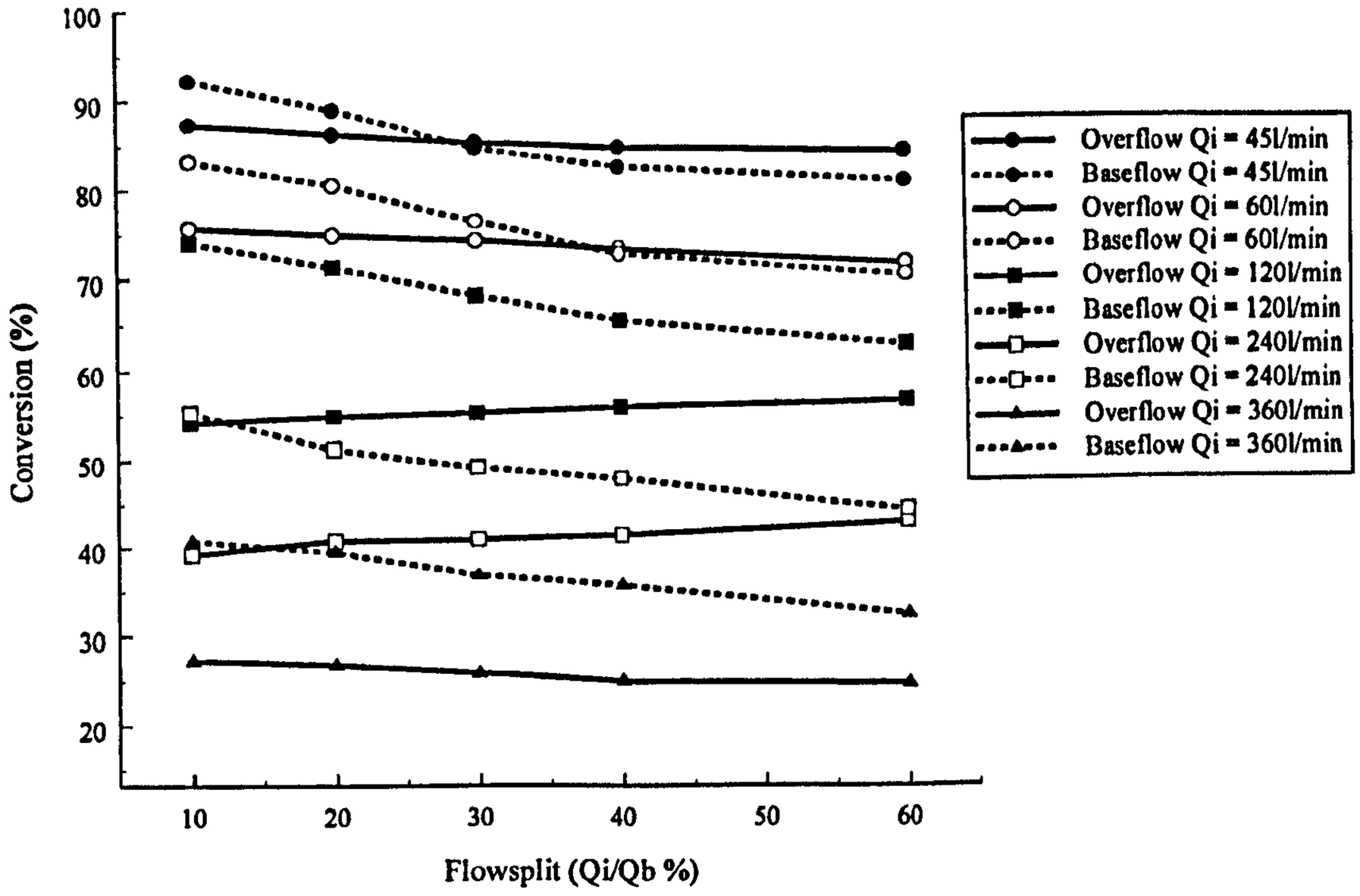

Fig. 7.19 Prototype HDVS Baseflow - Experimental Conversion Results

Figs. 7.20–7.23 compares the experimental conversion and the estimated flow model conversion values for an inlet flow rate of 120l/min. The results are presented in appendix F.4.2-F.4.7 and the correlation parameters (R^2 and ESS) in appendix 4.8. The relationship between the experimental conversion and the flow model estimation and therefore, the correlation parameters (R^2 and ESS) is very similar to that obtained for the model HDVS baseflow experiments (section 7.6.4). Additionally, the complete segregation model appears to provide the closest estimation of the experimental conversion data i.e. directly from the RTD curve, when the experimental conversion does not fall between the upper and lower limits (section 7.6.4). The advantage of the complete segregation model over other flow models is discussed in section 7.6.2.

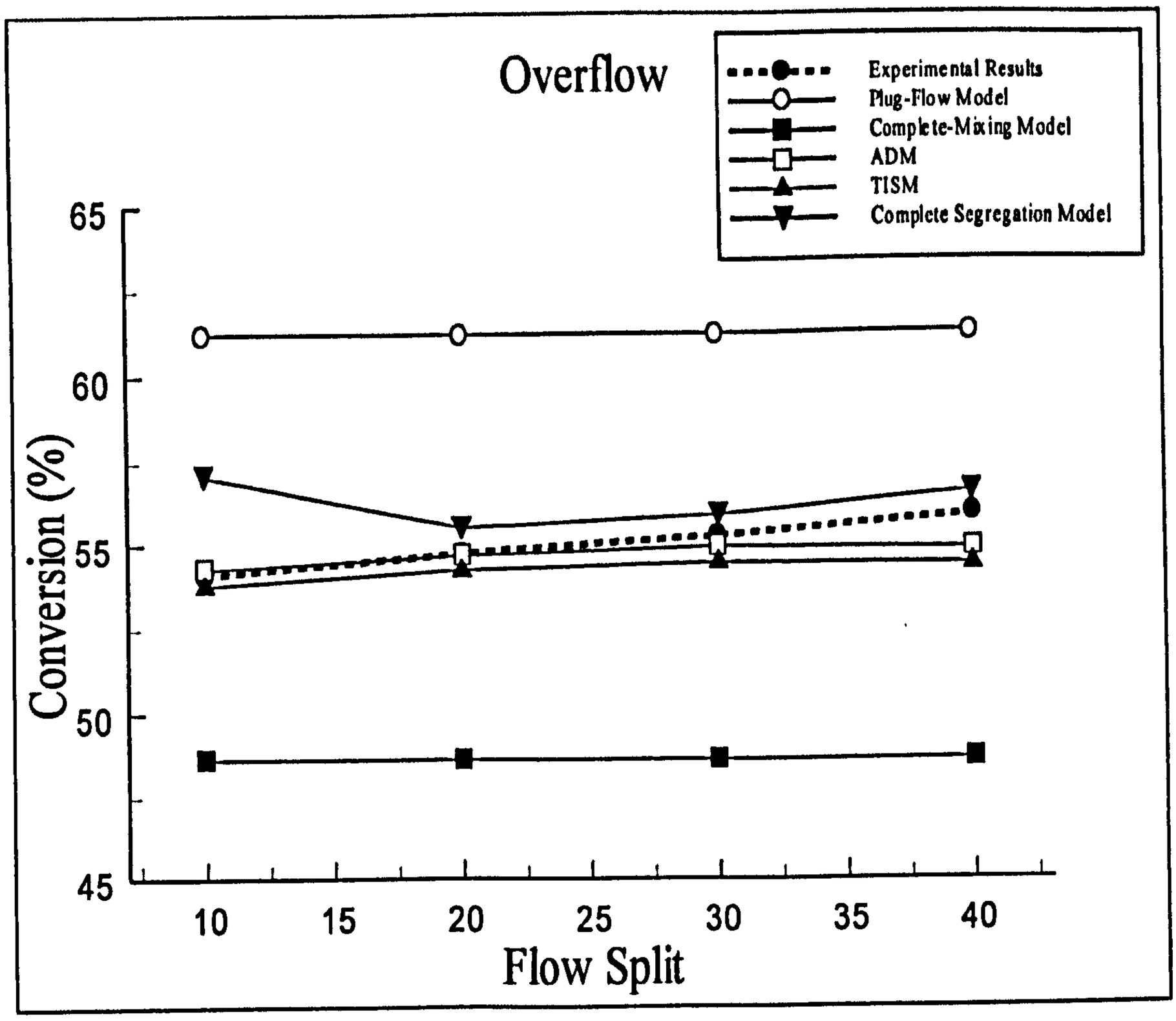

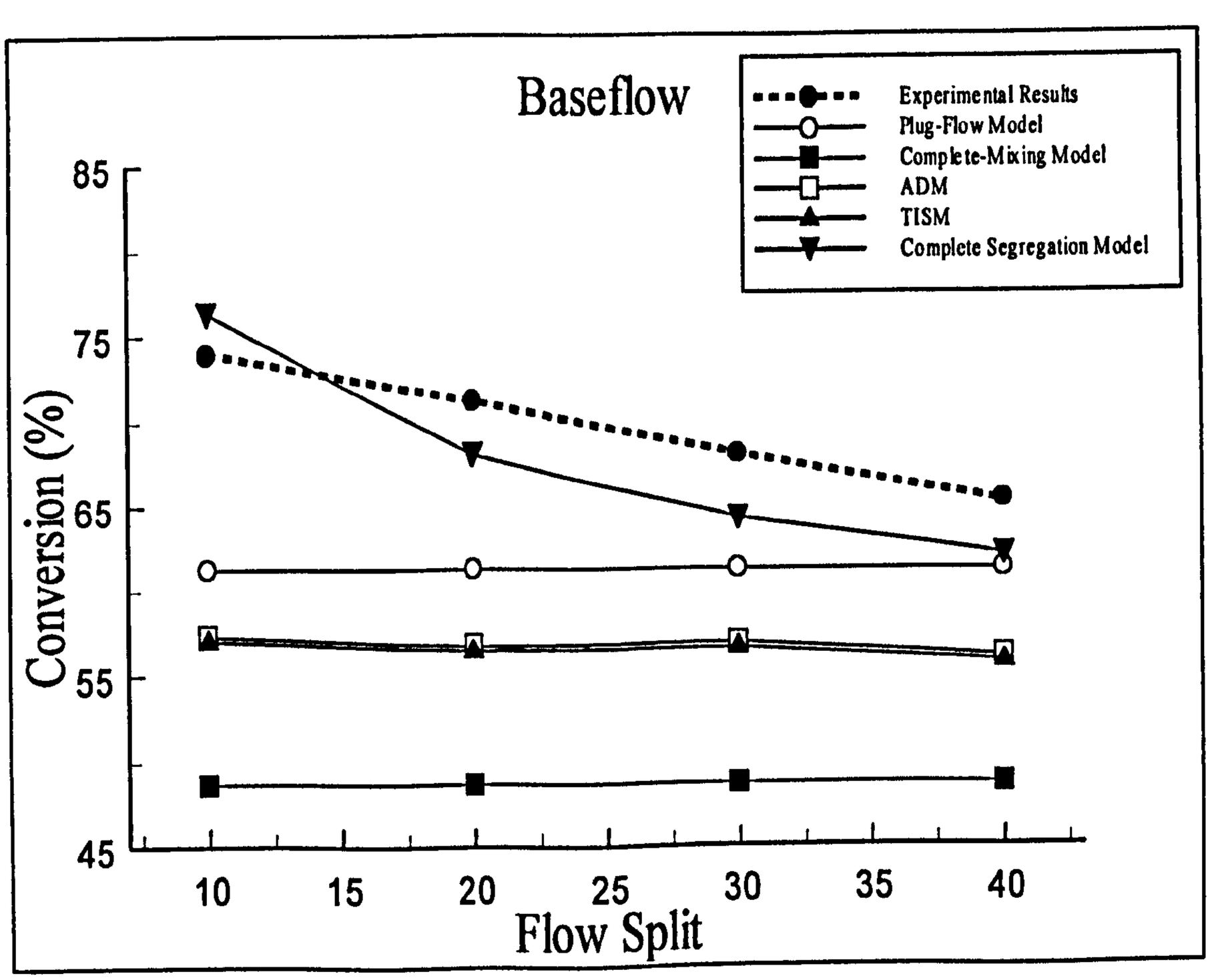

Fig. 7.20 Prototype HDVS Baseflow - Comparison of Experimental and Flow Model Conversion Results using the Theoretical Mean Residence Time and Method of Moments ADM and TISM Parameters for an Inlet Flow Rate of 120l/min

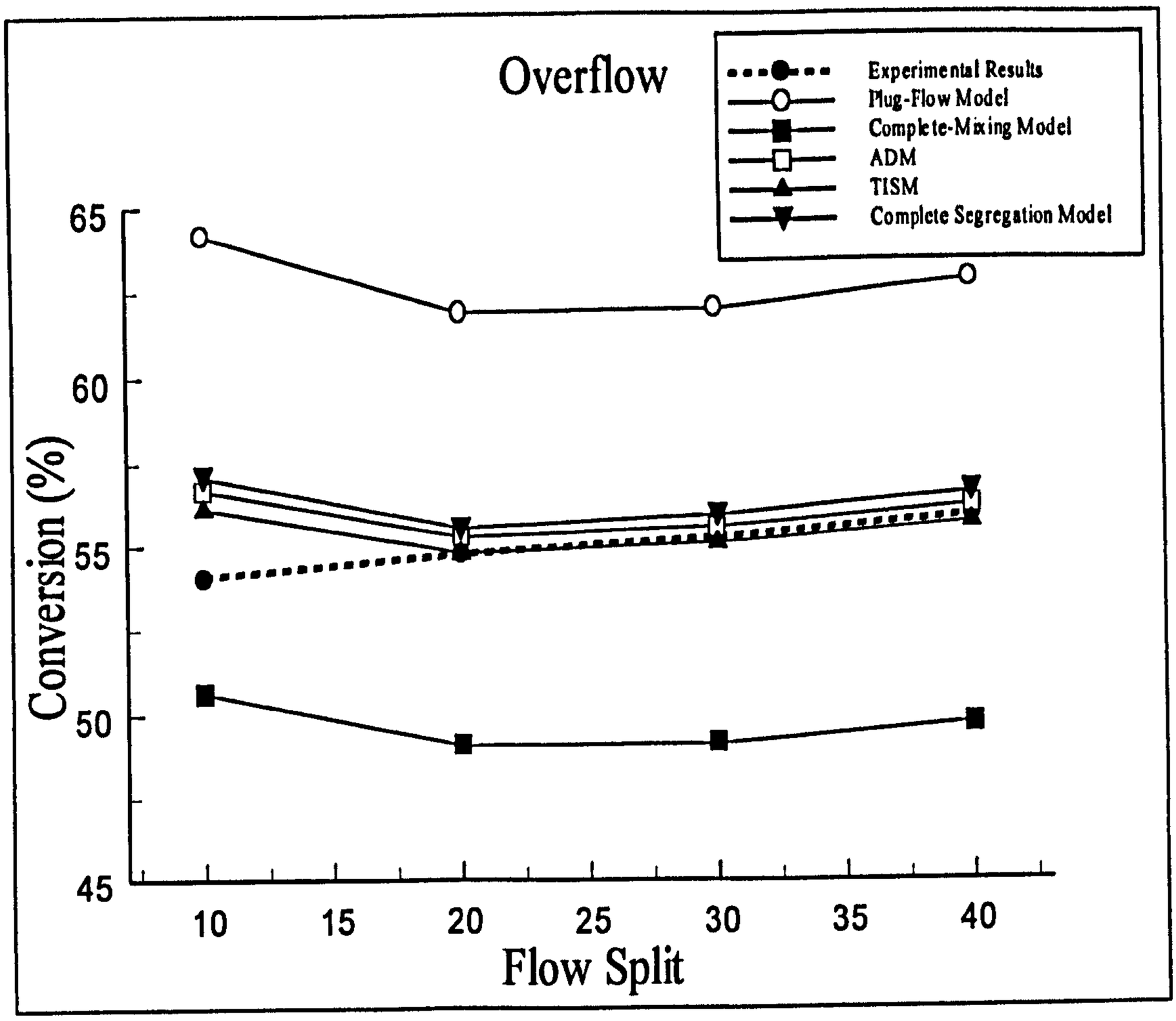

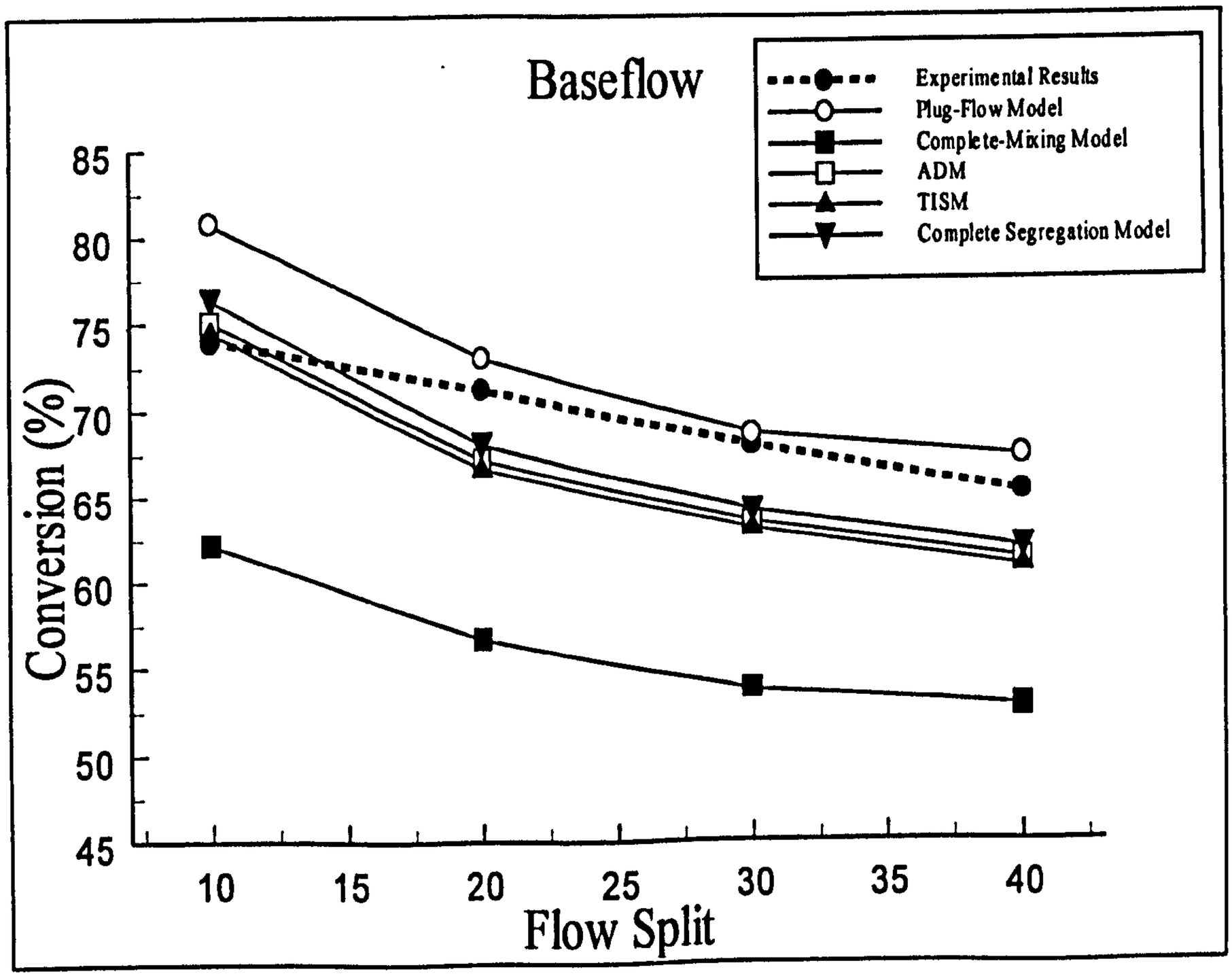

Fig. 7.21 Prototype HDVS Baseflow - Comparison of Experimental and Flow Model Conversion Results using the Experimental Mean Residence Time, ADM and TISM Parameters Calculated using the Method of Moments for an Inlet Flow Rate of 120l/min

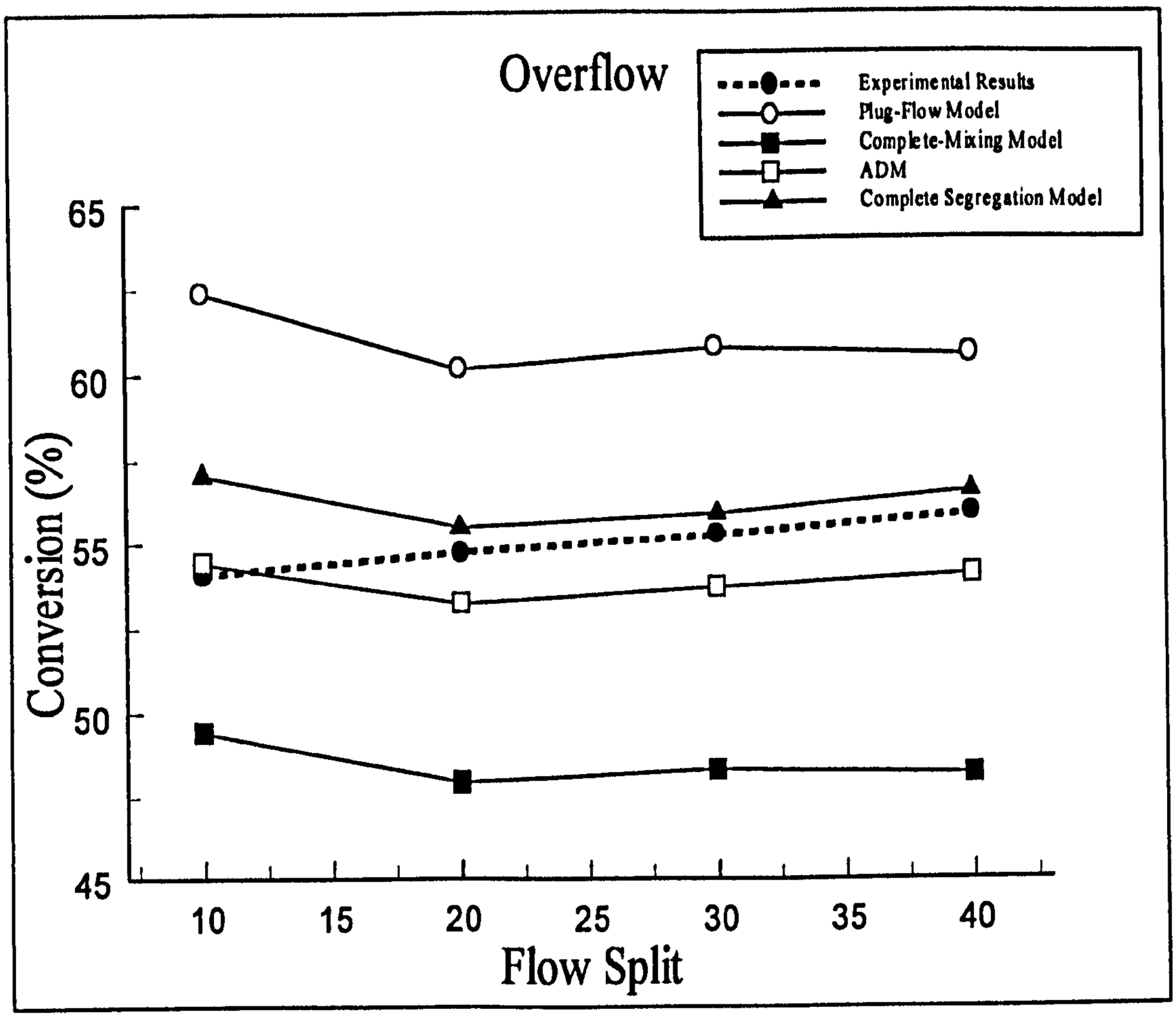

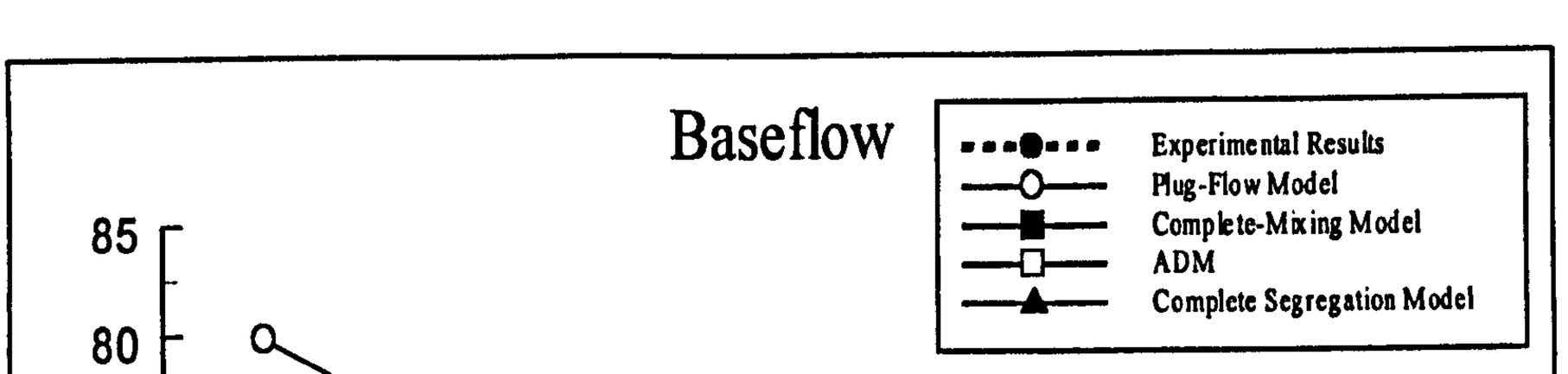

Fig. 7.22 Prototype HDVS Baseflow - Comparison of Experimental and Flow Model Conversion Results Calculated using the ADM and Non-Linear Regression for an Inlet Flow Rate of 120l/min

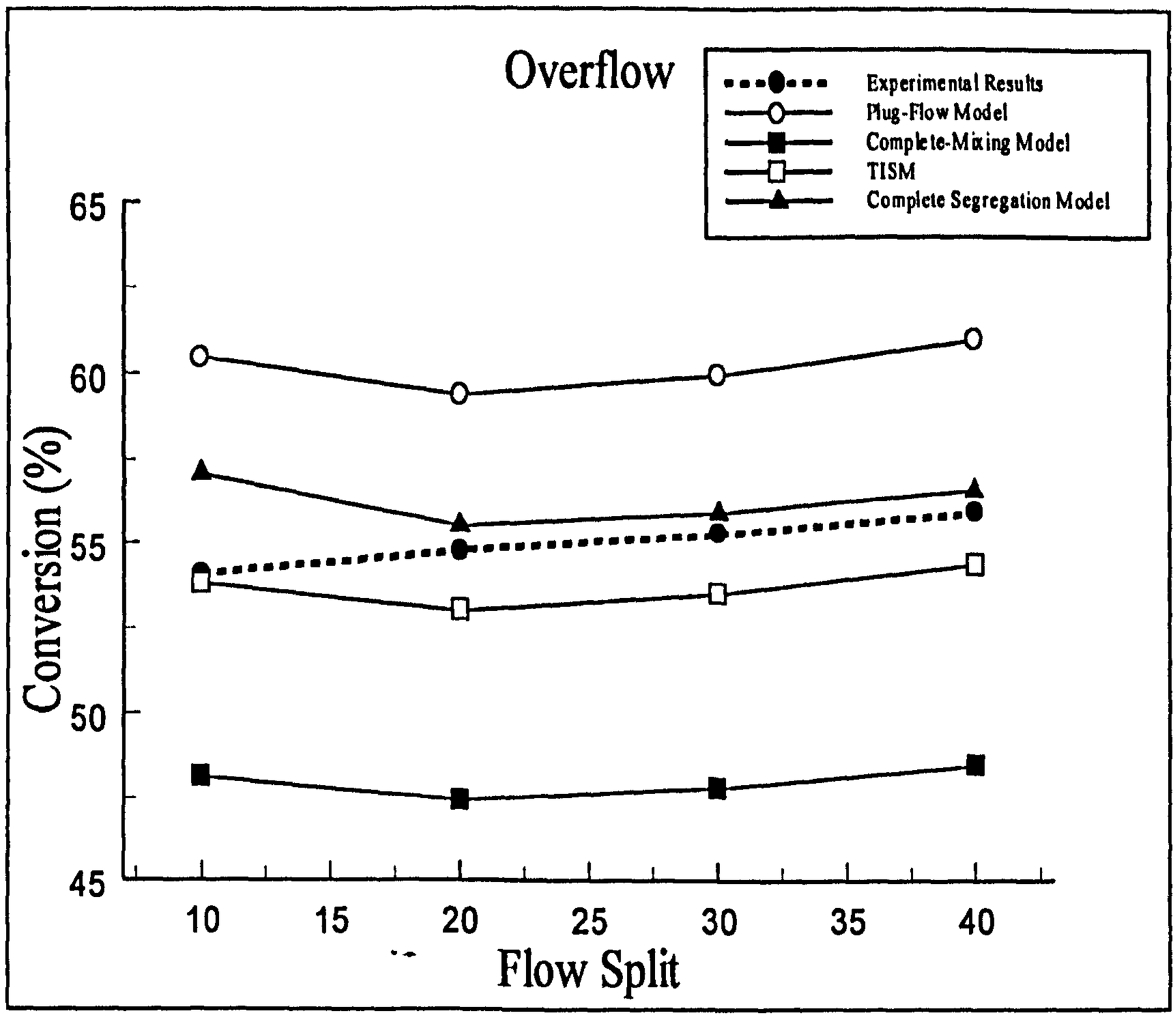

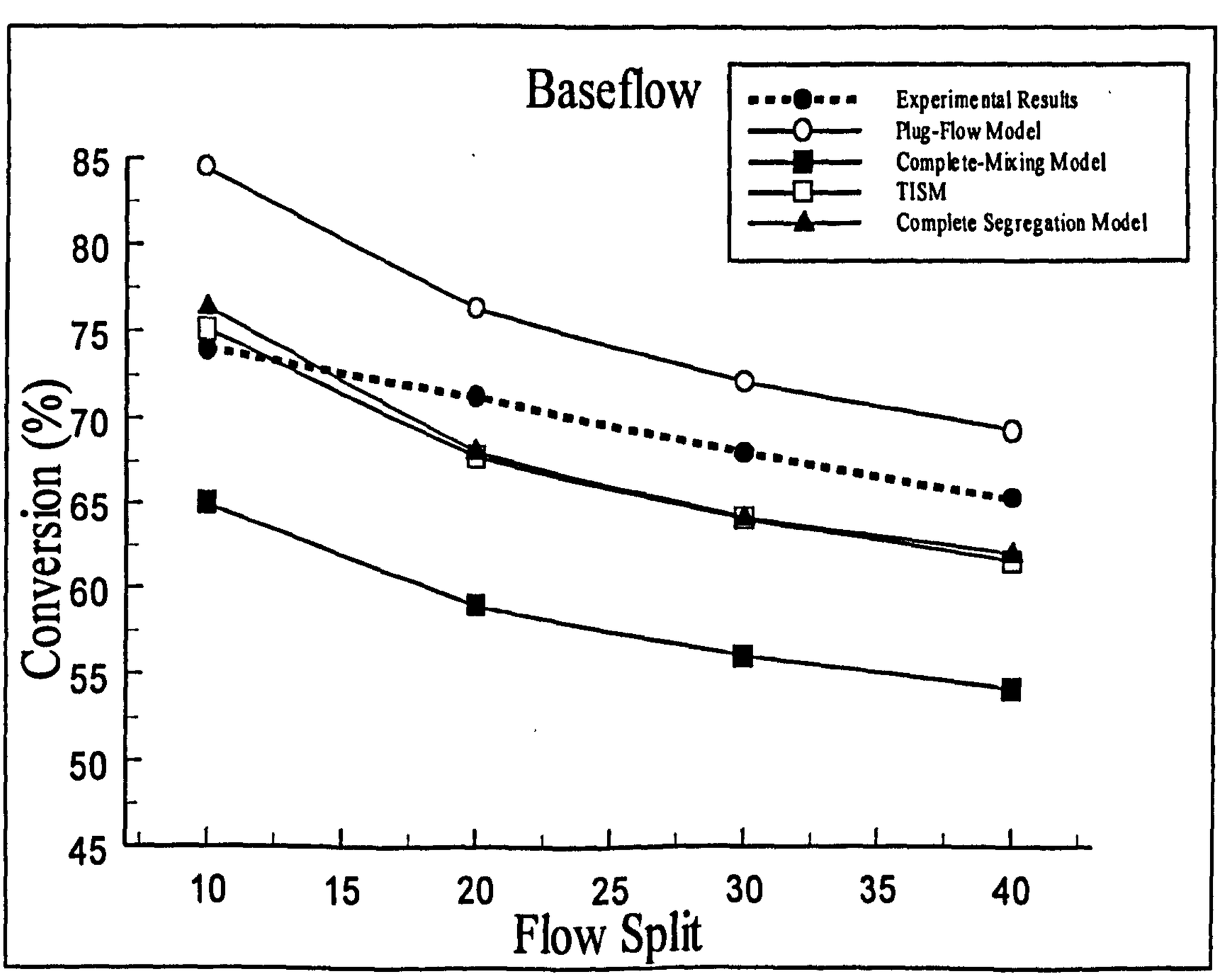

Fig. 7.23 Prototype HDVS Baseflow - Comparison of Experimental and Flow Model Conversion Results Calculated using the TISM and Non-Linear Regression for an Inlet Flow Rate of 120l/min

Rather than discussing each flow model and its correlation parameters individually they have been summarised in Table 7.2. This shows the best-fit flow model and the data analysis technique used to obtain the mean residence time for the range of inlet flow rates. The best-fit combination at each inlet flow rate for both the baseflow and overflow component is donated by an asterisk (*).

Table 7.2 Prototype HDVS Baseflow – Best-Fit Correlation Parameters for all Flow Model and Mean Residence Time Calculation Combinations

Data Analysis Technique used to Calculate the Mean Residence Time	Flow Rate (l/min)	O	B
Theoretical (eqn. 4.2)	45	ADM	ADM
	60	TISM*	ADM
	120	ADM*	ADM
	240	ADM	ADM
	360	ADM*	ADM
Method of Moments	45	TISM	CSEG*
	60	TISM	TISM
	120	TISM	CSEG
	240	PFM*	PFM*
	360	CMM	PFM*
Non-Linear Regression – ADM	45	ADM*	PFM
	60	ADM	ADM
	120	ADM	PFM*
	240	PFM	PFM
	360	CMM	PFM
Non-Linear Regression –TISM	45	TISM	PFM
	60	TISM	TISM*
	120	TISM	TISM
	240	PFM	TISM
	360	TISM	PFM

Where: PFM - Plug-Flow Model
CMM - Complete mixing Model
ADM - Axial Dispersion Model
TISM - Tanks-in-Series Model
CSEG - Complete Segregation Model

For each technique used to calculate the mean residence time the overflow component experimental conversion is generally described by an intermediate mixing regime between plug-flow and complete mixing for the range of inlet flow rates. Hence, there is no significant trend in the best-fit flow model and mean residence time

combination for the overflow component. A flow model indicating an intermediate mixing regime generally describes the baseflow component at low flow rates and at high flow rates the plug-flow mixing model provides the better correlation. This is also shown by the best-fit flow model and mean residence time combination for the baseflow component. These trends in the best-fit flow model are very similar to the ADM and TISM parameters and therefore the plug-flow mixing characteristics of the individual flow components (section 6.2.3). However, the mean residence time will still be the dominant factor in predicting the conversion (section 7.6.4).

Fig. 7.24 compares the overflow and baseflow component measured at SP2 and SP3 estimated H_2O_2 conversion using the complete segregation model (eqn. 7.11). This is presented to illustrate how the different mixing characteristics of the baseflow component measured at SP2 and SP3 affect the estimated conversion (Fig. 6.1). Additionally, the overflow component results should provide the same estimated conversion whether the baseflow RTD is measured at SP2 or SP3 (section 6.2.6). The overflow component results provide confidence in replicating RTD experiments on the prototype HDVS and the baseflow component measured at SP3 results are significantly greater than at SP2 for the same inlet flow rate. The baseflow component results support previous observations, as the baseflow component measured at SP3 i.e. including the sludge hopper, has greater plug-flow mixing characteristics compared to at SP2 and hence, provides better kinetic process efficiency (section 6.2.6).

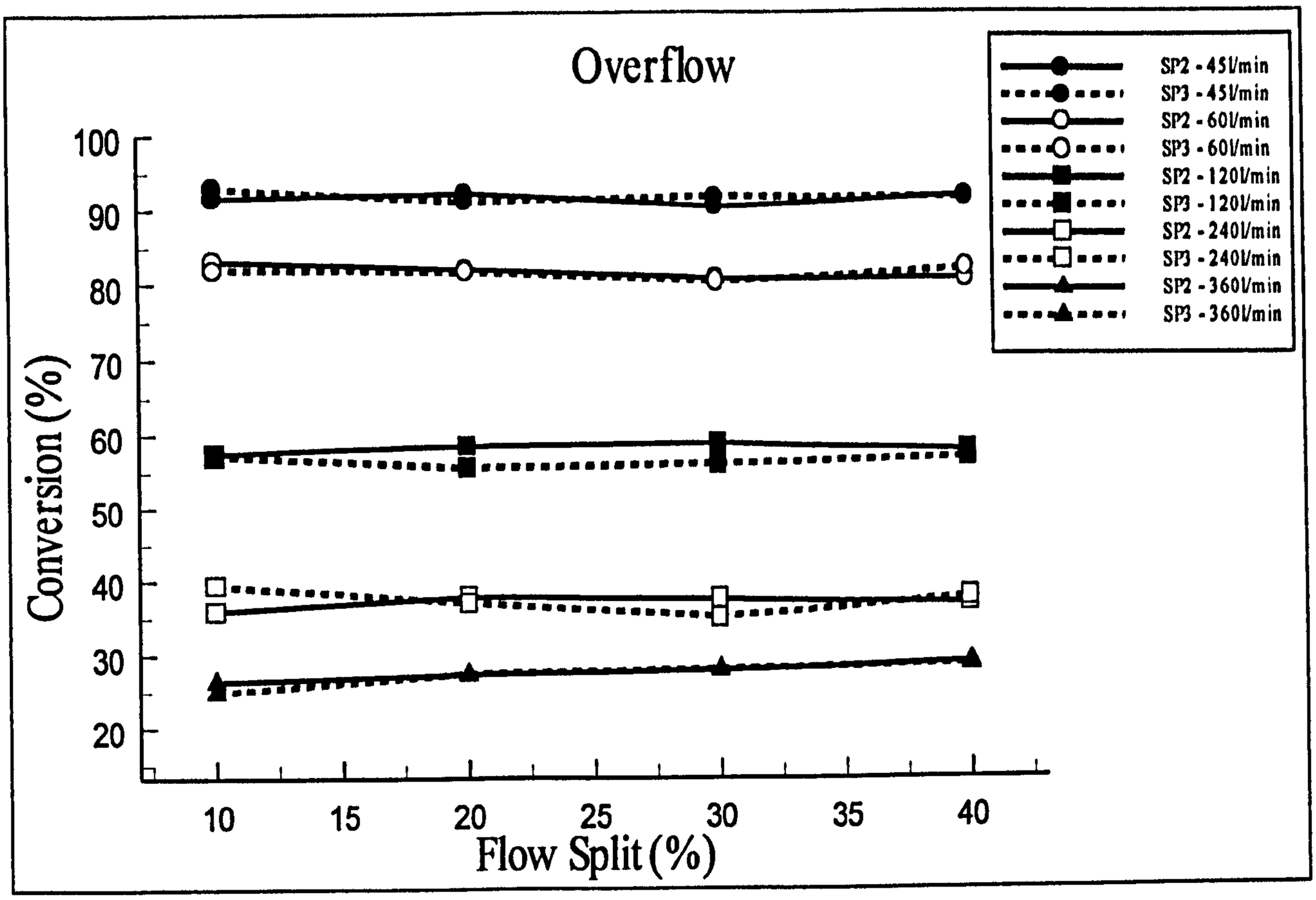

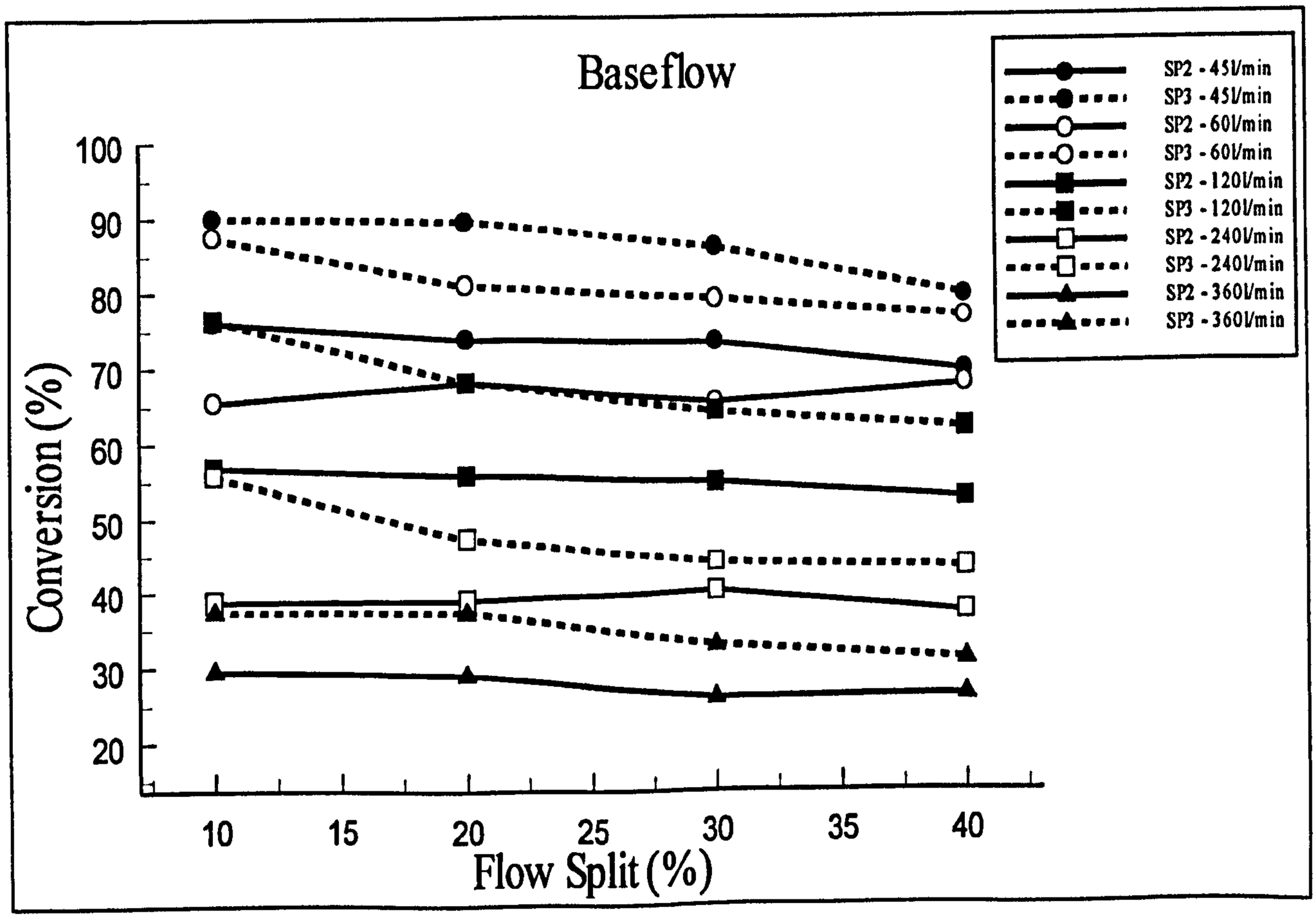

Fig. 7.24 Prototype HDVS Baseflow - Comparison of Complete Segregation Model Conversion Results for the Overflow and Baseflow Components using the SP2 and SP3 RTD Experimental Data

7.7 Chapter Overview

Investigation of the hydrogen peroxide (H_2O_2) conversion kinetics shows that the RTD and batch reactor data can be used to predict the efficiency of the continuously operated HDVS for kinetic process applications. This could eliminate the need for costly and time consuming pilot trials. For the HDVS operating without a baseflow component the experimental results are between the theoretical conversion boundaries i.e. plug-flow and complete mixing (section 7.3). These results provide confidence in the experimental data i.e. RTD curve, reaction rate constant (k) and the H_2O_2 conversion.

The RTD flow models that describe a well-mixed system generally provide a better estimation of the experimental H_2O_2 conversion and this supports previous descriptions of the HDVS's mixing regime (chapter 4-6). The HDVS RTD investigations have shown that the characterisation of the mixing regime within a system is subject to the limitations of the data analysis techniques. To minimise any possible errors the use of the complete segregation model to estimate the efficiency of a kinetic process within a system is recommended since it is a zero parameter model (section 7.5). The complete segregation model estimated H_2O_2 conversion overflow component results provide confidence in replicating RTD experiments on the HDVS and also show that the baseflow component measured at SP3 results are significantly greater than at SP2 for the same inlet flow rate. The baseflow component results support previous observations, as the baseflow component measured at SP3 i.e. including the sludge hopper, has greater plug-flow mixing characteristics compared to SP2 and hence, provides a better kinetic process performance (chapter 6).

8.0 Conclusions

This project presents the first stage in developing and aiding the existing design methodology for the optimisation of kinetic processes within a hydrodynamic vortex separator (HDVS). This has been achieved by characterising the mixing regime within a model (375mm diameter) and a prototype (750mm diameter) HDVS using residence time distribution (RTD) analysis. The model and prototype HDVS's were operated with and without a baseflow component and for these two operating conditions with and without the sludge hopper (Fig. 3.1). The RTD has been used to identify and describe any deviation from the two theoretical mixing regimes, i.e. plug-flow and complete mixing, due to non-ideal flow behaviour such as dispersion and short-circuiting. It therefore provides an accurate description of the hydraulic characteristics. Subsequently the use of this extensive characterisation of the mixing regime allows the optimisation of the HDVS for a range of kinetic process applications using different design methodologies.

The majority of existing research on the HDVS has focussed on its solids-liquid separation efficiency (chapter 2). Several HDVS research projects have investigated the internal mixing regime by conducting RTD and computational fluid dynamics (CFD) investigations. However, these RTD and CFD investigations were generally undertaken to support conclusions obtained from HDVS solids-liquid removal efficiency investigations. These RTD investigations were conducted on different styles of HDVS and were neither comprehensive nor consistent in the methods used to describe the RTD. The various HDVS's have different internal configurations, operating conditions and preferred applications to the HDVS investigated in this project. Additionally, the design of existing HDVS kinetic process applications does not consider the presence of non-ideal flow behaviour and generally assumes a theoretical mixing regime. Hence,

this project is the first research undertaken to characterise the mixing regime within the HDVS for the optimisation of kinetic process applications. Further work was also required to compare the experimental efficiency with that predicted from the RTD and batch reactor investigations. This was done by investigating the first-order decomposition of hydrogen peroxide (H_2O_2) using an enzyme (catalase).

The HDVS pulse injection RTD results describe a system with a complex mixing regime, which depends on the operating configuration and parameters i.e. sludge hopper, baseflow component, inlet flow rate and flow split. The HDVS has an imperfect plug-flow mixing regime and the non-ideal flow behaviour is associated with dispersion, dead volumes and short-circuiting. Additionally, when the HDVS is operated with a baseflow component the overflow and baseflow components have different mixing regimes and the total mixing regime characteristics are different to the HDVS operating without a baseflow component. The overflow component mixing characteristics are very similar for the HDVS operating with and without a baseflow component.

8.1 Hydrodynamic Vortex Separator (HDVS) Operating without a Baseflow Component Residence Time Distribution (RTD) Analysis

The HDVS operating with no baseflow component exhibits short-circuiting at high flow rates whilst fluid elements with residence times greater than the theoretical mean residence time are present at low flow rates (chapters 4 and 5). The flow rate that identifies this change in the HDVS mixing characteristics is termed the transition flow rate and is approximately 15l/min and 90l/min for the model and prototype HDVS operating with no baseflow and with and without the sludge hopper respectively. Subsequently, at low flow rates 'sluggish-flow' regions are present i.e. slow moving

fluid elements and at high flow rates dead volumes, which do not contribute to the mixing regime and effectively reduce the total active volume.

The 'sluggish-flow' regions contribute to the RTD curve tail section i.e. volume elements with long residence times. At low flow rates poor tracer recoveries (mass balance) and significantly extended mean residence time values were obtained. This is associated with the 'sluggish-flow' regions creating tracer hold-up for significant time periods. A mathematical weighting effect inherent in the method of moments and to a lesser extent in the non-linear regression parameter estimation calculation technique then becomes significant.

The inactive flow behaviour within the HDVS generally increases for flow rates up to the transition flow rate and then remains relatively stable for all higher flow rates. This implies that a greater volume is active in the mixing process at low flow rates and the mixing regime is stable at high flow rates. Hence, the mixing regime within any size of HDVS above its transition flow rate is likely to be stable and provide the same plug-flow mixing and inactive flow behaviour irrespective of the flow rate. The inactive flow behaviour within the model HDVS operating with no baseflow occupies approximately 20-40% of the total volume and similarly for the prototype HDVS 5-25%. Therefore the inactive flow behaviour occupies a smaller fraction of the total volume, as the HDVS is scaled-up. This study shows the importance of investigating the mixing regime within a system for a range of flow rates, which cover and exceed existing design flow rates for a variety of applications.

The HDVS operating without a baseflow component ADM (P_e) and TISM (N) parameters calculated using both the method of moments and non-linear regression, show that the plug-flow mixing characteristics increase and dispersion and mixing effects decrease as the flow rate decreases. The mixing regime is classified as high dispersion and equal to approximately 2-4 completely mixed tanks-in-series. The

evidence of a transition flow rate i.e. a change in HDVS mixing characteristics, is also provided by the ADM and TISM parameters as they are stable at high flow rates. Therefore, the stable mixing regime within the HDVS at high flow rates is associated with both the inactive flow behaviour and the plug-flow mixing characteristics.

The model and prototype HDVS ADM and TISM parameters are of a similar order of magnitude and therefore, they operate with a similar mixing regime. However, the prototype HDVS ADM and TISM parameters are generally greater than the model HDVS at a flow rate providing a similar theoretical mean residence time within each device. Therefore, the prototype HDVS has marginally improved plug-flow mixing characteristics compared to the model HDVS. Additionally, the prototype HDVS also has less inactive flow behaviour as mentioned above. Hence, the scale-up of the HDVS will provide a mixing regime with less short-circuiting and improved plug-flow mixing characteristics and therefore, more conducive for certain kinetic processes and particularly chemical disinfection processes. However the HDVS ADM and TISM parameters fall in the range where any variation could affect the performance of the HDVS for disinfection processes (Johnson *et al.*, 1997 and 1998). Hence, there is scope for the HDVS to be modified and its mixing regime improved to provide a greater element of plug-flow mixing.

The HDVS investigated throughout this project has a sludge hopper located at its base, which provides a collection volume for solids in its typical application of solid-liquid separation (Fig. 3.1). The inactive flow behaviour observed at low flow rates i.e. 'sluggish-flow' regions was attributed to the sludge hopper region due to its isolated location within the HDVS compared to the remaining volume. Subsequently the model and prototype HDVS operating with no baseflow was also investigated with the sludge hopper removed.

8.2 Hydrodynamic Vortex Separator (HDVS) Operating without the Sludge Hopper Residence Time Distribution (RTD) Analysis

The RTD investigations undertaken on the HDVS operating with no baseflow and without the sludge hopper confirmed that the sludge hopper contributes to the inactive flow behaviour within the HDVS. The HDVS operated with and without the sludge hopper has very similar mixing characteristics across the range of flow rates as discussed above. However, at flow rates below the transition flow rate the mixing characteristics do marginally change and particularly for the model HDVS. Therefore, removing the sludge hopper from the model HDVS has a greater effect on the mixing regime i.e. a reduction in 'sluggish-flow' volume, compared to the prototype HDVS.

The error between the theoretical and experimental mean residence time decreases at low flow rates when the HDVS is operated without the sludge hopper due to a reduction in the 'sluggish-flow' volume which subsequently reduces the method of moments and non-linear regression biased RTD parameter estimation. This is supported by a better tracer recovery (mass balance), particularly at low flow rates, which provides further evidence that the sludge hopper contributes to the 'sluggish-flow' volumes. However, the error between the theoretical and experimental mean residence time is not always eliminated and suggests that inactive flow behaviour still exists. Observations on the model HDVS using coloured dye suggested that inactive volumes could also exist around the cone area and at the top water level in the outer zone (Fig. 3.1).

For the HDVS operating without the sludge hopper the ADM and TISM parameters, calculated using the method of moments and non-linear regression, are greater than for the HDVS operating with the sludge hopper at the same flow rate. The HDVS operating without the sludge hopper Peclet numbers (P_e) show that the flow due to convection is generally greater than the flow due to dispersion compared to the

HDVS operating with the sludge hopper. The removal of the sludge hopper improves the plug-flow mixing characteristics of the HDVS by reducing the 'sluggish-flow' volume, which is associated with dispersion and mixing effects. This change in the flow characteristics between the HDVS operating with and without the sludge hopper is greater for the model HDVS compared to the prototype HDVS.

8.3 Hydrodynamic Vortex Separator (HDVS) Operating with a Baseflow Component Residence Time Distribution (RTD) Analysis

The HDVS overflow component short-circuits at high inlet flow rates and the baseflow component at low inlet flow rates however, the inclusion of the sludge hopper reduces the short-circuiting within the baseflow component (SP3). The baseflow component measured at SP3 short-circuits as the flow split is increased for the same inlet flow rate and at SP2 the short-circuiting remains constant for all flow splits (Fig. 6.1). Therefore there are two marginally different mixing regimes within the HDVS which are associated with the overflow and baseflow component. The short-circuiting is possibly related to the strength of the vortex generated within the HDVS and the internal configuration of the HDVS (Fig. 3.1).

The different mixing characteristics of the overflow and baseflow component are also shown by the ADM and TISM parameters and the HDVS total flow (overflow + baseflow) mixing regime characteristics. The baseflow component plug-flow mixing characteristics improve as the inlet flow rate increases and the overflow component as the inlet flow rate decreases. Additionally the plug-flow mixing characteristics for the baseflow component, measured at SP3, are significantly better than the characteristics measured at SP2 for the same inlet flow rate.

The total flow parameters clearly show that the introduction of a baseflow component, especially when the sludge hopper is included in the HDVS configuration (SP3), significantly increases the plug-flow mixing within the HDVS compared to the HDVS operating with no baseflow component. The ADM and TISM parameters for the individual flow components describe a mixing regime with high dispersion. However, the total flow parameters at high flow rates describe a system with moderate dispersion. The largest plug-flow mixing element within the HDVS operating with a baseflow component exists at the highest inlet flow rate. This has significant advantages for providing effective high-rate chemical treatment and particularly as the HDVS has the ability to operate at very high inlet flow rates for a small footprint compared to conventional treatment processes (Boner *et al.*, 1994).

The overflow component plug-flow mixing characteristics generally remain stable or marginally increase as the flow split increases i.e. as the overflow component flow rate decreases. However, the baseflow component has different plug-flow mixing characteristics with respect to the flow split, depending on the sample point location (Fig. 6.1). At SP2 the baseflow component ADM and TISM parameters are relatively stable and at SP3 they significantly decrease as the flow split increases for the same inlet flow rate. Therefore, for a fixed inlet flow rate the baseflow component measured at SP3 plug-flow mixing characteristics decrease and greater short-circuiting occurs as the flow split increases. However the baseflow component measured at SP2 mixing characteristics are the same across the range of flow splits for the same inlet flow rate.

The HDVS operating with a baseflow component sampling configuration provided a measured RTD from 3 locations within the HDVS (Fig. 6.1). Comparing the magnitude of the ADM and TISM parameters calculated from the RTD obtained at each location suggests that there are three different mixing regimes within the HDVS. These are the outer zone, inner zone and sludge hopper (Fig. 3.1). The former provides a

mixing regime closer to complete mixing and the remaining two regions provide improved plug-flow mixing characteristics. The sludge hopper region also provides a greater degree of quiescent flow behaviour and subsequently plug-flow conditions compared to the inner zone.

The sludge hopper appears to act a tubular reactor and provides plug-flow mixing when the HDVS is operated with a baseflow component however it contributes to the 'sluggish-flow' volume when the HDVS is operated without a baseflow component. This change in the sludge hopper's mixing characteristics results in better RTD tracer recoveries (mass balance) at all flow rates when the HDVS is operated with a baseflow component.

The RTD t_{10} parameter values for both the model and prototype HDVS operating with no baseflow have a similar relationship with the mean residence time and is therefore, independent of the size of the HDVS. The baseflow component t_{10} parameter is greater when the sludge hopper is included in the HDVS configuration. This has practical, environmental and financial implications by reducing the quantity of the reactant required e.g. disinfectant.

The RTD results presented in this project for a Swirl-Flo™ HDVS provide comparable results with those previously presented by other workers on the Storm King™ and Grit King™ HDVS's (Table 1.1). Therefore, there is no significant difference in the mixing regime between the different styles of HDVS. However, the existing HDVS RTD investigations are not consistent or comprehensive in their characterisation of the HDVS's mixing regime and prevents an accurate comparison (section 8.6).

8.4 Residence Time Distribution (RTD) Correlation Parameters

The ADM and TISM parameter estimation using the method of moments and non-linear regression provide a very good fit to the experimental data. However, the non-linear regression technique provides an improved correlation (R^2 and ESS) to the experimental data due to its flexibility, which is achieved by directly fitting the model to the experimental curve. The highest R^2 value did not necessarily result in the smallest ESS and therefore it is important to assess the goodness of fit using more than one correlation parameter and visually.

The HDVS operating without a baseflow component method of moments TISM and non-linear regression ADM and TISM correlation parameters generally improve as the flow rate decreases. The non-linear regression TISM parameter estimation technique is the superior data analysis combination for accurately describing the HDVS mixing regime. The HDVS operating with a baseflow component ADM and TISM RTD parameters and their correlation with the experimental data generally support these observations.

The RTD combined model correlation parameters improve as the flow rate increases. This is the opposite relationship generally achieved for the ADM and TISM and is related to the limited physical realism of the combined model. The correlation parameters for the combined model, ADM and TISM are subject to the limitations of each model relative to the HDVS's non-ideal flow behaviour across the range of inlet flow rates. Therefore, it may be better to use the ADM or TISM non-linear regression relationship at low flow rates and the RTD combined model at high flow rates. Observations regarding the physical realism provided by the combined model at low flow rates suggest the need for a different combined model configuration including additional tanks-in-series (N).

8.5 Hydrogen Peroxide (H_2O_2) Decomposition Investigation – Kinetic Analysis

The H_2O_2 decomposition experimental results support the description of the mixing regime provided by the RTD. Therefore, the design of the HDVS for kinetic processes can use the RTD and relevant batch reactor experiments eliminating the need for costly and time consuming pilot trials.

The complete segregation model is preferred for the estimation of the efficiency of a kinetic process within a system (section 7.5). This is because the complete segregation model is a zero parameter model and a solution is obtained directly from the RTD curve. The complete segregation model estimation of the H_2O_2 conversion provided confidence in replicating RTD experiments on the HDVS. The complete segregation model also showed that the baseflow component including the sludge hopper (SP3) provides greater H_2O_2 conversion compared to the baseflow component without the sludge hopper (SP2) (Fig. 6.1). This supports previous observations, as the baseflow component including the sludge hopper has better plug-flow mixing characteristics and hence, provides a better kinetic process performance.

The development and optimisation of the HDVS for its typical application of solids-liquid separation has evolved over 30 years (chapter 2). This provides an indication of the time periods required to produce a robust design methodology based on laboratory investigations and supported by full-scale field trials. The long term objectives and future research initiatives undertaken to complete the HDVS kinetic process design methodology should follow the same approach as undertaken for solids-liquid separation and are addressed in the recommendations for future research (section 8.6).

8.6 Recommendations for Future Research

This project is the first stage in characterising and optimising the HDVS for kinetic process applications. Subsequently continuing investigations into the experimental techniques and methods used during this project and additional investigations to meet the long term objectives i.e. HDVS kinetic process optimisation are necessary.

1. The information provided by a RTD curve depends on the nature of the tracer and injection method and the data analysis technique used to describe the RTD. Therefore, the results from different RTD studies cannot always be directly compared with confidence. It follows that a HDVS RTD protocol should be established, following the procedure employed in this project on the Swirl-Flo™ HDVS and additional investigations undertaken on the Grit-King™ and Storm King™ HDVS (Table 1.1). This would enable the different styles of HDVS to be consistently characterised using RTD analysis and the effect of their different internal configurations investigated. This also applies to other workers investigating mixing devices which all operate in similar manner. This has partially been addressed by the development of DISINFEX™ computer software, which contains a RTD database covering a variety of mixing devices (section 2.2.4).

2. For the model and prototype HDVS operating with no baseflow, a transition flow rate was identified at which point the mixing regime changes. This requires further investigation to obtain a more accurate estimation of the transition flow rate, by conducting RTD tests at flow rates in the vicinity of the transition flow rate i.e. model HDVS – 15l/min and prototype HDVS 90l/min.

3. To investigate any pulse tracer density effects, RTD tests should be conducted using a low-level radioactive or fluorescent tracer e.g. C^{14} or Rhodamine and the results compared to the RTD pulse tracer (LiCl) results presented in this project. Additionally, the convolution integral RTD data analysis technique could also be employed to minimise any potential problems with the tracer properties, input signal technique and inlet flow conditions (Levenspiel, 1972). This technique requires the input RTD to be measured at a point downstream of the tracer injection location but upstream of the entrance to the HDVS in addition to the exit RTD i.e. overflow and baseflow. Automated tracer grab sampling withdrawal and analysis would also be beneficial by increasing the experiment processing time and allowing multiple sample locations to be managed.

4. The RTD combined mathematical model provides the potential to investigate the scaling of the RTD between the model and prototype HDVS (chapter 5). The scaling technique should involve developing relationships between the HDVS inlet flow rate and the quantity of non-ideal flow behaviour calculated using the combined model i.e. fraction of stagnant and dead volume. The inlet flow rate can also be presented as the surface loading rate, which is a function of the HDVS diameter and inlet flow rate i.e. flow rate/cross-sectional area ($l/s/m^2$). The model HDVS surface loading rates for all inlet flow rates are in the same range as those investigated for the prototype HDVS, as hydraulic scaling relationships were used to determine the equivalent prototype HDVS flow rate in the model HDVS (chapter 3). This approach will provide a scaling relationship based on a physical dimension of the HDVS. Additionally, this scaling methodology could also be extended to include existing RTD data obtained from a full-scale HDVS (Dudley and Marks, 1993) and the inactive flow behaviour based on a physical estimation. The above approach can

also be used to establish scaling relationships for the normalised variance (eqn. 4.6). The normalised variance provides an indication of the spread of the RTD curve and therefore the degree of dispersion within the HDVS (section 4.3.1). Subsequently, the scaling of the model and prototype HDVS normalised variance can be compared to the ADM and TISM parameters presented in this project. The ADM and TISM parameters are related to the Morrill Dispersion Index (t_{90}/t_{10}) (Johnson *et al.*, 1998) and therefore, the proposed scaling method can also be compared with the CT approach (section 4.3.4) and the existing work carried out on the HDVS ADF at Columbus in the US (section 2.1.5).

5. The RTD combined model data analysis technique has currently been limited to the HDVS operating with no baseflow and can be extended to incorporate a baseflow component. This would involve changing the existing combined model configuration (Fig. 5.1) by removing the exchange flow rate (Q_2) and replacing it with a unidirectional flow from tank $V_2 \rightarrow V_4$ which will provide a second outlet i.e. baseflow component. Additionally, the RTD combined model could be used to compare the inactive flow behaviour within the different types of HDVS (Table 1.1).

6. During RTD combined model parameter optimisation simulations it was observed that either the coefficient of correlation (R^2) or the sum of the errors squared (ESS) correlation parameters, used throughout this study to assess the goodness of fit, did not always occur at its maximum or minimum value for the same simulation. This requires investigation to determine which combined model and experimental curve correlation parameters best describe the goodness of fit and will increase confidence

in the final RTD combined model parameters for the recommended scaling investigations discussed above.

7. A comprehensive batch reactor experimental investigation should be undertaken for a range of kinetic processes with different reaction mechanisms i.e. second and third-order reactions and particularly commonly used disinfectants e.g. bromine chloride, chlorine, chlorine dioxide, peracitic acid, sodium hypochlorite etc. This should investigate physical and chemical effects associated with pH, temperature, kinetic process concentration variation and the composition of the treated water i.e. mains water and primary and secondary treated wastewater and stormwater. This information can be combined with the comprehensive characterisation of the HDVS using RTD analysis presented in this project to predict the efficiency of the HDVS for a range of kinetic process applications and operating conditions. Subsequently, selected kinetic processes and particularly disinfection processes investigated at batch scale, should also be investigated on the continuously operated model and prototype HDVS for the same operating conditions and the actual performance compared to that predicted from RTD theory and batch reactor data (chapter 7).

8. The RTD combined model can be further developed to include reaction rate constants (k) (chapter 7) (Wen and Fan, 1975). This enables the combined model solution to estimate the performance of a kinetic process within the HDVS accounting for the degree of non-ideal flow behaviour associated with both dispersion and dead volumes. The RTD combined model solution including scaling relationships and kinetic parameters would provide an integrated hydrodynamic and kinetic design methodology for any size of HDVS.

The author appreciates that the recommendations for future work provide the framework for a long-term investigation. However, it is a transparent process and will provide a HDVS kinetic process design methodology matrix based on RTD and batch reactor data verified against field trials. The proposed design methodology can also be applied to different size HDVS's. By collating the stages in this design methodology into a computer modelling package (chapter 2), it will provide the design engineer, not necessarily familiar with all the stages in this project and those proposed for future research, with a design parameter input interface to optimise the HDVS for kinetic process applications.

References

Aldershof, B. K., Dennis, R. M. and Kunitsky, C. J. (1997) Study of the decomposition of four commercially available hydrogen peroxide solutions by Fenton's reagent. *Water Environment Research*, **69** (5), 1052-1056.

Alkhaddar, R. M., Higgins, P. R. and Phipps, D. A. (1999) The use of hydrodynamic vortex separators (HDVS) for distributed treatment of combined sewer overflows (CSO): Preliminary characterisation of the Storm King™ for in situ disinfection. Hydro *International Plc Conference on Sewer Networks and CSO Solutions for AMP3*, Leicester, UK.

Alkhaddar, R. M., Higgins, P. R. and Phipps, D. A. (2000) Characterisation for in situ disinfection of a hydrodynamic vortex separator (HDVS). *Proceedings of the 1st World Congress of the International Water Association*, Paris, 3-7 July.

Alkhaddar, R. M., Higgins, P. R., Phipps, D. A. and Andoh, R. Y. G. (1999) The residence time distribution of a prototype hydrodynamic vortex separator operating with a baseflow component. *Proceedings of the 8th International Conference on Urban Storm Drainage*, Sydney, Australia, **1**, 18-25.

American Waterworks Association (1991) *Surface-water treatment: the new rules.* AWWA, Denver.

Andoh, R. Y. G. (1993) *The Swirl-Flo™ process for treatment of wastewater for discharges to estuaries and coast: full-scale evaluation at Totnes Wastewater Treatment Works*. Hydro Research and Development Ltd, Bristol, Clevedon, UK.

Andoh, R. Y. G. (1994) The Storm King™ overflow hydrodynamic separator. *Hydro Research and Development Ltd Conference on Alleviating the Problems of Combined Sewer Overflows within the Piped System*, Warrington, UK.

Andoh, R. Y. G. (1998) Improving environmental quality using hydrodynamic separators. *Water Quality International*, January/February, 47-51.

Andoh, R. Y. G. (2000) Personnel communication.

Andoh, R. Y. G., Fagan, G. and Cook, R. (1993) The Swirl-Flo™ physico-chemical process for urban wastewater treatment. *Hydro Research and Development Ltd Symposium on Advances in Wastewater Treatment for Smaller Communities*, Weston-Super-Mare, UK.

Andoh, R. Y. G. and Harper, I. (1994) The Swirl-Flo™ process for high rate physico-chemical treatment at wastewater treatment works. *Water Environment Federation – A Global Perspective for Reducing CSOs: Balancing Technologies, Costs and Water Quality*, Louisville, Kentucky, US.

Andoh, R. Y. G. and Smisson, R. P. M. (1993) High rate sedimentation in hydrodynamic separators. *Proceedings of the 2nd International Conference on Hydraulic Modelling, Development and Application of Physical and Mathematical Models*, Stratford, UK, 341-358.

Andoh, R. Y. G. and Williams, C. A. (1995) *Meeting the EU UWWTD with the Swirl-Flo™ and Eff-Pac™ processes.* Hydro Research and Development Ltd, Bristol, Clevedon, UK.

Arnett, C. J. and Gurney, P. K. (1998) High rate solids removal and chemical and non-chemical UV disinfection alternatives for treatment of CSO's. *Innovation 2000, Conference on Treatment Innovation for the Next Century*, Cambridge, UK.

Balmforth, D. J. (1990) The pollution aspects of storm sewage overflows. *Journal of the Institute of Water and Environmental Management*, **4** (3), 219-226.

Balmforth, D. J., Lea, S. J. and Sarginson, E. J. (1984) Development of a vortex storm sewage overflow with peripheral spill. *Proceedings of the 3rd International Conference on Urban Storm Drainage,* Gotenborg, Sweden, 107-116.

Balmforth, D. J., Saul, A. J. and Clifforde, I. T. (1994) *Guide to the design of combined sewer overflow structures*, Report FR 0488, Foundation for Water Research.

Battaglia, A., Fox, P. and Pohland, F. G. (1993) Calculation of residence time distribution from tracer recycle experiments. *Water Research*, **27** (2), 337-341.

Bennett, M. J. and Farraday, R. V. (1990) A Study of pollution control at a stormwater overflow. *International Conference on Advances in Water Treatment and Environmental Management.* Lyon, France.

Boner, M. C., Ghosh, D. R., Harper, S. R. and Turner, B. G. (1995) Modified vortex separator and UV disinfection for combined sewer overflow treatment. *Water Science and Technology*, **31** (3-4), 263-274.

Boner, M. C., Ghosh, D. R., Hides, S. P. and Turner, B. G. (1993) High rate treatment of CSOs in Columbus, Georgia. *Proceedings of the 6th International Conference on Urban Storm Drainage,* Niagara Falls, Canada, 1671-1675.

Boner, M. C., Harper, S. R., Patrick, G. C., Ghosh, D. R. and Cairns, W. L. (1994) *Optimisation of vortex separator removal efficiencies for CSO Treatment.* Water Environment Research Foundation (WERF) Project 92-TCR-2.

Bosworth, R. C. L. (1948) Distribution of reaction times for laminar flow in cylindrical reactors. *Philosophical Magazine Series*, **7** (39), 847-862.

Brombach, H. (1987) Liquid-solid separation at vortex storm overflows. *Proceedings of the 4th International Conference on Urban Storm Drainage, Topics in Urban Storm Water Quality, Planning and Management,* Lausanne, Switzerland, 103-108.

Brombach, H. (1992) Solids removal from CSOs with vortex separators. *Novatech 92, International Conference on Innovative Technologies in the Domain of Urban Water Drainage*, Lyon, France, 447-459.

Brombach, H., Xanthopoulos, C., Hahn, H. H. and Pisano, W. C. (1993) Experience with vortex separators for combined sewer overflow control. *Water Science and Technology*, **27** (5-6), 93-104.

Brouckaert, C. J., Botha, C. J., Baddock, L. A. and Buckley, C. A. (1995) Impulse: a PC program for the determination of residence time distributions of biological and chemical reactors. *Water Supply,* **13** (2), 305-308.

BS 3680 2C: 1993 *Measurement of liquid flow in open channels. Methods of measurement using chemical tracers.*

BS 3680 2D: 1993 *Measurement of liquid flow in open channels. Methods of measurement using fluorescent tracers.*

Buffham, B. A. (1983) Internal and external residence time distributions. *Chemical Engineering Communication,* **22,** 105-107.

Buffham, B. A. and Mason, G. (1993) Holdup and dispersion: tracer residence times, moments and inventory measurements. *Chemical Engineering Science,* **48** (23), 3879-3887.

Buffham, B. A. and Nauman, E. B. (1975) On the limiting form of the residence–time distribution for a constant-volume recycle system. *Chemical Engineering Science,* **30,** 1519-1524.

Burrows, L. J., Stokes, A. J., West, J. R., Forster, C. F. and Martin, A. D. (1999) Evaluation of different analytical methods for tracer studies in aeration lanes of activated sludge plants. *Water Research,* **33** (2), 367-374.

Butler, D. and Davies, J. W. (2000) *Urban drainage,* E & FN Spon, London, UK.

Chick, H. (1908) An investigation of the laws of disinfection. *Journal of Hygiene,* **8,** 92-157.

Cholette, A. and Cloutier, I. (1959) Mixing efficiency determinations for continuous flow systems. *Canadian Journal of Chemical Engineering,* June, 105-112.

CIRIA (2000) *Sustainable urban drainage systems.* Research Project 555.

Conklin, A. R. (1996) Demonstration of the catalytic decomposition of Hydrogen Peroxide. *Journal of Chemical Education,* **73** (9), 838-839.

Council of the European Communities (1976). Council directive concerning the quality of bathing water (76/160/EEC). *Official Journal of the European Communities,* L31/1, February.

Council of the European Communities (1991). Council directive concerning urban wastewater treatment (91/271/EEC). *Official Journal of the European Communities,* L135/40, May.

Danckwerts, P. V. (1953) Continuous flow systems: distribution of residence times. *Chemical Engineering Science,* **2** (1), 3857-3866.

Danckwerts, P. V. (1958) The effect of incomplete mixing on homogeneous reactions. *Chemical Engineering Science,* **8,** 93-102.

Danckwerts, P. V., Jenkins, J. W. and Place, G. (1954) The distribution of residence-times in an industrial fluidised reactor. *Chemical Engineering Science*, **3**, 26-35.

Danckwerts, P. V. and Wilson, R. A. M. (1963) Flow-visualization by means of a time-reaction. *Journal of Fluid Mechanics*, **16** (3), 412-416.

Dawson, M. (1998) Cleaning up with disinfection design software. *Water Treatment and Supply*, November.

Deckwer, W. D. and Schumpe, A. (1993) Improved tools for bubble column reactor design and scale-up. *Chemical Engineering Science*, **48** (5), 889-911.

Denbigh, K. G., Dombrowski, N., Kisiel, A. J. and Place, E. R. (1962) The use of the "time-reaction" in residence time studies. *Chemical Engineering Science*, **17**, 573-577.

Dennis, R. M. (1984) *Oxidation of sodium cyanide in aqueous solutions by ultraviolet light and hydrogen peroxide*. PhD Thesis, Graduate School of Vanderbilt University.

Douglas, J. M. (1964) The effect of mixing on reactor design. *American Institute of Chemical Engineers (AIChE) Symposium Series*, **60** (48), 1-14.

Dudley, J. and Marks, H. (1993) *Evaluation of the Swirl-Flo™ Process*, WRc Report UC 1869.

Environment Select Committee (1998) *Sewage treatment and disposal*, HC 266-I.

Fagan, G. W. (1993) A quality assessment of dynamic experiences: the UK experience. *Proceedings of the 6th International Conference on Urban Storm Drainage*, Niagara Falls, Canada, 1663-1669.

Faram, M. G. and Andoh, R. Y. G. (2000) Application of simulation and predictive Techniques for the evaluation of hydrodynamic separators. *Proceedings of the Wastewater Treatment: Standards and Technologies to meet the Challenges of the 21st Century Joint Millennium Conference*, Leeds, UK, 223-230.

Fenner, R. A. and Tyack, J. N. (1997) Scaling laws for hydrodynamic separators. *American Society of Civil Engineers, Journal of Environmental Engineering*, **123** (10), 1019-1026.

Fenner, R. A. and Tyack, J. N. (1998) Physical modeling of hydrodynamic separators operating with underflow. *American Society of Civil Engineers, Journal of Environmental Engineering*, **124** (9), 881-886.

Fernández-Sempere, J., Font-Montesinos, R. and Espejo-Alcaraz, O. (1995) Residence time distribution for unsteady-state systems. *Chemical Engineering Science*, **50** (2), 223-230.

Field, R. (1974) Design of a combined sewer overflow regulator concentrator. *Journal of the Water Pollution Control Federation (WPCF)*, **46** (7), 1722-1741.

Field, R. and O'Connor, T. P. (1996) Swirl Technology: enhancement of design, evaluation and application. *American Society of Civil Engineers, Journal of Environmental Engineering,* **122** (8), 741-748.

Fogler, H. S. (1992) *Elements of chemical reaction engineering*, second edition. Prentice Hall International Editions.

Foundation for Water Research (1998) *Urban pollution management manual*, second edition, FR/CL 0002.

Gagné, B., Cigana, J., Couture, M., Meunier, C. and Comeau, Y. (1998) Determination of the vertical velocity distribution of floatables in CSOs. *Novatech 98, International Conference on Innovative Technologies in the Domain of Urban Water Drainage*, Lyon, France.

Ghosh, D. R. and Boner, M. C. (1992) Treatment of combined sewer overflows in a vortex separator. Control of Wet Weather Water Quality Problems, WERF Speciality Conference, June, USA, 1-14.

Gilliland, E. R. and Mason, E. A. (1952) Gas mixing in beds of fluidised solids. *Industrial and Engineering Chemistry*, **44**, 218-234.

Gustavsson, T. J. L., Fladda, G. H. and Masters, S. (1998) Residual peroxide measurement-an important parameter for monitoring and controlling the peroxide bleaching process. *Appita*, 341-345.

Haas, C. N. (1988) Micromixing and dispersion in chlorine contact chambers. *Environmental Technology Letters*, **9**, 35-44.

Haas, C. N. (1996) Moment analysis of tracer experiments. *American Society of Civil Engineers, Journal of Environmental Engineering,* **122** (12), 1121-1123.

Haas, C. N., Joffe, J., Anmangandla, U., Hornberger, J. C., Heath, M. S., Jacangelo, J. and Glicker, J. (1995) *Development and validation of rational design methods of disinfection*, AWWA Research Foundation.

Haas, C. N., Joffe, J., Heath, M. S. and Jacangelo, J. (1997) Continuous flow residence time distribution function characterisation. *American Society of Civil Engineers, Journal of Environmental Engineering,* **123** (2), 107-114.

Haas, C. N., Longley, K. and Selfridge, T. (1990) High-rate coliform disinfection of stormwater overflow. *Journal of the Water Pollution Control Federation (WPCF)*, **62** (3), 282-287.

Haas, C. N., Sheerin, J. G., Lue-Hing, C., Rao, K. C. and O'Brien, P. (1988) Effects of discontinuing disinfection on a receiving water. *Journal of the Water Pollution Control Federation (WPCF)*, **60** (5), 667-673.

Hahn, H. H. (1990) Sedimentation and flotation: Present status and necessary development: An introduction. *Water Supply*, **8**, 111-122.

Hall, E. R. (1985) Nonintrusive estimation of active volume in anaerobic reactors. *Canadian Journal of Water Pollution Research*, **20** (2), 44-54.

Hall, C. and Hughes, T. L. (1993) Ion chromatography tracer experiments during drilling. *SPE International Symposium on Oilfield Chemistry*. New Orleans, USA, March 2-5, 281-289.

Halliwell A. R. and Saul, A. J. (1980) The use of hydraulic models to examine the performance of storm-sewage overflows. *Proceedings of the Institution of Civil Engineers*, London, UK, **69** (2), 245-259.

Hamoda, M. F. and Abd-El-Bary, F. (1987) Operating characteristics of the aerated submerged fixed-film (ASFF) bioreactor. *Water Research,* **21** (8), 939-947.

Hansen, J. C. (1996) The iodide-catalyzed decomposition of hydrogen peroxide: a simple computer-interfaced kinetics experiment for general chemistry. *Journal of Chemical Education*, **73** (8), 728-732.

Harwood, R. and Saul, A. J. (1996a) *Field testing of a Storm King™ with Swirl Cleanse™ hydrodynamic separator combined sewer overflow.* Summary Report by the University of Sheffield for Hydro Research and Development Ltd, Clevedon, Bristol, UK, August.

Harwood, R. and Saul, A. J. (1996b) CFD and novel technology in combined sewer overflow. *Proceedings of the 7th International Conference on Urban Storm Drainage,* Hannover, Germany, 1025-1030.

Harwood, R. and Saul, A. J. (1999) The Influence of CSO chamber size on particle retention efficiency performance. *Proceedings of the 8th International Conference on Urban Storm Drainage,* Sydney, Australia, 1-9.

Hedges, P. D. (1991) The performance of a hydrodynamic separator combined sewer overflow. *Hydro Research and Development Ltd Conference on Practice and Performance*, London, UK.

Hedges, P. D. (1993) The relationship between field and model studies of a hydrodynamic separator combined sewer overflow. *Proceedings of the 6th International Conference on Urban Storm Drainage,* Niagara Falls, Canada, 1537-1541.

Hedges, P. D. (1994) The prediction of combined sewer overflow performance from models – a case study. *Water Science and Technology*, **29** (1-2), 373-382.

Hedges, P. D., Becker, F. A. and Smisson, R. P. M. (1998) The application of settling velocity as a parameter for characterising wastewater solids. *Water Science and Technology*, **37** (1), 45-52.

Higgins, P. R., Alkhaddar, R. M., Phipps, D. A. and Andoh, R. Y. G. (1998) Residence time distribution of a hydrodynamic vortex separator. *Proceedings of the 2nd International Conference on Advanced Wastewater Treatment, Recycling and Reuse*, Milan, Italy.

Higgins, P. R., Alkhaddar, R. M., Phipps, D. A. and Andoh, R. Y. G. (1999) Investigation into the retention-time distribution of a hydrodynamic vortex separator. *Journal of the Chartered Institution of Water and Environmental Management*, **13** (4), 255-261.

Himmelblau, D. M. and Bischoff, K. B. (1968) *Process analysis and simulation: deterministic systems*. John Wiley & Sons, New York.

Hvitved-Jacobsen, T. (1982) The impact of combined sewer overflows on the dissolved oxygen concentration of a river. *Water Research*, **16**, 1099-1105.

Irvine, K. N. and Pettibone, G. W. (1993). Dynamics of indicator bacteria populations in sediment and river water near a combined sewer outfall. *Environmental Technology Letters*, **14**, 531-542.

James, A. (1999) Personnel communication.

Johnson, P., Graham, N., Dawson, M. and Barker, J. (1998) Determining the optimal theoretical residence time distribution for chlorine contact tanks. *Journal of Water Services Research and Technology - Aqua*, **47** (5), 209-214.

Johnson, P., Graham, N. and Wilson, M. (1997) Predictive chlorine dosing: a new paradigm. *Journal of the Chartered Institution of Water and Environmental Management*, **11**, 413-422.

Kuznetsov, V. L., Elizarova, G. L., Usoltseva, A. N., Matvienko, L. G. and Shchegolikhina, O. I. (1997) Active sites of iron catalysts for oxidation reactions – H_2O oxidation and H_2O_2 decomposition. *Proceedings of the Materials Research Society Symposium*, **454**, 91-96.

Lawler, D. F. and Singer, P. C. (1993) Analyzing disinfection kinetics and reactor design: a conceptual approach versus the SWTR. *Journal of American Water Works Association (AWWA)*, November, 67-76.

Lee, E. T., Rehkopf, P. G., Warnicki, J. W., Friberg, T., Finegold, D. N. and Cape, E. G. (1997) A new method for assessment of changes in retinal blood flow. *Medical Engineering and Physics*, 19 (2), 125-30.

Levenspiel, O. (1972) *Chemical reaction engineering*, second edition. John Wiley & Sons, New York.

Levenspiel, O (1979) *The chemical reactor minibook*, John Wiley & Sons, New York.

Luyckx. G., Vaes. G. and Berlamont, J. (1998a) Experimental investigation on the efficiency of a hydrodynamic Storm King™ separator. *Novatech 98, International Conference on Innovative Technologies in the Domain of Urban Water Drainage*, Lyon, France, 443-450.

Luyckx. G., Vaes. G. and Berlamont, J. (1998b) Comparison between the separating efficiency of an improved high-side weir overflow and a hydrodynamic Storm King™ separator. *Proceedings of the 4th International Conference on Developments in Urban Drainage Modelling*, London, UK, 451-458.

Martin, N., Benezet-Toulze, M., Laplace, C., Faivre, M. and Langlais, B. (1992) Design and efficiency of ozone contactors for disinfection. *Ozone Science and Engineering*, **14** (5), 391-405.

Michelsen, M. L. (1972) A least squares method for residence time distribution analysis. *Journal of Chemical Engineering*, **4**, 171-179.

Montieth, H. D. and Stephenson, J. P. (1981) mixing efficiencies in full-scale anacrobic digesters by tracer methods. *Journal of the Water Pollution Control Federation (WPCF)*, **53** (1), 78-84.

Morgan-Sagastume, J. M., Jiménez, B. and Noyola, A. (1999) Alternative index for interpretation of RTD curves. *American Society of Civil Engineers, Journal of Environmental Engineering*, **125** (3) 290-294.

Morrill, A. B. (1932) Sedimentation basin research and design. *Journal of American Water Works Association (AWWA)*, **24** (9), 1442-1463.

Muhammad, N., Wheatley, A. D. and Smith, M. I. R. (2000) Design and development of Klargester oil/water interceptor. *Environment Agency and International Water Association Young Researchers Conference*, Nottingham, UK.

Mulliss, R., Revitt, D. M. and Shutes, R. B. E. (1997) The impacts of discharges from two combined sewer overflows on the water quality of an urban watercourse. *Water Science and Technology*, **36** (8-9), 195-199.

Naméche, T. and Vassel, J. L. (1996) New method for studying the hydraulic behaviour of tanks in series-application to aerated lagoons and waste stabilization ponds. *Water Science and Technology*, **33** (8), 105-124.

Naor, P. and Shinnar, R. (1963) Representation and evaluation of residence time distributions. *Industrial and Engineering Chemical Fundamentals*, **2** (4), 278-286.

Nauman, E. B. (1981) Residence time distributions and micromixing. *Chemical Engineering Communication*, **8**, 53-131.

Nauman, E. B. and Buffham, B. A. (1983) *Mixing in continuous flow systems*. John Wiley & Sons, New York.

Ni, X. (1994) RTD measurements in a pulsed baffled tube bundle. *Journal of Chemical Technology and Biotechnology*, **59**, 213-221.

Nieuwstad, T. J., Havelaar, A. H. and Van Olphen, M. (1991) Hydraulic and microbiological characterization of reactors for ultraviolet disinfection of secondary wastewater effluent. *Water Research*, **25** (7), 775-783.

NRA (1993) *General guidance note for preparatory work for AMP2 (version 2)*, October.

Oliveros, G and Smith, J. M. (1982) Dynamic studies of dispersion and channeling in fixed beds. *Journal of American Institute of Chemical Engineers (AIChE)*, **28** (5), 751-759.

Pisano, W. C. and Brombach, H. (1994) Operational experience with vortex solids separators for combined sewer overflow (CSO) control. *Water Science and Technology*, **29** (1-2), 383-391.

Pisano, W. C. and Zukovs, G. (1992) Demonstration of advanced high rate treatment for CSO control in Metropolitan Toronto. *Novatech 92, International Conference on Innovative Technologies in the Domain of Urban Water Drainage*, Lyon, France, 331-339.

Realey, G. J. (1989) *Stormwater disinfection trial at Bexhill-on-Sea using Oxymaster™*, WRc Report 888-S.

Realey, G. J. (1995) Impact of European Union Directives on the use of wastewater disinfection in England and Wales. *Seminar on Water and Wastewater Disinfection.* Chartered Institution of Water and Environmental Management, Birmingham, UK.

Robinson, B. A. and Tester, J. W. (1984) Dispersed fluid flow in fractured reservoirs: an analysis of tracer-determined residence time distributions. *Journal of Geophysical Research,* **89** (B12), 10374-10384.

Robinson, B. A. and Tester, J. W. (1986) Characterisation of flow maldistribution using inlet-outlet tracer techniques: an application of internal residence time distributions. *Chemical Engineering Science,* **41** (3), 469-483.

Rudd, T. and Hopkinson, L. M. (1989) Comparison of disinfection techniques for sewage and sewage effluents. *Journal of the Institute of Water and Environmental Management*, **3**, 612-618.

Ruff, S. (1994) Meeting new consents: the development of the Diverter™. *Hydro Research and Development Ltd Seminar on the Control of Urban Wastewater in the 90s*, Lymm, UK.

Ruff, S., Saul, A. J., Walsh, A. M. and Green, M. J. (1994) *The performance of a Storm King™ with an insitu Diverter™.* WRc Report No UC2324.

Samson, R., Van der Berg, I. and Kennedy, K. J. (1984) Influence continuous versus channels on mixing characteristics and performance of anaerobic downflow stationary fixed film (DSFF) reactors before and during waste treatment. *Proceedings of the 39th International Conference on Industrial Waste*, Purdue University, Indianapolis, USA, 677-685.

Saul, A. J. (1998) CSO state of the art review: a UK perspective. *Proceedings of the 4th International Conference on Developments in Urban Drainage Modelling,* London, UK, 617-626.

Saul, A. J. (2000) CSO screening for AMP3. *Hydro International Plc Conference on Sewer Networks and CSO Solutions for AMP3*, Warrington, UK.

Saul, A. J. and Harwood, R. (1998) Gross solid retention efficiency of hydrodynamic separator CSOs. *Proceedings of the Institution of Civil Engineers, Water, Maritime and Energy*, **130**, 70-83.

Saul, A. J. and Svejkovsky, K. (1994) Computational modelling of a vortex CSO structure. *Water Science and Technology*, **30** (1), 97-106.

Sawyer, C. N., McCarty, P. L. and Parkin, G. F. (1994) *Chemistry for environmental engineering,* fourth edition. McGraw-Hill International Editions.

Scottish Environment Protection Agency and Environment Agency (1997) *A guide to sustainable urban drainage.*

Shepherd, W., Guymer, I. and Saul, A. (2000) Soluble pollutant retention in a CSO structure. *WaPug Autumn Meeting,* Blackpool, UK.

Smisson, B. (1967) Design, construction, and performance of vortex overflows. *Symposium on storm sewage overflows*, Institution of Civil Engineers, May, 99-110.

Smisson, R. P. M. (1987) The development of dynamic separation. *Hydro Research and Development Ltd Internal Report*, Clevedon, Bristol, UK.

Smisson, R. P. M. (1989) Storm King™ dynamic separators for combined sewer overflows: Results to demonstrate compliance with performance requirements. *Hydro Research and Development Ltd Internal Report*, Clevedon, Bristol, UK.

Smith, B. (1999) CSO screening without power. *Hydro International Plc Conference on Alleviating Stormwater and CSO Problems*, Falkirk, UK.

Stedman, L. (1996) *Water Bulletin*, November.

Stedman, L. (1997) *Water Bulletin*, May.

Stevenson, D. G. (1995) The design if disinfection contact tanks. *Journal of the Chartered Institution of Water and Environmental Management*, **9**, 146-152.

Stover, E. L., Haas, C. N., Rakness, K. L. and Scheible, O. K. (1986) *USEPA Design Manual Municipal Wastewater Disinfection.* EPA/625/1-86/021.

Svarovsky, L. (1984) *Hydrocyclones*, Holt, Rinehart and Winston, London, England.

Tchobanoglous, G. and Burton, F. L. (1991) *Wastewater engineering treatment disposal reuse*, third edition. McGraw-Hill International Editions.

Teefy, S. M. and Singer, P. C. (1990) Performance and analysis of tracer tests to determine compliance of a disinfection scheme with the SWTR. *Journal of American Water Works Association (AWWA)*, December, 88-98.

Thomas, J. H. (1989) *The Egerton Park environmental survey.* Southern Water Authority, Southern Projects, UK.

Treleaven, C. R. and Tobgy, A. H. (1971) Conversion in reactors having separate reactant feed streams the state of maximum mixedness. *Chemical Engineering Science,* **26**, 1259-1269.

Trussell, R. R. and Chao, J. L. (1977) Rational design of chlorine contact facilities. *Journal of the Water Pollution Control Federation (WPCF).* **49** (4), 659-667.

Turner, B. G. and Boner, M. C. (1998) Economics of wet weather water quality controls. *Innovation 2000, Conference on Treatment Innovation for the Next Century,* Cambridge, UK.

Tyack, J. N. and Fenner, R. A. (1997) The use of scaling laws in characterising residence time in hydrodynamic separators. *Proceedings of the 2nd International Conference on the Sewer* and/as *a Physical, Chemical and Biological Reactor,* Aalborg, Denmark, 25-28 May.

Tyack, J. N. and Fenner, R. A. (1998a) Computational fluid dynamics modelling of velocity profiles within a hydrodynamic separator. *Proceedings of the 4th International Conference on Developments in Urban Drainage Modelling,* London, UK, 441-449.

Tyack, J. N. and Fenner, R. A. (1998b) Identification of flow regimes within a hydrodynamic separator. *Novatech 98, International Conference on Innovative Technologies in the Domain of Urban Water Drainage*, Lyon, France.

Tyack, J. N., Hedges, P. D. and Smisson, R. P. M. (1992) The use of sewage settling velocity grading in combined sewer overflow design. *Novatech 92, International Conference on Innovative Technologies in the Domain of Urban Water Drainage*, Lyon, France.

Tyack, J. N., Hedges, P. D. and Smisson, R. P. M. (1993) A device for determining the settling velocity grading of storm sewage. *Proceedings of the 6th International Conference on Urban Storm Drainage,* Niagara Falls, Canada, 1805-1810.

Walsh, A. M., Dempsey, P. and Thornton, A. J. (1994) *Investigation of alternatives to fixed storage for storm sewage*, WRc Report PT 1030.

Watson, H. E. (1908) A note on the variation of the rate of disinfection with change in the concentration of the disinfectant. *Journal of Hygiene*, **8**, 536-542.

Weiss, G. J. and Michelbach, S. (1996) Vortex separator: dimensionless properties and calculation of annual separation efficiencies. *Water Science and Technology*, **33** (9), 277-284.

Wen, C. Y. and Fan, L. T. (1975) *Models for flow systems and chemical reactors.* Marcel Dekker, Inc., New York.

Werner, T. M. and Kadlec, R. H. (1996) Application of residence time distributions to stormwater treatment systems. *Ecological Engineering*, 7, 213-234.

Westerterp, K. A., Van Swaaij, W. P. M. and Beenackers, A. A. C. M. (1984) *Chemical reactor design and operation.* John Wiley & Sons, Chichester, UK.

Wolf, D. and Resnick, W. (1963) Residence time distribution in real systems. *Industrial and Engineering Chemical Fundamentals*, **2** (4), 287-293.

Wolf. D. and White, D. H. (1976) Experimental study of the residence time distribution in plasticating screw extruders. *Journal of American Institute of Chemical Engineers (AIChE)*, **22** (1), 122-130.

World Health Organisation (1993) *Guidelines for drinking water*. WHO, Geneva.

Worrell, G. R. and Eagleton, L. C. (1964) An experimental study of mixing and segregation in a stirred tank reactor. *Canadian Journal of Chemical Engineering*, December, 254-258.

Young, H. W. and Young, J. C. (1988) Hydraulic characteristics of upflow anaerobic filters. *American Society of Civil Engineers, Journal of Environmental Engineering*, **114** (3), 621-638.

Zukovs, G. and Pisano, W. C. (1993) Demonstration of advanced high rate treatment for CSO control in Metropolitan Toronto. *Proceedings of the 6th International Conference on Urban Storm Drainage,* Niagara Falls, Canada, 1657-1662.

Zukovs, G. and Pisano, W. C. (1994) Process design of advanced storage-treatment facilities for CSO control. *Water Science Technology*, **30** (1), 121-130.

Zwietering, T. N. (1959) The degree of mixing in continuous flow systems. *Chemical Engineering Science,* **2** (1), 1-15.

PUBLICATIONS

PAGE/PAGES EXCLUDED UNDER INSTRUCTION FROM UNIVERSITY

THESIS CONTAINS CD/DVD